

Neuromethods 109

Springer Protocols



David W. Walker *Editor*

Prenatal and Postnatal Determinants of Development

 Humana Press

NEUROMETHODS

Series Editor
Wolfgang Walz
University of Saskatchewan,
Saskatoon, SK, Canada

For further volumes:
<http://www.springer.com/series/7657>

Prenatal and Postnatal Determinants of Development

Edited by

David W. Walker

*The Ritchie Centre,
Hudson Institute of Medical Research, Monash Medical Centre
&
Department of Obstetrics & Gynaecology,
Monash University - Clayton Campus
Melbourne, Australia*

 **Humana Press**

Editor

David W. Walker
The Ritchie Centre
Hudson Institute of Medical Research
Monash Medical Centre
&
Department of Obstetrics & Gynaecology
Monash University - Clayton Campus
Melbourne, Australia

ISSN 0893-2336 ISSN 1940-6045 (electronic)
Neuromethods
ISBN 978-1-4939-3013-5 ISBN 978-1-4939-3014-2 (eBook)
DOI 10.1007/978-1-4939-3014-2

Library of Congress Control Number: 2015955169

Springer New York Heidelberg Dordrecht London
© Springer Science+Business Media New York 2016

This work is subject to copyright. All rights are reserved by the Publisher, whether the whole or part of the material is concerned, specifically the rights of translation, reprinting, reuse of illustrations, recitation, broadcasting, reproduction on microfilms or in any other physical way, and transmission or information storage and retrieval, electronic adaptation, computer software, or by similar or dissimilar methodology now known or hereafter developed.

The use of general descriptive names, registered names, trademarks, service marks, etc. in this publication does not imply, even in the absence of a specific statement, that such names are exempt from the relevant protective laws and regulations and therefore free for general use.

The publisher, the authors and the editors are safe to assume that the advice and information in this book are believed to be true and accurate at the date of publication. Neither the publisher nor the authors or the editors give a warranty, express or implied, with respect to the material contained herein or for any errors or omissions that may have been made.

Printed on acid-free paper

Humana Press is a brand of Springer
Springer Science+Business Media LLC New York is part of Springer Science+Business Media (www.springer.com)

Series Preface

Experimental life sciences have two basic foundations: concepts and tools. The *Neuro-methods* series focuses on the tools and techniques unique to the investigation of the nervous system and excitable cells. It will not, however, shortchange the concept side of things as care has been taken to integrate these tools within the context of the concepts and questions under investigation. In this way, the series is unique in that it not only collects protocols but also includes theoretical background information and critiques which led to the methods and their development. Thus it gives the reader a better understanding of the origin of the techniques and their potential future development. The *Neuro-methods* publishing program strikes a balance between recent and exciting developments like those concerning new animal models of disease, imaging, in vivo methods, and more established techniques, including, for example, immunocytochemistry and electrophysiological technologies. New trainees in neurosciences still need a sound footing in these older methods in order to apply a critical approach to their results.

Under the guidance of its founders, Alan Boulton and Glen Baker, the *Neuro-methods* series has been a success since its first volume published through Humana Press in 1985. The series continues to flourish through many changes over the years. It is now published under the umbrella of Springer Protocols. While methods involving brain research have changed a lot since the series started, the publishing environment and technology have changed even more radically. *Neuro-methods* has the distinct layout and style of the Springer Protocols program, designed specifically for readability and ease of reference in a laboratory setting.

The careful application of methods is potentially the most important step in the process of scientific inquiry. In the past, new methodologies led the way in developing new disciplines in the biological and medical sciences. For example, Physiology emerged out of Anatomy in the nineteenth century by harnessing new methods based on the newly discovered phenomenon of electricity. Nowadays, the relationships between disciplines and methods are more complex. Methods are now widely shared between disciplines and research areas. New developments in electronic publishing make it possible for scientists that encounter new methods to quickly find sources of information electronically. The design of individual volumes and chapters in this series takes this new access technology into account. Springer Protocols makes it possible to download single protocols separately. In addition, Springer makes its print-on-demand technology available globally. A print copy can therefore be acquired quickly and for a competitive price anywhere in the world.

Saskatoon, Saskatchewan, Canada

Wolfgang Walz

Preface

The epidemiological and experimental evidence that stress, illness, or nutritional deprivation during pregnancy will impact on the structural and functional development of the brain is now compelling. This may cause not only catastrophic damage to the brain at birth, as shown by brain damage that leads to cerebral palsy, but also more subtle and long-term effects that manifest as behavioral disorders in the child and adult such as autism, schizophrenia, and compulsive/addictive behaviors. In addition to these extrinsic (environmental) influences, epigenetic, sex, and parental genomic effects have roles in determining the outcomes of pregnancy for the infant and child.

The purpose of this book is to provide the reader with an introduction to all the methods and major approaches now being used to study the structural and functional development of the brain. This area of research has gained greater prominence in recent years because so many more preterm babies survive, and their birth can occur at times when major cell migration and phenotypic transitions in the brain are still underway. Because of this we needed to cover topics such as early anatomical development, the emergence of function, and the processes that lead to damage and repair of the growing and immature brain; we have covered a broader area of research than would customarily be expected.

The book is divided into three parts—Development, Programming and Stress, and Brain Damage—Causes and Consequences.

In **Part 1 (Development)**, *Peter Kozulin, Gonzalo Almarza, Ilan Gobijs, and Linda J. Richards* introduce the concept of “in utero” electroporation (IUE) that provides a means of labeling neural progenitor cells and tracking their progeny in vivo. Using promoter-specific reporter constructs, and with precise transfection of progenitor subpopulations, they show how it is possible to induce or repress gene expression of neurons in a spatially and temporally specific manner at very early embryonic stages. *Isabel Martínez-Garay, Fernando García-Moreno, Navneet Vasistha, Andre Marques-Smith, and Zoltán Molnár* also report on the use of in utero electroporation to study key aspects of neural development, such as progenitor proliferation, neurogenesis, clonal and lineage analysis, neuronal migration, and circuit formation in various species from the chick to higher mammals with gyrencephalic brain development. This method can be also used to monitor and modulate the formation of cortical circuits in a controlled manner. Then, *Hui Xuan Ng and Joanne M. Britto* discuss how to study the placement of interneurons and pyramidal neurons during corticogenesis. Using transgenic technology to fluorescently label and isolate interneuron progenitor cells, they discuss how the cells isolated from the medial germinal epithelium can be transplanted in utero into the embryonic lateral ventricle; they further discuss how this might eventually become a cell-based therapy to rectify GABAergic dysfunction in the neocortex.

Techniques for studying the functional development of the infant human brain are introduced in the chapter by *Sampsa Vanhatalo and Peter Fransson*. The function of developing sensory systems can be readily studied using EEG even at a developmental stage when the sensory connections are only incompletely formed, and they develop the idea of deriving large-scale maps of functional connectivity from continuous records of the EEG and blood deoxygenation (fMRI) of the infant brain, despite the immaturity of neurovascular coupling making such functional tests a challenge. *Flora Wong* develops this theme by discussing the constraints in measuring cerebral blood flow in infants due to the

necessity to use noninvasive techniques. There is no general agreement on the best approach to measure cerebral blood flow, but despite the methodological differences, all of the commonly used techniques yield reasonably comparable results in terms of absolute values and of indicators of cerebrovascular reactivity.

Functional development of the brain during fetal life is discussed at length by *Dan Rurak*, including the changes of body movements, breathing activity, and cardiovascular function which together denote the development of fetal sleep-like states. Understanding these phenomena is important because fetal monitoring in human pregnancy is based on changes in fetal behavior that is used diagnostically to distinguish abnormal from normal fetal development, with implications for clinicians that may determine how the final stages of pregnancy are managed. Finally, for this part, the biophysical and hormonal cues related to photoperiod, how they affect fetal brain development, and why maternal chronodisruption disrupts the fetal circadian system are discussed by *Maria Serón-Ferré*, *Hans G. Richter*, and *Claudia Torres-Farfan*. The difficulties of finding an experimental animal model that resembles the human setting of chronodisruption during pregnancy (e.g., shift-work) and the need to identify changes at the level of the transcriptome, microRNA regulome (miR-Nome), and proteome are discussed.

In **Part 2 (Programming and Stress)**, different experimental approaches to evaluating the postnatal outcomes of pregnancy where maternal stress has occurred transiently or is present chronically are covered in five chapters. This area of research is receiving increasingly greater prominence due to the recognition that many forms of pathophysiology and ill-health in adolescent and adult life may have origins in early development, including fetal and early postnatal life (viz., Developmental Origins of Health & Adult Disease). *Beverley S. Muhlhauser* and *Jessica Gugusheff* discuss studies in rodent models that demonstrate how preference for particular foods can be programmed before birth and elucidate the biological mechanisms that drive these determinant (programming) effects in the mesolimbic reward pathway in the offspring. *Sarah J. Spencer* and *Trish A. Jenkins* provide a detailed description of several simple but elegant prenatal/postnatal animal models used to mimic the effects of early life overfeeding, and to study the impact of this on brain and metabolic development. *Helena C. Parkington* and *Harold A. Coleman* present methods for the effects of maternal obesity on offspring brain development, and for delineating effects on specific brain regions and outcomes reflected in behaviours appropriately assessed for gender and the animal species under study. The placenta is likely to be the crucial interface between the maternal and fetal “environments,” and *Hannha K. Palliser*, *Greer A. Bennett*, *Meredith A. Kelleher*, *Angela L. Cumberland*, *David W. Walker*, and *Jonathan J. Hirst* discuss metabolic and endocrine responses within the placenta, particularly in relation to precursor substances that enable synthesis of neuroactive neurosteroids in the fetal and newborn brain. A host of neurodevelopmental processes are modulated by serotonin (5-HT), which for some period of fetal life is largely of maternal and placental origin. *Juan C. Velasquez* and *Alexandre Bonnin* provide details of recently developed methods that can be applied to the study of how maternal-fetal transfer of therapeutic drugs such as selective serotonin reuptake inhibitors (SSRIs) cross the placenta and impact on the development of fetal brain circuits. They have shown that dysregulation of placental 5-HT transfer impacts a variety of critical signaling pathways that can lead to long-term effects on postnatal brain function.

Human epidemiological studies have indicated an association between infection during pregnancy and an increased risk of neurodevelopmental disorders such as schizophrenia in offspring. As infections arising from various causes have a similar debilitating effect in later life, it is thought that activation of the maternal immune response may be the critical factor

altering fetal brain development. *Udani Ratnayake* and *Rachel Hill* discuss various animal models of prenatal exposure to infection that result in behavioral abnormalities in the offspring that are comparable to those seen in schizophrenic patients and argue that such approaches, particularly viral illness modeled using polyribonucleosinic-polyribocytidilic acid (Poly I:C), provide a useful tool for understanding the neurodevelopmental basis of schizophrenia and for testing treatment strategies.

In **Part 3 (Brain Damage: Causes and Consequences)**, four teams of researchers address issues that arise from the continued and pressing need to predict, prevent, and treat perinatal brain injury—imperatives that have increased with the greater survival rates of premature infants. *Mary Tolcos*, *David H. Rowitch*, and *Justin Dean* discuss approaches to identifying causes of white matter injury, which they argue is due in part to impaired oligodendrocyte maturation, and which is not always replicated in experimental animal models of perinatal white matter injury. They propose that adopting a more standard approach to defining white matter injury is important for validating experimental findings against the *bona fide* human condition. *Stephen A. Back* and *A. Roger Hohimer* present evidence obtained from their extensive use of the preterm sheep fetus, chosen because cerebral development at this time shares many anatomical and physiological similarities with the preterm human infant. The experimental access to the fetus, made possible with such studies in pregnant sheep, has allowed them to define some of the cellular and vascular factors that contribute to preterm white and gray matter injury and to use clinically relevant technologies of neuroimaging and cerebral blood flow measurements that are not feasible in smaller laboratory animals. Likewise, *Lotte G. van den Heuvel*, *Guido Wassink*, *Alistair Jan Gunn*, and *Laura Bennet* describe their work with chronically instrumented preterm fetal sheep that is delineating the key factors that determine the pattern and severity of brain injury, and discuss how this might determine when and how injury to the immature brain should be treated.

Finally, neonatal seizure remains a major clinical problem worldwide and current anti-seizure drugs have limited efficacy and are potentially harmful to the developing brain, highlighting the need for new experimental approaches in this important area of neonatal medicine. *S. Tracey Bjorkman* describes a clinically relevant model of hypoxia/ischemia-induced seizures in the neonatal pig and again shows how such an approach may lead to new studies of seizure suppression in the newborn infant.

Melbourne, Australia

David W. Walker

Contents

<i>Series Preface</i>	v
<i>Preface</i>	vii
<i>Contributors</i>	xiii

PART I DEVELOPMENT

1 Investigating Early Formation of the Cerebral Cortex by In Utero Electroporation: Methods and Protocols	3
<i>Peter Kozulin, Gonzalo Almarza, Ilan Gobius, and Linda J. Richards</i>	
2 In Utero Electroporation Methods in the Study of Cerebral Cortical Development	21
<i>Isabel Martínez-Garay, Fernando García-Moreno, Navneet Vasistha, Andre Marques-Smith, and Zoltán Molnár</i>	
3 Isolation of GABAergic Cortical Neurons and Implications for Cell Transplantation Strategies in the Nervous System	41
<i>Hui Xuan Ng and Joanne M. Britto</i>	
4 Advanced EEG and MRI Measurements to Study the Functional Development of the Newborn Brain	53
<i>Sampsá Vanhatalo and Peter Fransson</i>	
5 Cerebral Blood Flow Measurements in the Neonatal Brain	69
<i>Flora Wong</i>	
6 Fetal Sleep and Spontaneous Behavior In Utero: Animal and Clinical Studies	89
<i>Dan Rurak</i>	
7 Circadian Rhythms in the Fetus and Newborn: Significance of Interactions with Maternal Physiology and the Environment	147
<i>María Serón-Ferré, Hans G. Richter, Guillermo J. Valenzuela, and Claudia Torres-Farfan</i>	

PART II PROGRAMMING AND STRESS

8 Prenatal Programming of the Mesolimbic Reward Pathway and Food Preferences	169
<i>Beverly S. Muhlhauser and Jessica Gugusheff</i>	
9 Perinatal and Postnatal Determinants of Brain Development: Recent Studies and Methodological Advances	189
<i>Sarah J. Spencer and Trisha A. Jenkins</i>	
10 Maternal Obesity in Pregnancy: Consequences for Brain Function in the Offspring	203
<i>Harold A. Coleman and Helena C. Parkinson</i>	

11 Models of Perinatal Compromises in the Guinea Pig: Their Use in Showing the Role of Neurosteroids in Pregnancy and the Newborn 221
Hannah K. Palliser, Greer A. Bennett, Meredith A. Kelleher, Angela L. Cumberland, David W. Walker, and Jonathan J. Hirst

12 Placental Transport and Metabolism: Implications for the Developmental Effects of Selective Serotonin Reuptake Inhibitors (SSRI) Antidepressants 245
Juan C. Velasquez and Alexandre Bonnin

13 Studies on the Effects Prenatal Immune Activation on Postnatal Behavior: Models of Developmental Origins of Schizophrenia 263
Udani Ratnayake and Rachel Anne Hill

PART III BRAIN DAMAGE—CAUSES AND CONSEQUENCES

14 Oligodendrocytes: Cells of Origin for White Matter Injury in the Developing Brain 281
Mary Tolcos, David H. Rowitch, and Justin Dean

15 Prenatal Determinants of Brain Development: Recent Studies and Methodological Advances 303
Stephen A. Back and A. Roger Hohimer

16 Using Pregnant Sheep to Model Developmental Brain Damage 327
Lotte G. van den Heuvel, Guido Wassink, Alistair J. Gunn, and Laura Bennet

17 Origin and Detection of Neonatal Seizures: Animal and Clinical Studies 343
S. Tracey Bjorkman

Index 359

Contributors

- GONZALO ALMARZA • *Queensland Brain Institute, School of Biomedical Sciences, The University of Queensland, Brisbane, QLD, Australia*
- STEPHEN A. BACK • *Department of Pediatrics, Oregon Health & Science University, Portland, OR, USA*
- LAURA BENNETT • *Department of Physiology, University of Auckland, Auckland, New Zealand*
- GREER A. BENNETT • *Mothers and Babies Research Centre, Hunter Medical Research Institute, Newcastle, NSW, Australia*
- S. TRACEY BJORKMAN • *Centre for Clinical Research, University of Queensland, Brisbane, QLD, Australia*
- ALEXANDRE BONNIN • *Department of Cell and Neurobiology, Zilkha Neurogenetic Institute, Keck School of Medicine of USC, University of Southern California, Los Angeles, CA, USA*
- JOANNE M. BRITTO • *The Florey Institute of Neuroscience & Mental Health, Parkville, Melbourne, VIC, Australia*
- HAROLD A. COLEMAN • *Department of Physiology, Monash University, Clayton, Melbourne, VIC, Australia*
- ANGELA L. CUMBERLAND • *Mothers and Babies Research Centre, Hunter Medical Research Institute, Newcastle, NSW, Australia*
- JUSTIN DEAN • *Department of Physiology, University of Auckland, Auckland, New Zealand*
- PETER FRANSSON • *Department of Clinical Neuroscience, Karolinska Institutet, Stockholm, Sweden*
- FERNANDO GARCÍA-MORENO • *Department of Physiology, Anatomy and Genetics, University of Oxford, Oxford, UK*
- ILAN GOBIUS • *Queensland Brain Institute, School of Biomedical Sciences, The University of Queensland, Brisbane, QLD, Australia*
- JESSICA GUGUSHEFF • *Sansom Institute for Health Research, University of South Australia, Adelaide, SA, Australia*
- ALISTAIR JAN GUNN • *Department of Physiology, University of Auckland, Auckland, New Zealand*
- LOTTE G. VAN DEN HEUIJ • *Department of Physiology, University of Auckland, Auckland, New Zealand*
- RACHEL ANNE HILL • *Psychoneuroendocrinology Laboratory, The Florey Institute of Neuroscience & Mental Health, Parkville, Melbourne, VIC, Australia*
- JONATHAN J. HIRST • *School of Biomedical Sciences and Pharmacy, University of Newcastle, Newcastle, NSW, Australia; Mothers and Babies Research Centre, Hunter Medical Research Institute, Newcastle, NSW, Australia*
- A. ROGER HOHIMER • *Department of Pediatrics, Oregon Health & Science University, Portland, OR, USA*
- TRISH A. JENKINS • *School of Health Sciences, Royal Melbourne Institute of Technology University, Melbourne, VIC, Australia*
- MEREDITH A. KELLEHER • *Mothers and Babies Research Centre, Hunter Medical Research Institute, Newcastle, NSW, Australia*
- PETER KOZULIN • *Queensland Brain Institute, School of Biomedical Sciences, The University of Queensland, Brisbane, QLD, Australia*

- ANDRE MARQUES-SMITH • *Department of Physiology, Anatomy and Genetics, University of Oxford, Oxford, UK; MRC Centre for Developmental Neurobiology, King's College London, London, England, UK; Developmental Neurobiology King's College London, London, England, UK*
- ISABEL MARTÍNEZ-GARAY • *Department of Physiology, Anatomy and Genetics, University of Oxford, Oxford, UK; Cardiff School of Biosciences, Cardiff University, Cardiff, Wales, UK*
- ZOLTÁN MOLNÁR • *Department of Physiology, Anatomy and Genetics, University of Oxford, Oxford, UK*
- BEVERLEY S. MUHLHAUSLER • *Sansom Institute for Health Research, University of South Australia, Adelaide, SA, Australia*
- HUI XUAN NG • *The Florey Institute of Neuroscience & Mental Health, Parkville, Melbourne, VIC, Australia*
- HANNAH K. PALLISER • *Mothers and Babies Research Centre, Hunter Medical Research Institute, Newcastle, NSW, Australia*
- HELENA C. PARKINGTON • *Department of Physiology, Monash University, Clayton, Melbourne, VIC, Australia*
- UDANI RATNAYAKE • *Behavioral Neuroscience Laboratory, The Florey Institute of Neuroscience & Mental Health, Parkville, Melbourne, VIC, Australia*
- LINDA J. RICHARDS • *Queensland Brain Institute, School of Biomedical Sciences, The University of Queensland, Brisbane, QLD, Australia*
- HANS G. RICHTER • *Instituto de Anatomía, Histología y Patología, Universidad Austral de Chile, Valdivia, Chile*
- DAVID H. ROWITCH • *Department of Pediatrics, Howard Hughes Medical Institute, University of California, San Francisco, CA, USA; Department of Neurological Surgery, Howard Hughes Medical Institute, University of California, San Francisco, CA, USA*
- DAN RURAK • *Division of Maternal Fetal Medicine, Department of Obstetrics & Gynecology, University of British Columbia, Vancouver, BC, Canada*
- MARIA SERÓN-FERRÉ • *Instituto de Ciencias Biomédicas, Universidad de Chile, Santiago, Chile*
- SARAH J. SPENCER • *School of Health Sciences, Royal Melbourne Institute of Technology University, Melbourne, VIC, Australia*
- MARY TOLCOS • *School of Health Sciences, Health Innovations Research Institute, RMIT University, Melbourne, Australia*
- CLAUDIA TORRES-FARFAN • *Instituto de Anatomía, Histología y Patología, Universidad Austral de Chile, Valdivia, Chile*
- GUILLERMO J. VALENZUELA • *Department of Women's Health, Arrowhead Regional Medical Center, San Bernardino, CA, USA*
- SAMPSA VANHATALO • *Department of Clinical Neurophysiology, Childrens Castle Hospital, University Hospital of Helsinki, Helsinki, Finland*
- NAVNEET VASISTHA • *Department of Physiology, Anatomy and Genetics, University of Oxford, Oxford, UK*
- JUAN C. VELASQUEZ • *Neuroscience Graduate Program, Keck School of Medicine of USC, Los Angeles, CA, USA*
- DAVID W. WALKER • *The Ritchie Centre, Hudson Institute of Medical Research, Monash Medical Centre & Department of Obstetrics & Gynaecology, Monash University - Clayton Campus, Melbourne, Australia*
- GUIDO WASSINK • *Department of Physiology, University of Auckland, Auckland, New Zealand*
- FLORA WONG • *Monash Newborn, Monash Health, Monash University, Clayton, Melbourne, VIC, Australia; Department of Paediatrics, Monash University, Clayton, Melbourne, VIC, Australia*

Part I

Development

Chapter 1

Investigating Early Formation of the Cerebral Cortex by In Utero Electroporation: Methods and Protocols

Peter Kozulin, Gonzalo Almarza, Ilan Gobius, and Linda J. Richards

Abstract

Cortical development requires a strict balance between neuronal proliferation, differentiation, and cellular migration within restricted developmental stages. The precise spatiotemporal gene manipulation used in developmental studies can be achieved by *in vitro* or *ex vivo* experiments or by the generation of transgenic animals. However, these approaches have significant limitations when trying to investigate the origin and molecular regulation of early cortical neurons. In utero electroporation (IUE) is an informative cell labeling technique that provides the ability to label neural progenitor cells and their progeny *in vivo* with promoter-specific reporter constructs as well as to induce or repress gene expression in a spatially and temporally specific manner. Technical improvements of this method have allowed the targeting of multiple neural cell types, as well as the precise transfection of subpopulations of neurons at increasingly earlier embryonic stages. Furthermore, neuronal projection studies and the use of multiple electroporations in the same embryo have made it possible to examine processes occurring at different developmental stages and/or cortical areas and link their anatomy to their function. In this chapter, we present the latest advances of the *in utero* electroporation technique for the study of early formation of the cerebral cortex, together with a description of the necessary tools.

Key words In utero, Electroporation, Brain, Cortical development, Transfection, Embryo, Mice

1 Introduction

During brain development, the neocortex arises from a homogeneous sheet of neuroepithelial cells in the telencephalon. Morphogen molecules such as Fgf8, Wnt, Bmps, and Shh secreted by patterning centers within the telencephalon induce the expression of transcription factors in gradients across the cortex, which serve to pattern the neuroepithelium into functional cortical areas [1–4]. Concomitantly, progenitor cells within the neuroepithelium undergo proliferation, differentiation, and migration to generate the six neuronal layers that characterize the mammalian neocortex. Furthermore, each cortical area is distinguished by its functional specificity for the processing of sensory input, motor activity, or cognitive function, as well as its distribution of input and output

projections which are guided toward their correct targets by specific guidance cues [5]. Although the influence of different morphogens in cortical patterning and subsequent neuronal wiring is not completely understood, sophisticated electroporation techniques have identified some of the mechanisms involved (for example see [6, 7]).

Electroporation is a method of transfection of plasmid DNA into cells that allows for exogenous gene expression via the use of cell-specific promoters, and gene loss-of-function studies via the transfection of small interfering RNAs (siRNAs). Since electroporation was first used in utero [8, 9], this technique has been an important tool for the study of neuronal origin and migration during early mammalian cortical development. By modifying the expression of transcription factors within the cortex in vivo, primarily using mouse and rat models, our knowledge of the migration, differentiation, and growth of multiple subpopulations of neurons originating from the ventricular and sub-ventricular zone zones has expanded [10–13]. Early-born interneurons that populate the cortex originate in the ganglionic eminences (reviewed in [14]), and can be labeled by IUE and then studied separately by their electrophysiological properties [15]. IUE has also been instrumental in the discovery of early-born cortical neurons from the edges of the neocortex which give rise to Cajal-Retzius cells [16, 17], and of new migratory streams of neurons such as those that contribute to the accessory olfactory bulb [18] and the amygdala [19].

The electroporation technique can be modified for the transfection of multiple expression constructs either together or with temporal and/or spatial variation for individual plasmids. The use of IUE at early stages allows the possibility of a second electroporation later in gestation, for example, to differentially label cortical layers generated at different developmental stages (Fig. 1). Alternatively, multiple plasmids can be co-electroporated simultaneously at a single age, and has been recently used to study activity-dependent axon targeting in the primary somatosensory cortex (S1) [20].

In this chapter we describe the methodology required to perform embryonic electroporation in mice at E10 for early cortical development studies. We also describe how to perform an additional electroporation at later developmental stages in order to differentially transfect other cortical layers.

2 Materials

For all equipment and reagents listed, the manufacturers and catalogue numbers are given as a guide only and can be substituted.

2.1 Mice

The IUE procedure in this chapter is described for use in CD1 mice given their relatively large litter size and their ability to cope with the anesthetic and surgical procedure. Other mouse strains such as

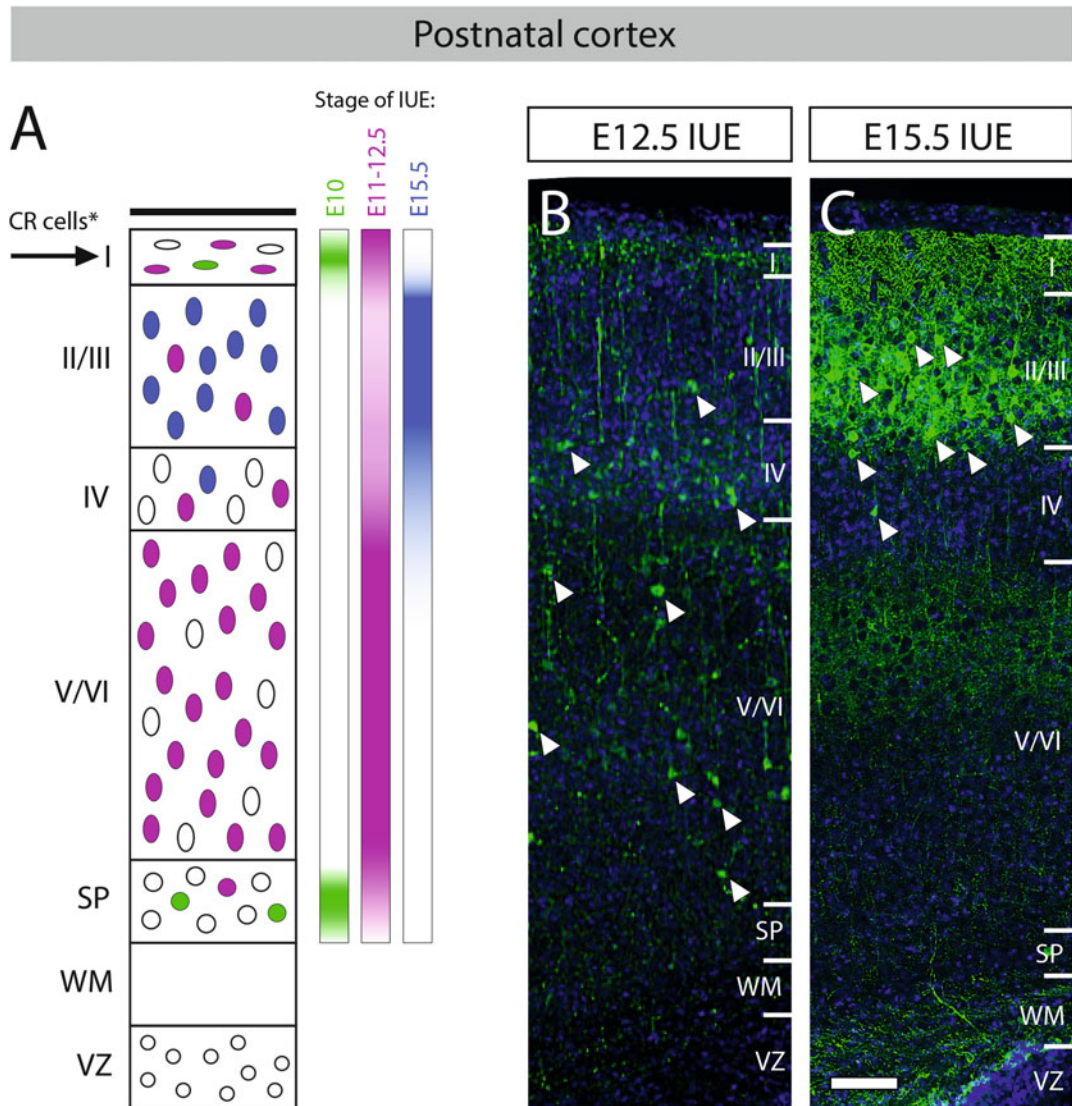


Fig. 1 Cortical layer targeting using in utero electroporation. **(a)** In this schematic of postnatal cortex, cells are represented with different colors according to the developmental stage at which they are electroporated as indicated on the *right*. The cortex develops in an inside-outside manner and electroporation at an early stage of E10 will target cells that eventually occupy the preplate and its derivatives (*green* cells), as indicated previously in cell birth-dating studies [16]. Electroporation at a later stage of E11–12.5 will target cells throughout the cortical plate (greater in layers V/VI) and the subplate, as indicated by the *purple* cells and the *arrowheads* in **(b)**. E15.5 electroporation will predominantly target neurons within the superficial cortical layers (II/III), but some electroporated neurons are also present in the underlying layer IV, as indicated by the *blue* cells and the *arrowheads* in **(c)**. The colored gradients on the *right* indicate the approximate profile of cell locations in postnatal cortex according to the stage of electroporation. Note that this schematic diagram is representative of IUE in the dorsal telencephalon but includes Cajal-Retzius (CR) cells in layer I (indicated by *). CR cells are generated in the cortical hem and can be targeted with an alternative IUE at E10–12.5 prior to their tangential migration away from this region (*see* Fig. 5h). **(b)** Coronal section of postnatal cortex after electroporation of pCAG-EGFP in E12.5 dorsal telencephalon shows GFP-positive neurons (*arrowheads*) throughout the cortex. **(c)** Electroporation of E15.5 dorsal telencephalon shows GFP-positive neurons (*arrowheads*) predominantly within cortical layers II/III. CR: Cajal-Retzius; I–VI: cortical layers; IUE: in utero electroporation; SP: subplate; VZ: ventricular zone; WM: white matter. Scale bar in **(b)** and **(c)**, 100 μm

C57BL/6 can also be used, but may exhibit a lower success rate. The day of appearance of the vaginal plug is embryonic day 0 (E0).

2.2 Anesthesia and Analgesic Solutions

Anesthesia of the pregnant dams is achieved via intraperitoneal injection of a mixture of 0.075 mg/g body weight ketamine, and 0.006 mg/g body weight xylazine, diluted in sterile PBS. Analgesia is achieved via subcutaneous injection of buprenorphine at 0.1 mg/g body weight.

2.3 Plasmid DNA

For effective gene expression it is important that the plasmids transfected via IUE are purified and endotoxin free, which can be achieved using a commercially available preparation kit, and are homogeneous once resuspended in water. If the plasmid solution contains precipitates and is not fully suspended, which can occur in higher concentration preparations, it can be further dissolved by heating the plasmid solution to 45 °C for 30 min.

Purified plasmid can be stored for a long term at –20 °C, and upon thawing can be stored at 4 °C for up to a month. In this protocol, plasmids were prepared using an endotoxin-free Maxi-prep kit (cat. 12362, Qiagen, Valencia, CA).

2.4 Electroporation and Microinjection Equipment

- ECM 830 Electroporator (BTX Harvard Apparatus, Holliston, MA) with electroporator foot pedal.
- Electrodes, forceps-style, 0.5 mm diameter (cat. CUY650P0.5, NepaGene, Chiba, Japan).
- Borosilicate glass capillaries, 1.2 mm O.D. × 0.9 mm I.D. (cat. TW120F-4, World Precision Instruments, Sarasota, FL).
- Picospritzer II microinjection system (Parker Hannifin, Hollis, NH) with microinjector foot pedal.
- Microcapillary holder (cat. MPH6S12, World Precision Instruments).
- Microloading pipette tips (cat. 0030 001.222, Eppendorf, Hamburg, Germany).
- Micropipette puller (cat. P-97, Sutter Instruments Co., Novato, CA) with square box filament.

2.5 General Equipment and Surgical Instruments

- Light source (cat. LG-PS2, Olympus, Shinjuku, Japan), with a fiber-optic arm for the illumination of E10 embryos through the uterine wall. The fiber-optic arm should be flexible to allow for easy manipulation and positioning against the uterus. Fiber-optic light is ideal since it emits minimal heat and will not damage the uterus or embryos.
- A secondary fiber-optic light (cat. LG-PS2, Olympus) source can also be positioned over the animal to help visualize the uterus and the surgery area.
- Silicone rubber heating pad, set to 37 °C.

- Water bath, set to 37 °C (cat. WB7, Ratek, Melbourne, Australia).
- Germinator 500 glass bead sterilizer, for sterilization of surgical instruments (cat. GRM5-1450, CellPoint Scientific, Gaithersburg, MD).
- Animal recovery chamber (ventilated), set at 37 °C.
- 2× Ring forceps, 6 mm diameter ring tip, 9 cm length (cat. 11106-09, Fine Science Tools, Vancouver, Canada).
- Micro-dissecting forceps with serrated edge, half-curved 1 mm tip, 4 in. length (cat. 160-18, George Tiemann & Co., Hauppauge, NY).
- Suture clamps, Gillies, 6.5 in. length (cat. 222-8-59, George Tiemann & Co.).
- Straight surgical scissors, 12 cm length (cat. 14002-12, Fine Science Tools).
- Syringe 1 ml (cat. SY1SC-TH-ET) and 27 G hypodermic needle (cat. HN-2713-ET) (Nipro, Osaka, Japan).
- Gauze swabs, sterile, 7.5 cm × 7.5 cm, 8 ply (cat. 72502-03, BSN Medical, Hamburg, Germany).
- Cotton tips, 15 cm (cat. 10102121, Surgical & Medical Products, Sydney, Australia).
- Silk sutures (Perma-Hand3-0, Ethicon).
- Pasteur pipettes, polyethylene, sterile, 3 ml (ThermoFisher Scientific, Loughborough, UK).
- Personal protective equipment/surgical attire: gown, face mask, hair net, gloves.
- Adhesive paper tape, 25 mm wide.

2.6 Reagents

- Ketamine-1000 (100 g/ml, Ceva, Lenexa, KS).
- Xylazil-20 (Xylazine, 20 mg/ml, Troy Laboratories, Glendening, Australia).
- Chlorhexidine (0.5 mg/ml, 0.05 %) and cetrimide (5 mg/ml, 0.5 %) topical antiseptic solution (cat. 16061505, Pfizer, New York, NY).
- Ringer's solution (NaCl 135 mM, KCl 5.4 mM, MgCl₂ 1 mM, CaCl₂ 1.8 mM, HEPES 5 mM) warmed to 37 °C.
- 1× phosphate-buffered saline (PBS), diluted from a 10× stock of Dulbecco's PBS (cat. 17-515Q, Lonza, Basel, Switzerland) in Milli-Q water, warmed to 37 °C.
- Hair removal cream (Nair, Church & Dwight Co., Sydney, Australia).

- Petroleum Jelly (Vaseline, Unilever, Leatherhead, UK).
- Fast Green (cat. F7258, Sigma, St. Louis, MO).
- Ethanol 70 %.

3 Methods

3.1 Preparation Before Surgery

3.1.1 Animals

Timed-pregnant females are used and the appearance of a vaginal plug is considered E0. For early-stage IUE, the embryos used are E10–10.5.

3.1.2 Surgery Area Preparation

Ensure that a sterile surgical environment is achieved by wearing surgical attire (gown, gloves, face mask, hair net) and wiping down surfaces, the fiber-optic light source, and all equipment with 70 % ethanol. Arrange the surgery area and equipment as shown in Fig. 2a. Turn on the heating pad, animal recovery chamber, glass bead sterilizer, and water bath, and place paper towel on the heat pad to soak up any excess PBS during the surgery. Place Ringer's and PBS solution into the water bath and warm to 37 °C.

Immerse the surgical instruments (forceps, scissors, and the suture clamp) in 70 % ethanol, allow to air-dry, and then further sterilize them by placing each of them into a glass bead sterilizer for several minutes.

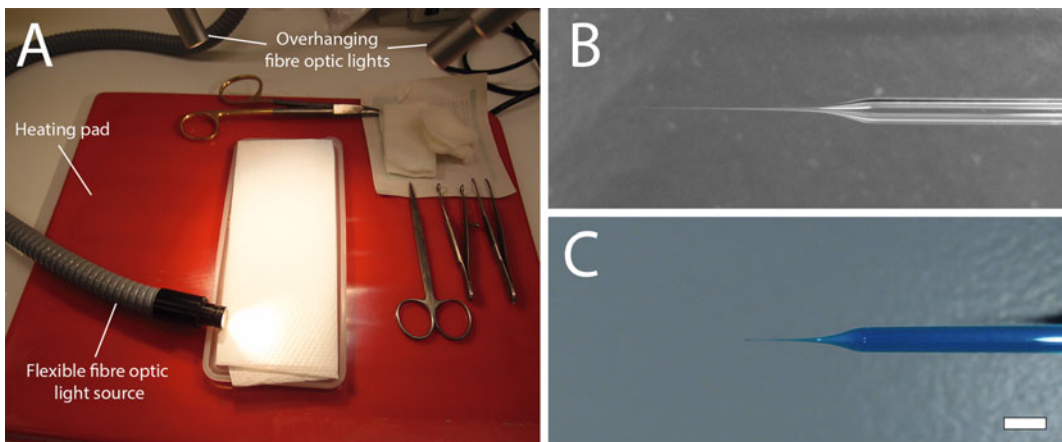


Fig. 2 Setup of surgery area and microcapillaries. **(a)** The surgery area is set up with the heating pad set at 37 °C, the paper towel in the center of the heating pad, the sterilized surgical tools (ring forceps, microdissecting forceps, scissors, suture clamps), and the flexible fiber-optic arm and overhanging light sources in position. **(b)** A fine, closed tip with a long taper is formed after the glass microcapillary is pulled. **(c)** The microcapillary tip must be cut at an oblique angle to produce a sharp tip that can penetrate the mouse uterine wall. At least two microcapillaries are cut and filled with plasmid DNA/Fast Green solution before surgery is commenced. Scale bar in **(b)** and **(c)**, 2 mm

- 3.1.3 Plasmid DNA** Prepare the desired concentration of plasmid DNA, typically between 0.5 and 2.0 $\mu\text{g}/\mu\text{l}$, into 0.025 % Fast Green solution (final concentration) made in sterile PBS. At this concentration, Fast Green is nontoxic to the embryo and allows the plasmid solution to be visualized during injection into the ventricle. The DNA/Fast Green preparation can be stored at 4 °C until needed.
- 3.1.4 Anesthetic and Analgesic Solutions** Prepare working solutions of a mixture of 15 mg/ml ketamine and 1.5 mg/ml xylazine, and 30 mg/ml buprenorphine, both in sterile PBS.
- 3.1.5 Microinjector** Connect the Picospritzer II microinjection system to a nitrogen gas line regulated at approximately 100 psi. Regulate the nitrogen pressure from the Picospritzer to the capillary holder at 10–15 psi, and the injection pulse time to 100 ms. Connect the foot pedal for hands-free initiation of microinjection pulse.
- 3.1.6 Microcapillaries** Using a micropipette puller, pull the ends of several borosilicate glass capillaries to form fine tips with a long (11–14 mm) taper (Fig. 2b). The precise settings to produce these tips depend on the size and age of the box filament, and the size of the glass capillaries, but generally require settings with a high level of heat, pull force, and pull velocity, but minimal (or no) use of air cooling. Using scissors or forceps cut approximately 6 mm off each microcapillary tip at an oblique angle, which will allow them to effectively penetrate through the uterine wall (Fig. 2c).
Load the desired volume of plasmid/Fast Green solution in the back of at least two capillaries using microloading pipette tips. If the capillary is longer than the pipette tip, the plasmid solution can be pushed to the injection end of the capillary by firmly holding the back end and forcefully flicking the capillary. Place one filled capillary in the holder connected to the Picospritzer II, and leave the other filled capillaries aside to allow for a rapid replacement in the event that the existing capillary is broken or more plasmid is required. Test the capillary injection onto a sterile surface to determine if the desired volume of plasmid (0.5–1.0 μl) can be delivered within a few seconds. If the injection capacity is insufficient, cut off an additional millimeter of the capillary tip to increase the tip diameter and its outflow. If different plasmids will be injected into each hemisphere, pull and load separate capillaries for each plasmid prior to beginning the surgery.
- 3.1.7 Electroporator** Connect the 0.5 mm diameter microelectrodes to the ECM 830 electroporator. Connect the electroporator foot pedal for hands-free activation of square wave pulses.

3.2 Procedure for Surgery and IUE

1. Weigh the animal and anesthetize with approximately 4.5 $\mu\text{l/g}$ body weight of the ketamine/xylazine working solution via intraperitoneal injection; for example for a 30 g pregnant dam, inject approximately 0.14 ml ketamine/xylazine.

Once the animal is sedated, inject 0.1 ml of the buprenorphine working solution subcutaneously. Place the mouse on the heat pad and, without compromising the animal's respiration, tape down the four limbs to stabilize the animal during surgery (Fig. 3a).

2. Place a liberal amount of Vaseline over the animal's eyes to prevent them from drying during surgery. Apply hair removal cream to the abdomen and wipe this area to remove the hair. Wash the abdomen thoroughly with PBS followed by chlorhexidine antiseptic solution to sterilize the area before incision.

Cut out a crescent-shaped hole, approximately 30 mm in length, from the center of a sterile gauze swab and place onto the hair-free area of the abdomen (Fig. 3a).

3. Perform a caesarian section via midline laparotomy to reveal the embryos. Grasp the abdominal skin or muscle with the serrated micro-dissecting forceps and use the surgical scissors to make

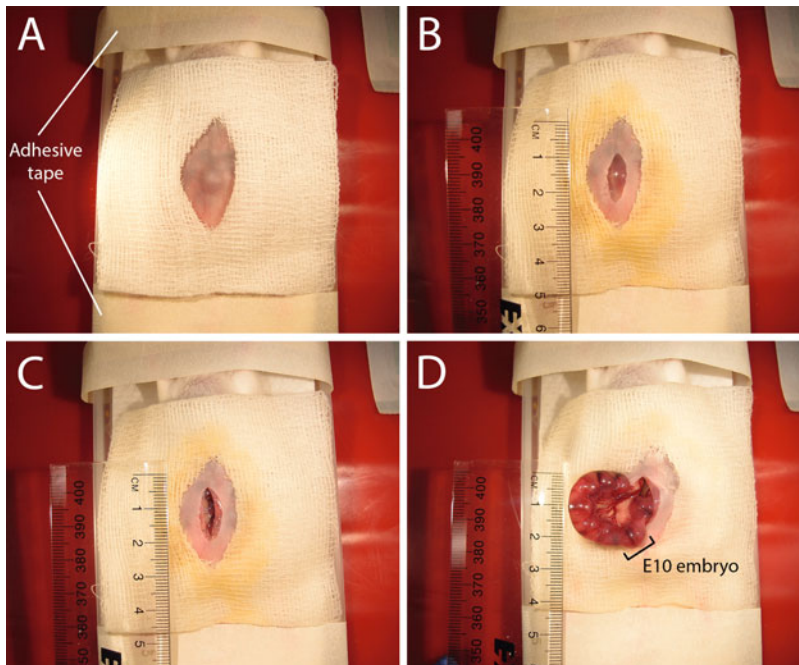


Fig. 3 Midline laparotomy and exposure of right uterine horn at E10. The dam is placed in a supine position on the paper towel and adhesive tape is used to secure the forelimbs and hindlimbs (a). A midline laparotomy is performed using serrated micro-dissecting forceps and surgical scissors on the abdominal skin (b) and muscle (c), and 3–4 embryos from one uterine horn are extracted from the abdominal cavity at a time for electroporation (d). The rostral-caudal length of one embryo within the uterus is indicated in (d)

two identical midline incisions, each approximately 12–14 mm, through the muscle and skin (Fig. 3b, c). During the muscle incision, take care to avoid piercing major blood vessels and organs such as the intestines or bladder.

4. Gently extract the uterine horns from the abdominal cavity with ring forceps and lay them on the gauze (Fig. 3d). Liberally administer warm PBS over the uterus and vasculature throughout the entire surgery to prevent the tissue from drying out and to maintain the mother at a stable warm temperature. To ensure that the embryos remain within the warm environment of the abdominal cavity for as much as possible during surgery, extract only 3–4 embryos at a time and reposition embryos back inside the abdominal cavity once they are electroporated before extracting the next embryos. Later stage embryos are larger and require extraction of the entire uterine horn to prevent contortion of the uterus and damage or occlusion of the uterine arteries.

The embryos can be rotated within the amniotic sac by using cotton tips and ring forceps; however, avoid applying too much pressure to each embryo since this could break the amniotic sac and potentially cause the embryo to reabsorb. For further information on handling the embryos during surgery and achieving a high survival rate, *see Note 5.1*.

5. At E11 the major cranial dural sinus vessels can be identified and used as a reference for determining the position of the telencephalic hemispheres. However, at E10 these major vessels are not apparent and visualization of the telencephalon at E10 is not possible through conventional overhead light sources. Instead, the telencephalon must be identified by placing the fiber-optic light source directly against the uterus in order to illuminate the embryos through the thick uterine wall and orienting the embryo with the dorsal side of the brain facing up (Fig. 4a, b). Once the position of the hemispheres has been identified (Fig. 4b, c), it is important to stabilize the embryos to avoid damaging the telencephalon during microinjection of the plasmid DNA. A convenient approach is to use the fingers and thumb of one hand to gently hold the light source against the uterus, and place a cotton tip under the uterus for further stabilization and positioning as shown in Fig. 4a. Once the cotton tip is positioned, hold the microcapillary or electrodes with the other hand (Fig. 5a, d).
6. Target the capillary tip to penetrate into the middle of one telencephalic hemisphere (Fig. 5b, c) and microinject 0.5–1.0 μ l of plasmid DNA (mixed with 0.025 % Fast Green dye in sterile PBS) into the lateral ventricular space. This injection volume typically requires 3–5 \times 100 ms pulses at 10–15 psi. It is important to inject the embryos carefully to avoid causing excess cortical damage and that the injection site is outside the intended region of electroporation (*see Note 5.2*).

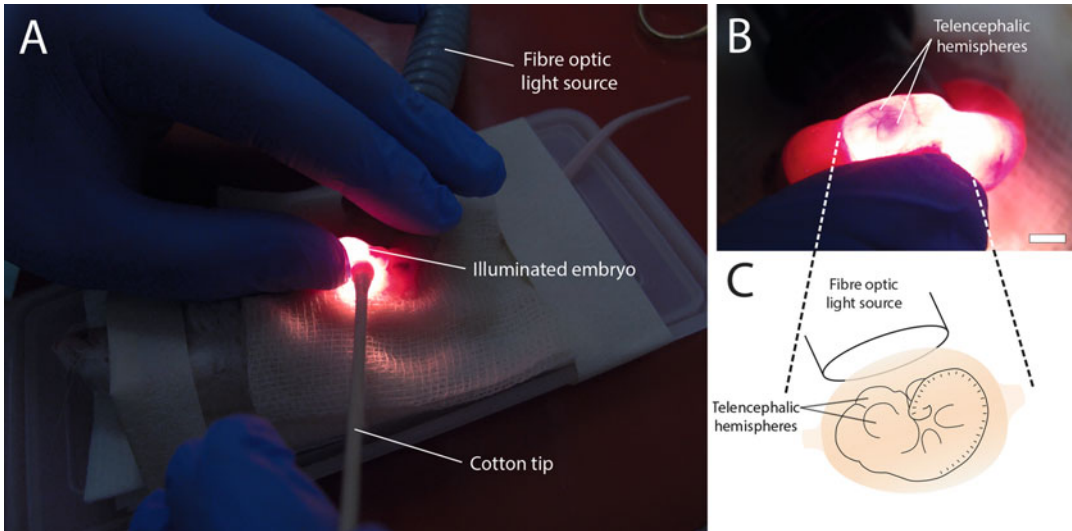


Fig. 4 E10 embryo illumination and stabilization immediately prior to plasmid DNA injection. The flexible fiber-optic light source is positioned directly against the uterus to illuminate each embryo, and a cotton tip is used to stabilize the position of the uterus (a). Once the embryo is oriented with the ventral side facing up, the telencephalic hemispheres can be identified (b). The orientation of the illuminated embryo and position of the telencephalic hemispheres shown in (b) are depicted in the schematic in (c). Scale bar in (b), 2 mm

Note that the ventricles are more openly connected at early embryonic stages and it is important not to inject excess plasmid; otherwise it may diffuse throughout the ventricular space and into the opposing hemisphere, resulting in undesired labeling. A small plasmid volume (no more than 1.0 μl) will ensure a more restricted area of electroporation and reduce the chance of transfecting cells in unwanted areas.

7. Position the positive electrode above the targeted cortical area and position the negative electrode on the uterus in such a way as to achieve the desired angle of electroporation. Figure 5e, f shows the position of the electrodes for the electroporation of the dorsal lateral telencephalon, and Fig. 5g shows a schematic (in coronal view) of the orientation of the electrodes relative to the embryo.

Electroporate the plasmid DNA into the target neuroepithelial tissue using five square wave pulses of 20–25 V, each at 50 ms, with 1-s interval. It is important that the electrodes have the correct orientation and are kept steady to ensure that the correct region is electroporated, and that some pressure is applied to the electrodes to ensure that their terminals are in complete contact with the uterine wall (Fig. 5e).

Medially positioned cortical areas such as the cingulate cortex or hippocampus are more difficult to electroporate because of their position within the developing brain, but can be accessed by an indirect method of electrode placement. For example, the

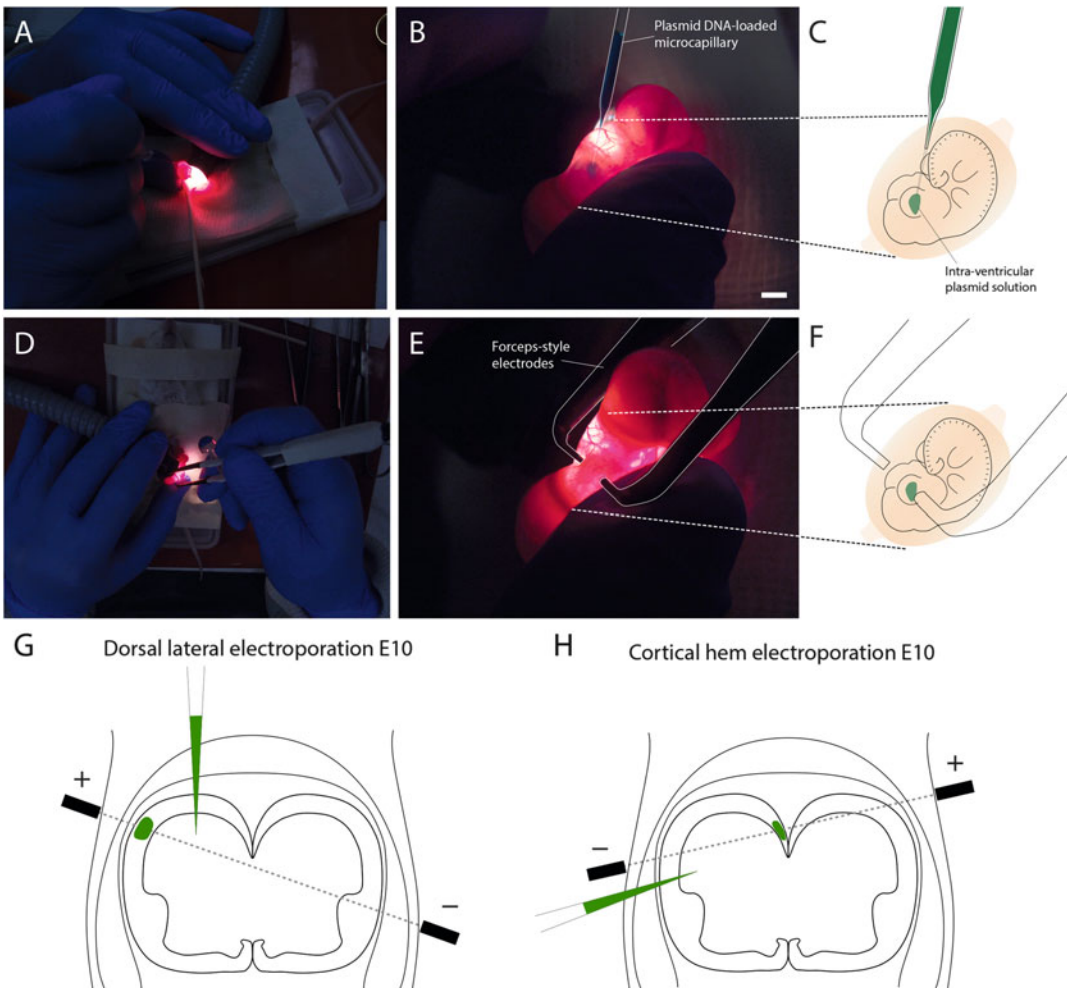


Fig. 5 Plasmid injection and electrode placement on an E10 embryo for the electroporation of dorsal lateral telencephalon. (a–c) Injection of plasmid DNA. Once the embryo is illuminated and secured in position (a), the plasmid DNA is injected into one hemisphere and is visualized with the use of Fast Green (b). The position of the injecting microcapillary with respect to the embryo is highlighted in *white outline* in (b), and the schematic in (c) depicts this microcapillary injection. (d–f) Electroporation. In order to achieve the desired angle of electrode orientation, the dam can be rotated on the heating pad (d). Once the embryo is stabilized, the electrodes are applied with a small degree of pressure to ensure that they are in complete contact with the surface of the uterus (e) and the electrical pulses are applied. The position of the electrodes with respect to the embryo is highlighted in *white outline* in (e), and the schematic in (f) depicts this electrode placement. (g) Dorsal lateral telencephalon electroporation. To target this region the positive electrode must be placed above the lateral portion of the same telencephalic hemisphere to where the plasmid DNA is injected. (h) Cortical hem electroporation. To target this region the positive electrode must be placed above the telencephalic hemisphere contralateral to where the plasmid DNA is injected. Scale bar in (b) and (e), 2 mm

cortical hem is located within the medial aspect of the dorsal telencephalon, but can be specifically targeted within one hemisphere using the electrode orientation shown in Fig. 5h.

8. Repeat steps 6 and 7 for each embryo, remembering to stabilize the embryo position prior to plasmid injection.
9. Once all embryos are electroporated, position the uterine horns back inside the abdominal cavity in their original positions and apply some warm PBS within the cavity. Apply a running suture to close the abdominal muscle incision (Fig. 6a), followed by a running suture to close the abdominal skin incision (Fig. 6b). Wipe the sutured skin with chlorhexidine solution.
10. Administer 1–2 ml of Ringer's solution subcutaneously to dilute the anesthetic and prevent dehydration of the animal.
11. Transfer the animal to the recovery chamber heated to 37 °C, monitor its recovery until it is able to walk and easily access its food and water supply, and then transfer back to its animal cage at room temperature.
12. Inspect the dam on the next day and administer analgesic solution subcutaneously if there are signs of pain or suffering. For further information on ensuring survival of the dam after surgery, *see* **Note 5.3**.
13. To prepare embryonic electroporated brains for histology, euthanize the dam at the desired stage of embryonic development, and dissect the embryos from the uterus. Dissect the brain from each electroporated embryo and drop-fix in 4 % paraformaldehyde (PFA) overnight at 4 °C. The next day, rinse brains in PBS and prepare fixed tissue for sectioning.

To prepare postnatal electroporated brains for histology, euthanize pups with an intraperitoneal injection of pentobarbital sodium solution (100 µg/g body weight). Perform transcardial perfusion of 0.9 % sodium chloride solution, and a perfusion of 4 % PFA. Dissect the brain from each electroporated pup and

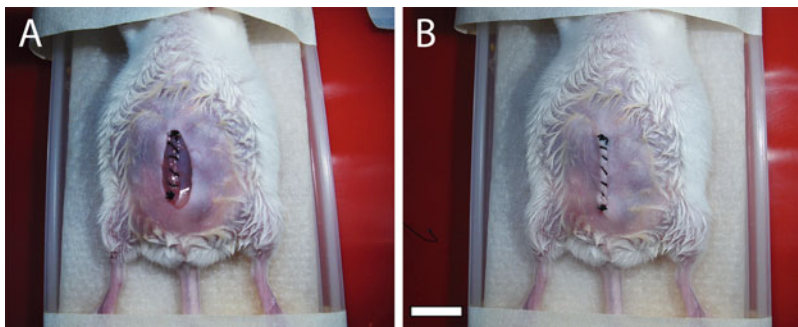


Fig. 6 Suturing of the abdominal muscle and skin. Once the embryos are electroporated, the uterine horns are positioned back inside the abdominal cavity in their original positions and warm PBS is applied into the cavity. The abdominal muscle is then closed using a running suture along the line of incision tied off with a knot at the rostral and caudal ends (a). This running suture method is repeated to close the abdominal skin incision (b). Scale bar, 10 mm

post-fix in 4 % PFA overnight at 4 °C. The next day, rinse brains in PBS and prepare fixed tissue for sectioning.

3.2.1 Multiple Electroporations

The procedure described above can be used for the electroporation of a cortical area at a single developmental stage; however, an additional electroporation on the same embryos can be performed at a later stage. Multiple electroporations performed over time can be used for the differential transfection of cortical layers generated at different stages. For example, performing electroporations 5 days apart, at E10 and E15, will differentiate cortical layers II/III from the subplate (*see* Fig. 1). For the second surgery, it is recommended to re-weigh the dam to ensure that an appropriately higher volume of anesthetic solution is injected given the relatively larger size of the embryos. In addition, remove the previous suture silk and perform the midline laparotomy along the previous incision to minimize the wound area. The voltage settings must also be increased to ensure efficient electroporation (for example, 30–35 V at E15).

For later stage embryos, it is also possible to perform two electroporations within the same embryo at a single developmental stage, and this technique has been commonly used to transfect different fluorescent protein expression plasmids to investigate or manipulate the development of different areas. For example, Zhou et al. [21] used this technique to electroporate different fluorophores between S1 and the primary motor cortex in E15.5 mice in order to distinguish the axon bundles from these two areas and their relative position within the corpus callosum. In addition, Suárez et al. [20] electroporated the inward-rectifying potassium channel, Kir2.1, into the right and left S1 at E15.5 to disrupt neuronal activity in both hemispheres. To perform multiple spatial electroporations, it is recommended to wait for 30 min between the two electroporations, during which time an additional small volume of anesthetic solution is applied to the dam to prolong the sedation and a PBS-soaked sterile gauze swab is placed over the caesarian section.

4 Outcome of In Utero Electroporation

By 2.5–3.0 days after electroporation of the dorsal telencephalon at E10 using the configuration shown in Fig. 5g, fluorescence is observed in a patch 400–500 µm wide in a lateral portion of the cortex. Transfected progenitor cells in the ventricular zone are observed radially migrating to the preplate layer (Fig. 7a') and also beginning to extend corticofugal axonal projections to subcerebral targets (Fig. 7a). By 5.5–6.0 days after electroporation, transfected progenitor cells are present in the subplate and cortical plate,

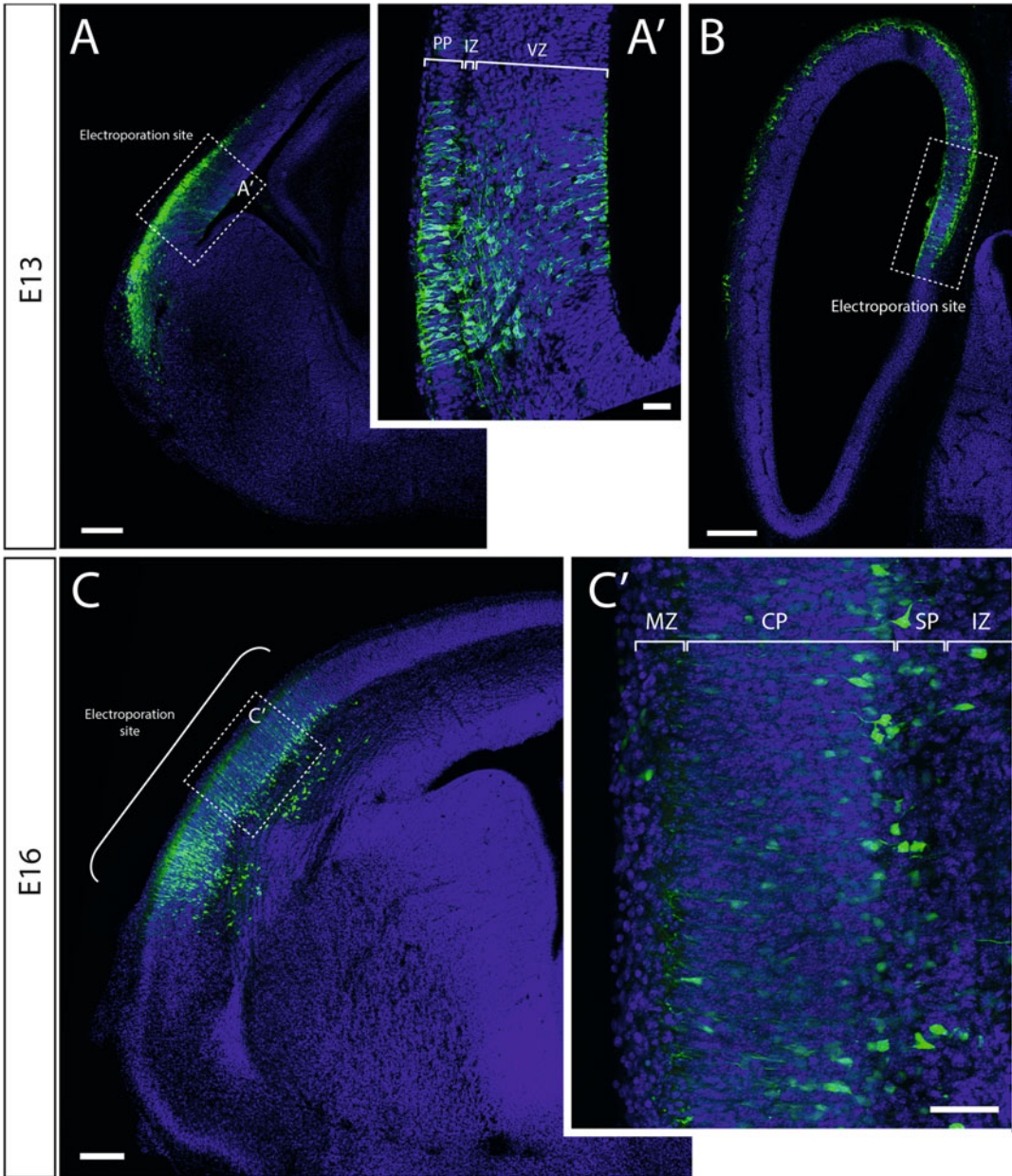


Fig. 7 Outcomes of electroporation of the developing cortex with pCAG-EGFP at E10. (a) Coronal view of E13 cortex after electroporation of pCAG-EGFP in E10 dorsal telencephalon shows 400–500 μm wide region of electroporation, and the initial extension of corticofugal projections from these EGFP-positive transfected cells. (a') At higher magnification, the site of electroporation is indicated by the region of radial migration of fluorescent progenitor cells to the PP layer from the VZ. (b) A horizontal section of E13 cortex after electroporation of pCAG-EGFP at E10 in the cortical hem shows tangential migration of transfected Cajal-Retzius cells from medial to lateral portions of the cortex. (c) A coronal view of E16 cortex after electroporation at E10 in the dorsal telencephalon. The density of fluorescent cells appears to increase at the caudal edge of the electroporation site since this coincides with the change in laminar structure at the edge of the neocortex. (c') Within the region of electroporation, transfected cells are present in the cortical plate and subplate. CP cortical plate, IZ intermediate zone, MZ marginal zone, PP preplate, SP subplate, VZ ventricular zone. Scale bar 200 μm in (a)–(c), and 50 μm in (a') and (b')

and are observed migrating radially with leading processes extending toward the pial surface (Fig. 7c, c').

2.5–3.0 days after electroporation of the cortical hem at E10 using the configuration shown in Fig. 5h, tangential migration of transfected Cajal-Retzius cells is observed throughout the cortex. In the horizontal section shown in Fig. 7b, fluorescent cells are observed migrating from the medially located cortical hem to lateral regions of the cortex.

A low or lack of fluorescent signal in the cortical tissue may indicate a problem with the plasmid, microcapillary, injection, or electrodes. See Note 5.4 for troubleshooting these problems.

5 Notes

5.1. Embryo Handling and Survival

Often an initial difficulty with the electroporation of embryos at E10 is the low survival rate of the embryos given their greater vulnerability to external manipulation compared with later stages of gestation. Ensure that the uterus is handled gently using the ring forceps and cotton tips. In particular avoid contact with the placenta of each embryo and the dorsal, vascularized surface of the uterus, and do not place the electrodes on these structures to prevent cauterization of the vasculature. In addition, avoid excessive pulling or twisting of the uterine horn, particularly of the terminal embryos adjacent to the ovaries and fundus/cervix, as this could cause reabsorption of all the embryos in the horn at early stages of gestation. It is also recommended to avoid electroporation of these terminal embryos.

Furthermore, a high embryo survival rate can be achieved by not using an electroporation voltage greater than 25 V, and after surgery, ensuring that the uterine horns are not twisted or contorted when placed back inside the abdominal cavity to prevent occlusion of the uterine blood supply.

5.2. Reducing Cortical Damage During Microinjection

A localized region (approximately 50 μm radius) of cortical damage is normally caused by microcapillary injection. To avoid causing excess cortical damage, ensure that the embryo is stabilized and that the microcapillary tip is not blunt and has an oblique angle cut before each injection. Furthermore, do not inject an excessive volume of plasmid solution into the telencephalon. The injection volume can be monitored by marking the volume increments along the outside of the microcapillary.

5.3. Dam Survival

Monitoring the dam's breathing is required during surgery to ensure that the animal is responding normally to the anesthesia, and should continue to be monitored closely after surgery while in the heated recovery chamber. To ensure that the dam recovers quickly from sedation, it is important that the appropriate dosage of ketamine and xylazine relative to the weight of the dam was given prior to surgery. The dosage recommended here should produce a maximum sedation time of 1 h. It is also important that there is no excessive bleeding during surgery, by ensuring that the laparotomy is performed carefully along the midline of the abdominal skin and muscle and avoiding damage to major blood vessels.

5.4. Troubleshooting a Low or Lack of Fluorescent Signal

- Check the plasmid by verifying the fluorescent protein sequence, and ensuring an appropriate promoter is used. The cytomegalovirus (CMV) early enhancer/chicken beta-actin (CAG) promoter drives high levels of expression in cortical neurons [22] and has been shown to be more efficient than the CMV promoter alone [23]. Plasmid expression can be tested *in vitro* first by transfection into an appropriate cell culture line.
- Microcapillary blockage: Check that the microcapillary tip is open and that there is outflow of plasmid DNA solution before injection. It should be possible to visualize the Fast Green solution entering the telencephalon during injection.
- Mis-targeting of the intended region of electroporation: Ensure that the embryo is illuminated to assist with the identification of the telencephalic hemispheres and that the microcapillary penetrates the embryonic tissue at the correct depth.
- Check the electrodes: Ensure that these are functional by testing an electric pulse in PBS solution and observing the appearance of bubbles during each pulse. Also avoid cleaning electrodes with ethanol as this may damage the platinum surface and reduce their conductivity.

6 Final Remarks

IUE is a valuable technique for the transfection of cortical cells and can be used to manipulate the expression of many different genes *in vivo*. While electroporation is often used in later stages of gestation to target the later born cortical plate neurons, this technique can be

performed at early stages of development to transfect cells in the early cortical plate. The protocol described in this chapter involves features optimized for early-stage IUE, such as techniques and equipment for improved visualization, injection, and electroporation of the embryos. Furthermore, the technique can be used for the transfection of multiple plasmids with temporal variation, allowing for the possibility of differential labeling between the subplate and cortical plate layers.

A further modification to the technique to enable cell lineage tracing within a target region is the integration of exogenous genes within the genome of electroporated cells via the incorporation of *Tol2* or *Piggybac* transposition sequences in the expression vector [24, 25]. Genome integration via IUE has previously been used for the expression of advanced reporters such as Brainbow transgenes, which contain multiple fluorophores co-expressed in random combinations upon Cre-mediated recombination. This technique provides a method for the detection of individual neuronal progenitor cells and their lineages, including those of cortical neurons by the differential expression of reporter genes [26].

Overall IUE provides significant advantages over conventional transgenic approaches by providing specific spatial and temporal precision. It provides a means for assaying neurons *in vivo* and can be used to generate chimeric tissue to investigate gene function. Combining this delivery technique with the sophisticated DNA construct technologies described above greatly extends the capabilities for investigating important questions in cortical development.

Acknowledgements

We thank R. Suárez and L. Fenlon for their input on the manuscript and providing histological images; Queensland Brain Institute (QBI) Microscopy Facility for microscopy assistance; the University of Queensland Biological Resources and QBI animal team for animal support. PK was supported by a National Health and Medical Research Council (NHMRC, Australia) Early Career (CJ Martin) Fellowship, GA was supported by a Becas Chile Fellowship, and LJR was supported by an NHMRC Principal Research Fellowship. IG was supported by NHMRC project grant GNT1048849.

References

1. Monuki ES, Porter FD, Walsh CA (2001) Patterning of the dorsal telencephalon and cerebral cortex by a roof plate-Lhx2 pathway. *Neuron* 32:591–604
2. O’Leary DDM, Chou S-J, Sahara S (2007) Area patterning of the mammalian cortex. *Neuron* 56:252–269
3. Borello U, Pierani A (2010) Patterning the cerebral cortex: traveling with morphogens. *Curr Opin Genet Dev* 20:408–415
4. Caronia-Brown G, Yoshida M, Gulden F et al (2014) The cortical hem regulates the size and patterning of neocortex. *Development* 141:2855–2865

5. Chédotal A, Richards LJ (2010) Wiring the brain: the biology of neuronal guidance. *Cold Spring Harb Perspect Biol* 2:a001917
6. Shimogori T, Grove EA (2005) Fibroblast growth factor 8 regulates neocortical guidance of area-specific thalamic innervation. *J Neurosci* 25:6550–6560
7. Assimacopoulos S, Kao T, Issa NP, Grove EA (2012) Fibroblast growth factor 8 organizes the neocortical area map and regulates sensory map topography. *J Neurosci* 32:7191–7201
8. Saito T, Nakatsuji N (2001) Efficient gene transfer into the embryonic mouse brain using *in vivo* electroporation. *Dev Biol* 240:237–246
9. Tabata H, Nakajima K (2001) Efficient *in utero* gene transfer to the developing mouse brain using electroporation: visualization of neuronal migration in the developing cortex. *Neuroscience* 103:865–872
10. Britanova O, De Juan RC, Cheung A et al (2008) *Satb2* is a postmitotic determinant for upper-layer neuron specification in the neocortex. *Neuron* 57:378–392
11. Shibata M, Kurokawa D, Nakao H et al (2008) MicroRNA-9 modulates Cajal-Retzius cell differentiation by suppressing *foxg1* expression in mouse medial pallium. *J Neurosci* 28:10415–10421
12. Rouaux C, Arlotta P (2013) Direct lineage reprogramming of post-mitotic callosal neurons into corticofugal neurons *in vivo*. *Nat Cell Biol* 15:214–221
13. Srivatsa S, Parthasarathy S, Britanova O et al (2014) *Unc5C* and *DCC* act downstream of *Ctip2* and *Satb2* and contribute to corpus callosum formation. *Nat Commun* 5:1–15
14. Faux C, Rakic S, Andrews W, Britto JM (2012) Neurons on the move: migration and lamination of cortical interneurons. *Neurosignals* 20:168–189
15. Borrell V, Yoshimura Y, Callaway EM (2005) Targeted gene delivery to telencephalic inhibitory neurons by directional *in utero* electroporation. *J Neurosci Methods* 143:151–158
16. Takiguchi-Hayashi K, Sekiguchi M, Ashigaki S et al (2004) Generation of reelin-positivemarginal zone cells from the caudomedial wall of telencephalic vesicles. *J Neurosci* 24:2286–2295
17. Bielle F, Griveau A, Narboux-Nême N et al (2005) Multiple origins of Cajal-Retzius cells at the borders of the developing pallium. *Nat Neurosci* 8:1002–1012
18. Huilgol D, Udin S, Shimogori T et al (2013) Dual origins of the mammalian accessory olfactory bulb revealed by an evolutionarily conserved migratory stream. *Nat Neurosci* 16:157–165
19. Remedios R, Huilgol D, Saha B et al (2007) A stream of cells migrating from the caudal telencephalon reveals a link between the amygdala and neocortex. *Nat Neurosci* 10:1141–1150
20. Suárez R, Fenlon LR, Marek R et al (2014) Balanced interhemispheric cortical activity is required for correct targeting of the corpus callosum. *Neuron* 82:1289–1298
21. Zhou J, Wen Y, She L et al (2013) Axon position within the corpus callosum determines contralateral cortical projection. *Proc Natl Acad Sci U S A* 110:E2714–E2723
22. Sahara S, Kawakami Y, Izpisua Belmonte J, O’Leary DD (2007) *Sp8* exhibits reciprocal induction with *Fgf8* but has an opposing effect on anterior-posterior cortical area patterning. *Neural Dev* 2:1–22
23. Yaguchi M, Ohashi Y, Tsubota T et al (2013) Characterization of the properties of seven promoters in the motor cortex of rats and monkeys after lentiviral vector-mediated gene transfer. *Hum Gene Ther Methods* 24:333–344
24. Yoshida A, Yamaguchi Y, Nonomura K et al (2010) Simultaneous expression of different transgenes in neurons and glia by combining *in utero* electroporation with the *Tol2* transposon-mediated gene transfer system. *Genes Cells* 15:501–512
25. Chen F, Maher BJ, LoTurco JJ (2014) Piggy-Bac transposon-mediated cellular transgenesis in mammalian forebrain by *in utero* electroporation. *Cold Spring Harb Protoc* 2014:741–749
26. Loulier K, Barry R, Mahou P et al (2014) Multiplex cell and lineage tracking with combinatorial labels. *Neuron* 81:505–520

Chapter 2

In Utero Electroporation Methods in the Study of Cerebral Cortical Development

Isabel Martínez-Garay, Fernando García-Moreno, Navneet Vasistha, Andre Marques-Smith, and Zoltán Molnár

Abstract

Research in the field of cortical development has benefited from technical advances in recent years, and tools are now available to label, monitor, and modulate cohorts of cerebral cortical neurons using in vivo approaches. Substantial populations of cerebral cortical neurons are generated in a specific sequence by the radial glia progenitors that line the ventricular surface during development. These radial progenitors self-renew and generate intermediate progenitors or neurons in a precisely choreographed fashion. Electroporation or electropermeabilization is a method that uses electric pulses to deliver molecules into cells and tissues. The in utero electroporation method has enabled the field to administer plasmids to these neural progenitors, allowing temporal and cell type-specific control for the manipulation of gene expression. For this reason, in utero electroporation has become a central technique in the study of key aspects of neural development, such as progenitor proliferation, neurogenesis, neuronal migration, and circuit formation. This method has also facilitated the exploitation of cell lineage and optogenetic techniques in various species from chick to gyrencephalic higher mammals. This chapter provides a description of the method and gives some examples for its utility in the study of cerebral cortical development and evolution.

Key words Electroporation, Cerebral cortical neurogenesis, Neuronal migration, Radial glia, Intermediate progenitors, *CLoNe*, Cell lineage, Optogenetics

The neocortex develops from the telencephalic vesicles over the course of a few days in mice [1]. The initial cell divisions primarily take place in the germinal zone surrounding the lateral ventricle—the ventricular zone (VZ)—from which cells migrate to the cortical plate. There are spatial and temporal distinctions in the generation of the neurons that will populate the cerebral cortex. Pyramidal neurons and interneurons are generated in different sections of the ventricular zone [2]. The glutamatergic pyramidal neurons arise from the VZ directly underneath the cortical wall and migrate radially towards the pial surface. On the other hand, interneurons arise from the lateral and medial ganglionic eminences (future striatum or basal ganglia) and migrate tangentially into the cortex

[3]. But irrespective of their site of origin, cortical neurons eventually settle in the cortex in an inside-out manner, such that late-born neurons settle in progressively more outward layers [4]. For pyramidal neurons this means that the later born cells must migrate past their older cousins to reach their final position in cortex. The processes of interneuron and pyramidal cell migration occur simultaneously and are likely to influence each other.

Because of the spatial and temporal characteristics of the developing cortex, in utero labeling methods can target specific cortical cell populations or cohorts at specific locations at specific stages of development. During the period of embryonic neurogenesis the radial glia progenitors are exposed to the ventricular surface through their end feet [5, 6]. This anatomical arrangement gives access to these progenitors to label them through different methodologies, including retrovirus-mediated gene transfer [7] or lipid-soluble carbocyanine dyes [8].

Current knowledge about the cellular mechanisms of proliferation and cell migration as well as the molecular cues that direct these processes was initially derived from cell culture and mutant mouse studies [9]. The routes of migration were analyzed by dye tracing techniques and retroviral labeling of clonally related cells both in wild-type and mutant mouse lines [10–12]. In recent years, further characterization of proliferation, fate specification, and migration mechanisms has been conducted using in utero electroporation as the main technique.

1 General Principles of In Utero Electroporation

In utero electroporation uses electric pulses to deliver DNA (plasmid constructs) to the progenitor cells lining the ventricles of the brain and it is performed on living embryos that are then allowed to further develop in utero until the desired embryonic or postnatal age [13–17]. The timing and location of the electroporation can be exploited in targeting specific cohorts of cortical neurons to study progenitor proliferation, neurogenesis, neuronal migration, axon pathfinding, and spine or circuit formation. This method also allows the combination of cell labeling with gain-of-function or loss-of-function experiments where specific mouse lines are not available. In addition, it has aided the exploitation of whole-cell lineage and optogenetic techniques [18–20].

The basic pattern of electroporation involves the injection of the plasmid DNA next to the cell group of choice. This injection is usually performed into the ventricular system for several reasons. First, the progenitors' endfeet line the ventricles, so that the DNA

can be delivered to them. Second, the ventricles are easy to target, enhancing reproducibility between experiments. And third, the potential damage to the tissue architecture caused by the injected volume is minimized when injecting into an already fluid-filled cavity instead of within the tissue. Following injection of the construct or constructs, electrodes are used to deliver electric pulses to the area of interest. These pulses induce the transient disruption of the plasma membrane lipids and promote the generation of pores. As a result, the cell permeability increases, allowing the introduction of the plasmids into the progenitor cells, which will then pass on the plasmids to their cellular offspring as they divide. Because DNA is negatively charged at normal pH, the polarity of the electrodes should be considered to direct the DNA into the tissue. The specific parameters for the electroporation have to be optimized for different areas of the nervous system, taking into account the specific region of interest and the age of the embryo. Transfection efficiency depends on the duration of the pulse, the number of electric pulses, and the pulse voltage [15]. Depending on where the plasmid DNA solution was injected and how the electrodes were oriented, different cell populations will be transfected. The achieved transfection is transient and it is specific for the time and area.

The use of different electrodes (paddle or needle) can refine the in utero electroporation technique because their position and size determine the size of the region transfected. This can vary from a few localized cells to the entire ventricular surface with a large cohort of labeled cells. The localized transfection is desired when the aim is to trace the migratory routes of cells. A more robust and general pattern of electroporation is required if the aim is to characterize gene function in a larger cell population.

There are several detailed descriptions and examples for applications in various systems in mouse: telencephalic inhibitory neurons [21, 22]; hippocampal primordium [23, 24]; precerebellar neurons [25]; adult hippocampal pyramidal neurons [26]; hippocampal dentate gyrus [27]; retinal ganglion cells [28]; developing cerebral cortex [29]; hypothalamic neurons [30]; and analysis of gene regulatory elements in the murine telencephalon [31]. More detailed description of in vivo electroporation in the embryonic mouse central nervous system is presented by Saito [32]. In publications of Walantus et al. [33], and Dixit et al. [34], the authors also present some very informative videos of the method. In the case of early neurogenic embryos (E10.5) an ultrasound-guided injection system such as VeVo 770 (Visual-Sonics) is recommended for visualization of the ventricles and the needle tip [30].

2 Specific Description of the Cerebral Cortical Electroporation in Mouse Modified from Shimogori [15] and Chen et al. [40]

2.1 Mouse Preparation

To induce general anesthesia, place the timed-pregnant mice in the induction chamber with 3.5 % isoflurane. When the dam is asleep and the breathing slows down, connect the anesthesia machine to the face mask with 3.5 % isoflurane. Put some artificial tears on the eyes before placing the animal on the heat blanket with the head in the face mask.

Shave the abdomen of the dam and rub it with antiseptic. A subcutaneous injection of buprenorphine (0.08 mg/kg) is given at the beginning of the surgery to allow action by the end of the surgery (usually within 20–30 min). Place a sterile drape over the animal. At this stage, isoflurane can be decreased to 2–1.5 %.

2.2 Surgery

Make a small incision on the skin following the vertical midline (2–3 cm or less, depending on the stage of the pregnancy). Use the ring forceps to separate the skin from the abdominal wall and then cut the midline abdominal wall (linea alba), making a shorter incision than before (2 cm or less).

Hold the skin and abdominal wall with the forceps and use the ring forceps to gently pull the mobile part of the uterine horns out. Pull gently in between embryos to avoid any damage and be very careful with the blood vessels. Once the uterine horns with the embryos are exposed, keep them always wet with warm (37 °C), sterile saline solution using a plastic Pasteur pipette. Place moistened cotton gauze draped around the incision.

2.3 Injection

Embryos are visualized through the uterus with a fiber-optic light source. Inject the plasmid DNA (usually 1 µg/µl) mixed with fast green (0.5 %) into the ventricle using a glass capillary. The glass capillaries are pulled beforehand to create very thin needles using a micropipette puller. To minimize damage to the uterine wall and to the skull and brain of the embryo, the size of the needles must be precisely controlled (the needle should be pulled to produce a thin tip along the last part of the electrode, no more than 50 µm). The Fast Green dye allows visualizing the filling of the ventricles.

2.4 Electroporation

Once the ventricles are filled with DNA and the indicator dye, the electrodes are dipped into the saline solution to wet them and placed on both sides of the embryo's head. The structure of the brain that needs to be electroporated dictates the placement of the electrodes, with the positive electrode next to the area to be electroporated, generally. The placenta and the heart should not receive the electrical shock. For more localized electroporation needle electrodes can be used. These electrodes are homemade [15] or commercially available. These have to be positioned (inserted into

the skull) according to the region of interest. Their size should be kept to the minimum to avoid damage to the uterine wall.

2.5 Closure of Incision

Once all desired embryos have been electroporated, they are rinsed again with warm sterile saline solution, and carefully placed back inside the dam. When the uterus is back in place, warm sterile saline solution is put into the abdominal cavity for further rinsing and for rehydration. The abdominal wall is sutured first, and then the skin is sutured or stapled. It is important to keep the surgery time to minimum and do not exceed 30 min. An injection of NSAID (e.g., Metacam, at 1–2 mg/kg) is given subcutaneously to the dam, which is then placed in a recovery chamber to keep her warm before being returned to the cage.

3 In Utero Electroporation and the 3 Rs

The use of animals as experimental subjects should always be done within the ethical framework provided by the three Rs: replacement, reduction, and refinement. Wherever possible cortical development should be studied *in vitro*. However the cortex is a very complex structure and some processes, like tridimensional neuronal migration, cannot be easily studied *in vitro* because they involve different cells types and defined tissue architecture. These aspects are more difficult to replicate in a dish. The *in utero* electroporation technique can reduce the overall number of animals used for loss-of-function (LOF) or gain-of-function (GOF) experiments. Some of these LOF and GOF experiments involve otherwise conditional KO lines, which can require larger colonies. Using electroporation decreases the need for transgenic mouse colonies, as genes can be knocked down using shRNA. Because *in utero* electroporation involves surgery with recovery, refinement of the whole process is especially critical. There are several considerations in anesthesia, surgical procedures, and postoperative care that can refine this method (*see* Box 1.).

Box 1 Refinement Strategies for *in Utero* Electroporation

- A combination of isoflurane and buprenorphine is used for anesthesia, and absence of pedal reflex is used to assess surgical depth.
- NSAIDs are used for postoperative pain relief and can be administered as jelly for continuous dosage after surgery.
- Aseptic surgical techniques are used in designated area within the procedure room.
- The mouse is kept on a heated pad during and after surgery.

(continued)

Box 1 (continued)

- Artificial tears are used to prevent the eyes from drying.
- During surgery the exposed uterus is kept wet with sterile, warm 1× PBS while exposed.
- Embryos are handled as gentle as possible. The two embryos nearest the cervix should not be injected.
- The mouse is kept hydrated during and after surgery.
- Recovery is closely monitored and the animal is checked several times a day after surgery.
- If there are any signs of discomfort after 14 h, another injection of buprenorphine is administered.
- Pulse parameters are determined in *in vitro* experiments and then adjusted for the age of the embryos.

Age	Volts (mV)	Pulse length (ms)	Interval (ms)	No. of pulses
E12.5	30–35	50	950	4–5
E13.5	35	75	950	5
E14.5	40–45	75–100	950	5
E15.5	50	100	950	5

4 Applications

4.1 Parameters

In utero electroporation is a very versatile technique that allows analysis of a variety of aspects of cortical development. There are four main parameters that can be adjusted according to the process that is being studied.

4.1.1 Time of Electroporation

Depending on the embryonic day that is chosen for the surgery, neurons predominantly located in different layers can be targeted. This allows analysis of specific populations and their intrinsic properties. Note the difference between the cortical neuronal population electroporated at E12.5 and E14.5, both examined at lateral cortex at E18.5. The electroporation at E12.5 primarily targets layer 6 and 5 neurons, whereas at E14.5 labels layer 2–4 neurons (Fig. 1).

4.1.2 Interval Between Electroporation and Harvesting of the Brains

By keeping the interval short (1–2 days), proliferation of neuronal precursors and neurogenesis can be studied. Longer intervals (3–4 days) allow the analysis of different migration modes (glia-guided migration and terminal translocation). To study laminar fate, neuronal differentiation, and dendritogenesis, the post-electroporation time can be extended until the embryos are born to harvest the brains postnatally. All panels in Fig. 2 have been

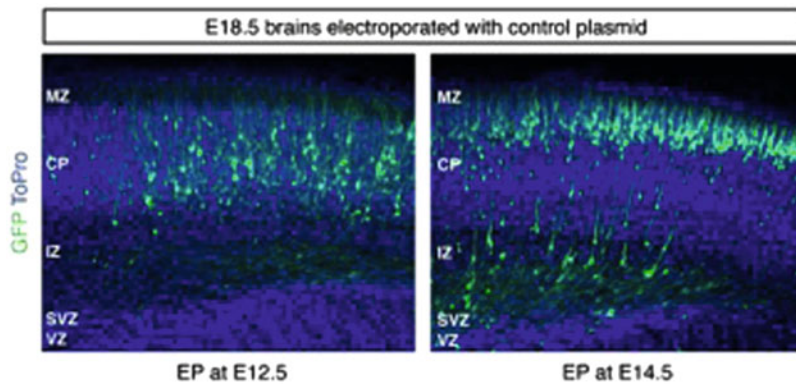


Fig. 1 Electroporation at different developmental stages targets different neuronal layers. Control plasmid expressing EGFP as a reporter was electroporated into the lateral ventricle of C57Bl6/J embryos at two different embryonic stages. One litter was electroporated at E12.5 and another at E14.5. Brains were dissected for analysis at E18.5. Electroporation at E12.5 targets mainly deep-layer neurons (layers VI and V, *left panel*), whereas upper layer neurons (layers IV and II/III, *right panel*) are labeled if the electroporation is performed at E14.5. Labeling in *blue* shows counterstaining of nuclei with ToPro for the observation of gross morphology. VZ ventricular zone, SVZ subventricular zone, IZ intermediate zone, CP cortical plate, MZ marginal zone

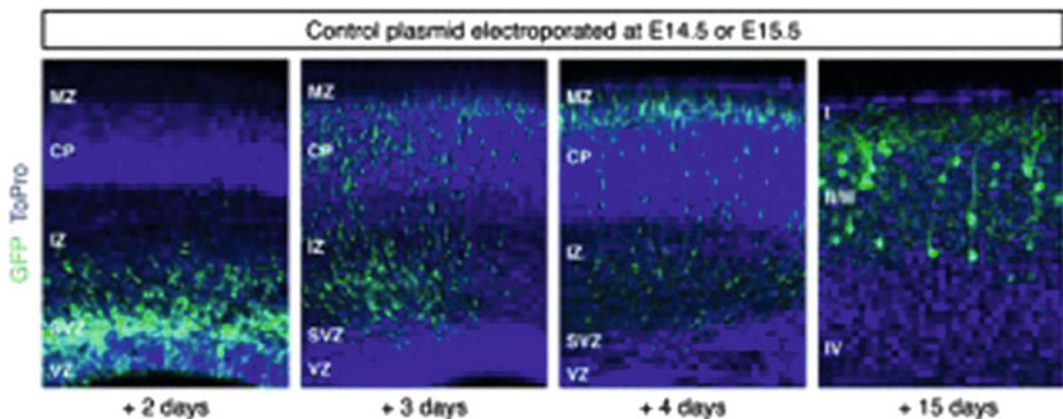


Fig. 2 In utero electroporation can be used to study different processes during corticogenesis. Control plasmid expressing EGFP as a reporter was electroporated into the lateral ventricle of C57Bl6/J embryos at either E14.5 or E15.5. Brains were harvested 2, 3, 4, or 15 days later. Two days after electroporation many progenitors are still labeled in the ventricular and subventricular zones (VZ and SVZ, respectively). One day later, labeling is almost restricted to migrating neurons, which span the majority of the cortical wall, from the SVZ to the top of the cortical plate (CP). Four days after electroporation most of the neurons have reached the top of the CP, although some of them are still migrating. After 15 days, electroporated neurons are differentiating in their layers, and their dendritic arbor and axonal projections can be analyzed. Labeling in *blue* shows counterstaining of nuclei with ToPro for the observation of gross morphology. VZ ventricular zone, SVZ subventricular zone, IZ intermediate zone, CP cortical plate, MZ marginal zone

electroporated at E14.5, but studied at different stages (2, 3, 4, or 15 days after electroporation).

4.1.3 *Various Types of DNA Injected*

There is a wide choice of DNA constructs that can be used for in utero electroporation depending on the experimental aims. The following list is not meant to be comprehensive, but it provides an overview of the possibilities:

- The simplest scenario involves using a eukaryotic expression plasmid with a reporter to label a specific cell population. The reporter gene expression can also be targeted to the nucleus, the cytoplasm, the cell membrane [18], or many other organelles.
- More than one plasmid can be electroporated. It is known that two vectors co-transfected at the same high concentration can virtually reach a global co-transfection [35]. Additionally, by artificially increasing the concentration of a construct A over other plasmid B we can make sure that all B-expressing cells will possess a copy of the construct A [18].
- For LOF experiments, plasmids encoding shRNAs against genes of interest can be used [36] or dominant negative forms of proteins or enzymes can be electroporated. In addition, if no appropriate Cre-expressing transgenic mouse line is available for LOF experiments in a cortical cohort, then electroporation of a plasmid encoding Cre-recombinase into floxed animals could be considered. Figure 3 shows an example of the effect of two different mutant proteins on the migration of cortical neurons. Electroporation was performed at E14.5 and the distribution of the neurons 4 days later varies depending on the construct electroporated. In Mutant 2 the cohort of migrating neurons is less advanced than in Mutant 1 or the Control.
- For GOF experiments, constitutively active forms of proteins or enzymes can be used, as well as overexpression of full-length proteins to analyze the effects of overexpression.
- Longer term lineage studies require a stable transfection of the progenitors, something that can be achieved with the inclusion of transposase [37–39] (see example and variations of the technique below).

4.1.4 *Promoter to Drive Expression of the DNA*

The use of a general promoter will direct expression of the plasmid from the moment it is internalized by the progenitors, being active both in progenitors and neurons. By using a neuronal specific promoter, expression can be restricted to the neuronal progeny, and cell type-specific promoters can further restrict expression to particular neuronal types. If a promoter of our choice drives the expression of Cre, STOP-floxed fluoroprotein cassettes can be selectively activated in the population that uniquely expresses our

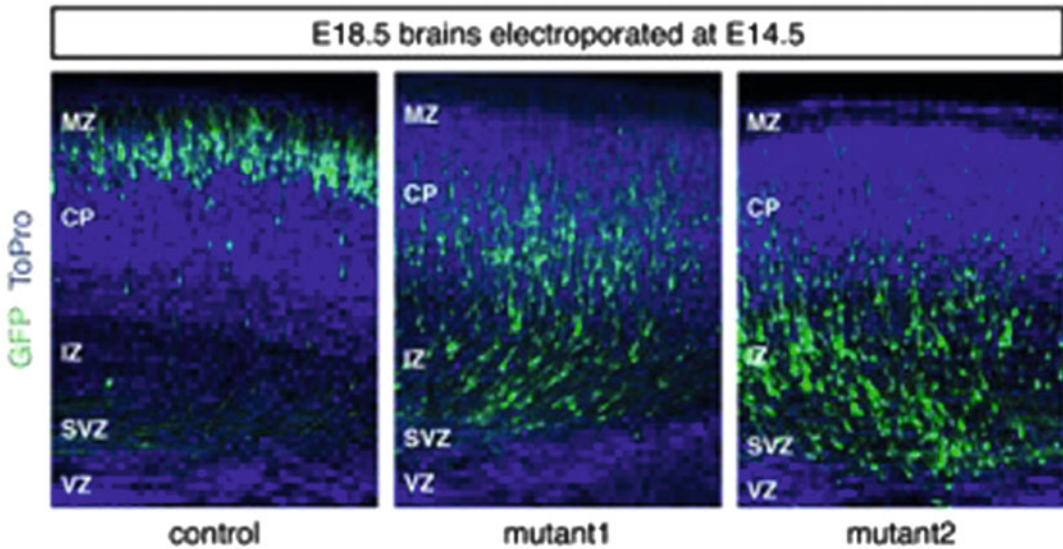


Fig. 3 Functional analysis of neuronal migration using in utero electroporation. C57Bl6/J embryos were electroporated at E14.5 with either control plasmid expressing EGFP as a reporter or bicistronic plasmids expressing dominant negative forms of two different proteins and EGFP. Brains were analyzed at E18.5. Neurons electroporated with control plasmid have reached the top of the CP after 4 days and form a tight band there. In contrast, neurons expressing the mutant proteins are still in the intermediate zone (IZ) or the lower half of the CP after the same amount of time, suggesting that the dominant negative forms of the proteins are interfering with normal migration. Labeling in *blue* shows counterstaining of nuclei with ToPro for the observation of gross morphology. VZ ventricular zone, SVZ subventricular zone, IZ intermediate zone, CP cortical plate, MZ marginal zone

favorite gene. As an example, *Emx2* or *Dlx1/2* enhancer sequences can trigger the expression of the reporter gene in either dorsal pallial or subpallial progenitors, respectively [18].

4.2 Examples

4.2.1 Electroporating STOP-Floxed Fluoroprotein Expressing Plasmids into Cre-Expressing Lines

In mouse models where a specific cortical progenitor population expresses Cre, one can reveal the lineage by electroporating stop-floxed fluoroproteins. Such an approach has been used to label the lineage from *Tbr2* intermediate progenitor neurons in *Tbr2^{Cre}* pregnant mice at 12.5 dpc (E12.5) [19].

4.2.2 CLoNe Method to Label Cortical Cell Lineages

More recently a binary *piggyBac* transposon system to induce genomic integration of a unique and permanent combination of fluorescent fluoroproteins has been developed to label cortical cell lineages [18]. These transgenes do not appear to inactivate after cell division, and this results in stable somatic cellular transgenesis of neurons and glia. This method uses a cocktail of transposase-expressing plasmid and STOP-floxed fluoroprotein-expressing plasmids that target the expression to nucleus, cell membrane, or cytoplasm [18].

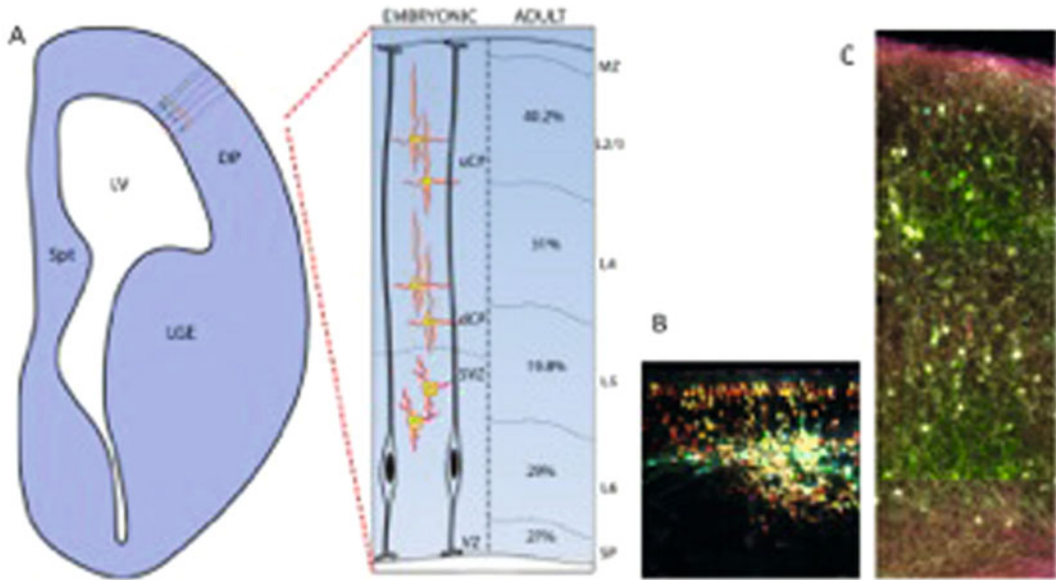


Fig. 4 Clonal lineage analysis of progenitor cells using Cre-activated fluoroproteins. Analysis of clonally derived cells can be carried out by in utero electroporation of STOP-floxed fluorescent labels. In this example, a mixture of fluorescent plasmids were electroporated into the lateral ventricle of *Tbr2*Cre mice to study and analyze the progenies of *Tbr2*⁺ intermediate progenitors in the *Tbr2*-Cre mouse at E12.5. **(a)** Schematic representation of the in utero electroporation site. Fluorescent proteins are expressed only in the cells expressing Cre (IPCs here) but not in radial glia (in *black outline*). The labels are stably inherited by the neurons. Percentages of labeled cells derived from IPCs in each layer can be described in this manner. **(b)** Labeling of IPCs and IPC-derived neurons is seen 2 days after electroporation. A variety of hues can be seen in the SVZ, IZ, and CP but not in the VZ. **(c)** Analysis at P7 reveals a multitude of neurons labeled in different hues. Neurons expressing similar set of fluorophores in the same regions can be recognized as clonally derived cells. *DP* dorsal pallium, *Spt* septum, *LV* lateral ventricle, *LGE* lateral ganglionic eminence, *VZ* ventricular zone, *SVZ* subventricular zone, *dCP* deeper cortical plate, *uCP* upper cortical plate, *SP* subplate, *L* layer, *MZ* marginal zone

In the case of the study of intermediate progenitors [19] this cocktail labels clonal progenies of focally electroporated progenitors that pass through a *Tbr2*⁺ lineage with the same combination of fluorophores, thus enabling their detection [18, 19, 37, 39, 40] (Fig. 4). The huge combinatorial variability of the fluorescent hue, inherited by sibling cell, reveals clonal relationship.

4.2.3 Silencing of Specific Neuronal Populations

Overexpression of the inwardly rectifying potassium channel Kir2.1 in neurons hyperpolarizes them, resulting in less excitable neurons and a decrease in neuronal activity [41]. In utero electroporation can be used to direct the expression of this channel to specific neuronal populations to silence them. In this way, the effects of neuronal activity or the lack thereof on cortical development can be assessed. This approach has been used to study thalamocortical axonal growth into the cortex [42] and callosal targeting by the axons of layer II–III neurons [43].

4.3 Electroporation of Optogenetic Actuators and Other Constructs for Studying Functional Circuit Development

In 1979, Francis Crick stated with extraordinary prescience the need in neurobiology for what would decades later become the great asset of optogenetic technology: "... a method by which all neurons of just one type could be inactivated leaving the others more or less unaltered" (Crick, p. 222) [44]. Broadly speaking, "optogenetics" [45–47] refers to a general methodological framework whereby optical stimulation methods are used to excite or inhibit restricted populations of neurons engineered to be directly [48] or indirectly [49–51] electrically responsive to light of a particular wavelength (Fig. 5). The most widely adopted approaches involve expression of light-sensitive bacterial opsins: variants of channelrhodopsin for neuronal activation and halo or archaerhodopsin for neuronal inactivation [48, 49, 52]. Other interesting optogenetic methods involve expression of ligand-gated ion channels foreign to the mammalian genome, obtained by synthetic design or mining and engineering the genome of nonmammalian species. Spatial specificity of activation is conferred in this approach

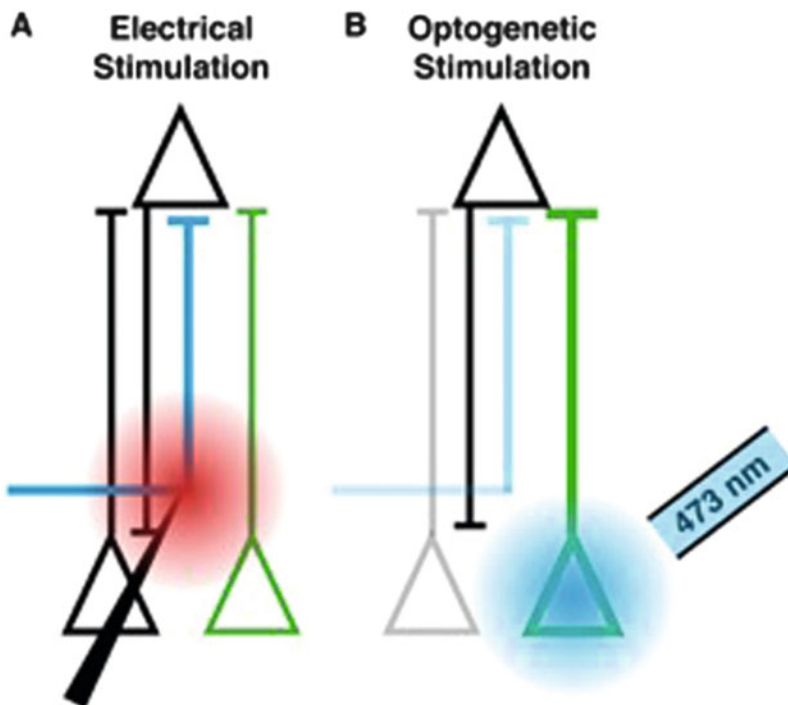


Fig. 5 Optogenetics in neural circuits. **(a)** Electrical stimulation can indiscriminately activate target axons (*green*), nearby axons from a different cell type (*black*), and axons of passage arriving from other areas (*blue*). In reciprocally connected structures it may also lead to antidromic activation of recorded cells (*black, top*). **(b)** Optogenetic stimulation circumvents these issues by restricting photoactuator expression to genetically defined cell types. Only neurons expressing the photoactuator (channelrhodopsin, in this example) will be activated by light (473 nm). These experimental conditions isolate the target pathway (*green, thick line*) for detailed study

by using and providing to the brain ligands which are made inert by photosensitive chemical “cages” [46, 50]. Upon focal stimulation with light of a particular wavelength, these ligands are rendered active within a restricted region of tissue and become free to diffuse and excite only cells which express the cognate receptor within a short distance of the stimulated area.

Light lends itself well as a medium for neuronal stimulation. It can be focused in three dimensions to excite extremely restricted volumes of brain tissue and it can be scanned quickly using a variety of technologies to iteratively stimulate neurons across regions of space. This allows experimenters to record a neuron using electrophysiology and use light to quickly probe multiple restricted brain areas containing putatively presynaptic channelrhodopsin-expressing neurons for synaptic inputs onto the recorded cell. This combined electrophysiological recording and iterative spatial stimulation of putative presynaptic clusters of neurons is generally termed circuit mapping. Recent developments in the application of optical physics to neuroscience and in genome engineering have led, amongst other advances, to two-photon optogenetic excitation for single-cell activation and spatial light modulation for projecting on brain tissue patterns rather than a single beam of light, enabling, amongst other applications, simultaneous activation/inactivation of neurons in spatially distant locations from each other [53–56]. Optogenetic technology has proved invaluable in providing a further level of specificity (cell type) to circuit mapping in vitro [57–60] and been instrumental in in vivo experiments for activation or inactivation of highly defined populations of neurons during specific behaviors, thereby clarifying their function for processes such as visual perception [61–63]. The potential held by cell type-specific functional manipulation methods for advancing our knowledge of brain function was in no way overstated by Francis Crick in 1979.

5 Optogenetics, Circuit Development, and In Utero Electroporation

Although key examples can certainly be found in developmental literature [64–67], circuit mapping has mostly been the province of the mature circuit physiologist. In spite of perhaps a smaller user base, optogenetics could be fundamental for addressing important questions in the field of brain development, examples of which are explored in this section.

The first advance provided by optogenetics which could be of use in development is its ability to unambiguously target stimulation to identified neurons and pathways. This is a key feature because several brain structures form reciprocal connections with each other, as exemplified by the thalamocortical and corticothalamic pathways [68]. The use of electrical stimulation is perilous in

such pathways, due to antidromic activation and stimulation of axons of passage (Fig. 5). Moreover, neurons involved in different networks and circuits, with specific projection patterns and distinct physiological characteristics, coexist side by side within the same brain areas. Cell type-specific activation enables the study of very-well-defined pathways avoiding the nonspecific activation of electrical stimulation methods (Fig. 5). A second interesting application is chronic activation or inactivation of specific neuron populations. Chronic blockade or enhancement of activity is a classical paradigm in the study of development [69]. Despite providing important insights, these experiments have traditionally involved application of drugs such as tetrodotoxin (sodium channel blocker) or muscimol (GABA agonist) in localized regions of the brain, indiscriminately affecting any cell in the targeted area, which can hamper interpretability. Chronic activation or inactivation experiments in mature mice involve the implantation of fiber optics in the brain for light delivery to opsin-transfected neurons, which, though challenging, could be ported into development, allowing inactivation/activation of specific cell types. Moreover, chronic activation experiments with channelrhodopsin offer an advantage over pharmacological or genetic enhancements of activity, as they permit refinement from simple “overactivation” to programmed stimulation, allowing the study of the role of spatiotemporally patterned activity in circuit development [70]. A key area of research in the development of optogenetic methods has been design and production of red-shifted optogenetic tools [71, 72]. The red-shifted light spectrum has longer wavelengths, facilitating tissue penetration by light, which could conceivably enable transcranial optogenetic stimulation [72]. This technology would have incredible potential for chronic manipulation studies in brain development as it circumvents fiber-optic implantation into the brain, problematic when dealing with fragile neonates.

Due to its ability to target neurons very early in development, in utero electroporation emerges as a choice candidate technique for delivery of optogenetic constructs for developmental experiments. Early expression is fundamental for the study of developing circuits as populations like subplate neurons or Cajal-Retzius cells form early circuits and perform important developmental functions, but are largely transient [73]. Moreover, the developing brain contains transient circuits that are fundamental conduits and generators of early network activity [73–75]. Understanding their developmental function requires the capability for early and cell type-selective targeting, which the combination of in utero electroporation and optogenetic technology can offer. Besides early targeting, an important advantage afforded by in utero electroporation is the large genetic payload provided by plasmids, compared to viral vector cassettes. Under the appropriate genetic conditions, this feature allows one-shot labeling/interference plus optogenetic

construct transfection of the same cell population. Besides reliably targeting the same neurons, this characteristic obviates an additional postnatal surgery, minimizing animal pain and distress. One interesting application would be co-electroporation of separate knockdown/overexpression and optogenetic constructs, allowing genetic interference with a cell population followed by postnatal functional verification of how its synaptic outputs are altered.

Combining in utero electroporation and optogenetics appears to be a profitable strategy for answering questions related to the organization of early neural circuits and the activity-dependent side of neural development. It may be however that optogenetic technology poses specific challenges to the developmental neurobiologist. Channelrhodopsins are known to have minute unitary conductances [46] and delays of over 10 days between transfection and optogenetic experimentation are commonly required for enough expression to be achieved [57, 58]. To the extent of our knowledge, the only study published using channelrhodopsin-based optogenetics in the brain prior to P10 targeted retinal ganglion cells to examine the retinogeniculate and retinocollicular pathways [70]. We have successfully used a heterologous channel (P2X₂) and caged ligand approach [46, 50] to map cell type-selective circuits in neonates (unpublished observations). Waiting time is a luxury developmental neuroscientists can rarely afford and it may be that current optogenetic constructs need to be optimized for earlier use and faster expression in development, in an application-dependent manner. Only experimentation will answer which neural systems, cell types, and constructs are most amenable to early optogenetic investigation. Nonetheless, the pace of progress in design and optimization of optogenetic constructs since their inception is encouraging [45–47] and will doubtlessly lead to exciting breakthroughs in developmental neurobiology.

6 Variations on the Technique

Different variations on the in utero electroporation technique have been developed that make it even more versatile:

- Sequential electroporation: More than one in utero electroporation is performed on the same animal, allowing the targeting of different neuronal populations [76].
- Use of a triple electrode: Improves reliability of the targeted area and allows access to previously difficult-to-reach areas, especially in the dorsal and rear brain sectors of the brain [24].
- Use of transposase-encoding vectors: Combined with plasmids containing the transposase recognition sequences, transfection becomes stable and the DNA of choice is incorporated into the recipient's cell genome and all its progeny [18, 19].

7 Electroporation in Different Species

- Ferret has been a very popular model for the understanding of the formation of cortical circuits and their plasticity, but genetic manipulations were limited. Recently in vivo electroporation methods have been developed in prenatal fetuses and postnatal ferret kits to deliver genetic constructs to cohorts of neurons of the cerebral cortex [77–80].
- Chick (*Gallus gallus*): Electroporation has been a widely used technique for the study of the development of the spinal cord and the peripheral nervous system (method reviewed in [81–83]). Additionally, in ovo electroporation in comparative studies on the development of homologous areas has revealed significant findings on the evolution of the neocortex [84–86].
- Reptile species: To a lower extent than avian species (such as chick and quail), in ovo electroporation of living reptile embryos has also been employed to unravel comparative features of the developing brain. Recently, Madagascar ground gecko (*Paroedura pictus*) and Chinese softshell turtle (*Pelodiscus sinensis*) have been proposed as good animal models to study this process through a reliable and feasible in ovo electroporation system [87, 88].

8 Limitations

In utero electroporation methods require considerable surgical skills to achieve constantly high success rates. While in utero electroporation can be used throughout the intrauterine period, younger ages (before E10 in mouse) can be more challenging because of the size of the brain and the less clear visibility through the uterine wall at these earlier stages of pregnancy.

Postnatal electroporation is also feasible, but the cortical neurons are no longer accessible by this period. Only a limited region of the subependymal zone (SVZ) can be electroporated to study the generation, migration, and integration of the neurons destined for the olfactory bulb [89, 90].

The scale of trauma caused to the integrity of the ventricular zone progenitors and subsequent lineage by electroporation is currently not known. It is known that electroporation can act on the destabilization of the cellular actin network and this effect is linked to the electric field rather than the entry of the delivered DNA [91]. These effects have not been studied systematically in cortical neurons, but should be further analyzed to exclude the possibility that electroporation itself can have an effect on neurogenesis or migration, since both mechanisms require intact actin network.

Although it has not been reported yet, the reporter genes (encoding various fluorescent proteins) could have their own undesired effects on the migrating neurons (e.g., Ca buffering, toxicity) in extreme conditions. The expressed Cre-recombinase itself can have an effect on the proliferation, migration, or differentiation of cortical neurons (Garcia-Moreno unpublished observations).

9 Conclusions

The difficulty to reproduce the complex architecture of the developing cortex in vitro prompted researchers to develop new ways to study corticogenesis. The in utero electroporation technique has allowed temporal and cell type-specific control in the manipulation of gene expression in progenitors and neurons, and has therefore become a very frequently used technique in the field. It is well suited to study several aspects of cerebral cortical development in vivo, such as progenitor proliferation, neurogenesis, neuronal migration, and circuit formation. We have provided here some examples for its versatility, but this chapter only gives a flavor of its utility in the study of cerebral cortical development. The list of references provides more detailed description of specific modifications.

References

1. Rakic P (1995) A small step for the cell, a giant leap for mankind: a hypothesis of neocortical expansion during evolution. *Trends Neurosci* 18(9):383–388
2. Kriegstein AR, Noctor SC (2004) Patterns of neuronal migration in the embryonic cortex. *Trends Neurosci* 27(7):392–399
3. Marin O, Rubenstein JL (2003) Cell migration in the forebrain. *Annu Rev Neurosci* 26:441–483
4. Rakic P (2000) Molecular and cellular mechanisms of neuronal migration: relevance to cortical epilepsies. *Adv Neurol* 84:1–14
5. Weigmann A, Corbeil D, Hellwig A, Huttner WB (1997) Prominin, a novel microvilli-specific polytopic membrane protein of the apical surface of epithelial cells, is targeted to plasmalemmal protrusions of non-epithelial cells. *Proc Natl Acad Sci U S A* 94(23):12425–12430
6. Dubreuil V, Marzesco AM, Corbeil D, Huttner WB, Wilsch-Bräuninger M (2007) Midbody and primary cilium of neural progenitors release extracellular membrane particles enriched in the stem cell marker prominin-1. *J Cell Biol* 176(4):483–495
7. Walsh C, Cepko CL (1993) Clonal dispersion in proliferative layers of developing cerebral cortex. *Nature* 362(6421):632–635
8. Molnár Z, Blakey D, Bystron I, Carney R (2006) Tract-tracing in developing systems and in post-mortem human material, Chapter 12. In: Zaborszky L, Wouterlood FG, Lanciego JL (eds) *Neuroanatomical tract-tracing 3: molecules - neurons - systems*. Springer, New York, NY, pp 336–393
9. Kriegstein AR (2005) Constructing circuits: neurogenesis and migration in the developing neocortex. *Epilepsia* 46(Suppl 7):15–21
10. de Carlos JAJ, López-Mascaraque LL, Valverde FF (1996) Dynamics of cell migration from the lateral ganglionic eminence in the rat. *J Neurosci* 16:6146–6156
11. Anderson S (1997) Interneuron migration from basal forebrain to neocortex: dependence on *Dlx* genes. *Science* 278:474–476
12. Wonders CP, Anderson SA (2006) The origin and specification of cortical interneurons. *Nat Rev Neurosci* 7(9):687–696
13. Fukuchi-Shimogori T, Grove EA (2001) Neocortex patterning by the secreted signaling molecule FGF8. *Science* 294(5544):1071–1074

14. Tabata H, Nakajima K (2003) Multipolar migration: the third mode of radial neuronal migration in the developing cerebral cortex. *J Neurosci* 23(31):9996–10001
15. Shimogori T (2006) Micro in utero electroporation for efficient gene targeting in mouse embryos. In: Friedmann T, Rossi J (eds) *Gene transfer: delivery and expression of DNA and RNA, a laboratory manual*. Cold Spring Harbor Laboratory Press, p 427–432
16. Shimogori T, Ogawa M (2008) Gene application with in utero electroporation in mouse embryonic brain. *Dev Growth Differ* 50(6):499–506
17. Matsui A, Yoshida AC, Kubota M, Ogawa M, Shimogori T (2011) Mouse in utero electroporation: controlled spatiotemporal gene transfection. *J Vis Exp* (54): pii: 3024
18. García-Moreno F, Vasistha NA, Begbie J, Molnár Z (2014) CLoNe is a new method to target single progenitors and study their progeny in mouse and chick. *Development* 141(7): 1589–1598
19. Vasistha NA, García-Moreno F, Arora S, Cheung AF, Arnold SJ, Robertson EJ, Molnár Z (2014) [Cortical and clonal contribution of Tbr2 expressing progenitors in the developing mouse brain](#). *Cereb Cortex*. pii: bh125.
20. Marques-Smith A (2014) Using optical stimulation to study the developing thalamocortical circuit in mouse somatosensory cortex. D Phil thesis, University of Oxford
21. Borrell V, Yoshimura Y, Callaway EM (2005) Targeted gene delivery to telencephalic inhibitory neurons by directional in utero electroporation. *J Neurosci Methods* 143(2):151–158
22. de Marco Garcia NV, Fishell G (2014) Subtype-selective electroporation of cortical interneurons. *J Vis Exp*. (90): e51518
23. Nakahira E, Yuasa S (2005) Neuronal generation, migration, and differentiation in the mouse hippocampal primordium as revealed by enhanced green fluorescent protein gene transfer by means of in utero electroporation. *J Comp Neurol* 483(3):329–340
24. dal Maschio M, Ghezzi D, Bony G, Alabastri A, Deidda G, Brondi M, Sato SS, Zaccaria RP, Di Fabrizio E, Ratto GM, Cancedda L (2012) High-performance and site-directed in utero electroporation by a triple-electrode probe. *Nat Commun* 3:960
25. Okada T, Keino-Masu K, Masu M (2007) Migration and nucleogenesis of mouse precerebellar neurons visualized by in utero electroporation of a green fluorescent protein gene. *Neurosci Res* 57(1):40–49
26. Navarro-Quiroga I, Chittajallu R, Gallo V, Haydar TF (2007) Long-term, selective gene expression in developing and adult hippocampal pyramidal neurons using focal in utero electroporation. *J Neurosci* 27(19):5007–5011
27. Ito H, Morishita R, Iwamoto I, Nagata K (2014) Establishment of an in vivo electroporation. *Hippocampus* 24(12):1449–1457
28. García-Frigola C, Carreres MI, Vegar C, Herrera E (2007) Gene delivery into mouse retinal ganglion cells by in utero electroporation. *BMC Dev Biol* 7:103
29. LoTurco J, Manent JB, Sidiqi F (2009) New and improved tools for in utero electroporation studies of developing cerebral cortex. *Cereb Cortex* 19(Suppl 1):i120–i125
30. García-Moreno F, Pedraza M, Di Giovannantonio LG, Di Salvio M, López-Mascaraque L, Simeone A, De Carlos JA (2010) A neuronal migratory pathway crossing from diencephalon to telencephalon populates amygdala nuclei. *Nat Neurosci* 13:680–689
31. Langevin LM, Mattar P, Scardigli R, Roussigné M, Logan C, Blader P, Schuurmans C (2007) Validating in utero electroporation for the rapid analysis of gene regulatory elements in the murine telencephalon. *Dev Dyn* 236(5):1273–1286
32. Saito T (2006) In vivo electroporation in the embryonic mouse central nervous system. *Nat Protoc* 1(3):1552–1558
33. Walantus W, Castaneda D, Elias L, Kriegstein A (2007) In utero intraventricular injection and electroporation of E15 mouse embryos. *J Vis Exp*. (6):239
34. Dixit R, Lu F, Cantrup R, Gruenig N, Langevin LM, Kurrasch DM, Schuurmans C (2011) Efficient gene delivery into multiple CNS territories using in utero electroporation. *J Vis Exp* (52): pii: 2957
35. Rana ZA, Ekmark M, Gundersen K (2004) Coexpression after electroporation of plasmid mixtures into muscle in vivo. *Acta Physiol Scand* 181:233–238
36. Paracchini S, Thomas A, Castro S, Lai C, Paramasivam M, Wang Y, Keating BJ, Taylor JM, Hacking DF, Scerri T, Francks C, Richardson AJ, Wade-Martins R, Stein JF, Knight JC, Copp AJ, Loturco J, Monaco AP (2006) The chromosome 6p22 haplotype associated with dyslexia reduces the expression of KIAA0319, a novel gene involved in neuronal migration. *Hum Mol Genet* 15(10):1659–1666
37. García-Marqués J, López-Mascaraque L (2013) Clonal identity determines astrocyte cortical heterogeneity. *Cereb Cortex* 23(6):1463–1472

38. Siddiqi F, Chen F, Aron AW, Fiondella CG, Patel K, LoTurco JJ (2014) Fate mapping by piggyBac transposase reveals that neocortical GLAST+ progenitors generate more astrocytes than Nestin+ progenitors in rat neocortex. *Cereb Cortex* 24:508
39. García-Marqués J, Nunez-Llaves R, López-Mascaraque L (2014) NG2-glia from pallial progenitors produce the largest clonal clusters of the brain: time frame of clonal generation in cortex and olfactory bulb. *J Neurosci* 34:2305–2313
40. Chen F, Maher BJ, LoTurco JJ (2014) piggyBac transposon-mediated cellular transgenesis in mammalian forebrain by in utero electroporation. *Cold Spring Harb Protoc* 2014 (7):741–749
41. Johns DC, Marx R, Mains RE, O'Rourke B, Marbán E (1999) Inducible genetic suppression of neuronal excitability. *J Neurosci* 19 (5):1691–1697
42. Mire E, Mezzera C, Leyva-Díaz E, Paternain AV, Squarzoni P, Bluy L, Castillo-Paterna M, López MJ, Peregrín S, Tessier-Lavigne M, Garel S, Galcerán J, Lerma J, López-Bendito G (2012) Spontaneous activity regulates Robo1 transcription to mediate a switch in thalamocortical axon growth. *Nat Neurosci* 15(8):1134–1143
43. Suárez R, Fenlon LR, Marek R, Avitan L, Sah P, Goodhill GJ, Richards LJ (2014) Balanced interhemispheric cortical activity is required for correct targeting of the corpus callosum. *Neuron* 82(6):1289–1298
44. Crick FH (1979) Thinking about the brain. *Sci Am* 241:219–232
45. Fenno L, Yizhar O, Deisseroth K (2011) The development and application of optogenetics. *Annu Rev Neurosci* 34(1):389–412
46. Miesenböck G (2011) Optogenetic control of cells and circuits. *Annu Rev Cell Dev Biol* 27:731–758
47. Bernstein JG, Garrity PA, Boyden ES (2012) Optogenetics and thermogenetics: technologies for controlling the activity of targeted cells within intact neural circuits. *Curr Opin Neurobiol* 22:61–71
48. Boyden ES, Zhang F, Bamberg E, Nagel G, Deisseroth K (2005) Millisecond-timescale, genetically targeted optical control of neural activity. *Nat Neurosci* 8:1263–1268
49. Zemelman BV, Lee GA, Ng M, Miesenböck G (2002) Selective photostimulation of genetically chARGed neurons. *Neuron* 33:15–22
50. Zemelman BV, Nesnas N, Lee GA, Miesenböck G (2003) Photochemical gating of heterogeneous ion channels: remote control over genetically designated populations of neurons. *Proc Natl Acad Sci U S A* 100:1352–1357
51. Lima SQ, Miesenböck G (2005) Remote control of behavior through genetically targeted photostimulation of neurons. *Cell* 121:141–152
52. Zhang F, Wang L-P, Brauner M, Liewald JF, Kay K, Watzke N, Wood PG, Bamberg E, Nagel G, Gottschalk A et al (2007) Multimodal fast optical interrogation of neural circuitry. *Nature* 446:633–639
53. Rickgauer JP, Tank DW (2009) Two-photon excitation of channelrhodopsin-2 at saturation. *Proc Natl Acad Sci U S A* 106:15025–15030
54. Vaziri A, Emiliani V (2012) Reshaping the optical dimension in optogenetics. *Curr Opin Neurobiol* 22:128–137
55. Packer AM, Peterka DS, Hirtz JJ, Prakash R, Deisseroth K, Yuste R (2012) Two-photon optogenetics of dendritic spines and neural circuits. *Nat Methods* 9:1202–1205
56. Packer AM, Roska B, Häusser M (2013) Targeting neurons and photons for optogenetics. *Nat Neurosci* 16:805–815
57. Petreanu L, Huber D, Sobczyk A, Svoboda K (2007) Channelrhodopsin-2-assisted circuit mapping of long-range callosal projections. *Nat Neurosci* 10:663–668
58. Petreanu L, Mao T, Sternson SM, Svoboda K (2009) The subcellular organization of neocortical excitatory connections. *Nature* 457:1142–1145
59. Kätzel D, Buetfering C, Wölfel M, Miesenböck G (2010) The columnar and laminar organization of inhibitory connections to neocortical excitatory cells. *Nat Neurosci* 14:100–107
60. Pfeffer CK, Xue M, He M, Huang ZJ, Scanziani M (2013) Inhibition of inhibition in visual cortex: the logic of connections between molecularly distinct interneurons. *Nat Neurosci* 16:1068–1076
61. Atallah BV, Bruns W, Carandini M, Scanziani M (2012) Parvalbumin-expressing interneurons linearly transform cortical responses to visual stimuli. *Neuron* 73:159–170
62. Wilson NR, Runyan CA, Wang FL, Sur M (2012) Division and subtraction by distinct cortical inhibitory networks in vivo. *Nature* 488:343
63. Lee S-H, Kwan AC, Zhang S, Phoumthipphavong V, Flannery JG, Masmanidis SC, Taniguchi H, Huang ZJ, Zhang F, Boyden ES et al (2012) Activation of specific interneurons improves V1 feature selectivity and visual perception. *Nature* 488:379
64. Dalva MB, Katz LC (1994) Rearrangements of synaptic connections in visual cortex revealed

- by laser photostimulation. *Science* 265:255–258
65. Bureau I, Shepherd GMG, Svoboda K (2004) Precise development of functional and anatomical columns in the neocortex. *Neuron* 42:789–801
 66. Viswanathan S, Bandyopadhyay S, Kao JPY, Kanold PO (2012) Changing microcircuits in the subplate of the developing cortex. *J Neurosci* 32:1589–1601
 67. Anastasiades PG, Butt SJB (2012) A role for silent synapses in the development of the pathway from layer 2/3 to 5 pyramidal cells in the neocortex. *J Neurosci* 32:13085–13099
 68. Grant E, Hoerder-Suabedissen A, Molnár Z (2012) Development of the corticothalamic projections. *Front Neurosci* 6:53
 69. Catalano SM, Shatz CJ (1998) Activity-dependent cortical target selection by thalamic axons. *Science* 281:559–562
 70. Zhang J, Ackman JB, Xu H-P, Crair MC (2012) Visual map development depends on the temporal pattern of binocular activity in mice. *Nat Neurosci* 15:298–307
 71. Zhang F, Prigge M, Beyrière F, Tsunoda SP, Mattis J, Yizhar O, Hegemann P, Deisseroth K (2008) Red-shifted optogenetic excitation: a tool for fast neural control derived from *Volvox carteri*. *Nat Neurosci* 11:631–633
 72. Lin JY, Knutsen PM, Muller A, Kleinfeld D, Tsien RY (2013) ReaChR: a red-shifted variant of channelrhodopsin enables deep transcranial optogenetic excitation. *Nat Neurosci* 16:1499–1508
 73. Luhmann HJ, Hanganu I, Kilb W (2003) Cellular physiology of the neonatal rat cerebral cortex. *Curr Opin Neurobiol* 60:345–353
 74. Minlebaev M, Colonnese M, Tsintsadze T, Sirota A, Khazipov R (2011) Early gamma oscillations synchronize developing thalamus and cortex. *Science* 334:226–229
 75. Tolner EA, Sheikh A, Yukin AY, Kaila K, Kanold PO (2012) Subplate neurons promote spindle bursts and thalamocortical patterning in the neonatal rat somatosensory cortex. *J Neurosci* 32:692–702
 76. Gil-Sanz C, Franco SJ, Martinez-Garay I, Espinosa A, Harkins-Perry S, Müller U (2013) Cajal-Retzius cells instruct neuronal migration by coincidence signaling between secreted and contact-dependent guidance cues. *Neuron* 79(3):461–477
 77. Borrell V (2010) In vivo gene delivery to the postnatal ferret cerebral cortex by DNA electroporation. *J Neurosci Methods* 186(2):186–195
 78. Kawasaki H, Iwai L, Tanno K (2012) Rapid and efficient genetic manipulation of gyrencephalic carnivores using in utero electroporation. *Mol. Brain* 5:24
 79. Kawasaki H, Toda T, Tanno K (2013) In vivo genetic manipulation of cortical progenitors in gyrencephalic carnivores using in utero electroporation. *Biol Open* 2(1):95–100
 80. Kawasaki H (2014) Molecular investigations of the brain of higher mammals using gyrencephalic carnivore ferrets. *Neurosci Res* 86:59, pii: S0168-0102(14)00117-5
 81. Itasaki N, Bel-Vialar S, Krumlauf R (1999) “Shocking” developments in chick embryology: electroporation and in ovo gene expression. *Nat Cell Biol* 1:E203–E207
 82. Krull CE (2004) A primer on using in ovo electroporation to analyze gene function. *Dev Dyn* 229:433–439
 83. Croteau LP, Kania A (2011) Optimisation of in ovo electroporation. *J Neurosci Methods* 201(2):381–384
 84. Nomura T, Takahashi M, Hara Y, Osumi N (2008) Patterns of neurogenesis and amplitude of reelin expression are essential for making a mammalian-type cortex. *PLoS One* 3:e1454
 85. Suzuki IK, Kawasaki T, Gojobori T, Hirata T (2012) The temporal sequence of the mammalian neocortical neurogenetic program drives mediolateral pattern in the chick pallium. *Dev Cell* 22:863–870
 86. García-Moreno F, Molnár Z (unpublished) A subset of early radial glial cells with delayed neurogenic program selectively contribute to the development and evolution of callosal connecting neurons
 87. Nomura T, Gotoh H, Ono K (2013) Changes in the regulation of cortical neurogenesis contribute to encephalization during amniote brain evolution. *Nat Commun* 4:2006
 88. Nomura T, Kawaguchi M, Ono K, Murakami Y (2013) Reptiles: a new model for brain evo-devo research. *J Exp Zool B Mol Dev Evol* 320:57–73
 89. Wang X, Chang L, Guo Z, Li W, Liu W, Cai B, Wang J (2013) Neonatal SVZ EGFP-labeled cells produce neurons in the olfactory bulb and astrocytes in the cerebral cortex by in-vivo electroporation. *Neuroreport* 24(7):381–387
 90. Feliciano DM, Lafourcade CA, Bordey A (2013) Neonatal subventricular zone electroporation. *J Vis Exp* (72): pii: 50197
 91. Louise C, Etienne D, Marie-Pierre R (2014) AFM sensing cortical actin cytoskeleton destabilization during plasma membrane electroporation. *Cytoskeleton (Hoboken)* 71(10):587–594

Isolation of GABAergic Cortical Neurons and Implications for Cell Transplantation Strategies in the Nervous System

Hui Xuan Ng and Joanne M. Britto

Abstract

The correct layer placement of interneurons and pyramidal neurons during corticogenesis is required for precise neuronal activity and subsequent functions of the neocortex. Interneurons are generated in the medial ganglionic eminence (MGE) and migrate from the ventral to dorsal telencephalon to reside within the developing cortical plate. Transplantation strategies are valuable in understanding the cellular and molecular basis of interneuron development, and more recently in the potential for cell-based therapies of neurological disorders. With the advancement of transgenic technologies, interneurons can be fluorescently labelled to aid separation from other cell types in brain tissue and visualization in host tissues post-transplantation. This chapter presents a method to generate a dissociated cell preparation from embryonic MGE and utilizes fluorescence-activated cell sorting (FACS) to isolate migrating interneurons from progenitors and non-interneuron cell types. The FACS protocol is optimized to increase the purity and quantity of sorted interneurons that can be recovered and used for further analysis. This chapter also details how to perform in utero transplantation of dissociated MGE cells into the lateral ventricle of an embryonic brain and methods for analysis of the host brain tissue post-transplantation. These experimental approaches can be applied to understanding interneuron circuit formation and cell-based therapies to rectify GABAergic dysfunction in the neocortex.

Key words In utero lateral injections, Cortex, Fluorescence-activated cell sorting

1 Introduction

The high-level cognitive processing of the neocortex depends upon the intricate balance and layer arrangement of excitatory glutamatergic neurons (pyramidal neurons) and inhibitory GABAergic neurons (interneurons). The layer-specific placement of interneurons is vital to shape the spatiotemporal pattern of neuronal activity and network oscillations implicated in cognitive processes [1, 2]. We are only starting to appreciate how loss of interneurons in a layer-specific manner is associated with the clinical symptoms of epilepsy, schizophrenia, autism spectrum, and bipolar disorders [3–5].

The assembly of functional circuits depends upon the migration of neurons from a site of origin to a final placement.

The two classes of neurons in the neocortex have different developmental origins and yet converge into the same layers following an equivalent “inside-out” layering sequence [6]. Current research aims at understanding how interneurons traverse vast distances to a finite layer placement and transplantation strategies have been an effective tool. The ability to match and mismatch donor/host tissue has aided fate mapping [7], migratory studies [8], and understanding the role of interneuron birth date and pyramidal neurons on layer placement [9, 10]. In recent years, the clinical relevance of cell-based therapies has been revealed in rodent models of neurological disorders. The transplanted interneurons increase the overall inhibitory tone of the brain and can reduce the frequency and severity of seizures in inherited or induced forms of epilepsy [11–13], reduce motor symptoms in Parkinson’s disease [14], and restore cognitive function in Alzheimer’s disease [15].

Genomic engineering to label discrete populations of cells has made it possible to visualize transplanted interneurons. For example, knock-in strategies, Cre/loxP recombination, and bacterial artificial chromosome transgenic technologies have created powerful tools to fluorescently label interneurons with synapse resolution. The *Glutamic Acid Decarboxylase 1* and 2 (GAD67 and GAD65) knock-in Green Fluorescent Protein (GFP) lines and Dlx5/6-Cre-IRES-GFP are pan-interneuron markers [16–18]. Cre driver lines open further the ability to label specific interneuron subtypes such as parvalbumin, somatostatin, and calretinin [19–21]. In combination with differing Cre reporter lines, interneurons can be generated to express YFP, CFP [22], GFP [23], or tdTomato [24].

We demonstrate an approach to isolate interneurons from the medial ganglionic eminence (MGE) of the GAD67-knock-in-GFP line. The expression of GFP appears when interneurons migrate from the ventricular zone and we describe how to use fluorescence-activated cell sorting (FACS) to separate the GFP-positive (GFP⁺) migrating interneurons from the GFP-negative (GFP⁻) progenitors and non-interneuron cell types. To conclude, we outline a protocol to transplant MGE cells into the lateral ventricle of an embryonic brain and approaches for post-transplantation analysis of host tissue.

2 Materials

1. GAD67-knock-in-GFP (GAD67^{+/gfp}) pregnant dams [17].
2. BDF1 wild-type strain generated by crossing C57BL/6 and DBA.
3. #5 or #55 fine forceps (Dumont).

2.1 Dissection and Dissociation of MGE Cells

1. Silicon-coated 6 or 10 cm petri dish (Sylgard, Dow Corning).
2. Hanks’ balanced salt solution (HBSS) with Ca²⁺, Mg²⁺, glucose, and phenol red (Gibco 24020-117).

3. Earle's balanced salt solution (EBSS; Worthington LK003188).
4. 20 U/ml Papain in EBSS, frozen in sterile 25 μ l aliquots (Worthington LK003176).
5. 2000 U/ml DNase in EBSS, frozen in sterile 500 μ l aliquots (Worthington LK003170).
6. Fetal bovine serum (FBS; Sigma-Aldrich 12003C).
7. Phosphate-buffered saline (PBS; Gibco 14190-136).
8. 5 ml round-bottom tube with cell strainer cap (BD Falcon 352235).

2.2 FACS

1. BD Biosciences FACS Aria™ III cell sorter.
2. 5 ml round-bottom tube (BD Falcon 352063).

2.3 Transplantation and Analysis of Host Brain Tissue

1. Sterile surgical supplies and bench space for two people to operate.
2. Warming tray (Thermoline).
3. Recovery box of suitable size with tissue soft bedding.
4. Pentobarbitone for general anesthesia and meloxicam administered preoperatively for analgesia (according to the Code of Practice for the Care and Use of Animals for Scientific Purposes).
5. Sterile PBS.
6. Micropipette with stainless steel plunger (Drummond 5-000-1001-X).
7. Sofsilk™ wax coated braided silk suture, 3/8 circle, 13 mm taper (Covidien VS-890).
8. AUTOCLIP® wound clip system (Becton Dickinson 427631).

3 Methods

This protocol is presented in three sections: preparation of MGE cells from the $GAD67^{+}/^{gfp}$ forebrain, FACS analysis to separate the GFP^{+} and GFP^{-} cell populations, and transplantation of dissociated MGE cells. Overall schematic is shown in Fig. 1.

3.1 Dissection and Dissociation of MGE Cells

1. Sterilize fine forceps for dissection with 80 % ethanol and air-dry before use.
2. Kill pregnant dam by using an animal ethics-approved method and clean abdomen with 80 % ethanol.
3. Make a 2–3 cm long midline incision through the skin and abdominal wall with scissors, remove uterine horns, and place in ice-cold HBSS in a 6 cm sterile dish.

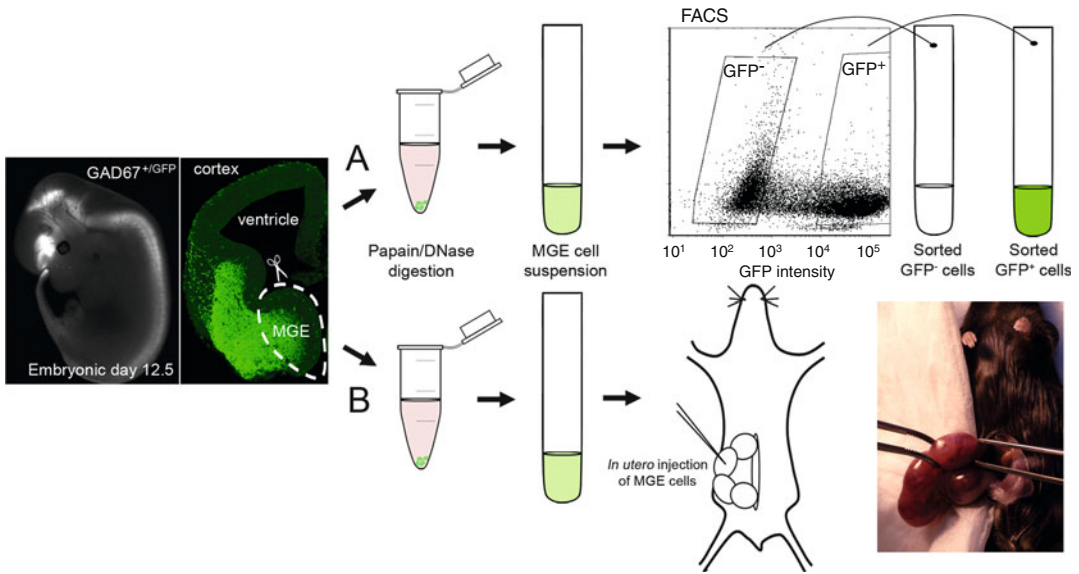


Fig. 1 Overview of approaches to utilize MGE-derived interneurons. The GFP fluorescence is present throughout the ventral neural tube at embryonic day 12.5 of a $GAD67^{+/GFP}$ embryo. The MGE is dissected from the brain and used to make a dissociated cell suspension for (a) FACS isolation of GFP^{+} interneurons and (b) in utero transplantation

4. All dissections are performed using the stereomicroscope to prevent damage to individual embryos. Using the fine forceps, remove embryos from uterine horn and place in a separate 6 cm dishes with ice-cold HBSS. Using the 488 nm filter, identify and separate $GAD67^{+/gfp}$ embryos using a fluorescent stereomicroscope and place in a separate 6 cm dish containing ice-cold HBSS.
5. Dissect brains and place in a clean 6 cm dish containing ice-cold HBSS.
6. The MGE can be accessed from the medial side of each hemisphere. To do this, remove the midbrain from forebrain and discard. Separate the two hemispheres by cutting through the midline using the forceps as scissors and position each hemisphere to gain access to the medial surface. Remove thalamus from each hemisphere taking care not to dissect into the medial ganglionic eminence.
7. Orient the hemisphere along the anterior and posterior axis and cut open the anterior neocortex to expose the ventral ganglionic eminences.
8. Using the forceps, pinch and remove the MGE from surrounding tissue and place into 1.7 ml tube containing 1 ml PBS on ice.
9. Centrifuge pooled MGE samples at $760 \times g \times 1$ min at room temperature.

10. Combine Papain and DNase aliquots and gas mixture with CO₂ gas until the pH indicator is between 7.2 and 7.4 (pH guide included in Worthington Papain Dissociation System).
11. Carefully remove PBS from cell pellet using a 1 ml pipette and resuspend cell pellet with Papain/DNase solution (pH 7.2–7.4).
12. Tap flick tube to separate tissue clumps and incubate at 37 °C, 5 % CO₂, for 30 min. Flick tube every 10 min to aid dissociation.
13. At the end of the incubation period, create a homogenous cell suspension by triturating sample 10× with a fire-polished glass pipette.
14. Neutralize Papain/DNase solution with an equal volume of FBS (500 µl), mix sample using a fire-polished glass pipette, and layer cell suspension onto 1 ml FBS in a 15 ml tube.
15. Pellet cells through FBS at 100 × *g* × 6 min at room temperature, aspirate supernatant, and resuspend cells in 2 % FBS/PBS (approximately 100 µl per brain).
16. To ensure that the single-cell suspension is suitable for FACS processing, pipette 300 µl of the cell suspension into the cell strainer caps attached to FACS tubes (BD Falcon 352235). Pulse spin to 100 × *g* to filter cells through the 35 mm nylon mesh. If more than one strainer is used, pool single-cell suspension into a single tube.
17. Calculate cell density using a hemocytometer and trypan blue exclusion to distinguish viable cells.

3.2 FACS Separation of GFP⁺ and GFP⁻ Cell Populations

The protocol described below is specific for the BD Biosciences FACS Aria™ III cell sorter and parameters may vary if other brands are used.

1. Set up and optimize the cell sorter. Using a 100 µm nozzle, start the fluidics and run 80 % ethanol through the sorter to sterilize the tubing through which experimental sample will flow. Perform automated setup, quality control, drop delay, and side stream optimization and install collection device.
2. Select the 488 nm laser for excitation and 530/30 emission filter for GFP signal detection.
3. Start the run and use approximately 5 × 10⁴ cells to gate defined cell populations. Each dot represents an individual cell and is now referred to as “events.” A numerical value of the number of events within each gate, the percentage of events from the previous gate, and percentage of events from the initial sample will be generated concurrently. An example of the FACS data from an embryonic day 15.5 MGE cell suspension is shown in Table 1 and Fig. 2.

Table 1
Example of numerical record generated from a FACS experiment of dissociated MGE from $GAD67^{+}/GFP$ at E15.5

Population	Gate	Number of events	Percentage—previous gate	Percentage—all events
Dissociated cell preparation	All events	58,157	–	100.0
Population excluding cell debris	P1	52,492	90.3	90.3
Population excluding doublets and cell aggregates (granularity)	P2	51,639	98.4	88.8
Population excluding doublets and cell aggregates (size)	P3	51,224	99.2	88.1
GFP ⁺ cell population	P4	30,455	59.5	52.4
GFP ⁻ cell population	P5	12,694	24.8	21.8

The GFP⁺ cells comprise 52 % after gating for cell debris, doublets, and aggregates as reflected from a sample collection of approximately 5.8×10^4 cells (events). Refer to Fig. 2 for corresponding FACS plots and gate outlines of P1–P5

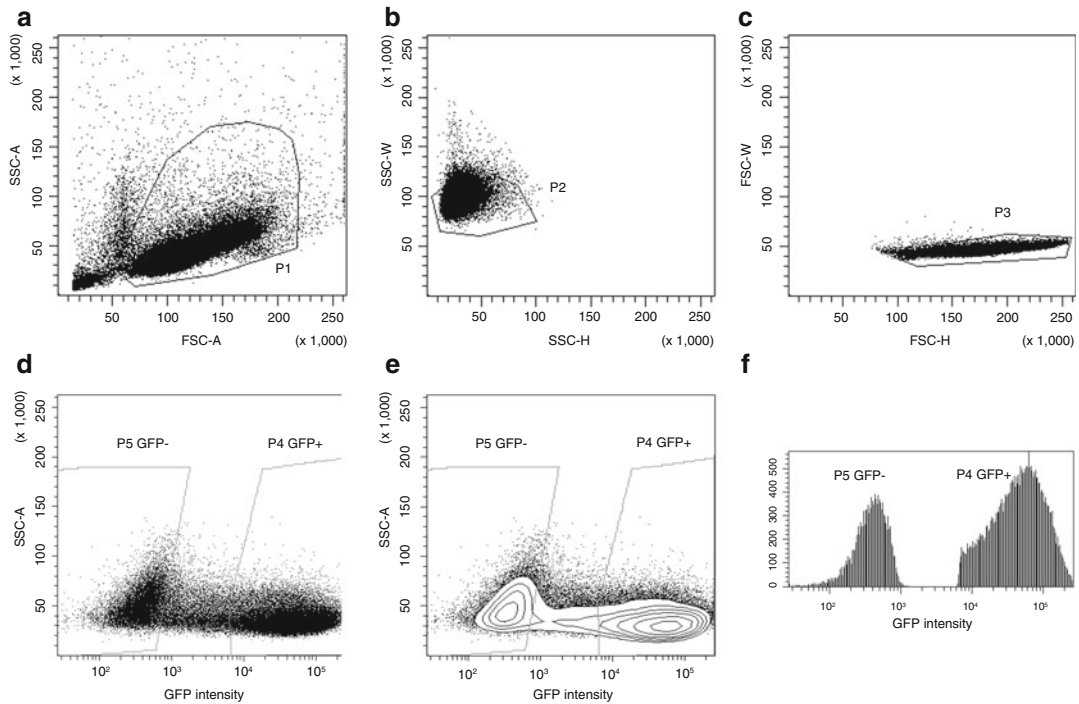


Fig. 2 FACS plots generated from sorting dissociated MGE from $GAD67^{+}/GFP$ at E15.5. Each stage of the gating process is required to produce a pure population of viable single cells. (a) FSC-A vs. SSC-A to exclude debris—outline of P1. (b) SSC-H vs. SSC-W to exclude doublets and cell aggregates—outline of P2. (c) FSC-H vs. FCS-W to exclude doublets and cell aggregates—outline of P3. (d) GFP intensity vs. SSC-A to separate GFP⁺ and GFP⁻ cell populations—outline of P4 and P5, respectively. (e) Corresponding contour plot GFP intensity vs. SSC-A to show cell density. (f) Frequency histogram of the gated GFP intensity showing clear separation of the GFP⁺ and GFP⁻ populations

4. Construct the following plots to define cell populations through gating. Each gate for the FACS Aria™ III is labelled as “P,” an arbitrary letter designation.
 - (a) FSC-A vs. SSC-A to exclude debris (P1).
 - (b) SSC-H vs. SSC-W and FSC-H vs. FCS-W to exclude doublets and cell aggregates (P2, P3).
 - (c) GFP intensity vs. SSC-A with corresponding contour plot of cell density. Use the contour plot to gate GFP⁺ and GFP⁻ populations (P4, P5).
 - (d) Frequency histogram of GFP intensity to show clear separation of the GFP⁺- and GFP⁻-gated populations.
5. Once the gating parameters are set, run the sample at a flow rate of less than 10,000 event/s, sheath pressure of 20 psi, and drop precision mode of 1.5.
6. Collect sorted populations into 5 ml FACS tubes and maintain cell sample and collection tubes at 4 °C.
7. Conduct a post-sort analysis on each of the sorted populations to ensure a purity reading of greater than 99 %.
8. Recover sorted cells by centrifugation at $400 \times g \times 5$ min.

3.3 Transplantation of Dissociated MGE Cells

Prepare MGE cells as described in “Dissection and dissociation of MGE cells” from **steps 1–13**.

1. Neutralize Papain/DNase solution with equal volume of FBS (500 μ l) and mix sample using a fire-polished glass pipette.
2. Take aliquot of cell suspension and calculate cell density using trypan blue exclusion to distinguish viable cells. Layer remaining cells on 1 ml FBS in a 15 ml tube.
3. Pellet cells through FBS at $100 \times g \times 6$ min at room temperature, aspirate supernatant, and resuspend cells in 0.1 % DNase/HBSS to obtain a cell density between 8×10^4 and 2×10^5 cells/ μ l.
4. Anesthetize pregnant dam with an intraperitoneal injection of pentobarbitone.
5. Place anesthetized dam on the warming tray to expose the abdomen and wipe with 80 % ethanol. Make a 2 cm long midline incision through the skin and abdominal wall with scissors and place gauze on either side of incision.
6. Carefully remove one uterine horn out of the abdomen and place onto gauze without attaching the forceps to the placenta or embryo. Use the space between embryos to manoeuvre the uterine horns to avoid damage to blood vessels (Fig. 1).
7. Keep the uterus wet at all times with PBS when exposed to air.

8. One person positions the embryos to the surface of the uterine wall by placing forceps on either side of the embryo at the crown and rump (Fig. 1). The embryo can be rotated gently for correct positioning of the cortical hemispheres to be upright.
9. The second person injects 1 μ l of cell suspension into the lateral ventricle using a pulled micropipette. Inject all embryos except those directly adjacent to the cervix, a technique previously shown to increase survival and reduce delivery complications.
10. Reposition the uterine horn into the abdominal cavity and repeat **steps 6–9** for the second uterine horn.
11. Suture the abdominal wall and clip the skin to close the wound. Record the number and position of embryos injected.
12. Wipe excess fluid from the pregnant dam, gently wrap in tissue paper, and place in recovery box on the warming tray. Check every hour for movement, and when animal stirs, place in home cage with food and water in easy reach. Place home cage on warming tray.
13. Replace cage into the animal-holding facility once the animal is walking around the cage and check after 24 h for normal movement and grooming.
14. Injected embryos can be collected at embryonic or postnatal stages to examine integration of GFP⁺ interneurons.
15. Post-transplantation host brain tissue is fixed by myocardial perfusion or drop-fixed in 4 % paraformaldehyde. The tissue can be prepared for cryosections and the position of GFP⁺ cells assessed by the location of the soma in the cortical plate.
16. To examine the arborization of integrated interneurons, prepare 150–200 μ m thick vibratome sections and mount slices for microscopy. This can be viewed under a fluorescent stereomicroscope or confocal microscope (Fig. 3).
17. To intensify GFP signal, conduct slice immunohistochemistry using an anti-GFP primary antibody (1:1000; Abcam ab13970) and Alexa Fluor 488 secondary (1:500; Life Technologies A-11039).

4 Notes

1. The stereomicroscope is used for all dissections due to the size of the brain at embryonic days (E) 12–15. This allows for precision in the dissection and avoidance of non-ganglionic eminence tissue in the cell preparation. The minuscule size of the ganglionic eminence warrants at least nine E12.5–E15.5

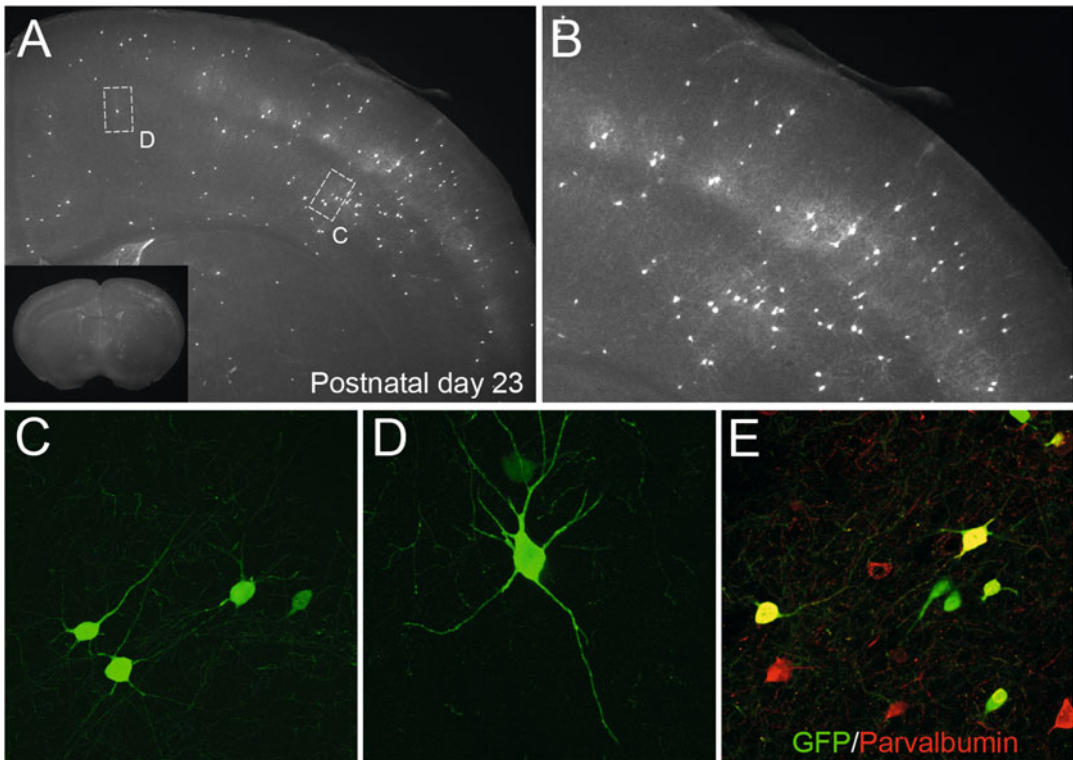


Fig. 3 Transplantation of dissociated MGE from $GAD67^{+/GFP}$ at E14.5 transplanted into an E15.5 wild-type host. (a) Stereomicroscope image showing a coronal vibratome brain slice at postnatal day 23. GFP^{+} cells have integrated throughout the cortical depth. (b) Stereomicroscope image at higher magnification. (c) Projection of confocal images using Z-stacks to capture interneuron arborization at $40\times$ and (d) $63\times$ magnification. (e) Double immunohistochemistry with anti-GFP and anti-parvalbumin to label endogenous and transplanted interneurons

$GAD67^{+/GFP}$ embryos to generate enough cells for FACS or transplantation.

2. Tack-free silicon is used to coat the petri dishes to prevent damage to the brain tissue and fine forceps tips. Silicon is made by mixing the elastomer and curing agent (as per the manufacturer's instructions) and poured into the petri dish to a height of approximately 2–3 mm. Keep enough space in the dish for dissection media.
3. This protocol describes the dissociation of tissue by Papain/DNase enzymatic digestion rather than trypsin or collagenase/dispase. These other enzymes are valid; however, our experience showed low MGE cell viability and subsequent cell loss during FACS. If trypsin or collagenase/dispase is the choice of enzyme, optimize timing of incubation and concentration to maintain cell viability.

4. Do not vortex the samples or shake vigorously during the Papain/DNase digestion as this induces cell death. The glass pipette used is fire-polished to smooth the edges and narrow the aperture. If the dissections are performed with clear cuts and minimal tissue shearing, cells do not stick to the glass pipette. If this becomes a problem, use Sigmacote[®] (SL2-25 ml) to siliconize the glass pipettes and follow the manufacturer's instructions for removal. Sterilize after coating with 80 % ethanol and air-dry.
5. Avoid using a nozzle smaller than 100 μm on the FACS cell sorter as this increases the flow pressure and impacts on cell viability. The flow rate is kept below 10,000 event/s to ensure higher sorting efficiency and a maximal collection of cells. Increasing the flow rate elevates the number of cells that are excluded from the sorting process.
6. Avoid placing the GFP⁺ and GFP⁻ gates too close during FACS. It is preferable to be conservative in the gating to ensure a high purity of the sorted GFP⁺ and GFP⁻ populations. It is recommended to conduct a post-sorting analysis to verify the purity of each sorted sample. Gating and FACS settings should be revised if the purity levels are less than 99 %.
7. Try not to use polystyrene tubes to collect sorted cells, as this material is prone to cracking during centrifugation especially when sorted cells are pooled from multiple collection tubes. Polypropylene tubes are more durable and show less cell adhesion.
8. The number of embryos per litter varies with the background strain of mice. We use BDF1 (generated by crossing C57BL/6 and DBA strains) for the wild-type plugs as the litter sizes range from 8 to 10 with increased viability of embryos. C57BL/6 can be used successfully; however, more rounds of surgery are required.
9. Different anesthetics can be used to prepare the pregnant dams for surgery. We routinely use pentobarbitone; however, isoflurane can be used to reduce the recovery and monitoring time frame post-surgery.
10. The protocol outlines collection of entire MGE tissue for FACS and transplantation. If more discrete regions of the MGE are required, dissections can be collected from vibratome slices of fresh embryonic brain tissue.
11. Vibratome sections can be generated at varying thickness for immunohistochemistry; however, be aware of the objective working distance for microscopy. If problems arise with slice width consistency, embed fixed brains in 1 % low-melting-point agarose to provide additional tissue support.

References

1. Freund TF (2003) Interneuron diversity series: rhythm and mood in perisomatic inhibition. *Trends Neurosci* 26:489
2. Whittington MA, Traub RD (2003) Interneuron diversity series: inhibitory interneurons and network oscillations in vitro. *Trends Neurosci* 26:676
3. Powell EM, Campbell DB, Stanwood GD, Davis C, Noebels JL, Levitt P (2003) Genetic disruption of cortical interneuron development causes region- and GABA cell type-specific deficits, epilepsy, and behavioral dysfunction. *J Neurosci* 23:622
4. Lewis DA, Hashimoto T, Volk DW (2005) Cortical inhibitory neurons and schizophrenia. *Nat Rev Neurosci* 6:312
5. Rubenstein JL, Merzenich MM (2003) Model of autism: increased ratio of excitation/inhibition in key neural systems. *Genes Brain Behav* 2:255
6. Rakic P (2006) A century of progress in corticogenesis: from silver impregnation to genetic engineering. *Cereb Cortex* 16(Suppl 1):i3
7. Wonders CP, Taylor L, Welagen J, Mbata IC, Xiang JZ, Anderson SA (2008) A spatial bias for the origins of interneuron subgroups within the medial ganglionic eminence. *Dev Biol* 314:127
8. Wichterle H, Turnbull DH, Nery S, Fishell G, Alvarez-Buylla A (2001) In utero fate mapping reveals distinct migratory pathways and fates of neurons born in the mammalian basal forebrain. *Development* 128:3759
9. Valcanis H, Tan SS (2003) Layer specification of transplanted interneurons in developing mouse neocortex. *J Neurosci* 23:5113
10. Hammond V, So E, Gunnarsen J, Valcanis H, Kalloniatis M, Tan SS (2006) Layer positioning of late-born cortical interneurons is dependent on Reelin but not p35 signaling. *J Neurosci* 26:1646
11. Xu Q, Cobos I, De La Cruz E, Rubenstein JL, Anderson SA (2004) Origins of cortical interneuron subtypes. *J Neurosci* 24:2612
12. Baraban SC, Southwell DG, Estrada RC, Jones DL, Sebe JY, Alfaro-Cervello C, Garcia-Verdugo JM, Rubenstein JL, Alvarez-Buylla A (2009) Reduction of seizures by transplantation of cortical GABAergic interneuron precursors into Kv1.1 mutant mice. *Proc Natl Acad Sci U S A* 106:15472
13. Calcagnotto ME, Ruiz LP, Blanco MM, Santos-Junior JG, Valente MF, Patti C, Frussa-Filho R, Santiago MF, Zipancic I, Alvarez-Dolado M, Mello LE, Longo BM (2010) Effect of neuronal precursor cells derived from medial ganglionic eminence in an acute epileptic seizure model. *Epilepsia* 51 (Suppl 3):71
14. Martinez-Cerdeno V, Noctor SC, Espinosa A, Ariza J, Parker P, Orasji S, Daadi MM, Bankiewicz K, Alvarez-Buylla A, Kriegstein AR (2010) Embryonic MGE precursor cells grafted into adult rat striatum integrate and ameliorate motor symptoms in 6-OHDA-lesioned rats. *Cell Stem Cell* 6:238
15. Tong LM, Djukic B, Arnold C, Gillespie AK, Yoon SY, Wang MM, Zhang O, Knoferle J, Rubenstein JL, Alvarez-Buylla A, Huang Y (2014) Inhibitory interneuron progenitor transplantation restores normal learning and memory in ApoE4 knock-in mice without or with abeta accumulation. *J Neurosci* 34:9506
16. Stenman J, Toresson H, Campbell K (2003) Identification of two distinct progenitor populations in the lateral ganglionic eminence: implications for striatal and olfactory bulb neurogenesis. *J Neurosci* 23:167
17. Tamamaki N, Yanagawa Y, Tomioka R, Miyazaki J, Obata K, Kaneko T (2003) Green fluorescent protein expression and colocalization with calretinin, parvalbumin, and somatostatin in the GAD67-GFP knock-in mouse. *J Comp Neurol* 467:60
18. Lopez-Bendito G, Sturgess K, Erdelyi F, Szabo G, Molnar Z, Paulsen O (2004) Preferential origin and layer destination of GAD65-GFP cortical interneurons. *Cereb Cortex* 14:1122
19. Meyer AH, Katona I, Blatow M, Rozov A, Monyer H (2002) In vivo labeling of parvalbumin-positive interneurons and analysis of electrical coupling in identified neurons. *J Neurosci* 22:7055
20. Tanahira C, Higo S, Watanabe K, Tomioka R, Ebihara S, Kaneko T, Tamamaki N (2009) Parvalbumin neurons in the forebrain as revealed by parvalbumin-Cre transgenic mice. *Neurosci Res* 63:213
21. Taniguchi H, He M, Wu P, Kim S, Paik R, Sugino K, Kvitsiani D, Fu Y, Lu J, Lin Y, Miyoshi G, Shima Y, Fishell G, Nelson SB, Huang ZJ (2011) A resource of Cre driver lines for genetic targeting of GABAergic neurons in cerebral cortex. *Neuron* 71:995
22. Srinivas S, Watanabe T, Lin CS, William CM, Tanabe Y, Jessell TM, Costantini F (2001) Cre reporter strains produced by targeted insertion

- of EYFP and ECFP into the ROSA26 locus. *BMC Dev Biol* 1:4
23. Novak A, Guo C, Yang W, Nagy A, Lobe CG (2000) Z/EG, a double reporter mouse line that expresses enhanced green fluorescent protein upon Cre-mediated excision. *Genesis* 28:147
24. Madisen L, Zwingman TA, Sunkin SM, Oh SW, Zariwala HA, Gu H, Ng LL, Palmiter RD, Hawrylycz MJ, Jones AR, Lein ES, Zeng H (2010) A robust and high-throughput Cre reporting and characterization system for the whole mouse brain. *Nat Neurosci* 13:133

Advanced EEG and MRI Measurements to Study the Functional Development of the Newborn Brain

Sampsa Vanhatalo and Peter Fransson

Abstract

In this chapter we review the methodological progress that has recently been made for studying brain development in infants using noninvasive techniques. In particular, we focus on methodological platforms based on electroencephalography (EEG) and functional magnetic resonance imaging (fMRI). Key aspects of experimental setup, data acquisition, data preprocessing, and analysis are described and discussed with emphasis on recordings performed on the infant brain. The measurement and estimation of large-scale brain network connectivity using fMRI and EEG has become an important tool to study brain development. To this end, we describe central findings regarding the large-scale brain network architecture of the infant brain. Further, data analysis strategies pertaining to the investigation brain connectivity are described together with a discussion of their advantages and pitfalls.

Key words Functional connectivity, fMRI, Neonatal EEG, Phase synchrony, Resting-state network

1 Introduction

Functional development of the infant brain may be viewed from the standpoint of interactions across brain networks [1] or by studying individual neuronal systems, such as visual or somatosensory pathways. Function of developing sensory systems can be readily studied using EEG even at the phase when the sensory connections are only growing to their destinations [2–4]; however immaturity of neurovascular coupling makes comparison of such functional tests challenging between EEG and fMRI. Hence, this chapter focuses on conceptually easier comparison of how large-scale connectivity can be studied from the electric activity (EEG) and blood deoxygenation (fMRI) of the infant brain.

The electric (EEG) network studies in the neonatal brain have recently experienced a paradigm shift as a result of concerted development at all levels of methodology, ranging from the theoretical aspects to recording methods and improvements in signal analysis paradigms. Theoretical and basic neuroscience work has

convincingly shown that the neonatal EEG consists of transient events that are important for the early wiring process [5–7]. The neonatal EEG is also shown to have both a very high spatial complexity [8, 9] and a very wide spectral content [10], which together call for a significant increase in the density of electrodes, as well as better reliability in recording low- and high-frequency contents. Progress in recording methodology has opened possibilities to greatly improve the information content of neonatal EEG recording: Increase in spatial resolution has resulted from the development of neonatal compatible, high-density EEG caps/nets [11, 12], as well as from the introduction of higher (up to 256) channel numbers in the modern EEG amplifiers. Spectral content of the EEG signal has been greatly improved by combination of better amplifier design [13] and mechanically more stable EEG caps [12]. Finally, many signal analysis methods originally developed for studying connectivity in the adult EEG activity have recently been modified and adopted into neonatal EEG studies.

The possibility to examine functional connectivity in the infant brain using functional magnetic resonance imaging has been made feasible due to the recent development of resting-state blood oxygenation level-dependent (BOLD) fMRI (*see ref. [14] for a review*). In contrast to task-evoked fMRI in which local changes in brain blood oxygenation in response to external stimuli are detected, studies using resting-state fMRI connectivity exploit the fact that spontaneous, low-frequency (0.01–0.1 Hz) BOLD signal changes are synchronized in time across multiple functional networks that span long-range anatomical structures [15, 16].

Studies of brain connectivity using EEG and fMRI methods are both based on analyzing temporal dependencies between time series collected from the brain. Hence, several aspects of data analysis and interpretation of results are comparable technically, but also physiologically. In this chapter, this comparability is made easier by describing the common strategies of data analysis together for both research modalities, followed by comparison of the physiological underpinnings of EEG and fMRI in the neonatal context.

2 Signal Acquisition and Preprocessing

2.1 EEG Acquisition

A major practical challenge in studies of EEG connectivity is to obtain high enough signal-to-noise ratio. The most common artefacts (e.g., eye blinks, 50/60 Hz noise, muscle activity) may readily confound connectivity estimates, especially those based on signal amplitudes. Therefore, the single most important step is the reduction of potential sources of noise in the recording room as well as during the recording session. Baby-related artefacts are usually best

avoided by few obvious practices: Have the sensors firmly attached (see also below), assure a comfortable sleep by feeding just before EEG recording, and make sure that the environment is dark and quiet. External artefacts are usually best avoided by removing other electric devices from the vicinity of the baby and bed. For practical examples of neonatal EEG recording, the reader is referred to multimedia presentations in ref. [4], and the educational website of NEMO consortium [17].

The EEG recording setup, including measurement devices, channel counts, as well as the length of recording sessions, is defined by the research question. For instance, analysis of conventional interhemispheric synchrony can be readily done from few minutes' recordings and four recording electrodes to yield one bipolar signal for each hemisphere [18]; however a detailed, event-related connectivity map may need very high numbers of electrodes and hours of recording time. These recording requirements relative to logistic constraints in all neonatal studies are important to assess realistically before commencing actual recordings. Many advanced studies done with adult subjects are not practically achievable with neonatal subjects [19–21].

Commercial amplifiers have significant differences with respect to their use in neonatal studies: They are differently approved for use in clinical patient populations, which is the case in many study recruits. Amplifiers do also have very different artefact sensitivity that is usually dependent on amplifier's input impedance (translates to sensitivity to skin impedance and 50/60 Hz noise) as well as common mode rejection ratio (*a.k.a.* CMRR).

Another major factor is the design of EEG caps. Many commercial caps may have comparable numbers of electrodes, but they vary greatly with respect to their real-life performance in moving babies with different head shapes and sizes. Studies of connectivity mostly require longer recordings with continuous EEG signal from sleeping babies; the signal cannot be segmented as is commonly done in studies on evoked responses; hence the EEG cap/net needs high mechanical stability [12].

Electrodes can be positioned individually or by using electrode caps. Individual placement allows better fixation on the scalp with less movement artefacts. The time allowed for EEG placement between feeding and sleeping is usually so short that the higher electrode numbers needed for an adequate connectivity study can only be applied by using EEG caps. Another advantage of the EEG cap is that the relative positions of electrodes are automatically adjusted, and the user only needs to position the cap symmetrically with respect to anatomical landmarks. However, the high spatial complexity of scalp EEG signal [8] together with the known individual anatomical variability in the scalp-cortex relationships [22] implies that the EEG locations are always relatively rough approximates. An optimal source-level knowledge of cortical activity in the

neonate would require up to hundreds of electrodes, as well as head models based on individual MRI images. Both of them are, however, unachievable in the healthy newborns due to technical and ethical constraints. Hence, there is a need to find balance between optimal and practical aspects, and, as in any good science, the awareness of this compromise is a key to proper interpretation of the results.

2.2 EEG Preprocessing

Preprocessing of EEG data includes *epoch selection*, *montage selection*, *artefact removal (or correction)*, as well as *filtering*. Some analysis software may perform preprocessing as an integrated procedure in the analysis workflow. It may be practical to save a copy of preprocessed datasets separately so that multiple connectivity estimates can be computed and directly compared from the same data.

The length of epoch(s) needed for connectivity analysis is typically from few minutes to tens of minutes; hence only sleep epochs with less movements are useful in the neonates. Longer EEG epochs yield more reliable connectivity estimates. Many paradigms are so sensitive to epoch length that it is advisable to have the same length from all subjects in the study group. Sleep state should also be comparable (either quiet or active sleep) in all subjects, because brain network function changes markedly between sleep states [23].

The data needs to be re-montaged, and the choice of montage affects the results. All analyses of connectivity attempt to quantify interaction between two or more brain areas/signals, while electric signals are always acquired as a potential difference between two brain areas. A meaningful connectivity analysis necessitates off-line generation of new montages whereby the spatial identity of the EEG signals is made relatively independent. The common choices for montage are grand average or Laplacian montage. They are both good when the numbers of recorded signals are high. Artefacts in single channels may readily confound all signals in average reference montage, while the choice of smoothing parameters and an even coverage of scalp by electrodes pose challenges to Laplacian montage. Recent studies on adults have increasingly examined computed source (brain cortex) signals instead of the recorded EEG (or magnetoencephalography, MEG) signals [19, 24]. This approach will give theoretically better spatial resolution; however its use in neonates has been recently challenged by the lack of reliable infant head models as well as by the already very high spatial specificity of the neonatal EEG signal [8, 25].

Most importantly, the clinically popular bipolar derivations will be unhelpful and misleading in connectivity studies (apart from the analysis of conventional interhemispheric synchrony), and the use of referential recordings (e.g., Cz or mastoid reference) is inherently introducing very strong common mode that seriously affects the connectivity estimates.

Artefacts can be removed manually or automatically. Automatic artefact removal by using independent component analysis (ICA) [26] can be useful for stereotypic artefacts, such as eye blinks or heart (ECG) from a multichannel EEG signal. Most artefacts in the infant sleep EEG are, however, not suited for automated correction. They can be sometimes removed by filtering (50/60 Hz noise, some EMG, or respiration) if the connectivity measure does not depend on the frequency band covered by the artefact. Most often the method of choice is to visually scan the EEG epochs and prune the segments with visually obvious artefacts. This is intuitively clear; however it requires expertise with neonatal EEG reading.

2.3 *fMRI Acquisition*

Researchers who wish to conduct functional MRI studies of the infant brain should pay particular attention to reduce the level of noise as much as possible during image acquisition. A substantial reduction of the amount of MR scanner noise that reaches the inner ear of the infant is of essence since all MRI studies of infants are done during sleep to avoid head movement. Typical strategies to reduce MR scanner noise inside the scanner include individually molded earplugs together with neonatal and pediatric ear muffs. Additionally, we have successfully used a custom-made sound-dampening hood inside the scanner that is tightly attached to the upper half of semicircle of the magnet bore which reduced the noise level with up to 24 dB [27].

A typical infant MR scanning session lasts between 45 and 60 min and might include structural, diffusion, and resting-state fMRI data acquisitions, depending on the objectives of the study. For resting-state fMRI of the infant brain, BOLD images are acquired using echo-planar imaging (EPI) MR sequence parameter settings that are similar to those used for adult fMRI imaging, which entails a TR (repetition time) of 2–3 s to cover the whole brain, an image slice thickness of 3–4 mm, and echo time (TE) that is sufficiently long enough to be sensitive to the effects of deoxygenated haemoglobin through T2* relaxation (typically, TE is set to 40–50 ms at 1.5 T magnet strength, while a shorter TE of 25–30 ms is used at 3 T). The length of the resting-state EPI fMRI scan has varied between 3 and 14 min in different studies, but it has been reported that an improvement in test-retest reliability and similarity of resting-state connectivity measures have been achieved by increasing the scan length from 5 up to 13 min [28]. Given the proneness of infant scanning to susceptibility to head movement artefacts (see also troubleshooting section below) it is recommended that the total scan length is set towards the higher end of the 5–13-min scan range.

Whereas most studies on resting-state fMRI connectivity have been conducted in awake subjects, all studies in infants to date have been carried out during light sedation [29, 30] or natural sleep

[31–33]. The fact that resting-state fMRI studies in infants by necessity have been conducted during sleep is a factor that should be considered when the results are to be compared to resting-state data acquired during wakefulness. Previous research has shown that light sleep increases the connectivity patterns and it affects the temporal and spatial properties of resting-state connectivity compared to the awake state [34, 35].

2.4 fMRI Preprocessing

After data acquisition, image data is commonly preprocessed in several steps before the analysis of functional connectivity is conducted. First, functional MR image data is realigned and resampled with respect to head movement during scanning using a rigid-body model that in total includes six parameters (translation (x,y,z) , rotation (ϕ,ψ,θ)). These six parameters related to head movement across time are often subsequently used in the connectivity analysis to regress out residual signal variance related to head movement. Second, functional image volumes are co-registered and normalized, i.e., resampled to a suitable brain template that often is an anatomical MR brain image that is composed as an average of MR scans from an ensemble of individuals. The spatial normalization step is mandatory if one wishes to assess brain connectivity at a group level since the image normalization assures that the fMRI data from all subjects are in the same anatomical space of reference. For the case of infant fMRI, several brain templates have been made freely available (e.g., ref. [36]). Subsequent to spatial normalization to a group atlas template, the functional EPI volumes are spatially filtered to improve sensitivity by low-pass filtering of image data which, for example, suppresses high-frequency spatial noise (matched filter theorem [37]). As a last step, resting-state fMRI image data are temporally band-pass filtered since the frequency range of interest for the spontaneous BOLD signal fluctuations resides in the 0.01–0.1 Hz range [38].

The influence from head movement on resting-state fMRI connectivity has recently gained attention. It has been shown that even small head movements during fMRI scanning might cause an underestimation of long-range connectivity and an overestimation of short-range connectivity [39]. Generally, it is therefore recommended that head movements are carefully monitored during scanning and that image post-processing strategies that aim to minimize the influence from movement are included in the image data preprocessing pipeline. In addition to the usual custom of including regressors of no interest in the model of resting-state connectivity that are related to residual motion, it is advisable to apply censoring (“scrubbing”) of the raw fMRI data to discard data volumes that show large motion-induced signal variability. An example of such a measure is the frame-wise displacement (FD) that indexes the amount of movement of the head from one image volume to the next [40]. It should be noted that the issue of subject head

movement is of particular concern when comparing functional connectivity in different cohorts of subjects, e.g., healthy controls versus patients.

3 Measures of Connectivity

In above, we have described the pathway to obtaining individual time series signals from each brain area of interest. The next step is to estimate interactions between these signals. Some analytic strategies have been used for both EEG and fMRI despite the fundamental differences in the signal characteristics and the underlying mechanisms. There is a large body of theoretical and application literature on various mathematical measures to analyze interaction between two time series (for a review, *see*, e.g., refs. [41, 42]). Most importantly, there are no universal, omnipotent, and/or unchallengeable measures for brain connectivity. The methods employed in the literature are mutually different, both theoretically and conceptually. They also have different mathematical and physiological basis; some are supported by basic physiology while others may be purely developed from mathematical grounds without empiric physiological foundation. Most common overall strategies are to look at amplitude fluctuations, synchrony in the phase of oscillations, and causal relationships between two signals. It is preferable to avoid measures with ambiguous analytic interpretation, such as coherence that mixes variations in amplitude co-variability and phase synchrony. Recent methodological development has opened promising pathways for genuinely data-driven analyses with minimal pre-assumptions (e.g., ref. [43]). Since the need of accuracy in neuronal interactions increases dramatically (from seconds to milliseconds) from amplitude fluctuations to causal relationships, almost all neonatal studies have focused on estimating amplitude-based measures only.

It may be common to implicitly assume that brain networks are stable over time, especially because such networks are far easier to visualize intuitively. This idea has been proven wrong recently. The electric signals with their inherent high-frequency content have been shown to change its connectivity patterns at subsecond time scales [44, 45]. However, even slowly varying resting-state fMRI signals acquired at rest are not stationary in time and their connectivity profile may change over time [46].

The most straightforward and simplest way to analyze resting-state fMRI connectivity is by extracting the signal intensity time series at a small seed region of interest (ROI) that is a priori selected by the researcher. Next, the extracted BOLD signal time series is correlated with all other image voxels in the brain [38]. The seed-based correlation method is advantageous if the hypotheses regarding brain connectivity that are to be tested are a priori well defined

and localized to brain structures that are anatomically well circumscribed. The obvious drawback with seed-based resting-state correlation analysis is its inherent user selection bias in terms of spatial specificity which might imply that connectivity patterns of interest are neglected by the analysis. On the other hand, the user selection bias problem may at least partly be overcome by defining a manifold of ROIs, e.g., on points that are equidistantly positioned along a grid pattern that covers the entire cortex. However, the grid approach to seed-based correlation analysis comes with the methodological burden of multiple comparisons, which means that the statistical inference must take into account the fact that many tests of connectivity are made on the same data.

A complementary approach to hypothesis-driven methods to investigate the network structure of brain connectivity is to use data-driven, exploratory data analysis methods. For resting-state fMRI analysis, the independent component analysis (ICA) approach (or blind source separation) has become the method of choice [47]. Generally speaking, ICA will decompose the four-dimensional functional EPI MR data set into separate spatiotemporal components under the assumption that the BOLD signal intensity time course and their accompanying spatial maps are statistically independent. It should be noted that while it can be expected that each independent component will likely be the result of a single signal source that has a unique temporal characteristic, it is by no means that only resting-state networks contribute to the BOLD signal variability during resting-state conditions. Several non-neuronal sources for BOLD signal intensity variability exist: residual signal variability from head movements, blood flow-related signals residing in macroscopic vessels, interactions between macroscopic magnetic susceptibility, and subject head movement, just to mention a few. The fact that the BOLD resting-state fMRI data contains elements from neuronal as well as various non-neuronal sources implies that the researcher is required to assess the plausibility that any given component produced by an ICA represents a resting-state network or if it is likely to be caused by non-neuronal signal sources. This assessment can for example be guided by inspecting their anatomical localization: That is, is the component mainly situated in gray matter or not? Similarly, one can take advantage of the fact that the main part of the BOLD fMRI signal variance related to resting-state networks is within the low frequency interval (0.01–0.1 Hz). Consequently, if the majority of the signal variance for a given component resides in the low-frequency range and is anatomically confined to gray matter, chances are higher that it represents a resting-state network. Further confirmation can be obtained by checking the reproducibility of networks across individuals and separate cohorts. An example of an ICA analysis of resting-state fMRI data obtained from 12 infants is shown in Fig. 2 (*see* also results section below and ref. [29]).

Several software packages for doing ICA analysis of resting-state fMRI data are publically available (Gift toolbox; melodic toolbox).

Analysis of EEG signal is commonly based on analyzing each electrode pair (bivariate analysis) along one of the four main alternatives that are explained in more mathematical detail in the respective references: (1) temporal fluctuations in amplitude [48, 49], (2) synchrony of the phase in two oscillations [19, 50], (3) combination of amplitude in one signal and phase in the other (“nested oscillation” [10]), or (4) nonlinear dependency of other kind between two signals (e.g., synchronization likelihood [51]). These methods estimate relationships in the temporal behavior between neuronal signals; however more stringent methods have later been developed to allow estimation of directed interactions (e.g., ref. [52]). Such causal dependencies between brain areas are yet to be disclosed in spontaneous brain activity in the infant. Moreover, work in adults [54] and experimental models [53] have also developed methods that allow analysis of spatial ensembles, such as avalanches [54] that are known to characterize the large-scale cortical activity.

A fundamental step in all connectivity analysis is estimation of significance of the findings. All connectivity analyses will return some value from any two time series, even if the signals have virtually no relationship (e.g., ECG from one subject correlated to EEG of another subject). For instance, two biosignals, such as the EEGs from any two babies, may share features (e.g., temporal autocorrelations) that may give rise to spurious relationships. Also recording artefacts, such as movements or blinks, may readily result in elevated connectivity estimates, and their effect should be ruled out before or by the time of result interpretation. It is hence advisable to perform significance testing at individual level to avoid systematic confounders in the datasets. The most common method is to use surrogate statistics where real connectivity value is compared to a set of connectivity values obtained from surrogate signals. The surrogate signals can be generated from the original signal in several ways (e.g., time shifting, epoch shuffling, phase shuffling, reversing), and the rule of thumb is to preserve as much as possible of the original signal after destroying the signal feature of interest. Use of surrogates allows expressing the connectivity values as normalized measures or simply to declare the finding significant at individual level [49]. Importantly, statistical testing in hundreds (EEG) or thousands (fMRI) of signal pairs does also need to consider corrections for multiple comparison that is usually done by controlling the false detection rate (FDR [55]).

It is sometimes possible in group comparisons to use plain connectivity estimates without individual-level significant testing; however one will then run the risk that findings are confounded by different spurious effects in the study groups.

4 Analysis of Networks

The above-described analyses will return adjacency matrices, which summarizes strengths of given connectivity estimates between all possible pairs of signals. While this is an effective technical summary, it will rarely be helpful for the neuroscientist, because it does not visualize or quantify the kind of network that underlies the matrix.

A simple way to visualize the matrix is to plot topographic images where individual connections are either thresholded or their strengths are coded (Fig. 1), or one may focus on only analyzing selected combinations of signals (e.g., look at occipito-occipital interactions).

Recent work in systems neuroscience has demonstrated both spatially and temporally dynamic nature of brain networks, which has set the request to find more global network quantifiers and descriptors. The most promising framework here is developed within graph theory to create complete maps of the large-scale structural as well as a functional architecture of the brain, i.e., the structural and functional brain connectome [56]. This approach is based on graph theoretical concepts such as node strength, network efficiency, small worldness, and betweenness centrality [57]. The basic constituents of brain network graphs are nodes and edges, where nodes represent individual brain regions, while edges between two nodes reflect connection strengths, i.e., the connectivity estimates. The core idea behind applying graph theory to neuronal connectivity data is to let patterns of resting-state fMRI functional connectivity and/or EEG data to be represented as a connectivity matrix or equivalently, a graph, in which the entries of

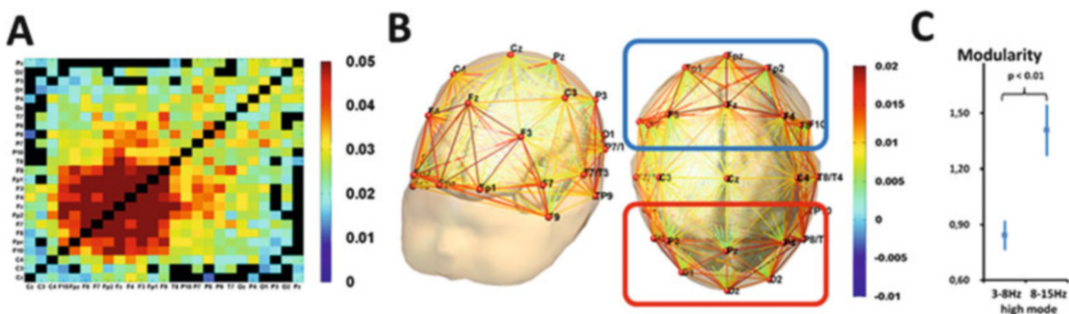


Fig. 1 Analysis of EEG connectivity using spatial amplitude correlations in the neonatal data. (a) Adjacency matrix that shows strengths of amplitude correlations between all channel pairs. The *black* cells are statistically insignificant as defined by using surrogate data. (b) Topographic visualization of the adjacency matrix shows the distribution and strengths (coded by the colors of the lines) of connections. (c) Graph theoretical approach, here using modularity index, quantifies the presence of modules irrespective of their anatomical locations. This plot shows a significant difference in modularity between amplitude correlations at different frequency bands (figure modified from ref. [49])

the matrix signify the strength of connectivity between all nodes in the network. The size of the connectivity matrix is governed by the number of nodes in the network, where each node is represented by, e.g., a single MR image voxel (or a voxel cluster), or an EEG signal. More detailed information regarding graph theoretical properties of brain network connectivity graphs as well as more advanced analysis pathways are presented in recent reviews [57, 58].

5 Example Results

5.1 EEG

Figure 1a shows an example of an adjacency matrix where strengths of long-range amplitude correlations are summarized between all electrode pairs. Statistical thresholding is employed at the individual and group levels, and the signal pairs below FDR-corrected threshold are blacked out. Thereafter, a topographical (3D) visualization is used to plot the significant connections on the baby scalp to illustrate their spatial distribution. While such maps are purely qualitative, they will help in intuitive understanding of the findings. In this particular case, the topographic visualization does also demonstrate the presence of apparent clusters in the frontal and occipital connections, which idea was supported by subsequent graph analysis (for full details of the analytic procedure, please *see ref.* [49]).

5.2 fMRI

Figure 2 shows the resting-state networks in the infant brain as given by an ICA analysis of resting-state fMRI data acquired in 12 infants scanned full term. Each infant was scanned for 10 min (TR = 2 s, 300 EPI volumes). At the age of birth, resting-state fMRI networks are present that resemble the network architecture seen in adults but with important differences. Whereas strong bilateral pattern of connectivity in the sensorimotor, visual, and auditory cortices (Fig. 3a–c) is clearly implemented at birth, networks that span higher order associative cortices are incomplete and/or fragmented. For example, the default mode network that in adults encompasses the posterior medioparietal cortex, medial prefrontal cortex, and the bilateral parietal cortex [59] is at the age of birth fragmented into a posterior and an anterior subnetwork (Fig. 3d, e). Subsequent research has shown that the connectivity pattern within the default network is fully developed at the age of 2 [32]. It has also been shown that most of the resting-state networks observed during the time of birth are present already during the third trimester [30, 33]. Taken together, recent research suggests that different resting-state networks in the human brain have different developmental trajectories [60].

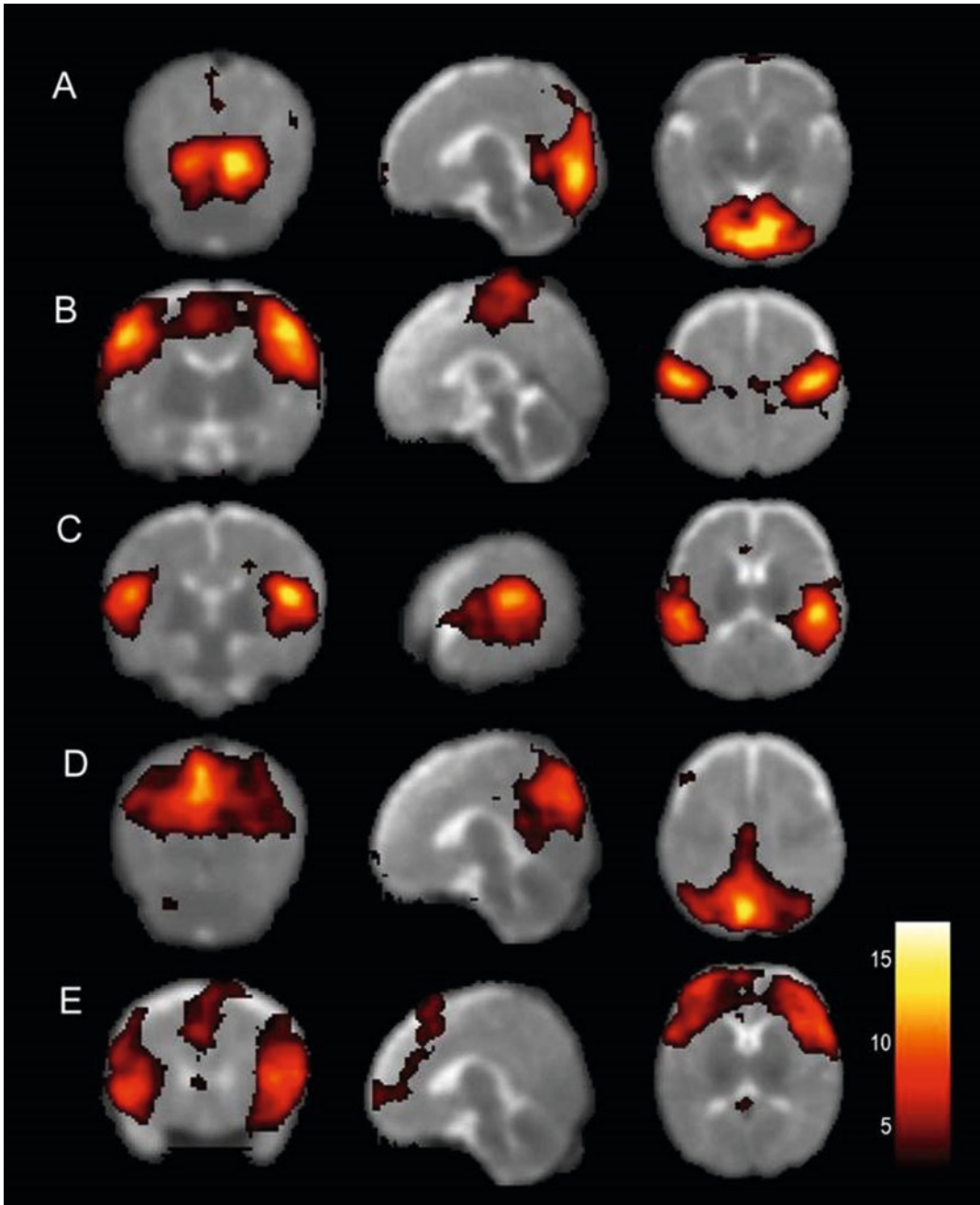


Fig. 2 Resting-state networks in the infant brain (adapted from Fransson et al., PNAS 2007)

6 Comparison of the EEG and fMRI in the Neonatal Studies

There is abundant literature on the combination of EEG and resting-state fMRI in the adults, including several fundamental studies on the mechanisms of neurovascular coupling in adults.

However, methodological constraints have precluded co-registration of EEG and fMRI in the human infants, and only correlational work exists with parallel analysis of distinctly recorded datasets [49, 61]. These works have suggested that the power law—like frequency scaling—is found in both modalities [61]; however it can only be inspected at orders of magnitude different range of frequencies (fMRI: 0.01–0.15 Hz vs. EEG 0.2–30 Hz). A more recent study showed that the cortical electric activity in the infants is amplitude-wise correlated at relatively rapid temporal scales (via spontaneous activity transients [10]) only, and such correlations are too rapid to be detected from the fMRI in human infants [49].

Studies on the neurovascular coupling after natural cortical activity in human infants have shown both highly variable and very delayed hemodynamic responses [62, 63], which together with recent experimental works [64] challenge the idea of direct relationships between EEG and fMRI in infants. The implication of this is that the networks disclosed by fMRI and EEG are by default different. One might observe spatially comparable networks by using analytical manipulations as such by regressing EEG data with fMRI data; however it is always advisable to be cautious with analytic pathways that may introduce strong bias or are based on physiologically unreasoned a priori assumptions.

Apart from the elusive neurovascular coupling in infants, spatial correlation between fMRI and EEG does also result in challenges. The EEG recordings are always sparse relative to fMRI voxels, and no unique solution exists for their spatial coordination. In addition, a reasonable bivariate connectivity analysis of the cortical space requires cortical parcellation, which is inherently ill posed, because no a priori knowledge exists about physiologically coherent activity patches.

Finally, time scales in the EEG and fMRI activity are different. Virtually nothing in the electric brain is stationary for tens of seconds that is the underlying assumption when analyzing networks in the fMRI signal. The need to do longer recordings with EEG is purely due to signal-to-noise ratio where more repetitions of the presumed networks are needed for their statistical capture.

References

1. Stam CJ, van Straaten ECW (2012) The organization of physiological brain networks. *Clin Neurophysiol* 123:1067–1087
2. Milh M, Kaminska A, Huon C, Lapillonne A, Ben-Ari Y, Khazipov R (2007) Rapid cortical oscillations and early motor activity in premature human neonate. *Cereb Cortex* 17:1582–1594
3. Vanhatalo S, Lauronen L (2006) Neonatal SEP: back to bedside with basic science. *Semin Fetal Neonatal Med* 11:464–470
4. Stjerna S et al. (2012) Preterm EEG: a multimodal neurophysiological protocol. *J Vis Exp* (60): e3774, <http://dx.doi.org/10.3791/3774>
5. Hanganu-Opatz IL (2010) Between molecules and experience: role of early patterns of coordinated activity for the development of cortical maps and sensory abilities. *Brain Res Rev* 64: 160–176
6. Colonnese M, Khazipov R (2012) Spontaneous activity in developing sensory circuits:

- implications for resting state fMRI. *Neuroimage* 62:2212–2221
7. Kilb W, Kirischuk S, Luhmann HJ (2011) Electrical activity patterns and the functional maturation of the neocortex. *Eur J Neurosci* 34:1677–1686
 8. Odabaec M et al (2013) Spatial patterning of the neonatal EEG suggests a need for a high number of electrodes. *Neuroimage* 68: 229–235
 9. Grieve PG et al (2004) Quantitative analysis of spatial sampling error in the infant and adult electroencephalogram. *Neuroimage* 21: 1260–1274
 10. Vanhatalo S, Palva M, Andersson S, Rivera C, Voipio J, Kaila K (2005) Slow endogenous activity transients and developmental expression of K-Cl cotransporter 2 in the immature human cortex. *Eur J Neurosci* 22:2799–2804
 11. Welch MG et al (2014) Electroencephalographic activity of preterm infants is increased by Family Nurture Intervention: a randomized controlled trial in the NICU. *Clin Neurophysiol* 125:675. doi:10.1016/j.clinph.2013.08.021
 12. Vanhatalo S et al (2008) High-fidelity recording of brain activity in the extremely preterm babies: feasibility study in the incubator. *Clin Neurophysiol* 119:439–445
 13. Vanhatalo S et al (2005) Full-band EEG (FbEEG): an emerging standard in electroencephalography. *Clin Neurophysiol* 116:1–8
 14. Fox MD, Raichle ME (2007) Spontaneous fluctuations in brain activity observed with functional magnetic resonance imaging. *Nat Rev Neurosci* 8:700–711
 15. Biswal B, Yetkin FZ, Haughton VM, Hyde JS (1995) Functional connectivity in the motor cortex of resting human brain using echoplanar MRI. *Magn Reson Med* 34:537–541
 16. Damoiseaux JS, Rombouts SA, Barkhof F, Scheltens P, Stam CJ, Smith SM, Beckmann CF (2006) Consistent resting-state networks across healthy subjects. *Proc Natl Acad Sci U S A* 103:13848–13853
 17. NEMO (2011) An educational multimedia package directed and authored by Vanhatalo S. <http://www.nemo-europe.com/en/educational-tools.php>
 18. Räsänen O, Metsäranta M, Vanhatalo S (2013) Development of a novel robust measure for interhemispheric synchrony in the neonatal EEG: Activation Synchrony Index (ASI). *Neuroimage* 69:256–266
 19. Palva JM et al (2010) Neuronal synchrony reveals working memory networks and predicts individual memory capacity. *Proc Natl Acad Sci* 107:7580–7585. doi:10.1073/pnas.0913113107
 20. Pasquale F, Penna SD, Snyder AZ, Lewis C, Mantini D, Marzetti L, Belardinelli P, Ciancetta L, Pizzella V, Romani GL, Corbetta M (2010) Temporal dynamics of spontaneous MEG activity in brain networks. *Proc Natl Acad Sci U S A* 107:6040–6045
 21. Brookes MJ, Woolrich M, Luckhoo H, Price D, Hale JR, Stephenson MC, Barnes GR, Smith SM, Morris PG (2011) Investigating the electrophysiological basis of resting state networks using magnetoencephalography. *Proc Natl Acad Sci U S A* 108:16783
 22. Kabdebon C, Leroy F, Simmonet H, Perrot M, Dubois J, Dehaene-Lambertz G (2014) Anatomical correlations of the international 10-20 sensor placement system in infants. *Neuroimage* 99:342–356
 23. Palmu K, Kirjavainen T, Salokivi T, Palva M, Vanhatalo S (2013) Sleep wake cycling in early preterm infants, and its potential monitoring using a novel automated measure from the EEG monitoring. *Clin Neurophysiol* 124: 1807–1814
 24. Schoffelen J-M, Gross J (2009) Source connectivity analysis with MEG and EEG. *Hum Brain Mapp* 30:1857–1865. doi:10.1002/hbm.20745
 25. Odabaec M, Tokariev A, Layeghy S, Mesbah M, Colditz PB, Ramon C, Vanhatalo S (2014) Neonatal EEG at scalp is focal and implies high skull conductivity in realistic neonatal head models. *Neuroimage* 96C:73–80
 26. De Vos M, Deburchgraeve W, Cherian PJ, Matic V, Swarte RM, Govaert P, Visser GH, Van Huffel S (2011) Automated artifact removal as preprocessing refines neonatal seizure detection. *Clin Neurophysiol* 122: 2345–2354
 27. Nordell A, Lundh M, Horsch S, Hallberg B, Åden U, Nordell B, Blennow M (2009) The acoustic hood: a patient-independent device improving acoustic noise protection during neonatal magnetic resonance imaging. *Acta Paediatrica* 98:1278–1283
 28. Birn RM, Molloy EK, Patriat R, Parker T, Meier TB, Kirk GR, Nair VA, Mayerand ME, Prabhakaran V (2013) The effect of scan length on the reliability of resting-state fMRI connectivity estimates. *Neuroimage* 83: 550–558
 29. Fransson P, Skiöld B, Horsch S, Nordell A, Blennow M, Lagercrantz H, Åden U (2007) Resting-state networks in the infant brain. *Proc Natl Acad Sci U S A* 104:15531–15536

30. Doria V, Beckmann CF, Arichi T, Merchant N, Groppo M, Turkheimer FE, Counsell SJ, Murgasova M, Aljabar P, Nunes RG et al (2010) Emergence of resting state networks in the preterm human brain. *Proc Natl Acad Sci U S A* 107:20015–20020
31. Fransson P, Skiöld B, Engström M, Hallberg B, Mosskin M, Åden U, Lagercrantz H, Blennow M (2009) Spontaneous brain activity in the newborn brain during natural sleep—an fMRI study in infants born at full term. *Pediatr Res* 66:301–305
32. Gao W, Zhu H, Giovanello KS, Smith JK, Shen D, Gilmore JH, Lin W (2009) Evidence on the emergence of the brain’s default network from 2-week-old to 2-year-old healthy pediatric subjects. *Proc Natl Acad Sci U S A* 106:6790–6795
33. Smyser CD, Inder TE, Shimony JS, Hill JE, Degnan AJ, Snyder AZ, Neil JJ (2010) Longitudinal analysis of neural network development in preterm infants. *Cereb Cortex* 20:2852–2862
34. Horowitz SG, Fukunaga M, de Zwart JA, van Gelderen P, Fulton SC, Balkin TJ, Duyn JH (2008) Low frequency BOLD fluctuations during resting wakefulness and light sleep: a simultaneous EEG-fMRI study. *Hum Brain Mapp* 29:671–682
35. Sämann PG, Wehrle R, Hoehn D, Spoormaker VI, Peters H, Tully C, Holsboer F, Czisch M (2011) Development of the brain’s default mode network from wakefulness to slow wave sleep. *Cereb Cortex* 21:2082–2093
36. Gousias IS, Hammers A, Counsell SJ, Srinivasan L, Rutherford MA, Heckemann RA, Hajnal JV, Rueckers D, Edwards AD (2013) Magnetic resonance imaging of the newborn brain: automatic segmentation of brain images into 50 anatomical regions. *PLoS One* 8(4):e59990
37. Rosenfeld A, Kak AC (1982) Digital picture processing. Academic, Orlando, FL
38. Dijk KRAV, Hedden T, Venkataraman A, Evans KC, Lazar SW, Buckner RL (2010) Intrinsic functional connectivity as a tool for human connectomics: theory, properties, and optimization. *J Neurophysiol* 103:297–321
39. Power JD, Barnes KA, Snyder AZ, Schlaggar BL, Petersen SE (2012) Spurious but systematic correlations in functional connectivity in MRI networks arise from subject movement. *Neuroimage* 59:2142–2154
40. Power JD, Mitra A, Laumann TO, Snyder AZ, Schlaggar BL, Petersen SE (2014) Methods to detect, characterize, and remove motion artifacts in resting-state fMRI. *Neuroimage* 84:320–341
41. Hutchison RM, Womelsdorf T, Allen EA, Bandettini PA, Calhoun VD, Corbetta M, Della Penna S, Duyn JH, Glover GH, Gonzalez-Castillo J, Handwerker DA, Keilholz S, Kiviniemi V, Leopold DA, de Pasquale F, Sporns O, Walter M, Chang C (2013) Dynamic functional connectivity: promise, issues, and interpretations. *Neuroimage* 80:360–378
42. Cohen MX (2014) Analyzing neural time series data: theory and practice. MIT Press, Cambridge, MA
43. Mehrkanoon S, Breakspear M, Boonstra TW (2014) Low-dimensional dynamics of resting-state cortical activity. *Brain Topogr* 27:338–352
44. Betzel RF, Erickson MA, Abell M, O’Donnell BF, Hetrick WP, Sporns O (2012) Synchronization dynamics and evidence for a repertoire of network states in resting EEG. *Front Comput Neurosci* 6:74
45. Brookes MJ, O’Neill GC, Hall EL, Woolrich MW, Baker A, Palazzo Corner S, Robson SE, Morris PG, Barnes GR (2014) Measuring temporal, spectral and spatial changes in electrophysiological brain network connectivity. *Neuroimage* 91:282–299
46. Chang C, Glover GH (2010) Time-frequency dynamics of resting-state brain connectivity measured with fMRI. *Neuroimage* 50:81–98
47. Beckmann CF, DeLuca M, Devlin JT, Smith SM (2005) Investigations into resting-state connectivity using independent component analysis. *Philos Trans R Soc Lond B Biol Sci* 360:1001–1013
48. Hipp JF, Hawellek DJ, Corbetta M, Siegel M, Engel AK (2012) Large-scale cortical correlation structure of spontaneous oscillatory activity. *Nat Neurosci* 15:884–890
49. Omidvarnia A, Fransson P, Metsäranta M, Vanhatalo S (2014) Functional bimodality in the early electric networks in the human newborn brain. *Cereb Cortex* 24:2657–2668
50. Tokariev A et al (2012) Phase synchrony in the early preterm EEG: development of methods for estimating synchrony in both oscillations and events. *Neuroimage* 60:1562–1573
51. Boersma M, Smit DJA, de Bie HMA, Van Baal GCM, Boomsma DI, de Geus EJC, Delemarre-van de Waal HA, Stam CJ (2011) Network analysis of resting state EEG in the developing young brain: structure comes with maturation. *Hum Brain Mapp* 32:413–425
52. Lobier M, Siebenhühner F, Palva S, Palva JM (2014) Phase transfer entropy: a novel phase-based measure for directed connectivity in

- networks coupled by oscillatory interactions. *Neuroimage* 85(Pt 2):853–872
53. Brockmann MD, Pöschel B, Cichon N, Hanganu-Opatz IL (2011) Coupled oscillations mediate directed interactions between prefrontal cortex and hippocampus of the neonatal rat. *Neuron* 71:332–347. doi:[10.1016/j.neuron.2011.05.041](https://doi.org/10.1016/j.neuron.2011.05.041)
 54. Shriki O, Alstott J, Carver F, Holroyd T, Henson RN, Smith ML, Coppola R, Bullmore E, Plenz D (2013) Neuronal avalanches in the resting MEG of the human brain. *J Neurosci* 33:7079–7090
 55. Singh AK, Asoh H, Phillips S (2011) Optimal detection of functional connectivity from high-dimensional EEG synchrony data. *Neuroimage* 58:148–156
 56. Sporns O (2013) The human connectome: origins and challenges. *Neuroimage* 80:53–61
 57. Rubinov M, Sporns O (2010) Complex network measures of brain connectivity: uses and interpretations. *Neuroimage* 52:1059–1069
 58. Stam CJ, Tewarie P, Van Dellen E, van Straaten EC, Hillebrand A, Van Mieghem P (2014) The trees and the forest: characterization of complex brain networks with minimum spanning trees. *Int J Psychophysiol* 92:129–138
 59. Raichle ME, MacLeod AM, Snyder AZ, Powers WJ, Gusnard DA, Shulman GL (2001) A default mode of brain function. *Proc Natl Acad Sci U S A* 98:676–682
 60. Fransson P, Åden U, Blennow M, Lagercrantz H (2011) The functional architecture of the infant brain as revealed by resting-state fMRI. *Cereb Cortex* 21:145–154
 61. Fransson P, Metsäranta M, Blennow M, Åden U, Lagercrantz H, Vanhatalo S (2013) Early development of spatial patterns of power-law frequency scaling in fMRI resting-state and EEG data in the newborn brain. *Cereb Cortex* 23:638–646
 62. Arichi T, Moraux A, Melendez A, Doria V, Groppo M, Merchant N, Combs S, Burdet E, Larkman DJ, Counsell SJ, Beckmann CF, Edwards AD (2010) Somatosensory cortical activation identified by functional MRI in preterm and term infants. *Neuroimage* 49:2063–2071
 63. Roche-Labarbe N, Wallois F, Ponchel E, Kongolo G, Grebe R (2007) Coupled oxygenation oscillation measured by NIRS and intermittent cerebral activation on EEG in premature infants. *Neuroimage* 36:718–727
 64. Colonnese MT, Phillips MA, Constantine-Paton M, Kaila K, Jasanoff A (2008) Development of hemodynamic responses and functional connectivity in rat somatosensory cortex. *Nat Neurosci* 11:72–79

Cerebral Blood Flow Measurements in the Neonatal Brain

Flora Wong

Abstract

Cerebrovascular lesions and hypoxic-ischaemic brain injury are important causes of acquired neonatal brain injury in term and preterm newborn infants, which lead to significant morbidity and long-term mortality. Improved understanding of the cerebral hemodynamics and metabolism in the immature brain, and blood flow responses to physiological and external stimuli would aid understanding of the pathogenesis of neonatal brain injury. There has been increasing research interest and clinical demand to study the neonatal brain, with the exploration of the bedside and real-time measurement of cerebral hemodynamics in guiding therapy and predicting outcome. The major techniques which allow the assessment of cerebral blood flow (CBF) with relative ease at the bedside in the neonatal intensive care unit include near-infrared spectroscopy (NIRS), and transcranial Doppler ultrasonography. Diffuse optical correlation spectroscopy (DCS) is a new technique for which portable devices are currently being developed to continuously monitor relative changes in microvascular CBF at the bedside. DCS can potentially be combined with NIRS to provide continuous simultaneous measurement of changes in CBF and oxygenation, and enables the quantification of cerebral metabolic rate of oxygen. Functional studies have also been utilized with NIRS and magnetic resonance imaging to elucidate the connections between localized cortical activity and cerebral hemodynamic responses during early human development. To utilize and translate cerebral hemodynamic measurements in clinical management, future research should aim to establish clinically relevant parameters and references range for cerebral perfusion and oxygenation for the neonatal population.

Key words Neonate, Cerebral blood flow, Cerebral oxygenation, Near-infrared spectroscopy, Neonatal brain injury, Diffusion correlation spectroscopy

1 Background

With many infants now born preterm at 24–32-week gestation [1], a full understanding of the physiological regulation of cerebral blood flow (CBF) in the immature brain is becoming increasingly important. Survival of infants born extremely preterm (<28-week gestation) has increased sharply (50–70 %) over the last two decades [2, 3], but this has been accompanied by higher rates of neurodevelopmental disability, which exceed 50 % in most studies [3–5]. The pathological correlates of neurodevelopmental disability with preterm birth include various acquired cerebral lesions, most

notably periventricular leukomalacia (PVL) and germinal matrix hemorrhage–intraventricular hemorrhage (GMH-IVH) [6, 7]. Although the aetiology of cerebral lesions in the preterm infant is complex, it is generally accepted that hypoxia and poor cerebral perfusion lead to some regions of the preterm brain and, particularly white matter, falling into a condition best described as hypoxia-ischemia [8].

Improving our ability to assess changes in cerebral oxygenation and regulation of CBF will enhance our understanding of how these changes may contribute towards acquired brain injury. Clinically, investigation of CBF in infants is constrained by the necessity to use noninvasive techniques. There is no general agreement on the best approach to measure CBF. Each of the techniques has its own merits and limitations regarding use in newborn infants. Nevertheless, it is important to note that, despite their methodological diversity, all these measurement methods yield fairly comparable results on cerebral circulation, in terms of both absolute values of CBF and characteristics of cerebrovascular reactivity. In the 1940s, Kety and Schmidt pioneered the measurement of CBF, using nitrous oxide and the Fick principle wherein the rate of uptake and clearance of an inert diffusible gas are proportional to blood flow [9]. The invasive nature of this measurement technique, requiring repeated blood sampling from the internal jugular veins, together with the fact that equilibrium of nitrous oxide between the circulation and the brain tissue occurs very slowly, however, largely limited its use even in the experimental setting.

In the past, techniques which require use of a radioactive substance (e.g., xenon-133) or high radiation exposure (e.g., positron emission tomography (PET) scans) were also used to measure cerebral perfusion in neonates. In the past two decades, near-infrared spectroscopy (NIRS), transcranial Doppler (TCD), and MRI-based methods are the main modalities used in clinical research of neonatal cerebral hemodynamics.

2 Techniques and Applications

2.1 *Xenon-133 Clearance Technique*

Since the 1960s and the advent of radioisotope imaging, the Kety-Schmidt method was gradually replaced by the tracing and measurement of the strong gamma emitter xenon-133, a freely diffusible inert gas that does not interfere with cerebral metabolism. The xenon-133 clearance technique utilizes administration of xenon-133, either by intra-arterial or intravenous injection or by inhalation to diffuse into the brain. As xenon-133 is not metabolized, the rate of clearance in the brain is proportional to CBF. Detection of the brain clearance of xenon-133, specifically the gamma radiation thereof, is made possible by placing external scintillators over the skull. The measurement represents global CBF. The technique is

able to provide quantitative data with portable equipment [10], but involves exposure to radiation and is no longer deemed to be appropriate for newborn infants. Measurement also requires several minutes, so that rapid changes in CBF cannot be recorded.

2.2 Positron Emission Tomography

Regional CBF, together with glucose and oxygen consumption, can be observed using PET. The positron-emitting isotope (H_2^{15}O) is injected and positrons then collide with electrons in tissues, leading to annihilation of the particles and the emission of two photons at an angle of 180° to each other. Suitable detectors can determine the location of the annihilation event, and, by comparing the clearance of the positron-emitting isotope with the location of the annihilation event, determine regional CBF with a resolution of 3–4 mm. The ability to obtain regional hemodynamic and metabolic information is a great advantage. However, the use of PET in the newborn [11] is limited by the relatively high exposure to ionizing radiation, having to transport the infant to nearby cyclotron facility, and the need to draw a substantial volume of arterial blood to quantify CBF results.

2.3 Single-Photon Emission Computed Tomography

Relative but non-quantitative regional CBF with ~1 cm resolution has been observed in newborn infants using single-photon emission computed tomography (SPECT). This requires injection of a radioactive tracer ($^{99\text{m}}\text{Tc-HMPAO}$) that fixes in tissue at first pass and acts as a chemical microsphere. The radioactive ligand becomes trapped in the brain and can be imaged at some later time during its decay, offering the potential for observing CBF during clinical events. The disadvantage is that only the distribution, not the absolute level of CBF, is obtained [12]. Again, the method cannot be easily applied at the bedside.

2.4 Arterial Spin- Labeled Perfusion- Magnetic Resonance Imaging

A novel technique, arterial spin-labeled perfusion-magnetic resonance imaging (ASL-pMRI), allows noninvasive measurement of CBF using electromagnetically labeled arterial blood water as an endogenous contrast agent [13]. One of the most significant advantages of ASL-pMRI over previous techniques is the ability to assess CBF without using intravascular contrast agents or radioactive labeled tracers.

ASL-pMRI magnetically labels arterial blood by inversion or saturation proximal to the tissue of interest. After a delay in time, image acquisition occurs allowing the labeled blood to flow into the imaging slices. Perfusion is determined by pair-wise comparison with separate images that are acquired without labeling (control).

Sensitivity of the ASL-pMRI measurement decreases in regions of very low CBF, which is a challenge in neonatal measurements as CBF in infants is significantly lower than that of older children and adults [14, 15]. The measurement only represents a discrete time

point and cannot be used at the bedside, or for prolonged periods of assessment. The technique can potentially be combined with the use of functional MRI to assess cerebral perfusion and oxygenation changes associated with neural activity. Despite the limitations, studies in normal neonates using ASL-pMRI have reported normal range of CBF in preterm and term infants [16] as well as age-related changes throughout childhood [17].

2.5 Functional Magnetic Resonance Imaging

Functional magnetic resonance imaging (fMRI) is based on the detection of blood oxygenation level-dependent (BOLD) signal changes, in relation to neural activity, in response to a stimulus or during spontaneous neural fluctuations. The BOLD effect is due to the physical phenomenon that deoxyhemoglobin is paramagnetic and reduces the MR signal [18]. The existence of the BOLD effect depends on the localized changes of CBF that occur with neural activity, so that when neural activity increases, CBF increases and exceeds the cerebral metabolic rate of oxygen ($CMRO_2$); hence decreasing the local oxygen extraction fraction and the decreased concentration of deoxyhemoglobin then creates the BOLD response. Therefore, the BOLD signal depends strongly on the relative changes in CBF and $CMRO_2$. BOLD signal changes are usually expressed as a relative percentage signal change or as a statistical significance level based on a statistical model.

An increase in neuronal activity results in a local increase in blood oxygenation and a corresponding increase in BOLD signal (i.e., a positive BOLD response). A positive BOLD contrast response can be elicited from around postnatal days 13–15 in the rat brain, which equates to approximately 28–32 weeks in human gestation [19], and increasing age is associated with an increase in the peak amplitude of BOLD responses, and co-activation of the ipsilateral cortex and supplementary areas in addition to the primary sensory areas [19]. fMRI studies in human newborn, however, have produced inconsistent results, complicated with methodological difficulties [20]. Some studies suggest that in contrast to the adult response and the postnatal rat studies, sensory stimulation induces a decrease in BOLD signal (often termed “negative BOLD”) during early human infancy [21, 22]. Interpretation of results is further complicated by the use of sedative medication and/or anaesthesia, which is often necessary for neonatal subjects during MRI examination to reduce distress and motion artefact [20, 23]. Interpretation and the physiological origin of the negative BOLD response remain controversial. Several theories have been proposed [24], including an increase in neuronal activity and $CMRO_2$ without a compensatory increase in CBF, or a decrease in CBF due to the “hemodynamic steal” of blood by an adjacent activated cortical region.

3 Cotside Measurement

All of the above techniques are not suitable for cotside use, or for continuous monitoring. Currently, there are two major techniques that allow the assessment of CBF with relative ease at the bedside in NICU: NIRS, and transcranial Doppler ultrasonography (TCD).

3.1 Transcranial Doppler Ultrasonography

TCD was introduced into clinical practice in 1982 and allows continuous noninvasive monitoring of CBF velocity at the bedside [25].

TCD follows the same principles and assumptions of the Doppler effect to measure blood flow velocity in large vessels [26]. A piezoelectric transducer generates an ultrasound beam, typically of 2 MHz for adults or higher frequencies for neonates. The insonating ultrasound pressure wave is reflected by the red blood cells in a large vessel with a frequency shift that is directly proportional to the velocity of the scattering elements [26]. In the presence of laminar flow, the reflected Doppler frequency shift will comprise a distribution of frequencies, rather than a single value. Spectral analysis can then be used to obtain measures of blood flow velocity; usually either the maximum frequency (i.e., maximum velocity) or its intensity-weighted mean is extracted to represent the mean velocity for the time interval measured. CBF velocity can be obtained continuously in the anterior, middle, posterior, and basilar cerebral arteries. An important assumption for TCD measurements is that the diameter of the insonated vessel does not change during the course of a study and it remains constant in response to physiologic variables such as blood pressure changes. In addition, CBF velocity is not quantitative of absolute CBF as the cross-sectional dimension of the vessel is unknown, and it is not representative of global CBF as only one cerebral artery is insonated at any one time. Nonetheless, TCD can be utilized to assess (1) qualitative changes in flow velocities, (2) cerebrovascular resistance, and (3) CBF autoregulation [26–28].

The use of TCD is limited only to short periods of assessment in neonates due to safety concerns over exposure to high-energy transmission over longer periods. Ultrasound waves, especially when used for color Doppler imaging, may induce temperature elevations in human tissue over time that have the potential to cause damage. The power used should be kept in line with published guidelines such as those by the British Medical Ultrasound Society (www.bmus.org), with the lowest setting compatible with obtaining diagnostic images. Other technical limitations include operator dependence and the difficulty in maintaining angle of insonation for optimal and prolonged measurement.

3.2 Near-Infrared Spectroscopy

3.2.1 Principle

NIRS is a noninvasive optical technique to assess microvascular cerebral oxygenation, where CBF (or cerebral blood volume (CBV)) is inferred from changes that occur in oxy- and deoxyhemoglobin concentrations. NIRS can also provide serial quantitative measurements of CBF, CBV, and cerebral venous saturation at the bedside.

Biological tissue is relatively transparent to light in the near-infrared (NIR) part of the spectrum (in the wavelength range 700–1000 nm) allowing several centimeters of tissue to be illuminated. At shorter wavelengths, in the visible spectrum, hemoglobin absorbs strongly. At longer wavelengths, water absorbs increasingly. Within this NIR window, the chromophores oxyhemoglobin (HbO₂), deoxyhemoglobin (HHb) and cytochrome c oxidase have light absorption characteristics which vary with oxygenation status. This allows spectroscopic measurements of light attenuation to be used to assess blood and tissue oxygenation. The attenuation (or loss) of NIR light will be due to both absorption and scattering effects within these tissues. If scattering is assumed to be constant, the measured changes in the attenuation of the NIR light can therefore be used to calculate the changes in blood oxyhemoglobin (ΔHbO_2), deoxyhemoglobin (ΔHHb), and total hemoglobin ($\Delta\text{HbT} = \text{HbO}_2 + \text{HHb}$) in the illuminated tissue. With knowledge of the optical pathlength in tissue [29], the changes in HbO₂, HHb, and HbT can be expressed in μmolar units. The changes in concentration of these chromophores can be used as surrogate markers of CBF and CBV [30].

Theoretically, if the source to detector distance is increased, light penetration would increase and detected light would provide information about deeper tissue [31]. However, in the NIR spectrum, for every centimeter of additional distance between the source and the sensor, light is attenuated by a factor of 10–100 [32]. For adequate levels of light detection, source-detector distances should not be more than 5 cm. Furthermore, because of the random propagation of light in tissue, the depth of measurement is no more than 2–3 cm [33]. This depth is more than enough for measurements within the newborn brain. Notably, as the intensity of the light sources can vary across NIRS systems, a source-detector separation distance that is ideal for one system may not be for another.

3.2.2 Instruments and Measurements

Three fundamental NIRS techniques exist to interrogate tissue oxygenation in vivo (Fig. 1). *Continuous wave (CW) spectroscopy* measure changes in attenuation by recording the intensity of light between a pair of optodes. *Frequency-resolved spectroscopy* measures both intensity and phase shift of an intensity-modulated light source. *Time-resolved spectroscopy* measures the time of flight of photons between source and detector and has been applied in optical tomography of the neonatal brain [34].

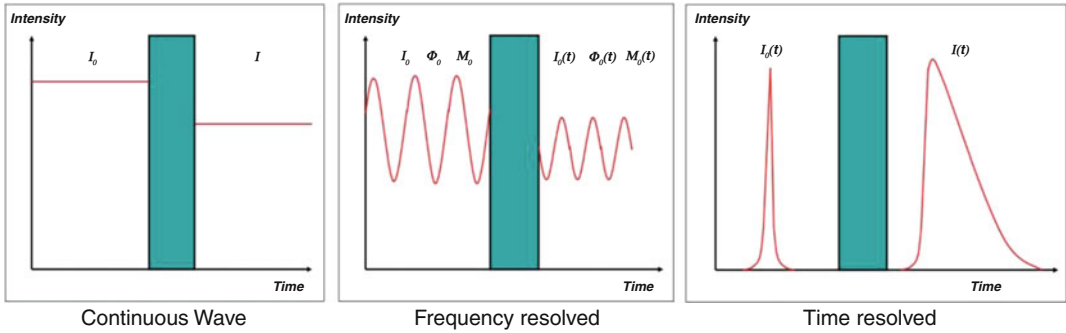


Fig. 1 Three fundamental types of optical spectroscopy and imaging techniques [38]. The continuous wave instrument measures the transmitted intensity (I) after incident light intensity (I_0) through an absorber. The intensity (I), phase shift (Φ), and modulation depth (M) relative to the input signal are measured in the frequency-resolved instrument. The time-resolved instrument records individual photons and measures their flight times to construct a histogram of the distribution of arrival times

The frequency-resolved technique employs continuous laser light on which is superimposed very-high-frequency intensity modulations in the MHz range. In addition to measurement of transmitted intensity, the phase shift and modulation depth relative to the input signal are also measured. This phase shift is proportional to the optical pathlength through the tissue sample and is wavelength specific. In vivo measurement of optical pathlength has been described in both adults and infants [35]. The strength of this technique is that phase shift measurements allow absorption and scattering to be quantified and thereby the calculation of absolute chromophore concentrations [36, 37]. However, in order to obtain accurate estimates of absorption and scattering coefficients, measurements over a wider frequency range than other NIR methods need to be performed, which proves to be difficult in practice [38].

The time-resolved spectroscopy measures the time passage of a picosecond pulse of light through tissue. The shortest distance between the light source and detector is known as the ballistic trajectory, which is a path only a very few photons will traverse; the majority will be scattered to a greater or lesser degree before either being absorbed, scattered out of range of the detector, or eventually reach the detector. A histogram of photon density against arrival time at the detector can be built up known as the temporal point spread function (TPSF), from which the scattering and absorption coefficients can be calculated [39, 40], allowing absolute quantification of oxygenation and CBV. The need to generate several wavelengths of this picosecond light source as well as a fast detector makes this a very expensive technique [41].

The continuous-wave (CW) NIRS measures the attenuation of constant intensity source light after it has diffused through the tissue. Changes in optical attenuation can be converted into changes in chromophore concentration. Data are collected at multiple wavelengths, equal to or exceeding the number of

chromophores measured [35]. The most common prototype of NIRS used in clinical research is the CW NIRS.

CW NIRS can be used to obtain absolute intermittent quantification of CBF (in ml/100 g/min) and CBV (in ml/100 g), by employing spontaneous or induced (by hemodynamic or biochemical manipulation) parameter changes in tissue. Measurement of CBF by NIRS employs a modification of the Fick principle. The technique uses a purely intravascular and non-diffusible tracer, such as a bolus of oxygen as an endogenous tracer [42], or the NIR dye indocyanine green injected as an exogenous tracer [43]. If the tracer (Q) is rapidly introduced into the arterial supply of the brain, the amount that has accumulated in the brain may be measured later at a time t . If this time is less than the transit time through the brain, no tracer will have appeared in the venous blood. Thus CBF can be determined from the ratio of tracer accumulated at time t to the quantity of tracer introduced. This quantity is equal to the integral of the arterial concentration of tracer at time t ($Ca(t)$) with respect to time. Therefore,

$$\text{CBF} = \frac{Q(t)}{\int_0^t Ca(t) dt}$$

Commercially available NIRS instruments from companies, such as Hamamatsu, Covidien, and Casmed, are typically CW devices. Although the cost of a CW NIRS device is typically much less than that of a time-resolved or frequency-resolved instrument, CW instruments are highly sensitive to room light and to surface coupling between skin and/or hair and the optical probe, and lead to interferences between the calculated tissue absorption and scattering [44].

Cerebral oximetry. The clinical drive for absolute values of cerebral hemodynamics without the need for biochemical or hemodynamic manipulation has led to the development of “cerebral oximetry” using NIRS techniques. Using multi-distanced sensors and different algorithms [32, 41, 45], absolute values of cerebral tissue oxygen saturation can be calculated from the changes in oxy- and total hemoglobin. This is often expressed as tissue oxygenation index (TOI) or regional cerebral oxygen saturation (rScO₂), depending on the NIRS prototype and algorithms used [32]. The measurement is absolute on a scale from 0 to 100 %.

Multichannel optical topography systems which use arrays of multiple sources and detectors have been developed to provide two-dimensional maps of the cortical hemodynamic response (and therefore brain activity) [46]. However, it is difficult to design an easy-to-apply and comfortable method by which to attach multiple source and detector optodes to the infant head. There have been increasingly sophisticated designs for NIRS probes and head-gear custom-made for infant studies [46, 47]. Developments have also been made in a number of commercial NIRS systems such as

the ETG Optical Topography system (The Hitachi Medical Corporation, <http://www.hitachimedical.com>) and the Imagent (ISS Inc., <http://www.iss.com>).

3.2.3 Clinical Application in Neonatal Measurements

NIRS has been favored in monitoring the infant brain partly because of the convenient optical geometry of the infant head with the thin skull and extracerebral layers. Several additional hemodynamic parameters have been derived from NIRS measurements. These include (1) cerebral venous saturation [48]; (2) cerebral oxygen delivery which refers to the combination of CBF and cerebral arterial oxygen content; (3) cerebral metabolic rate of oxygen consumption (CRMO₂) [49], which indicates the rate at which oxygen is used within the cerebral tissue and represents cerebral metabolic activity; and (4) cerebral fractional tissue oxygen extraction which refers to the percentage of oxygen being extracted from the arterial blood by the cerebral tissue and represents the balance between oxygen delivery and consumption [50].

Simultaneous continuous measurement of the oxygenation index, i.e., $[\Delta\text{HbO}_2 - \Delta\text{HHb}]$ or TOI from NIRS, and arterial blood pressure, can be used to determine if blood pressure changes are reflected in cerebral perfusion and oxygenation [51, 52]. A strong correlating relationship between the two signals may indicate the lack of CBF autoregulation, and has been quantified by a measure of the correlation in the frequency domain, called coherence. Several studies have reported the association between high coherence in preterm infants (impaired autoregulation) at very low frequencies, i.e., the co-fluctuation of the signals over periods of 25 s–5 min, and adverse clinical indices including low CRIB score, and germinal matrix/intraventricular hemorrhage [51–54].

Most neonatal NIRS studies focused particularly on infants at risk of brain injury, and aimed to determine if NIRS measurements would indicate subsequent neurodevelopmental abnormalities. Previous studies in animals and humans using NIRS have found a cerebral oxygenation of 40–50 % [55–57] to be the limits below which significant cerebral hypoxia with poor neurologic outcome occurs. Preterm infants in the NICU with cerebral oxygenation <50 % for >10 % of time during the first 72 h of life had a lower neurodevelopmental score at 18 months [58]. Several reviews of neonatal cerebral hemodynamic studies utilizing NIRS measurements have been published [32, 59, 60].

3.2.4 Functional NIRS, and Comparison with fMRI

NIRS has been applied to functional brain imaging in infants to elucidate the connections between localized cortical activity and hemodynamic responses during early human development. Brain activity due to a specific stimulation leads to an increase in the local oxygen consumption immediately followed by an increase in blood flow [61]. Typical changes in HbO₂ and HHb during functional

activation of the adult brain involve an increase in the concentration of HbO_2 , which is accompanied by a lesser decrease in HHb concentration. The situation appears to be very different in the neonate and in particular in preterm infants [62–66]. Depending on the age of infants and possibly other unknown factors, the HHb sometimes increases or decreases during activation. For functional NIRS (fNIRS), changes in HbO_2 and HbT may therefore be more reliable markers of brain activity than changes in HHb. This may be due to immaturity of the flow-metabolism coupling which may affect the pattern of response to neural activity.

Adult studies suggest that the characteristics of the vascular response measured by NIRS are comparable to the BOLD response seen in fMRI. It is important to note that unlike fMRI BOLD, fNIRS provides a separate measure of quantified changes in both HbO_2 and HHb. It has also been shown that the HHb signal follows the BOLD signal more closely than does the HbO_2 signal [67, 68]. The balance of cerebral oxygen consumption and cerebral blood flow/volume increase determines whether HHb may increase, decrease, or remain the same, depending on factors such as age, the region studied, and sleep/sedation status [23, 69–71]. Therefore, HHb alone is not a reliable marker for functional activation, especially in neonatal studies in which various patterns of HHb response have been reported. As an increase in HbO_2 with no significant HHb change would not represent activation in a BOLD signal study, the BOLD signal may miss many activations in neonates.

Though fMRI and fNIRS measure the same hemodynamic response, generally fMRI techniques have an intrinsically limited acquisition rate usually at a minimum of 1 Hz [72] whereas fNIRS has high temporal resolution and can acquire data rapidly, up to hundreds of hertz [67]. However, depth resolution of fNIRS is dependant on the age of the infant and the optical properties of the tissue [31]; the technique offers lower spatial resolution compared with MRI, and is unable to assess brain structures for anatomical reference.

3.2.5 Interpretation

Oxygenation indices derived from NIRS, such as the Hb difference signal (HbD), calculated by $\Delta\text{HbO}_2 - \Delta\text{HHb}$, or the TOI, have been used and validated as surrogates of CBF [73, 74]. Notably, while TOI reflects CBF, it is more sensitive to variations of CBF of low frequency (≤ 0.1 Hz) than to more rapid, higher frequency changes. Changes in cerebral oxygenation measured by NIRS are likely to occur at a slower rate than CBF due to the time delay in achieving equilibrium of oxygenation in the venous blood pool, as changes in cerebral oxygen extraction are slow to compensate for changes in CBF [74].

Furthermore, NIRS provides a weighted average of the saturations within the venous and arterial compartments in the region of

tissue illuminated; this weighting is difficult to determine precisely and may differ over time. There is also inhomogeneous regional blood distribution and variation in the relative proportion of arterial and venous volumes within the brain. Although it is critical for fully interpreting cerebral oxygenation measurements, available data on cerebral arterial and venous volume fractions are very limited, especially in the newborn brain. Using various imaging techniques, the baseline cerebral arterial volume fraction has been found to be 25 % in normal adults [75] and 25–30 % in adult animals [76] under normoxic conditions. During hypoxemia, significant arterial vasodilatation occurs at lower arterial oxygenation, making the assumed cerebral arterial-venous volume ratio of 25:75 erroneously low [77]. Other common conditions in sick infants, such as hypercapnia, hypotension, or vasoparalysis due to hypoxic-ischaemic injury, could also increase baseline CBV and change the cerebral arterial-venous volume ratio. Further studies are warranted to investigate the arterial-venous volume ratio in these conditions, together with the corresponding effects on measurements of mixed cerebral oxygenation by NIRS.

Another difficulty in interpretation of NIRS measurement lies with the lack of detail in the underlying physiological components of the signal output from which the change in cerebral oxygenation is derived. For example, reduced cerebral oxygenation may be due to reduced CBF, increased cerebral oxygen extraction, increased oxygen demand, or a combination of these factors, but it is often difficult to differentiate between these possible mechanisms based on conventional NIRS measurements. This lack of mechanistic insight also makes the clinical interpretation and application of the NIRS measurements more difficult.

3.2.6 Limitation, Accuracy, and Precision

Although a significant improvement on previous techniques, NIRS is not without its own limitations. These include a relatively high signal-to-noise ratio, susceptibility to movement artefact, and intra-patient and inter-patient variation [78]. The anatomical structure of the head as well as the curvature of the skull vary within and between individuals. A major challenge is to ensure that the probe sits flat and securely against the head. Hair will cause attenuation of the light and further increase the signal artefacts due to movement of the infant, leading to decrease in signal-to-noise ratio and unreliable measurements. Another concern is the nonspecific, regional measurement of tissue oxygenation which includes measurement of all tissues between the light source and the detector including skin, bone, cerebrospinal fluid, and brain matter to an unknown depth [79]. In the neonate, this is a relatively smaller problem because the skin, scalp, and skull are thin [31].

It is difficult to assess the accuracy of NIRS-based cerebral oximetry in the neonatal population because there is no gold

standard or other means of measuring mixed cerebral oxygen saturation and it is not feasible to sample blood from cerebral veins in human newborns. Other studies in older children and adults have compared values of cerebral oximetry with values in the jugular bulb or central venous return. However, jugular or central venous saturations represent global measurements including extracerebral tissue, and they may differ significantly from the actual cerebral venous saturation. Accuracy, as defined by the mean difference (bias) in Bland-Altman analysis, is typically within 5 % [80–84]. We have performed the comparison with sagittal sinus venous saturation in newborn lambs assuming a cerebral arterial-to-venous volume ratio of 25:75 [77], and found that the mean difference was 0.07 % for NIRS-measured mixed cerebral oxygenation between 40 and 60 %. However the mean difference widened to 9–10 % for NIRS-measured mixed cerebral oxygenation of <40 %, probably due to cerebral arterial vasodilatation during hypoxemia, increased cerebral arterial-to-venous volume ratio, and therefore dominance of the cerebral arterial saturation towards the NIRS measurement [77].

In vitro precision of NIRS-based tissue oximetry determined on optical phantoms is good, with values of 1–2 % [45]. However, in vivo precision is less satisfactory with wider limits of agreement and poor repeatability, in the range of 5–8 % [85, 86], in comparison with pulse oximetry which also uses red/infrared light for measurement with the repeatability of 2–3 %. The problem appears to be associated with the replacement of sensors. Possibly the sensors are sensitive to small local heterogeneities of the surface geometry and optical properties of tissue (hair, blood vessels, sub-arachnoidal space, gyral folding) [79]. For clinical application, a precision less than 3 % is desirable.

3.3 Diffusion Correlation Spectroscopy

Diffuse optical correlation spectroscopy (DCS) is a new technique for which portable devices are currently being developed to measure changes in CBF at the bedside. DCS continuously monitors relative changes in microvascular CBF (absolute calculations have not been quantified to date) [87–89] as opposed to NIRS that monitors cerebral blood oxygen saturation and volume. DCS detects blood flow by quantifying temporal fluctuations of NIR light fields emerging from the tissue surface. NIR laser light is introduced into the brain tissue where it is scattered by moving red blood cells in tissue vasculature before emerging from the tissue surface. This “dynamic” scattering from moving red blood cells [60] causes the detected intensity to fluctuate with time. Based on the photon arrival times at the detector location, an intensity temporal autocorrelation function of the collected light is calculated. A blood flow index (BFI) with units of cm^2/s is derived from the intensity temporal autocorrelation function. Changes in cerebral

BFI relative to the baseline measurement reflect changes in CBF. DCS requires only one wavelength and can be chosen based on laser availability and cost. Being a relatively new technique, most DCS instruments have been custom-built and not commercially available.

DCS measures of relative blood flow have been extensively validated using comparisons to literature [90, 91], to Doppler ultrasound in preterm human brain [92], to arterial spin-labeled perfusion MRI in human brain [91, 93], and to flow and fluorescent microspheres in animal brains [87]. It has also been used to measure blood flow in many organs, including muscle, and breast [94, 95]. In both adults and children, validation studies have demonstrated that the changes in cerebral BFI relative to the baseline measurement measured by DCS correlate with relative changes in CBF measured by other modalities [87].

DCS can be used in the neonatal population, as it is portable, does not involve radiation, and offers continuous and noninvasive measurement of relative changes in regional cortical CBF. As continuous-wave NIRS devices that measure regional cerebral oxygenation are already in widespread use in research and also clinically in some ICUs, DCS can potentially be combined with NIRS to provide continuous simultaneous measurement of changes in CBF and cerebral oxygenation. The combination of NIRS with DCS also enables the quantification of regional $CMRO_2$ [96], a parameter that may indicate neuronal status and activity. This information provides the clinician with a more complete assessment of cerebral physiology than either $rScO_2$ or CBF alone. For example, an increase in $rScO_2$ may be due to a CBF rise which exceeds metabolic demand, or may be due to a reduced $CMRO_2$. Conversely, if decreases in $rScO_2$ are observed, simultaneous CBF measurements can help ascertain whether these decreases are due to reduced oxygen delivery (e.g., CBF decreases due to decreased blood pressure or cardiac output) or due to increased oxygen consumption not matched by oxygen delivery. Future potential for DCS combined with NIRS to inform clinical management based on optimizing regional cerebral $rScO_2$ in relation to $CMRO_2$ should be explored, as an alternative to strategies based on a single cerebral $rScO_2$ measurement or secondary systemic parameters, such as blood pressure or arterial oxygen saturation. DCS can also be potentially combined with other modalities such as Doppler ultrasound or electroencephalography, to augment information on cerebral physiology and inform clinical management.

There are still relatively few published reports on DCS use, particularly in newborn and infants which is a very suitable population for DCS due to the thinner extra-cerebral layers. The signal-to-noise ratio is higher with higher reproducibility of BFI and greater sensitivity to cortical tissue as compared to adult. Examples of neonatal studies utilizing DCS include demonstration of cerebral

hemodynamics in VLBW preterm infants during a small postural change [92], and dose-dependent increases in CBF following treatment of metabolic acidosis using sodium bicarbonate [97]. Such information may be especially important in adjusting clinical management to avoid large and rapid CBF fluctuations which may lead to brain injury, in particular intraventricular hemorrhage in preterm infants. The combination of NIRS-measured cerebral oxygenation and DCS-measured BFI has been utilized to derive quantitative information on changes in cerebral oxygen metabolism in infants who suffered hypoxic-ischaemic encephalopathy and underwent therapeutic hypothermia [98] and in infants who underwent neonatal cardiac surgery [99] and developmental changes in cerebral oxygen metabolism in preterm infants [100], as well as in functional studies to understand the coupling relationship between neuronal metabolism and CBF in the preterm brain [101].

There are several limitations of DCS measurements. While changes in cerebral BFI relative to the baseline measurement reflect changes in CBF, the quantification of absolute BFI is limited [102, 103], and remains to be determined across a wide range of subjects and tissue types. Another significant limitation of DCS is its susceptibility to motion artifacts. Blood flow measurements in DCS are derived from light intensity fluctuations due to moving red blood cells, and therefore additional movement of the probe can increase the signal-to-noise ratio in the measurement. In addition, the penetration depth of DCS is limited. Like NIRS, a common rule of thumb for DCS is that it measures a tissue depth underneath the optical probe that is roughly one-third to one-half of the source-detector separation; thus, typical DCS experimental setups with source-detector separations of 2–3 cm would interrogate and measure superficial cortical regions. To increase the penetration depth, larger source-detector separations are required. Nevertheless, the use of larger source-detector separation configurations leads to a lower signal-to-noise ratio, especially since DCS optimally requires single-mode detection fibers for measurement of the intensity autocorrelation function, which has relatively low throughput. This low signal-to-noise ratio becomes even more problematic in the presence of hair and/or dark skin.

4 Summary

There has been increasing research interest and clinical demand to study the neonatal brain, with the exploration of the bedside and real-time measurement of cerebral hemodynamics in guiding therapy and predicting outcome. The research modalities have the potential to be combined to provide complementary information on preterm cerebrovascular physiology, and its relation to brain

injury and therapy. Importantly, the measurements are required to be reliable and reproducible, and reference/target ranges are yet to be established.

Effective brain-oriented neonatal intensive care is mainly impeded by two major obstacles: firstly, the lack of clinically relevant parameters for cotside monitoring of cerebral perfusion and oxygenation; secondly, not knowing whether maintaining the cerebral hemodynamic parameters within a “normal” range would translate into improved outcomes for preterm infants. Prospective trials demonstrating the use of these tools in guiding treatment, and evidence that maintaining predefined and targeted cerebral hemodynamic measurements improves clinically relevant outcomes for preterm infants, are clearly important [104]. Future research should also aim to determine the limits beyond which changes in cerebral hemodynamics become injurious to the developing preterm brain.

References

- Martin JA, Kung HC, Mathews TJ, Hoyert DL, Strobino DM, Guyer B et al (2008) Annual summary of vital statistics: 2006. *Pediatrics* 121(4):788–801
- Costeloe KL, Hennessy EM, Haider S, Stacey F, Marlow N, Draper ES (2012) Short term outcomes after extreme preterm birth in England: comparison of two birth cohorts in 1995 and 2006 (the EPICure studies). *BMJ* 345:e7976
- Doyle LW, Roberts G, Anderson PJ (2010) Outcomes at age 2 years of infants < 28 weeks' gestational age born in Victoria in 2005. *J Pediatr* 156(1):49–53.e1
- Wolke D, Samara M, Bracewell M, Marlow N (2008) Specific language difficulties and school achievement in children born at 25 weeks of gestation or less. *J Pediatr* 152(2):256–262
- Moore T, Hennessy EM, Myles J, Johnson SJ, Draper ES, Costeloe KL et al (2012) Neurological and developmental outcome in extremely preterm children born in England in 1995 and 2006: the EPICure studies. *BMJ* 345:e7961
- Woodward LJ, Anderson PJ, Austin NC, Howard K, Inder TE (2006) Neonatal MRI to predict neurodevelopmental outcomes in preterm infants. *N Engl J Med* 355(7):685–694
- Nongena P, Ederies A, Azzopardi DV, Edwards AD (2010) Confidence in the prediction of neurodevelopmental outcome by cranial ultrasound and MRI in preterm infants. *Arch Dis Child Fetal Neonatal Ed* 95(6):F388–F390
- Khwaja O, Volpe JJ (2008) Pathogenesis of cerebral white matter injury of prematurity. *Arch Dis Child Fetal Neonatal Ed* 93(2):F153–F161
- Kety SS, Schmidt CF (1946) The effects of active and passive hyperventilation on cerebral blood flow, cerebral oxygen consumption, cardiac output, and blood pressure of normal young men. *J Clin Invest* 25(1):107–119
- Skov L, Pryds O, Greisen G (1991) Estimating cerebral blood flow in newborn infants: comparison of near infrared spectroscopy and ¹³³Xe clearance. *Pediatr Res* 30(6):570–573
- Altman DI, Perlman JM, Volpe JJ, Powers WJ (1993) Cerebral oxygen metabolism in newborns. *Pediatrics* 92(1):99–104
- Borch K, Greisen G (1998) Blood flow distribution in the normal human preterm brain. *Pediatr Res* 43(1):28–33
- Wang J, Licht DJ, Jahng GH, Liu CS, Rubin JT, Haselgrove J et al (2003) Pediatric perfusion imaging using pulsed arterial spin labeling. *J Magn Reson Imaging* 18(4):404–413
- Baron JC (2001) Perfusion thresholds in human cerebral ischemia: historical perspective and therapeutic implications. *Cerebrovasc Dis* 11(Suppl 1):2–8
- Meek JH, Tyszczuk L, Elwell CE, Wyatt JS (1998) Cerebral blood flow increases over the first three days of life in extremely preterm neonates. *Arch Dis Child Fetal Neonatal Ed* 78(1):F33–F37

16. Miranda MJ, Olofsson K, Sidaros K (2006) Noninvasive measurements of regional cerebral perfusion in preterm and term neonates by magnetic resonance arterial spin labeling. *Pediatr Res* 60(3):359–363
17. Biagi L, Abbruzzese A, Bianchi MC, Alsop DC, Del Guerra A, Tosetti M (2007) Age dependence of cerebral perfusion assessed by magnetic resonance continuous arterial spin labeling. *J Magn Reson Imaging* 25(4):696–702
18. Buxton RB (2010) Interpreting oxygenation-based neuroimaging signals: the importance and the challenge of understanding brain oxygen metabolism. *Front Neuroenergetics* 2:8
19. Colonnese MT, Phillips MA, Constantine-Paton M, Kaila K, Jasanoff A (2008) Development of hemodynamic responses and functional connectivity in rat somatosensory cortex. *Nat Neurosci* 11(1):72–79
20. Seghier ML, Lazeyras F, Huppi PS (2006) Functional MRI of the newborn. *Semin Fetal Neonatal Med* 11(6):479–488
21. Heep A, Scheef L, Jankowski J, Born M, Zimmermann N, Sival D et al (2009) Functional magnetic resonance imaging of the sensorimotor system in preterm infants. *Pediatrics* 123(1):294–300
22. Seghier ML, Lazeyras F, Zimine S, Maier SE, Hanquinet S, Delavelle J et al (2004) Combination of event-related fMRI and diffusion tensor imaging in an infant with perinatal stroke. *Neuroimage* 21(1):463–472
23. Marcar VL, Schwarz U, Martin E, Loenneker T (2006) How depth of anesthesia influences the blood oxygenation level-dependent signal from the visual cortex of children. *AJNR Am J Neuroradiol* 27(4):799–805
24. Mullinger KJ, Mayhew SD, Bagshaw AP, Bowtell R, Francis ST (2014) Evidence that the negative BOLD response is neuronal in origin: a simultaneous EEG-BOLD-CBF study in humans. *Neuroimage* 94:263–274
25. Aaslid R, Markwalder TM, Nornes H (1982) Noninvasive transcranial Doppler ultrasound recording of flow velocity in basal cerebral arteries. *J Neurosurg* 57(6):769–774
26. Panerai RB (2009) Transcranial Doppler for evaluation of cerebral autoregulation. *Clin Auton Res* 19(4):197–211
27. Boylan GB, Young K, Panerai RB, Rennie JM, Evans DH (2000) Dynamic cerebral autoregulation in sick newborn infants. *Pediatr Res* 48(1):12–17
28. Kaiser JR, Gauss CH, Williams DK (2005) The effects of hypercapnia on cerebral autoregulation in ventilated very low birth weight infants. *Pediatr Res* 58(5):931–935
29. Delpy DT, Cope M (1997) Quantification in tissue near-infrared spectroscopy. *Philos Trans Roy Soc Lond Ser B Biol Sci* 352:649–659
30. Elwell C (1995) A practical user's guide to near infrared spectroscopy. Hamamatsu Photonics KK, Hamamatsu City
31. Fukui Y, Ajichi Y, Okada E (2003) Monte Carlo prediction of near-infrared light propagation in realistic adult and neonatal head models. *Appl Opt* 42(16):2881–2887
32. Wolf M, Greisen G (2009) Advances in near-infrared spectroscopy to study the brain of the preterm and term neonate. *Clin Perinatol* 36(4):807–834, vi
33. Brown DW, Picot PA, Nacini JG, Springett R, Delpy DT, Lee TY (2002) Quantitative near infrared spectroscopy measurement of cerebral hemodynamics in newborn piglets. *Pediatr Res* 51(5):564–570
34. Hebden JC (2003) Advances in optical imaging of the newborn infant brain. *Psychophysiology* 40(4):501–510
35. Duncan A, Meek JH, Clemence M, Elwell CE, Tyszczuk L, Cope M et al (1995) Optical pathlength measurements on adult head, calf and forearm and the head of the newborn infant using phase resolved optical spectroscopy. *Phys Med Biol* 40(2):295–304
36. Ferrari M, Mottola L, Quaresima V (2004) Principles, techniques, and limitations of near infrared spectroscopy. *Can J Appl Physiol* 29(4):463–487
37. Kohl M, Watson R, Chow G, Roberts I, Delpy D, Cope M (1997) Monitoring of cerebral hemodynamics during open-heart surgery in children using near infrared intensity modulated spectroscopy. *Proc SPIE* 2979:408–416
38. Schmidt FE (1999) Development of a time-resolved optical tomography system for neonatal brain imaging. PhD thesis. London: University College London
39. Chance B, Nioka S, Kent J, McCully K, Fountain M, Greenfeld R et al (1988) Time-resolved spectroscopy of hemoglobin and myoglobin in resting and ischemic muscle. *Anal Biochem* 174(2):698–707
40. Hebden JC, Gibson A, Yusof RM, Everdell N, Hillman EM, Delpy DT et al (2002) Three-dimensional optical tomography of the premature infant brain. *Phys Med Biol* 47(23):4155–4166
41. Nicklin SE, Hassan IA, Wickramasinghe YA, Spencer SA (2003) The light still shines, but not that brightly? The current status of perinatal near infrared spectroscopy. *Arch Dis Child Fetal Neonatal Ed* 88(4):F263–F268

42. Edwards AD, Wyatt JS, Richardson C, Delpy DT, Cope M, Reynolds EO (1988) Cotside measurement of cerebral blood flow in ill newborn infants by near infrared spectroscopy. *Lancet* 2(8614):770–771
43. Patel J, Marks K, Roberts I, Azzopardi D, Edwards AD (1998) Measurement of cerebral blood flow in newborn infants using near infrared spectroscopy with indocyanine green. *Pediatr Res* 43(1):34–39
44. Corlu A, Choe R, Durduran T, Lee K, Schweiger M, Arridge SR et al (2005) Diffuse optical tomography with spectral constraints and wavelength optimization. *Appl Opt* 44(11):2082–2093
45. Suzuki STS, Ozaki T, Kobayashi Y (1999) A tissue oxygenation monitor using NIR spatially resolved spectroscopy. *Proc SPIE* 3597:582–592
46. Blasi A, Fox S, Everdell N, Volein A, Tucker L, Csibra G et al (2007) Investigation of depth dependent changes in cerebral haemodynamics during face perception in infants. *Phys Med Biol* 52(23):6849–6864
47. Franceschini MA, Joseph DK, Huppert TJ, Diamond SG, Boas DA (2006) Diffuse optical imaging of the whole head. *J Biomed Opt* 11(5):054007
48. Wong FY, Barfield CP, Campbell L, Brodecky VA, Walker AM (2008) Validation of cerebral venous oxygenation measured using near-infrared spectroscopy and partial jugular venous occlusion in the newborn lamb. *J Cereb Blood Flow Metab* 28(1):74–80
49. Kissack CM, Garr R, Wardle SP, Weindling AM (2005) Cerebral fractional oxygen extraction is inversely correlated with oxygen delivery in the sick, newborn, preterm infant. *J Cereb Blood Flow Metab* 25(5):545–553
50. Naulaers G, Meyns B, Miserez M, Leunens V, Van Huffel S, Casaer P et al (2007) Use of tissue oxygenation index and fractional tissue oxygen extraction as non-invasive parameters for cerebral oxygenation. A validation study in piglets. *Neonatology* 92(2):120–126
51. Tsuji M, Saul JP, du Plessis A, Eichenwald E, Sobh J, Crocker R et al (2000) Cerebral intravascular oxygenation correlates with mean arterial pressure in critically ill premature infants. *Pediatrics* 106(4):625–632
52. Wong FY, Leung TS, Austin T, Wilkinson M, Meek JH, Wyatt JS et al (2008) Impaired autoregulation in preterm infants identified by using spatially resolved spectroscopy. *Pediatrics* 121(3):e604–e611
53. Soul JS, Hammer PE, Tsuji M, Saul JP, Bassan H, Limperopoulos C et al (2007) Fluctuating pressure-passivity is common in the cerebral circulation of sick premature infants. *Pediatr Res* 61(4):467–473
54. O’Leary H, Gregas MC, Limperopoulos C, Zaretskaya I, Bassan H, Soul JS et al (2009) Elevated cerebral pressure passivity is associated with prematurity-related intracranial hemorrhage. *Pediatrics* 124(1):302–309
55. Hagino I, Anttila V, Zurakowski D, Duebener LF, Lidov HG, Jonas RA (2005) Tissue oxygenation index is a useful monitor of histologic and neurologic outcome after cardiopulmonary bypass in piglets. *J Thorac Cardiovasc Surg* 130(2):384–392
56. Phelps HM, Mahle WT, Kim D, Simsic JM, Kirshbom PM, Kanter KR et al (2009) Post-operative cerebral oxygenation in hypoplastic left heart syndrome after the Norwood procedure. *Ann Thorac Surg* 87(5):1490–1494
57. Hou X, Ding H, Teng Y, Zhou C, Tang X, Li S (2007) Research on the relationship between brain anoxia at different regional oxygen saturations and brain damage using near-infrared spectroscopy. *Physiol Meas* 28(10):1251–1265
58. Alderliesten T, Lemmers PM, van Haastert IC, de Vries LS, Bonestroo HJ, Baerts W et al (2014) Hypotension in preterm neonates: low blood pressure alone does not affect neurodevelopmental outcome. *J Pediatr* 164:986
59. Fyfe KL, Yiallourou SR, Wong FY, Horne RS (2014) The development of cardiovascular and cerebral vascular control in preterm infants. *Sleep Med Rev* 18:299
60. Goff DA, Buckley EM, Durduran T, Wang J, Licht DJ (2010) Noninvasive cerebral perfusion imaging in high-risk neonates. *Semin Perinatol* 34(1):46–56
61. Thompson JK, Peterson MR, Freeman RD (2003) Single-neuron activity and tissue oxygenation in the cerebral cortex. *Science* 299(5609):1070–1072
62. Greisen G, Hellstrom-Vestas L, Lou H, Rosen I, Svenningsen N (1985) Sleep-waking shifts and cerebral blood flow in stable preterm infants. *Pediatr Res* 19(11):1156–1159
63. Bartocci M, Bergqvist LL, Lagercrantz H, Anand KJ (2006) Pain activates cortical areas in the preterm newborn brain. *Pain* 122(1–2):109–117
64. Bartocci M, Winberg J, Papendieck G, Mus-tica T, Serra G, Lagercrantz H (2001) Cerebral hemodynamic response to unpleasant odors in the preterm newborn measured by near-infrared spectroscopy. *Pediatr Res* 50(3):324–330

65. Meek JH, Firbank M, Elwell CE, Atkinson J, Braddick O, Wyatt JS (1998) Regional hemodynamic responses to visual stimulation in awake infants. *Pediatr Res* 43(6):840–843
66. Slater R, Cantarella A, Gallella S, Worley A, Boyd S, Meek J et al (2006) Cortical pain responses in human infants. *J Neurosci* 26(14):3662–3666
67. Huppert TJ, Hoge RD, Diamond SG, Franceschini MA, Boas DA (2006) A temporal comparison of BOLD, ASL, and NIRS hemodynamic responses to motor stimuli in adult humans. *Neuroimage* 29(2):368–382
68. Toronov V, Walker S, Gupta R, Choi JH, Gratton E, Hueber D et al (2003) The roles of changes in deoxyhemoglobin concentration and regional cerebral blood volume in the fMRI BOLD signal. *Neuroimage* 19(4):1521–1531
69. Meek J (2002) Basic principles of optical imaging and application to the study of infant development. *Dev Sci* 5(3):371–380
70. Marcar VL, Strassle AE, Loenneker T, Schwarz U, Martin E (2004) The influence of cortical maturation on the BOLD response: an fMRI study of visual cortex in children. *Pediatr Res* 56(6):967–974
71. Wilcox T, Bortfeld H, Woods R, Wruck E, Boas DA (2008) Hemodynamic response to featural changes in the occipital and inferior temporal cortex in infants: a preliminary methodological exploration. *Dev Sci* 11(3):361–370
72. Lloyd-Fox S, Blasi A, Elwell CE (2010) Illuminating the developing brain: the past, present and future of functional near infrared spectroscopy. *Neurosci Biobehav Rev* 34(3):269–284
73. Tsuji M, duPlessis A, Taylor G, Crocker R, Volpe JJ (1998) Near infrared spectroscopy detects cerebral ischemia during hypotension in piglets. *Pediatr Res* 44(4):591–595
74. Wong FY, Nakamura M, Alexiou T, Brodecky V, Walker AM (2009) Tissue oxygenation index measured using spatially resolved spectroscopy correlates with changes in cerebral blood flow in newborn lambs. *Intensive Care Med* 35(8):1464–1470
75. An H, Lin W (2002) Cerebral venous and arterial blood volumes can be estimated separately in humans using magnetic resonance imaging. *Magn Reson Med* 48(4):583–588
76. Lee SP, Duong TQ, Yang G, Iadecola C, Kim SG (2001) Relative changes of cerebral arterial and venous blood volumes during increased cerebral blood flow: implications for BOLD fMRI. *Magn Reson Med* 45(5):791–800
77. Wong FY, Alexiou T, Samarasinghe T, Brodecky V, Walker AM (2010) Cerebral arterial and venous contributions to tissue oxygenation index measured using spatially resolved spectroscopy in newborn lambs. *Anesthesiology* 113(6):1385–1391
78. van Bel F, Lemmers P, Naulaers G (2008) Monitoring neonatal regional cerebral oxygen saturation in clinical practice: value and pitfalls. *Neonatology* 94(4):237–244
79. Leung TS, Elwell CE, Delpy DT (2005) Estimation of cerebral oxy- and deoxyhaemoglobin concentration changes in a layered adult head model using near-infrared spectroscopy and multivariate statistical analysis. *Phys Med Biol* 50(24):5783–5798
80. Daubeney PE, Pilkington SN, Janke E, Charlton GA, Smith DC, Webber SA (1996) Cerebral oxygenation measured by near-infrared spectroscopy: comparison with jugular bulb oximetry. *Ann Thorac Surg* 61(3):930–934
81. Nagdyman N, Fleck T, Barth S, Abdul-Khalik H, Stiller B, Ewert P et al (2004) Relation of cerebral tissue oxygenation index to central venous oxygen saturation in children. *Intensive Care Med* 30(3):468–471
82. Nagdyman N, Fleck T, Schubert S, Ewert P, Peters B, Lange PE et al (2005) Comparison between cerebral tissue oxygenation index measured by near-infrared spectroscopy and venous jugular bulb saturation in children. *Intensive Care Med* 31(6):846–850
83. Weiss M, Dullenkopf A, Kolarova A, Schulz G, Frey B, Baenziger O (2005) Near-infrared spectroscopic cerebral oxygenation reading in neonates and infants is associated with central venous oxygen saturation. *Paediatr Anaesth* 15(2):102–109
84. Ranucci M, Isgro G, De la Torre T, Romitti F, Conti D, Carlucci C (2008) Near-infrared spectroscopy correlates with continuous superior vena cava oxygen saturation in pediatric cardiac surgery patients. *Paediatr Anaesth* 18(12):1163–1169
85. Lemmers PM, van Bel F (2009) Left-to-right differences of regional cerebral oxygen saturation and oxygen extraction in preterm infants during the first days of life. *Pediatr Res* 65(2):226–230
86. Sorensen LC, Greisen G (2006) Precision of measurement of cerebral tissue oxygenation index using near-infrared spectroscopy in preterm neonates. *J Biomed Opt* 11(5):054005

87. Durduran T, Yodh AG (2014) Diffuse correlation spectroscopy for non-invasive, microvascular cerebral blood flow measurement. *Neuroimage* 85(Pt 1):51–63
88. Culver JP, Durduran T, Cheung C, Furuya D, Greenberg JH, Yodh AG (2003) Diffuse optical measurement of hemoglobin and cerebral blood flow in rat brain during hypercapnia, hypoxia and cardiac arrest. *Adv Exp Med Biol* 510:293–297
89. Zhou C, Yu G, Furuya D, Greenberg J, Yodh A, Durduran T (2006) Diffuse optical correlation tomography of cerebral blood flow during cortical spreading depression in rat brain. *Opt Express* 14(3):1125–1144
90. Culver JP, Durduran T, Furuya D, Cheung C, Greenberg JH, Yodh AG (2003) Diffuse optical tomography of cerebral blood flow, oxygenation, and metabolism in rat during focal ischemia. *J Cereb Blood Flow Metab* 23(8):911–924
91. Durduran T, Yu G, Burnett MG, Detre JA, Greenberg JH, Wang J et al (2004) Diffuse optical measurement of blood flow, blood oxygenation, and metabolism in a human brain during sensorimotor cortex activation. *Opt Lett* 29(15):1766–1768
92. Buckley EM, Cook NM, Durduran T, Kim MN, Zhou C, Choe R et al (2009) Cerebral hemodynamics in preterm infants during positional intervention measured with diffuse correlation spectroscopy and transcranial Doppler ultrasound. *Opt Express* 17(15):12571–12581
93. Yu G, Floyd TF, Durduran T, Zhou C, Wang J, Detre JA et al (2007) Validation of diffuse correlation spectroscopy for muscle blood flow with concurrent arterial spin labeled perfusion MRI. *Opt Express* 15(3):1064–1075
94. Yu G, Durduran T, Lech G, Zhou C, Chance B, Mohler ER 3rd et al (2005) Time-dependent blood flow and oxygenation in human skeletal muscles measured with noninvasive near-infrared diffuse optical spectroscopies. *J Biomed Opt* 10(2):024027
95. Zhou C, Choe R, Shah N, Durduran T, Yu G, Durkin A et al (2007) Diffuse optical monitoring of blood flow and oxygenation in human breast cancer during early stages of neoadjuvant chemotherapy. *J Biomed Opt* 12(5):051903
96. Verdecchia K, Diop M, Lee TY, St. Lawrence K (2013) Quantifying the cerebral metabolic rate of oxygen by combining diffuse correlation spectroscopy and time-resolved near-infrared spectroscopy. *J Biomed Opt* 18(2):27007
97. Buckley EM, Naim MY, Lynch JM, Goff DA, Schwab PJ, Diaz LK et al (2013) Sodium bicarbonate causes dose-dependent increases in cerebral blood flow in infants and children with single-ventricle physiology. *Pediatr Res* 73(5):668–673
98. Dehaes M, Aggarwal A, Lin PY, Rosa Fortuno C, Fenoglio A, Roche-Labarbe N et al (2014) Cerebral oxygen metabolism in neonatal hypoxic ischemic encephalopathy during and after therapeutic hypothermia. *J Cereb Blood Flow Metab* 34(1):87–94
99. Buckley EM, Lynch JM, Goff DA, Schwab PJ, Baker WB, Durduran T et al (2013) Early postoperative changes in cerebral oxygen metabolism following neonatal cardiac surgery: effects of surgical duration. *J Thorac Cardiovasc Surg* 145(1):196–203, 205.e1; discussion 203–205
100. Roche-Labarbe N, Carp SA, Surova A, Patel M, Boas DA, Grant PE et al (2010) Noninvasive optical measures of CBV, StO(2), CBF index, and rCMRO(2) in human premature neonates' brains in the first six weeks of life. *Hum Brain Mapp* 31(3):341–352
101. Roche-Labarbe N, Fenoglio A, Radhakrishnan H, Kocienski-Filip M, Carp SA, Dubb J et al (2014) Somatosensory evoked changes in cerebral oxygen consumption measured non-invasively in premature neonates. *Neuroimage* 85(Pt 1):279–286
102. Jain V, Buckley EM, Licht DJ, Lynch JM, Schwab PJ, Naim MY et al (2014) Cerebral oxygen metabolism in neonates with congenital heart disease quantified by MRI and optics. *J Cereb Blood Flow Metab* 34(3):380–388
103. Zhou C, Eucker SA, Durduran T, Yu G, Ralston J, Friess SH et al (2009) Diffuse optical monitoring of hemodynamic changes in piglet brain with closed head injury. *J Biomed Opt* 14(3):034015
104. Pellicer A, Greisen G, Benders M, Claris O, Dempsey E, Fumagally M et al (2013) The SafeBoosC phase II randomised clinical trial: a treatment guideline for targeted near-infrared-derived cerebral tissue oxygenation versus standard treatment in extremely preterm infants. *Neonatology* 104(3):171–178

Fetal Sleep and Spontaneous Behavior In Utero: Animal and Clinical Studies

Dan Rurak

Abstract

The term fetal behavior includes fetal sleep states, which in precocial mammalian species (i.e., those born relatively mature at birth) develop in late gestation, along with the fetal physiological processes, such as fetal body movements and breathing activity, cardiovascular function, blood gas, and acid-base status, which are linked to fetal sleep states. Since ~1970, as a result of technological and technical advances, there has been significant advances in our understanding of fetal behavior in man and animals, and also the development of fetal monitoring techniques in human pregnancy that are based on the changes in fetal behavioral variables that are altered in pathophysiological complications of pregnancy. In species such as sheep, guinea pigs, and primates, including the human, fetal sleep states, comprised primarily of quiet sleep and REM sleep, develop in the second half of gestation. Fetal motility in the form of body and breathing movements develop earlier in gestation, but when fetal sleep states develop they become linked to these states. In all species, fetal breathing is episodic occurring about 40 % of the time. In the fetal lamb, fetal breathing activity occurs only in REM sleep, whereas in primates, breathing occurs in both sleep states although the character of the breathing movements changes with sleep state. Fetal body movements occur in both sleep states, but vigorous body movements occur mainly during brief periods of a more aroused state, in which vigorous breathing and fetal swallowing also occur. However this aroused state is unlikely to represent wakefulness. Although they do not fulfil the functions that they will after birth, fetal breathing and body movements are important for the development of the lung and musculoskeletal system, respectively. Uterine activity, in the form of pre-labor contractions, which appear to occur in all species, can also affect fetal behavioral activity, particularly in species, like sheep, where the contractions are quiet long (5 min). There are also circadian rhythms in breathing and body movements, and various other fetal variables, with a higher incidence breathing and motility at night. Evidence from sheep indicates that the fetal circadian rhythms are derived from the maternal melatonin rhythm via maternal to fetal transfer of maternal melatonin. Fetal movements are associated with transient changes in fetal heart rate, usually accelerations, and this response forms the basis of the non-stress test and is an element of the fetal biophysical profile score, which are commonly used diagnostic methods to assess fetal well-being in human pregnancies. The transient accelerations in fetal heart rate increase cardiac output and umbilical blood flow. In contrast to the situation after birth, fetal vascular oxygenation fluctuates consistently with transient decreases due to episodic fetal breathing and body movements and uterine contractions. In sheep, increasing the frequency of these uterine contractions above the normal rate, via pulsatile maternal intravenous oxytocin administration, has maturational effects on neural and cardiovascular functions. Overall the data indicate that in late gestation, the healthy fetus exhibits an organized constellation of cyclic activities, including motility, breathing activity, ingestion, and cardiorespiratory function, all of which are linked to the regular alterations in behavioral states. In all species studied, there is a progressive decrease in fetal motility with advancing gestation and there are also reductions in fetal motility with fetal metabolic compromise. More studies are required in the human and

other species to more precisely define the changes in fetal behavioral and related variables with advancing gestation and with deteriorations in fetal metabolic status.

Key words Fetal behavior, Fetal breathing, Fetal body movements, Fetal circadian rhythms, Antenatal uterine activity, Fetal monitoring

1 Introduction

In this chapter, the methodologies used to discern fetal behavior in animals and man will be discussed along with information on fetal behavior that these methods have provided. The term fetal behavior includes fetal sleep states, which in precocial mammalian species (i.e., those born relatively mature at birth) develop in late gestation, along with the fetal physiological processes, such as fetal body movements and breathing activity, cardiovascular function, blood gas, and acid-base status, which are linked to fetal sleep states. Since ~1970, as a result of technological and technical advances, there has been significant advances in our understanding of fetal behavior in man and animals, and also the development of fetal monitoring techniques in human pregnancy that are based on the changes in fetal behavioral variables that are altered in pathophysiological complications of pregnancy.

2 Fetal Behavior in Sheep

Study of normal fetal physiology is obviously complicated by the inaccessibility of the fetus. Thus, gaining of understanding of fetal functions in animals has resulted from the development of the surgical and monitoring methodologies to establish chronically instrumented fetal preparations. This involves aseptic surgery in anesthetized animals and gaining access to the fetus via incisions in the maternal abdomen and uterus, followed by implantation of vascular catheters and other devices in the fetus (Fig. 1). The distal ends of the catheters and other cables can be brought to the exterior through a small incision in the maternal flank, followed by closure of all incisions. After allowing several days (4–7 days) for

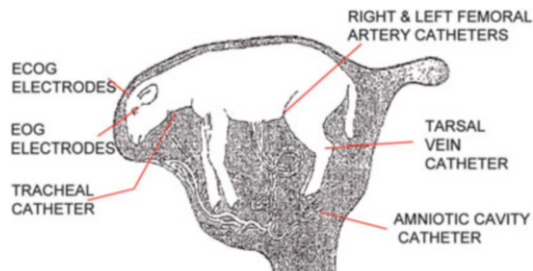


Fig. 1 Diagram of a typical chronically instrumented fetal sheep preparation

recovery of the animal from the surgery, the fetus can be monitored in utero; using appropriate polygraph equipment and other monitoring equipment, blood and other fluid samples can be collected from the fetus, drugs and other compounds can be administered, and experiments can be conducted. In theory, the fetus can be studied for the remainder of gestation, although in most cases, the study duration is less than this. This methodology was first described in pregnant sheep by Meschia et al. [1].

Although the use of chronically instrumented fetal lambs has provided a wealth of data of normal fetal development and the changes that occur in models of fetal compromise, the study of such preparations involves considerable expenses and they are logistically demanding. There can also be a significant incidence of preparation failure due to in utero fetal death or premature delivery or failure of the implanted catheters and other devices. Strict adherence to aseptic procedures is necessary both during the surgical instrumentation of the fetus and with the subsequent handling of the implanted fetal catheters. In addition, there is evidence that even in preparations that go to term with the delivery of a live newborn, fetal growth can be impaired and there can also be a significant incidence of preterm birth, something that does not normally occur in sheep [2, 3]. Moreover in pregnant sheep carrying the twins or triplets, the impairment in growth affects all fetuses, not just the one that was surgically instrumented. However, acclimation of the animals to the laboratory environment and lab personnel as well as bringing sheep from the same peer group into the lab may reduce the incidences of these problems [3]. During monitoring and experimental sessions, the measurement of the very small voltages associated with fetal ECoG and EMG activity requires the use of appropriate high-gain amplifiers and adequate shielding to prevent interference from the mains voltage.

The first such chronically instrumented fetal preparation that focused upon fetal sleep states and related processes was reported by Dawes et al. [4]. In this study, both acutely exteriorized, unanesthetized fetal lambs delivered into a warm saline bath with the umbilical circulation intact and chronically instrumented fetal lambs were studied and the gestational age ranged from 40-day gestation (0.27 of term) to term (~147 days). In some of the chronically instrumented fetal lambs between 110- and 138-day gestation, electrocortical (ECoG) activity and eye movements were recorded from stainless steel screws implanted through burr holes biparietally that were in contact with the dura and with similar screws implanted along the superior orbital ridge, respectively. Two types of activity were observed: one with fast (10–20 Hz), low-voltage electrocortical activity, associated with rapid eye movements (REM) that occurred for 54–69 % of the time and the other associated with slow (3–12 Hz), high-voltage electrocortical activity and no eye movements (Fig. 2). The authors concluded that the former activity represented REM sleep and the latter non-REM or quiet sleep. In addition, as discussed further below, fetal breathing activity, measured with a non-occlusive

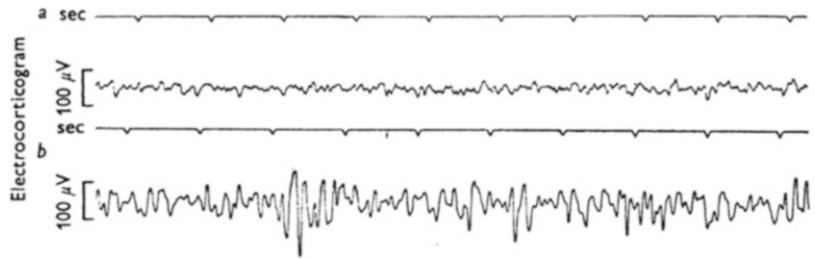


Fig. 2 Records of a biparietal dural electrocorticogram in a chronically instrumented fetal lamb at 143-day gestation. **(a)** Low-voltage rapid activity, **(b)** high-voltage slow activity (from [4] with permission)

catheter implanted in the trachea, an oesophageal catheter, or an electromagnetic flow meter implanted in the trachea, only occurred in REM sleep (Fig. 3). It was also noted that in fetuses less than 128-day gestation, it was difficult to identify the two sleep states as the ECoG voltage was consistently low (20–40 μV).

Subsequent research in this area identified another sleep state in late gestational fetal lambs [5–7]. In addition to recording the fetal ECoG and eye movements, these researchers recorded EMG activity from a fetal neck muscle and in the case of Ruckebusch et al. [5, 7], from several limb muscles as well. The rationale for recording neck muscle EMG is that postnatally there is tonic activity of this muscle during quiet sleep, and loss of activity during REM sleep and phasic activity during wakefulness [6]. In both studies, a portion of low-voltage ECoG activity was associated with phasic nuchal muscle activity and, in the Ruckebusch et al. study, phasic limb muscle activity. Harding et al. [6] also reported that fetal swallowing activity also occurred in this state (Fig. 4) and Rigatto et al. [8] reported that the early monosynaptic response to peripheral nerve stimulation was enhanced during this state, compared to the responses in quiet sleep and much greater than the response in REM sleep. The authors noted that this pattern of responsiveness was similar to that observed during wakefulness after birth. Moreover, this aroused state could be elicited by external stimulation [5, 7]. The duration of these episodes averaged 2.0 ± 0.1 min and the mean interval between successive episodes was 2.3 ± 0.2 h in nine fetal lambs at 109–134-day gestation [6]. This compares to durations of quiet sleep and REM sleep of 6.8–9.7 and 9.5–15.0 min (95% confidence intervals) in fetal lambs at 131–140-day gestation [9]. These studies concluded that the brief low-voltage ECoG episodes were different from REM sleep and may represent fetal wakefulness or an awake-like state of arousal. However, it also pointed out that with the recording methods employed in these studies it was not possible to unequivocally demonstrate fetal wakefulness [6]; direct observation of the fetus is required.

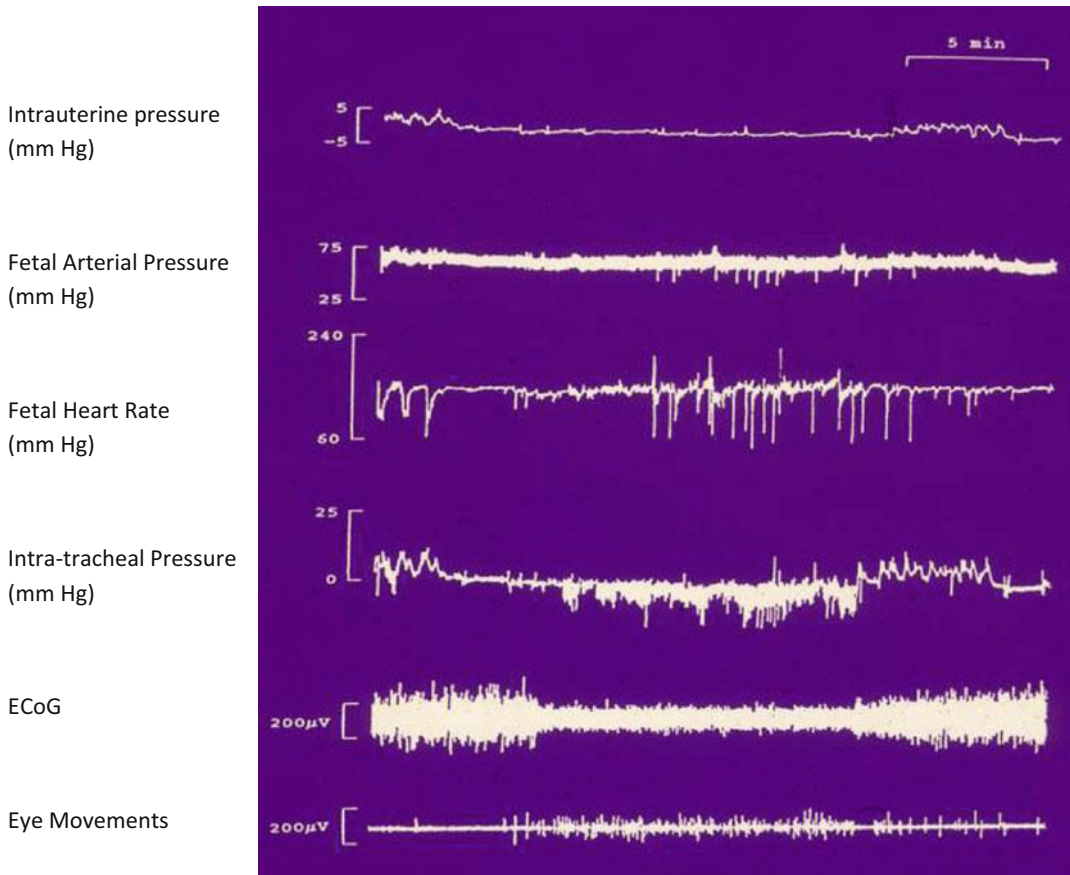


Fig. 3 A section of a polygraph record from a chronically instrumented fetal sheep at 134-day gestation last for about 45 min (ECoG—electrocortical activity). Antepartum uterine contractions can be discerned at the beginning and near the end of the intrauterine pressure trace

Direct observation of the fetal lamb has been accomplished in two studies in pregnant sheep. Dawes et al. [4] observed fetal lambs at 115–147 days that were delivered into a warm saline bath (39–40 °C) adjacent to the ewes under epidural anesthesia and with intact umbilical circulation. In addition to REM and quiet sleep, brief periods of apparent wakefulness were observed, which involved the lamb moving its limbs, raising its head, and opening its eyes. The lambs also responded vigorously to tactile and auditory stimuli. However, this behavioral state was not usually associated with breathing. In subsequent experiments on mature fetal lambs (Paul Johnson, Dan Rurak, Geoffrey Dawes, unpublished data), wakefulness was only observed when the bath temperature was reduced. When fetal core temperature reached ~37 °C (compared to a normal temperature of 39.5 °C), wakefulness was observed, which included the lamb raising its head out of the bath. This was associated with the onset of continuous pulmonary ventilation. When

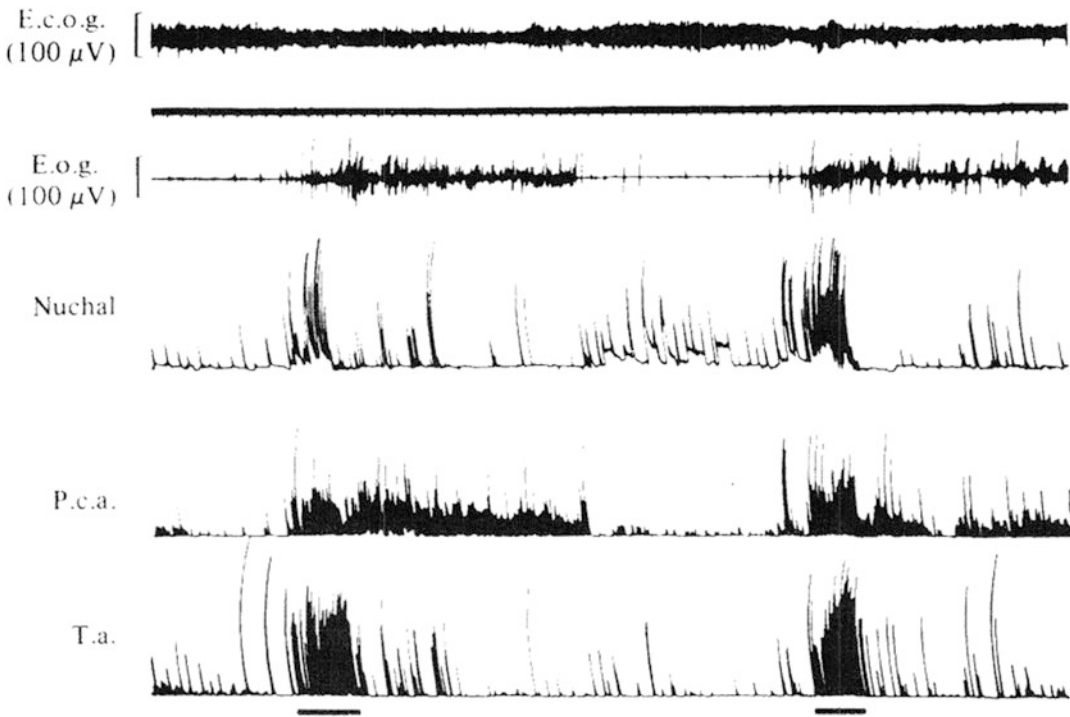


Fig. 4 Polygraph recording from a chronically instrumented fetal lamb at 142-day gestation. *E.c.o.g.* electrocortical activity, *E.o.g.* electroocular activity (eye movements), *Nuchal* EMG recording from a neck muscle, *P.c.a.* EMG recording from the posterior cricoarytenoid muscle (a laryngeal muscle that contracts in phase with breathing movements), *T.a.* EMG recording from the thyroarytenoid muscle (a laryngeal muscle that contracts in phase with swallowing). The EMG signals are in an integrated form. Bouts of fetal swallowing are *underlined* (from [6] with permission)

the bath and fetal core temperature was raised back to normal, pulmonary ventilation ceased, and the lamb's head sunk back into the bath. This routine of cooling and returning the bath temperature to the in utero value was repeated several times in individual fetuses and in every instance cooling resulted in the appearance of wakefulness, which ceased when the bath temperature was raised. Similar results were reported by Harned and Ferreiro [10], although in the case, the bath temperature was lowered gradually to 25–26 °C and this was always associated with arousal and the onset of pulmonary ventilation. Harned et al. [11] also report that following delivery of term fetal lambs by caesarean section and the initiation of continuous breathing, immersion of the lambs in a bath at 39–40 °C resulted in a marked suppression of breathing and this response was present for the first few days after birth. Cooling of the fetal lamb in utero via pumping cold tap water through coiled tubing implanted in the amniotic cavity (external cooling) or in the fetal stomach via the oesophagus (internal cooling) resulted in the onset of continuous breathing and with the external cooling, this

occurred before fetal core temperature started to decrease [12]. Collectively these observations suggest that surface and core cooling of the fetus following birth could be important for the initiation of arousal and wakefulness and continuous breathing, and also that the wakefulness of the exteriorized fetal lamb observed by Dawes et al. [4] may have resulted from inadvertent surface cooling of the animals.

The other study that involved direct observation of fetal lambs involved viewing chronically instrumented fetuses through a plexiglass window implanted in the flank of the pregnant ewe [13]. In these studies, the fetal head was kept within the viewing window via a harness placed around the lamb's muzzle. The implanted electrocortical, nuchal muscle EMG activity and eye movements allowed identification of REM and quiet sleep and the brief periods of arousal reported in previous studies [6, 7]. However, wakefulness, defined as opening of the eyes and purposeful movements of the head, was never observed.

Mellor and colleagues [14, 15] have carefully considered the evidence for and against the occurrence of wakefulness in the mammalian fetus. They have concluded that wakefulness does not occur prior to birth, because of the presence of a number of suppressors of arousal in utero. These include the warmth of the intrauterine environment, perhaps more particularly the lack of a temperature gradient between the fetal core and body surface. In addition there are several compounds present in fetal blood and in the brain that suppress arousal, including adenosine, the neuroactive steroids, allopregnanolone and pregnanolone, and prostaglandin E₂. All these compounds are produced by the placenta as well as other tissues, including the fetal brain [15], and their concentrations fall rapidly at birth, as does neonatal surface temperature, allowing for the rapid onset of wakefulness following delivery.

3 Fetal ECoG Activity in Other Species

Most of the animal research on fetal behavioral variables has been conducted on pregnant sheep. However data from other species are available. Stark and colleagues have studied fetal behavioral states in chronically instrumented fetal baboons [16]. These studies were conducted in late gestation (0.8–0.9 of term) and used methodologies similar to those employed in the fetal lamb studies, with electrodes implanted on the fetal frontal and parietal cortex for monitoring ECoG activity and electrodes implanted subcutaneously on either side of the orbit to record eye movements [16, 17]. In some fetuses, six ECoG electrodes were implanted pairwise on either side of the cranial midline, at 1 cm intervals in an anterior-posterior orientation in order to examine local coherence of the ECoG recordings [18]. Two major patterns of ECoG activity were

observed. One, termed trace alternant, comprised periodic bursts of high-amplitude activity ($\sim 100 \mu\text{V}$) alternating with low-amplitude activity ($\sim 25 \mu\text{V}$) and associated with few eye movements and low heart rate variability. It was concluded that this represented quiet sleep. The other state exhibited a more stable pattern with amplitudes of $50\text{--}75 \mu\text{V}$, associated with eye movements and increased heart rate variability, and was identified as REM sleep. These signals are qualitatively different from those obtained from fetal lambs (Figs. 2 and 3), but are similar to the electroencephalographic recordings obtained from human newborns [19]. The quiet and REM sleep episodes were separated by transition periods, which using statistical analysis were determined to be up to 7 min in duration, but which averaged 3.6 min. The average duration for the quiet sleep and REM sleep episodes averaged to 6.0 and 20.1 min, respectively. Another difference from the fetal lamb results is that in the baboon fetus at 0.8–0.9 of gestation, recognizable behavioral states (quiet and REM sleep) occur for only 41.2 % of the time. For 34.3 % of the time the state was termed intermediate. For 24.6 % of the time, there were the appropriate coincident associations of electrocortical pattern, eye movements, and heart rate, but these did not meet the criteria for state for several reasons including being bounded by intermediate states. As noted above, in the fetal lamb, cycling between quiet sleep and REM sleep is not obvious before about 128 days. The authors suggested that the differences between the baboon and sheep results may reflect differences in brain development between the species, but it could also be due in part to difference in the way the data was analyzed in the sheep and baboon studies. It could not be determined if the transition periods in the baboon were associated with fetal arousal periods, as in the fetal lamb (*see* Fig. 4), because recordings of fetal postural and other skeletal muscles were not obtained.

Fetal behavioral state data has also been obtained from the guinea pig [20, 21]. In the Umans et al. study [21] fetal guinea pigs were instrumented with electrocortical and ECG electrodes. As in the sheep and baboon, two alternating patterns of electrocortical activity were observed: high-voltage, slow activity and low-voltage, fast activity and these patterns first appeared at about 50-day gestation (~ 0.7 of term). As with the baboon studies, the periods of fetal arousal that have been observed in the fetal lamb could not be detected in the guinea pig because the appropriate electrodes were not implanted.

4 Automated Analysis of Fetal Electrocortical Signals

Much of the research on fetal sleep states has involved visual analysis of the polygraph traces [4, 22]. This can provide information on the incidences of the various states and their average durations, but

not about the frequency and amplitude characteristics of the signal. Szeto and colleagues have done much research in this area, and this process has been aided by the progressive development of desktop computers and computerized data acquisition systems [23, 24]. The basic approach was to record the electrocortical signals on an FM tape recorder, with subsequent processing of this signal involving analog-to-digital conversion, and then processing by an IBM PC to conduct a fast Fourier transform and generate a power spectrum of the data, using a combination of commercially available and custom-built software [23]. Analysis of the power spectra at different gestational age ranges from less than 120 to 139 days indicated that clearly distinguishable episodes of high-voltage slow activity and low-voltage fast activity were observed at 114–117-day gestation. With advancing gestational age, the main change occurred with low-voltage fast activity, involving a shift to higher frequency bands. A somewhat simpler process was also employed, which did not involve generation of a complete power spectrum of the electrocortical frequency bands. Instead the frequency below which 90 or 95 % of the power in the spectrum resides, the spectral edge frequency was calculated, and this process was used to provide a quantitative measure of the maturation of electrocortical activity in the fetal lamb with advancing gestation [25]. At gestational ages below 122–125 days only one spectral edge peak was present, whereas above this age range two peaks were present representing low-voltage fast and high-voltage slow electrocortical states (Fig. 8). This is later than the age (114–117 days) at which two electrocortical patterns were distinguishable with visual analysis of the power spectra (see above). However the spectral edge frequency analysis indicates that the main developmental change occurred with low-voltage fast activity, which involved an increase in the spectral edge frequency with advancing gestational age. This is similar to findings resulting from analysis of the electrocortical power spectra (see above) (Fig. 5).

The use of electrocortical power spectra and spectral edge frequency analysis has provided valuable information about the frequency characteristics of the signal and the ontogenetic changes that occur with advancing gestation and also the changes in sleep state that occur with the onset of labor [26]. However for examining relationships between sleep state and other physiologic processes in the fetus, such as breathing and body movements and cardiovascular function, a system that automatically identified the patterns of electrocortical activity, particularly in real time, would be desirable. McNerney and Szeto [27] described such a system. This employed methods similar to those used to determine the electrocortical power spectra and spectral edge frequency following digitization of the electrocortical signal and fast Fourier transformation. Then three criteria were employed to distinguish between quiet and REM sleep and also between two transitional states: total

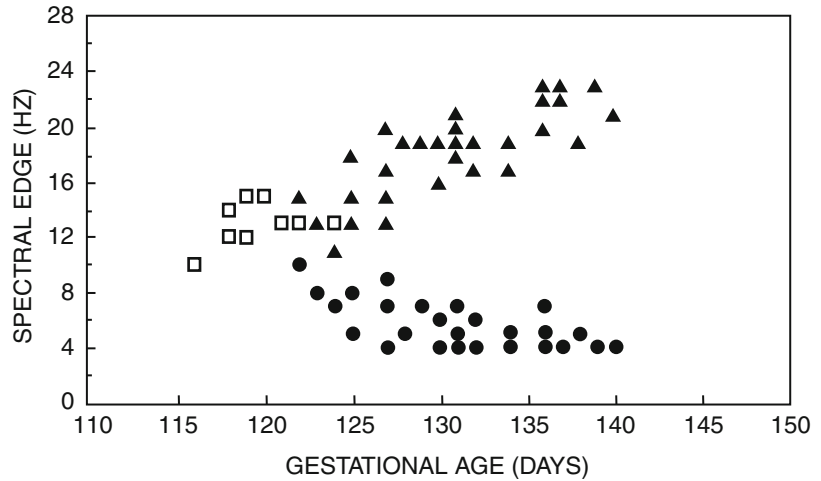


Fig. 5 Spectral edge frequencies of high-voltage fast (*solid triangles*) and low-voltage slow (*solid circles*) electrocortical activities in fetal lambs as a function of gestation age. The *open squares* represent data from fetuses where only one dominant frequency was present. From [25] with permission

power, percent power in the 1–4 Hz bandwidth (i.e., characteristic of high-voltage slow activity), and percent power in the 15–31 Hz bandwidth (i.e., characteristic of low-voltage fast activity). Using these criteria, the various sleep states could be automatically identified. However, because of the limited power of desktop computers of the day, the analysis was conducted off-line and was restricted to 2–3-h segments. Nonetheless, the study did identify one feature of the electrocortical pattern what was not obvious from visual analysis of the electrocortical pattern; the transitional states are not restricted to the periods of change from quiet sleep to REM sleep and vice versa, but transitional epochs also occur briefly within these states. Akay et al. [28] used an alternative method from fast Fourier transformation for analyzing the electrocortical signal in chronically instrumented fetal lambs. The method employed wavelet transformation for a number of reasons, with the main one being that wavelet transform analysis is better than fast Fourier transformation for analyzing non-stationary signals, which is the case with electrocortical activity. In addition, it was hoped that wavelet transform analysis would be better at detecting the time in gestation when distinct high- and low-voltage patterns first become apparent since as noted above, with fast Fourier transformation (spectral edge frequency), this was first detected at 122–125-day gestation, whereas it was detected visually at 114–117 days. The wavelet transform analysis was analyzed with 2-h electrocortical records and four frequency bands were examined: 16–31, 8–16, 4–8, and 2–4 Hz at gestational age ranges of 110–122, 123–135, and 136–144 days. In contrast to the findings with fast Fourier analysis,

which indicated that the main developmental change in electrocortical pattern involved low-voltage fast activity, with an increase in power of the higher frequency changes (i.e., 16–31 Hz), wavelet transform analysis indicates changes in both low-voltage fast and high-voltage slow activity with advancing gestation. From 110 to 130 days, the main change was with high-voltage slow activity, with a progressive increase in the power of the 2–8 Hz band. In contrast from 130- to 145-day gestation, the main change occurred with low-voltage fast activity with an increase in the power of the 16–32 Hz band. Moreover, use of fast Fourier transformation of the data did not detect these changes [28]. This study suggests that waveform analysis is better than fast Fourier analysis for analyzing the frequency characteristics of the fetal electrocorticogram. However, the method could still only be used off-line with data recorded on an FM tape recorder and then digitized and was limited to 2-h time blocks. In addition, it is not clear from the paper how the complex calculations involved in wavelet transform analysis were conducted. Commercial software (MatLab, Mathworks Inc., Natick, MA) is now available and has been used for EEG analysis in adult subjects [29]. It does not however appear to have been applied to fetal ECoG or EEG signals.

More recently, Keen et al. [30] developed an automated analysis method for the amplitude and frequency components of the fetal lamb ECoG that employs the Powerlab computerized data acquisition system (ADInstruments, Colorado Springs, CO). The spectrum function of the Powerlab system was used to estimate the 95 % spectral edge frequency, ECoG amplitude, and the spectral power in the 1–4, 4–8, 8–12, and 12–25 Hz frequency bands. The automated analysis incorporated four variables: ECoG amplitude, 95 % spectral edge frequency, and the relative spectral power in the 1–4 and 12–25 Hz frequency bands. The cutoff values for these variables in terms of the various ECoG states had to be determined for each animal, which could then be used for the ECoG analysis of that animal. The automated analysis identified periods of low-voltage fast and high-voltage low activity and also transitional periods between the main ECoG states. In addition for 10 % of the time, a specific ECoG state could not be defined with the criteria used and this was assigned as an indeterminate voltage/frequency pattern. Although the Powerlab spectrum analysis is done off-line, the calculated variables can be displayed as new channels in the Powerlab chart display, which facilitates analysis of the relationship between the ECoG variables and the other fetal variables recorded. In the initial publication from this group [30], the fetal lambs studied were at 132–134-day gestation. However in an additional publication [31], the fetuses were studied at 116–119-, 121–122-, 124–126-, 128–129-, and 131–134-day gestation. The developmental changes in ECoG pattern mainly comprised an increase in ECoG voltage amplitude of the high-voltage,

low-frequency state, but not the low-voltage fast state, and an increase in the 95 % spectral edge frequency for the low-voltage state, and a slight decrease in spectral edge frequency of the high-voltage state. In addition there was an increase in the voltage amplitude of the indeterminate frequency/voltage pattern with advancing gestation. There was also a decrease in the mean percent time spent in the low-voltage state (from 54.2 ± 2 % to 46 ± 2 %) and an increase in the mean percent time spent in the high-voltage state (from 26.3 ± 3 % to 37 ± 2 %). However, even in late gestation, the fetal lamb spends more time in the low-voltage than the high-voltage state. Moreover, the changes in percent time were accompanied by an increase in the mean durations of both the low-voltage (from 3.3 ± 2.2 to 5.8 ± 0.6 min) and high-voltage (1.9 ± 0.2 to 4.7 ± 0.5 min) states. The transitional states also showed changes. For transitions from low to high voltage, the mean duration more than doubled (from 40 to 87 s), whereas there was no change in the duration of transitions for high to low voltage. Some of these developmental changes, particularly for spectral edge frequency, are similar to earlier reports [25]. Keen et al. [31] also examined the ECoG variables in fetuses subjected to chronic hypoxemia achieved via embolization of the umbilical circulation. Overall, the various analytical methods employed to examine ECoG characteristics in fetal lambs have provided considerable information on the various ECoG states and on the developmental changes in these states. With the development of methodologies that allow for long-term automated identification of the various ECoG states in relation to other fetal variables, it seems that more information could be obtained on the relationship of fetal ECoG states to other fetal functions and on the impact of other normal intrauterine processes on the ECoG states.

Myers et al. [32] describe a quantitative method for classification of the ECoG states in the fetal baboon. The methodology employed was similar to that employed in the earlier studies conducted on fetal lambs: implantation of dural ECoG electrodes biparietally, with one additional electrode on the frontal cortex. The ECoG signal was acquired, amplified, and recorded on a polygraph recorder and FM tape recorder, with the ECoG analysis being conducted off-line. Fast Fourier transforms were conducted, and the 80 % spectral edge frequency was estimated. An additional analysis was performed to identify the trace alterant pattern that is present in the fetal baboon and other primates. The ECoG signal was first processed by a high-pass filter to attenuate the low-frequency components and then subjected to linear full-wave rectification and electronically smoothed. The ratio of relative spectral power in the 0.03–0.20 Hz frequency band (i.e., the frequency band of the trace alterant pattern divided by the relative spectral power in the 12–24 Hz frequency band) was termed the EEG ratio and accurately identified the periods of trace alterant activity. In a

subsequent publication [18], this group examined another aspect of ECoG/EEG activity that has not been examined in other studies of fetal sleep states. This is the spatial integration of ECoG voltage and frequency oscillations across the cerebral cortex, which relates to the development of cortical networks. For this purpose, three pairs of cortical dural electrodes implanted with an additional reference electrode were implanted in five fetal baboons at 128–132-day gestation (term ~175 days). The ECoG data was sampled and digitized using a commercial computerized data acquisition system and periodicities in the EEG spectral power ratios and coherence data were analyzed off-line over 5-min blocks. Because of gaps in the data largely due to maternal movement artefacts, fast Fourier transformation could not be used; rather Lomb periodograms, which can deal with data gaps, were employed. The ECoG frequency bands analyzed were 1–4, 4–7, 8–12, 12–30, and >30 Hz. The magnitude of the coherence between pairs of electrodes was estimated using a published formula. The data analyzed was obtained between 137 and 151 days and over this time, both ECoG cycling and local synchrony of the ECoG signals became increasingly well organized with a cycle length of ~1 h. This suggests that with advancing gestation both ECoG-state cycling and the integration of cortical activity develop in parallel.

5 Behavioral States in the Human Fetus

The EEG of the human fetus has been measured during labor after rupture of the membranes and application of a suction cup EEG electrode assembly to the fetal scalp [33–35]. However, two of these publications [33, 34] mainly presented the methodology employed to obtain the EEG signals, with little or no data presented. In contrast, Thaler et al. [35] used fast Fourier transform and 90 % spectral edge frequency to characterize the EEG pattern in 14 subjects from 38- to 42-week gestation. They characterized episodes of low-voltage fast and high-voltage slow activities, which had average durations of 41.3 ± 2.3 (SE) and 26.2 ± 2.0 min, respectively, and these values are significantly different ($P > 0.001$, paired t test). The percentage of time spent in the low- and high-voltage states average 60.1 % and 39.9 %, respectively. The durations are much longer than the durations of the ECoG states in the late-gestation fetal lamb (see above). A part of this difference may relate to the fact that in the human study, the EEG records were obtained in labor, and Shinozuka and Nathanielsz [26] have found changes in the percentage time and durations of the high- and low-voltage states in the fetal lamb during labor. Because other fetal variables, such as eye movements and postural muscle activity, were not measured, assignment of sleep

states is not possible. Nonetheless, the data presented by Thaler et al. [35] indicate that the EEG cycling occurs in the human fetus at term.

The recording of EEG signals from the scalp of the human fetus is only possible during labor. For assessment of behavioral states during pregnancy, other methods, based upon real-time ultrasound and Doppler ultrasound, have been employed. Two main approaches have been developed. One of these was developed by researchers in the Netherlands and was based upon behavioral state studies conducted on term and preterm infants by Prechtel and colleagues [36]. For the fetal studies, two real-time ultrasound scanners were used, one to monitor eye movements, which as Bots et al. had demonstrated could be monitored with ultrasound [37], and the other to monitor fetal body movements. Fetal heart rate was monitored with a conventional cardiocograph and all data was recorded on a videocassette recorder [38] with the analysis being conducted off-line. In this initial study, 14 low-risk pregnancies were monitored at 2-week intervals from 32 to 40 weeks of gestation. All three signals obtained (eye movements, body movements, heart rate) showed periodic changes. Moreover, the pattern of change of the variables at times appeared to be temporally linked in terms of the simultaneity of the changes, their recurrence, and stability. Four behavioral states were noted: state 1F—general quiescence with brief gross body movements, absent eye movements, and stable heart rate; state 2F—frequent and periodic gross body movements, continuous eye movements, and heart rate with a wider oscillation and frequent accelerations associated with body movements.; state 3F—gross body movements absent, continuous eye movements, and heart rate with a wider oscillation but no accelerations; and state 4F—vigorous, continual body movements, continuous eye movements, and unstable heart rate, with large and long-lasting accelerations. The behavioral states observed in human infants include the following: state 1, eyes closed, regular respiration, and no movements; state 2, eyes closed, irregular breathing, and small movements; state 3 eyes open, and no movements; state 4, eyes open, and gross movements; and state 5, crying [36]. There is clearly not a fetal equivalent to state 5. Also, the 3F state occurs rarely [38] or not at all [39, 40]. Thus in the human fetus in late gestation, there are three main states: 1F, 2F, and 4F. The 1F and 2F states appear similar to quiet and REM sleep, respectively, and state 4F to the brief periods of arousal identified in the fetal lamb (see above). However, Nijhuis et al. [38] were careful not to denote states to the 1F and 2F patterns because fetal EEG recordings during pregnancy were not available. Pillai and James [39] compared the ultrasound assessments of behavioral states of 18 healthy term fetuses (>37-week gestation) with the recordings from the same subjects at 3 and 5 days after birth. The number of eye movements, limb movements, and body movements/10 min

were not significantly different between states 1F (fetal) and 1 (neonatal) and 2F and 2. In terms of comparisons between F4 and 4, eye and limb movements/10 min were not different, but the number of body movements was significantly greater in the neonate compared to the fetus. Heart rate patterns in the various fetal and neonatal states were also comparable, although mean heart rate in states 1, 2, and 4 were ~20 beats lower than the corresponding fetal values, which reflects the progressive fall in heart rate that occurs during development [41]. Given that in the newborn states 1 and 2 are denoted as quiet and REM sleep [19, 36, 42], respectively, it seems reasonable to consider that the fetal states 1F and 2F represent quiet and REM sleep. Supporting evidence for this view comes from comparison of the % time spent by the term fetus in state 1 (33.3) and state 2 (52.5) that is similar to % time spent by the human fetus in labor in high-voltage (39.9) and low-voltage (60.1) EEG states [35]. In terms of state 4F, it occurs 10.2 % of the time at >39-week gestation [39]. For the reasons discussed above on the aroused state in the fetal lamb, it seems unlikely that state 4 represents true wakefulness. The human fetus is exposed to many or all of the factors that suppress arousal in the fetal lamb, including lack of a temperature gradient, high levels of neuroactive steroids in fetal blood [43, 44], and high fetal circulating prostaglandin E₂ concentrations at both mid-pregnancy and term [45, 46].

In terms of the developmental aspects of behavioral states in the human fetus, Nijhuis et al. [38] noted that prior to about 36-week gestation, while there were cycles of heart rate, eye movements, and body movements, these cycles were usually not coincident and did not start and end at the same time. With advancing gestation, these criteria were met for the three variables monitored particularly at 36–38 weeks. Visser et al. [47] studied 11 fetuses at 30–32-week gestation. In six of these cases, the cycles of heart rate, eye movements, and body movements were coincident, although they accepted changes in body and eye movements within 4 or 6 min of the heart rate change to be simultaneous. Pillai et al. [48, 49] studied 45 healthy pregnant women at monthly intervals starting at 12–14-week gestation. Fetal diaphragmatic, limb, body, and mouthing movements were monitored with ultrasound and fetal heart rate with a standard heart rate monitor. Before 28 weeks, there was a high rate of fetal movement, with only short (<4 min) periods of quiescence. Thereafter the periods of quiescence increased progressively to term, so that rest-activity cycles were present. The fetal behavioral states (predominantly states 1F and 2F), which exhibited simultaneity and coincidence of the variables monitored, were first noted at ~32-week gestation and were present in over 80 % of the recordings at 36-week gestation. These collective results indicate the progressive development of organized fetal behavioral states in the second half of pregnancy and are similar to the results obtained from the animal species discussed above.

The other method that has been employed in human pregnancy to study fetal behavioral states utilizes a fetal actocardiograph [50, 51]. This device is similar to a Doppler fetal heart rate monitor, with the difference being that the Doppler return signals resulting from fetal movement, which have lower Doppler shift frequencies than the Doppler signals returning from the fetal heart, are not filtered out. Doppler signals resulting from maternal movements, which are of lower frequency than the fetal signals, are filtered out, so that the actocardiograph displays fetal heart rate and movement traces, which can also be digitized and processed online [50, 52]. The fetal movements are displayed as spikelike upward deflections of the trace, so that the device provides information on the vigor and duration of movement bouts. Comparison of actocardiograph-identified fetal movements with those obtained with real-time ultrasound observation indicates that the actocardiograph can detect 95.9 % of those observed with ultrasound [53]. The advantage of the actocardiograph is that the measurements can be obtained by a single operator and are quantitative. The disadvantage is that fetal eye movements, which are used in the ultrasound determination of fetal behavioral state (see above), are not detected with the actocardiograph. However, Visser et al. have reported that fetal behavioral states 1F (quiet sleep) and 2F (REM sleep), which comprise the bulk of fetal behavior, can be reliably identified using visual analysis of fetal heart rate patterns alone [54], so that the combination of heart rate and fetal movements provided by the actocardiograph should suffice, particularly since the movement trace indicates periods of vigorous fetal movement and thus can identify state 4F. Also details on the types of fetal movement cannot be obtained, although Besinger and Johnson [53] report that fetal limb, spinal, and rolling movements can be distinguished with the actocardiograph by differences in the amplitude and duration of the movements. DiPietro et al. used the actocardiograph to study the development of human fetal behavioral patterns from 20 to 33–89 weeks at 4-week intervals and also examined the fetal heart rate response to vibroacoustic stimulation [52]. Concordant states, as defined above and comprising concordant periods of fetal activity and heart rate pattern, developed in a nonlinear pattern from 20 weeks to term, while the periods of non-concordance decreased. The biggest changes occurred between 20 and 28 weeks, with a slower rate of change thereafter (Fig. 6). State 4F first appeared at 24-week gestation and increased to 11–16 % from 32 weeks to term. This is slightly higher than the value of 8.9 % reported for the term fetus by Pillai and James [55]. It also appears that the estimates of percentage time spent in state 1F is lower and in state 2F higher with the actocardiograph method compared to real-time ultrasound observations (*see* above). However whether this is due to methodological differences

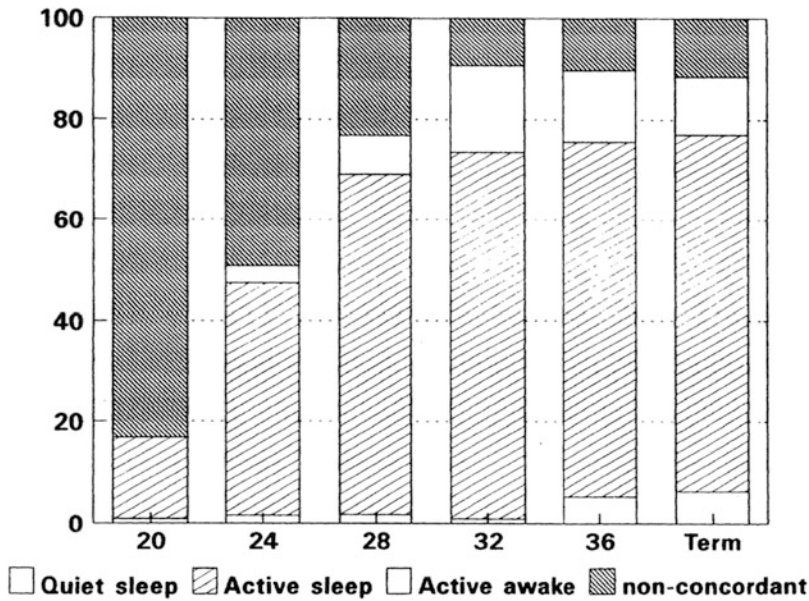


Fig. 6 Percentage of total observation time spent in states 1F, 2F, and 4F and the % of non-concordant time. From [52] with permission

or the different patient populations studied is not clear. It appears that for many types of studies, either method is acceptable.

A newer technology that has been employed to study human fetal behavioral states is fetal magnetoencephalography (MEG). The technique exploits the fact that the flow of electric current through tissues of the body generates a magnetic field that can be detected noninvasively with appropriate sensors [56, 57]. The instruments used for fetal MEG are comprised of ~150 superconducting primary sensors and ~30 reference sensors, which are arranged in an array that conforms to the contours of the abdomen of a pregnant woman [58]. During use of the device, the mother is seated in a lean forward position so that her abdomen conforms to the array. In addition the device must be used in magnetically shielded room. Processing of the MEG signals includes removal of the signals resulting from the mother, mainly the ECG, by an algorithm, while the signal generated by the fetal ECG is separated from the original MEG signals and used to derive R-R intervals and thus a cardiogram. In addition, by tracking changes in the amplitude of MEG signals resulting from the QRS signals and the center of gravity of this signal in relation to the other MEG sensors, fetal movements can be detected, so that an actocardiogram can be produced [59]. MEG signals emanating from the fetal brain were identified by ultrasound localization of the fetal head [57] or via 3 localization coils placed around the maternal abdomen [58]. One limitation of the MEG approach is relatively short monitoring times, largely as a result of maternal discomfort and which have

ranged from 12 to 30 min [57, 58, 60]. This is shorter than the average duration of a cycle of low- and high-voltage ECoG activity (65.8 min) in human fetuses during labor [35], and also shorter than the median length of a cycle of states 1F and 2F (40.5 min) at 38-week gestation [38]. Much of the research with fetal MEG recordings has involved assessment of fetal CNS responses to auditory and visual stimuli [56, 57]. Eswaran et al. [57] used MEG recordings to examine EEG patterns between 27- and 39-week gestation. Prior to 35-week gestation, the predominant pattern was short bursts of EEG activity separated by flat or lower voltage intervals, which was termed “trace discontinue.” After 35 weeks, a trace alterant pattern was observed, similar to that seen in the fetal baboon and in the preterm infant. Haddad et al. [60] correlated the MEG patterns with actocardiograph recordings of fetal behavioral state between 30- and 37-week gestation. The authors referred to the pattern in state 1F as discontinuous and that in state 2F as continuous. The differences in EEG pattern between the two states are less than those seen in the fetal lamb and the fetal baboon. Haddad et al. also estimated the 90 % SEF in states 1F and 2F [60]. However, there was no difference between the two states, with the values in the range of 15–20 Hz. This is different from the 90 % SEF found with EEG recording from human fetuses during labor, where the value in high-voltage EEG activity (state 1F, quiet sleep) was 4–11 Hz and in the low-voltage state (state 2F, REM sleep) the value was 12–14 Hz [35]. The reason for these differences between the fetal MEG recordings and the direct EEG recording during labor is not clear. One way to resolve this issue would be to obtain MEG recordings from fetuses in late gestation and then direct EEG recording from the same fetuses during labor or in the neonatal period.

The data summarized above indicate that the sleep states develop prenatally in the sheep, guinea pig, baboon, and human. All of these species are termed precocial, in that they are born neurologically mature. The situation is different for most rodents and carnivores, which are termed altricial and are born neurologically immature. This difference in neurological maturity between precocial and altricial species is manifest in various ways. This includes the time during post-conceptual development when the brain growth spurt occurs [61]. In the guinea pig, sheep, and rhesus monkey, it largely occurs prior to birth; in the human and pig, it spans the perinatal period, and in the rat and rabbit it is largely a postnatal event. Romijn et al. [62] compared four parameters of the cerebral cortex (numerical synapse formation, development of glutamate decarboxylase activity, the development of choline acetyltransferase activity, and the development of electrical activity) in the human and rat and concluded that the degree of cerebral cortical maturation in the human infant at birth occurred in the rat at postnatal days 12–13. Jouvett-Mounier [20] recorded

EEG activity in the rat, cat, and guinea pig from birth to day 50. Cortical electrical activity was observed at birth in all three species, but in the rat and cat, this was very largely REM sleep and in the rat it was confounded by EMG signals resulting from body movements. Wakefulness and quiet sleep were largely absent and regular cycling between the sleep states and wakefulness did not occur until the third postnatal week. In contrast in the guinea pig, cycling among REM sleep, quiet sleep, and wakefulness was present at birth, although the amount of REM sleep was about double that in the adult. Clancy et al. [63] have created a Web-based system (<http://translatingtime.net/home>) for translating neurodevelopment from 18 mammalian laboratory species, including hamster, rat, rabbit, spiny mouse, guinea pig, ferret, cat, rhesus monkey, sheep, and human, and which incorporates over 100 neurodevelopmental events. This site is very useful for comparing the neurodevelopment trajectory in one of the species to the human or any other species on the list.

6 Fetal Breathing Movements

There has been considerable interest in fetal breathing since at least the nineteenth century. An extensive review of this literature is provided by Wilds [64]. Fetal breathing movements were first directly identified in chronically instrumented fetal lambs by Merlet et al. [65] and Dawes et al. [4]. In the former study, the breathing movements were detected from recordings from an oesophageal catheter which recorded the intrathoracic pressure changes resulting from the breathing activity. In the Dawes et al. study, an oesophageal catheter was also employed and also a cannulated electromagnetic flow meter was implanted in the trachea to record the tracheal fluid movements associated with breathing [4]. Two types of breathing movements were observed: single, large-amplitude inspiratory efforts, which often occurred as a series of a few, and rapid, irregular breathing movements. Both studies showed one of the salient features of rapid, irregular breathing activity; it is episodic and not continuous and in the fetal lamb; the breathing is restricted to periods of low-voltage fast ECoG activity, which as discussed above is comprised mainly of REM sleep and a small amount of an aroused state (*see* Fig. 3). Overall, the breathing movements occurred about 1/3 of the time [4]. In the Dawes et al. study, another interesting observation was that in a twin lamb preparation, one of the fetuses, which was hypoxemic and hypoglycemic, the amount of breathing activity was less than in the other twin, but was not completely absent [4]. A subsequent study [66] reported that an acute 1-h period of fetal hypoxemia, achieved by lowering maternal inspired O₂ concentration, reduced the proportion of time during which fetal breathing occurred from

23.0 ± 2.0 to 4.1 ± 2.1 ml/h. However with longer periods of fetal hypoxemia, fetal breathing activity is initially reduced, but after ~ 24 h returns to the normal incidence [67, 68].

The single inspiratory efforts observed in the fetal lamb were initially referred to as gasping and occupied 4 % of the time [4]. Harding et al. provided further information on these inspiratory efforts by recording EMG activity in laryngeal abductor, which opens the glottis (posterior cricoarytenoid, PCA), and adductor muscles, which close to glottis (thyroarytenoid, TA), in addition to tracheal pressure and diaphragmatic EMG activity in fetal lambs at 110–130-day gestation and also in postnatal lambs [69]. These isolated movements occurred at intervals of 0.5–2 min and were largely restricted to quiet sleep. The intratracheal pressure changes were biphasic or triphasic and were usually of larger amplitude than the rapid irregular breathing. The PCA was inactive during the diaphragmatic EMG burst, suggesting that the glottis was closed. Following the inspiratory effort there was a prolonged burst of TA activity (Fig. 7). The authors concluded that these single inspiratory efforts most closely resembled the regurgitative activity associated with rumination after birth. This activity, as well as rapid, irregular breathing, obviously does not fulfil the functions that they do after birth.

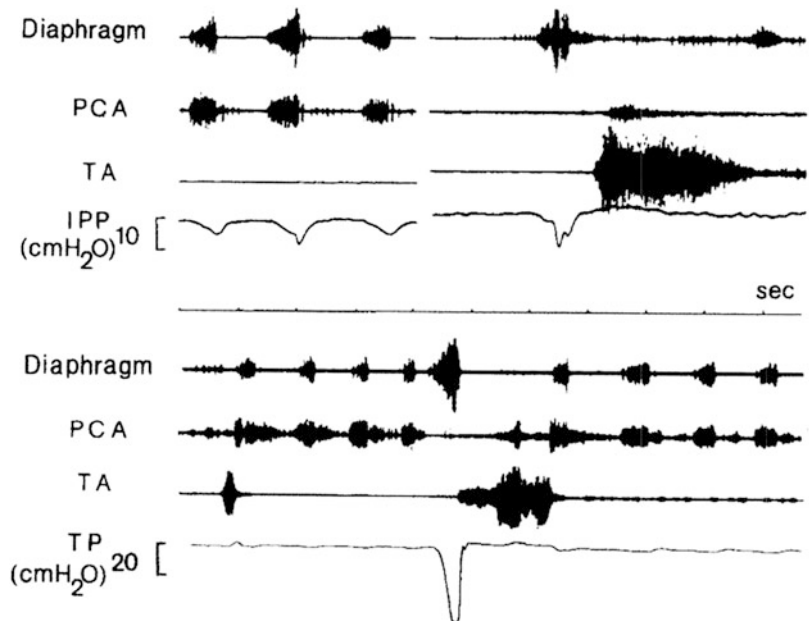


Fig. 7 Polygraph recording from a fetal lamb (*upper record*) and ruminating lamb (*lower record*). In the *fetal record*, rapid irregular breathing is illustrated on the *left* and a large inspiratory effort on the *right*. The *lamb record* illustrates a large transient decrease in tracheal pressure in the absence of PCA activity, which represents regurgitation. From [69] with permission

Two experimental approaches have been used to identify anatomic location in the fetal lamb brain responsible for the apnea during quiet sleep and acute hypoxemia. Dawes et al. [70] employed fetal brain sections, either at caudal (pons, midbrain, caudal hypothalamus) or rostral (hypothalamus, anterior commissure, optic chiasma) (Fig. 8) in pregnant sheep at 118–123-day gestation. Fetal breathing was measured by a non-occlusive catheter implanted in the fetal trachea and with EMG electrodes implanted on the diaphragm. With the caudal sections, the incidence of fetal breathing movements increased to near continuous and occurred in both REM and quiet sleep. Acute fetal hypoxemia resulted in an increase in the rate and amplitude of the breathing, similar to the situation after birth. With the rostral sections, the incidence of breathing was not altered but it was dissociated from fetal sleep state. Acute hypoxemia resulted in a marked decrease in the amount of breathing, identical to the situation in intact fetuses. These results led the authors to conclude that the fetal midbrain generates the episodic pattern of fetal breathing, but that for the tight link between fetal breathing and low-voltage ECoG activity, the cortex is also involved. Gluckman and colleagues [71, 72] made use of a stereotactic brain atlas for a 120-day gestation fetal lamb [73] to place small bilateral lesions in the brain stem of fetal lambs in an attempt to localize the sites involved in episodic fetal breathing and the hypoxic inhibition of this activity (Fig. 9). They found that bilateral lesions in an area in the rostral lateral pons near the later parabrachial and Kolliker-Fuse nuclei resulted in the

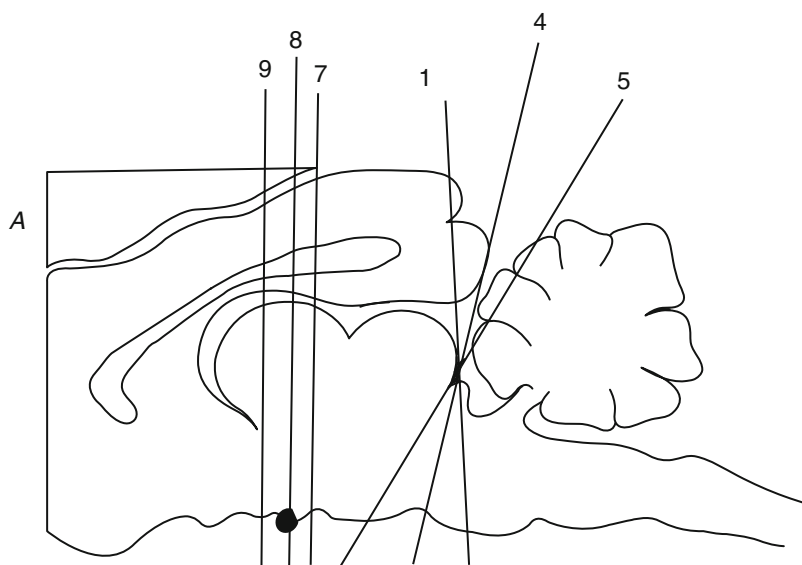


Fig. 8 Schematic diagram of a portion of the fetal lamb brain showing the location of the rostral and caudal brain sections. The *numbers* refer to the different fetuses studies. Modified from [70] with permission

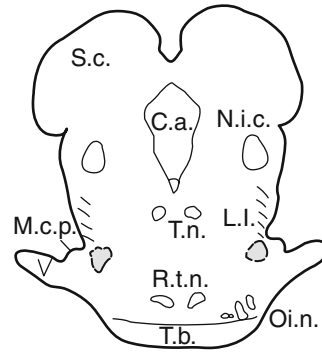


Fig. 9 Diagram of the midbrain of a fetal lamb showing the location of the bilateral lesions that resulted in the hypoxic stimulation of fetal breathing (*shaded areas*). *S.c.* superior colliculus, *C.a.* cerebral aqueduct, *N.i.c.* nucleus of inferior colliculus, *L.l.* lateral lemniscus, *T.n.* trochlear nerve nuclei, *M.c.p.* middle cerebral peduncle, *V.* fifth cranial nerve (trigeminal), *R.t.n.* reticulotegmental nucleus pons, *T.b.* trapezoid body, *O.i.n.* olivary nuclei. Modified from [71] with permission

stimulation of fetal breathing during acute fetal hypoxia, as opposed to the inhibition seen in fetuses with lesions elsewhere in the midbrain and in intact fetuses [71]. However, these lesions did not result in continuous fetal breathing, but in some the incidence of breathing was increased and breathing episodes extended into quiet sleep. There was also an apparent decrease in the rate of breathing and it became more irregular, although detailed analysis of these variables was not done. In a subsequent study [72], the effects of acute fetal hypercapnia (achieved by increasing maternal inspired CO_2 concentration) and metabolic acidemia (achieved by fetal i.v. infusion of lactate) were examined in fetal lambs with the lateral pontine lesions, with lesions elsewhere in the midbrain and intact fetuses. Hypercapnia and acidemia resulted in a stimulation of breathing only in the group with lateral pontine lesions in both low- and high-voltage ECoG states, so that breathing became continuous or near continuous. The authors concluded that the area in the rostral lateral pons that was lesioned is involved in the inhibitory effects of acute hypoxia on fetal breathing and also with the normal absence of breathing in quiet sleep, with this inhibition being related to an increased threshold for fetal breathing that is sensitive to H^+/CO_2 . These results differ from those of Dawes et al., in which the caudal brain sections resulted in near-continuous breathing in the absence of experimental changes in vascular Pco_2 and pH [70]. Johnston and Gluckman [72] explained this difference by the fact that in the Dawes et al. study the increase in fetal breathing with caudal brain section occurred progressively over a ~2-week period, and they noted that there is often a small fall in vascular pH with increasing perioperative age, which could have

stimulated the breathing. Although there is a progressive decrease in arterial pH in the fetal lamb with advancing gestational age [74], the decrease in pH over a 2-week period would only be 0.02 pH unit, which seems an insufficient stimulus for fetal breathing.

The above studies suggest that midbrain elements are involved in both the episodic nature and hypoxic inhibition of breathing in the fetal lamb. In fetal lambs subjected to decortication (total cortical isolation from lower brain regions), the episodic nature of fetal breathing is maintained associated with REM and lack of tonic nuchal muscle activity [75]. However, the low-voltage, fast ECoG activity pattern was not present, although the high-voltage, slow ECoG pattern characteristic of quiet sleep was. During fetal breathing episodes, the average integrated ECoG power was significantly less than that during quiet sleep. In addition, tonic diaphragmatic EMF activity occurred during a portion of quiet sleep. The breathing responses to hypercapnia and hypoxemia were maintained in the decorticate fetuses [76]. These results suggest that the cerebral cortex is not involved in the episodic nature of fetal breathing, the maintenance of high-voltage, slow ECoG activity during NREM sleep, or the responses to hypercapnia and hypoxemia. However, the cortex would seem to be involved in the presence of low-voltage, fast ECoG activity during REM sleep and in the inhibition of tonic diaphragmatic EMG activity during NREM sleep. Koos et al. [77] examined the effects of lesions in the fetal thalamus on the breathing responses to acute hypoxia. Two approaches were used: brain transection in this region and local injection of ibotenic acid bilaterally in the medial thalamus via guide cannula inserted at the time of surgery and made accessible by a silicone rubber membrane implanted in the flank of the ewe. Ibotenic acid destroys cells by activating *N*-methyl-D-aspartate and metabotropic receptors to result in a rise in intracellular calcium levels; nerve fibres passing through the lesioned area seem not to be affected. Breathing responses to acute hypoxemia were assessed before and after ibotenic acid injection. Before injection, hypoxemia resulted in a marked reduction in fetal breathing and eye movements. Following injection two types of responses were observed. In 7 of 11 lesioned fetuses, the breathing response to hypoxemia was abolished and in all of these animals there was bilateral damage to the parafascicular complex in the medial thalamus. In remaining four fetuses, the lesions did not abolish the decrease in fetal breathing with acute hypoxemia and none of these lesions involved the parafascicular complex. These results clearly identify this complex, which is part of the rostral portion of the reticular activating system as being involved in the inhibition of fetal breathing during acute hypoxemia. Further research on the midbrain pathways involved in the control of the episodic nature and other aspects of fetal breathing seems warranted, particularly on the pathways linking the midbrain, thalamic, and cortical elements that have been identified as being involved in these processes.

There is evidence obtained from the fetal lamb that two endogenous compounds are involved in the episodic nature and hypoxic inhibition of fetal breathing. Both adenosine and prostaglandin E₂ have already been mentioned as compounds implicated in the suppression of arousal in the fetus. Koos and colleagues have extensively investigated the role of adenosine in the hypoxic inhibition of fetal breathing. Their findings include the inhibition of fetal breathing and eye movements during a 1-h intracarotid infusion of adenosine with no effect on the incidence of low-voltage, fast ECoG activity, whereas with a 9-h adenosine infusion fetal breathing and eye movements recovered after 6–8 h, similar to the situation with chronic hypoxemia (see above) [78]. Acute fetal hypoxemia results in an increase in brain extracellular adenosine concentration, which was measured via microdialysis probes inserted into the rostral brain stem [79]. Intra-arterial administration of an adenosine A_{2a} receptor antagonist, but not an A₁ receptor antagonist, abolished the decreases in fetal breathing and eye movements during acute hypoxemia [80]. In contrast to the situation in intact fetuses, adenosine administration stimulates fetal breathing in fetuses with brain transection in the caudal brain stem [81], similar to the approach employed by Dawes et al. [70], which was discussed above and which also results in a stimulation of fetal breathing during acute hypoxemia. In fetuses with caudal brain stem transections, denervation of peripheral chemoreceptors by carotid body denervation and bilateral vagal nerve section eliminated the adenosine-elicited stimulation of fetal breathing, indicating that these peripheral chemoreceptors are responsible for the adenosine-elicited hyperpnea [81]. In contrast, the stimulatory effects of acute hypoxemia appear to involve both peripheral and central chemoreceptors. In fetuses with bilateral thalamic lesions that involve the parafascicular complex mentioned above [77], the inhibitory effects of adenosine on fetal breathing were abolished. However the region of brain disruption that abolished the adenosine effects appeared to be smaller than that which abolished the inhibitory effects of hypoxemia, and none of the lesions that disrupted the adenosine responses abolished the inhibitory effects of hypoxemia [82]. This led the authors to conclude that the inhibitory effects of acute hypoxemia on fetal breathing involve both adenosine and non-adenosine-mediated mechanism.

The prostaglandin E₂ concentration in fetal blood is high in part because of PGE₂ production by the placenta [83] and release into the fetal circulation and likely low systemic clearance of PGE₂ in the fetus because of the very low rate of pulmonary blood flow. The first evidence for a role of PGE₂ in the episodic pattern of fetal breathing in sheep was provided by Wallen et al. [84], who infused meclofenamate, a nonselective cyclooxygenase inhibitor, i.v. to fetal lambs. This resulted in a marked reduction in the circulating PGE₂ concentration, associated with a marked rise in the incidence of

fetal breathing to near continuous. Increasing doses of PGE₂ were then co-infused and this resulted in a progressive reduction of the amount of fetal breathing to the control level. Interestingly, at the highest PGE₂ infusion rate, the resulting plasma PGE₂ concentration was about 1/3 the control value; yet the incidence of fetal breathing was reduced to about 1/2 the control value, suggesting an increase in the sensitivity of the response. In situ hybridization techniques have also demonstrated the presence of prostaglandin H-synthase-1, an enzyme involved in prostaglandin synthesis, in various regions of the fetal brain from the cortex to the medulla, suggesting that these brain regions, which include those implicated in the episodic nature of fetal breathing, can synthesize PGE₂ locally [85]. In vitro receptor autoradiography was used to demonstrate high-density binding for PGE₂ in several nuclei within the fetal brain stem, including the hypoglossal, tractus solitarius, parabrachial, and spinal trigeminal-oral nuclei and more moderate binding in several other nuclei [86]. Note that the parabrachial nucleus was the site of lesions that resulted in the loss of hypoxia-induced inhibition of fetal breathing and the onset of continuous breathing with hypercapnia and academia [71, 72]. Tai et al. examined mRNA levels of the various PGE₂ receptor subtypes in various CNS regions from the spinal cord to cerebellum [87]. The mRNA levels of EP1 and EP2 receptors appeared higher in the medulla, pons diencephalon, and hippocampus than in the cerebellum and cortex, whereas this did not seem to be the case with EP3 and EP4 receptors. The levels of all receptors in the pons and medulla were highest in the newborn, with similar levels in the fetus and adult. Further support for the hypothesis that PEG₂ is at least in part responsible for the episodic breathing in the fetal lambs comes from studies that have examined the changes in systemic and CNS PGE₂ levels in the perinatal period. Jones et al. [88] stereotactically implanted a sampling catheter in the third ventricle of fetal lambs for collection of CSF fluid and measured PGE₂ concentration in this fluid and in plasma in late gestation before and following caesarean delivery once the ewes were in early labor. CSF PGE₂ concentration increased progressively over the last ~12 days of gestation, peaked at the time of delivery, and decreased to levels similar to those present in the fetus, and at 24 h after birth were near the detection limit of the assay. Plasma PGE₂ concentration tended to be higher than that in the CSF and did not change prior to delivery, when they peaked and then declined initially to levels present in the fetus and after 24 h to much lower levels. Intravenous infusion of PGE₂ to late-gestation fetal lambs to achieve PGE₂ concentrations of the range present in labor resulted in a marked reduction in the incidence of fetal breathing and also a reduction in the amount of low-voltage, fast ECoG activity [89]. Following cessation of the infusion, the plasma PGE₂ concentration fell, but only to the level present in the fetus prior to the start of the infusion. However

this resulted in a marked increase in the incidence of fetal breathing to 74 % of the time, with the breathing occurring at times in the high-voltage ECoG state. There was also an increase in the amount of the low-voltage ECoG state. Collectively these results provide strong evidence for a role for PGE₂ in the episodic breathing pattern that is characteristic of the fetus and also for the withdrawal of PGE₂ being involved in the onset of continuous breathing at birth.

7 Characteristics of Fetal Breathing in Sheep

As noted previously Dawes et al. monitored fluid movement in the fetal airway associated with fetal breathing [4]. Inward and outward movement of fluid was measured with each fetal breath, but the volume of fluid moved rarely exceeded 0.5 ml. Similar results were reported by Maloney et al. [90] who measured tracheal fluid flow with an electromagnetic flow meter in an exteriorized catheter whose proximal and distal ends were implanted pointing towards and away from the lung, respectively, in conjunction with measurement of diaphragmatic EMG activity and tracheal pressure. During fetal breathing, each diaphragmatic burst was accompanied by a decrease in tracheal pressure and inflow of fluid towards the lung. Because the fluid in the fetal airway has a much higher inertia and viscosity than a gaseous mixture, the airway and intrapleural pressure changes associated with fetal breathing are much higher than with breathing after birth. Thus it is common to present these pressure changes in mmHg rather than cm water that is used with postnatal breathing. During spontaneous fetal breathing, the amplitude averages 2–4 mmHg and the rate averages ~20/min [91, 92]. However another characteristic of fetal breathing is considerable variability in both rate and depth. Because of this variability and also because of the episodic nature, analysis of breathing characteristics and the factors that affect normal fetal breathing has proved difficult particularly using automated methods. Chapman et al. [91] made an initial attempt at automated analysis of fetal breathing movement measured as tracheal pressure changes. Using an early minicomputer with limited power, fetal tracheal pressure recordings were sampled at 100 Hz, digitized, and analysed in 12-min blocks. Consecutive 12-min blocks that comprised complete breathing episodes during normal conditions and during experimental hypercapnia were analyzed. Normal breathing episodes are characterized by transient accelerations in rate over a basal level that occur 1–3 times/min and last for 10–30 s. The basal level ranges from near 0 to 30–40/min and during the accelerations, rate can increase up to 280/min, although the normal increase is to 125–150/min. Breath amplitude also exhibits considerable variability, increasing from the normal range of

2–4 mmHg to as much as 30 mmHg. The effects of hypercapnia are to significantly increase the constancy of breath intervals and to normalize the frequency distribution of breath intervals and also to increase breath amplitude [91, 93]. However, there are also times during spontaneous fetal breathing when there is a decrease in the variation in breath interval and increase in breath amplitude. This pattern of more regular, vigorous breathing was characterized by Chapman et al. as a percentage variation in breath interval of ≤ 25 and an amplitude > 5 mmHg [91]. The amount of such regular breathing varies from episode to episode and is sometimes absent. Factors that may initiate such breathing are discussed below.

The large airway and intrapleural pressure changes associated with fetal breathing can affect pulsatile cardiovascular variables, particularly with large-amplitude breathing. Arterial pressure and aortic and umbilical arterial blood flows are all modulated by the breathing movements, resulting in a significant disruption of the normal pulsatile signals [4, 94]. Fetal breathing also affects pulmonary hemodynamics in the sheep fetus. Polglase et al. [95] measured left pulmonary arterial flow (with a transonic flow meter), pulmonary arterial pressure and left atrial pressure, and calculated pulmonary vascular resistance during fetal apnea, low-amplitude breathing, and high-amplitude breathing (> 3.5 mmHg). During the large-amplitude breathing, but not the low-amplitude breathing, pulmonary blood flow and pulmonary arterial pressure increased and pulmonary vascular resistance fell. During large-amplitude breathing there was also a change in the pulsatile pulmonary arterial flow profile, with decreases in both peak systolic flow and retrograde flow during diastole.

In the fetal lamb, there are significant changes in the pattern of breathing with gestational age. However, the precise pattern that is observed depends upon the method used to monitor the breathing. When the breathing is measured using diaphragmatic EMG activity, there is near-continuous breathing prior to ~ 110 -day gestation [92, 96, 97]. After 110-day gestation, the breathing becomes episodic and at ~ 120 days the episodic breathing is largely restricted to REM sleep, as discussed above [4]. In contrast, when fetal breathing is measured using real-time ultrasound, the incidence of breathing increases from a low value of 6 % at 55–64-day gestation to values of ~ 45 % between 95 and 134 days, which is similar to the estimates obtained using diaphragmatic EMG activity and tracheal pressure [98]. At no point is the breathing continuous. Between 134 days and term, the incidence of breathing decreases and a similar finding has been obtained using diaphragmatic EMG activity [99]. An explanation for these discrepant findings likely involves the developmental changes in contractile proteins in the diaphragm and other respiratory muscles, particularly the myosin heavy-chain isoforms [98]. In the fetal lamb as in other species, there is a developmental change from embryonic to perinatal to neonatal

fast myosin heavy-chain isoforms [100, 101]. In rats the maximum tetanic force and maximal unloaded shortening velocity in diaphragms obtained at different post-ages increased with increasing postnatal age and these changes were correlated with the ratio of fast/embryonic + neonatal + slow MHC isoforms [102]. Thus in younger fetal lambs, diaphragmatic EMG discharges may not lead to effective respiratory muscle contractions and chest and abdominal wall movements and so may not be visible with ultrasound observation. Clewlow et al. [92] reported that in fetal lambs aged 95–106-day gestation, when diaphragmatic EMG activity is continuous, the resulting tracheal pressure changes were often small and difficult to detect. In contrast in older fetuses, there is a reasonable correlation between diaphragmatic EMG activity and tracheal pressure [91] and there are also corresponding movements of the chest wall and abdomen [103]. Thus in late gestation (>120-day gestation), breathing movements in the fetal lamb can likely be monitored with diaphragmatic EMG activity, tracheal pressure measurement, or ultrasound observation of chest and abdominal wall movement.

8 Fetal Breathing in Other Species

Fetal breathing activity has been identified in all the mammalian species investigated. However the number of species that have been studied is relatively small. In addition to the large amount of data from sheep, published results are available for the baboon, rhesus monkey, pig, guinea pig, rat, and human [104–111]. In earlier work using pregnant rabbits, dogs, and rats, in which anesthesia of the maternal abdominal and perineal regions was achieved by section of the lumbar spine episodic fetal breathing was observed through the uterine wall or after incision in the uterus through the intact fetal membranes [112, 113]. Some of the recent data have obtained data from chronically instrumented preparations [105, 106, 108], whereas in the human and rat, noninvasive real-time ultrasound has been employed [109, 110]. As in the sheep, breathing movements in most of these other species are of at least two types: individual large inspiratory efforts that often occur as a series and episodes of rapid, irregular breathing movements. In the rhesus monkey, the individual inspiratory efforts have been termed gasping and they often occurred in association with the deflection of other recording channels, suggesting fetal movement [105]. In the human these movements have been termed hiccups, characterized by large inward and outward of the chest wall, associated with shaking of the fetal body [114]. Pillai and James reported that fetal hiccups in the human were more common prior to 24-week gestation, with ~1.5 episodes/h, with a rapid decrease to ~0.5/h thereafter [115]. Hiccups have also been observed in

fetal pigs and baboons [108, 111, 116]. Kendall reported three types of breathing activity in the fetal guinea pig: slow breathing at a rate of 1–8/min with inspiratory efforts of 1–20 mmHg; rapid irregular breathing, which lasted for a few seconds up to 40 min; and rapid, regular breathing, which occurred in bouts with a mean duration of 3.14 min and an average peak inspiratory pressure of 9.35 mmHg. It would appear that either the slow breathing or the rapid, regular breathing could be similar to the hiccups reported in the other species. The functions and mechanisms controlling hiccups are not known.

In the baboon and human, fetal breathing movements have been recorded in association with fetal behavioral state. In contrast to the situation in the fetal lamb, breathing is not restricted to REM sleep, but occurs in quiet sleep as well [104, 117–119]. In the baboon, the incidence of fetal breathing in quiet sleep was significantly less than in REM sleep and also the breathing rate, amplitude, and variability in rate were lower in quiet sleep [104]. In the rhesus monkey, the fetal breathing movements occurred more frequently during the periods with eye movements and bouts of REM only occurred during breathing periods [104]. In the human studies, the presence of fetal breathing during quiet periods and state 1F and an increase in regularity of breathing rate in these states compared to the active state and state 2F have been reported [117–119]. In one of these studies [119], the incidence of fetal breathing declined progressively from ~40 to ~6 % during the 2-h monitoring period, but there were no differences in the incidence of breathing between states 1F and 2F.

In the human, fetal breathing has been measured using a number of methods. Timor-Tritsch et al. [117] utilized two tocodynamometers applied to the maternal abdomen over the upper and lower portions of the fetus as determined by palpation. This indicates that fetal breathing movements can at times at least be transmitted through the maternal abdominal wall, a fact that was noted much earlier in the nineteenth century by Ahfeld and colleagues, who reported fluctuations in the maternal abdominal wall at rates of 38–78 min near the umbilicus, which they suggested represented fetal breathing. A subsequent researcher recorded these movements with a kymograph [64]. However these results were not generally accepted because of the absence of direct evidence that the movement was due to fetal breathing, such as fetal chest wall movements (*see* [64, 113]). Moreover, the ability to detect fetal breathing using this approach likely depends upon factors such as the gravity of the mother, the orientation of the fetus within the uterus, and changes in fetal position and orientation over time. Ultrasound methods provided the first direct evidence that fetal breathing movements did indeed occur in the human. This was first accomplished using A-scan ultrasound, in which ultrasound echoes returning from internal structures were displayed as vertical peaks

with respect to the distance from the transducer [120]. The method was verified by comparing A-scan estimates of fetal chest wall movement with recordings of tracheal pressure in chronically instrumented fetal lambs. Fetal chest wall movements were recorded in seven pregnant women and were observed in all except in one small-for-dates pregnancy, which provided evidence that fetal breathing movements might have diagnostic utility. In a subsequent study [121], these researchers demonstrated that the rhythmic maternal abdominal movements reported by Ahfeld and colleagues were associated with fetal chest wall movements at the same rate recorded with A-scan ultrasound. However, the A-scan technology provides little or no information on fetal position and changes in position. Consequently, real-time ultrasound rapidly supplanted the A-scan technique, once developed. With real-time ultrasound, movements of the fetal diaphragm, chest, abdominal wall, and abdominal contents associated with breathing can be observed and recorded with an event marker [114]. The breathing is clearly episodic and the pattern of episodes is similar to that observed in sheep and other species. In a subsequent study, Patrick et al. [110] used real-time ultrasound to monitor fetal breathing activity for 24 h at 34–35 weeks in 11 pregnant women. Postprandial increases in fetal breathing occurred after maternal meals at breakfast, lunch, and dinner. There was also a prolonged increase at night, reflective of a fetal circadian rhythm, which will be discussed further below. The postprandial increases in fetal breathing were associated with transient increases in maternal plasma glucose concentration. Adamson et al. [122] utilized an ultrasound tracking device developed by Cousin et al. [123] to measure chest and abdominal wall movement in seven human fetuses at 38–40-week gestation before and following maternal i.v. injection of a glucose dose. This resulted in a significant increase in the incidence in fetal breathing and in the amplitude of abdominal wall movement during fetal breathing, and a nonsignificant increase in rib cage movement. Unfortunately, this tracking device does not appear to have been used in other studies of the characteristics of fetal breathing in the human.

Aside from real-time ultrasound and direct observation of pulsations of the maternal abdominal wall, several other methods have been used to monitor fetal breathing in the human. Doppler ultrasound was employed to monitor pulsations from the fetus that were synchronous with pulsations on the maternal abdomen and similar pulsations recorded from an isolated lamb's lung in a saline bath, into which saline was pumped and withdrawn suggesting that the sonogram obtained from the human fetus originated from the fetal lung [124]. Trudinger and Cook used continuous-wave Doppler ultrasound to measure pulsations in umbilical venous blood flow velocity waveforms associated with fetal breathing movements in

eight primiparous human patients at 2-week intervals from 28 weeks to term. With each fetal inspiratory effort there was a decrease in umbilical venous blood flow velocity followed by a return to the normal level during expiration. This transient decrease was attributed to an increase in abdominal pressure, and hence a decrease in the umbilical arterial-venous pressure gradient, due to the descent of the fetal diaphragm with inspiration. Trudinger and Cook used the umbilical venous pulsations associated with fetal breathing to calculate inspiratory and expiratory times, breath to breath, an estimate of breath amplitude, and the coefficient of variation of breath amplitude as a function of gestational age and found the results similar to those obtained using real-time ultrasound observation of fetal chest and abdominal wall movement [125]. Fetal breathing-elicited alterations of Doppler ultrasound flow waveforms have also been noted for the mitral and tricuspid valves [126], middle cerebral artery [127], and descending aorta [128]. These findings indicate that breathing movements in the human fetus modulate cardiovascular function similar to the situation in the fetal lamb.

Fetal biomagnetography has also been used to monitor human fetal breathing. Gustafson et al. [129] used an 83-channel fetal biomagnetometer to obtain signals from pregnant women at 36–38 weeks over 18-min periods. Processing of the signals yielded the maternal and fetal ECG and an intermittent rhythmic signal obtained from channels over the fetal diaphragm. Simultaneous display of fetal heart rate and diaphragmatic contractions indicated the presence of a respiratory sinus arrhythmia, similar to that observed after birth. Van Leeuwen et al. exploited this phenomenon via use of a 61-channel biomagnetometer, with processing of the signals to obtain both fetal ECG and diaphragmatic signals and developed an automated system to identify periods of fetal breathing from the respiratory sinus arrhythmia in the R-R intervals. As with the use of fetal biomagnetography to measure the fetal EEG, use of the technique to monitor fetal breathing requires use of a magnetically shielded room.

The rat is the only altricial species, for which information on fetal breathing is available. Kobayashi et al. used real-time ultrasound to monitor fetal chest wall and diaphragmatic movements in pregnant rats for 30-min periods. As in the fetal lamb and human, two types of respiratory movements were observed: single respiratory efforts similar to hiccoughs in the human and intermittent periods of clusters of fetal breathing movements. The isolated respiratory efforts first occurred at gestational day 16 and the clustered fetal breathing at day 18. The total number of episodes of clustered breathing increased progressively on gestational ages 19 and 20 and on the latter day comprised ~15 % of the time. This appears less than the incidence of breathing in late gestation in the

sheep and human (40–45 %). Fetal breathing in the rat also is first evident at a later gestational age (0.85 of term) compared to the sheep (0.34 of term) and human (0.25 of term). A useful research technique that has been used in the rat is the isolated brain stem-medulla preparation, from which recordings can be obtained from cranial and spinal motor neurons and also from medullary centers, including the pre-Bötzinger complex and the retrotrapezoid nucleus and parafacial respiratory group, which are involved in the generation of the respiratory rhythm [130, 131]. Recordings from both sites exhibited phasic discharges at gestational age 16, which increased in frequency with advancing gestational age until term [132, 133]. This is the same time frame as for the ultrasound observations of fetal breathing in the rat that was discussed above. This suggests a different pattern of respiratory development in the rat compared to the sheep, in which as discussed above phasic discharge from the medullary respiratory centers begins before observable chest wall movement. This further suggests that in the rat the development of the medullary respiratory centers must develop in parallel with the development of the respiratory muscles, a situation that appears different from the sheep.

Studies of respiratory rhythm generation have also been conducted in a precocial rodent, the spiny mouse (*Acomys cahirinus*) [134], which has a longer gestational length (39 days) than in the rat and mouse and is born in a more mature state [131]. Greer et al. [134] utilized whole-body plethysmographic measurements to determine the frequency and depth of breathing at postnatal days 0–1 and found the pattern to be similar to that obtained in neonatal rats. Histological examination of the phrenic nerve at birth in the two species indicated that the nerve in the spiny mouse is much more advanced in terms of myelination than in the rat. The isolated brain stem-spinal cord of the neonatal spiny mouse appeared more mature than in the rat in terms of features such as cerebellar development, increased ventral root thickness, and increased tissue compactness. However, these isolated preparations from the spiny mouse did not generate a spontaneous respiratory rhythm, which is similar to the findings in postnatal rats at days 4–5. Using the more reduced medullary slice preparation, a spontaneous respiratory rhythm was observed and the rate of respiratory discharge was slightly but significantly faster than in the neonatal rat. Several findings of this study suggest that in the spiny mouse the respiratory system is more mature than in the rat, such as the greater maturation of the phrenic nerve and the more mature appearance of the isolated brain stem-spinal cord preparation. However, demonstration of greater functional maturity would require ultrasound assessment of fetal breathing activity in this species, particularly in terms of the stage of gestation at which the breathing movements first occur.

9 Fetal Body Movements

The fetus moves have been recognized by pregnant women, likely since early in human evolution. Although most pregnant women can detect various types of fetal movement (rolling and stretching, isolated limb movements, trunk movements, and hiccups), the variability in maternal awareness of fetal movements precludes its use as a research method to characterize fetal motility and also its usefulness as a diagnostic screening method [135–137]. Until the development of ultrasound visualization methods, study of the details of fetal movement patterns was difficult, even in animal species. This is because instrumentation of the fetus to study fetal movements would have to be extensive to identify different movement types. Ruckebusch et al. provided some of the first data on motility in chronically instrumented fetal lambs [5]. The surgical preparation included electrodes for recording ECoG activity and eye movements and paired EMG electrodes inserted 5 mm apart in each of the triceps brachii, splenius, and longissimus dorsi muscles and in two animals in the tenth intercostal space. These electrodes allowed detection of movements of the forelimb, neck, and trunk. Paired electrodes were also implanted in the myometrium of the uterine horn containing the operated fetus and two 0.3 mm insulated iron discs were attached to the opposite sides of the uterine horn. These discs recorded impedance changes associated with fetal movements and these were also identified by the fetal muscle EMGs, which were all connected to the same amplifier. Of the ten fetuses chronically instrumented, five provided successful recordings. The fate of the unsuccessful preparations is not detailed, but likely involved fetal death, preterm birth, and catheter or electrode failures. This success rate is typical for complex chronically instrumented fetal preparations.

The authors defined three types of fetal movements. Simple fetal movements (SFM), which involved activities such as extension of the head or forelimb, were not associated with impedance changes and did not affect fetal heart rate. Complex fetal movements (CFM) were 2–3 large amplitude deflections of the limb, trunk, and neck muscle EMGs, with associated changes in fetal heart rate (accelerations or decelerations) and 2/3 of the time with impedance changes. Gross fetal activity (GFA) was associated with both EMG and impedance changes in separate and repeated bouts of complex movements lasting for 3–10 min. There were about 15 bouts of GFA per day and they were restricted to low-voltage ECoG activity without REM that is consistent with the aroused state discussed above. SFM and CFM occurred during both quiet and REM sleep, although it appeared that they were more of these movement types during quiet sleep. There was a higher incidence of fetal movements, particularly GFA, during the night.

Another approach was assessing fetal movements in sheep which was employed by Natale et al. [138]. They conducted surgery at 116-day gestation to implant ECoG and eye movements, and electrodes consisting of insulated twisted stainless steel wire in the triceps and biceps muscles of each forelimb. Ultrasound transducers were implanted on each forelimb, with the transmitter placed at the head of the humerus and the receiver at the head of the ulna. The ultrasound signals were processed by a custom-built device that measured the transit time between the transmitter and receiver and also linked these signals to the EMG signals from the biceps and triceps muscles. This allowed identification of passive movement, which involved limb movements without EMG activity and active movements with limb movements associated with EMG activity. Simple active movements were defined a single rapid extension and/or flexion of the limb, whereas complex movements were defined as having a longer duration and consisting of repetitive limb movements. Active limb movements occurred in all fetal sleep states, with the average number of movements/min being 2.00 ± 0.35 for quiet sleep, 1.65 ± 0.35 for REM sleep, and 2.42 ± 0.30 and 2.24 ± 0.12 for the brief arousal episodes between quiet sleep and REM sleep and REM sleep and quiet sleep. None of these values are significantly different although it appears that complex limb movements were more frequent during the arousal periods. A 1-h period of fetal hypoxemia, achieved by lowering maternal inspired oxygen, resulted in a marked reduction in fetal limb movements, similar to the effect of acute fetal hypoxemia on fetal breathing. In three of the fetuses recordings were obtained during spontaneous labor and delivery. The fetus continued to cycle between quiet and REM sleep, with brief arousal periods. However, there was a significant reduction in limb movements in all sleep states, particularly REM sleep. The remaining limb movement largely occurred during uterine contractions.

Real-time ultrasound is the primary method used to assess fetal motility in human pregnancy, although as discussed earlier other methods such as actocardiography have also been employed. The advantage of ultrasound is that it provides visualization of the fetus and thus qualitative information on fetal movements. Moreover, this advantage has been enhanced by the development of 3-D ultrasound, which provides a static three-dimensional image of the fetus, and 4-D ultrasound, which gives dynamic three-dimensional viewing of the entire fetus [139]. Patrick et al. [140] provided the first report of ultrasound observation of human fetal body movements over 24 h. The movements recorded included rolling movements and stretching movements; isolate limb movements were not recorded. In contrast to the situation with fetal breathing (see above), there were no increases in fetal body movements associated with maternal meals. However, there was an increase in body movements during the night. There was

considerable variability in the data, with the number of body movements in any hour ranging from 0 to 130 and the longest period of quiescence being 75 min, which highlights the fact that prolonged quiescence is a normal feature of fetal behavior.

As discussed earlier in relation to human fetal behavior, fetal movements appear to be modulated by behavioral state, with general quiescence and brief gross body movements and absent eye movements in state 1F (quiet sleep), frequent and periodic gross body movements and continuous eye movements in state 2F (REM sleep), and vigorous, continual body movements and continuous eye movements in state 4F (arousal). More information on the variation in fetal movements in relation to the behavioral states is provided by Pillai and James [49, 115] and de Vries and Fong [141], particularly in relation to startles as a form of movement during state 1F and differences in mouthing, tongue, and jaw movements between states 1F and 2F. There are also data on the ontogeny of fetal movements as a function of gestational age [49, 142, 143]. Fetal motility is first discernible at 7–8-week gestation (~0.19 of term). These are first comprised of sideways bending of the head, which thereafter extend caudally to incorporate the arms and rump [143]. By 10–12 weeks the movements become more forceful and are sufficient to cause displacement of the fetus. Breathing movements are first present at 10–11 weeks, with other movement types occurring progressively as gestation proceeds [142]. Ten Hof et al. [144] used ultrasound to monitor longitudinally human fetal body movements later in gestation. Fetal body movements were measured biweekly for 60 min in 29 singleton pregnancies from 24 weeks to term. The percentage and number of fetal movements decreased progressively, and this was the case during episodes of fetal heart rate patterns (FHRP) A (stable heart rate, with isolated accelerations linked to movements, consistent with state 1F, quiet sleep) and B (wider oscillations in rate with frequent accelerations during movement, consistent with state 2F, REM sleep). Moreover, the median duration of FHRP A episodes increased from 14.5 min at 32–34 weeks to 36.0 min at 38–40 weeks, and near term there were hardly any movement during FHRP A episodes. Collectively these human results suggest a progressive increase in the amount and types of fetal body movements in the first half of gestation, followed by a progressive reduction in the second half.

Ultrasound has also been used to study fetal motility in several other species, including the guinea pig, pig, and sheep [98, 107, 145]. In the guinea pig study, van Kam et al. [107] conducted a detailed study of fetal body and breathing movements involving ultrasound observation for 30 min every 2–4 days from 24 days until term (68 days). The pregnant guinea pigs were trained during 3–4 sessions to remain quiet during scanning. Fetal motility began at ~24 days (0.35 of term) with sideways movement of the head and

rump. Other forms of movement commenced between 24 and ~35 days; the movement patterns displayed were similar to those in the human [141]. The movements versus gestational age relationships were best described by polynomial equations. The percentages of time occupied by sideways bending, general movements, and fetal breathing all increased and then decreased. However the gestational age at which the peaks in these activities occurred differed, being ~30 days for sideways bending, ~45 days for general movements, and ~50 days for fetal breathing. The percentage time at rest curve was the inverse of the motility curves; it decreased until ~45 days, and then increased thereafter.

In the pig study, fetal body movements were monitored for 60 min every 3–5 days over the last 3 weeks of pregnancy [145]. General and head movements and total fetal activity decreased progressively with advancing gestational age, whereas isolated limb movements were best described by a quadratic equation, in that the % of time with limb movements increased until about 2 weeks prior to term, and then decreased. The duration of the longest period of quiescence increased progressively.

Rurak and Wittman [98] used real-time ultrasound to measure motility and abdominal diameter in eight fetal lambs at weekly intervals for 30 min from 55 days to term. The body movements that were recorded were movements of the limbs and body of the fetus sufficient to cause transient displacement of the fetal trunk. Isolated limb movements, when observed, were not recorded. Fetal body movement counts/min were relatively constant between 55 and ~90 days, and declined progressively thereafter, a relationship best described by piecewise linear regression with two elements (Fig. 10). The breakpoints in the regression curves ranged from 65- to 110-day gestation and averaged 91.9 ± 5.2 days.

Data on fetal lamb motility from earlier in gestation has been obtained using other approaches. Barcroft and colleagues [146] conducted studies of pregnant sheep between ~30- and 60-day gestation while under spinal anesthesia and immersed in a saline bath at body temperature. Following abdominal and uterine incisions, the fetus could be viewed through the intact amniotic membrane. Although spontaneous fetal movements were not reported, movements in response to tapping the fetal head first occurred at 34–35 days (0.32 of term). Initially only the fetal head was involved in movement, but by the 38th day there is generalized body movement (“spasm”) and also movement of the diaphragm, and by the 40th day there is a rhythm of successive spasms. Generalized body movement and rhythmic diaphragmatic movement increased in response to touching the fetus until about 50-day gestation. Between 50 and 60 days, the fetus became increasingly unresponsive except following umbilical cord occlusion.

The observations of Barcroft and colleagues on acute sheep preparations have been extended to studies on fetal lambs from

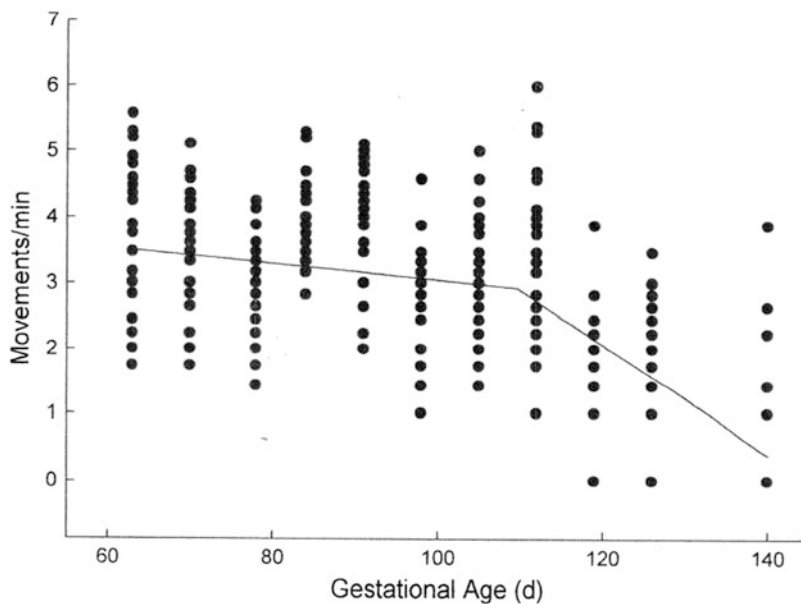


Fig. 10 Movement counts/min monitored with real-time ultrasound in eight fetal lambs during each 30-min monitoring session at each gestational age studied. The *regression line* was calculated using piecewise linear regression with two elements. From [98] with permission

45- to 95-day gestation with chronically implanted EMG electrodes on respiratory (diaphragm, external intercostal) and non-respiratory (e.g., longissimus dorsi) muscles by Berger and colleagues [97, 147]. At 45 days, the predominant activity observed was sustained EMG bursts lasting for up to several minutes and which involved both respiratory and non-respiratory muscles. This is perhaps analogous to the generalized body movement (spasm) reported by Barcroft [146]. There was also repetitive burst activity that involved the diaphragm only and had the characteristics of a respiratory rhythm [97]. With advancing age, these repetitive bursts became segregated from the sustained EMG bursts. Moreover in fetuses subjected to spinal cord transection, the repetitive bursting in the diaphragm was lost, suggesting that they are generated from supraspinal locations, perhaps the developing respiratory rhythm generator in the medulla [97]. In addition, the findings also suggest developing supraspinal influences on fetal motility that early in gestation involve only pathways in the spinal cord [147]. The reasons for the quiescence observed in the 50–60-day fetuses in the Barcroft study [145] and fetal motility observed at this gestational age by Berger and colleagues [97, 147] and Rurak and Wittman [98] are not clear. It may relate to the acute surgical condition of the former study, and perhaps an increasing sensitivity of the fetus to these conditions with increasing gestation. Nonetheless, the results overall suggest that by at least 45-day

gestation, the fetal lamb is capable of making both body and breathing movements. Detailed ultrasound observations of the fetus prior to this age could provide more detailed information on the development of motility in this species.

Fraser and colleagues have used a variety of techniques, including radiography, fluoroscopy, and Doppler ultrasound to observe several aspects of motility in fetal sheep, cows, and horses [148–152]. The types of movement described include rapid opening and closing of the mouth in the late-gestation sheep fetus [152] and changes in motility over gestation in fetal cows and horses. Doppler ultrasound was employed to assess motility and distinguished simple from complex movements by specific changes in the pitch of the audio signal from the ultrasound unit [148, 149, 151]. In the fetal horse, simple fetal movements were first detected at 90-day gestation, increased in incidence to ~180 days, remained at a plateau until ~250 days, then decreased until ~280 days, and remained at the level until term. There was also an increase in the duration of quiescent periods with advancing gestation. In the cow, simple fetal movements increased between 4 and ~6.5 m and then decreased, although the magnitude of the decrease appeared to be less than that in the fetal horse and lamb. In all three species in late gestation, specific “righting reflexes” were also observed. These are postural and positional changes (foreleg extension, head elevation) undertaken by the fetuses of these quadruped species in the prepartum period in preparation for birth. They occur over the last 2 days of gestation in the sheep, 1 day prepartum in the cow, and in early labor in the horse [152]. These movements appear to be the only purposeful movements exerted by the fetus, in that they are a form of activity that occurs in late gestation that results in the fetus attaining a posture that facilitates efficient delivery. Fraser and Broom [152] have estimated that righting reflexes in the fetal lamb involve 3500 movements following which there is typically quiescence until labor. The mechanisms involved in righting reflexes are unclear. It would seem that studies involving measurement of EMG activity in fetal limb and neck muscles, similar to the methods employed by Ruckebusch et al. [5], combined with real-time observation of the fetus could provide more information on this phenomenon.

As discussed above in this section, a number of methods have been employed to assess fetal motility. Real-time ultrasound offers advantages over invasive methods in that viewing of the fetus allows for information of the types of fetal movements to be obtained and in addition in animal studies it can be utilized earlier in gestation than is possible for chronically instrumented preparations. The studies conducted to date with ultrasound in animal species demonstrate that it is possible to use this method in conscious pregnant animals, particularly if the animals are acclimated to the procedure. Moreover with the development of portable, battery-powered ultrasound units, such as the GE VScan unit, it is much more

feasible to conduct studies on pregnant large animal outside of the laboratory environment, for example on farms.

Overall the available information on fetal motility indicates several general features. During the first half of gestation, the various forms of fetal body movements and fetal breathing develop in a coordinated fashion, while in the second half, fetal body and breathing movements become linked to fetal behavioral state and there is also a more or less progressive decrease in the amount of body and breathing movements, except that in quadruped species there are righting reflexes that orientate the fetus in preparation for labor. The decline in fetal body movements with advancing gestational age has been attributed to the development of fetal behavior and a reduction in the space available for movement due to the increasing size of the fetus in a relatively fixed amniotic fluid volume [107]. The latter proposition is supported by the observation in human pregnancy that reduced amniotic fluid volume in patients with premature membrane rupture was associated with significantly reduced fetal movements, as well as a decrease in the speed and amplitude of general movements [153, 154]. Conversely, prophylactic amnioinfusion to treat oligohydramnios results in an increase in fetal body movements [155]. However it also seems possible that the decline in fetal motility with advancing gestation is linked to the increase in fetal plasma concentrations of two of the compounds that have been postulated to suppress fetal arousal and fetal breathing. In the fetal lamb, Nguyen et al. [156] have reported that the plasma concentrations of neurosteroids (allopregnanolone, progesterone, pregnanolone) in the fetal lamb increase in the second half of pregnancy, although the time course of the changes varies for the individual steroids. There were also increases in the content of the various steroids in the different brain regions examined. In addition in fetal lambs, the plasma concentration of PGE₂, which inhibits fetal breathing, will increase progressively beginning at 20 days before parturition (~127 day's gestation) [157]. In human pregnancy, the maternal serum concentrations of progesterone, pregnanolone, and allopregnanolone increase progressively with advancing gestational age and at delivery the concentrations of allopregnanolone and progesterone were higher in cord blood than in maternal blood [158]. The increases in fetal neurosteroid and PGE₂ could inhibit fetal arousal and breathing, respectively. In the ultrasound study of fetal lamb motility conducted by Rurak and Wittman [98], there was also a breakpoint in the curve relating fetal abdominal diameter to gestational age, with the rate of increase in diameter decreasing after the movement breakpoint. The mean gestational age of this breakpoint (113.1 ± 3.9 days) was significantly different for the breakpoint for fetal motility (91.9 ± 5.2 days). Moreover, there was a significant linear relationship between the movement and abdominal diameter breakpoints in the individual fetuses, which suggests that these two processes may be causally

related. As discussed in more detail in Rurak and Wittman [98], the decline in fetal motility and growth may be a response of the fetus to the decline in weight-normalized uterine and umbilical blood flows that has been reported in various species, which leads to progressive decreases in fetal vascular PO_2 , O_2 content, and O_2 delivery and in the fetal lamb at least O_2 consumption. As fetal motility and growth impose metabolic costs on the fetus, the decline in fetal motility and growth may function to maintain the balance between oxygen delivery and consumption.

10 Fetal Circadian Rhythms

As noted above, there are circadian rhythms in fetal breathing and body movements in the human fetus and in fetal body movements in the fetal lamb [5, 140]. There are also circadian rhythms in breathing, ECoG states, plasma prolactin concentration, arterial pressure, heart rate, carotid blood flow, and urine flow in the fetal lamb [159–162]. A similar circadian rhythm in behavioral state has been reported in the fetal baboon [163]. In addition in human fetuses at 36 weeks, Doppler ultrasound variables obtained from the middle cerebral artery and fetal heart rate variables change significantly from morning to afternoon, which may also reflect a circadian rhythm in these variables [164]. These observations are somewhat surprising since following birth, circadian rhythms are initially absent during the neonatal period. The plasma melatonin rhythm in term lambs is not present until 3–4 weeks after birth [165]. In the human infant, the melatonin rhythm, assessed by the urinary excretion of a melatonin metabolite, develops between ~9 and 12 weeks following birth [166], which is similar to the time of onset in the circadian rhythms of core body temperature, day-night cortisol concentrations and rest-activity [167].

Studies in pregnant sheep have provided evidence that the fetal circadian rhythms are derived from the maternal melatonin circadian rhythm. There are 24-h rhythms in the plasma melatonin concentration in both the ewe and fetus with the peak concentrations occurring from ~1800 to 0600 [168, 169]. Melatonin readily crosses the placenta and maternal pinealectomy abolishes the melatonin rhythms and results in basal concentrations in both the ewe and fetus [169–171]. Maternal pinealectomy also abolishes the nocturnal increase in fetal breathing although it unmasks an increase in the morning (09.00–12.00). This increase occurred following the morning feed of the ewes and was attributed to the resulting increased supply of glucose and other nutrients to the fetus that would occur at this time [172, 173]. However maternal pinealectomy did not affect the prolactin rhythm in the ewe and fetus although altering the time of the dark period shifted the prolactin peak to the time of the altered dark period [173]. Overall

these results suggest that the fetal circadian rhythms are derived from the maternal melatonin cycle, with the difference being that the melatonin peak in the mother is associated with sleep (human) and sleep/drowsiness (sheep), whereas in the fetus it is associated with increased motility.

11 Antepartum Uterine Activity and Fetal Behavior

The uterus is not totally quiescent during pregnancy. In human pregnancy, antepartum uterine activity was first described in 1871 by John Braxton-Hicks, and the contractions are named after him [174]. However, it is likely that such contractions were recognized long before this, if only by pregnant women. In pregnant sheep, antepartum uterine activity was not described until 1979 by Jansen et al. [175]. In the sheep, these contractions (also known as contractures) last for about 5 min and have a peak amplitude of ~ 5–7 mmHg. They are thus very different from the contractions that occur during labor in terms of both amplitude and duration. They can be measured by monitoring intra-amniotic pressure with an implanted catheter (*see* Fig. 3) or perhaps more accurately by monitoring myometrial EMG activity with implanted electrodes [176]. Antepartum uterine contractions have also been observed in the rhesus monkey, guinea pig, and rabbit [177]. The mechanisms involved in the generation of these contractions are not entirely clear. In pregnant sheep, Lye and Freitag [177] transplanted small strips of myometrium alone and myometrium plus endometrium to the omental fat and recorded EMG activity in the strips and uterus. The frequency of EMG bursts in the implanted strips was higher and the duration of the bursts shorter than in the uterus. This led to the conclusion that the contractions were not due to circulating factors in the ewe, but rather to mechanisms operating within the myometrium.

The available data of the effects of antepartum uterine activity on the fetus have largely been obtained from pregnant sheep. Jansen et al. [175] first reported that the contractures were associated with a transient reduction in fetal right atrial and arterial Po_2 , which were measured continuously with a catheter with an attached Po_2 electrode at its tip. Uterine tissue Po_2 , measured with a galvanic electrode, decreases during contractions as well [178]. There is also an increase in arterial Pco_2 [179]. These changes in fetal blood gas status are likely at least in part due to a transient reduction in uterine blood flow during the contractures [180, 181]; however, umbilical blood flow is unchanged [179]. These contractions also squeeze the fetus resulting in a change in shape of the thorax [181, 182] and can result in an increase in intracranial pressure [183]. There is also a transient increase in fetal arterial and venous pressures, likely due to translocation of blood from the placenta to the

fetal vascular space [184]. All of the above data on contracture-related effects were obtained by collecting measurements from the fetus before, during, and after a spontaneous contraction. This obviously requires the ability to predict when a contraction is going to occur, in order to obtain the pre-contraction data close to the onset of the contraction. An alternative approach is to elicit similar contractions by administering small doses of oxytocin intravenously to the ewe [177, 185]. Using this approach, Lye et al. [186] demonstrated a transient increase in fetal plasma ACTH levels associated with the fall in vascular P_{O_2} during the contractions. Woudstra et al. [187] subsequently demonstrated that the contracture-related rise in fetal plasma ACTH concentration was abolished when the fall in fetal vascular P_{O_2} was abolished by maternal oxygen administration. There are also changes in fetal behavior associated with antepartum uterine contractions. Two studies have reported that contractions are associated with a change in behavioral state, more often from a low-voltage pattern (largely REM sleep) to a high-voltage pattern (quiet sleep) and a cessation of fetal breathing if it was occurring before the onset of the contraction [182, 188]. However these changes do not occur with every contraction; rather the changes occurred with 55 to 74 % of them [182]. The mechanisms involved in this linkage between uterine activity and fetal behavioral state have not been elucidated, but could involve some of the effects noted above, such as the transient fetal hypoxemia or the increase in intracranial pressure.

In human pregnancy, Wilkinson and Robinson [189] monitored fetal breathing with real-time ultrasound and recorded uterine activity with an external tocograph. If fetal breathing movements were occurring prior to a Braxton-Hicks contraction, the rate of breathing decreased from ~ 30 /min prior to the contraction onset to ~ 17 /min just prior to the contraction peak and then increased to ~ 35 /min as the contraction waned. This is different from the breathing responses to contractures in the fetal lamb, where as noted above the breathing usually ceases. The effect of Braxton-Hicks contractions on human fetal behavior has also been examined [190]. However, behavior was coded only as state 1F (quiet sleep) and non-state 1F (more active states). There was no association between uterine contractions and fetal behavioral state. There was, however, an effect of the contractions on fetal body and breathing movements if they were present at the onset of the contraction, although the precise changes depended on the duration of the contraction, particularly for fetal breathing. With contractions of durations >45 and <120 s the breathing rate fell during the contraction, but rose again as the contraction waned, similar to the findings of Wilkinson and Robinson [189]. With contraction durations >120 and <300 s, the breathing rate declined towards the peak of the contraction and continued to decrease for the rest of the contraction and for at least the next

90 s. With body movements, they increased during the first $\frac{1}{2}$ of the contraction and decreased during the second $\frac{1}{2}$. With the longer duration contractions the initial increase in body movements was larger than with the shorter duration ones. These results are different from those reported for the fetal lamb and this may be due to the different characteristics of antepartum uterine activity in the two species. As mentioned above the duration of contractures in the sheep is relatively constant at about 5 min. In contrast, the mean duration of Braxton-Hicks contractions in human pregnancy is 114 s (1.9 min) and only 25 % have durations from 2 to 5 min [190]. However, with the longest duration contraction (14 min) observed by Mulder and Visser [190], there was a deceleration in fetal heart rate and a change for a non-state F1 to F1 state.

The data summarized above indicate that antepartum uterine contractions have significant acute effects on the fetus, particularly the fetal lamb. Some of these effects, such as the transient rise in plasma ACTH concentrations, via stimulatory effects on fetal adrenal, increase cortisol secretion, particularly in late gestation [191], and thereby have maturational effects of various fetal organs and tissues [192]. Thus along with eliciting acute effects, antepartum uterine contractions could also have maturational actions. One experimental approach to test this hypothesis would be to inhibit such activity on a long-term basis. In pregnant sheep contractures can be acutely inhibited with the adrenergic β agonists, such as salbutamol [193], that were at one time used as tocolytics in human pregnancy [194]. However, these agents would be unlikely to inhibit uterine activity on a long-term basis [195] and these also elicit significant cardiovascular and metabolic effects on the mother [196] and fetus [197], which could result in significant confounding effects. An alternative approach was employed by Nathanielsz and colleagues: pulsatile, intravenous administration of small dose of oxytocin to increase the rate of contractures above the basal rate by ~ 130 %, with a minimum duration of oxytocin infusion being 6 days [198, 199]. Some of these studies involved examination of the fetal responses to experimental perturbations such as acute hypoxemia and hypotension [199, 200]. However, the studies most relevant to the current discussion relate to the maturational effects of the increased contraction frequency. Shinozuka et al. [201] employed the oxytocin administration regimen from 96- to 133-day gestation, after which the cardiovascular responses to acute hypotension (induced by i.v. administration of sodium nitropruside) and hypertension (induced by i.v. injection of phenylephrine) were assessed. Arterial P_{O_2} was lower and O_2 content higher in the oxytocin group compared to the control group. This has been reported previously [200] and shown to be due to a leftward shift in the blood oxygen dissociation curve. Between 126- and 140-day gestation, fetal arterial pressure was higher and fetal heart rate was lower in oxytocin-administered group compared to the control

group. Moreover the slopes of the gestational age-related increase in arterial pressure and decrease in heart rate were lower in the former compared to the latter group. There were also alterations in the heart rate responses to acute hypotension and hypertension. Sadowsky et al. [198] examined the effects of maternal oxytocin administration on behavior in late-gestation fetal lambs. They specifically examined the peak voltage in high-voltage ECoG activity by mathematical analysis of the amplified and filtered ECoG activity. In both the control and experimental groups, this voltage increased with advancing gestational age, and this is a measure of the maturation of the high-voltage ECoG pattern. Moreover the rate of increase in this voltage was significantly higher (by 53 %) than in the control group, and the time spent in the high-voltage state was also higher in the oxytocin-administered group. As noted previously, Szeto et al. [9, 24] reported a decrease in the amount of REM sleep with advancing gestation and an increase in the spectral edge frequency for the high-voltage pattern and a decrease in the spectral edge frequency for low voltage. The changes noted in the high-voltage peak voltage observed by Sadowsky et al. [198] are consistent with these changes and suggest that an increased frequency of uterine contractions increases the rate of behavioral maturation in the fetal lamb. What remains to be determined is whether long-term maternal oxytocin administration has any effects on post-natal development. Are the fetuses from such pregnancies more mature at birth?

Overall these results indicate that the antepartum uterine contraction elicits significant acute effect on the human and sheep fetus, and in the latter species may also be involved in maturational effects on neural and cardiovascular functions. The results also suggest that these contractions have greater effects on fetal lambs compared to the human fetus and this may be due to the longer duration of the contractions in sheep. This may relate to the differences in the degree of maturation at birth in these two species. Birth weight in fetal lambs is similar to that in human newborns, but the state of maturation, particularly in terms of locomotory abilities, is greater than in the human. Yet gestational length in sheep (147 days) is just over $\frac{1}{2}$ that in the human (270 days), which indicates that the rate of both growth and maturation must be greater than that in the human. It may be that the longer duration contractions in sheep contribute to the greater rate of maturation. It is of interest that the duration of antepartum uterine contractions in the pig (8 min) is long and they also occur at a higher frequency ($\sim 6/h$) than in sheep [202]. Guinea pigs are very mature at birth and have a gestational length of 67 days. The duration of antepartum uterine contractions in the rabbit is up to 5 minutes and it occurs at a rate of 1–4 min. Rabbits are an altricial species, but have a gestation length of only ~ 31 days, so that uterine contraction-elicited maturational effects may be important for the

fetal rabbit reaching a state of maturation that permits postnatal survival. In contrast, the duration of antepartum uterine contractions in the rhesus monkey is only about 2 min, similar to the human. More research in various species on antepartum uterine activity and its short- and long-term effects on the fetus is required to gain a better understanding of the effects of this activity on fetal development and maturation.

Fetal Behavior and Cardiorespiratory Function: As noted above, fetal body movements are associated with transient changes in heart rate, usually accelerations in healthy fetuses. This association has been noted in sheep, humans, and various other species [203] and in human pregnancy is the basis of the non-stress test and is a component of the biophysical profile score, both of which are tests of fetal well-being [204–206]. The existence of a causal relationship between fetal body movements and heart rate accelerations was tested in the sheep and human using the same experimental approach: temporary paralysis of the fetus with a neuromuscular blocking agent [207, 208]. In both studies, this led to abolition or a marked reduction in fetal motility, but no change in the number of heart rate accelerations, although in the human study, there was a 60 % reduction in fetal heart rate variability. This suggests that it is not the body movements that lead to the tachycardia; rather both are likely increased by augmented stimulatory output from the fetal brain. An increase in heart rate will lead to an increase in cardiac output, and thus likely transient increased flow to fetal organs and tissues [209], and will also in some cases result in a transient rise in arterial pressure. Thus in healthy fetuses there are frequent transient increases in fetal heart rate, cardiac output, arterial pressure, and organ blood flows associated with fetal movements (Fig. 11). Bouts of fetal motility also increase fetal oxygen consumption [94, 210]. Conversely, temporary paralysis of the fetal lamb with a neuromuscular blocking agent or anesthesia of the fetus by intravenous injection of sodium pentobarbitone decreases fetal oxygen consumption by 15–20 % [211–213]. Moreover, fetal motility and the abolition of fetal motility have opposite effects on fetal oxygenation, with fetal activity bouts leading to a reduction in fetal vascular P_{O_2} and the abolition of fetal motility leading to a rise in vascular P_{O_2} . An explanation for this phenomenon resides within the maternal-placental-fetal supply line for oxygen. If we compare this system to the postnatal lung, umbilical blood flow is equivalent to pulmonary blood flow and uterine blood flow is the equivalent to pulmonary ventilation. With the postnatal lung, increases in oxygen demands, such as with exercise, result in increases in both pulmonary blood flow and pulmonary ventilation. With the placenta, umbilical blood flow increases with fetal movements, but there is no evidence that

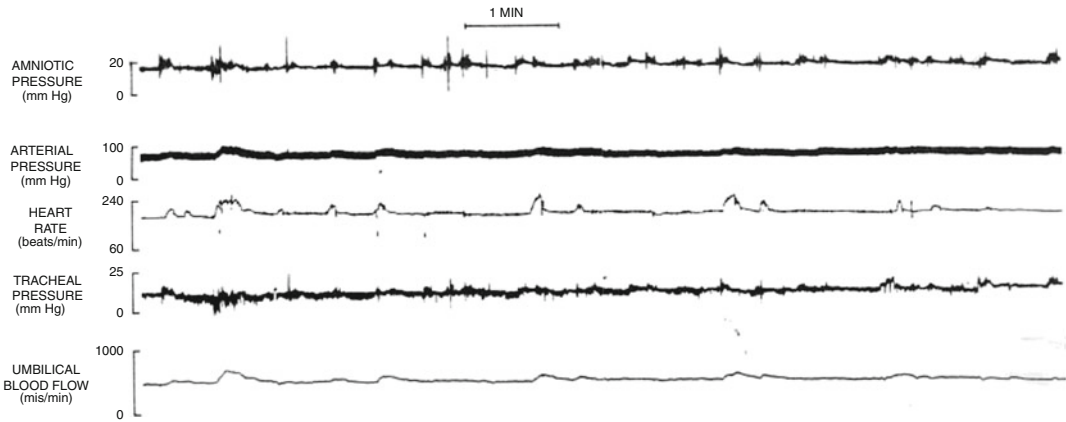


Fig. 11 Polygraph recording from a fetal lamb at 127-day gestation displaying amniotic pressure, arterial pressure, heart rate, tracheal pressure, and mean umbilical blood flow (measured by an electromagnetic flow transducer implanted around the common umbilical artery). The transient accelerations in heart rate, especially the larger ones, are associated with transient hypertension and increased umbilical blood flow. Rurak and Wittman, unpublished data

uterine blood flow responds to transient changes in fetal oxygen requirements. Thus when fetal oxygen demands rise during fetal “exercise” more oxygen is removed from maternal uterine blood as it flows through the placenta and its oxygen levels decrease resulting in a greater fall in P_{O_2} . As there appears to be an equilibration of maternal and fetal vascular P_{O_2} within the placental exchange areas, fetal vascular P_{O_2} will also fall. Thus in healthy fetal lambs, episodic fetal breathing and body movements are associated with transient reductions in vascular P_{O_2} , with greater degrees of hypoxemia occurring with more vigorous movements [94, 210]. Uterine contractions also contribute to the variability in fetal oxygenation, since as discussed above fetal vascular P_{O_2} falls during these antepartum contractions and they also can lead to a change in behavioral state. There is also evidence that fetal motility might be stimulated during contractions. If an episode of fetal breathing is occurring when a contraction starts, there is often a transient increase in breath amplitude before the breathing ceases [214]. In addition there is an increase in carcass blood flow and total body oxygen consumption in the fetal lamb during contractions, both of which are consistent with increased fetal motility [179, 215]. The stimulus for the increased motility has not been established. However it could be due to the modest hypoxemia that occurs initially during the contraction. Testing the possibility that modest hypoxemia stimulates fetal breathing by precisely lowering fetal vascular P_{O_2} by 2–3 mmHg via reducing the maternal inspired O_2 concentration is difficult to achieve. An alternative approach is to raise fetal

vascular P_{O_2} by increasing the maternal inspired O_2 concentration and then after equilibration of the values to return fetal vascular P_{O_2} back to the normal range by switching the mother back to room air. This relative fetal hypoxemia has been shown to elicit the same cardiovascular responses (hypertension, femoral arterial vasoconstriction) as do true reductions in P_{O_2} [216]. Rurak and Cooper employed this approach to determine the effects of relative hypoxemia on breathing movements in the fetal lamb [217]. Maternal and fetal vascular P_{O_2} were raised by having the ewe breathe a 50 % oxygen mixture. This resulted in a rise of fetal arterial P_{O_2} from 17 to 25 mmHg and when the inspired gas mixture was changed back to room air, fetal P_{O_2} declined to the control value over ~5 min. When this relative hypoxemia was applied during a non-breathing period, breathing was not initiated. However when applied during breathing episodes, in 12 of 16 trials the amplitude of the breathing movements increased for the remainder of the breathing episode, which lasted for a further 8.6 min for a total duration of 15.2 min (Fig. 12). In the remaining four trials, the relative hypoxemia was applied on average 15.1 min after the breathing episode had started and the episode lasted only for a further 2.1 min. Moreover, in the 12 experiments in which breath amplitude increased, fetal arterial P_{O_2} fell significantly below the control value by ~1 mmHg during the augmented breathing, suggesting that the modest hypoxemia can stimulate fetal breathing, and also that the increased breathing activity can further reduce fetal P_{O_2} via increased O_2 consumption. Thus, as a consequence episodic uterine activity and fetal motility, fetal vascular P_{O_2} , and other blood gas parameters fluctuate continuously, with transient decreases occurring during uterine contractions and bouts of fetal motility. These fluctuations are most accurately characterized using continuous methods to measure fetal blood gas variables [175, 178, 193, 218]. This situation is very different from that after birth, since in adults even severe exercise is associated with maintenance of arterial oxygenation at least at sea level [219]. Harding et al. [193] convincingly demonstrated in chronically instrumented fetal lambs that antepartum uterine contractions and episodic fetal motility were responsible for the fluctuations in arterial oxygenation. Arterial oxygenation was measured continuously by either a catheter with a P_{O_2} electrode at its tip or a catheter oximeter to measure blood O_2 saturation. These measurements were obtained for a 4-h period under control conditions, following temporary paralysis of the fetus with a neuromuscular blocking agent and then co-administration of the neuromuscular blocker and salbutamol, a β_2 adrenergic agonist, which can temporarily inhibit uterine activity. The latter treatment abolished the transient reductions in arterial oxygenation.

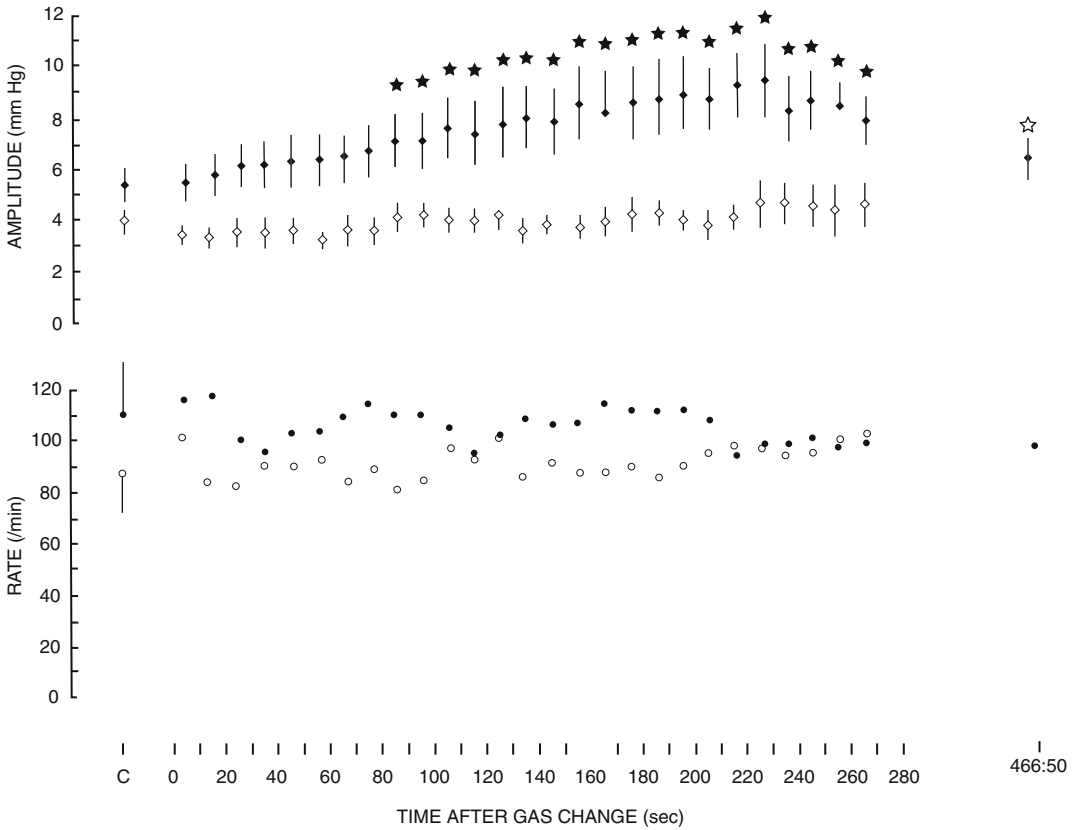


Fig. 12 Closed circles: Mean \pm SE tracheal pressure changes (breath amplitude) and breathing rate in 12 experiments of fetal lambs at 121–140-day gestation, where maternal inspired O_2 concentration was changed for 50–21 %. *C* = average values for the 30 s prior to the gas change. The numbers on the abscissa give the time in seconds following the gas change. The final point (466 ± 50) gives the mean values over the last 30 s of the breathing episode, filled star, $P < 0.05$ for the change from *C*; open star, $P > 0.05$ of the change from 230 s. Open circles: Mean \pm SE breathing amplitude and rate over 5 min in the middle portions of nine spontaneous fetal breathing records. From [217] with permission

12 Summary

Overall, from the results from the studies of fetal behavior, it appears that at least in late gestation, the fetus exhibits an organized constellation of cyclic activities, including motility, breathing activity, ingestion, and cardiorespiratory function, all of which are linked to regular alterations in behavioral states. Antepartum uterine activity impinges on these processes and there is considerable evidence that other external stimuli such as maternal body sounds (e.g., maternal pulse and bowel sounds) and external sounds and vibration also have effects [220]. The healthy fetus is characterized by continuous variability in behavior and related functions, with

alterations between active and quiescent states, with the incidence of quiescence progressively increasing in late gestation. The function of fetal body and breathing movements appears to be a form of “practice” for the postnatal period, when breathing must be continuous and mobility is required. Experimental abolition of fetal body and breathing movements, for example by daily intrauterine injections of curare to fetal rats from gestation days 19–21, results in a constellation of anomalies, including multiple joint contractures, pulmonary hypoplasia, growth restriction, comprised mainly by reduced muscle and bone mass, polyhydramnios, and a shortened umbilical cord [221]. These are very similar to the anomalies associated with the Pena-Shokeir phenotype (fetal akinesia deformation sequence) in human pregnancy [222]. Abolition of breathing movements alone via cervical spinal cord section or phrenic nerve section, reduction in the intrapleural pressure changes associated with fetal breathing movements via thoracoplasty, and drainage of lung fluid to reduce lung volume all reduce lung growth and maturation [223–226].

As described above, there is now a great deal of information on fetal behavior in humans and various animal species. However, there are much more data to be acquired. This includes a more detailed description of the changes in fetal behavioral parameters and related variables that occur during late gestation until the onset of labor. As was described above, data from a number of species indicate a decrease in motility with advancing gestation. However, whether there are changes in the other variables that are linked to fetal behavioral changes, such as arterial pressure, heart rate, and transient reductions in fetal vascular P_{O_2} is less clear. Also, the changes in fetal behavior and related variables that occur with chronic fetal compromise, such as that associated with intrauterine growth restriction (IUGR), warrant further study. Ribbert et al. [227] longitudinally followed 19 IUGR fetuses for 2–14 days that were ultimately delivered by caesarean section and monitored Doppler flow variables, fetal heart rate variations, and fetal body movements and fetal breathing. Abnormal Doppler flow variables were present in the majority of the fetuses from the onset of the study onwards. Fetal heart rate variability fell during the last 2 days prior to delivery and fetal body movements also decreased, whereas the fetal breathing changes were more variable. Because this study was conducted on pregnant women, the daily monitoring period was only 1 h. The use of chronically instrumented fetuses in sheep or other animal species would allow for 24-h recording of these and other related variables, such as circadian rhythms, and using catheter P_{O_2} electrodes or catheter oximeters, fetal vascular P_{O_2} , both in normal pregnancies and models of fetal compromise, could provide much useful data.

References

1. Meschia G, Cotter J, Makowski E, Barron D (1966) Simultaneous measurement of uterine and umbilical blood flows and oxygen uptakes. *Q J Exp Physiol* 52:1–18
2. Clark KE, Mack C, Khoury J (1990) Effects of chronic instrumentation on fetal growth. *J Dev Physiol* 14:343–347
3. Besette NW, Rurak DW (2010) Chronic fetal and maternal instrumentation in pregnant sheep: effect on gestation length and birth weight. *Reprod Fertil Dev* 22:459–467
4. Dawes GS, Fox HE, Leduc BM, Liggins GC, Richards RT (1972) Respiratory movements and rapid eye movement sleep in the foetal lamb. *J Physiol* 220:119–143
5. Ruckebusch Y, Gaujoux M, Eghbali B (1977) Sleep cycles and kinesis in the foetal lamb. *Electroencephalogr Clin Neurophysiol* 42:226–237
6. Harding R, Sigger JN, Poore ER, Johnson P (1984) Ingestion in fetal sheep and its relation to sleep states and breathing movements. *Q J Exp Physiol* 69:477–486
7. Ruckebusch Y (1972) Development of sleep and wakefulness in the foetal lamb. *Electroencephalogr Clin Neurophysiol* 32:119–128
8. Rigatto H, Blanco CE, Walker DW (1982) The response to stimulation of hindlimb nerves in fetal sheep, in utero, during the different phases of electrocortical activity. *J Dev Physiol* 4:175–185
9. Szeto HH, Hinman DJ (1985) Prenatal development of sleep-wake patterns in sheep. *Sleep* 8:347–355
10. Harned HS Jr, Ferreiro J (1973) Initiation of breathing by cold stimulation: effects of change in ambient temperature on respiratory activity of the full-term fetal lamb. *J Pediatr* 83:663–669
11. Harned HS Jr, Herrington RT, Ferreiro JI (1970) The effects of immersion and temperature on respiration in newborn lambs. *Pediatrics* 45:598–605
12. Gluckman PD, Gunn TR, Johnston BM (1983) The effect of cooling on breathing and shivering in unanaesthetized fetal lambs in utero. *J Physiol* 343:495–506
13. Rigatto H, Moore M, Cates D (1986) Fetal breathing and behavior measured through a double-wall Plexiglas window in sheep. *J Appl Physiol* 61:160–164
14. Mellor DJ, Diesch TJ, Gunn AJ, Bennet L (2005) The importance of ‘awareness’ for understanding fetal pain. *Brain Res Brain Res Rev* 49:455–471
15. Mellor DJ, Diesch TJ (2007) Birth and hatching: key events in the onset of awareness in the lamb and chick. *N Z Vet J* 55:51–60
16. Stark RI, Haiken J, Nordli D, Myers MM (1991) Characterization of electroencephalographic state in fetal baboons. *Am J Physiol* 261:R496–R500
17. Grieve PG, Myers MM, Stark RI (1994) Behavioral states in the fetal baboon. *Early Hum Dev* 39:159–175
18. Isler JR, Garland M, Stark RI, Grieve PG (2005) Local coherence oscillations in the EEG during development in the fetal baboon. *Clin Neurophysiol* 116:2121–2128
19. Scher MS, Loparo KA (2009) Neonatal EEG/sleep state analyses: a complex phenotype of developmental neural plasticity. *Dev Neurosci* 31:259–275
20. Jouviet-Mounier D, Astic L, Lacote D (1970) Ontogenesis of the states of sleep in rat, cat, and guinea pig during the first postnatal month. *Dev Psychobiol* 2:216–239
21. Umans JG, Cox MJ, Hinman DJ, Dogramajian ME, Senger G, Szeto HH (1985) The development of electrocortical activity in the fetal and neonatal guinea pig. *Am J Obstet Gynecol* 153:467–471
22. Morrison JL, Chien C, Gruber N, Rurak D, Riggs KW (2001) Fetal behavioural state changes following maternal fluoxetine infusion in sheep. *Dev Brain Res* 131:47–56
23. Vo TD, Dwyer G, Szeto HH (1986) A distributed microcomputer-controlled system for data acquisition and power spectral analysis of EEG. *J Neurosci Methods* 16:141–148
24. Szeto HH, Vo TD, Dwyer G, Dogramajian ME, Cox MJ, Senger G (1985) The ontogeny of fetal lamb electrocortical activity: a power spectral analysis. *Am J Obstet Gynecol* 153:462–466
25. Szeto HH (1990) Spectral edge frequency as a simple quantitative measure of the maturation of electrocortical activity. *Pediatr Res* 27:289–292
26. Shinozuka N, Nathanielsz PW (1998) Electrocortical activity in fetal sheep in the last seven days of gestation. *J Physiol* 513(Pt 1):273–281
27. McNerney ME, Szeto HH (1990) Automated identification and quantitation of four patterns of electrocortical activity in the near-term fetal lamb. *Pediatr Res* 28:106–110
28. Akay M, Akay YM, Cheng P, Szeto HH (1994) Time-frequency analysis of the

- electrocortical activity during maturation using wavelet transform. *Biol Cybern* 71: 169–176
29. Hatz F, Hardmeier M, Bousleiman H, Ruegg S, Schindler C, Fuhr P (2015) Reliability of fully automated versus visually controlled pre- and post-processing of resting-state EEG. *Clin Neurophysiol* 126(2):268–274
 30. Keen AE, Frasch MG, Sheehan MA, Matuszewski BJ, Richardson BS (2011) Electrocortical activity in the near-term ovine fetus: automated analysis using amplitude frequency components. *Brain Res* 1402:30–37
 31. Keen AE, Frasch MG, Sheehan MA, Matuszewski B, Richardson BS (2011) Maturation changes and effects of chronic hypoxemia on electrocortical activity in the ovine fetus. *Brain Res* 1402:38–45
 32. Myers MM, Stark RI, Fifer WP, Grieve PG, Haiken J, Leung K, Schulze KF (1993) A quantitative method for classification of EEG in the fetal baboon. *Am J Physiol* 265: R706–R714
 33. Wilson PC, Levy LF, Spies S, Chadwicke J (1979) The technique of fetal electroencephalography during labour. *Br J Obstet Gynaecol* 86:266–268
 34. Weller C, Dyson RJ, McFadyen IR, Green HL, Arias E (1981) Fetal electroencephalography using a new, flexible electrode. *Br J Obstet Gynaecol* 88:983–986
 35. Thaler I, Boldes R, Timor-Tritsch I (2000) Real-time spectral analysis of the fetal EEG: a new approach to monitoring sleep states and fetal condition during labor. *Pediatr Res* 48:340–345
 36. Prechtl HF (1974) The behavioural states of the newborn infant (a review). *Brain Res* 76:185–212
 37. Bots RS, Nijhuis JG, Martin CB Jr, Prechtl HF (1981) Human fetal eye movements: detection in utero by ultrasonography. *Early Hum Dev* 5:87–94
 38. Nijhuis JG, Prechtl HF, Martin CB Jr, Bots RS (1982) Are there behavioural states in the human fetus? *Early Hum Dev* 6: 177–195
 39. Pillai M, James D (1990) Are the behavioural states of the newborn comparable to those of the fetus? *Early Hum Dev* 22:39–49
 40. Pillai M, James D (1990) Behavioural states in normal mature human fetuses. *Arch Dis Child* 65:39–43
 41. Finley JP, Nugent ST (1995) Heart rate variability in infants, children and young adults. *J Auton Nerv Syst* 51:103–108
 42. Mirmiran M, Maas YG, Ariagno RL (2003) Development of fetal and neonatal sleep and circadian rhythms. *Sleep Med Rev* 7:321–334
 43. Hill M, Parizek A, Bicikova M, Havlikova H, Klak J, Fait T, Cibula D, Hampl R, Cegan A, Sulcova J, Starka L (2000) Neuroactive steroids, their precursors, and polar conjugates during parturition and postpartum in maternal and umbilical blood: 1. Identification and simultaneous determination of pregnanolone isomers. *J Steroid Biochem Mol Biol* 75:237–244
 44. Bicikova M, Klak J, Hill M, Zizka Z, Hampl R, Calda P (2002) Two neuroactive steroids in midpregnancy as measured in maternal and fetal sera and in amniotic fluid. *Steroids* 67:399–402
 45. Toh S, Mitchell AA, Louik C, Werler MM, Chambers CD, Hernandez-Diaz S (2009) Selective serotonin reuptake inhibitor use and risk of gestational hypertension. *Am J Psychiatry* 166:320–328
 46. Ogino M, Abe Y, Okahara T, Jimbo T (1986) Comparison of plasma prostanoid levels in the human cord artery in normal and fetal distressed deliveries. *Endocrinol Jpn* 33: 75–80
 47. Visser GH, Poelmann-Weesjes G, Cohen TM, Bekedam DJ (1987) Fetal behavior at 30 to 32 weeks of gestation. *Pediatr Res* 22: 655–658
 48. Pillai M, James DK, Parker M (1992) The development of ultradian rhythms in the human fetus. *Am J Obstet Gynecol* 167: 172–177
 49. Pillai M, James D (1990) Development of human fetal behavior: a review. *Fetal Diagn Ther* 5:15–32
 50. Maeda K, Tatsumura M, Nakajima K (1991) Objective and quantitative evaluation of fetal movement with ultrasonic Doppler actocardiogram. *Biol Neonate* 60(Suppl 1):41–51
 51. DiPietro JA, Hodgson DM, Costigan KA, Hilton SC, Johnson TR (1996) Development of fetal movement—fetal heart rate coupling from 20 weeks through term. *Early Hum Dev* 44:139–151
 52. DiPietro JA, Hodgson DM, Costigan KA, Hilton SC, Johnson TR (1996) Fetal neuro-behavioral development. *Child Dev* 67:2553–2567
 53. Besinger RE, Johnson TR (1989) Doppler recording of fetal movement: clinical correlation with real-time ultrasound. *Obstet Gynecol* 74:277–280
 54. Visser GH, Mulder EJ, Stevens H, Verweij R (1993) Heart rate variation during fetal

- behavioural states 1 and 2. *Early Hum Dev* 34:21–28
55. Pillai M, James D (1990) The importance of the behavioural state in biophysical assessment of the term human fetus. *Br J Obstet Gynaecol* 97:1130–1134
 56. Anderson AL, Thomason ME (2013) Functional plasticity before the cradle: a review of neural functional imaging in the human fetus. *Neurosci Biobehav Rev* 37:2220–2232
 57. Eswaran H, Haddad NI, Shihabuddin BS, Preissl H, Siegel ER, Murphy P, Lowery CL (2007) Non-invasive detection and identification of brain activity patterns in the developing fetus. *Clin Neurophysiol* 118:1940–1946
 58. Sonanini A, Stingl K, Preissl H, Brandle J, Hoopmann M, Kagan O, Wallwiener D, Abele H, Kiefer-Schmidt I (2014) Fetal behavioral states are stable over daytime—evidence by longitudinal and cross-sectional fetal biomagnetic recordings. *J Perinat Med* 42:307–314
 59. Govindan RB, Vairavan S, Ulsar UD, Wilson JD, McKelvey SS, Preissl H, Eswaran H (2011) A novel approach to track fetal movement using multi-sensor magnetocardiographic recordings. *Ann Biomed Eng* 39:964–972
 60. Haddad N, Govindan RB, Vairavan S, Siegel E, Temple J, Preissl H, Lowery CL, Eswaran H (2011) Correlation between fetal brain activity patterns and behavioral states: an exploratory fetal magnetoencephalography study. *Exp Neurol* 228:200–205
 61. Dobbing J, Sands J (1979) Comparative aspects of the brain growth spurt. *Early Hum Dev* 3:79–83
 62. Romijn HJ, Hofman MA, Gramsbergen A (1991) At what age is the developing cerebral cortex of the rat comparable to that of the full-term newborn human baby? *Early Hum Dev* 26:61–67
 63. Clancy B, Kersh B, Hyde J, Darlington RB, Anand KJ, Finlay BL (2007) Web-based method for translating neurodevelopment from laboratory species to humans. *Neuroinformatics* 5:79–94
 64. Wilds PL (1978) Observations of intrauterine fetal breathing movements—a review. *Am J Obstet Gynecol* 131:315–338
 65. Merlet C, Hoerter J, Devilleneuve C, Tchobroutsky C (1970) Demonstration of respiratory movements in lamb fetus in utero during the last month of gestation. *C R Acad Sci Hebd Seances Acad Sci D* 270:2462–2464
 66. Boddy K, Dawes GS, Fisher R, Pinter S, Robinson JS (1974) Foetal respiratory movements, electrocortical and cardiovascular responses to hypoxaemia and hypercapnia in sheep. *J Physiol* 243:599–618
 67. Koos BJ, Kitanaka T, Matsuda K, Gilbert RD, Longo LD (1988) Fetal breathing adaptation to prolonged hypoxaemia in sheep. *J Dev Physiol* 10:161–166
 68. Bocking AD, Gagnon R, Milne KM, White SE (1988) Behavioral activity during prolonged hypoxemia in fetal sheep. *J Appl Physiol* (1985) 65:2420–2426
 69. Harding R, Johnson P, McClelland ME (1980) Respiratory function of the larynx in developing sheep and the influence of sleep state. *Respir Physiol* 40:165–179
 70. Dawes GS, Gardner WN, Johnston BM, Walker DW (1983) Breathing in fetal lambs: the effect of brain stem section. *J Physiol* 335:535–553
 71. Gluckman PD, Johnston BM (1987) Lesions in the upper lateral pons abolish the hypoxic depression of breathing in unanaesthetized fetal lambs in utero. *J Physiol* 382:373–383
 72. Johnston BM, Gluckman PD (1989) Lateral pontine lesions affect central chemosensitivity in unanesthetized fetal lambs. *J Appl Physiol* (1985) 67:1113–1118
 73. Gluckman PD, Parsons Y (1983) Stereotaxic method and atlas for the ovine fetal forebrain. *J Dev Physiol* 5:101–128
 74. Rurak D, Bessette NW (2013) Changes in fetal lamb arterial blood gas and acid-base status with advancing gestation. *Am J Physiol Regul Integr Comp Physiol* 304(10):R908–R916
 75. Ioffe S, Jansen AH, Chernick V (1984) ECoG and breathing activity in fetal lambs after undercut of cerebral cortex. *J Appl Physiol Respir Environ Exerc Physiol* 57:1195–1201
 76. Ioffe S, Jansen AH, Chernick V (1986) Effects of hypercapnia and hypoxemia on fetal breathing after decortication. *J Appl Physiol* (1985) 61:1071–1076
 77. Koos BJ, Chau A, Matsuura M, Punla O, Kruger L (1998) Thalamic locus mediates hypoxic inhibition of breathing in fetal sheep. *J Neurophysiol* 79:2383–2393
 78. Koos BJ, Matsuda K (1990) Fetal breathing, sleep state, and cardiovascular responses to adenosine in sheep. *J Appl Physiol* (1985) 68:489–495
 79. Koos BJ, Mason BA, Punla O, Adinolfi AM (1994) Hypoxic inhibition of breathing in fetal sheep: relationship to brain adenosine concentrations. *J Appl Physiol* (1985) 77:2734–2739

80. Koos BJ, Maeda T, Jan C, Lopez G (2002) Adenosine A(2A) receptors mediate hypoxic inhibition of fetal breathing in sheep. *Am J Obstet Gynecol* 186:663–668
81. Koos BJ, Chao A, Doany W (1992) Adenosine stimulates breathing in fetal sheep with brain stem section. *J Appl Physiol* (1985) 72:94–99
82. Koos BJ, Chau A, Matsuura M, Punla O, Kruger L (2000) Thalamic lesions dissociate breathing inhibition by hypoxia and adenosine in fetal sheep. *Am J Physiol Regul Integr Comp Physiol* 278:R831–R837
83. Kelleman A, Binienda Z, Ding XY, Rittenhouse L, Mitchell M, Nathanielsz PW (1992) Prostaglandin production in the umbilical and uterine circulations in pregnant sheep at 129–136 days gestation. *J Dev Physiol* 17:63–67
84. Wallen LD, Murai DT, Clyman RI, Lee CH, Mauray FE, Kitterman JA (1986) Regulation of breathing movements in fetal sheep by prostaglandin E2. *J Appl Physiol* 60:526–531
85. Norton JL, Adamson SL, Bocking AD, Han VK (1996) Prostaglandin-H synthase-1 (PGHS-1) gene is expressed in specific neurons of the brain of the late gestation ovine fetus. *Brain Res Dev Brain Res* 95:79–96
86. Tai TC, MacLusky NJ, Adamson SL (1994) Ontogenesis of prostaglandin E2 binding sites in the brainstem of the sheep. *Brain Res* 652:28–39
87. Tai TC, Lye SJ, Adamson SL (1998) Expression of prostaglandin E2 receptor subtypes in the developing sheep brainstem. *Brain Res Mol Brain Res* 57:161–166
88. Jones SA, Adamson SL, Bishai I, Lees J, Engelberts D, Coceani F (1993) Eicosanoids in third ventricular cerebrospinal fluid of fetal and newborn sheep. *Am J Physiol* 264:R135–R142
89. Hollingworth SA, Jones SA, Adamson SL (1996) Rebound increase in fetal breathing movements after 24-h prostaglandin E2 infusion in fetal sheep. *J Appl Physiol* (1985) 80:166–175
90. Maloney JE, Adamson TM, Brodecky AV, Cranage S, Lambert TF, Ritchie BC (1975) Diaphragmatic activity and lung liquid flow in the unanesthetized fetal sheep. *J Appl Physiol* 39:423–428
91. Chapman RL, Dawes GS, Rurak DW, Wilds PL (1980) Breathing movements in fetal lambs and the effect of hypercapnia. *J Physiol* 302:19–29
92. Clewlow F, Dawes GS, Johnston BM, Walker DW (1983) Changes in breathing, electrocortical and muscle activity in unanaesthetized fetal lambs with age. *J Physiol* 341:463–476
93. Dawes GS, Gardner WN, Johnston BM, Walker DW (1982) Effects of hypercapnia on tracheal pressure, diaphragm and intercostal electromyograms in unanaesthetized fetal lambs. *J Physiol* 326:461–474
94. Rurak DW, Cooper CC, Taylor SM (1986) Fetal oxygen consumption and PO2 during hypercapnia in pregnant sheep. *J Dev Physiol* 8:447–459
95. Polglase GR, Wallace MJ, Grant DA, Hooper SB (2004) Influence of fetal breathing movements on pulmonary hemodynamics in fetal sheep. *Pediatr Res* 56:932–938
96. Bowes G, Adamson TM, Ritchie BC, Dowling M, Wilkinson MH, Maloney JE (1981) Development of patterns of respiratory activity in unanesthetized fetal sheep in utero. *J Appl Physiol* 50:693–700
97. Cooke IR, Berger PJ (1996) Development of patterns of activity in diaphragm of fetal lamb early in gestation. *J Neurobiol* 30:385–396
98. Rurak D, Wittman B (2013) Real-time ultrasound assessment of body and breathing movements and abdominal diameter in fetal lambs from 55 days of gestation to term. *Reprod Sci* 20(4):414–425
99. Berger PJ, Walker AM, Horne R, Brodecky V, Wilkinson MH, Wilson F, Maloney JE (1986) Phasic respiratory activity in the fetal lamb during late gestation and labour. *Respir Physiol* 65:55–68
100. Finkelstein DI, Andrianakis P, Luff AR, Walker DW (1992) Developmental changes in hindlimb muscles and diaphragm of sheep. *Am J Physiol* 263:R900–R908
101. Cannata DJ, Crossley KJ, Barclay CJ, Walker DW, West JM (2011) Contribution of stretch to the change of activation properties of muscle fibers in the diaphragm at the transition from fetal to neonatal life. *Front Physiol* 2:109
102. Johnson BD, Wilson LE, Zhan WZ, Watchko JF, Daood MJ, Sieck GC (1994) Contractile properties of the developing diaphragm correlate with myosin heavy chain phenotype. *J Appl Physiol* 77:481–487
103. Poore ER, Walker DW (1980) Chest wall movements during fetal breathing in the sheep. *J Physiol* 301:307–315
104. Stark RI, Daniel SS, Kim YI, Leung K, Myers MM, Tropper PJ (1994) Patterns of fetal breathing in the baboon vary with EEG sleep state. *Early Hum Dev* 38:11–26

105. Martin CB Jr, Murata Y, Petrie RH, Parer JT (1974) Respiratory movements in fetal rhesus monkeys. *Am J Obstet Gynecol* 119:939–948
106. Kendall JZ (1977) Respiratory movements in the fetal guinea pig in utero. *J Appl Physiol Respir Environ Exerc Physiol* 42:661–663
107. van Kan CM, de Vries JI, Luchinger AB, Mulder EJ, Taverne MA (2009) Ontogeny of fetal movements in the guinea pig. *Physiol Behav* 98:338–344
108. Stark RI, Daniel SS, Kim YI, Leung K, Rey HR, Tropper PJ (1993) Patterns of development in fetal breathing activity in the latter third of gestation of the baboon. *Early Hum Dev* 32:31–47
109. Kobayashi K, Lemke RP, Greer JJ (2001) Ultrasound measurements of fetal breathing movements in the rat. *J Appl Physiol* (1985) 91:316–320
110. Patrick J, Natale R, Richardson B (1978) Patterns of human fetal breathing activity at 34 to 35 weeks' gestational age. *Am J Obstet Gynecol* 132:507–513
111. Harding R, Fowden AL, Silver M (1991) Respiratory and non-respiratory thoracic movements in the fetal pig. *J Dev Physiol* 15:269–275
112. Rosenfeld M, Snyder FF (1936) Fetal respiration in rabbits. *Proc Soc Exp Biol Med* 33:576–578
113. Bonar BE, Blumenfeld CM, Fenning C (1938) Studies of fetal respiratory movements: 1. Historical and present day observations. *Am J Dis Child* 55:1–11
114. Patrick J, Fetherston W, Vick H, Voegelin R (1978) Human fetal breathing movements and gross fetal body movements at weeks 34 to 35 of gestation. *Am J Obstet Gynecol* 130:693–699
115. Pillai M, James D (1990) Hiccups and breathing in human fetuses. *Arch Dis Child* 65:1072–1075
116. Stark RI, Daniel SS, Garland M, Jaille-Marti JC, Kim YI, Leung K, Myers MM, Tropper PJ (1994) Fetal hiccups in the baboon. *Am J Physiol* 267:R1479–R1487
117. Timor-Tritsch IE, Dierker LJ Jr, Hertz RH, Chik L, Rosen MG (1980) Regular and irregular human fetal respiratory movement. *Early Hum Dev* 4:315–324
118. Nijhuis JG, Martin CB Jr, Gommers S, Bouws P, Bots RS, Jongsma HW (1983) The rhythmicity of fetal breathing varies with behavioural state in the human fetus. *Early Hum Dev* 9:1–7
119. Mulder EJ, Boersma M, Meeuse M, van der Wal M, van de Weerd E, Visser GH (1994) Patterns of breathing movements in the near-term human fetus: relationship to behavioural states. *Early Hum Dev* 36:127–135
120. Boddy K, Robinson JS (1971) External method for detection of fetal breathing in utero. *Lancet* 2:1231–1233
121. Boddy K, Mantell CD (1972) Observations of fetal breathing movements transmitted through maternal abdominal wall. *Lancet* 2:1219–1220
122. Adamson SL, Bocking A, Cousin AJ, Rapoport I, Patrick JE (1983) Ultrasonic measurement of rate and depth of human fetal breathing: effect of glucose. *Am J Obstet Gynecol* 147:288–295
123. Cousin AJ, Rapoport I, Campbell K, Patrick JE (1983) A tracking system for pulsed ultrasound images: application to quantification of fetal breathing movements. *IEEE Trans Biomed Eng* 30:577–584
124. Boyce ES, Dawes GS, Gough JD, Poore ER (1976) Doppler ultrasound method for detecting human fetal breathing in utero. *Br Med J* 2:17–18
125. Trudinger BJ, Knight PC (1980) Fetal age and patterns of human fetal breathing movements. *Am J Obstet Gynecol* 137:724–728
126. van der Mooren K, Wladimiroff JW, Stijnen T (1991) Effect of fetal breathing movements on fetal cardiac hemodynamics. *Ultrasound Med Biol* 17:787–790
127. Burghouwt M, Wladimiroff JW (1992) Modulation of middle cerebral artery flow velocity waveforms by breathing movements in the normal term fetus. *Ultrasound Med Biol* 18:821–825
128. Marsal K, Lindblad A, Lingman G, Eik-Nes SH (1984) Blood flow in the fetal descending aorta; intrinsic factors affecting fetal blood flow, i.e. fetal breathing movements and cardiac arrhythmia. *Ultrasound Med Biol* 10:339–348
129. Gustafson KM, Allen JJ, Yeh HW, May LE (2011) Characterization of the fetal diaphragmatic magnetomyogram and the effect of breathing movements on cardiac metrics of rate and variability. *Early Hum Dev* 87:467–475
130. Greer JJ (2012) Control of breathing activity in the fetus and newborn. *Compr Physiol* 2:1873–1888
131. Ratnayake U, Quinn T, Daruwalla K, Dickinson H, Walker DW (2014) Understanding the behavioural phenotype of the precocial spiny mouse. *Behav Brain Res* 275C:62–71
132. Greer JJ, Smith JC, Feldman JL (1992) Respiratory and locomotor patterns generated in

- the fetal rat brain stem-spinal cord in vitro. *J Neurophysiol* 67:996–999
133. Pagliardini S, Ren J, Greer JJ (2003) Ontogeny of the pre-Botzinger complex in perinatal rats. *J Neurosci* 23:9575–9584
 134. Greer JJ, Carter JE, Allan DW (1996) Respiratory rhythm generation in a precocial rodent in vitro preparation. *Respir Physiol* 103:105–112
 135. Hantoushzadeh S, Sheikh M, Shariat M, Farahani Z (2015) Maternal perception of fetal movement type: the effect of gestational age and maternal factors. *J Matern Fetal Neonatal Med* 28(6):713–717
 136. Hijazi ZR, East CE (2009) Factors affecting maternal perception of fetal movement. *Obstet Gynecol Surv* 64:489–497, quiz 499
 137. Froen JF, Heazell AE, Tveit JV, Saastad E, Fretts RC, Flenady V (2008) Fetal movement assessment. *Semin Perinatol* 32:243–246
 138. Natale R, Clewlow F, Dawes GS (1981) Measurement of fetal forelimb movements in the lamb in utero. *Am J Obstet Gynecol* 140:545–551
 139. Kurjak A, Tikvica A, Stanojevic M, Miskovic B, Ahmed B, Azumendi G, Di Renzo GC (2008) The assessment of fetal neurobehavior by three-dimensional and four-dimensional ultrasound. *J Matern Fetal Neonatal Med* 21:675–684
 140. Patrick J, Campbell K, Carmichael L, Natale R, Richardson B (1982) Patterns of gross fetal body movements over 24-hour observation intervals during the last 10 weeks of pregnancy. *Am J Obstet Gynecol* 142:363–371
 141. de Vries JI, Fong BF (2006) Normal fetal motility: an overview. *Ultrasound Obstet Gynecol* 27:701–711
 142. de Vries JI, Visser GH, Prechtl HF (1982) The emergence of fetal behaviour: I. Qualitative aspects. *Early Hum Dev* 7:301–322
 143. Luchinger AB, Hadders-Algra M, van Kan CM, de Vries JI (2008) Fetal onset of general movements. *Pediatr Res* 63:191–195
 144. Ten Hof J, Nijhuis IJ, Mulder EJ, Nijhuis JG, Narayan H, Taylor DJ, Westers P, Visser GH (2002) Longitudinal study of fetal body movements: nomograms, intrafetal consistency, and relationship with episodes of heart rate patterns A and B. *Pediatr Res* 52:568–575
 145. Cohen S, Mulder EJ, van Oord HA, Jonker FH, Parvizi N, van der Weijden GC, Taverne MA (2010) Fetal movements during late gestation in the pig: a longitudinal ultrasonographic study. *Theriogenology* 74:24–30
 146. Barcroft J (1946) *Researches on pre-natal life*. Blackwell, Oxford
 147. Berger PJ, Kyriakides MA, Cooke IR (1997) Supraspinal influence on the development of motor behavior in the fetal lamb. *J Neurobiol* 33:276–288
 148. Fraser AF, Hastie H, Callicott RB, Brownlie S (1975) An exploratory ultrasonic study of quantitative foetal kinesis in the horse. *Appl Anim Ethol* 1:395–404
 149. Fraser AF (1976) Some features of an ultrasonic study of bovine foetal kinesis. *Appl Anim Ethol* 2:379–383
 150. Husa L, Bieger D, Fraser AF (1988) Fluoroscopic study of the birth posture of the sheep fetus. *Vet Rec* 123:645–648
 151. Fraser AF (1989) A monitored study of major physical activities in the perinatal calf. *Vet Rec* 125:38–40
 152. Fraser AF, Broom DM (1990) *Farm animal behaviour and welfare*. Balliere Tindall, New York
 153. Sherer DM, Spong CY, Minior VK, Salafia CM (1996) Decreased amniotic fluid volume at <32 weeks of gestation is associated with decreased fetal movements. *Am J Perinatol* 13:479–482
 154. Sival DA, Visser GH, Prechtl HF (1990) Does reduction of amniotic fluid affect fetal movements? *Early Hum Dev* 23:233–246
 155. Garzetti GG, Ciavattini A, De Cristofaro F, La Marca N, Arduini D (1997) Prophylactic transabdominal amnioinfusion in oligohydramnios for preterm premature rupture of membranes: increase of amniotic fluid index during latency period. *Gynecol Obstet Invest* 44:249–254
 156. Nguyen PN, Billiards SS, Walker DW, Hirst JJ (2003) Changes in 5 α -pregnane steroids and neurosteroidogenic enzyme expression in fetal sheep with umbilicoplacental embolization. *Pediatr Res* 54:840–847
 157. Young IR, Thorburn GD (1994) Prostaglandin E₂, fetal maturation and ovine parturition. *Aust N Z J Obstet Gynaecol* 34:342–346
 158. Luisi S, Petraglia F, Benedetto C, Nappi RE, Bernardi F, Fadalti M, Reis FM, Luisi M, Genazzani AR (2000) Serum allopregnanolone levels in pregnant women: changes during pregnancy, at delivery, and in hypertensive patients. *J Clin Endocrinol Metab* 85:2429–2433
 159. Boddy K, Dawes GS, Robinson JS (1973) A 24-hour rhythm in the foetus. In: Cross K, Comline R, Dawes GS, Nathanielsz P (eds) *Foetal and neonatal physiology: proceedings*

- of the barcroft symposium. Cambridge University Press, Cambridge, pp 63–66
160. Brace RA, Moore TR (1991) Diurnal rhythms in fetal urine flow, vascular pressures, and heart rate in sheep. *Am J Physiol* 261: R1015–R1021
 161. Morrison JL, Rurak DW, Chien C, Kennaway DJ, Gruber N, McMillen IC, Riggs KW (2005) Maternal fluoxetine infusion does not alter fetal endocrine and biophysical circadian rhythms in pregnant sheep. *J Soc Gynecol Investig* 12:356–364
 162. Jensen EC, Bennet L, Guild SJ, Booth LC, Stewart J, Gunn AJ (2009) The role of the neural sympathetic and parasympathetic systems in diurnal and sleep state-related cardiovascular rhythms in the late-gestation ovine fetus. *Am J Physiol Regul Integr Comp Physiol* 297:R998–R1008
 163. Stark RI, Garland M, Daniel S, Myers MM (1998) Diurnal rhythm of fetal behavioral state. *Sleep* 21:167–176
 164. Rurak D, Lim K, Sanders A, Brain U, Riggs W, Oberlander TF (2011) Third trimester fetal heart rate and Doppler middle cerebral artery blood flow velocity characteristics during prenatal selective serotonin reuptake inhibitor exposure. *Pediatr Res* 70:96–101
 165. Nowak R, Young IR, McMillen IC (1990) Emergence of the diurnal rhythm in plasma melatonin concentrations in newborn lambs delivered to intact or pinealectomized ewes. *J Endocrinol* 125:97–102
 166. Kennaway DJ, Goble FC, Stamp GE (1996) Factors influencing the development of melatonin rhythmicity in humans. *J Clin Endocrinol Metab* 81:1525–1532
 167. Joseph D, Chong NW, Shanks ME, Rosato E, Taub NA, Petersen SA, Symonds ME, Whitehouse WP, Wailoo M (2015) Getting rhythm: how do babies do it? *Arch Dis Child Fetal Neonatal* Ed 100:F50–F54
 168. Yellon SM, Longo LD (1987) Melatonin rhythms in fetal and maternal circulation during pregnancy in sheep. *Am J Physiol* 252: E799–802
 169. Zemdegs IZ, McMillen IC, Walker DW, Thorburn GD, Nowak R (1988) Diurnal rhythms in plasma melatonin concentrations in the fetal sheep and pregnant ewe during late gestation. *Endocrinology* 123:284–289
 170. Yellon SM, Longo LD (1988) Effect of maternal pinealectomy and reverse photoperiod on the circadian melatonin rhythm in the sheep and fetus during the last trimester of pregnancy. *Biol Reprod* 39:1093–1099
 171. McMillen IC, Nowak R (1989) Maternal pinealectomy abolishes the diurnal rhythm in plasma melatonin concentrations in the fetal sheep and pregnant ewe during late gestation. *J Endocrinol* 120:459–464
 172. McMillen IC, Nowak R, Walker DW, Young IR (1990) Maternal pinealectomy alters the daily pattern of fetal breathing in sheep. *Am J Physiol* 258:R284–R287
 173. Houghton DC, Walker DW, Young IR, McMillen IC (1993) Melatonin and the light-dark cycle separately influence daily behavioral and hormonal rhythms in the pregnant ewe and sheep fetus. *Endocrinology* 133:90–98
 174. Dunn PM (1999) John Braxton Hicks (1823–97) and painless uterine contractions. *Arch Dis Child Fetal Neonatal* Ed 81: F157–F158
 175. Jansen CA, Krane EJ, Thomas AL, Beck NF, Lowe KC, Joyce P, Parr M, Nathanielsz PW (1979) Continuous variability of fetal PO₂ in the chronically catheterized fetal sheep. *Am J Obstet Gynecol* 134:776–783
 176. Harding R, Poore ER, Bailey A, Thorburn GD, Jansen CA, Nathanielsz PW (1982) Electromyographic activity of the nonpregnant and pregnant sheep uterus. *Am J Obstet Gynecol* 142:448–457
 177. Lye SJ, Freitag CL (1988) An in-vivo model to examine the electromyographic activity of isolated myometrial tissue from pregnant sheep. *J Reprod Fertil* 82:51–61
 178. Towell ME, Regier I, Lysak I, Saylor D, Bessman SP (1983) Maternal and fetal tissue PO₂ in the pregnant ewe measured with galvanic PO₂ electrodes. *Adv Exp Med Biol* 159: 37–48
 179. Llanos AJ, Court DJ, Block BS, Germain AM, Parer JT (1986) Fetal cardiorespiratory changes during spontaneous prelabor uterine contractions in sheep. *Am J Obstet Gynecol* 155:893–897
 180. Sunderji SG, El Badry A, Poore ER, Figueroa JP, Nathanielsz PW (1984) The effect of myometrial contractures on uterine blood flow in the pregnant sheep at 114 to 140 days' gestation measured by the 4-aminoantipyrine equilibrium diffusion technique. *Am J Obstet Gynecol* 149:408–412
 181. Harding R, Poore ER (1984) The effects of myometrial activity on fetal thoracic dimensions and uterine blood flow during late gestation in the sheep. *Biol Neonate* 45:244–251
 182. Nathanielsz PW, Bailey A, Poore ER, Thorburn GD, Harding R (1980) The relationship

- between myometrial activity and sleep state and breathing in fetal sheep throughout the last third of gestation. *Am J Obstet Gynecol* 138:653–659
183. Walker DW, Harding R (1986) The effects of raising intracranial pressure on breathing movements, eye movements and electrocortical activity in fetal sheep. *J Dev Physiol* 8:105–116
184. Shields LE, Brace RA (1994) Fetal vascular pressure responses to nonlabor uterine contractions: dependence on amniotic fluid volume in the ovine fetus. *Am J Obstet Gynecol* 171:84–89
185. Lye SJ, Wlodek ME, Challis JR (1984) Relation between fetal arterial PO₂ and oxytocin-induced uterine contractions in pregnant sheep. *Can J Physiol Pharmacol* 62:1337–1340
186. Lye SJ, Wlodek ME, Challis JR (1985) Possible role of uterine contractions in the short-term fluctuations of plasma ACTH concentration in fetal sheep. *J Endocrinol* 106:R9–R11
187. Woudstra B, Kim C, Aarnoudse J, Nathanielsz P (1991) Myometrial contracture-related increases in plasma adrenocorticotropin in fetal sheep in the last 3rd of gestation are abolished by maintaining fetal normoxemia. *Endocrinology* 129:1709–1713
188. Hofmeyr GJ, Bamford OS, Gianopoulos JG, Parkes MJ, Dawes GS (1985) The partial association of uterine contractions with changes in electrocortical activity, breathing, and PaO₂ in the fetal lamb: effects of brain stem section. *Am J Obstet Gynecol* 152:905–910
189. Wilkinson C, Robinson J (1982) Braxton-Hicks contractions and fetal breathing movements. *Aust N Z J Obstet Gynaecol* 22:212–214
190. Mulder EJ, Visser GH (1987) Braxton Hicks' contractions and motor behavior in the near-term human fetus. *Am J Obstet Gynecol* 156(3):543–549
191. Norman LJ, Lye SJ, Wlodek ME, Challis JR (1985) Changes in pituitary responses to synthetic ovine corticotrophin releasing factor in fetal sheep. *Can J Physiol Pharmacol* 63:1398–1403
192. Liggins GC (1994) The role of cortisol in preparing the fetus for birth. *Reprod Fertil Dev* 6:141–150
193. Harding R, Sigger JN, Wickham PJ (1983) Fetal and maternal influences on arterial oxygen levels in the sheep fetus. *J Dev Physiol* 5:267–276
194. King J, Grant A, Keirse M, Chalmers I (1988) Beta-mimetics in preterm labor—an overview of the randomized controlled trials. *Br J Obstet Gynaecol* 95:211–222
195. Casper R, Lye S (1986) Myometrial desensitization to continuous but not to intermittent beta-adrenergic agonist infusion in the sheep. *Am J Obstet Gynecol* 154:301–305
196. Benedetti T (1986) Life-threatening complications of beta-mimetic therapy for preterm labor inhibition. *Clin Perinatol* 13:843–852
197. Vanderweyde M, Wright M, Taylor S, Axelson J, Rurak D (1992) Metabolic effects of ritodrine in the fetal lamb. *J Pharmacol Exp Ther* 262:48–59
198. Sadowsky DW, Martel JK, Jenkins SL, Poore MG, Cabalum T, Nathanielsz PW (1992) Pulsatile oxytocin administered to ewes at 120 to 140 days gestational age increases the rate of maturation of the fetal electrocortigram and nuchal activity. *J Dev Physiol* 17:175–181
199. Owiny JR, Sadowsky D, Zarzeczny S, Nathanielsz PW (1995) Effect of pulsatile intravenous oxytocin administration to pregnant sheep over the last third of gestation on fetal ACTH and cortisol responses to hypotension. *J Soc Gynecol Investig* 2:13–18
200. Shinozuka N, Yen A, Nathanielsz P (1999) Alteration of fetal oxygenation and responses to acute hypoxemia by increased myometrial contracture frequency produced by pulse administration of oxytocin to the pregnant ewe from 96 to 131 days' gestation. *Am J Obstet Gynecol* 180:1202–1208
201. Shinozuka N, Yen A, Nathanielsz P (2000) Increased myometrial contracture frequency at 96–140 days accelerates fetal cardiovascular maturation. *Am J Physiol Heart Circ Physiol* 278:H41–H49
202. Porter D (1971) Quantitative changes in myometrial activity in guinea-pig during pregnancy. *J Reprod Fertil* 27:219–226
203. Wittmann BK, Rurak DW, Gruber N, Brown S (1981) Real-time ultrasound observation of breathing and movements in the fetal lamb. *Am J Obstet Gynecol* 141:807–810
204. Mandruzzato G, Meir YJ, Natale R, Maso G (2001) Antepartal assessment of IUGR fetuses. *J Perinat Med* 29:222–229
205. Walton JR, Peaceman AM (2012) Identification, assessment and management of fetal compromise. *Clin Perinatol* 39:753–783
206. Bocking AD (2003) Assessment of fetal heart rate and fetal movements in detecting oxygen deprivation in-utero. *Eur J Obstet Gynecol Reprod Biol* 110(Suppl 1):S108–S112

207. Bocking A, Harding R, Wickham P (1985) Relationship between accelerations and decelerations in heart-rate and skeletal-muscle activity in fetal sheep. *J Dev Physiol* 7:47–54
208. Spencer J, Ryan G, Ronderosdumit D, Nicolini U, Rodeck C (1994) The effect of neuromuscular blockade on human fetal heart-rate and its variation. *Br J Obstet Gynaecol* 101:121–124
209. Rudolph A, Heymann M (1976) Cardiac-output in fetal lamb—effects of spontaneous and induced changes of heart-rate on right and left-ventricular output. *Am J Obstet Gynecol* 124:183–192
210. Rurak DW, Gruber NC (1983) Increased oxygen consumption associated with breathing activity in fetal lambs. *J Appl Physiol* 54:701–707
211. Rurak DW, Gruber NC (1983) The effect of neuromuscular blockade on oxygen consumption and blood gases in the fetal lamb. *Am J Obstet Gynecol* 145:258–262
212. Wilkening RB, Boyle DW, Meschia G (1989) Fetal neuromuscular blockade: effect on oxygen demand and placental transport. *Am J Physiol* 257:H734–H738
213. Rurak DW, Taylor SM (1986) Oxygen consumption in fetal lambs after maternal administration of sodium pentobarbital. *Am J Obstet Gynecol* 154:674–678
214. Harding R, Poore ER, Cohen GL (1981) The effect of brief episodes of diminished uterine blood flow on breathing movements, sleep states and heart rate in fetal sheep. *J Dev Physiol* 3:231–243
215. Llanos AJ, Block BS, Court DJ, Germain AM, Parer JT (1988) Fetal oxygen uptake during uterine contractures. *J Dev Physiol* 10:525–529
216. Dawes G, Duncan S, Lewis B, Merlet C, Owenthom JB, Reeves J (1969) Hypoxaemia and aortic chemoreceptor function in foetal lambs. *J Physiol* 201:105–116
217. Rurak DW, Cooper C (1984) The effect of relative hypoxemia on the pattern of breathing movements in fetal lambs. *Respir Physiol* 55:23–37
218. Woudstra BR, de Wolf BT, Smits TM, Nathanielsz PW, Zijlstra WG, Aarnoudse JG (1995) Variability of continuously measured arterial pH and blood gas values in the near term fetal lamb. *Pediatr Res* 38:528–532
219. Torre-Bueno JR, Wagner PD, Saltzman HA, Gale GE, Moon RE (1985) Diffusion limitation in normal humans during exercise at sea level and simulated altitude. *J Appl Physiol* 58(3):989–995
220. Abrams RM, Gerhardt KJ (2000) The acoustic environment and physiological responses of the fetus. *J Perinatol* 20(8 Pt 2):S31–S36
221. Moessinger AC (1983) Fetal akinesia deformation sequence: an animal model. *Pediatrics* 72:857–863
222. Hall JG (2009) Pena-Shokeir phenotype (fetal akinesia deformation sequence) revisited. *Birth Defects Res A Clin Mol Teratol* 85(8):677–694. doi:10.1002/Bdra.20611
223. Alcorn D, Adamson T, Maloney J, Robinson P (1980) Morphological effects of chronic bilateral phrenectomy or vagotomy in the fetal lamb lung. *J Anat* 130:683–695
224. Alcorn D, Adamson T, Lambert T, Maloney J, Ritchie B, Robinson P (1977) Morphological effects of chronic tracheal ligation and drainage in fetal lamb lung. *J Anat* 123:649–660
225. Wigglesworth JS, Desai R (1979) Effect on lung growth of cervical cord section in the rabbit fetus. *Early Hum Dev* 3:51–65
226. Liggins GC, Vilos GA, Campos GA, Kitterman JA, Lee CH (1981) The effect of bilateral thoracoplasty on lung development in fetal sheep. *J Dev Physiol* 3:275–282
227. Ribbert LS, Visser GH, Mulder EJ, Zonneveld MF, Morssink LP (1993) Changes with time in fetal heart rate variation, movement incidences and haemodynamics in intrauterine growth retarded fetuses: a longitudinal approach to the assessment of fetal well being. *Early Hum Dev* 31:195–208

Circadian Rhythms in the Fetus and Newborn: Significance of Interactions with Maternal Physiology and the Environment

María Serón-Ferré, Hans G. Richter, Guillermo J. Valenzuela, and Claudia Torres-Farfan

Abstract

Timing of balanced and precise daily delivery of oxygen, nutrients, hormones, and biophysical cues from mother to fetus is essential for fetal growth and successful transition to extrauterine life. Such timing is provided by an arrangement of biological clocks operating in the mother and fetus. However, adverse intrauterine conditions including effects of altering the photoperiod (chronodisruption) during gestation on fetal growth/development and postnatal physiology may translate into adult disease, in which the role played by fetal circadian system remains unclear. Here we review the development of the circadian system, changes experienced by the maternal circadian system during pregnancy, evidence that chronodisruption during pregnancy has long-term effects on the offspring, and current experimental approaches utilized to investigate these issues. However, we are aware that we are just now obtaining new pieces of information that needs to be broadened and studied searching for a diurnal model more comparable to humans. Physiological and pathophysiological questions related to the mother-fetus pair and neonate *in vivo* need to be addressed as well as the corresponding consequences in adulthood, with expanded and new techniques: among the latter, effects on the transcriptome, microRNA regulome (miRNome), and proteome of different maternal-fetal, neonatal, and adult tissues.

Key words Circadian clocks, Fetal circadian system, Maternal chronodisruption, Melatonin, Fetal adrenal function, Glucocorticoid rhythm, DOHaD

1 Introduction

Timing of balanced and precise daily delivery of oxygen, nutrients, hormones, and biophysical cues from mother to fetus is essential for fetal growth and successful transition to extrauterine life. Substantial research efforts over the last couple of decades have indicated that adverse intrauterine conditions may translate into adult disease. More recently, we and others have focused on the detrimental effects of altering the photoperiod (chronodisruption) during gestation on fetal growth/development and postnatal physiology.

A fascinating challenge is to discover the actual impact of maternal circadian misalignment, not only on the physiology and developmental trajectory of the fetus, but also on the adult offspring's health and disease status. The evidence available suggests that maternal chronodisruption disrupts the fetal circadian system. However, this novel research avenue still faces multiple challenges. These include working on an experimental model that more closely resembles the human setting of shift work during pregnancy, and identifying changes not only in systemic pathophysiological read-outs, but also in the transcriptome, microRNA regulome (miR-Nome), and proteome from different fetal tissues.

2 Circadian Clocks

Chronodisruption is defined as “a breakdown of phasing internal biological systems appropriately relative to the external, i.e. environmental changes” [1]. Such internal temporal order of physiological systems depends on biological clocks. Individuals living on Earth evolved predictive mechanisms to accommodate their physiology and behavior to our planet's daily day/night changes. The outcome of these mechanisms is an integrated system of biological clocks that oscillate with a period of close to a day (*circa dies*, 24 h) driving circadian rhythms at the cellular and systemic level, thus generating an internal temporal order in physiological functions tuned to the external environment. Conceptually, a circadian clock comprises three parts, an input signal that entrains the internal clock to clock time, an oscillator with a period of 24 h, and output rhythmic signals. In adult mammals, the circadian system is organized as a master clock, located in the suprachiasmatic nucleus (SCN) of the hypothalamus that commands peripheral circadian clocks located in brain areas other than the SCN and in almost every organ of the body. The SCN, connected to the retina by the retino-hypothalamic tract, entrains to the light:dark (LD) cycle. This information is conveyed to peripheral circadian clocks through innervation by the autonomic nervous system or through the effects on all organs of circadian rhythms like temperature, melatonin, and glucocorticoids (reviewed by [2]).

At the cellular level, circadian function in the SCN and peripheral circadian clocks is sustained by the interconnected stimulatory and inhibitory transcriptional-translational feedback loops of the clock genes named *Period1-3*, *Cryptochrome1-2*, *Bmal1*, and *Clock* [3–6]. This circuit drives genes involved in major cellular functions through binding to E-boxes in their promoters (clock-controlled genes) or by using other transcription factors as intermediaries like *DBP* and *Egr1* [7–9]. The overall result is the 24-h oscillation of 10–30 % of the transcriptome in practically every tissue of the body, impacting a wide range of physiological

functions. The integral network of signals linking the SCN and peripheral oscillators results in overt circadian rhythms in physiological processes like thermoregulation, sleep, melatonin/ACTH/corticosteroid secretion, metabolic status, and feeding (reviewed by [2]) tuned to the daily light:dark cycle.

3 Development of the Circadian System: Fetal and Newborn Period

A number of studies show that the developing circadian system is organized differently from that of the adult. It is well established that development of circadian rhythms is part of the offspring's development program and proceeds normally in the absence of a functional maternal SCN. However, these rhythms are no longer synchronized indicating that maternal signals synchronize these rhythms. Comparison of the data available in nonhuman primates and rodents led us to propose that the fetal SCN is not a master clock and that the fetal SCN and other fetal organs are peripheral maternal circadian oscillators, potentially entrained by different maternal signals (reviewed by [10–13]) (Fig. 1).

3.1 The Fetal SCN

By mid-gestation, the fetal SCN is recognizable by histology. Day/night differences in diverse SCN functions such as metabolic activity, vasopressin mRNA and c-Fos mRNA, and protein expression are present during fetal life in nonhuman primates, sheep, and rodents SCN [14–19]. Innervation of the SCN by the retino-hypothalamic tract occurs in utero in human, nonhuman primates, and sheep, and postnatally in rodents [12, 20–22]. Clock gene oscillation is present in the fetal nonhuman primates' SCN, but starts postnatally in the rat SCN [23, 24]. Despite the lack of clock gene oscillation in the rat SCN, circadian clock gene oscillation is present in several fetal organs.

3.2 Fetal Peripheral Oscillators

In rats, circadian expression in several fetal organs starts before that of the fetal SCN [12, 25–29]. As shown in Fig. 2, at 18 days of gestation, fetuses gestated under a light:dark photoperiod (12:12 LD) show day/night changes in clock gene expression in the fetal heart, pineal, and hippocampus, already entrained to the LD cycle. A recent study shows 24-h clock gene expression in the fetal colon at 20 days of gestation [30]. Studies performed on the fetal adrenal of rats and nonhuman primates, at about 90 % gestation, established the fetal adrenal as a strong peripheral clock by linking clock gene expression with evidence of circadian adrenal steroid production. In both species, the clock genes *Bmal1* and *Per2* are expressed in antiphase, and mRNAs coding for the melatonin receptor and steroidogenic enzymes oscillate with a period of 24-h sustaining rhythms of corticosterone and DHAS (rat and monkey, respectively) in fetal plasma (Fig. 3). Recent work has shown daily

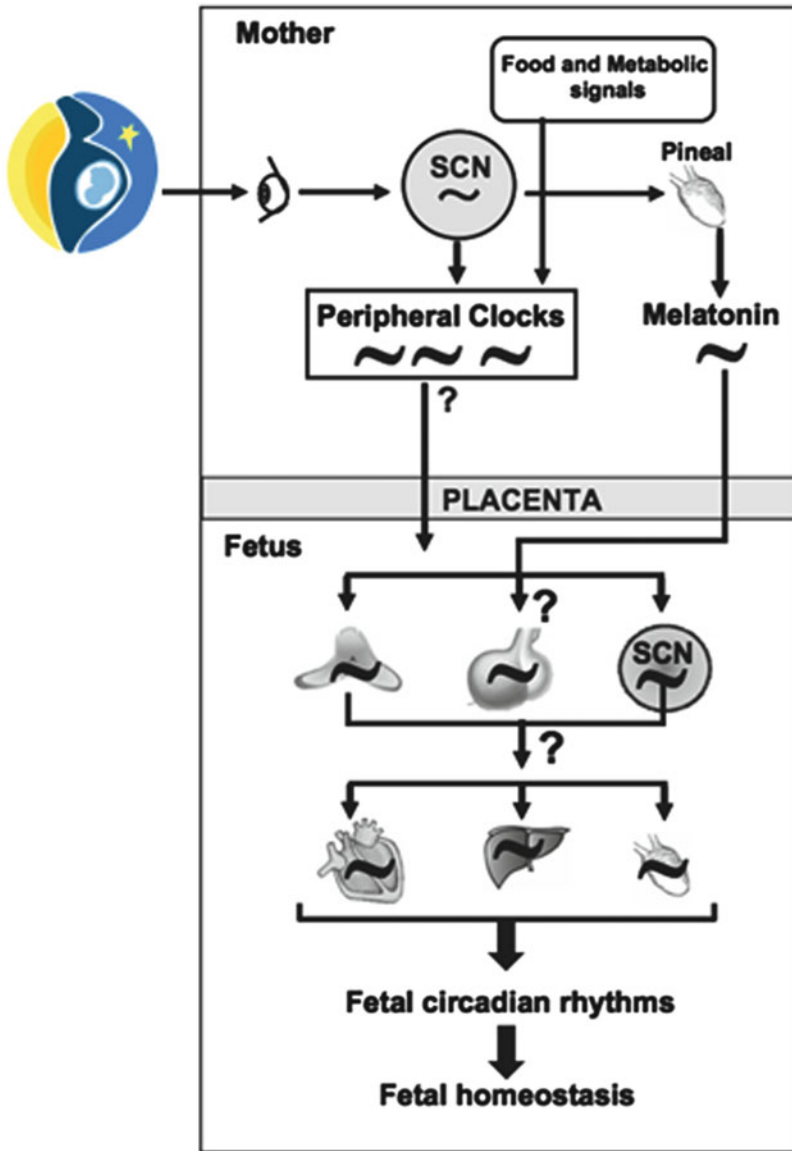


Fig. 1 Schematic representation of the proposed entrainment pathways of the fetal circadian system. The rat fetal adrenal and the primate fetal SCN could be entrained by the rhythms of maternal melatonin whereas other fetal peripheral clocks are phase entrained by (1) the maternal SCN through humoral or metabolic signals that cross the placenta or (2) a fetal peripheral circadian clock. We propose that a potential candidate for this task is the fetal adrenal gland through circadian glucocorticoid production (modified from [12])

oscillatory expression of the clock genes *Bmal1* and *Per2*, and of clock-controlled genes (melatonin receptor *Mtnr1b*, glucose transporter *Slc2a4*, glucocorticoid receptor *Nr3c1*, and NMDA receptor subunits 1B-3A-3B) in the rat fetal hippocampus at 18 days [31]. Studies performed in rat kidneys at embryonic day 20 [32] show a 24-h oscillation of the clock genes *Clock*, *Per2*, and *Rev-erba* and

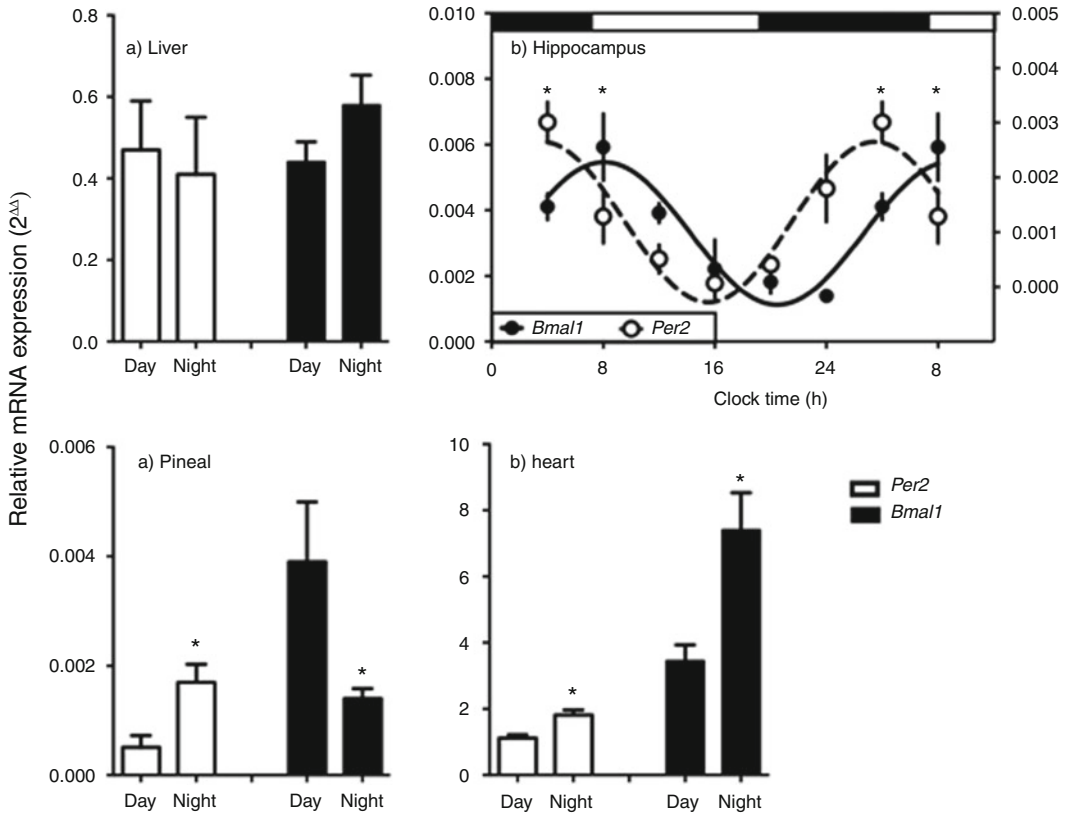
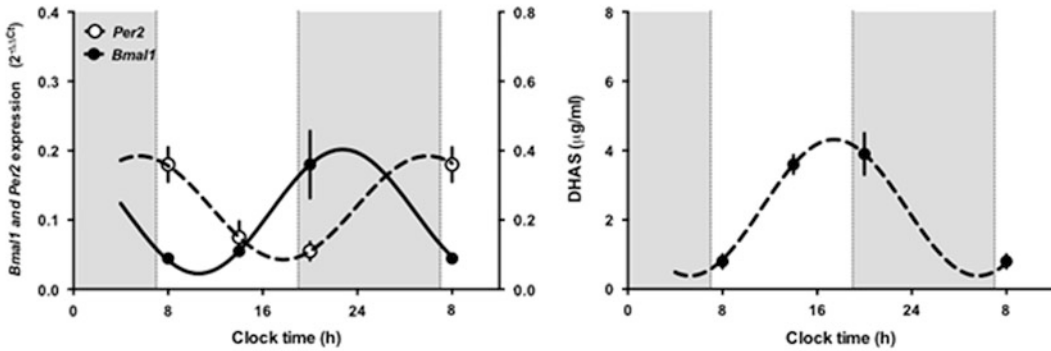


Fig. 2 Day/night and circadian pattern of *Per2* and *Bmal1* expression (mean \pm SEM) in rat fetal tissues at 18 days' gestation from Seron-Ferre et al. [12], and Vilches et al. [45]. *Per2* and *Bmal1* mRNA expression in heart, liver, and pineal was measured in fetuses from six groups of five pregnant rats; three groups were euthanized at day time (between 08.00 and 14.00) and the other three under red light at nighttime (between 20.00 and 02.00), fetuses ($n = 9/\text{dam}$) were delivered by hysterotomy, and tissues were dissected and preserved in TRizol until RNA extraction. *Per2* and *Bmal1* expression was measured by real-time PCR. *: different from daytime ($P < 0.05$, T test); **: Different to other clock time (ANOVA and Newman-Keuls). The lines in the hippocampus graph represent the theoretical 24-h cosinor function fitting the mean data. The dark bars indicate lights-off hours

several clock-controlled genes (epithelial sodium channel ENaC; serum and glucocorticoid-regulated kinase 1, SGK1; sodium hydrogen antiporter3, NHE3, and arginine vasopressin receptor 2, AVPR2). The genes studied in the fetal adrenal, kidney, and hippocampus are clock-controlled genes in the same organs when adult. Of note, the fetal adrenal and kidney have important physiological roles during fetal life: the adrenal as source of glucocorticoids important for fetal organ maturation and in some species, for triggering parturition [33]. The fetal kidneys contribute amniotic fluid production, which is important for several aspects of well-being [34].

Postnatal changes in clock gene expression have been investigated in the rat colon, kidney, and liver. As a rule, expression profile

a) Primate



b) Rat

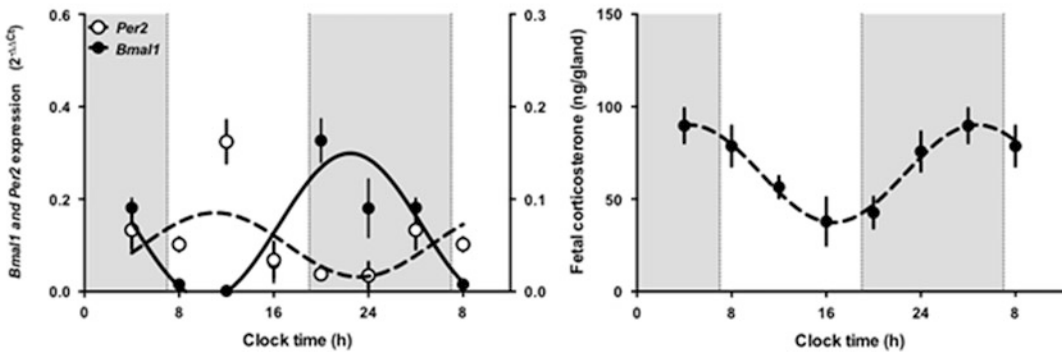


Fig. 3 Circadian pattern of *Per2* and *Bmal1* expression in fetal adrenal gland and plasma adrenal steroids in capuchin monkey (90 % of gestation, term about 160 days) and rat (18 days' gestation). From Torres-Farfan et al. 2004; 2011, respectively [23, 29]. Data are mean \pm SEM. The *lines* in each graph represent the theoretical 24-h cosinor function fitting the mean data. The *dark bars* indicate lights-off hours

similar to that of the adult is attained by 30 days of age. Using culture of organ slices from *Per2-luc* rats, Nishide et al. [35] followed the developmental changes in *Per2* expression between E20 and P19 and compared the expression with that of the same organs in the adult. These authors found oscillation in *Per2* expression at all ages studied in the SCN, lung, kidney, and liver. In another set of experiments, a large number of organs were studied at P5, P10, and P15, finding postnatal developmental phase changes in the pineal, lung, heart, muscle, kidney, spleen, thymus, testis, and stomach, whereas the phases of the SCN, adrenal, and liver were more or less maintained. This pattern of development fits with the observation that overt endocrine and behavioral rhythms with phases similar to those of the adult are detected 2–4 weeks after birth (e.g., corticosterone [36], pineal *N*-acetyltransferase [37], and eating and drinking [38]).

3.3 Entraining Signals for the Fetus and Newborn

Developing embryos and fetuses do not respond directly to external *zeitgebers* (“time givers”) like light, but instead to an internal representation of day/night alternation provided by the mother.

As will be reviewed in the next section, the maternal environment presents circadian rhythms. There is compelling evidence for two maternal signals acting during gestation on entrainment of fetal and newborn rhythms: maternal feeding time and maternal melatonin. A third maternal rhythm may be maternal core temperature.

The time of food availability induces important behavioral and metabolic adaptations in the mother and also in the offspring. In SCN-lesioned pregnant rats, restricting feeding to a 4-h period restores synchronization of the pups' drinking rhythms [39]. However, in the presence of an intact maternal SCN, a maternal restricted feeding schedule does not affect the fetal SCN. Maternal exposure to constant light (a condition that disrupts activity and melatonin rhythms in the mother) flattens the AVP and c-Fos rhythms in the fetal SCN, allowing entrainment to the restricted feeding schedule [17]. These data are interpreted as indicating that an LD signal derived from the mother SCN prevails over the food signal in causing or entraining the AVP and c-Fos mRNA rhythms in the fetal SCN.

There is strong evidence for maternal melatonin being an entraining signal for some fetal peripheral clocks. The maternal pineal gland produces melatonin in a circadian fashion, with high plasma levels at nighttime and very low levels at daytime (Fig. 4). Melatonin has the ability to cross all physiological barriers, such as the placenta [40] and the blood-brain barrier [41]. Thus the fetus, in which the pineal does not synthesize melatonin, in L:D conditions, is exposed to the maternal melatonin rhythm, and hence indirectly to LD information [42, 43]. When pregnant dams are exposed to constant light at night, plasma melatonin is suppressed in both diurnal and nocturnal animals [44, 45]. Melatonin receptors are widely distributed in fetal tissues from rat, mouse, hamster, sheep, human, and capuchin monkey [12, 29, 44, 46]. In the latter species, melatonin receptor expression followed a circadian pattern in the SCN and adrenal gland at 90 % of gestation [23]. We also reported that melatonin receptor expression displays a circadian rhythm in the rat fetal adrenal at 18 days of gestation [29]. Taken together, the circadian rhythms of both melatonin receptor expression and plasma melatonin supplied by the mother support that melatonin may act as a *zeitgeber* for different fetal peripheral oscillators. The experimental paradigm to test this hypothesis has been to compare the effects of maternal melatonin deprivation (either by maternal exposure to constant light or maternal pinealectomy) and daily maternal melatonin replacement with rhythms in fetuses and newborns whose mothers maintain a rhythm of melatonin (being gestated in LD). We demonstrated that the lack of melatonin suppressed clock gene expression rhythm and clock-controlled genes in the rat fetal adrenal and fetal hippocampus [29, 31, 45]. In addition, it decreased fetal adrenal corticosterone production [45]. Other researchers have shown that maternal pinealectomy

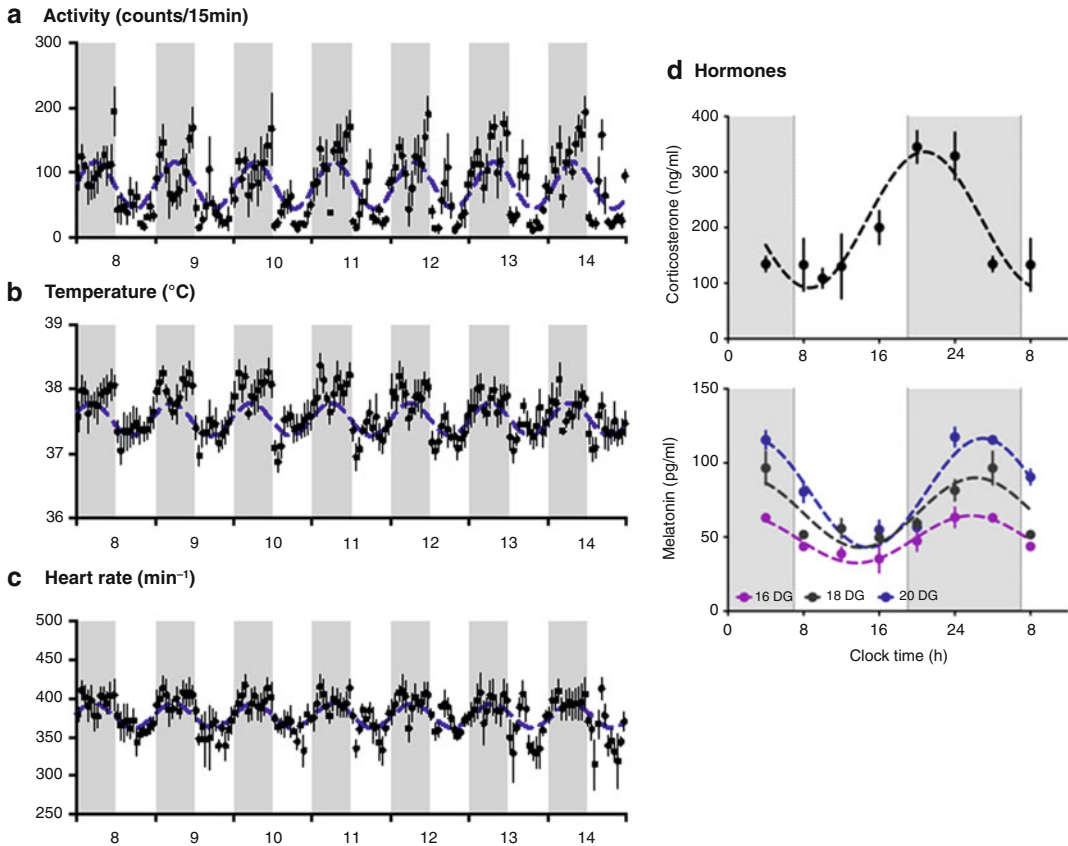


Fig. 4 Circadian rhythms in pregnant rats. Temperature (**a**), activity (**b**), and heart rate (**c**) were measured at 15-min intervals by telemetry (Mini-Mitter Co.) in pregnant rats at week 2 of gestation. A telemetric transponder was implanted in the abdominal cavity—7–10 days before mating (Torres-Farfan unpublished data). The acrophases occurred at midnight for all the variables measured. The *blue line* represents the theoretical 24-h cosinor function fitting the mean data ($n = 5$). (**d**) shows the circadian rhythms of corticosterone and melatonin in pregnant rats at 18 days of gestation (modified from [29]). The *dark bars* indicate lights-off hours

during gestation desynchronizes the pup's drinking rhythm [47]. In this and the previous experiments, daily maternal melatonin replacement during late gestation reversed the effects of gestational melatonin deprivation. Using the same experimental paradigm, we showed that maternal melatonin is a *zeitgeber* for the fetal primate's SCN [23], and that chronic maternal exposure to constant light results in a free running of the temperature rhythm in the newborn [48]. In this last study, the maternal temperature rhythm was not affected by exposure to constant light, suggesting that at least under melatonin deprivation, the maternal temperature rhythm is not an entraining signal for the fetal SCN nor the temperature rhythm in nonhuman, newborn primates [48]. The previous experiments were designed to test the role of melatonin as a *zeitgeber* for fetal organs. In another study, with maternal exposure to

constant light, without melatonin replacement, the overall effects on the fetal rat heart were studied utilizing microarrays, finding differential expression for 383 transcripts in LL relative to LD fetal heart (280 up-regulated and 103 downregulated). The altered gene networks included local steroidogenesis, as well as cardiac hypertrophy, stenosis, and necrosis/cell death. microRNA analysis revealed up-regulation of miRNAs 218-1 and 501 and concurrent downregulation of their validated target genes [49].

An important clinical situation in which the circadian information between mother and fetus is lost is the preterm newborn. Habitually, these newborns remain in intensive care units (ICU) for several weeks, exposed to constant light or constant dim light to facilitate medical care. In clinical studies, Rivkees [50] reported that exposure of premature infants to a regular LD cycle in the hospital nursery induces distinct patterns of rest-activity that are apparent within 1 week after discharge, suggesting that the circadian clock of developing infants is entrained by lighting conditions. As mentioned previously, the connection between the SCN and the retina is established during gestation in the human, and human preterm infants are able to detect light. Two recent studies investigated the effects of exposing preterm newborns to an LD cycle. Watanabe et al. [51] determined the wavelengths detected by the preterm newborn eye. Based on these findings they created an artificial night by covering the incubator for 9.5 h with a red filter absorbing wavelengths under 610 nm. Newborns exposed to the filter at night showed more daytime than nighttime activity at 38-week gestational age and a better growth rate. Vásquez-Ruiz et al. [52] created a night environment by placing a removable acrylic helmet covered by a blanket over the newborn head. They found that infants maintained in an LD cycle required a shorter stay in the hospital, tolerated food better, and gained weight faster than infants in LL, exhibiting improved oxygen saturation, less heart rate variation, and also day/night variation in salivary melatonin. Altogether, these results suggest entrainment by the LD cycle and stress the importance of an entraining signal for newborn physiology.

4 The Maternal Circadian System During Pregnancy

Pregnancy and the ensuing process, lactation, are physiological contexts in which maternal physiology changes to fulfill the increasing metabolic demands of the fetus, to provide input for timely parturition, and to prepare for providing food and care for the newborn. As a result, the cardiorespiratory system, immune system, renal, hepatic and gastrointestinal function, and endocrine system differ from that of nonpregnant women [53]. Pregnancy induces remodeling in areas of the “expectant brain” involved in food

intake and stress response, and in the autonomic system control (reviewed by [54]). In addition, a series of studies by Schrader et al. [55–57], measuring rhythms of *cFos* and *Per2* protein expression, support a functional reorganization of the SCN and ventral subparaventricular zone during early pregnancy, and of extra-SCN oscillators, such as the oval nucleus of the bed nucleus of the *stria terminalis*. The same authors found changes in daily patterns of immunoreactive FOS in early pregnant rats in areas related to sleep/wake control, finding an attenuation of daily rhythms of FOS expression in areas known to support wakefulness, whereas FOS expression was maintained in areas that correlate with sleep [56]. At peripheral levels, changes in maternal liver expression of clock genes between pregnant and nonpregnant rats have been described by Wharfe et al. and Varcoe et al. [58, 59]. Therefore, chronobiotic perturbations may be acting on a circadian system that may present differences from that of a nonpregnant female at the central and peripheral levels.

Several maternal functions show circadian rhythms under LD conditions. As shown in Fig 4, activity and temperature show regular circadian oscillation in pregnant rats. The figure also shows circadian rhythms of plasma corticosterone and melatonin. Consistent with other studies in rats and in humans, the amplitude of the maternal melatonin rhythm increases through gestation (reviewed by [60]). In addition, in both species there is an increase in the concentration of maternal plasma glucocorticoids, whilst the plasma glucocorticoid rhythm is maintained, and the hypothalamic-adrenal axis response to stress is markedly decreased (reviewed by [61, 62]). Other hormones like leptin, prolactin, progesterone, and estrogens also present circadian rhythms during pregnancy. And close to term, preceding parturition, there is a prominent rhythm in maternal oxytocin and circadian rhythms in uterine activity. In addition, metabolic variables like plasma glucose, cholesterol, free fatty acids, and triglyceride concentrations show a circadian rhythm [58]. Other maternal rhythms like activity and temperature show species-specific changes during pregnancy. In the diurnal Nile grass rat, activity- and temperature-phase rhythms were similar to those in nonpregnant animals, but the amplitude was decreased [63]. In contrast, in the nocturnal rat there were differences in both amplitude and phase of the temperature and activity rhythms [64].

Chronodisruption is expected to affect maternal rhythms. Clock gene defects are associated with pathologies in humans [65] and metabolic disorders in experimental animals [66–68]. A question arising from the previous observations is the possible impact of chronodisruption during pregnancy in the mother and offspring. Two experimental models of chronodisruption during pregnancy have been studied: constant light exposure and chronic phase shift model in which pregnant rats are exposed to chronic LD phase shifts lasting 3 days throughout gestation.

4.1 Constant Light

In rats and nonhuman primates, exposure to constant light during pregnancy suppresses the maternal melatonin rhythm and maintains the glucocorticoid rhythm. Exposure of constant light to pregnant capuchin and rhesus monkeys has no effect over the maternal cortisol, progesterone, estradiol, and temperature rhythms [44, 48, 69]. Effects of constant light on other maternal endocrine rhythms have not been studied in rats. However, the activity rhythm response differs between species. Exposing pregnant rats to constant light results in a free running activity rhythm and, eventually, in the disappearance of this rhythm [17] whereas it had minor effects in the capuchin [48]. Effects on metabolic rhythms have not been measured during exposure to constant light in rats or nonhuman primates.

4.2 Chronic Phase Shift

In rats, this model of chronodisruption produces profound circadian alterations eliminair in rats [58]. The authors found that at 20 days of gestation, melatonin secretion was not affected, but maternal 24-h profiles of corticosterone, leptin, glucose, insulin, free fatty acids, triglycerides, and cholesterol concentrations were altered. The pattern, but not the amount of food consumption, changed, and weight gain was decreased specially in early gestation. At 20 days of gestation, body weight was about 5 % lower than control rats, retroperitoneal fat pad and liver weight were reduced, and the expression of gluconeogenic and circadian clock genes in maternal and fetal liver became either arrhythmic or were in anti-phase to the controls. The authors suggest that the reduced maternal weight gain in early gestation may be involved in determining the offspring phenotype of increased adiposity, hyperinsulinemia, hyperleptinemia, and poor glucose tolerance [70] which is discussed in the following section.

5 Effects of Chronodisruption During Pregnancy on the Offspring

A number of studies have established a clear relationship between antenatal deleterious environments and the development of adult diseases including hypertension, metabolic syndrome, obesity, and neurologic/mental disorders [71–75]. In keeping with the importance of the fetal environment and postnatal outcome, perturbations of the fetal circadian system by melatonin deprivation during gestation have long-term consequences in the offspring. Metabolic effects (glucose intolerance, impaired glucose-stimulated insulin secretion, and hepatic insulin resistance) have been detected in the adult offspring of pinealectomized rats reared in LD [76]. In adult offspring gestated in LL, we observed complete lack of day/night differences in plasma melatonin and decreased day/night differences in plasma corticosterone. Moreover, overall hippocampal day/night difference of gene expression was decreased, which

was accompanied by a significant deficit of spatial memory [31]. In the heart, we found persistent downregulation of the mRNA coding for a subunit of the voltage-gated potassium Kv4 channel complex (Kcnp2), and hypertrophy of the left ventricle (thicker ventricle wall and increase in cardiomyocyte area and nuclear diameter [48]).

Another situation receiving attention is the effect on the offspring of maternal chronodisruption induced by shift work during pregnancy. Shift work may disrupt the maternal melatonin rhythm and impose abnormal maternal sleep and feeding patterns. Epidemiological studies in women show that shift work increases the risks of spontaneous abortion, premature delivery, and low-birth-weight babies [77]. As already reviewed, in the rat, simulated shift work during pregnancy [58] induces profound maternal metabolic changes and decreases early pregnancy weight gain. As shown by the same group in a previous study [70], simulated shift work during pregnancy had long-term effects on the offspring. At 3 months of age, offspring showed increased adiposity and hyperleptinemia. By 12 months of age, they showed altered glucose tolerance and insulin resistance that characterizes the metabolic syndrome. In contrast, there were no effects on the circadian temperature rhythm, suggesting that chronic LD phase shifts experienced during pregnancy did not result in long-term effects on the offspring SCN function. The authors suggest that the reduced maternal weight gain in early gestation may play an important role in determining the offspring metabolic phenotype [70].

Collectively, the present data point to the long-term adverse effects of gestational chronodisruption on a broad range of functions, including metabolic syndrome, heart hypertrophy, and cognitive function. The important health issues involved require establishing the mechanisms involved.

6 Analysis of Circadian Data

Examination of circadian rhythms in the fetus may offer important information about the impact of maternal environment on fetal development as well as its potential negative impact in adulthood. Several experimental models are being utilized to collect data on circadian changes. These models focus on specific variables at the individual and tissue level with the goal of exploring the impact of several interventions over these variables. This implies a characterization of a circadian pattern for the variable as well as identification of the perturbation of this pattern using adequate statistical methods.

In general, circadian studies require careful control of the LD cycles, feeding time, and housekeeping procedures to which the animals are exposed to avoid introducing circadian signals. Animal manipulation and procedures during nighttime should be done

under red light. In addition establishing a circadian profile of a given variable (e.g., hormones, metabolites, gene expression) requires frequent sampling at fixed intervals (at least every 4 h) around the clock. Strict protocols to preserve the samples are required as the researchers themselves are usually chronodisrupted. Fortunately, some biophysical and behavioral variables are amenable to continuous measurements over several days, with minimal human intervention.

6.1 Experimental Models

6.1.1 In Vivo Studies

Two experimental approaches have been used to study circadian rhythms *in vivo*. One is to obtain repeated measures over a long time interval from the same animal. The other is to obtain discontinuous sampling from different animals in which each animal contributes with a single sample for a given clock time. Large-size animals like sheep and nonhuman primates, in which the fetus and mother can be chronically instrumented, allow detection of overt circadian rhythms in biophysical variables like heart rate, blood pressure, fetal breathing, temperature, and electromyographic activity, by performing continuous recordings for extensive periods of time in the same individual. In addition, placements of vascular catheters allow obtaining blood samples from the same individual at fixed intervals around the clock to measure hormones and metabolites. Whenever possible, it is recommended to extend the sampling period for 48 h. The use of telemetric devices allows continuous recordings of temperature, activity, heart rate, and blood pressure during pregnancy in small animals like the rat. As rhythms can be detected in individual animals, less animals are needed to obtain significant information. These procedures have been used in the studies reported by us and others [48, 78–80].

The second alternative, usually of choice, is to obtain fetal samples blood and tissues at fixed intervals around the clock. Rapid sterile dissection and tissue collection require a collective effort of the team involved in the experiments. Depending on the variables to be measured, tissues can be fixed for histology, immunohistochemistry, and *in situ* hybridization, preserved for molecular biology measurements, frozen for biochemical measurements, etc. Additionally, tissues can be collected for *ex vivo* experiments. This experimental approach requires the utilization of a large number of animals but allows for performing many studies thereafter. These procedures have been used in the studies reported by us and others [12, 23, 29, 31, 58, 59, 81, 82].

6.1.2 Ex Vivo Studies

An option is to use organotypic cultures; this implies that the whole (or pieces) of organs are cultured for 48 h or longer. A large amount of tissue is required with this approach in order to perform relatively

frequent collection of tissue (every 4–6 h) over more than 24 h. In this experimental approach, pieces of tissue are taken at fixed and frequent time intervals. Moreover, drugs or hormones can be added to the medium, investigating their direct effects on clock gene oscillation. Measuring the temporal pattern of expression of several clock genes as well as clock-controlled genes in the explants provides evidence for circadian functional clocks being present in the tissue. This experimental approach does not require a big team for dissections, and the use of red light in the night is not necessary [23, 29, 35]. A variation of the previous approach consists of continuous measurement of a gene reporter expression over several days (for instance tissue from transgenic animals expressing *Per-2* coupled to luciferase). This type of experiment provides very important information about the ability of a tissue to maintain independent oscillation and allows for following any changes in the characteristics of the reporter rhythm (amplitude and acrophase over several days). Furthermore, this approach allows for the study of rhythm perturbations by some treatments. Conditions of sterility and avoidance of contamination are important in *ex vivo* models. These procedures have been used in the studies reported by us and others [83–85].

6.2 Assays

6.2.1 *Plasmatic Hormones*

As in other biological experiments, assays should be highly sensitive to minimize the amount of blood or tissue required. This applies to blood measurements and also to molecular biology techniques. With regard to hormone levels, probably the most difficult hormone to measure is melatonin, for which there are few commercial kits available. To the best of our knowledge, the melatonin RIA is a sensitive assay. However, there are difficulties/challenges which require careful treatment of the samples to avoid hemolysis and high lipid concentrations. Additionally, the RIA manipulation should be made in lab where melatonin has not been used recently, because the assay is easily contaminated by the environment. In our experience, the technician that performs the experiment should stop using melatonin if he or she is taking melatonin for sleep problems (a common problem in people that work on circadian rhythms). On the other hand, commercial kits to measure other hormones (cortisol, corticosterone, aldosterone, etc.) in general are easier than melatonin and work efficiently for us [12, 29, 45, 86, 87].

6.2.2 *mRNA Expression*

To measure mRNA levels, we routinely used qRT-PCR. This method is usually sensitive enough to allow good discrimination in gene expression, at different clock times. To use this technique, it is necessary to consider the best housekeeping for a particular organ. In this context, sometimes it is necessary to test several potential housekeeping genes. Recently, we found that maternal

chronodisruption induced major changes in fetal liver 18S-rRNA. This situation did not occur in the fetal adrenal gland, an organ in which 18S-rRNA was not modified by the maternal treatments [45]. The major advantage of qRT-PCR is that several mRNAs could be measured in the same sample. In addition, qRT-PCR is used to validate data obtained by microarrays.

6.3 Statistical Methods Utilized to Detect Circadian Rhythms

An important consideration is the method utilized to decide that the changes of a variable over time are circadian. Refinetti et al. [88] provide a comprehensive review of strengths and weakness of the different statistical methods used to detect circadian rhythms and provide a list of programs available for these methods. A simple definition of a rhythm is the oscillation of a variable with a constant period. The period of a rhythm is the duration of a full cycle. Three parameters characterize a circadian rhythm: period close to 24 h, amplitude, and phase of the oscillation. A simple method for circadian rhythm assessment is cosinor analysis. This method fits the data to the cosine function:

$$x_i = M + A \cos 360 T^{-1}(t_i - \varphi)$$

in which x_i is the value of the variable at the time t_i expressed in hours, M is the mesor (mean of the data in 24 h), A is the amplitude (difference between the mesor and value of the variable at the acrophase), φ is the acrophase (time at which the variable reaches its maximal value), and T is the period (24 h). Time is usually expressed in hours as clock time or zeitgeber time (hours from the start of the light period, or in some cases hours from the start of the activity rhythm). Cosinor analysis applies to data obtained in individuals, organs, and cells. More sophisticated analysis is available for experiments that involve data obtained over long-term intervals, as discussed by Refinetti et al. [88]. In our experiments, we have usually investigated the presence of clock time-related changes in the mean data of a variable by ANOVA. If these are present, we utilize cosinor analysis. Comparison of mesor and amplitudes can be done utilizing standard statistical tests (Student's T test or ANOVA, when adequate). Circular statistical tests are required to both assess and compare the random distribution of acrophases (Watson-Williams and Rayleigh tests, respectively [89]).

7 Concluding Remarks

From our review, it becomes clear that maternal circadian signals during pregnancy are important for entrainment of fetal and newborn circadian rhythms. The response of this system to environmental perturbations (food restriction, stress, shifts in the LD cycle among others) may have long-term effects in the offspring. However, this novel research avenue still faces multiple challenges.

These include working on an experimental model that more closely resembles the human setting of shift work during pregnancy; exploring further organs as targets of developmental chronodisruption; and identifying changes not only in systemic pathophysiological readouts, but also in the transcriptome, microRNA regulome (miRNome), and proteome from different fetal tissues. The long-standing aim of the work discussed here is to offer insight into mechanism as well as potential human translational targets for intervention against the developmental programming of disease triggered by prenatal chronodisruption.

Acknowledgments

ANILLO ACT-1116; FONDECYT 1110220 and 1120938 (Chile).

We thank Monica Prizant for editorial assistance.

References

- Erren TC, Reiter RJ (2009) Defining chronodisruption. *J Pineal Res* 46:245–247
- Bass J, Takahashi JS (2010) Circadian integration of metabolism and energetics. *Science* 330:1349–1354
- Reppert SM, Weaver DR (2002) Coordination of circadian timing in mammals. *Nature* 418:935–941
- Richter HG, Torres-Farfan C, Rojas-García PP, Campino C, Torrealba F, Seron-Ferre M (2004) The circadian timing system: making sense of day/night gene expression. *Biol Res* 37:11–28
- Ishida A, Mutoh T, Ueyama T, Bando H, Masubuchi S, Nakahara D, Tsujimoto G, Okamura H (2005) Light activates the adrenal gland: timing of gene expression and glucocorticoid release. *Cell Metab* 2:297–307
- Watanabe T et al (2006) Peripheral clock gene expression in CS mice with bimodal locomotor rhythms. *Neurosci Res* 54:295–301
- Fustin JM, Dardente H, Wagner GC, Carter DA, Johnston JD, Lincoln GA, Hazlerigg DG (2009) *Egr1* involvement in evening gene regulation by melatonin. *FASEB J* 23:764–773
- Levi F, Schibler U (2007) Circadian rhythms: mechanisms and therapeutic implications. *Annu Rev Pharmacol Toxicol* 47:593–628
- Resuehr HE, Resuehr D, Olcese J (2009) Induction of *mPer1* expression by GnRH in pituitary gonadotrope cells involves *EGR-1*. *Mol Cell Endocrinol* 311:120–125
- Sumova A, Bendova Z, Sladek M, El-Hennamy R, Mateju K, Polidarova L, Sosniyenko S, Illnerova H (2008) Circadian molecular clocks tick along ontogenesis. *Physiol Res* 57(Suppl 3):S139–S148
- Jud C, Albrecht U (2006) Circadian rhythms in murine pups develop in absence of a functional maternal circadian clock. *J Biol Rhythms* 21:149–154
- Seron-Ferre M et al (2012) Circadian rhythms in the fetus. *Mol Cell Endocrinol* 349:68–75
- Davis FC, Reppert SM (2001) Development of mammalian circadian rhythms. In: Takahashi JS, Turek FW, Moore RY (eds) *Circadian clocks*, Handbooks of behavioral neurobiology. Kluwer Academic/Plenum Publishers, New York, NY, pp 247–291
- Reppert SM, Schwartz WJ (1984) Functional activity of the suprachiasmatic nuclei in the fetal primate. *Neurosci Lett* 46:145–149
- Reppert SM, Schwartz WJ (1983) Maternal coordination of the fetal biological clock in utero. *Science* 220:969–971
- Davis FC, Gorski RA (1985) Development of hamster circadian rhythms. I. Within-litter synchrony of mother and pup activity rhythms at weaning. *Biol Reprod* 33:353–362
- Novakova M, Sladek M, Sumova A (2010) Exposure of pregnant rats to restricted feeding schedule synchronizes the SCN clocks of their fetuses under constant light but not under a light-dark regime. *J Biol Rhythms* 25:350–360

18. Constandil L, Parraguez VH, Torrealba F, Valenzuela G, Seron-Ferre M (1995) Day-night changes in c-fos expression in the fetal sheep suprachiasmatic nucleus at late gestation. *Reprod Fertil Dev* 7:411–413
19. Breen S, Rees S, Walker D (1996) The development of diurnal rhythmicity in fetal suprachiasmatic neurons as demonstrated by fos immunohistochemistry. *Neuroscience* 74:917–926
20. Seron-Ferre M, Valenzuela GJ, Torres-Farfan C (2007) Circadian clocks during embryonic and fetal development. *Birth Defects Res C Embryo Today* 81:204–214
21. Torrealba F, Parraguez VH, Reyes T, Valenzuela G, Seron-Ferre M (1993) Prenatal development of the retinohypothalamic pathway and the suprachiasmatic nucleus in the sheep. *J Comp Neurol* 338:304–316
22. Muller C, Torrealba F (1998) Postnatal development of neuron number and connections in the suprachiasmatic nucleus of the hamster. *Brain Res Dev Brain Res* 110:203–213
23. Torres-Farfan C et al (2006) Maternal melatonin effects on clock gene expression in a non-human primate fetus. *Endocrinology* 147:4618–4626
24. Bendova Z, Sumova A, Illnerova H (2004) Development of circadian rhythmicity and photoperiodic response in subdivisions of the rat suprachiasmatic nucleus. *Brain Res Dev Brain Res* 148:105–112
25. Ko MS et al (2000) Large-scale cDNA analysis reveals phased gene expression patterns during preimplantation mouse development. *Development* 127:1737–1749
26. Johnson MH, Lim A, Fernando D, Day ML (2002) Circadian clockwork genes are expressed in the reproductive tract and conceptus of the early pregnant mouse. *Reprod Biomed Online* 4:140–145
27. Saxena MT, Aton SJ, Hildebolt C, Prior JL, Abraham U, Piwnica-Worms D, Herzog ED (2007) Bioluminescence imaging of period1 gene expression in utero. *Mol Imaging* 6:68–72
28. Sladek M, Jindrakova Z, Bendova Z, Sumova A (2007) Postnatal ontogenesis of the circadian clock within the rat liver. *Am J Physiol Regul Integr Comp Physiol* 292:R1224–R1229
29. Torres-Farfan C, Mendez N, Abarzua-Catalan L, Vilches N, Valenzuela GJ, Seron-Ferre M (2011) A Circadian clock entrained by melatonin is ticking in the rat fetal adrenal. *Endocrinology* 152:1891–1900
30. Polidarova L, Olejnikova L, Pauslyova L, Sladek M, Sotak M, Pacha J, Sumova A (2014) Development and entrainment of the colonic circadian clock during ontogenesis. *Am J Physiol Gastrointest Liver Physiol* 306:G346–G356
31. Vilches N, Spichiger C, Mendez N, Abarzua-Catalan L, Galdames HA, Hazlerigg DG, Richter HG, Torres-Farfan C (2014) Gestational chronodisruption impairs hippocampal expression of NMDA receptor subunits Grin1b/Grin3a and spatial memory in the adult offspring. *PLoS One* 9:e91313
32. Meszaros K, Pruess L, Szabo AJ, Gondan M, Ritz E, Schaefer F (2014) Development of the circadian clockwork in the kidney. *Kidney Int* 86:915
33. Liggins GC (1994) The role of cortisol in preparing the fetus for birth. *Reprod Fertil Dev* 6:141–150
34. Underwood MA, Gilbert WM, Sherman MP (2005) Amniotic fluid: not just fetal urine anymore. *J Perinatol* 25:341–348
35. Nishide SY, Hashimoto K, Nishio T, Honma K, Honma S (2014) Organ-specific development characterizes circadian clock gene *Per2* expression in rats. *Am J Physiol Regul Integr Comp Physiol* 306:R67–R74
36. Hiroshige T, Honma K, Watanabe K (1982) Ontogeny of the circadian rhythm of plasma corticosterone in blind infantile rats. *J Physiol* 325:493–506
37. Deguchi T (1975) Ontogenesis of a biological clock for serotonin:acetyl coenzyme A N-acetyltransferase in pineal gland of rat. *Proc Natl Acad Sci U S A* 72:2814–2818
38. Reppert SM, Schwartz WJ (1986) Maternal suprachiasmatic nuclei are necessary for maternal coordination of the developing circadian system. *J Neurosci* 6:2724–2729
39. Weaver DR, Reppert SM (1989) Periodic feeding of SCN-lesioned pregnant rats entrains the fetal biological clock. *Brain Res Dev Brain Res* 46:291–296
40. Okatani Y, Okamoto K, Hayashi K, Wakatsuki A, Tamura S, Sagara Y (1998) Maternal-fetal transfer of melatonin in pregnant women near term. *J Pineal Res* 25:129–134
41. Reiter RJ (1998) Oxidative damage in the central nervous system: protection by melatonin. *Prog Neurobiol* 56:359–384
42. Yellon SM, Longo LD (1988) Effect of maternal pinealectomy and reverse photoperiod on the circadian melatonin rhythm in the sheep and fetus during the last trimester of pregnancy. *Biol Reprod* 39:1093–1099
43. McMillen IC, Nowak R (1989) Maternal pinealectomy abolishes the diurnal rhythm in plasma melatonin concentrations in the fetal

- sheep and pregnant ewe during late gestation. *J Endocrinol* 120:459–464
44. Torres-Farfan C et al (2004) Maternal melatonin selectively inhibits cortisol production in the primate fetal adrenal gland. *J Physiol* 554:841–856
 45. Mendez N et al (2012) Timed maternal melatonin treatment reverses circadian disruption of the fetal adrenal clock imposed by exposure to constant light. *PLoS One* 7:e42713
 46. Torres-Farfan C et al (2008) Evidence of a role for melatonin in fetal sheep physiology: direct actions of melatonin on fetal cerebral artery, brown adipose tissue and adrenal gland. *J Physiol* 586:4017–4027
 47. Bellavia SL, Carpentieri AR, Vaque AM, Macchione AF, Vermouth NT (2006) Pup circadian rhythm entrainment—effect of maternal ganglionectomy or pinealectomy. *Physiol Behav* 89:342–349
 48. Seron-Ferre M et al (2013) Impact of chronodisruption during primate pregnancy on the maternal and newborn temperature rhythms. *PLoS One* 8:e57710
 49. Galdames HA, Torres-Farfan C, Spichiger C, Mendez N, Abarzua-Catalan L, Alonso-Vazquez P, Richter HG (2014) Impact of gestational chronodisruption on fetal cardiac genomics. *J Mol Cell Cardiol* 66:1–11
 50. Rivkees SA, Mayes L, Jacobs H, Gross I (2004) Rest-activity patterns of premature infants are regulated by cycled lighting. *Pediatrics* 113:833–839
 51. Watanabe S, Akiyama S, Hanita T, Li H, Nakagawa M, Kaneshi Y, Ohta H (2013) Designing artificial environments for preterm infants based on circadian studies on pregnant uterus. *Front Endocrinol (Lausanne)* 4:113
 52. Vasquez-Ruiz S, Maya-Barrios JA, Torres-Narvaez P, Vega-Martinez BR, Rojas-Granados A, Escobar C, Angeles-Castellanos M (2014) A light/dark cycle in the NICU accelerates body weight gain and shortens time to discharge in preterm infants. *Early Hum Dev* 90:535
 53. Cunningham FG, Leveno K, Bloom S, Hauth J, Rouse D, Spong CY (2009) Maternal and fetal anatomy and physiology. In: Fried A, Davis K (eds) *Williams obstetrics*. McGraw-Hill Professional Publishing, New York, NY, pp 107–136
 54. Brunton PJ, Russell JA (2008) The expectant brain: adapting for motherhood. *Nat Rev Neurosci* 9:11–25
 55. Schrader JA, Nunez AA, Smale L (2010) Changes in and dorsal to the rat suprachiasmatic nucleus during early pregnancy. *Neuroscience* 171:513–523
 56. Schrader JA, Smale L, Nunez AA (2012) Pregnancy affects FOS rhythms in brain regions regulating sleep/wake state and body temperature in rats. *Brain Res* 1480:53–60
 57. Schrader JA, Nunez AA, Smale L (2011) Site-specific changes in brain extra-SCN oscillators during early pregnancy in the rat. *J Biol Rhythms* 26:363–367
 58. Varcoe TJ, Boden MJ, Voultsios A, Salkeld MD, Rattanaray L, Kennaway DJ (2013) Characterisation of the maternal response to chronic phase shifts during gestation in the rat: implications for fetal metabolic programming. *PLoS One* 8:e53800
 59. Wharfe MD, Mark PJ, Waddell BJ (2011) Circadian variation in placental and hepatic clock genes in rat pregnancy. *Endocrinology* 152:3552–3560
 60. Tamura H, Nakamura Y, Terron MP, Flores LJ, Manchester LC, Tan DX, Sugino N, Reiter RJ (2008) Melatonin and pregnancy in the human. *Reprod Toxicol* 25:291–303
 61. de Weerth C, Buitelaar JK (2005) Physiological stress reactivity in human pregnancy – a review. *Neurosci Biobehav Rev* 29:295–312
 62. Brunton PJ, Russell JA (2010) Prenatal social stress in the rat programmes neuroendocrine and behavioural responses to stress in the adult offspring: sex-specific effects. *J Neuroendocrinol* 22:258–271
 63. Schrader JA, Walaszczyk EJ, Smale L (2009) Changing patterns of daily rhythmicity across reproductive states in diurnal female Nile grass rats (*Arvicanthis niloticus*). *Physiol Behav* 98:547–556
 64. Kittrell EM, Satinoff E (1988) Diurnal rhythms of body temperature, drinking and activity over reproductive cycles. *Physiol Behav* 42:477–484
 65. Ebisawa T (2007) Circadian rhythms in the CNS and peripheral clock disorders: human sleep disorders and clock genes. *J Pharmacol Sci* 103:150–154
 66. Jilg A, Lesny S, Peruzki N, Schwegler H, Selbach O, Dehghani F, Stehle JH (2010) Temporal dynamics of mouse hippocampal clock gene expression support memory. *Hippocampus* 20:377–388
 67. MarcheVA B, Ramsey KM, Peek CB, Affinati A, Maury E, Bass J (2013) Circadian clocks and metabolism. *Handb Exp Pharmacol* (217): 127–155
 68. Sadacca LA, Lamia KA, deLemos AS, Blum B, Weitz CJ (2011) An intrinsic circadian clock of the pancreas is required for normal insulin release and glucose homeostasis in mice. *Diabetologia* 54:120–124

69. Matsumoto T, Hess DL, Kaushal KM, Valenzuela GJ, Yellon SM, Ducsay CA (1991) Circadian myometrial and endocrine rhythms in the pregnant rhesus macaque: effects of constant light and timed melatonin infusion. *Am J Obstet Gynecol* 165:1777–1784
70. Varcoe TJ, Wight N, Voultios A, Salkeld MD, Kennaway DJ (2011) Chronic phase shifts of the photoperiod throughout pregnancy programs glucose. *PLoS One* 6:e18504
71. Osmond C, Barker DJ (2000) Fetal, infant, and childhood growth are predictors of coronary heart disease, diabetes, and hypertension in adult men and women. *Environ Health Perspect* 108:545–553
72. Fowden AL, Giussani DA, Forhead AJ (2006) Intrauterine programming of physiological systems: causes and consequences. *Physiology (Bethesda)* 21:29–37
73. Nathanielsz PW (2006) Animal models that elucidate basic principles of the developmental origins of adult diseases. *ILAR J* 47:73–82
74. Nuyt AM (2008) Mechanisms underlying developmental programming of elevated blood pressure and vascular dysfunction: evidence from human studies and experimental animal models. *Clin Sci (Lond)* 114:1–17
75. Barker DJ (2006) Adult consequences of fetal growth restriction. *Clin Obstet Gynecol* 49:270–283
76. Ferreira DS et al (2012) Maternal melatonin programs the daily pattern of energy metabolism in adult offspring. *PLoS One* 7:e38795
77. Zhu JL, Hjollund NH, Andersen AM, Olsen J (2004) Shift work, job stress, and late fetal loss: the National Birth Cohort in Denmark. *J Occup Environ Med* 46:1144–1149
78. Taylor NF, Martin MC, Nathanielsz PW, Seron-Ferre M (1983) The fetus determines circadian oscillation of myometrial electromyographic activity in the pregnant rhesus monkey. *Am J Obstet Gynecol* 146:557–567
79. Figueroa JP, Honnebier MB, Jenkins S, Nathanielsz PW (1990) Alteration of 24-hour rhythms in myometrial activity in the chronically catheterized pregnant rhesus monkey after a 6-hour shift in the light-dark cycle. *Am J Obstet Gynecol* 163:648–654
80. Jensen EC, Bennet L, Guild SJ, Booth LC, Stewart J, Gunn AJ (2009) The role of the neural sympathetic and parasympathetic systems in diurnal and sleep state-related cardiovascular rhythms in the late-gestation ovine fetus. *Am J Physiol Regul Integr Comp Physiol* 297:R998–R1008
81. Houdek P, Polidarova L, Novakova M, Mateju K, Kubik S, Sumova A (2015) Melatonin administered during the fetal stage affects circadian clock in the suprachiasmatic nucleus but not in the liver. *Dev Neurobiol* 75:131
82. Li C, Yu S, Zhong X, Wu J, Li X (2012) Circadian rhythms of fetal liver transcription persist in the absence of canonical circadian clock gene expression rhythms in vivo. *PLoS One* 7:e30781
83. Akiyama S et al (2010) The uterus sustains stable biological clock during pregnancy. *Tohoku J Exp Med* 221:287–298
84. Ratajczak CK, Herzog ED, Muglia LJ (2010) Clock gene expression in gravid uterus and extra-embryonic tissues during late gestation in the mouse. *Reprod Fertil Dev* 22:743–750
85. Ohta H et al (2008) Maternal feeding controls fetal biological clock. *PLoS One* 3:e2601
86. Seron-Ferre M, Ducsay CA, Valenzuela GJ (1993) Circadian rhythms during pregnancy. *Endocr Rev* 14:594–609
87. Seron-Ferre M, Rizzo R, Valenzuela GJ, Germain AM (2001) Twenty-four-hour pattern of cortisol in the human fetus at term. *Am J Obstet Gynecol* 184:1278–1283
88. Refinetti R, Lissen GC, Halberg F (2007) Procedures for numerical analysis of circadian rhythms. *Biol Rhythm Res* 38:275–325
89. Zar J (1974) Circular distributions. In: McElroy W, Swanson C (eds) *Biostatistical analysis*. Prentice-Hall, Englewood Cliffs, NJ, pp 310–328

Part II

Programming and Stress

Chapter 8

Prenatal Programming of the Mesolimbic Reward Pathway and Food Preferences

Beverly S. Muhlhausler and Jessica Gugusheff

Abstract

The drive to consume palatable foods, high in fat and sugar, goes beyond the need to satisfy hunger and has a strong hedonic component. Studies in rodent models have demonstrated that the preference for these foods can be programmed before birth, and that feeding dams on cafeteria diets during pregnancy and lactation is associated with an increased preference for palatable foods in the offspring after weaning. More recently, attention has turned towards elucidating the biological mechanisms which drive these effects, with studies to date focussing on the impact of maternal cafeteria diets on the development of the mesolimbic reward pathway in the offspring. This chapter discusses the methods we have used to study the impact of maternal “junk food” diets during pregnancy and lactation on food preferences and gene expression of key components of the opioid and dopamine signalling systems in two key regions of the mesolimbic reward pathway in the offspring.

Key words Fetal programming, Reward, Cafeteria diet, Dopamine, Opioids, Neonate, Ontogeny, Animal model

1 Background

Obesity is currently a major public health issue in both the developed and developing world, with current estimates suggesting that over one billion adults worldwide are either overweight (BMI > 25 kg/m²) or obese (BMI > 30 kg/m²) [1]. The substantial increase in the prevalence of obesity over the past 30–40 years has led to growing interest in determining the genetic and environmental factors which contribute to its development, and a plethora of studies aimed at elucidating the key drivers of weight gain and excess adiposity in human populations. These studies have all pointed to environmental factors in modern society, in particular the increased availability of high-fat high-sugar palatable foods (“junk foods”) [2], as having an important role in promoting weight gain and obesity in individuals.

The drive to consume palatable diets goes beyond the need to satisfy hunger, since fat and sugar, and possibly other components of these diets, can activate the same mesolimbic reward pathway as alcohol, nicotine, and recreational drugs [3, 4]. Activation of the reward pathway results in the release of endogenous opioids which bind to opioid receptors on inhibitory GABAergic neurons in the ventral tegmental area (VTA) of the brain, and releases their inhibition of dopamine synthesis in dopaminergic neurons in this brain region [5]. These dopaminergic neurons project to a region in the forebrain, the nucleus accumbens (NAc) where the dopamine is released. This results in an increase in extracellular dopamine concentrations in the NAc, which translates into the acute pleasurable sensation associated with the consumption of rewarding stimuli [3, 6].

The preference for and ability to control consumption of high-fat, high-sugar foods differs significantly between individuals, and this has led to studies focussed on the determinants of individual food preferences. A number of studies have now suggested that the preference for “junk foods” can be programmed before birth, and we and others have demonstrated that maternal intake of “natural rewards” including high-fat, high-sugar diets, is associated with an increased propensity towards the overconsumption of these types of foods in the offspring [7–11]. More recent studies have attempted to define the mechanisms which underlie the early life origins of food preferences by investigating the effect of maternal high-fat, high-sugar diets on the mesolimbic reward pathway. These studies have demonstrated that a number of key components of this pathway, including the mu-opioid receptor and D1 and D2 dopamine receptors, are altered in adolescent and adult offspring of mothers fed a cafeteria/high-fat diet during pregnancy and lactation [12, 13]. Thus, rodent studies focussed on the impact of maternal diet on the development of the reward pathway and subsequent food preferences can provide valuable insights into the mechanisms which underlie the propensity towards overconsumption of these food types.

This chapter describes the methods we have used to study the food preferences of offspring exposed to a “junk food” diet before birth and whilst suckling as well as provide specific detail on how to measure changes in reward pathway development in these animals using molecular and histological approaches.

2 Equipment/Material/Setup

2.1 *Animals*

The impact of the maternal diet during pregnancy and lactation on food preferences and the reward pathway of the offspring have been studied almost exclusively in rodents. The specific breed/strain has varied between studies, and has included Wistar rats [14, 15],

Sprague-Dawley rats [7], and mixed background mice [11, 12]. The results have been relatively consistent between these various species/breeds, which suggests that the programming effects observed are conserved across rodent species. As such, the selection of breed/species for these experiments can be based more on other factors, such as availability/access, cost, ease of handling, litter size, and temperament.

Ideally, the female rats that we used in studies of the developmental programming effects of maternal cafeteria diets are between 6 and 8 weeks of age and around 200–250 g in weight when the experiment begins, which ensures that they are at their peak fertility at the time of mating. The cafeteria diet we have used in our studies typically produces a weight gain of ~20 % of initial body weight in the first 2 weeks, and the fertility of the animals declines markedly with increasing body weight. Most successful mating is generally obtained with male rats that are older and slightly larger than the females, ideally over 400 g in body weight and >3 months of age. Before beginning a study involving an animal model it is important that approval from an animal ethics committee has been obtained and appropriate housing in an animal research facility has been organized. All procedures should be conducted according to the Australian code for the care and use of animals for scientific purposes (or local equivalent) [16]. The animal housing facility will require scales for weighing both the rats (to the nearest 0.01 g for pups and nearest 0.1 g for older animals) and the food (preferably to the nearest 0.001 g), a light microscope, and full postmortem facilities including a CO₂ gas chamber for euthanasia.

2.2 Composition of the Cafeteria Diet

The cafeteria diet is a well-established model of junk food feeding in the rodent [17]. The exact composition of this diet varies between studies but all include a selection of readily available “junk foods” which are typically energy dense, nutrient poor, and relatively high in fat, sugar, and salt. In our studies, we have used a cafeteria diet comprising of peanut butter, hazelnut spread, sweetened breakfast cereal, cheese- and bacon-flavored snacks, chocolate biscuits, and a mixture of lard and standard laboratory chow [10] (Fig. 1a). Other examples of cafeteria diets which have been provided to dams during pregnancy and/or lactation in studies of developmental programming include those used by Bayol and colleagues, which consisted of biscuits, marshmallows, jam doughnuts, cheese, potato crisps, chocolate chip muffins, butter flapjacks, and caramel/chocolate bars [9] and that used by Langley-Evans and colleagues, which consisted of biscuits, potato crisps, chocolate, cheddar cheese, golden syrup cake, pork pie, cocktail sausage, liver and bacon pate, strawberry jam, and peanuts [15]. In all cases, these diets provide between 50 and 60 % of calories as fat (predominately saturated fat), compared with ~12 % energy from fat provided by the standard rodent chow, and contain relatively low levels of

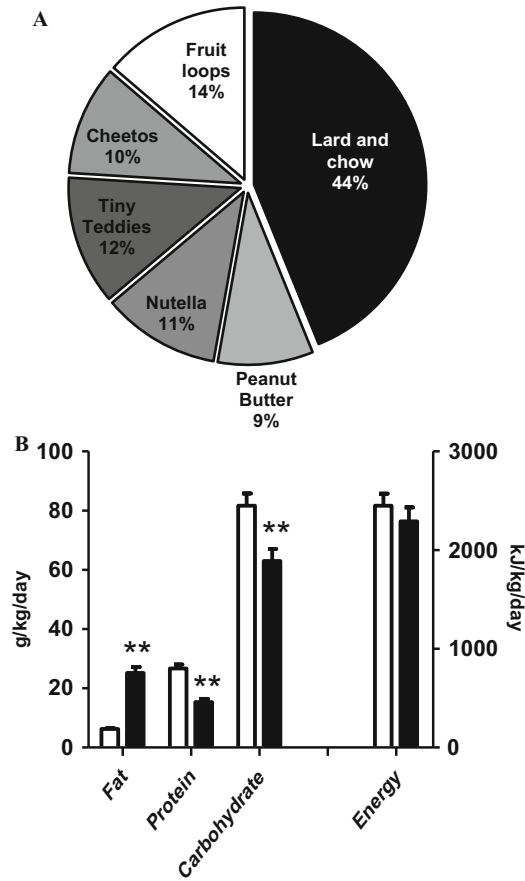


Fig. 1 (a) Representative pie chart depicting the contribution of different components of the cafeteria diet to food intake of “junk food”-fed dams during pregnancy. (b) Bar graph comparing the typical macronutrient (in g/kg/day) and overall energy intake (in kJ/kg/day) of control (*open bars*) and junk food-fed (*closed bars*) dams during lactation. The junk food-fed dams consume more fat but less protein and carbohydrate, reflecting the energy sources in each diet

protein. The dams who are fed on the cafeteria diet typically consume higher amounts of fat and lower amounts of protein compared to controls, although not necessarily higher amounts of total energy (Fig. 1b).

In addition to cafeteria diets, it is also possible to use formulated diets which are prepared by a feed manufacturer (or in-house) to a predefined recipe. These diets are typically in the form of a pellet-based or liquid diet, which are provided to dams on either a per kg body weight basis or *ad libitum*. The advantage of these formulated diets is that it is possible to precisely control the composition of the diet that the rats consume, since the macronutrient and micronutrient content is consistent across the diet. It is also

easier to measure food intake/food refusals than for the cafeteria diet. However, we have consistently used the cafeteria diet in our studies in order to mimic the typical poor-quality Western diets which are both energy/fat dense and micronutrient poor. This approach also allows for the direct comparison of the specific types of foods that are preferred by the mother and her offspring, to distinguish the programming of macronutrient preference from the programming of a taste for specific flavors.

Whichever type of diet you use, it is important to accurately determine the nutritional composition. In the case of the formulated diet, this is more straightforward since the composition is predefined. In the case of the cafeteria diet, it is often necessary to rely on the nutritional information provided on the packaging of the various foods included in the diet, which may not always be accurate, particularly in the case of minor dietary components. While macronutrient and energy content information is likely to be relatively reliable, should your study design rely on accurate information in relation to minor dietary components, for example the content of individual fatty acids, then we recommend that you arrange for independent testing of the foods you plan to use prior to the experiment. This information will enable the macronutrient/micronutrient intake of your dams to be determined accurately.

2.3 Rat Brain Atlas

A detailed rat brain atlas is critical for accurately identifying the key regions of the mesolimbic reward pathway in histological sections as well as isolating different brain regions for downstream applications. There are a number of high-quality atlases available, including some online versions which can be downloaded for free. The key criteria to consider when selecting the atlas include the level of detail provided, the type of staining used for images, and the distance (in μm) between adjacent images. In addition, it is often helpful for the atlas to include both sagittal and coronal sections. In studies of the reward pathway involving offspring younger than 4 weeks of age, you will need to acquire a brain atlas which is specific for the developing brain, since the reward pathway in rodents does not reach adult configuration until 21–28 days after birth [18, 19]. A good example of a neonatal rat brain atlas is “*A stereotaxic atlas of the developing rat brain*” by Sherwood and Timiras [20].

2.4 Equipment for Molecular and Histological Analyses

The impact of maternal high-fat/high-sugar diets on the reward pathways of the offspring can be studied at both the gene and protein level. For gene expression analyses, our approach has been to isolate the NAc and VTA from the whole brain at the time of postmortem (details below) and extract total RNA from each brain area. Following reverse transcription to cDNA, using standard approaches, the mRNA expression of target genes can then be determined using qRT-PCR. This obviously requires access to a

qRT-PCR machine optimized for these assays. The amount of tissue that is available is typically very limited (<100 mg for both the VTA and NAc), which makes it challenging to isolate both RNA and protein from the same sample. Consequently, additional animals may need to be sampled at each time point (preferably same-sex littermates) in order to measure both gene expression and protein abundance in the same experiment. Gene and protein expression can also be determined using section-based approaches, which have the advantage that (in combination with a detailed rat brain atlas) they enable the site of mRNA/protein expression for each of the gene to be visualized. If undertaking these studies you will require access to either a microtome (for fixed section) or a cryostat (for frozen sections). A number of different approaches exist for both immunohistochemistry and in situ hybridization, and it is important to check well in advance of tissue collection whether there are any specific requirements for the way tissues are collected, processed, and stored. If you plan to use radioactive probes for in situ hybridization studies, then the appropriate licenses and authorizations also need to be obtained.

3 Methods

3.1 Cafeteria Diet Feeding During Pregnancy and Lactation

After the female rats are acclimatized to the animal-housing facility (typically ~1 week after arrival) they can be assigned to either the control or junk food diet. Since maternal starting weight is likely to be a factor in determining the weight of the offspring at birth, it is preferable to ensure that the average weight of animals assigned the control and junk food groups does not differ at baseline. From this point, the control group is provided with *ad libitum* access to standard laboratory chow and the junk food group with *ad libitum* access to the cafeteria diet as described above. It is important to accurately monitor the actual food intake of the animals during this time, which can be done by subtracting the amount of each food type that is left uneaten in the cage from the amount initially provided. Since many of the individual components of the cafeteria diet are perishable, food intake in the cafeteria group should be monitored every 2 days and fresh food provided. The food intake of the control group should be monitored at the same interval, so that this is consistent between groups, but it is not necessary to provide fresh food on each occasion provided that still sufficient food is remaining. Rats will typically consume ~20–25 g of standard chow each day during pregnancy, and this amount will increase during lactation, so it is important to ensure that sufficient food is available throughout the experimental period.

After ~2 weeks on these diets, the females are monitored daily to determine their estrus cycle stage (using either vaginal smears or an estrus probe). We have achieved the greatest mating success by

placing 1–2 female rats with one male on the evening of diestrous/proestrous and leaving the pair(s) together for 24 h. The females are placed into the male's cage, rather than the other way around (*Note 1*). It is also worth noting here that there is an emerging body of evidence in support of the importance of paternal, as well as maternal, influences on developmental programming [21]. As a result, it is important that the same small group of males are used to mate females in all the different treatment groups in your experiment in order to exclude the possibility of confounding due to paternal effects.

While there are several methods used to assess mating success, we have routinely used the presence of sperm in the vaginal smears at the end of the 24-h mating period as an indication of successful mating, and this is then designated as gestation day 1. The control/junk food diet is then provided to the dams in the respective treatment groups *ad libitum* throughout pregnancy and lactation. Daily energy requirements of the animals increase during pregnancy, and particularly in lactation, so the amount provided will need to be increased during these times. It is important to continue monitoring food intake during pregnancy and lactation, and body weight of the dams should also be measured at least once per week across this period.

The gestation period in the rat is typically between 21 and 22 days, and we have not identified any effect of maternal cafeteria diets on gestation length in our previous studies. In the few days before pups are due, dams should be provided with nesting material (e.g., shredded newspaper). It is not normally necessary for a researcher to be present when the dam delivers her pups, unless you wish to document the exact time of delivery (for obtaining an accurate measure of gestation length). After delivery, the dam and her pups should be left undisturbed for at least 12 h after the pups are born, to allow for the dam to establish feeding and to minimize maternal stress, which can lead to cannibalism and failure to appropriately nurture her pups (*Note 2*). The total number of pups born and the number of pups stillborn or cannibalized should be recorded as soon as practicable after birth. Within 24 h of delivery, all pups should be sexed and individually weighed and litters culled to eight pups (four male and four female pups where possible). The practice standardizes the nutritional environment during the suckling period, since variations in litter size are known to impact on the dam's milk production and hence pup growth [22]. The pups remain with their mother until weaning (postnatal day 21).

3.2 Determination of Food Preferences in the Offspring

In our past experiments we have determined food preferences in the offspring of control- and junk food-fed dams at various postnatal ages; however the methods applied are essentially the same. In the “food preference” test, the offspring are provided with *ad libitum* access to both the standard rat chow and the same cafeteria diet as

detailed above. Food intake is determined every 2 days and fresh food provided at this time. It is important to ensure that the intake of each individual food item is recorded as accurately as possible. In order to provide a reliable measure, the food preference study should be conducted for at least a 2-week period.

It is preferable that the pups are housed individually during the food preference test. However, if this is not possible due to economic or logistic reasons, then the intake of each individual animal in the cage can be determined by dividing the total amount of each food type consumed by the number of pups per cage. Obviously, this does not take into account variations in food intake between individual animals, and will be less precise than measures taken on individual animals. If it is necessary to group house the offspring, then animals should be housed with same-sex littermates only as rats and mice are sexually mature from ~5 weeks of age.

Since food intake is expected to be related to body weight, i.e., heavier animals are expected to consume more than lighter animals, we would generally recommend that the calculated food/macronutrient intakes are normalized to the pup's bodyweight. This is particularly important in light of our previous findings that body weight is lower in offspring of cafeteria-fed dams compared to controls [13]. In cases where there are multiple pups per cage, the values can be normalized to the average weight of these pups.

The food intake data collected during the 2–3-week food preference test period can be used to calculate a number of parameters:

1. *The preference for each individual food type*—calculated by dividing the intake of each food type over the course of the study by the number of days on which food intake is recorded, and can provide information as to whether the preference for specific food types in the cafeteria group is correlated between the dam and her offspring.
2. *The preference for different macronutrients*—determined by multiplying the amount of each specific food consumed by the foods' macronutrient composition (obtained from the nutritional information provided by the manufacturer/feed company or compositional analysis conducted either in-house or by an external supplier). This enables the relative intake of fat, protein, and carbohydrate in the control and cafeteria groups to be determined, and hence differences in preference for the respective macronutrients to be determined.
3. *Overall energy intake*—the energy intake from each individual food is determined by multiplying the amount of each specific food consumed (in g or g/day) by its energy content (again, from the nutritional composition information provided or empirical assessment) in kJ/g. The energy intake from each food (including the standard chow) is then added together to

obtain an overall energy intake for each experimental animal. Separating the overall contribution of the junk foods vs. the standard chow to overall energy intake can provide a measure of relative preference for the junk food and control chow diets between the treatment groups.

4. *The macronutrient composition of the diet*—this is determined by multiplying the total of each macronutrient in g/day (determined as described above) by its energy content per gram (17 kJ/g for carbohydrate, 17 kJ/g for protein, and 37 kJ/g for fat). This figure can then be divided by the total energy intake of the animals to determine the percentage energy provided by fat, carbohydrate, and protein, respectively, in each of the treatment groups.

There are a number of ways that these data can be summarized and presented. We have typically examined the average intake of individual foods, macronutrients, and energy across the entire food preference period (i.e., total values for each divided by the number of days that food preferences are recorded), as well as shorter intervals. We have often noted that both the patterns of food intake in the offspring and the extent of differences between treatment groups can vary over time, and would therefore recommend examining the parameters above within individual weeks (or even days) of the food preference period before combining all information together to obtain an overall average.

3.3 Tissue Collection

Following humane euthanasia of the animal, a blood sample can be collected by cardiac puncture. This can be used to obtain plasma or serum for subsequent analysis of blood hormones and metabolites, and also reduces the pooling of blood in internal body cavities which can occur if the animal is decapitated after euthanasia. In order to get a more complete picture of the metabolic consequences of maternal cafeteria feeding on the offspring, we generally undertake a full postmortem collection of key internal organs and tissues, including the heart, liver, adrenal glands, kidneys, lungs, thymus, spleen, pancreas, and all dissectible fat depots for the determination of total fat mass and fat distribution.

Appropriate tissue collection and processing are important for ensuring the accuracy of the results of downstream assessments of the reward pathway. Careful removal of the intact brain is critical for obtaining high-quality histological sections and to ensure accurate isolation of specific brain regions. If other tissues are being collected from the animal, we would recommend that there be a dedicated team member responsible for processing the brain, to minimize the interval between euthanasia and brain retrieval/processing. The removal of the brain is easier if the animal is decapitated after euthanasia. In younger animals (up to ~6 weeks of age), this can be done using a sharp scalpel to make a deep cut

across the skin on the throat and through the spine. In older animals, a scalpel should still be used to cut the skin on the throat/neck; however, a pair of large dissection scissors is usually required to cut through the spine.

Once the head has been removed, the skin on the skull can be removed by using a scalpel blade to make a single incision from the front to the back of the head. Once this incision is made, the skin can be peeled back or cut, using tweezers and fine scissors, to reveal the skull (*Note 3*). Once the skull is visible, the excess muscle should be cut from around the base. Once this is done, use small curved scissors to carefully cut around the left side of the skull, starting at the base and going as far as possible towards the nose. Repeat this step for the right side. It should now be possible to carefully remove the top of the skull (*Note 4*). Using a spatula, gently remove the brain from the skull, taking particular care to detach the olfactory bulbs and optic tracts. The brain can then be weighed before being processed for analysis.

How the brain is processed from this point will depend on the subsequent experiments you are planning to perform. If you are planning to conduct histology/immunohistochemistry, perfusion fixing of the brain is recommended; however it is important to note that the animal cannot be decapitated if planning to be perfused, and it will not be possible to collect any other tissues from the animal for gene/protein analyses. As a result, we have generally chosen to instead place the brain (or one half of the brain after cutting laterally down the midsection) in a tissue cassette and fix in 4 % paraformaldehyde for 24 h before embedding the section in paraffin, and the quality of the sections has been more than sufficient for downstream applications. If the brain is cut into half prior to embedding, it is preferable to put the brain into the tissue cassette with the cut side facing down, since this will make it easier to cut sections after embedding. For frozen sections, the brain can be frozen on dry ice (the slower freezing of the tissue preserves tissue integrity better than snap freezing in liquid nitrogen) and the samples then transferred to an ultra-cold ($-80\text{ }^{\circ}\text{C}$) freezer for storage.

For most of our studies, we have isolated the two key regions of the mesolimbic reward pathway (VTA and NAc) from the whole brain at the time of tissue collection, and snap frozen and stored these regions for subsequent molecular analysis.

3.4 Isolating the VTA and NAc from the Whole Brain

The VTA and NAc are relatively small brain regions, and the isolation process is much easier if the brain is partially frozen. When the whole brain has been removed from the skull, it should be placed on a glass dish which has been pre-cooled and sitting on a bed of dry ice. Once the brain is partially frozen, to the point where it is solid enough to cut without distortion but not so hard that the scalpel has difficulty moving through it, then you can begin

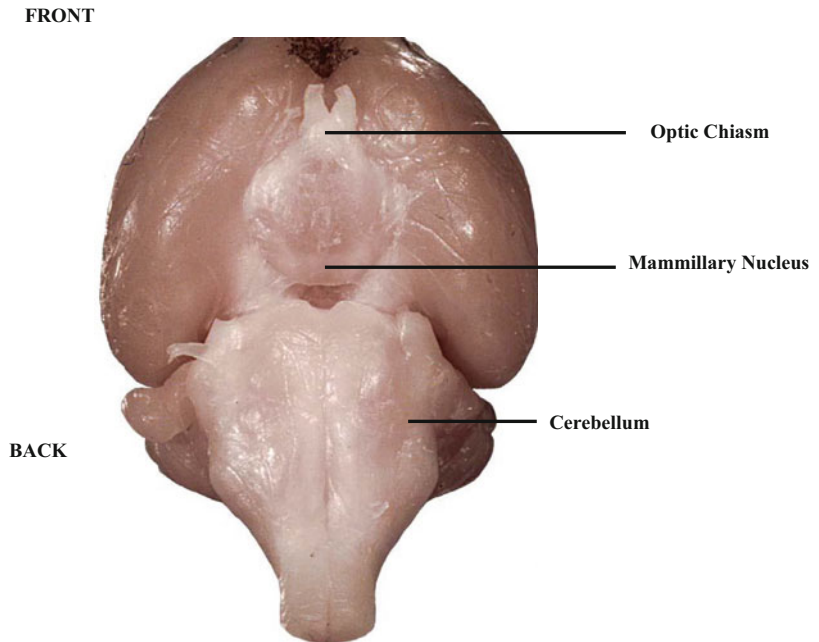


Fig. 2 Photograph of the ventral base of the brain indicating the key landmarks used for identifying starting points for dissection of the individual brain regions (NAc and VTA)

dissecting. First, the brain can be cut into half vertically down the midline; this way one half of the brain can be used for sectioning (fixed in 4 % paraformaldehyde) and the other for the isolation of the desired brain areas. *See Fig. 2* for a representation of key landmarks for start of cutting.

3.4.1 VTA Isolation

To isolate the VTA, make one incision 12 mm from the front of the brain (at the interpeduncular nucleus, bregma -6.84 mm) and a second incision 10 mm from the front of the brain (at the mammillary nucleus, bregma -4.96 mm). This will result in the isolation of a coronal section of 2 mm thickness. This section should then be placed face up on the glass dish and a cut made 1 mm from the base of the section to remove the substantia nigra. A further cut of 1 mm off the base of the section will isolate the VTA.

3.4.2 NAc Isolation

To isolate the NAc, first mark the section 5 mm back from the front of the brain at the optic chiasm (bregma -0.24), but do not cut all the way through. Next, make an incision 3 mm back from the front of the brain (bregma -1.68 mm) and cut through. Cut through the brain at the optic chiasm and you will again be left with a 2 mm coronal section. This section can then be placed face up and the rhinal fissure (RF) used as a landmark to locate and isolate the NAc, which is 1 mm above the RF (*Note 5*). This method has been used

Table 1
Primer sequences for μ , PENK, D1, D2, TH, and DAT

		Sequence	Size (bp)	Accession number	Working concentration
μ	F	5'-GTA GTG GGC CTC TTC GGA AAC-3'	75	NM_001038598	300 nM
	R	5'-GTT GGT GGC AGT CTT CAT TTT G-3'			
PENK	F	5'-GGA CTG CGC TAA ATG CAG CTA-3'	126	NM_017139	100 nM
	R	5'-GTG TGC ATG CCA GGA AGT TG-3'			
D1	F	5'-CGG GCT GCC AGC GGA GAG-3'	86	NM_012546	60 nM
	R	5'-TGC CCA GGA GAG TGG ACA GG-3'			
D2	F	5'-AGA CGA TGA GCC GCA GAA AG-3'	96	NM_012547	900 nM
	R	5'-GCA GCC AGC AGA TGA TGA AC-3'			
TH	F	5'-GCC CCC ACC TGG AGT ATT TTG-3'	83	NM_012740	300 nM
	R	5'-AGA CAC CCG ACG CAC AGA GC-3'			
DAT	F	5'-AGC TGG CTC TCG GAC AGT TC-3'	141	NM_012694	600 nM
	R	5'-GTG CCC ATG CGA TGA TGA C-3'			

in numerous publications in our laboratory [10, 13, 23, 24] and is based on a previously published work by Bell and colleagues [25] as well as the rat brain atlas [26].

While it is possible to isolate these regions from the whole brain after it is fully frozen, this is much more difficult and we therefore recommend that this be done at the time of tissue collection. Once the brain regions are isolated, standard extraction methods can be used to obtain RNA, DNA, and/or protein from these sections. In our previous studies we have measured gene expression of key components of the opioid/dopaminergic pathways in the VTA and NAc using real-time PCR in offspring of junk food-fed mothers as young as 3 weeks of age [10, 13]. The PCR primers that have been validated for use in our laboratory include the mu-opioid receptor, proenkephalin, D1 receptor, D2 receptor, tyrosine hydroxylase, and the dopamine active transporter (*see* Table 1 for primer sequences).

3.5 Identifying the VTA and NAc in Neonatal Rat Brain Sections

The use of downstream applications involving brain sections, such as in situ hybridization (for mRNA) and immunohistochemistry (protein), can be particularly informative for determining changes in development of brain pathways, since they make it possible to visualize precisely where genes/proteins are localized. Immunohistochemistry, in particular, makes it possible to examine the density of projections between brain regions which are known to be influenced by prenatal exposures [27, 28]. The use of section-based approaches is especially useful in neonatal offspring younger than 3 weeks as it is difficult to isolate specific nuclei such as the VTA

from the developing brain. Importantly, using frozen sections cut along the sagittal plane, it is possible to examine the gene/protein abundance of key opioid and dopaminergic genes in both the VTA and the NAc within the same section, and also visualize the projections between these two brain regions.

3.5.1 Sectioning Frozen Brain Tissue (Sagittal Sections)

If starting with a whole brain, begin by cutting the brain in half vertically along the midline. Then place the hemisected brain face down into a 15 mm × 15 mm × 5 mm cryostat mould and fill the mould with optimum cutting temperature (OCT) compound. This mould can then be attached to the chuck of the cryostat (using OCT) to facilitate the cutting of 15 µm sagittal sections which should be mounted onto Menzel-Glaser Super Frost Plus slides (25 × 75 × 1.0 mm, Menzel-Glaser, Braunschweig, Germany). The optimal cutting temperature for brains is between −10 and −15 °C. In our studies, we typically mount three individual sections on each slide and cut sections in blocks of eight slides. Thus, the first eight sections cut for an animal in each individual block are mounted on eight separate slides, the second set of eight sections are mounted consecutively below the first, and the third set of eight sections below this (Fig. 3). This approach means that each of the eight slides (each containing three individual sections) is roughly equivalent in relation to the brain regions they contain and can be used as replicates in subsequent experiments, thereby allowing for the measurement of up to eight different genes. It is recommended that you cut at least 120 sections per animal to ensure that the area of interest is included.

The mRNA expression/protein abundance of key genes within the reward pathway can vary markedly between different areas within the same brain region in the same experimental animal. As a result, selecting sections from equivalent regions in all animals is

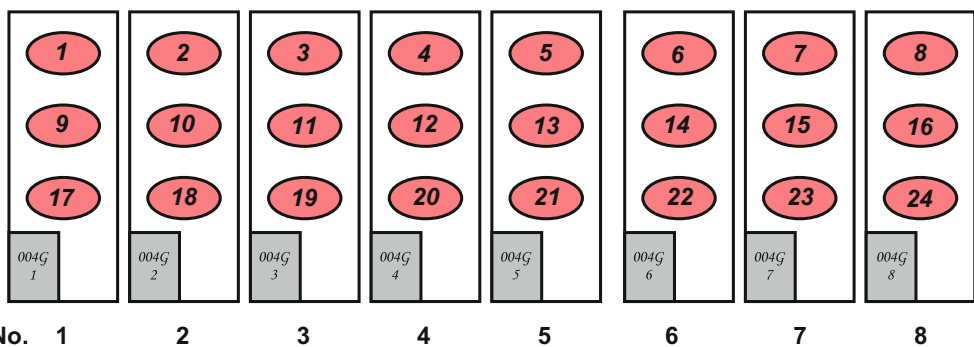


Fig. 3 Schematic diagram representing the approach used for mounting individual brain sections on slides for downstream in situ hybridization and immunohistological procedures. The numbers on the sections (1–24) indicate the order in which the sections are cut from the block. The subsequent 24 sections should be mounted on the next block of 8 slides

critical to achieving reliable and meaningful results. While it is possible to rely on stereotaxic coordinates and gross landmarks to some extent, we have found it more reliable to use stained sections, in conjunction with a rat brain atlas specific for the age group involved, to select sections. To do this, one slide can be selected at random from each block of eight slides and stained with either hemotoxylin and eosin or cresyl violet, using standard methods. In relation to the reward pathway, we have found the hippocampus and the anterior commissure to be the most reliable landmarks for selecting representative sections. In these sections, the NAc can be located by following along the line of the corpus callosum towards the base of the brain, whilst the VTA is located above the interpeduncular fossa.

3.5.2 Sectioning Fixed Brain Tissue (Sagittal Sections)

Fixed paraffin-embedded brain tissues should be cut at $\sim 4 \mu\text{m}$ using a microtome and mounted on Menzel-Glaser Super Frost Plus slides ($25 \times 75 \times 1.0 \text{ mm}$, Menzel-Glaser, Braunschweig, Germany). Paraffin sections are generally cut in “ribbons” rather than individually like frozen sections; however the same criteria for selecting appropriate tissue sections for subsequent analyses apply.

Methods for determining gene expression in the reward pathway by in situ hybridization and visualizing proteins by immunohistochemistry have been published by others, and will not be discussed further here. It is worth noting, however, that while in situ hybridization, in particular radioactive methods, can be used to provide a quantitative measure of the expression of key reward pathway components in specific brain regions/neurons (*Note 6*), immunohistochemistry is not truly quantitative.

3.6 Assessing Functional Effects on the Reward System

While changes in gene/protein expression in the reward pathway induced by maternal cafeteria diets can provide insights into the underlying mechanisms, it is also important to assess whether such changes have functional consequences. Following on from our finding of reduced mRNA expression of the mu-opioid receptor in the VTA in offspring of junk food dams at 3 weeks of age, we developed a protocol for assessing opioid sensitivity of the offspring in relation to feeding behavior. The activation of opioid signalling is associated with the drive to consume palatable foods, and opioid receptor blockade is typically associated with a reduced intake of these food types [29, 30]. We therefore reasoned that an opioid receptor blocker would be less effective at suppressing the intake of a palatable cafeteria diet in offspring of junk food-fed dams (who had lower opioid receptor levels) compared to the offspring of controls.

In order to do this, offspring of both control- and junk food-fed dams were given a daily intraperitoneal injection of either naloxone hydrochloride dihydrate (5 mg/kg) (*Note 7*) or an equivalent volume of saline for 10 days after weaning, and the intake of a

cafeteria diet was assessed over this period. Immediately prior to each injection it is important to weigh the pups to ensure accurate dosing. Following the administration of the naloxone/saline injections, the pups can be returned to their home cage and provided with free access to both the control and the cafeteria diet. The food intake of the rats should be recorded as described above at both 2 and 24 h post-injection. The 2-h time point is important, since naloxone (at the dose administered) only persists in brain at concentrations capable of inhibiting food intake for this time [31]. Comparing the specific food, macronutrient and energy intake of the offspring in the 2-h period following injection between the saline- and naloxone-treated offspring in the same maternal treatment group provides an indication of the extent to which naloxone can suppress palatable food intake (*Note 8*). Comparing the magnitude of this effect between the treatment groups enables you to determine if there are differences in the sensitivity of opioid signalling between offspring of control- and junk food-fed dams. Using this approach, we have previously demonstrated that offspring of junk food-fed dams are less sensitive to naloxone's suppressive effects on fat intake, supporting the hypothesis that the down-regulation of opioid receptors has functional consequences for the regulation of reward signalling [13].

There are now a large number of compounds which can be used to inhibit or activate specific signalling pathways within the mesolimbic reward system, which could be used to undertake similar experiments to our naloxone study, and thereby provide new information as to the relative role of different signalling systems within the reward pathway to the early life origins of food preference and reward function.

3.7 How Much Time Is Required?

The use of rodent models allows the long-term effects of a maternal junk food diet on the offspring to be determined within a relatively short time frame, since the gestation and lactation periods in rodents are much shorter than in larger mammals and humans and rodents are generally considered adults for the purposes of feeding behavior studies from about 3–4 months of age [32]. The total time that it will take to complete a study similar to those described in this chapter is heavily dependent on the number of experimental animals required (i.e., can all animals be included in a single cohort) and at what age the assessments in the offspring are conducted (i.e., neonate, juvenile, or adult). In determining the total time required for the experiment, it is also important to consider the number and complexity of any analyses you wish to do on the blood/tissues from the animals after collection. On the basis of our previous studies in Albino Wistar rats, an experiment which includes 20 dams and aims to determine food preferences and gene expression in the reward pathway using qRT-PCR at two

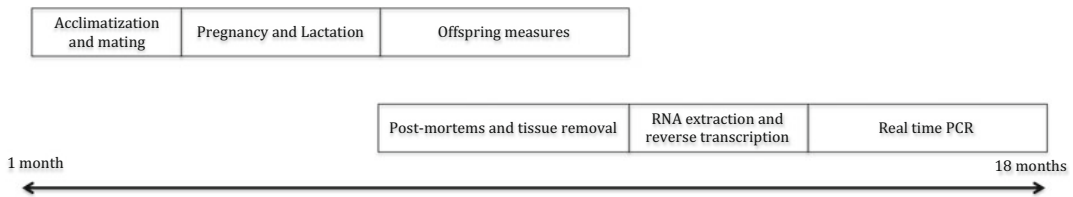


Fig. 4 Example timeline for an experiment. For a cohort of 20 dams, at least 18 months should be allocated for the completion of the study. Acclimatization and mating will take approximately a month, whilst pregnancy and lactation in the dams take 6 weeks; however as mating should be spaced out across 2 weeks, allow at least 8 weeks for this process. It should be noted that significant delays will arise if the dams have difficulty getting pregnant; in a cohort of 20 dams our experience suggests that 3–4 dams will either fail to get pregnant or not produce a viable litter; this should be considered when planning final animal numbers. Measuring offspring outcomes until adulthood will require an additional 3 months at minimum. The length of time required for molecular analysis depends on the number of tissues and offspring time points investigated; for a study in which we examined the VTA and NAc of male and female offspring at 3 and 12 weeks of age 9–12 months were needed between the collection of brain tissue and obtaining the final results

offspring time points (neonate and adult) in both sexes would require at least 18 months for full completion (Fig. 4) (*Note 9*).

3.8 Data Analysis

To analyze the data standard statistical analyses can be applied. Before commencing analysis, it is critical to ensure that the raw data have been carefully checked for errors, and that outlying values are investigated and either corrected, repeated, or excluded from the analysis. The Grubbs test is a free online tool that can be used to identify statistical outliers. Note that you should always retain a copy of the original spreadsheet/database which includes all outliers and provide a justification for exclusion of any values. The process of data cleaning is vital for minimizing the potential for erroneous results. Once data are cleaned and checked, they can be entered into an appropriate statistical package. We recommend that you check that the mean and standard deviation values which are obtained using the statistical package are the same as those in your original spreadsheet before proceeding with any data analysis—to ensure that all data are entered correctly and in the correct column.

The first step in the data analysis process is to determine whether the variables of interest are normally distributed. A number of tests of “normality” are available; however we strongly recommend reviewing the actual normality plots rather than relying only on the values that these tests provide.

Where there are only two groups for comparison (e.g., when comparing control- and junk food-fed dams), group differences can be determined using a Student’s unpaired *t*-test. In the case of offspring measures, we have consistently found marked differences in the effect of the maternal junk food diet between sexes. Therefore, all analyses of offspring outcomes should include sex, as well as treatment, as a factor, in a two-way ANOVA. In the case of assessing

the effect of naloxone treatment on food intake in the control and junk food offspring, a 3-way ANOVA, including maternal diet, sex, and injection group, should be used. In both of these cases, both main and interaction effects should be explored. For comparing longitudinal measures obtained in the same dam/pup, such as body weight gain and food intake, a repeated measures ANOVA, with treatment and offspring sex (if applicable), should be performed. In all analyses, the dam should be used as the unit of analysis, rather than the individual pup, and if there are multiple male or multiple female pups per litter assessed at a given time point, then a nested analysis will need to be performed in order to account for this.

4 Notes (Troubleshooting)

This section offers tips, advice, and modifications to the methods that are designed to help you achieve optimal results.

1. The fertility of the dams fed the cafeteria diet prior to mating is generally lower than controls, particularly if they have gained an excessive amount of weight prior to mating, and we have rarely achieved pregnancy success in dams who are >450 g in weight (average weight of control dams at the time of mating is ~300 g). To improve the success rate, ensure that the dams are mated with older, proven males that are larger in size. We also recommend limiting the length of time that the dams are maintained on the cafeteria diet prior to mating to 2 weeks or less to limit any negative impact of the diet on maternal metabolic/reproductive health before pregnancy. In addition to difficulties in conceiving, excess weight gain before mating makes it difficult to definitively establish if the dam is pregnant, since the increased weekly weight gain which occurs during pregnancy is often difficult to separate from the diet-induced weight increases. Therefore, it is particularly important that clear amounts of sperm are seen in post-mating vaginal smear of junk food-fed dams to be confident that they are pregnant.
2. Several studies have suggested that the junk food diet, particularly if it has a low micronutrient content, has the potential to lead to a heightened maternal stress response. For this reason, it is particularly important to take extra care to minimize other external forms of stress to ensure the continued viability of the pregnancy. Make certain that the dams are provided with sufficient nesting material (shredded newspaper, cardboard boxes, etc.), that the area in which they are housed is as quiet as possible, and that food intake is monitored (loss of appetite is a clear sign of stress). After the pups are born, we recommend that you wait for 24 h before disturbing the cage to weigh/cull the pups, to give extra time for maternal bonding. If there are

prolonged issues with pup cannibalization (a symptom of maternal stress), it might be useful to investigate the micronutrient content of the cafeteria diet provided and if there is a notable deficiency provide the dams with a limited amount of standard rodent chow which can assist in correcting micronutrient deficiencies and therefore improving pup viability.

3. When removing brain tissue from very young offspring (less than 2 weeks of age), partially freeze the whole head before cutting into the skull. This will harden the brain tissue and help minimize any accidental damage that may be caused when attempting to detach the skull. In these very young offspring a scalpel blade and forceps rather than scissors are the best tools for skull removal.
4. In older animals (more than 3 months of age), the skull becomes quite thick and difficult to cut. In these animals, it may be easier to use the scissors to make a small cut in the middle of the base of the skull and then use forceps to pull the two halves of the skull away from the head, rather than cut around the side of the skull as described in the methods.
5. When isolating the NAc, if the rhinal fissure cannot be located, instead cut 0.5 mm below the anterior commissure. The anterior commissure is a small oval shape approximately 1/3 of the way from the base of the coronal section.
6. Before using any in situ hybridization protocol, ensure that it has been designed for use on frozen sections and optimized for use with your specific samples. Many in situ hybridization protocols for fixed sections and some for frozen include a Proteinase K protein digestion step, to break cross-links and allow better probe binding. However, for fresh frozen sections cut at 15 μm as described in the methods, this step should either be omitted or replaced with a less stringent enzyme to maintain the integrity of the sections.
7. Naloxone hydrochloride dihydrate is a restricted drug, so when planning experiments ensure that sufficient time is allowed to obtain the appropriate licenses. The naloxone should be stored away from light and kept at 4 °C for the duration of the experiment. Prior to administration dissolve the naloxone in sterile saline at the appropriate concentration for the dose required.
8. When investigating the effects of naloxone on feeding behavior, it is best to administer the drug at the onset of the dark cycle, since this is the time when rodents naturally increase their food intake, making the appetite-suppressive effects of naloxone easier to detect. This is particularly important when observing the effects of naloxone in newly weaned offspring that only consume relatively small amounts of food.

9. The length of time a study takes to complete naturally depends on the specific experimental outcomes being investigated. However, when planning experiments involving animal models it is important to note that they will often take longer than originally planned. Common delays that are faced include the need to wait for approval from an ethics committee, difficulty in getting the dams pregnant, litters that are too small to be included in the study, and delays in acquiring reagents for molecular analysis.

5 Conclusion

In the context of the current epidemic of obesity and metabolic disease, it has become important to understand the biological mechanisms, which can increase an individual's susceptibility to overeating and obesity. There is compelling evidence from clinical, epidemiological, and experimental animal studies that the origins of obesity can begin very early in life, and that the nutritional environment an individual is exposed to before birth and in early infancy is a key determinant of their later metabolic health. In this chapter, we have described methods and approaches which can be applied to determine the impact of perinatal exposure to highly palatable "junk food" diets on food preferences and the reward pathway in the offspring. While we are beginning to understand more about the importance of perinatal nutrition in determining subsequent food preferences, and in directing the development of the reward pathway, more studies in this area are required to improve our understanding of the role of specific components of the reward pathway in these programming effects and thus identifying potential targets for intervention. The methods described in this chapter can be modified to focus on the role of specific components of the mesolimbic reward system on these programming effects, e.g., by the use of targeted antagonists or agonists, or to begin to test to the efficacy of nutritional/pharmacological interventions to reverse these effects. By understanding the effect of a maternal junk food diet on reward pathway development in the offspring and designing targeted interventions, we may be able to prevent the continuation of what has become an intergenerational cycle of obesity.

References

1. Chen L, Magliano DJ, Zimmet PZ (2011) The worldwide epidemiology of type 2 diabetes mellitus-present and future perspectives. *Nat Rev Endocrinol* 8:228–236
2. Putnam J, Allshouse J, Kantor LS (2002) U.S. Per capita food supply trends: more calories, refined carbohydrates, and fats. *Food Rev* 25:2
3. Adinoff B (2004) Neurobiologic processes in drug reward and addiction. *Harv Rev Psychiatry* 12:305–320
4. Saper CB, Chou TC, Elmquist JK (2002) The need to feed: homeostatic and hedonic control of eating. *Neuron* 36:199–211
5. Zheng H et al (2009) Appetite control and energy balance regulation in the modern

- world: reward-driven brain overrides repletion signals. *Int J Obes (Lond)* 33:S8–S13
6. Berridge KC (1996) Food reward: brain substrates of wanting and liking. *Neurosci Biobehav Rev* 20:1–25
 7. Chang GQ et al (2008) Maternal high-fat diet and fetal programming: increased proliferation of hypothalamic peptide-producing neurons that increase risk for overeating and obesity. *J Neurosci* 28:12107–12119
 8. Kirk SL et al (2009) Maternal obesity induced by diet in rats permanently influences central processes regulating food intake in offspring. *PLoS One* 4:e5870
 9. Bayol SA, Farrington SJ, Stickland NC (2007) A maternal ‘junk food’ diet in pregnancy and lactation promotes an exacerbated taste for ‘junk food’ and a greater propensity for obesity in rat offspring. *Br J Nutr* 98:843–851
 10. Ong ZY, Muhlhausler BS (2011) Maternal “junk-food” feeding of rat dams alters food choices and development of the mesolimbic reward pathway in the offspring. *FASEB J* 25:2167–2179
 11. Teegarden SL, Scotta AN, Bale TL (2009) Early life exposure to a high fat diet promotes long-term changes in dietary preferences and central reward signaling. *Neuroscience* 162:924–932
 12. Vucetic Z et al (2010) Maternal high-fat diet alters methylation and gene expression of dopamine and opioid-related genes. *Endocrinology* 151:4756–4764
 13. Gugusheff JR, Ong ZY, Muhlhausler BS (2013) A maternal “junk-food” diet reduces sensitivity to the opioid antagonist naloxone in offspring postweaning. *FASEB J* 27:1275–1284
 14. Bayol SA et al (2008) Offspring from mothers fed a ‘junk food’ diet in pregnancy and lactation exhibit exacerbated adiposity that is more pronounced in females. *J Physiol* 586:3219–3230
 15. Wright TM et al (2011) Exposure to maternal consumption of cafeteria diet during the lactation period programmes feeding behaviour in the rat. *Int J Dev Neurosci* 29:785–793
 16. NHMRC (2013) Australian code for the care and use of animals for scientific purposes, 8th edition. National Health and Medical Research Council of Australia, Canberra, ACT
 17. Sampey BP et al (2011) Cafeteria diet is a robust model of human metabolic syndrome with liver and adipose inflammation: comparison to high-fat diet. *Obesity* 19:1109–1117
 18. McDowell J, Kitchen I (1987) Development of opioid systems: peptides, receptors and pharmacology. *Brain Res* 434:397–421
 19. Antonopoulou J et al (2002) Postnatal development of the dopaminergic system of the striatum in the rat. *Neuroscience* 110:245–256
 20. Sherwood NM, Timiras PS (1970) A stereotaxic atlas of the developing rat brain. University of California Press, Berkeley, CA
 21. Ng S-F et al (2010) Chronic high-fat diet in fathers programs [bgr]-cell dysfunction in female rat offspring. *Nature* 467:963–966
 22. Plagemann A et al (1999) Increased number of galanin-neurons in the paraventricular hypothalamic nucleus of neonatally overfed weanling rats. *Brain Res* 818:160–163
 23. Gugusheff JR, Ong ZY, Muhlhausler BS (2014) Naloxone treatment alters gene expression in the mesolimbic reward system in ‘junk food’ exposed offspring in a sex-specific manner but does not affect food preferences in adulthood. *Physiol Behav* 133:14–21
 24. Ong ZY, Muhlhausler BS (2013) Consuming a low-fat diet from weaning to adulthood reverses the programming of food preferences in male, but not female, offspring of ‘junk food’-fed rat dams. *Acta Physiol (Oxf)* 210:127–141
 25. Bell RL et al (2006) Protein expression changes in the nucleus accumbens and amygdala of inbred alcohol-preferring rats given either continuous or scheduled access to ethanol. *Alcohol* 40:3–17
 26. Paxinos G, Watson C (2012) The rat brain in stereotaxic coordinates, 7th edn. Elsevier Academic Press, San Diego, CA
 27. Bouret SG, Draper SJ, Simerly RB (2004) Trophic action of leptin on hypothalamic neurons that regulate feeding. *Science* 304:108–110
 28. Bouret SG, Draper SJ, Simerly RB (2004) Formation of projection pathways from the arcuate nucleus of the hypothalamus to hypothalamic regions implicated in the neural control of feeding behavior in mice. *J Neurosci* 24:2797–2805
 29. Olszewski PK, Levine AS (2007) Central opioids and consumption of sweet tastants: when reward outweighs homeostasis. *Physiol Behav* 91:506–512
 30. Zhang M, Gosnell BA, Kelley AE (1998) Intake of high-fat food is selectively enhanced by muopioid receptor stimulation within the nucleus accumbens. *J Pharm Exp Ther* 285:908–914
 31. Marks-Kaufman R, Kanarek RB (1981) Modifications of nutrient selection induced by naloxone in rats. *Psychopharmacology* 74:321–324
 32. Quinn R (2005) Comparing rat’s to human’s age: how old is my rat in people years? *Nutrition* 21:775–777

Perinatal and Postnatal Determinants of Brain Development: Recent Studies and Methodological Advances

Sarah J. Spencer and Trisha A. Jenkins

Abstract

Perinatal diet is an important factor in programming brain development and susceptibility to obesity. There are currently several elegant and simple prenatal and postnatal animal models in use to mimic the effects of early life overfeeding and to study its impact on brain and metabolic development. In this chapter we will discuss the background to some of these models, with a specific focus on manipulating rodent litter sizes to alter the early life nutritional environment.

Key words Diet, Fostering, Hypothalamic–pituitary–adrenal axis, Lipopolysaccharide, Litter size, Obesity, Perinatal programming, Suckling

1 Introduction

1.1 The Importance of Perinatal Diet in Programming Obesity, Metabolic Dysfunction, and Appetite in the Offspring

Obesity has become epidemic in our society and, as such, obesity in parents at conception and throughout pregnancy has become very common. Around 60 % of women of childbearing age are classified as overweight or obese in the US and Australia [1, 2]. In addition to the effects of diet and obesity at conception and during pregnancy, a baby may also have to contend with an inappropriate diet in the days, weeks, and months following birth. Diet during these vulnerable early programming stages of life can have significant influences on feeding, satiety, and metabolic circuitry in the brain, but also on brain development in general, including on cognitive function [3, 4].

The first dietary influence to potentially affect baby's brain development is an indirect one; the effect of paternal diet on the sperm. There is currently limited evidence for the extent of this effect on brain development, but we do know paternal obesity in humans influences sperm concentration and motility and can damage sperm DNA [5]. When other factors are controlled for, paternal obesity at conception leads to increased adiposity in daughters (but not sons) when they reach adolescence [6]. In rat models, paternal

obesity is linked to pancreatic beta-cell dysfunction and a predisposition to diabetes, with, again, these effects being manifest in female but not male offspring [7].

Perhaps more intuitively obvious is the maternal effect on the offspring. Maternal metabolic state during pregnancy can have pronounced effects on offspring brain development. Overweight or obese mothers are significantly more likely to have or develop type 2 or gestational diabetes and these conditions predispose the baby to abnormal pancreatic development, insulin resistance, diabetes, and obesity [8–11]. Even in the absence of diabetes, a “junk food” diet, one high in fat, sugar, and salt, during pregnancy can also influence a baby’s brain development [12–14]. For instance, a maternal diet high in fat is linked with changes to central reward processing, altering the way the rewarding aspects of food are perceived throughout life, leading to a preference for fatty, sugary foods [3]. Cognitive function in general can be altered in the offspring of obese or high-fat-diet-fed mothers, with these children having poorer psychomotor and cognitive development scores than children from lean mothers [4]. These dietary influences from both the father and mother can occur in the absence of or in addition to any specific genetic effects. Thus, experimental animal models, where the genetic variable is removed, consistently reveal an important early life dietary influence on brain development.

Postnatally, a baby’s vulnerability to dietary influences continues. Obese and overweight babies and children are significantly more likely to grow to be obese and overweight adults [15, 16]. There are a variety of factors that contribute to this. Potentially, the most important dietary contribution to a baby’s brain development is the speed with which it gains weight after birth [17–19]. Particularly in, but not restricted to, small for gestational age babies, intensive feeding immediately postnatally is important in ensuring appropriate brain and lung development, but can also lead to increased risk of obesity and its associated central dysfunction [17–19]. Stettler and colleagues have found for every 100 g a baby gains in weight in the week after birth, its chances of developing obesity as an adult are increased by 28 % [20]. Factors influencing weight gain include the baby’s general health as well as the composition of its diet. Maternal diet can influence the composition and amount of breast milk available. For instance, there are indications that a maternal diet high in conjugated linoleic acid isomers (found in organic meats and dairy) may reduce adiposity and the likelihood of obesity in the baby. At least, conjugated linoleic acid isomers in diet can reduce fat accrual in adults [21, 22] and can also be passed on to the baby through the breast milk [23]. Maternal breast milk omega-3 levels are even significantly correlated with better performance in mathematics tests in the offspring [24]. Similarly, baby formula content may also be important in programming a baby’s development throughout life.

High-protein, but not low-protein formulas are associated with obesity long-term [25], and formulas fortified with long-chain polyunsaturated fatty acids are associated with faster processing speeds in cognitive tests later in life than standard formulas [26]. Feeding frequency and the timing of introduction of solid food may also influence a baby's brain development and its propensity to develop obesity [27].

While there are indications that factors such as breast versus formula-feeding and timing of solid food introduction in humans are very important in a baby's development, research in this area is clouded by the huge number of additional variables inherent in any human study of this kind. Socioeconomic and other environmental factors, parental age, definitions of exclusive breast-feeding, breast versus bottle versus different types of formula-feeding, and social stigma encouraging reporting errors all make it difficult to draw solid conclusions from the data [28]. Animal models are therefore essential for us to delineate the effects of early life overfeeding as well as the mechanisms for these changes.

2 Models of Perinatal Overfeeding

Several animal models of perinatal overfeeding are in routine use to study the programming influence of diet on brain and metabolic development [29–33]. These include:

1. Paternal high fat diet prior to and/or at conception.
2. Maternal high fat diet prior to and/or at conception and/or during pregnancy.
3. In utero growth restriction.
4. Maternal high fat/high protein diet during lactation.
5. “Pup-in-a-cup” artificial rearing.
6. Sucking pups in small litters.
7. Combinations of any of the above.

2.1 *Equating Developmental Ages and Stages*

It is difficult and controversial to accurately equate developmental stages between species. However, higher order mammals do undergo significant development of brain pathways contributing to feeding regulation, satiety, and metabolism in the third trimester of gestation. The rodent reaches a similar stage of development of these pathways in the first and second week of life. For instance, the projections from the arcuate nucleus to the paraventricular nucleus of the hypothalamus (PVN) are essential for body weight regulation and these are functional in primates and other higher order mammals but immature in the rodent at birth [34]. It is thus

generally considered that late gestation and the early postnatal period in the rodent are roughly equivalent to the third trimester of pregnancy in the human, particularly with regard to metabolic systems. For this reason, we will concentrate on postnatal rodent models of early life dietary intervention in this chapter. In particular, we will discuss the impact of suckling rodent pups in small litters to induce neonatal overfeeding.

2.2 Postnatal Models of Overfeeding; Manipulations in Maternal and Pup Diet

Alteration of the maternal diet is a well-recognized technique of changing the nutritional content of milk for lactating rodents. Nutrients can be directly administered to the mother or added to the maternal diet during pregnancy and/or pre-weaning [35]. A well-established model of postnatal overfeeding involves feeding the mother a high fat diet. This causes excessive weight gain in the pup, which is, considering variability due to diet composition and strain, generally maintained until adulthood [36].

Within the literature many diets have been investigated, ranging from chow altered to contain increased amounts of fats and/or carbohydrates to the high-fatcafeteria-style diet [37]. Each has their own advantages: the chow diet can be made to contain varying concentrations and types of fats and sugars so consumption of different components is easily calculated; while the cafeteria-style diet, which is the feeding of “human” food, such as pies and cakes, to rodents, is seen to be much more palatable and perhaps more similar to the human condition, but absolute amounts of ingestion of the various elements are sometimes difficult to assess [38].

The effect of maternal obesity on the offspring has been investigated from gestation through to lactation. Offspring from obese mothers gain more weight and exhibit increased adiposity, glucose intolerance, and increases in blood pressure and other metabolic markers, than those from lean dams [39, 40]. Central disturbances in the development of hypothalamic feeding circuits are also apparent [41]. Moreover, this excess weight gain and metabolic disturbance is carried through to adulthood, and is independent of post-weaning diet. Meanwhile, pups born to lean mothers then nursed by obese dams exhibit increases in weight and plasma triglyceride levels compared to pups born and nursed by lean mothers [42]. This example demonstrates the complicated nature of maternal dietary influences, that is maternal obesity at both pregnancy and the time of nursing have influences on programming obesity and metabolic dysfunction in the offspring.

The rodent pup-in-a-cup artificial rearing model allows the researcher to have complete control of dietary content and quantity in the immediate postnatal period. This neonatal overfeeding procedure allows the lipid, protein, and carbohydrate composition of milk to be manipulated by artificially rearing pups in foam cups in a temperature-controlled bath and feeding via tubes implanted directly into the gut [43, 44]. Studies have been performed from

neonatal day one, though results should be considered in the context of the underlying influence of loss of normal maternal and sibling interactions during pre-weaning, absence of ano-genital licking to stimulate digestion, and some suggestion of reduced brain growth [45].

3 Postnatal Models of Overfeeding; Litter Size Manipulation to Induce Overfeeding

An alternative well-accepted rodent model to mimic human overfeeding during the perinatal period is to manipulate the litter size in which the pups are suckled. Pups are suckled in either small litters, where they have greater access to their mother's milk, or in standardized control litters. This type of overfeeding during the early postnatal period leads to increased weight gain and body fat in early life that persists throughout the juvenile period and into adulthood [46–48].

3.1 *Materials and Methods*

Suckling rat (or mouse) pups in small litters is an extremely simple and effective method of inducing changes in neonatal diet. It will be discussed here for Wistar rats but can be adapted for use in mice and other animals. It requires:

1. At least three time-mated pregnant dams (scheduled to give birth on the same day).
2. Spare cages labeled with the dam's identification code.
3. Scales for weighing.
 - (a) Observe all dams periodically on the date of birth and commence litter size manipulation 2–3 h after birthing is complete. This timing avoids additional pups accidentally being added to the litter after manipulation and limits stress placed on the dam during birth.
 - (b) Gently remove all pups from their nests and place them in whole-litter groups in labeled clean cages. Ensure pups remain together in a bunch so they retain as much heat as possible. At this point it is useful to track numbers of pups born and numbers stillborn.
 - (c) Randomly pick one male and one female from litters other than the natural litter of the foster-dam until the desired litter size is reached. We use small litters of 4 and control litters of 12 [46–49]. We also use this model to induce neonatal underfeeding by creating large litters of 20 pups [49–51].

- (d) Weigh the pups in a group and return them to the nest, taking care to disturb the nest site as little as possible. Excess pups should be euthanized in a different room.
- (e) Leave the dams and pups undisturbed for as long as possible before cleaning cages or otherwise disturbing them. Cage cleaning, feeding, and all other procedures should be standardized between cages. Pups are generally weaned into same-sex littermate pairs at postnatal day (P)21.

While these litter manipulations are designed to manipulate the amount of food the pup has access to, they are well within the normal physiological range. Wistar rats give birth to an average of 12–15 pups but are known to regularly give birth and raise as many as 18 or as few as 2.

3.2 Troubleshooting

Pup temperature during manipulation: As young neonates, pups behaviorally thermoregulate in the nest, circulating closer to the dam and the centre of the nest to stay warm [52]. Prolonged periods away from the dam lead to a significant drop in body temperature that should be avoided as it potentially contributes to pup rejection by the foster-dam [53]. Keep the pups together as a birth-litter during manipulation and conduct the procedure as quickly as possible to avoid excessive cooling. We typically manipulate only three to six litters at one time to reduce the time the pups are away from the dam to approximately 5 min. If excessive cooling is anticipated and unavoidable, an incubator or heating lamp can be used. Heating blankets are not recommended due to the possibility the pups may overheat.

Pup attrition: Unanticipated pup death occasionally occurs, even in untouched litters, and this can be due to a variety of factors. Occasionally pups are born with congenital abnormalities that mean they are either not viable for long after birth or are less competitive for food and maternal attention. When selecting pups for reallocation, take care to avoid those that are weaker, smaller, or paler in color than their siblings to minimize the chances of selecting an individual with an existing abnormality.

Severe stress can, in some cases, induce the dams to kill and cannibalize healthy pups [54, 55]. One should take extreme care when removing pups from the nest and introducing the new pups to minimize contact with the dam and to avoid disturbing her nest-site. Cages should be left unchanged for as long as feasible after birth/litter manipulation. This will depend upon animal facility policy, cage size, cage ventilation, etc., but we have found careful cage changes 3 days after birth do not adversely affect the dams or their litters.

Fostering issues: Fostering eliminates pregnancy-related variables from the model. Wistar rats are very good foster parents [53, 56]

and we have seen no cases of refusal to care for a new litter. We have also found no differences in crude measurements, including weight and fat pads, in litters that were not fostered but were culled to small size ([46], unpublished). There is some suggestion foster mothers may give more attention to their own pups in a mixed litter or otherwise treat foster-pups differently [57]. For this reason, we ensure no dam receives any of her naturally born pups.

Greater difficulties with fostering may present with other rat strains and with mice. One can minimize rejection by taking great care to not stress the dam. It has also been suggested that rubbing bedding material onto the experimenter's gloves and onto the new pups to disguise foreign smells assists with acceptance [53].

3.3 Comments and Considerations on the Model

Gender balance: The size and gender composition of the litters will depend upon the experimental protocol, but for a standard model to induce overfeeding during the neonatal period we ensure a 50-50 balance of males and females within a litter. There is some evidence dams offer differences in attention to males and females [58, 59] and, although it might be desirable to generate all-male litters when all-male studies are being designed for, we chose to eliminate this variable as it is not possible to do this for small and control litters equally.

Litter representation for statistical analysis: Typically when a whole-litter manipulation is conducted, that litter is then regarded as an “*n*” of one for the purposes of group composition and statistical analysis [60]. In this regard, one also needs to consider the ethically appropriate use of animals in research and how to avoid maximizing information obtained from each animal. We can also consider all our pups are fostered and are therefore not from the same pregnancy. For our experiments we typically take one to two males and one to two females from each litter for allocation to each experimental group, thereby controlling for mothering effects but maximizing appropriate animal use.

Maternal attention and other non-nutritive elements to the model: This model is certainly effective at increasing the food available to the pups suckled in the small litters. Previous studies have shown rats suckled in small litters receive more milk and milk that is higher in fat than those from control litters, despite the dam reducing her milk production [29]. We should note, however, that this model has elements independent of food intake that could also contribute to weight gain and brain development.

Rats raised in small litters are, for instance, given more opportunities for interaction with their dam [29]. Maternal attention is an important component of an animal's development that can permanently influence brain function long-term. For instance, seminal studies by Meaney and colleagues have shown that pups that receive more licking, grooming, and intensive (arched back)

nursing during their suckling period have hyperactive hypothalamic–pituitary–adrenal (HPA) axes [61–64]. These effects of maternal care are likely to be due, at least in part, to the tactile stimulation inducing thyroid hormone and serotonin responses that stimulate nerve growth factor inducible factor A expression, which increases histone acetylation of the glucocorticoid receptor [65]. Increased maternal attention therefore leads (in otherwise untreated pups) to comparatively enhanced glucocorticoid receptor transcription, more efficient glucocorticoid negative feedback onto the HPA axis, and attenuated HPA axis responses to stress [65, 66]. Although there is no question pups raised in small litters receive more maternal attention, it is clear that this is not sufficient to override the nutritive and other effects of the model with respect to its effects on HPA axis function. Thus, neonatally overfed rats have exacerbated, not attenuated, HPA axis responses to stress and immune challenge [46, 47, 67]. How the overfeeding is able to override the long-term effects of maternal care in this way is not known.

Other factors that should be considered with the model are the potential for differences in body temperature regulation in a small litter with respect to a control one. In addition, neonatally overfed pups will receive a diet that is higher in several nutritional elements, not just fat. For instance, they will also receive proportionally more leptin, which can act as a trophic factor in the brain in early life [68–71].

3.4 Typical/ Anticipated Results

Neonatal overfeeding from being suckled in a small litter leads to accelerated growth and weight gain that persists into early adulthood. Thus rats from small litters weigh significantly more as early as P7 and maintain this elevated weight into adulthood of 12 [46–49]. Those from large litters have the opposite phenotype [49–51] (Fig. 1).

Animal models of early life overfeeding have shown us postnatal diet can be extremely important in programming brain development. For instance, rats raised in small litters, where they have greater access to their dam's milk than those in control litters do, have accelerated maturation of their HPA axes. In this case, the excess milk, fat, and other nutrients leads to an adult-like profile of adrenocorticotrophic hormone and corticosterone in small litter rats, as well as increases in PVN glucocorticoid receptor mRNA [67]. They also respond with a greater hormonal and central response to stress than controls do [47, 49]. It is likely that this change in HPA axis maturation contributes long-term to the way the animal responds to stress and immune challenge. Thus, neonatally overfed adult female rats have exacerbated neuronal activation in the PVN, the apex of the HPA axis, in response to psychological stress compared with control rats [46]. Neonatally overfed male

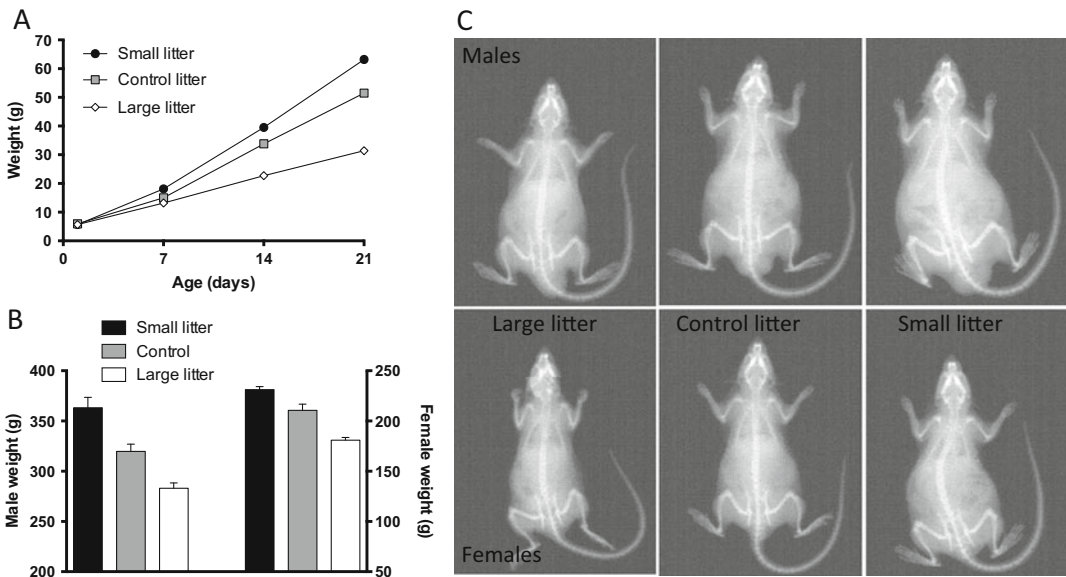


Fig. 1 Representative data showing how litter size affects long-term body weight. **(a)** Pre-weaning weights. **(b)** Adult weights. **(c)** Adult dual-energy X-ray absorptiometry scans showing fat mass. Similar data have been published previously [46–51]

and female adult rats have a similar exacerbated PVN response to an immune challenge with the bacterial endotoxin lipopolysaccharide (LPS) [47]. This latter is likely to be a reflection of slower glucocorticoid negative feedback, culminating in less suppression of the HPA axis response to the immune challenge and also less, or slower glucocorticoid-mediated suppression of nuclear factor κ B-dependent cytokine transcription. In short, these changes mean neonatally overfed animals have dysregulated central and peripheral responses to stress and immune challenge. Again, neonatally underfed (large litter) rats have the opposite responses [50, 51].

Neonatal overfeeding in animal models may also contribute to aberrant development of brain pathways regulating feeding, satiety, and metabolism. In the rat and mouse, connectivity between various parts of the hypothalamus occurs at critical stages of development [68–71]. The growth of these connections is stimulated by a surge in circulating leptin. In early life, leptin is obtained principally from the diet. Excessive leptin, as occurs with neonatal overfeeding by raising rats in small litters [48], can potentially signal this hypothalamic connectivity to start developing too soon, or to overdevelop. In either case, the result is a potential impairment in satiety signaling.

This potential for central changes in satiety signaling in neonatally overfed animals is reflected in changes in feeding, and metabolism in these rats. Thus, many groups have seen neonatal overfeeding leads to hyperphagia [72–75]. We have also seen changes in

metabolism [48], and it has been suggested alterations in brown adipose tissue thermogenesis contribute to the phenotype [76].

4 Conclusion

Obesity has become a significant problem in the developing world, and the impact of early life diet on how our children develop is an important factor to explore. There are now several simple and replicable rodent models available that allow us to investigate this question. Litter size manipulation is one of these. This relatively non-invasive technique to alter early life nutrition, as outlined here, allows us to interrogate the neurological changes that occur with early life diet and, ultimately, test strategies to ameliorate the effects of an overweight/obese phenotype initiated in early life.

Acknowledgements

This work was supported by a Discovery Project Grant from the Australian Research Council (ARC) to SJS (DP130100508). SJS is an ARC Future Fellow (FT110100084) and an RMIT University VC Senior Research Fellow.

References

1. Flegal KM, Carroll MD, Ogden CL, Johnson CL (2002) Prevalence and trends in obesity among US adults, 1999–2000. *JAMA* 288 (14):1723–1727
2. Colagiuri S, Lee CM, Colagiuri R, Magliano D, Shaw JE, Zimmet PZ et al (2010) The cost of overweight and obesity in Australia. *Med J Aust* 192(5):260–264
3. Ong ZY, Muhlhausler BS (2011) Maternal “junk-food” feeding of rat dams alters food choices and development of the mesolimbic reward pathway in the offspring. *FASEB J* 25 (7):2167–2179
4. Casas M, Chatzi L, Carsin AE, Amiano P, Guxens M, Kogevinas M et al (2013) Maternal pre-pregnancy overweight and obesity, and child neuropsychological development: two Southern European birth cohort studies. *Int J Epidemiol* 42(2):506–517
5. Kasturi SS, Tannir J, Brannigan RE (2008) The metabolic syndrome and male infertility. *J Androl* 29(3):251–259
6. Figueroa-Colon R, Arani RB, Goran MI, Weinsier RL (2000) Paternal body fat is a longitudinal predictor of changes in body fat in premenarcheal girls. *Am J Clin Nutr* 71 (3):829–834
7. Ng SF, Lin RC, Laybutt DR, Barres R, Owens JA, Morris MJ (2010) Chronic high-fat diet in fathers programs beta-cell dysfunction in female rat offspring. *Nature* 467 (7318):963–966
8. Aerts L, Holemans K, Van Assche FA (1990) Maternal diabetes during pregnancy: consequences for the offspring. *Diabetes Metab Rev* 6(3):147–167
9. Silverman BL, Metzger BE, Cho NH, Loeb CA (1995) Impaired glucose tolerance in adolescent offspring of diabetic mothers. Relationship to fetal hyperinsulinism. *Diabetes Care* 18 (5):611–617
10. Plagemann A, Harder T, Kohlhoff R, Rohde W, Dorner G (1997) Glucose tolerance and insulin secretion in children of mothers with pregestational IDDM or gestational diabetes. *Diabetologia* 40(9):1094–1100
11. Weiss PA, Scholz HS, Haas J, Tamussino KF, Seissler J, Borkenstein MH (2000) Long-term-follow-up of infants of mothers with type 1 diabetes: evidence for hereditary and nonhereditary transmission of diabetes and precursors. *Diabetes Care* 23(7):905–911
12. Albuquerque KT, Sardinha FL, Telles MM, Watanabe RL, Nascimento CM, Tavares do

- Carmo MG et al (2006) Intake of trans fatty acid-rich hydrogenated fat during pregnancy and lactation inhibits the hypophagic effect of central insulin in the adult offspring. *Nutrition* 22(7–8):820–829
13. Srinivasan M, Katewa SD, Palaniyappan A, Pandya JD, Patel MS (2006) Maternal high-fat diet consumption results in fetal malprogramming predisposing to the onset of metabolic syndrome-like phenotype in adulthood. *Am J Physiol Endocrinol Metab* 291(4):E792–E799
 14. Ashino NG, Saito KN, Souza FD, Nakutz FS, Roman EA, Velloso LA et al (2012) Maternal high-fat feeding through pregnancy and lactation predisposes mouse offspring to molecular insulin resistance and fatty liver. *J Nutr Biochem* 23(4):341–348
 15. Whitaker RC, Wright JA, Pepe MS, Seidel KD, Dietz WH (1997) Predicting obesity in young adulthood from childhood and parental obesity. *N Engl J Med* 337(13):869–873
 16. Biro FM, Wien M (2010) Childhood obesity and adult morbidities. *Am J Clin Nutr* 91(5):1499S–1505S
 17. Lucas A (1998) Programming by early nutrition: an experimental approach. *J Nutr* 128 (Suppl 2):406S
 18. Gluckman PD, Hanson MA (2004) Living with the past: evolution, development, and patterns of disease. *Science* 305(5691):1733–1736
 19. Singhal A, Kennedy K, Lanigan J, Fewtrell M, Cole TJ, Stephenson T et al (2010) Nutrition in infancy and long-term risk of obesity: evidence from 2 randomized controlled trials. *Am J Clin Nutr* 92(5):1133–1144
 20. Stettler N, Stallings VA, Troxel AB, Zhao J, Schinnar R, Nelson SE et al (2005) Weight gain in the first week of life and overweight in adulthood: a cohort study of European American subjects fed infant formula. *Circulation* 111(15):1897–1903
 21. Park Y, Albright KJ, Storkson JM, Liu W, Pariza MW (2007) Conjugated linoleic acid (CLA) prevents body fat accumulation and weight gain in an animal model. *J Food Sci* 72(8):S612–S617
 22. Racine NM, Watras AC, Carrel AL, Allen DB, McVean JJ, Clark RR et al (2010) Effect of conjugated linoleic acid on body fat accretion in overweight or obese children. *Am J Clin Nutr* 91(5):1157–1164
 23. Rist L, Mueller A, Barthel C, Snijders B, Jansen M, Simoes-Wust AP et al (2007) Influence of organic diet on the amount of conjugated linoleic acids in breast milk of lactating women in the Netherlands. *Br J Nutr* 97(4):735–743
 24. Lassek WD, Gaulin SJ (2013) Maternal milk DHA content predicts cognitive performance in a sample of 28 nations. *Matern Child Nutr*
 25. Koletzko B, von Kries R, Monasterolo RC, Subias JE, Scaglioni S, Giovannini M et al (2009) Infant feeding and later obesity risk. *Adv Exp Med Biol* 646:15–29
 26. Willatts P, Forsyth S, Agostoni C, Casaer P, Riva E, Boehm G (2013) Effects of long-chain PUFA supplementation in infant formula on cognitive function in later childhood. *Am J Clin Nutr* 98(2):536S–542S
 27. Seach KA, Dharmage SC, Lowe AJ, Dixon JB (2010) Delayed introduction of solid feeding reduces child overweight and obesity at 10 years. *Int J Obes* 34(10):1475–1479
 28. Durmus B, van Rossem L, Duijts L, Arends LR, Raat H, Moll HA et al (2011) Breast-feeding and growth in children until the age of 3 years: the Generation R Study. *Br J Nutr* 105(11):1704–1711
 29. Fiorotto ML, Burrin DG, Perez M, Reeds PJ (1991) Intake and use of milk nutrients by rat pups suckled in small, medium, or large litters. *Am J Physiol* 260(6 Pt 2):R1104–R1113
 30. West JR (1993) Use of pup in a cup model to study brain development. *J Nutr* 123(Suppl 2):382–385
 31. Vuguin PM (2007) Animal models for small for gestational age and fetal programming of adult disease. *Horm Res* 68(3):113–123
 32. Lukaszewski MA, Eberle D, Vieau D, Breton C (2013) Nutritional manipulations in the perinatal period program adipose tissue in offspring. *Am J Physiol Endocrinol Metab* 305(10):E1195–E1207
 33. Williams L, Seki Y, Vuguin PM, Charron MJ (2014) Animal models of in utero exposure to a high fat diet: a review. *Biochim Biophys Acta* 1842(3):507–519
 34. Bouret SG, Simerly RB (2007) Development of leptin-sensitive circuits. *J Neuroendocrinol* 19(8):575–582
 35. Perez-Cano FJ, Franch A, Castellote C, Castell M (2012) The suckling rat as a model for immunonutrition studies in early life. *Clin Dev Immunol* 2012:537310
 36. Plagemann A, Heidrich I, Gotz F, Rohde W, Dorner G (1992) Obesity and enhanced diabetes and cardiovascular risk in adult rats due to early postnatal overfeeding. *Exp Clin Endocrinol* 99(3):154–158

37. Panchal SK, Brown L (2011) Rodent models for metabolic syndrome research. *J Biomed Biotechnol* 2011:351982
38. Speakman J, Hambly C, Mitchell S, Krol E (2008) The contribution of animal models to the study of obesity. *Lab Anim* 42(4):413–432
39. Buckley AJ, Keseru B, Briody J, Thompson M, Ozanne SE, Thompson CH (2005) Altered body composition and metabolism in the male offspring of high fat-fed rats. *Metabolism* 54 (4):500–507
40. Samuelsson AM, Matthews PA, Argenton M, Christie MR, McConnell JM, Jansen EH et al (2008) Diet-induced obesity in female mice leads to offspring hyperphagia, adiposity, hypertension, and insulin resistance: a novel murine model of developmental programming. *Hypertension* 51(2):383–392
41. Chen H, Simar D, Morris MJ (2009) Hypothalamic neuroendocrine circuitry is programmed by maternal obesity: interaction with postnatal nutritional environment. *PLoS One* 4(7):e6259
42. Desai M, Jellyman JK, Han G, Beall M, Lane RH, Ross MG (2014) Rat maternal obesity and high fat diet program offspring metabolic syndrome. *Am J Obstet Gynecol* 211(3):237.e1–237.e13
43. Hall WG (1975) Weaning and growth of artificially reared rats. *Science* 190 (4221):1313–1315
44. Beierle EA, Chen MK, Hartwich JE, Iyengar M, Dai W, Li N et al (2004) Artificial rearing of mouse pups: development of a mouse pup in a cup model. *Pediatr Res* 56(2):250–255
45. Diaz J, Moore E, Petracca F, Schacher J, Stamper C (1982) Artificial rearing of rat pups with a protein-enriched formula. *J Nutr* 112(5):841–847
46. Spencer SJ, Tilbrook A (2009) Neonatal overfeeding alters adult anxiety and stress responsiveness. *Psychoneuroendocrinology* 34 (8):1133–1143
47. Clarke MA, Stefanidis A, Spencer SJ (2012) Postnatal overfeeding leads to obesity and exacerbated febrile responses to lipopolysaccharide throughout life. *J Neuroendocrinol* 24 (3):511–524
48. Stefanidis A, Spencer SJ (2012) Effects of neonatal overfeeding on juvenile and adult feeding and energy expenditure in the rat. *PLoS One* 7 (12), e52130
49. Smith JT, Spencer SJ (2012) Prewaning over- and underfeeding alters onset of puberty in the rat without affecting kisspeptin. *Biol Reprod* 86(5):145, 141–148
50. Bulfin LJ, Clarke MA, Buller KM, Spencer SJ (2011) Anxiety and hypothalamic-pituitary-adrenal axis responses to psychological stress are attenuated in male rats made lean by large litter rearing. *Psychoneuroendocrinology* 36 (7):1080–1091
51. Clarke M, Cai G, Saleh S, Buller KM, Spencer SJ (2013) Being suckled in a large litter mitigates the effects of early-life stress on hypothalamic-pituitary-adrenal axis function in the male rat. *J Neuroendocrinol* 25(9):792–802
52. Farrell WJ, Alberts JR (2007) Rat behavioral thermoregulation integrates with nonshivering thermogenesis during postnatal development. *Behav Neurosci* 121(6):1333–1341
53. Suckow MA, Weisbroth SH, Franklin CL (2005) *The laboratory rat*. Academic, New York, NY
54. Lane-Petter W (1968) Cannibalism in rats and mice. *Proc R Soc Med* 61(12):1295–1296
55. DeSantis DT, Schmaltz LW (1984) The mother-litter relationship in developmental rat studies: cannibalism vs caring. *Dev Psychobiol* 17(3):255–262
56. <http://www.arc.wa.gov.au>
57. Cierpial MA, Murphy CA, McCarty R (1990) Maternal behavior of spontaneously hypertensive and Wistar-Kyoto normotensive rats: effects of reciprocal cross-fostering of litters. *Behav Neural Biol* 54(1):90–96
58. Sharpe RM, Morris A, Wyatt AC (1973) The effect of the sex of litter-mates on the subsequent behaviour and breeding performance of cross-fostered rats. *Lab Anim* 7 (1):51–59
59. Moore CL, Morelli GA (1979) Mother rats interact differently with male and female offspring. *J Comp Physiol Psychol* 93 (4):677–684
60. Lazic SE (2010) The problem of pseudoreplication in neuroscientific studies: is it affecting your analysis? *BMC Neurosci* 11:5
61. Liu D, Diorio J, Tannenbaum B, Caldji C, Francis D, Freedman A et al (1997) Maternal care, hippocampal glucocorticoid receptors, and hypothalamic-pituitary-adrenal responses to stress. *Science* 277(5332):1659–1662
62. Caldji C, Tannenbaum B, Sharma S, Francis D, Plotsky PM, Meaney MJ (1998) Maternal care during infancy regulates the development of neural systems mediating the expression of fearfulness in the rat. *Proc Natl Acad Sci U S A* 95(9):5335–5340
63. Francis DD, Meaney MJ (1999) Maternal care and the development of stress responses. *Curr Opin Neurobiol* 9(1):128–134
64. Weaver IC, Cervoni N, Champagne FA, D’Alessio AC, Sharma S, Seckl JR et al (2004) Epigenetic programming by maternal behavior. *Nat Neurosci* 7(8):847–854

65. Hellstrom IC, Dhir SK, Diorio JC, Meaney MJ (2012) Maternal licking regulates hippocampal glucocorticoid receptor transcription through a thyroid hormone-serotonin-NGFI-A signaling cascade. *Philos Trans R Soc Lond B Biol Sci* 367(1601):2495–2510
66. Champagne F, Meaney MJ (2001) Like mother, like daughter: evidence for non-genomic transmission of parental behavior and stress responsivity. *Prog Brain Res* 133:287–302
67. Boullu-Ciocca S, Dutour A, Guillaume V, Achard V, Oliver C, Grino M (2005) Postnatal diet-induced obesity in rats upregulates systemic and adipose tissue glucocorticoid metabolism during development and in adulthood: its relationship with the metabolic syndrome. *Diabetes* 54(1):197–203
68. Schmidt I, Fritz A, Scholch C, Schneider D, Simon E, Plagemann A (2001) The effect of leptin treatment on the development of obesity in overfed suckling Wistar rats. *Int J Obes Relat Metab Disord* 25(8):1168–1174
69. Bouret SG, Draper SJ, Simerly RB (2004) Formation of projection pathways from the arcuate nucleus of the hypothalamus to hypothalamic regions implicated in the neural control of feeding behavior in mice. *J Neurosci* 24(11):2797–2805
70. Bouret SG, Draper SJ, Simerly RB (2004) Trophic action of leptin on hypothalamic neurons that regulate feeding. *Science* 304(5667):108–110
71. Bouret SG, Simerly RB (2006) Developmental programming of hypothalamic feeding circuits. *Clin Genet* 70(4):295–301
72. Oscai LB, McGarr JA (1978) Evidence that the amount of food consumed in early life fixes appetite in the rat. *Am J Physiol* 235(3):R141–R144
73. Lopez M, Tovar S, Vazquez MJ, Nogueiras R, Seoane LM, Garcia M et al (2007) Perinatal overfeeding in rats results in increased levels of plasma leptin but unchanged cerebrospinal leptin in adulthood. *Int J Obes* 31(2):371–377
74. Rodrigues AL, De Souza EP, Da Silva SV, Rodrigues DS, Nascimento AB, Barja-Fidalgo C et al (2007) Low expression of insulin signaling molecules impairs glucose uptake in adipocytes after early overnutrition. *J Endocrinol* 195(3):485–494
75. Rodrigues AL, de Moura EG, Passos MC, Dutra SC, Lisboa PC (2009) Postnatal early overnutrition changes the leptin signalling pathway in the hypothalamic-pituitary-thyroid axis of young and adult rats. *J Physiol* 587(Pt 11):2647–2661
76. Xiao XQ, Williams SM, Grayson BE, Glavas MM, Cowley MA, Smith MS et al (2007) Excess weight gain during the early postnatal period is associated with permanent reprogramming of brown adipose tissue adaptive thermogenesis. *Endocrinology* 148(9):4150–4159

Maternal Obesity in Pregnancy: Consequences for Brain Function in the Offspring

Harold A. Coleman and Helena C. Parkington

Abstract

It is perhaps not surprising that an inhospitable intrauterine environment can result in neurodevelopmental disorders, given the enormous changes in brain development that occur during gestation. Here we discuss: (1) Obesity is a state of low-grade inflammation and is thus a candidate for having an unfavorable impact on brain function in the offspring. (2) Maternal obesity has recently been associated with offspring attention deficit hyperactivity disorder and autism spectrum disorder. A recent study found differences in amniotic fluid mRNA for 20 genes in fetuses of obese versus lean women, and several of these genes impact on brain sculpting. (3) The balance between excitable and inhibitory neural function can be disturbed as a consequence of maternal obesity and can lead to hyperexcitability-linked cognitive decline later in life. (4) While most studies of brain development and function have focused on neurons, inflammation and oxidative stress have major effects on microglia and astrocytes, key cells in the sculpting of synapses, neural plasticity, and the formation of neural networks. (5) Animal models are, of necessity, widely used and the temporal trajectory of neurodevelopment to accommodate the requirements of the different species has recently been modeled. While detailed studies are essential for understanding mechanism, it is critical to test the outcomes of manipulating the system on behavior. In this regard considerable care is required to ensure that the most appropriate behavioral test and animal model are used. Thus, there is considerable scope for consolidating our understanding of the effects of maternal obesity on brain function in the offspring.

Key words Fetal origins of neurodevelopmental disorders, Hippocampal hyperexcitability, Inflammation, Astrocytes, Microglia, Excitatory/inhibitory balance, Maternal obesity

1 Introduction

Optimal pregnancy outcomes rely on a supportive intrauterine environment. The population is becoming overweight and obese and this has resulted in an increase in obesity in pregnancy. Obesity is a low-grade inflammatory state, which constitutes an inhospitable environment not only for the pregnant woman but also for the fetus she is carrying. Maternal obesity contributes to complications of pregnancy, which include increased incidences of diabetes, hypertension, preeclampsia, prolonged pregnancy, and failure to progress in labor necessitating emergency caesarean delivery.

A recent Australian report on 75,432 Queenslanders, over a period of just 12 years, found a correlation between maternal obesity and a twofold increase in morbidity needing neonatal intensive care and a threefold incidence in neonatal deaths [1]. In addition, offspring of obese mothers are further at increased risk of obesity in childhood and beyond, thus transmitting the problems of obesity to the next generation, condemning them to a vicious cycle. In adults, high BMI and metabolic syndrome are associated with a reduction in grey and white matter volumes [2], lower cognitive performance, and poor memory and executive function [3]. These problems are now emerging in the young (from mid-teens) [2–4]. Intellectual disability and neurodevelopmental abnormalities, e.g., reduced cognitive capacity, developmental delay, attention deficit hyperactivity disorder (ADHD), and autism spectrum disorders [5, 6] are a significant emotional burden on the individuals involved and their families, and to society in general.

2 Fetal Gene Regulation in Obese Pregnancies

For any maternal obesity effects that result in inappropriate brain architecture, neuron identity or density, then behavioral outcomes in the offspring might be anticipated. A recent study by Edlow, Bianchi, and colleagues used cell-free fetal RNA analysis of amniotic fluid during the second trimester of human pregnancy and reported significant changes in 20 genes in obese pregnancies compared with age-matched lean counterparts [7]. Genes for brain-specific apoD protein (involved in lipid metabolism and oxidative stress), presynaptic synaptotagmin, and carbonic anhydrase 11 (involved in blood–brain-barrier function and microglial activation) were significantly upregulated, whereas presynaptic cytomatrix protein was downregulated. In addition, genes involved in the control of apoptosis (e.g., anti-apoptotic Bcl 2/3) and inflammation (e.g., Bcl, canopy 3 homolog) were upregulated, while genes encoding serine/threonine kinase (STK) 24 and ATPase class VI (involved in metabolism) were downregulated compared with gene expression in the lean controls. During gestation, some neurons go through apoptosis, a process of programmed cell death, which is an important mechanism determining normal brain architecture and fetal neurodevelopment. Architectural disturbances and reduced pruning are disturbed in autism [8]. STK24 levels in pyramidal neurons are associated with epilepsy in humans and rats.

3 The Hypothalamus

The hypothalamus is the major brain region involved in the regulation of feeding. Activity is influenced by hormones, important among which are those released by peripheral organs involved in

metabolic regulation, e.g., leptin produced by white adipocytes, insulin secreted by β -pancreatic cells, ghrelin released from the stomach. How the levels of these hormones change in the fetus and the effects of maternal obesity are not always clear. Also, our understanding of the timing of the development of feeding circuits remains incompletely understood. Neurons of the arcuate nucleus in the hypothalamus are critically involved in feeding circuits, and these neurons form important networks within other hypothalamic nuclei and within limbic nuclei. Leptin, transported across the blood-brain-barrier into the brain, acts on arcuate neurons to suppress feeding. This hormone also has a stimulatory effect on arcuate neuron axon growth and networking and, in adults, this effect is reversible. During a critical period of development (within the first 1–2 weeks of life in rodents), the stimulatory effects of leptin are not reversible and hence establish feeding patterns that persist for the long term [9]. Rodents have a spurt of leptin production in the first week of life, which has an irreversible effect on feeding circuitry, and this spurt is exaggerated in pups of obese dams [10]. Insulin receptors are present in hypothalamus, amygdala, cerebellum and hippocampus in fetal rodents [11]. Although the origins of insulin, peripheral or brain, remains a matter of debate, mRNA has been detected in the hypothalamus and hippocampus [12]. Insulin enhances neurite outgrowth and presynaptic activity in cerebellum and hippocampus [13]. Ghrelin stimulates neuron and astrocyte proliferation in the late-gestation hypothalamus [14]. Sculpting of neural circuits and networking involves cell death to balance proliferation and axonal growth. Thus, of importance is the report that failure of apoptosis in mice results in disruption of arcuate nucleus networking and metabolic regulation [15], and hence the changes in apoptotic mechanisms in the offspring of obese women, mentioned above, is of concern. While feeding circuits are not established in rodents until weeks 1–2 of life, they are established before birth in humans. Studies focussing on individuals that had been gestated during the Dutch Famine (1944–1945) have revealed critical windows for nutrient availability in humans. Famine in early gestation resulted in obesity in adulthood, while late gestation famine was associated with low adult fat mass and reduced insulin sensitivity.

While the central importance of the hypothalamus in the regulation of feeding control is recognized and the role of obesity during development on this system has been reviewed very recently [16], obesity and its consequences, elevated circulating glucose, lipid, hormones, e.g., leptin, insulin, ghrelin, and inflammation have effects in the brain that extend well beyond the hypothalamus. These effects include reduced motoneurone excitability in vagal circuits involved in gastrointestinal signaling of satiety, a result of a high fat diet during the perinatal period [17]. Overall, these

widespread effects are hardly surprising since the control of feeding is so important to survival that it also incorporates hedonic mechanisms. The importance of the reward system and the involvement of dopaminergic mechanism in the control of feeding was demonstrated experimentally four decades ago [18] Reward systems are widespread throughout the neocortex, including prefrontal cortex, amygdala, basal ganglia, and hippocampus. The remainder of this review will focus on the effects of maternal obesity on these brain regions.

4 Hippocampus

The hippocampus is a major brain center involved in memory, learning, and decision making, and it also provides important input into emotional regulation, addiction and reward. Evidence indicates that obesity can exacerbate brain aging and thereby promote the development of cognitive alterations including dementia [19]. Hippocampal volume is negatively associated with BMI [20] and hippocampal dysfunction is likely to be a key contributor to age-associated memory impairment [21].

4.1 *Hippocampal Oscillations*

A striking feature of the hippocampus is its ability to generate strong oscillations in electrical activity due to powerful recurrent collateral connections, particularly in the CA3 region. Oscillations are critical for hippocampal function, with those in the gamma (~20–80 Hz) and theta (~4–10 Hz) bands being particularly important for learning and memory. Hypoactivity of the hippocampus occurs in subjects with well-established Alzheimer's disease (AD) and is associated with impaired memory. Conversely, excessive activity can result in uncontrolled, runaway oscillations that can result in epileptic seizures. Thus the hippocampus is finely tuned by a balance between excitatory and inhibitory mechanisms.

4.2 *Effects of Obesity on Seizures and Epileptic Activity*

Interaction between diet and epileptic seizures has long been appreciated, and Hippocrates used fasting 2500 years ago to inhibit epileptic seizures. However, very few studies have addressed the issue of the effects of obesity on seizure activity. One of the difficulties is that changes due to obesity may be imperceptibly slow over many years or may not manifest until decades after the onset of obesity in susceptible individuals, making it difficult to link neuropathologic features with obesity [22]. Nevertheless, various studies have shown increased rates of obesity in patients with seizure disorders. Many of these associations were presumed to be secondary to the seizures due to lifestyle issues including less exercise, and the effects of antiepileptic drugs which can affect metabolism [22]. Thus, the issue of causality has been difficult to assess. For nearly a century the ketogenic diet (high fat, low carbohydrate, adequate

protein) has been used for refractory epilepsy, with various ketogenic diets proven clinically effective by randomized or blinded trials [22]. Since decreased calorie intake can be beneficial for brain function, does the converse apply? Is a high calorie intake detrimental to the brain?

Significantly, in a study of children, those with newly diagnosed epilepsy had higher BMIs than controls [23]. Importantly, these children were not using antiepileptic drugs, thus ruling out an involvement of such drugs in contributing to the BMI. In adults, the incidence of seizures in overweight or obese individuals was more than double that expected for a normally distributed population [23]. A study of UK adults found a trend for a higher rate of seizures in the obese [24]. In Icelandic adults socioeconomic status (SES) was a risk factor for epilepsy, with no evidence of downward social drift [25]. Other studies indicate that the incidence of epilepsy is now higher in the elderly relative to pediatric populations, concordant with the rise of chronic diseases such as obesity, diabetes, and cerebrovascular disease [22]. Laboratory studies show that obesity is associated with enhanced kainic acid-induced seizures [22]. Thus the small number of studies supports the idea that obesity exacerbates the occurrence of seizures.

4.3 Limbic System

Hippocampal oscillations are not necessarily restricted to the hippocampus but can propagate to other components of the limbic system such as entorhinal cortex and amygdala, structures typically affected during temporal lobe epilepsy. These components of the limbic system play an important role, not only in memory but also in emotional behavior and reward, during which components interact and affect each other. Dysfunction in these systems can contribute to depression and anxiety illnesses [26, 27].

4.4 Dementia

A significant body of evidence has recently accumulated indicating that, somewhat surprisingly, hyperactivity of the hippocampus is associated with impaired learning and memory. This excessive activity occurs in the CA3/dentate gyrus region of the hippocampus [21, 28–30]. Aged rats with normal cognitive function have normal hippocampal activity, whereas aged rats with impaired learning and memory have hyperactive hippocampi [21]. Similarly, aged humans with mild cognitive impairment (MCI) also display hyperactive hippocampi [28, 31], as do hAPP mouse models of AD [32]. Indeed, it has been suggested that increased hippocampal activity may be an early indicator of AD [31]. This is consistent with observations that patients with MCI who have epilepsy, and patients with AD who have epilepsy or subclinical epileptiform activity, present with symptoms of cognitive decline ~7 years earlier than those without epilepsy or epileptiform activity [33]. In rodents and humans, suppression of hippocampal hyperactivity restored learning and memory [28, 30, 32–35]. These results indicate a

critical role of hippocampal hyperactivity in underlying the deficits in learning and memory. Importantly, these results also demonstrate proof-of-principle that targeting hippocampal hyperactivity can have significant therapeutic value. Unfortunately, such approaches currently have a number of side effects with, for example, some antiepileptic medications affecting metabolism to increase obesity [22].

4.5 Mechanisms Underlying Hippocampal Hyperactivity

As discussed, hippocampal activity involves a fine balance between excitatory and inhibitory mechanisms. Thus, hyperactivity could arise from increased excitatory and/or decreased inhibitory mechanisms. Mechanisms impacting this balance can include changes in expression of ion channels and transporters involved in cellular excitability, synaptic transmission, and neurotransmitter and substrate uptake and release processes by neurons and astrocytes. Genetic mutations can underlie hippocampal hyperactivity in some epilepsies, but these are less likely to be important for obesity-induced hippocampal hyperactivity. Inhibitory interneurons are considered to be more vulnerable to dysfunction than excitatory neurons [36, 37] and to be “exquisitely sensitive” to even minor environmental perturbations [38], hence more recent studies have tended to focus on these cells. Using GAD67 as a marker of GABAergic neurons, Spiegel et al. [39] found no difference with age in CA1, but age-related decreases in CA3 and dentate gyrus. Aged rats with memory deficits and hippocampal hyperactivity had significantly reduced numbers of somatostatin-positive (SOM) interneurons in the hilar region of the dentate gyrus than young or aged unimpaired rats. There was no change in hilar NPY immunoreactivity. Loss of hilar SOM neurons in aged impaired rats is consistent with the loss of inhibition and excess dentate gyrus/CA3 activity commonly observed when memory loss occurs in aging. The same group also reported hippocampal hyperactivity and decreased expression of GABA_A α 5 receptor subunit in CA3 of aged rats [29]. As these receptors are involved in tonic inhibition, their loss is consistent with CA3 hyperactivity. Other changes include decreased expression of chaperone/protein folding genes, mitochondrion and oxidative phosphorylation groups, AMPAR subtypes, and the Kv4.2 channel and its interacting protein [29]. A decreased excitability of GABAergic interneurons in the hAPP mouse model of Alzheimer’s disease makes a critical contribution to abnormalities in network synchrony and memory deficiencies [35]. The defect was attributed to decreased expression of Na_v1.1 sodium channels in parvalbumin interneurons.

Hippocampal synaptic plasticity and function have been comprehensively reviewed in Nature Neuroscience [26], including dorsal versus ventral hippocampus. While it is clear that excitatory neurons and inhibitory GABA interneurons are crucial for memory processing and behaviors, the relative importance of various

locations, hippocampus, or nearby subiculum, amygdala, entorhinal, prefrontal, or sensory/motor cortices likely differ for different facets of memory and behavior.

4.6 Treatments That Suppress Hippocampal Hyperactivity

Treatments aimed at decreasing hippocampal hyperactivity have included the antiepileptic drugs. Levetiracetam and valproate are effective in reducing hippocampal hyperactivity and improving memory performance in aged rats [30], in the hAPP mouse model of AD [32], and in humans with mild cognitive impairment [28]. Positive allosteric modulators of GABA_A $\alpha 5$ receptors [34], or overexpressing NPY_{13–36} have been successful in enhancing CA3 inhibitory activity in aged impaired rats [30]. However, many of these agents have significant side-effects and a greater understanding of mechanisms is needed to ameliorate or prevent obesity-induced hyperactivity in the brain.

5 Astroglia

Astrocytes contribute to normal neural electrical activity in a number of critical ways. They play a major role in neurotransmitter uptake, with GABA and glutamate being particularly relevant. It has been estimated that 80–90 % of extracellular glutamate is taken up by transporters located on astrocytes. In this way, astrocytes can influence extracellular levels of GABA and glutamate and thereby levels of tonic inhibition or excitation and excitotoxicity, respectively. Once taken up by astrocytes, GABA and glutamate are converted into glutamine by glutamine synthase within the glutamate–glutamine cycle and the glutamine is then transported out of the astrocytes and taken up by transporters on the glutamatergic and GABAergic neurons. The glutamine is converted into glutamate, and in GABAergic cells, on to GABA by glutamate decarboxylase (GAD). Astrocytes may also contribute to refueling the neurons by taking up glucose, converting it into lactate, and exporting the lactate to the neurons where it is used to fuel neuronal metabolic processes. These functions of astrocytes mean that any malfunctioning of astrocytes can have a major influence on neural activity in a number of ways as discussed above. Of relevance in this context, astrocytes are targets for leptin [40], insulin [41] and ghrelin [42] and these hormones have been reported to influence function of the astrocyte transporters discussed above, ion channels and to result in excessive stimulation.

5.1 Microglia

Microglia are very sensitive to perturbations by environmental challenges [43]. Microglia play an important role in learning and memory as a result of their interactions with the synapse [44], and may be involved in cognitive dysfunction associated with aging [45]. Some aspects of their function are likely to be due to their

multiple fine processes that are dynamically extended and retracted, particularly in the region of synapses [45]. Microglial function is also mediated via the release of the neurotrophin BDNF (brain-derived neurotrophic factor). BDNF interacts with TrkB signaling in neurons to influence synaptic function and learning and memory [44]. Effects of microglial-derived BDNF can also include influences on inhibitory mechanisms [45, 46]. More traditionally, microglia are viewed as the primary immune responsive cells within the brain and the most likely source of pro-inflammatory cytokines [43, 45, 47]. As discussed below, an inflammatory state can have significant influences on cognitive function.

6 Inflammation

Obesity is a low-grade inflammatory state. While acute inflammation is essential for survival, chronic low-grade production of inflammatory cytokines plays a pivotal role in many diseases. Toll-like receptors (TLR) are plasma membrane receptors central to the initiation of inflammatory cascades. Nuclear factor κ B (NF- κ B) is disinhibited and enters the nucleus to activate production of inflammatory cytokines. NF- κ B can be activated by intracellular stress (endoplasmic reticulum and oxidative stress). A number of inflammatory cytokines contribute to brain damage [48]. Cyclooxygenase is central to prostanoid production, important in neurovascular coupling. Nitric oxide synthase (NOS) results in NO production, toxic to glutamatergic neurons. Interleukins IL-1, IL-6 suppress neurogenesis, interfere with synaptic networking, resulting in abnormal brain electrical activity [49], and impair cerebral blood flow. Tumor necrosis factor α (TNF- α) has been linked to memory loss in adults [50]. Also, STK24, downregulated in second trimester amniotic fluid, is involved in immune defense. Inflammatory cytokines, oxidative stress, and protein nitrosylation via ongoing NO exposure have been linked to schizophrenia and depression in humans [51]. In adults, a high-fat diet is associated with inflammation in the brain and impairment of cognitive function [52, 53]. More recently, it has been concluded that obesity per se is not sufficient to precipitate neurological decline, but that it is due to pro-inflammatory mediators, particularly NOX2 (NADPH oxidase 2) [54]. Obesity and/or neuro-inflammation are associated with a range of effects on neural activity that can involve not only changes in synaptic plasticity, but also changes in the excitation/inhibitory balance that can result from effects on the astrocyte glutamate–glutamine cycle [55].

Astrocytes are sensitive to inflammation, with TLRs occurring in astrocytes [56] as well as in neurons [57]. While brief activation of TLRs can stimulate signaling that is protective, e.g., upregulation of ion channels, receptors, and calcium signaling [58],

over-activation (during prolonged inflammation) stimulates NADPH oxidase and the production of reactive oxygen species (ROS) [59]. Increased ROS production [60] can also result in destabilization of the astrocyte/cerebrovascular relationship resulting in impairment of regional blood flow regulation and the blood–brain barrier. In astrocytes and neurons, ROS cause mitochondrial dysfunction, disruption of calcium homeostasis, altered function of redox-sensitive proteins, with disturbed signaling, DNA damage, and cell death (demyelination and neurodegeneration). Disruption of their function is associated with many pathologies [55]. Over-activation results in changes in astrocyte shape and rearrangement of processes servicing synapses. Thus, the support provided to neurons is reduced following activation of astrocytes [61].

An important process that is impaired in reactive astrocytes is the glutamate–glutamine cycle. This cycle is relied upon by GABAergic signaling to a much greater extent than glutamatergic synapses, which may depend more on direct uptake of glutamate into neurons and/or have a higher basal cytoplasmic reserve of this amino acid than interneurons. Consequently, dysfunction of the glutamate–glutamine cycle has deleterious effects on inhibitory before excitatory synaptic responses [55, 62]. The inhibitory deficits associated with reactive astrocytosis can be sufficient to result in hyperexcitability of hippocampal networks [55]. Astrocytosis, inflammation, and significantly reduced levels of glutamine synthetase are often prominent features in some forms of epilepsy, including temporal lobe epilepsy (TLE) in humans [47, 62, 63]. Epilepsies are characterized by recurrent, unpredictable seizures that involve hyperexcitability and hypersynchronous neuronal activity. TLE is one of the most prevalent forms of localization-related epilepsies in humans and is characterized by spontaneous recurrent seizures that involve structures such as the hippocampus, amygdala, and entorhinal cortex [62]. It has recently been suggested that the glutamate–glutamine cycle plays such an important role in brain function that diminished glutamine synthetase can cause TLE [62].

Mitochondrial dysfunction occurs in obesity [54], epilepsy [64], and AD [65], and may be caused by oxidative stress. Mitochondria can also be a significant source of oxidative stress, though this is not necessarily detrimental to cells [66]. Mitochondrial dysfunction increases with age and may be increased by some anti-epileptic drugs, e.g., valproic acid, phenobarbital, carbamazepine, phenytoin [67]. Diminished mitochondrial function predisposes to disrupted calcium handling with consequences for neurotransmission and excitability, and hence with the potential to influence hippocampal excitatory/inhibitory balance.

7 Gender

The brains of females and males are not the same, with differing expression of 1680 genes in the hippocampus alone! [68] Processes involved in synaptic plasticity feature significantly in sexual dimorphism, with some differences also occurring between “male” and “female” astrocytes [69]. Prenatal stress reduces the number of differentially expressed genes to just 191 genes in hippocampus [68]. Following decades of research in this area, McCarthy has recently written that “our understanding of the how, when, and why steroids direct brain development remains rudimentary” [70]. Sex steroids, synthesized in the brain, are differentially distributed between the sexes, brain regions, and during critical developmental periods in pregnancy and early life [71], and estradiol masculinizes the brain [70]. STK24 and docosahexaenoic acid, the only omega-3 fatty acid in brain, are influenced by estrogen. The extent of neuronal dendritic arborization is determined by estrogen in some neurons [72]. In cortical and hippocampal pyramidal cells, dendritic spine number is decreased by estrogen, and the estrogen receptor β (ER β) has been implicated [73]. ER β activation increases GAD, the enzyme responsible for synthesis of the inhibitory transmitter GABA, and enhances astrocyte projection density [73]. ER α reduces excitatory NMDA receptor levels. These observations could explain the gender bias in early life disadvantage [74], peripubertal anxiety [75], and some neurological disorders [4].

8 Stress

As with inflammation, acute stress is essential for survival, but chronic stress plays a major role in many diseases and, although cardiovascular disease is prominent, stress has also been implicated in cancers and neurological dysfunction such as depression, some epilepsies, and post traumatic stress disorder (PTSD). The major players are cortisol/corticosterone, which act on the genome via high-affinity mineralocorticoid receptors (MR) and low-affinity glucocorticoid receptors (GR). GR and MR are highly expressed in hippocampus but some aspects of the stress response are independent of these receptors. Putative membrane-bound MR/GR may be involved but a role for noradrenaline (NA) is a possibility. Normal NA levels in the prefrontal cortex (which interconnects intimately with the hippocampus) are critical for optimal working memory, whereas high levels of NA suppress working memory, effects achieved via glutamatergic transmission [76]. Corticotrophin-releasing hormone (CRH) can also influence neural structure and function, and is a potent convulsant in infant rats [77]. The stress and inflammatory systems interact. Glia produce

IL-1 β , IL-6, and TNF- α in response to stressors [47, 78]. Acute stress can suppress the immune system and anxiety responses to stress can be suppressed under conditions of chronic inflammation, likely involving reduced brain-derived neurotrophic factor (BDNF) [79, 80]. A recent behavioral study has demonstrated that just 1 week of fat feeding triggered anxiety-like behaviors and impaired learning and memory in young mice post weaning, associated with decreased hippocampal and cortical BDNF and nerve growth factor (NGF). The question remains as to the situation during early development, in utero, and the mechanisms involved.

9 Some Important Methodological Considerations

9.1 Recent Developments

The presence of fetal cell-free mRNA in the mother was first described in 2000 by Lo and colleagues [81]. This technique is very powerful as it permits monitoring of gene expression in the living fetus from around the 15th week of pregnancy. In addition to informing on fetal genetic abnormalities, analysis of cell-free mRNA may also provide information on developmental processes, as in the very recent study of high BMI pregnancies by Edlow [7]. In that study new information on events in the fetal brain was provided and thus approaches such as this have powerful potential.

Most studies of brain development and function have focused on neurons. However, it is well established that microglia and astrocytes provide considerable support in the adult brain [82]. Microglia defend the brain under attack and their processes continuously scan, removing debris and dead cells. They also sculpt synapses, augmenting or reducing both pre- and post-synaptic elements eg terminals, dendritic spines. Inflammation activates glia, and obesity is a pro-inflammatory state. It has recently been demonstrated that microglial progenitors present in the yolk sac invade the developing brain in a narrow time-window, via the meninges and ventricles at E6.5 and via the early establishment of the cerebral vasculature at E7.2-7.5 in mice [83]. In human fetuses, invasion via the meninges and ventricles occurs around week 5 [84] and intravascular influx occurs during week 10 [85]. Maternal obesity predisposes to autism spectrum disorders (ASD) in the offspring [5], and a greater density of activated microglia has been reported in ASD [86]. A mechanistic link requires investigation.

While the housekeeping role of astrocytes at synapses is well accepted, the possibility that astrocytes may also influence synaptic efficiency has been suggested [87], and even release of “neurotransmitter” has been mooted very recently [88, 89]. This possibility of a direct role for astrocytes in synaptic transmission is currently under vigorous debate [90, 91]. Calcium plays a major role in astrocyte function and approaches to recording changes in

astrocyte calcium levels with a view to shedding greater light on this debate has been critically reviewed [92]. The role of astrocytes, or not, in the establishment of neural networks during development requires study, as is their potential involvement in attention deficit hyperactivity disorder and ASD.

9.2 Methodological Integration

Translation of knowledge to prevent or ameliorate human disease is a major aim of biomedical research and an important step in achieving this is to perform studies in animal models using approaches that can also be tested in human subjects. So, while *in vitro* slice electrophysiological techniques can be invaluable in providing insights into complex mechanisms at a significant level of detail, and the potential of this approach can be enhanced by the use of genetically modified animals, knock-down of signalling agents using transfection methods, the use of siRNA, and optogenetic technologies, integrating observations from these approaches with prior behavioural testing of the intact animal is critical for a more complete understanding of potential therapeutic strategies. Considerable care is required so that the most appropriate behavioural tests are used and considerations and pitfalls have been thoroughly reviewed and require careful attention [93, 94].

Combining detailed mechanistic studies with prior imaging technologies may also provide more tangible links towards translation. Magnetic resonance imaging (MRI) is widely used in clinical practice and has also been used in non-human studies. While humans remain fully conscious during MRI testing, laboratory species invariably require anaesthesia in order to prevent movement, which would invalidate measurements. MRI detects changes in blood oxygen (deoxyhaemoglobin levels) or changes in cerebral blood volume and all anaesthetic agents available influence basal blood flow and cerebral volume [95]. Furthermore, available anaesthetics alter the responsiveness and/or sensitivity to most neurotransmitters in the brain [95], confounding this method of enquiry. Attempts have been made to circumvent these problems with non-human MRI measurements. Restraint has been used but this introduces stress which, on its own, has repercussions on brain activity (see above). Habituation to restraint does not obviate this problem [96]. In a very elegant study, Scott and colleagues trained rats to place their heads voluntarily into a headport for 8 seconds which permitted quick clamping of the head in a precise location and recording of changes in intracellular free calcium of neurons in layers 2-5 of the cortex, using a two-photon laser-scanning microscopy [97]. Further development of this system will likely provide much-needed insights into cell signalling in intact, conscious experimental animals.

9.3 Animal Models

While epidemiological studies that report on the association between maternal obesity and outcomes in the offspring in human populations are critically important, more precise

manipulation of the system to directly address cause-and-effect requires the use of non-human animal models. Brain development does not occur in a regular homogeneous progression. Rather, specific developmental events can occur rapidly or have specific requirements such as to give rise to sensitive, critical windows of vulnerability. Less than optimal conditions in the critical window can result in long-lasting dysfunction and may underpin neurobehavioral deficits after birth [98]. As a result, one of the first considerations when choosing a non-human animal model is the issue of its critical window compared with that in humans for the neurobehavioral condition of interest. Dobbing and Sands [99] provided a detailed description of the spurt in brain growth in six most commonly-used laboratory species. However, the relationship between this brain growth spurt and a critical window is not clear. Some light has been thrown on this issue in a very elegant recent study by Workman and colleagues [100]. They generated a model of neural development in 18 species, including human, macaque, several rodent species, sheep, cat and several marsupials. The model included brain stem, cerebellum, limbic system, thalamus, striatum, cortex, sensory peripheral system and retina, and these regions were further divided. Developmental events such as neurogenesis, axon extension, network formation, myelination, brain volume, behavioural milestones were also provided. This repository will be invaluable when choosing the most appropriate model when interrogating the mechanisms underpinning specific neurobehavioral problems and should result in faster translation from bench to bedside.

10 In Conclusion

Maternal obesity appears to have wide ranging effects across a broad range of brain regions and functions in the offspring. These effects can include increases in the propensity for the offspring to be obese through effects on circuitry controlling feeding and metabolism, thereby reinforcing the obesity epidemic. A range of neural disorders are likely to be exacerbated by maternal obesity, with long term sequelae for the individuals affected and those around them. Cognition is a major brain function that may be negatively impacted by maternal obesity and this may contribute to enhanced dementia in the affected individuals in later life. However, research into the effects of maternal obesity on brain function in the offspring, other than in the hypothalamus, is very much in its infancy. There is enormous scope for consolidating current concepts, and for studies to determine in greater depth and breadth the effects of maternal obesity and the underlying mechanisms in brain function of the offspring.

References

1. McIntyre HD et al (2012) Overweight and obesity in Australian mothers: epidemic or endemic? *Med J Aust* 196:184–188
2. Gunstad J et al (2008) Relationship between body mass index and brain volume in healthy adults. *Int J Neurosci* 118:1582–1593
3. Cohen RA (2010) Obesity-associated cognitive decline: excess weight affects more than the waistline. *Neuroepidemiology* 34: 230–231
4. AP Association (2000) Diagnostic and statistical manual of mental disorders. APA, Washington, DC, Revised 4th edition
5. Krakowiak P et al (2012) Maternal metabolic conditions and risk for autism and other neurodevelopmental disorders. *Pediatrics* 129: e1121–e1128
6. Sullivan EL et al (2014) Maternal high fat diet consumption during the perinatal period programs offspring behavior. *Physiol Behav* 123:236–242
7. Edlow AG et al (2014) Maternal obesity affects fetal neurodevelopmental and metabolic gene expression: a pilot study. *PLoS One* 9:e88661
8. Maximo JO et al (2014) The implications of brain connectivity in the neuropsychology of autism. *Neuropsychol Rev* 24:16
9. Bouret SG et al (2004) Trophic action of leptin on hypothalamic neurons that regulate feeding. *Science* 304:108–110
10. Kirk SL et al (2009) Maternal obesity induced by diet in rats permanently influences central processes regulating food intake in offspring. *PLoS One* 4:e5870
11. Kar S et al (1993) Quantitative autoradiographic localization of [125I]insulin-like growth factor I, [125I]insulin-like growth factor II, and [125I]insulin receptor binding sites in developing and adult rat brain. *J Comp Neurol* 333:375–397
12. Blazquez E et al (2014) Insulin in the brain: its pathophysiological implications for States related with central insulin resistance, type 2 diabetes and Alzheimer's disease. *Front Endocrinol* 5:161
13. Heidenreich KA et al (1989) Insulin receptors mediate growth effects in cultured fetal neurons. II. Activation of a protein kinase that phosphorylates ribosomal protein S6. *Endocrinology* 125:1458–1463
14. Inoue Y et al (2010) Transitional change in rat fetal cell proliferation in response to ghrelin and des-acyl ghrelin during the last stage of pregnancy. *Biochem Biophys Res Commun* 393:455–460
15. Coupe B et al (2012) Loss of autophagy in pro-opiomelanocortin neurons perturbs axon growth and causes metabolic dysregulation. *Cell Metab* 15:247–255
16. Bouret S et al (2015) Gene-environment interactions controlling energy and glucose homeostasis and the developmental origins of obesity. *Physiol Rev* 95:47–82
17. Bhagat R et al (2015) Exposure to a high fat diet during the perinatal period alters vagal motoneurone excitability, even in the absence of obesity. *J Physiol* 593:285–303
18. Zis AP et al (1975) Neuroleptic-induced deficits in food and water regulation: similarities to the lateral hypothalamic syndrome. *Psychopharmacologia* 43:63–68
19. Uranga RM et al (2010) Intersection between metabolic dysfunction, high fat diet consumption, and brain aging. *J Neurochem* 114: 344–361
20. Convit A et al (2003) Reduced glucose tolerance is associated with poor memory performance and hippocampal atrophy among normal elderly. *Proc Natl Acad Sci U S A* 100:2019–2022
21. Wilson IA et al (2006) Neurocognitive aging: prior memories hinder new hippocampal encoding. *Trends Neurosci* 29:662–670
22. Lee EB et al (2014) The neuropathology of obesity: insights from human disease. *Acta Neuropathol* 127:3–28
23. Daniels ZSB et al (2009) Obesity is a common comorbidity for pediatric patients with untreated, newly diagnosed epilepsy. *Neurology* 73:658–664
24. Gao S et al (2008) The incidence rate of seizures in relation to BMI in UK adults. *Obesity* 16:2126–2132
25. Hesdorffer DC et al (2005) Socioeconomic status is a risk factor for epilepsy in Icelandic adults but not in children. *Epilepsia* 46: 1297–1303
26. Bannerman DM et al (2014) Hippocampal synaptic plasticity, spatial memory and anxiety. *Nat Rev Neurosci* 15:181–192
27. Stoop R et al (2000) Functional connections and epileptic spread between hippocampus, entorhinal cortex and amygdala in a modified horizontal slice preparation of the rat brain. *Eur J Neurosci* 12:3651–3663
28. Bakker A et al (2012) Reduction of hippocampal hyperactivity improves cognition in

- amnesic mild cognitive impairment. *Neuron* 74:467–474
29. Haberman RP et al (2011) Prominent hippocampal CA3 gene expression profile in neurocognitive aging. *Neurobiol Aging* 32:1678–1692
 30. Koh MT et al (2010) Treatment strategies targeting excess hippocampal activity benefit aged rats with cognitive impairment. *Neuropharmacology* 35:1016–1025
 31. Putcha D et al (2011) Hippocampal hyperactivation associated with cortical thinning in Alzheimer's Disease signature regions in nondemented elderly adults. *J Neurosci* 31:17680–17688
 32. Sanchez PE et al (2012) Levetiracetam suppresses neuronal network dysfunction and reverses synaptic and cognitive deficits in an Alzheimer's disease model. *Proc Natl Acad Sci U S A* 109:E2895–E2903
 33. Vossel KA et al (2013) Seizures and epileptiform activity in the early stages of Alzheimer disease. *JAMA Neurol* 70:1158–1166
 34. Koh MT et al (2013) Selective GABA_A α5 positive allosteric modulators improve cognitive function in aged rats with memory impairment. *Neuropharmacology* 64:145–152
 35. Verret L et al (2012) Inhibitory interneuron deficit links altered network activity and cognitive dysfunction in Alzheimer model. *Cell* 149:708–721
 36. Luhmann HJ et al (1992) Hypoxia-induced functional alterations in adult rat neocortex. *J Neurophysiol* 67:798–811
 37. Perez Velazquez JL et al (2007) Typical versus atypical absence seizures: network mechanisms of the spread of paroxysms. *Epilepsia* 48:1585–1593
 38. Hsu F-C et al (2003) Repeated neonatal handling with maternal separation permanently alters hippocampal GABA_A receptors and behavioral stress responses. *Proc Natl Acad Sci U S A* 100:12213–12218
 39. Spiegel AM et al (2013) Hilar interneuron vulnerability distinguishes aged rats with memory impairment. *J Comp Neurol* 521:3508–3523
 40. Spanswick D et al (1997) Leptin inhibits hypothalamic neurons by activation of ATP-sensitive potassium channels. *Nature* 390:521–525
 41. Spanswick D et al (2000) Insulin activates ATP-sensitive K⁺ channels in hypothalamic neurons of lean, but not obese rats. *Nat Neurosci* 3:757–758
 42. Briggs DI et al (2014) Evidence that diet-induced hyperleptinemia, but not hypothalamic gliosis, causes ghrelin resistance in NPY/AgRP neurons of male mice. *Endocrinology* 155:2411–2422
 43. Walker FR et al (2013) Acute and chronic stress-induced disturbances of microglial plasticity, phenotype and function. *Curr Drug Targets* 14:1262–1276
 44. Parkhurst CN et al (2013) Microglia promote learning-dependent synapse formation through Brain-Derived Neurotrophic Factor. *Cell* 155:1596–1609
 45. Wake H et al (2012) Physiological function of microglia. *Neuron Glia Biol* 7:1–3
 46. Zheng K et al (2011) TrkB signaling in parvalbumin-positive interneurons is critical for gamma-band network synchronization in hippocampus. *Proc Natl Acad Sci U S A* 108:17201–17206
 47. Devinsky O et al (2013) Glia and epilepsy: excitability and inflammation. *Trends Neurosci* 36:174–184
 48. Tornatore L et al (2012) The nuclear factor kappa B signaling pathway: integrating metabolism with inflammation. *Trends Cell Biol* 22:557–566
 49. Green HF et al (2012) Unlocking mechanisms in interleukin-1b-induced changes in hippocampal neurogenesis -a role for GSK-3b and TLX. *Transl Psychiatry* 2:e194
 50. Ganz PA et al (2012) Does tumor necrosis factor-alpha (TNF-alpha) play a role in post-chemotherapy cerebral dysfunction? *Brain Behav Immun* 30(Suppl):S99–S108
 51. Anderson G et al (2013) Schizophrenia is primed for an increased expression of depression through activation of immunoinflammatory, oxidative and nitrosative stress, and tryptophan catabolite pathways. *Prog Neuropsychopharmacol Biol Psychiatry* 42:101
 52. Beilharz JE et al (2014) Short exposure to a diet rich in both fat and sugar or sugar alone impairs place, but not object recognition memory in rats. *Brain Behav Immun* 37:134–141
 53. Pistell PJ et al (2010) Cognitive impairment following high fat diet consumption is associated with brain inflammation. *J Neuroimmunol* 219:25–32
 54. Pepping JK et al (2013) NOX2 deficiency attenuates markers of adiposopathy and brain injury induced by high-fat diet. *Am J Physiol Endocrinol Metab* 304:E392–E404
 55. Ortinski PI et al (2010) Selective induction of astrocytic gliosis generates deficits in neuronal inhibition. *Nat Neurosci* 13:584–U93

56. Elovitz MA et al (2006) Elucidating the early signal transduction pathways leading to fetal brain injury in preterm birth. *Pediatr Res* 59:50–55
57. Tang SC et al (2007) Pivotal role for neuronal Toll-like receptors in ischemic brain injury and functional deficits. *Proc Natl Acad Sci U S A* 104:13798–13803
58. Kushnir R et al (2011) Peripheral inflammation upregulates P2X receptor expression in satellite glial cells of mouse trigeminal ganglia: a calcium imaging study. *Neuropharmacology* 61:739–746
59. Block ML et al (2007) Microglia-mediated neurotoxicity: uncovering the molecular mechanisms. *Nat Rev Neurosci* 8:57–69
60. Ma D et al (2013) The neurotoxic effect of astrocytes activated with toll-like receptor ligands. *J Neuroimmunol* 254:10–18
61. Steele ML et al (2012) Reactive astrocytes give neurons less support: implications for Alzheimer’s disease. *Neurobiol Aging* 33 (423):e1–e13
62. Coulter DA et al (2012) Astrocytic regulation of glutamate homeostasis in epilepsy. *Glia* 60:1215–1226
63. Wetherington J et al (2008) Astrocytes in the epileptic brain. *Neuron* 58:168–178
64. Khurana DS et al (2013) Mitochondrial dysfunction in epilepsy. *Semin Pediatr Neurol* 20:176–187
65. Wang X et al (2014) Oxidative stress and mitochondrial dysfunction in Alzheimer’s disease. *Biochim Biophys Acta* 1842:1240
66. Accardi MV et al (2014) Mitochondrial reactive oxygen species regulate the strength of inhibitory GABA-mediated synaptic transmission. *Nat Commun* 5(3168):1–12
67. Finsterer J et al (2012) Mitochondrial toxicity of antiepileptic drugs and their tolerability in mitochondrial disorders. *Expert Opin Drug Metab Toxicol* 8:71–79
68. Biala YN et al (2011) Prenatal stress diminishes gender differences in behavior and in expression of hippocampal synaptic genes and proteins in rats. *Hippocampus* 21:1114–1125
69. Liu M et al (2007) Role of P450 aromatase in sex-specific astrocytic cell death. *J Cereb Blood Flow Metab* 27:135–141
70. McCarthy MM (2013) Sexual differentiation of the brain in man and animals. *Am J Med Genet C Semin Med Genet* 163:3–15
71. Konkle AT et al (2011) Developmental time course of estradiol, testosterone, and dihydrotestosterone levels in discrete regions of male and female rat brain. *Endocrinology* 152: 223–235
72. Amateau SK et al (2002) A novel mechanism of dendritic spine plasticity involving estradiol induction of prostaglandin-E2. *J Neurosci* 22:8586–8596
73. Tan XJ et al (2012) Reduction of dendritic spines and elevation of GABAergic signaling in the brains of mice treated with an estrogen receptor beta ligand. *Proc Natl Acad Sci U S A* 109:1708–1712
74. Oomen CA et al (2009) Opposite effects of early maternal deprivation on neurogenesis in male versus female rats. *PLoS One* 4:e3675
75. Hayward C et al (2002) Puberty and the emergence of gender differences in psychopathology. *J Adolesc Health* 30:49–58
76. Zhang Z et al (2013) Norepinephrine drives persistent activity in prefrontal cortex via synergistic alpha 1 and alpha2 adrenoceptors. *PLoS One* 8:e66122
77. Baram TZ et al (1991) Corticotropin-releasing hormone is a rapid and potent convulsant in the infant rat. *Brain Res Dev Brain Res* 61:97–101
78. Cowley TR et al (2012) Rosiglitazone attenuates the age-related changes in astrocytosis and the deficit in LTP. *Neurobiol Aging* 33:162–175
79. Clark SM et al (2014) Immune status influences fear and anxiety responses in mice after acute stress exposure. *Brain Behav Immun* 38:192
80. Shiraev T et al (2009) Differential effects of restricted versus unlimited high-fat feeding in rats on fat mass, plasma hormones and brain appetite regulators. *J Neuroendocrinol* 21: 602–609
81. Poon LL et al (2000) Presence of fetal RNA in maternal plasma. *Clin Chem* 46:1832–1834
82. Bilimoria PM et al (2014) Microglia function during brain development: new insights from animal models. *Brain Res* 1617:7–17
83. Ginhoux F et al (2010) Fate mapping analysis reveals that adult microglia derive from primitive macrophages. *Science* 330:841–845
84. Monier A et al (2007) Entry and distribution of microglial cells in human embryonic and fetal cerebral cortex. *J Neuropathol Exp Neurol* 66:372–382
85. Verney C et al (2010) Early microglial colonization of the human forebrain and possible involvement in periventricular white-matter injury of preterm infants. *J Anat* 217:436–448
86. Morgan JT et al (2010) Microglial activation and increased microglial density observed in

- the dorsolateral prefrontal cortex in autism. *Biol Psychiatry* 68:368–376
87. Tasker JG et al (2012) Glial regulation of neuronal function: from synapse to systems physiology. *J Neuroendocrinol* 24:566–576
 88. Rusakov DA (2012) Astroglial glutamate transporters trigger glutaminergic gliotransmission. *J Physiol* 590:2187–2188
 89. Rusakov DA (2012) Depletion of extracellular Ca²⁺(+) prompts astroglia to moderate synaptic network activity. *Science signaling* 5:pe4
 90. Hamilton NB et al (2010) Do astrocytes really exocytose neurotransmitters? *Nat Rev Neurosci* 11:227–238
 91. Smith K (2010) Neuroscience: settling the great glia debate. *Nature* 468:160–162
 92. Khakh BS et al (2015) Astrocyte calcium signaling: from observations to functions and the challenges therein. *Cold Spring Harb Perspect Biol* 7(4):a020404
 93. Alleva E et al (2000) Important hints in behavioural teratology of rodents. *Curr Pharm Des* 6:99–126
 94. Ohl F et al (2003) Behavioural screening in mutagenised mice—in search for novel animal models of psychiatric disorders. *Eur J Pharmacol* 480:219–228
 95. Haensel JX et al (2015) A systematic review of physiological methods in rodent pharmacological MRI studies. *Psychopharmacology (Berl)* 232:489–499
 96. Reed MD et al (2013) Behavioral effects of acclimatization to restraint protocol used for awake animal imaging. *J Neurosci Methods* 217:63–66
 97. Scott BB et al (2013) Cellular resolution functional imaging in behaving rats using voluntary head restraint. *Neuron* 80:371–384
 98. Meredith RM (2014) Sensitive and critical periods during neurotypical and aberrant neurodevelopment: a framework for neurodevelopmental disorders. *Neurosci Biobehav Rev* 50:180–188
 99. Dobbing J et al (1979) Comparative aspects of the brain growth spurt. *Early Hum Dev* 3:79–83
 100. Workman AD et al (2013) Modeling transformations of neurodevelopmental sequences across mammalian species. *J Neurosci* 33:7368–7383

Chapter 11

Models of Perinatal Compromises in the Guinea Pig: Their Use in Showing the Role of Neurosteroids in Pregnancy and the Newborn

Hannah K. Palliser, Greer A. Bennett, Meredith A. Kelleher, Angela L. Cumberland, David W. Walker, and Jonathan J. Hirst

Abstract

Placental progesterone production during late gestation has a major role in maintaining elevated neurosteroid levels during pregnancy. These levels of key neurosteroids, including allopregnanolone, are critical for optimal brain development during late gestation and the early neonatal period. The long gestation period (~70), in utero brain development and placental progesterone synthesis of the guinea pig makes this species very suitable for studying the mechanisms by which pregnancy compromises impact neurosteroid pathways. We have used models of intrauterine growth restriction and preterm birth to show that these challenges may suppress neurosteroid action and this likely contributes to the adverse outcomes following these conditions. Reduced allopregnanolone levels during late gestation result in reduced myelination and injurious brain cell death suggesting supplementation treatments may improve outcomes following compromised pregnancy. Guinea pig models of episodic prenatal maternal stress have been used to examine how these events lead to adverse behavioral outcomes for the offspring. We found that prenatal stress disrupts the neurosteroid pathways between the dam and fetus. Together this work indicates that compromises and stress during pregnancy and in the early neonatal period disrupt neurotropic and protective neurosteroid pathways leading to deficiencies that contribute to the adverse neurological and behavioral outcomes following these challenges. The use of neurosteroid-based supplementation therapies may represent a future range of therapeutic approaches that could be used to improve outcomes following stressful events in pregnancy and following premature birth.

Key words Stress, Neurosteroid, Cortisol, Fetus, Neonate, Growth restriction, Preterm birth

1 Introduction

The growing appreciation of the importance of pregnancy and the perinatal period in determining the future vulnerability to adult disease has highlighted the importance of using animal models in which life events and their effects on adult health can be examined in a manageable time frame. The timing of these adverse events during pregnancy and in the perinatal period appears critical to the

ultimate long-term outcome and this seems particularly so with potential effects on brain development. The choice of animal models is particularly important in studies of neurosteroid actions in pregnancy due to the marked differences in the endocrinology of pregnancy between common laboratory species [1]. This further indicates that the selection of the animal model has a major bearing on the translatability of observations to long-term outcomes in human health. We and others have used guinea pig models of acute and chronic stress in pregnancy and the perinatal period to examine effects of changes to the neurosteroid environment of the developing brain [2]. In addition, how ongoing changes to neurosteroid-regulated excitability may subtly influence behavior and that potentially contribute to behavioral disorders after birth and into adolescence.

The most important difference between the guinea pig, compared to other laboratory rodents, is the long gestation period of ~70 days. This gestation period results in the delivery of a highly developed fetus at birth, with the fetus undergoing major phases of maturation, and importantly brain development while in utero [3]. Brain growth rates more closely approximates humans with rapid myelination occurring in late gestation [4]. This also means development is subject to the relatively hypoxic environment that typifies fetal life and so is more similar to human developmental conditions. Furthermore, the large size of the fetus and mass of the combined litter creates considerable maternal load. Therefore, even marginal interference with the uterine blood supply can lead to detrimental effects on fetal growth [5]. This seems to occur normally to some extent in the guinea pig as there is considerable pregnancy loss in most colonies with stillbirth rates up to 20 % [6]. This suggests the fetus is highly vulnerable to interventions that adversely influence nutrient supply.

2 Key Endocrine Changes in Pregnancy and at Labor Onset in the Guinea Pig

The endocrinology of pregnancy in the guinea pig has important similarities to human pregnancy, particularly the production of progesterone by the placenta and the maintenance of relatively high levels throughout late pregnancy until the time of birth [1]. This, as in the human, is accompanied by rising neurosteroid levels in the plasma and brain during late gestation. These levels are also maintained until term in the guinea pig and decline following the loss of the placenta after birth [2]. Most colonies show a greater spread of gestational ages at delivery compared to other rodent species with this spread of ages both within colonies and between colonies [7]. This suggests that the blocking of uterine activation by progesterone is less powerful in this species. Indeed, like the

human, labor in the guinea pig is initiated despite the high gestational progesterone concentration and is thought to involve loss of uterine progesterone sensitivity [8]. In the human there is a decline in progesterone sensitivity due to changes in progesterone receptor (PR) expression in the uterine myometrium. Mesiano et al. [9] showed that the ratio of the full-length receptor isoform (PRB) to the truncated (PRA) isoform decreased toward term in human myometrium. As PRB mediates the inhibitory effect of progesterone and PRA reduced the effects of PRB, these changes lead to a loss of progesterone action on the myometrium. We have found that similar changes in numbers are seen in the guinea pigs with overall PR concentrations falling near term, indicating that withdrawal of progesterone-induced myometrial suppression leads to labor onset in the guinea pig [8].

Similarities in PR changes and progesterone action during the initiation labor in the guinea pigs have proved useful for studies of the mechanisms contributing to these changes. We were first to show that fetal placental insufficiency and the associated growth retardation (*see* below) in the guinea pig resulted in a relatively small (5 %) but significant reduction in gestation length [10]. Further studies showed that placental insufficiency was associated with marked changes in the PR expression. However, in contrast to a decline in receptor expression and resultant progesterone-mediated inhibition of labor, we found total PR levels had increased in myometrium following placental insufficiency. This rise may be compensatory or protective to maintain pregnancies as long as possible [10]. This intriguing finding suggests that the earlier labor in these pregnancies is driven by potent mechanisms that can overcome relatively greater progesterone-produced and -associated inhibitory actions. These findings further support the guinea pig as a useful species in which to examine the mechanisms that lead to loss of progesterone-induced inhibition of myometrial activity.

Together the above studies show that the long gestation period and the maturity of the fetus at birth as well as similarities in pregnancy endocrinology mean that the guinea pig is useful for studying the effects of pregnancy compromise on timing of labor. In addition, the adverse effects of these compromises on the fetus can be investigated as the large size of the fetus and placenta has allowed the development of a number of models of pregnancy compromise, and perinatal stress. We have longstanding interest in the effect of adverse events in pregnancy on endocrine changes and how changes effect placental function and in turn can influence the interaction of neurosteroids and the development of the fetal brain [2]. The guinea pigs and the models of compromises established in this species are ideal for investigation of the role of neurosteroids in these processes.

Neurosteroids are steroid hormones that modulate neurotransmission in the central nervous system. These steroids have major roles in regulating CNS development and setting the overall excitability of the brain particularly during late gestation [11]. The most potent neurosteroids known to regulate CNS excitability are allopregnanolone (5 α -pregane-3 α -ol-20-one) and 5 α -tetrahydrocorticosterone (THDOC), which are derived from progesterone and deoxycorticosterone (DOC), respectively. These steroids do not bind to progesterone or glucocorticoid receptors like their precursors, but instead bind as agonists to a steroid binding site on the gamma-amino butyric acid type-A (GABA_A) receptor [11]. In binding to these receptors allopregnanolone increases the action of GABA and enhances GABAergic inhibitory transmission. Other steroids including pregnenolone and some allopregnanolone isomers have an antagonist action at the GABA_A receptor reducing inhibition and may also enhance excitatory glutamatergic activity [12]. The lipophilic nature of these steroids and the extra synaptic location of steroid-sensitive receptors results in a widespread action within brain areas markedly influencing tonic excitability [11]. Together, the overall levels of these steroids regulate excitability of the CNS, although little is known regarding these actions in pregnancy.

3 Protective Role of Neurosteroids

During pregnancy, high progesterone production by the placenta leads to commensurately high concentrations of allopregnanolone in the fetal brain. These levels are the highest seen throughout life and lead to tonic suppression of activities during late gestation [13]. The adult brain contains all of the enzymatic mechanisms required for the synthesis of progesterone and its metabolism to allopregnanolone [14]. These include the 5 α -reductase as well as 20 α -hydroxysteroid oxidoreductase that are expressed in glial cell and neurons [15]. However, we found that concentrations of allopregnanolone in the brain decline markedly at birth suggesting a supply of progesterone metabolites from the placenta is required to maintain fetal brain concentrations. Indeed, progesterone treatment of newborn guinea pigs raises allopregnanolone levels in the brain [16]. These observations show that placental progesterone production in long gestation species, including guinea pigs and likely women, leads to increased availability of allopregnanolone precursors (progesterone and 3 α -dihydroprogesterone) in the fetal circulation. This in turn leads to the remarkably high levels of allopregnanolone seen in the fetal brain and which decline rapidly after birth [17]. We were the first to show that allopregnanolone has a major role in controlling CNS activity in fetus during the

second half of gestation, and that this action continues into neonatal life [16, 18]. Furthermore, we have showed that appropriate fetal concentrations of these steroids are required to maintain normal fetal excitability and behavioral state in late gestation [13]. Partial suppression of precursor availability increases excitability and alters the incidences of fetal REM-like and non-REM-like behavior and arousal and hence the sleep-like patterns that typify late gestation fetal life [13]. Moreover, marked suppression of allopregnanolone production leads to seizure-like activity [19]. Importantly, this action also reduces the vulnerability that may result in hypoxic/ischemic episodes during pregnancy and at labor onset.

Neurosteroids directly influence brain development, particularly neurites, synaptogenesis and astrocytes and myelination [20, 21]. There is also growing evidence that changes in neurosteroid exposure during pregnancy can have adverse effects on development and lead to long-term changes in behavior, including hyperactivity, anxiety, and depression [22, 23]. Fetal behavioral states are important for normal late gestation brain development and changes in behavioral states may contribute to the effects of premature decline on neurosteroid levels that occur with preterm birth (*see* below). Together these data suggest that loss of the normally high neurosteroid environment in the fetus will adversely affect outcome [24]. We have used the pregnant guinea pig model to mimic the loss of neurosteroid exposure following premature delivery. In this work the 5α -reductase inhibitor, finasteride, was used to suppress allopregnanolone levels and thus highlight the importance of neurosteroids to normal late gestation neurodevelopment. We firstly showed that finasteride treatment markedly potentiated cell death in the brain caused by an episode of hypoxia [24]. These data showed that normal gestational neurosteroid levels reduce vulnerability to hypoxia-induced damage and make up an endogenous neuroprotective mechanism during late gestation. In further studies in the guinea pig we showed that finasteride treatment heightened the deficiencies in myelination and changes astrocyte activation that were seen in growth-restricted pregnancies [5]. These studies support the contention that allopregnanolone in the brain promotes normal development and may counter the effects on growth restriction resulting from inadequate nutrient supply in late gestation.

4 Evaluation of Outcome Following Growth Restriction in the Guinea Pig

Both rats and guinea pigs have a bicornate uterus and while the litter size in the guinea pig is smaller typically 2–5 fetus [7]. However, in contrast to the rats, guinea pigs with smaller litter sizes may have all fetuses in a single horn, with the remaining horn empty.

Additionally, spacing of implantation sites is less organized with small fetuses apparently close or crowned rather than an orderly spacing. The blood supply to the uterine horns in both guinea pigs and rats is by an arcade artery arising anteriorly from the utero-ovarian artery and posteriorly from the iliac arteries [25]. Several groups of investigators have used ligation of the posterior end of the arcade artery to reduce uterine blood flow and create growth restriction in the ipsilateral horn. Rees et al. [26] successfully used this approach to produce marked growth restriction in fetal guinea pigs that also show marked brain injury. The ligation procedure was done at mid gestation in the guinea pig and resulted in marked asymmetric growth restriction. This however was accompanied by increased incidence of fetal death, with fetuses in the ipsilateral horn and nearest to the ligation most effected. Rees and colleagues further showed that ligation of the uterine artery led to major adverse outcomes including mark reduction in myelination [27]. Turner and Trudinger [28] modified this technique by using diathermy to ablate a proportion of the branches of the uterine arcade artery that tend to supply perfusion of the maternal side of each placenta (Fig. 1). This procedure was performed between 31 and 35 days of gestation and was found to significantly reduce fetal weight but with a reduced incidence of intrauterine death compared to the arcade artery ligation procedure. However, given the differences in spacing of the fetus and number of fetuses per horn the reduction in fetal weight is variable, but more consistent than the artery ligation procedure. We used a modification of this procedure to evaluate the effect of growth restriction on neurosteroid pathways [5]. We consistently ablated every second artery branch to each placenta of all fetuses. Although we were careful to include small vessels, as these vessels may grow with advancing gestation, we were mindful that some vessels that were not obvious to us may expand with increasing demand over gestation. This approach produced growth restriction with marked reduction in total fetal weight and individual organ weights (Fig. 2). Brain weight was also reduced, but to a lesser extent, and there was pronounced brain sparing compared to other organs suggesting the procedure resulted in a good model of human intrauterine growth restriction (IUGR).

The growth restriction we produced resulted in reduced myelination in the CA1 region of the hippocampus as shown by reduced myelin basic protein staining [5]. There was also a marked increase in the expression of glial fibrillary acidic protein (GFAP) indicating greater activation of astrocytes typical of upregulation of injurious or inflammatory processes (Fig. 3a). We further examined the effect of reduced neurosteroid synthesis by treating the pregnant dams with finasteride. Finasteride treatment markedly reduced allopregnanolone levels in the fetal brain [5]. This treatment led to a significant reduction in myelination in the subcortical white matter and increase in activated astrocyte immunostaining (Fig. 3a) and

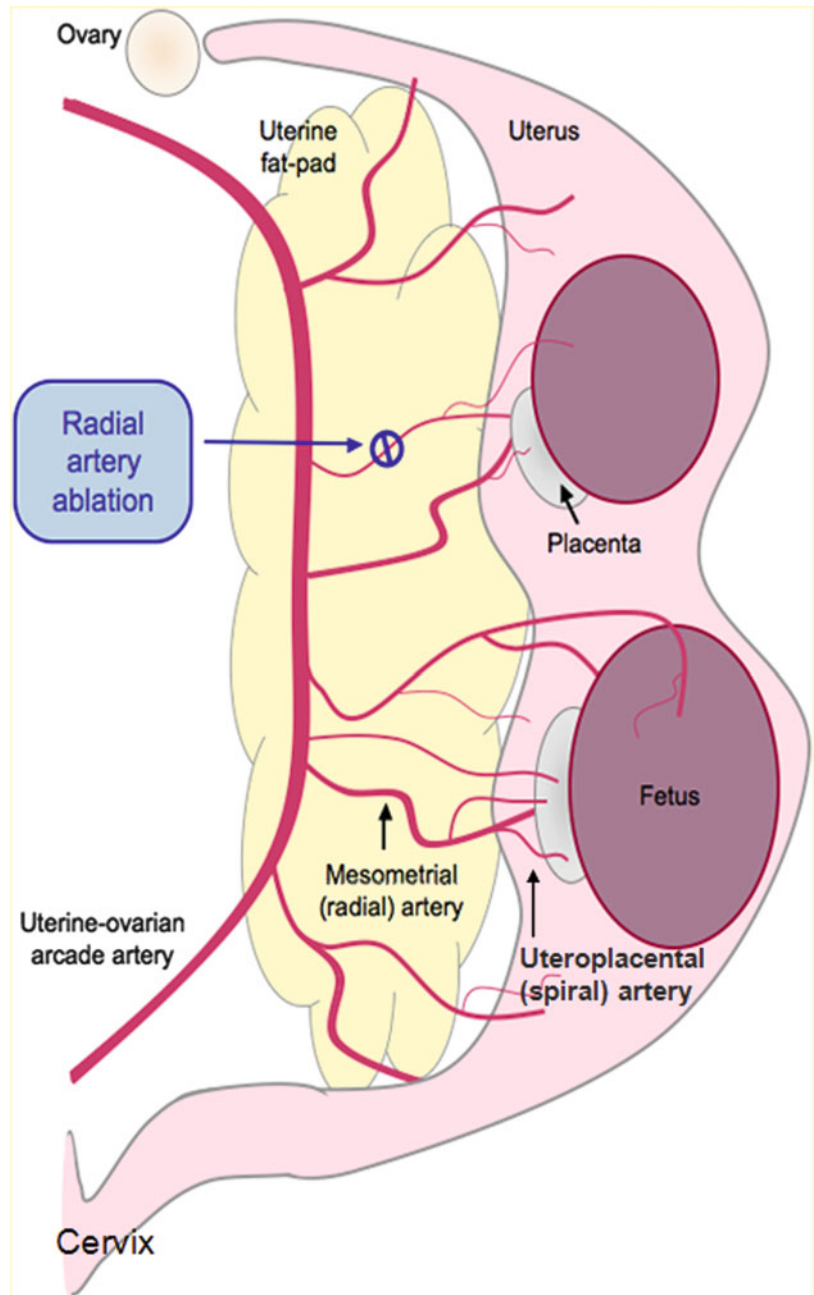


Fig. 1 Diagram showing pregnant uterine horn and placental blood supply in the guinea pig. The uterus that is supplied with arterial oxygenated blood from the uterine-ovarian arcade artery, which branches into mesometrial (radial) and uteroplacental (spiral) arteries to supply the placenta and fetus. At mid-gestation placental insufficiency by the cauterization of ~50 % of the radial/spiral arteries supplying each placenta with a typical site of radial artery ablation is shown. Adapted from [25]

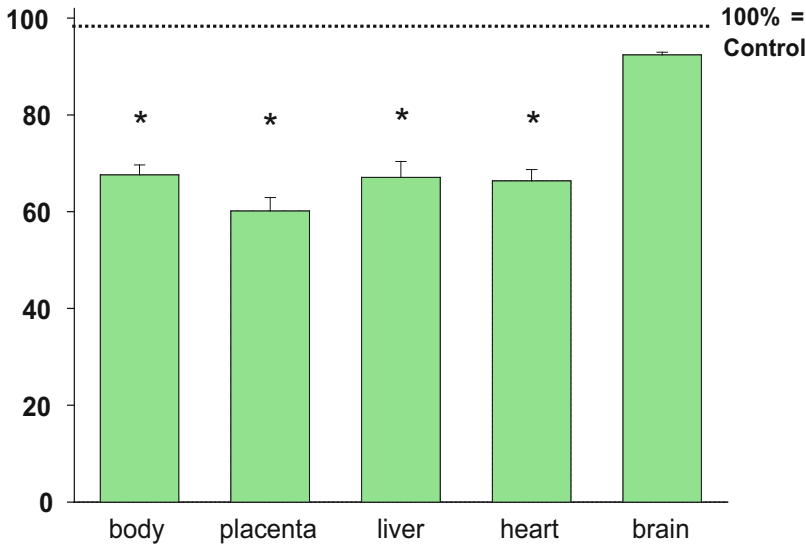


Fig. 2 The mean body and organ weights for fetal guinea pigs after artery ablation treatment with values presented as a % of weights observed in sham-operated animals. Asymmetric growth restriction in fetuses is shown by the lesser effect of the procedure on brain weight with animals that received artery ablation treatment. *Asterisks* indicate significant differences between from the sham operated group ($*p < 0.05$)

there was also a marked reduction in myelination in the subcortical white matter (Fig. 3b). These changes suggest that the treatment reduced growth and potential raised vulnerability to cell damage. The changes were also accompanied by trends toward reduced 5 α -reductase-2 enzyme expression in brain homogenates [5]. Together these findings suggest that loss of neurosteroid levels may contribute to the reduction in brain development in growth-restricted pregnancies. Furthermore, the studies suggest that reduced exposure to gestational levels as occurs with preterm birth may have major adverse effects on brain growth.

5 Preterm Birth and Progesterone Replacement in Guinea Pigs: Effects on Allopregnanolone Levels and Neurodevelopment

Preterm birth (birth at <37 weeks gestation) is a major contributor to the burden of disease and mortality in newborn infants. We have shown that progesterone and allopregnanolone levels in the brain remain at late gestation levels until loss of the placenta at birth and that may be critical to the developing brain [16]. As indicated above a reduction of allopregnanolone synthesis in the late-gestation guinea pig reduces myelination and enhances the expression of GFAP-positive astrocytes, suggestive of brain insult (Fig. 3) [5]. We have examined the effect of loss of normal allopregnanolone levels and neurodevelopmental outcomes in preterm guinea pig neonates [16]. We used the guinea pig, a species with precocial

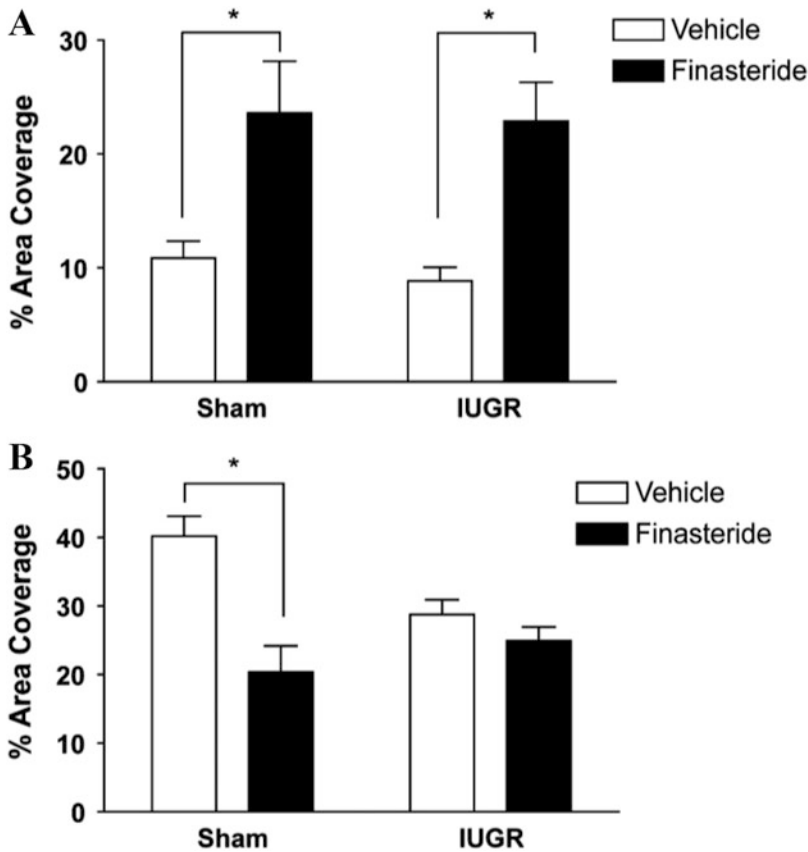


Fig. 3 Glial fibrillary acidic protein (GFAP) immunostaining (**a**) and myelin basic protein (MBP) immunostaining (**b**) in the sub-cortical white matter of the guinea pig brain. Staining is expressed as percentage coverage of total area. Fetuses were normally grown (sham operated) that were vehicle treated (sham, *open* bars), intrauterine growth restricted and vehicle treated (IUGR, and *open* bars), normally grown and finasteride treated (sham, and *open* bars) or growth restricted and finasteride treated (IUGR and *black* bars). Each bar represents mean \pm SEM. Asterisks indicate significant differences between groups link by lines ($*p < 0.05$, $n = 10\text{--}12$ fetuses) (M Kelleher Ph.D. Thesis, University of Newcastle, 2013)

brain development [4], and relatively high concentrations of placentally derived progesterone [29], to study the transition from gestational allopregnanolone levels to those seen preterm neonatal brain. The animals were delivered by cesarean section at 63 days of gestation and maintained until 24 h of age. Postnatal care involved the use of periods of continuous positive airway pressure (CPAP) to establish regular breathing, an adequate tidal volume, and functional residual capacity. We maintained the animals in a heated and humidified chamber. Preterm animals had a significantly greater mortality rate of 60 % at 24 h following delivery, compared to a 3 % mortality rate in term neonates with male neonates making up a higher proportion of those animals that did not reach 24 h (67 %) [16]. Furthermore, it was not possible to deliver animals early than 62 days without a very marked fall in survival rate (unpublished observations).

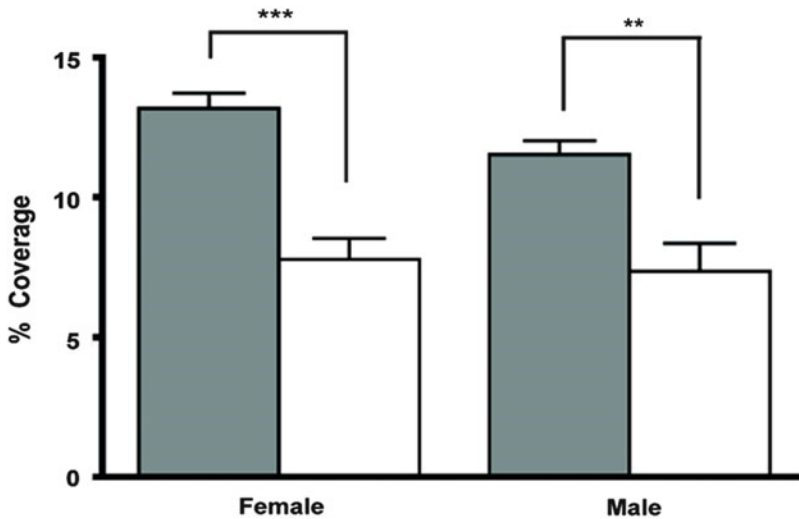


Fig. 4 Reduced myelination as measured by myelin basic protein immunostaining in the hippocampal CA1. Values for term female and term male (grey bars) or preterm female and preterm male (open bars) fetal brains and are expressed as mean percent area coverage \pm S.E.M ($n = 6$). Asterisks indicate significant differences between term and preterm groups (** $p < 0.01$, *** $p < 0.001$)

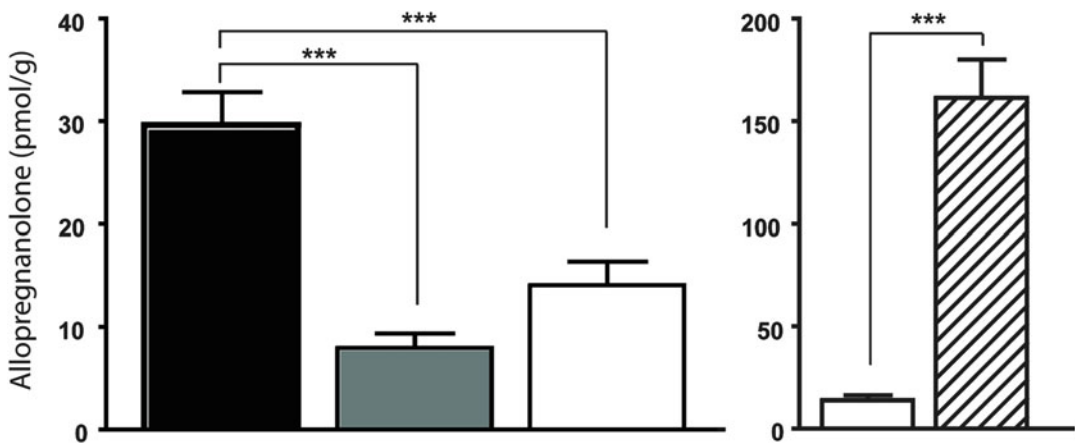


Fig. 5 Brain allopregnanolone concentrations in fetal ($n = 12$, black), term neonatal ($n = 9$, grey), and preterm neonatal animals ($n = 11$, open; left panel). Preterm neonates (open right panel) compared with progesterone treated preterm neonates ($n = 10$, hashed; right panel, note different scale). Each bar represents mean \pm SEM. Asterisks indicate significant differences between groups indicated by lines (** $p < 0.001$) [16]

Consistent with the immaturity of these animals, we found lower myelin basic protein staining in the CA1 region of the hippocampus of both male and females guinea pigs, indicative of reduced myelination, compared to term controls (Fig. 4). We have previously reported there was a dramatic drop in allopregnanolone levels after birth in the sheep brain and we found a similar decline in concentrations after term birth compared to late-gestation fetal

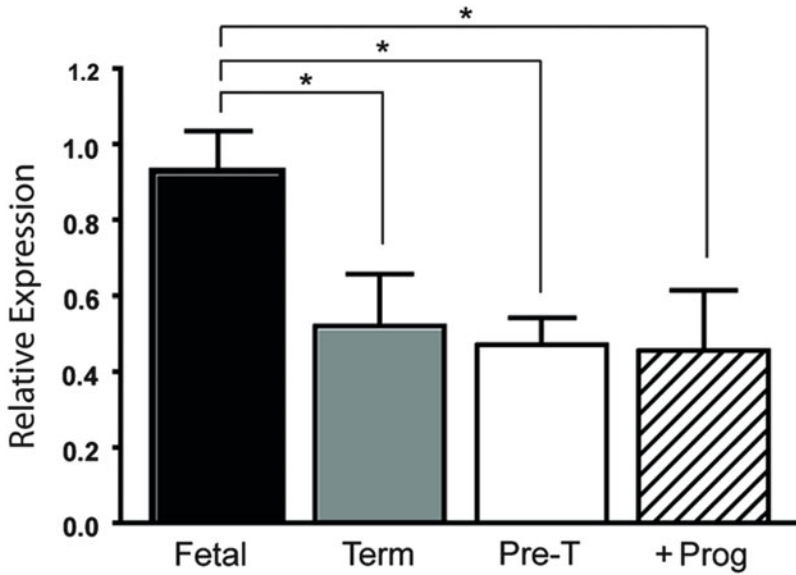


Fig. 6 Expression of 5 α -reductase type 2 in brain from fetal ($n = 16$, Fetal, *black bars*), from term neonatal ($n = 11$, Term, *grey bars*), preterm neonatal ($n = 12$, Pre-T, *open bars*) and preterm progesterone treated neonatal guinea pigs ($n = 8$, +Prog, *hashed bars*). The neonatal guinea pig brains were obtained at 24 h of age. Bars represent mean \pm SEM. Asterisks indicate significant differences between groups linked by lines ($*p < 0.05$) [16]

levels in the guinea pig (Fig. 5). Plasma allopregnanolone concentrations also declined after preterm birth although the fall was somewhat less than that seen at term suggesting lower metabolism rates in the preterm neonate [16]. In the brain however levels declined rapidly after both normal and preterm birth (Fig. 5). In addition, brain 5 α -reductase-2 expression was significantly lower in the preterm neonates at 24 h of age compared to expression levels observed during gestation (Fig. 6). Interestingly, 5 α -reductase-1 expression was not effected. However, previous studies of allopregnanolone production in fetal sheep have shown 5 α -reductase-2 as the most important isoform in regulating allopregnanolone levels within the fetal brain and in the early neonatal period [17]. These data show that both allopregnanolone levels and synthetic capacity are reduced after preterm birth. Furthermore, the work showed that the transition from fetal to neonatal life in the preterm guinea pig and the loss of placental progesterone result in a premature decrease in allopregnanolone concentrations in the brain. The finding that 5 α -reductase-2 expression was also reduced within the brain suggests that both the endogenous supply of progesterone and the capacity of the brain to synthesize neuroactive progesterone metabolites are compromised in the preterm neonate. This further shows that brain maturation in the preterm neonate from delivery to term equivalent age takes place in a markedly lower neurosteroid environment compared to animals that remain in

utero. Whether this deficiency accounts for the lower myelination seen in these neonates or whether there is adequate catch up awaits further study.

We have investigated the effects of progesterone replacement in an additional group of preterm guinea pig neonates during the first 24 h after birth. Progesterone treatment did markedly raise allopregnanolone concentrations in the brain (Fig. 5). This work supports the potential use of exogenous progesterone replacement to increase allopregnanolone precursor supply. The findings demonstrate that administration of progesterone to preterm neonates, in amounts that elevated plasma concentrations [16], resulted in increased levels of metabolites for allopregnanolone synthesis. In addition, despite the reduced expression of 5α -reductase-2, the exogenous administration of progesterone was sufficient to raise brain allopregnanolone concentrations. This observation provides support for the augmentation of allopregnanolone levels in the brain via endogenous synthetic mechanisms, allowing retroactive steroid concentrations to become re-established following preterm birth. Short-term administration of progesterone to preterm neonates over 24 h did not have an effect on neuropathological findings our studies. Long-term progesterone replacement, however, during the preterm postnatal period, warrants further examination of effects on allopregnanolone concentrations and potentially brain development and functional neurological outcomes.

These findings are also of interest in view of the existing use of perinatal progesterone treatments. Progesterone and synthetic progestins have been investigated for use as preventative treatments for preterm birth [30]. There is currently, however, little information on the effect of such treatments on fetal and neonatal allopregnanolone concentrations. The finding that neurosteroid levels in the preterm neonate are at least partially dependent on progesterone concentrations suggest some caution is needed over the potential effect of treatments on brain development. Together, these findings suggest preterm delivery in the guinea pig resulted in reduced myelination and a premature reduction in neonatal brain concentrations of allopregnanolone. Current observations indicate that these alterations may be reversed by postnatal treatment with progesterone. Additionally, progesterone and its neuroactive steroid metabolites may have particularly important effects on postnatal processes of myelination, a key neurodevelopmental pathway affected by preterm birth.

6 Neurosteroids and Prenatal Stress in a Guinea Pig Model

Psychosocial stress in pregnancy is a biopsychosocial factor that can be defined as the “imbalance that a pregnant woman feels when she cannot cope with demands, which may be expressed behaviorally

and physiologically” [31]. Some common causes of maternal psychosocial stress in pregnancy include anxiety and depression, family disruptions and quarrels, spousal uncertainty, and pregnancy anxiety. Physiological responses to prenatal stress may include neuroendocrine responses, particularly increased circulating cortisol. We have previously shown that repeated doses of synthetic glucocorticoids markedly reduces $5\alpha R2$ expression in a sex-specific manner, specifically reducing levels in male fetal guinea pig brains and lowering allopregnanolone levels [32], suggesting the important suppressive effect of these neurosteroid synthetic capacity. This suggests that prenatal stress that chronically raises cortisol levels may depress neurosteroid levels in the fetal brain.

The adverse consequences of maternal stress in pregnancy are becoming more widely recognized and are associated with poor pregnancy outcomes including neurodevelopmental consequences in the offspring [33, 34]. Epidemiological studies have demonstrated that maternal psychological stress during pregnancy has marked effects on the fetus, adversely affecting neurological outcomes and leading to behavioral problems in childhood [33, 34]. Maternal state anxiety has been found to be associated with hyperactivity and inattention problems for the offspring at 5 years of age [35]. Women reporting high anxiety in late gestation, and increased cortisol, were found to be twice as likely to have children who develop emotional and behavioral problems at 4 and 7 years of age, particularly male infants with hyperactivity and attention disorders [36] and decreased grey matter density at 6–9 years [37]. Furthermore, extensive studies have also shown that affected offspring demonstrates increased hypothalamo-pituitary axis (HPA) activity [33, 36, 37], which has the potential to exacerbate those who may be exposed to further stress in postnatal life. Both the degree and timing of stress throughout the course of pregnancy is influential to the risk of adverse outcomes. Interestingly, relatively short episodes of acute anxiety appear sufficient to cause adverse outcomes. For example, high levels of objective stress exposure in pregnancies following the Quebec ice storm showed negative effects on intellectual capacity, such as cognitive and language abilities, in children born after this traumatic event [38, 39]. These studies also suggested vulnerability differed with gestational age, with stress exposure during the first 28 weeks of gestation having the greatest impact [33]. These events resulted in markedly increased maternal cortisol, suggesting cortisol-induced suppression of neurosteroid synthesis may contribute to neurological perturbations and behavioral problems, although the potential linkage pathways occurring in the infant are unclear [35, 40].

Clinical studies indicate repeated exposure to synthetic glucocorticoids may adversely affect neonatal outcome [41]. Animal

studies have shown that repeated treatment with betamethasone causes delays in maturation of neurons, myelination and glia and reduced brain weight and head size [42–44]. In contrast to synthetic steroids, the fetus is normally protected from the high concentrations of cortisol in maternal plasma by the placenta, due to the presence of 11β -hydroxysteroid dehydrogenase type-2 (11β -HSD2). This enzyme converts cortisol to the markedly less potent glucocorticoid, cortisone, so that limited amounts of maternal cortisol actually reaches the fetal circulation [45]. However, during stress, elevated maternal cortisol concentrations may exceed the metabolic capacity of the placenta allowing a larger proportion of maternal cortisol to cross the fetal circulation [45]. Furthermore, exposure to prolonged compromise may reduce the expression of 11β -HSD2 [46]. Despite the substantive evidence of adverse effects of prenatal stress and associated increases in maternal cortisol, the mechanism by which these changes affect brain development remains unclear [47]. The majority of studies assessing pre- or postnatal stress and rises in cortisol have centered on the ongoing effects on the HPA system of affected offspring. Whilst these animal studies have identified that programming of the HPA axis has been found to play an important role, we are interested in the effect of elevated cortisol exposure on the neurodevelopmental and protective role of neurosteroids.

We used a guinea model of prenatal stress that was developed by Kapoor and colleagues [48, 49]. This model involves the induction of stress by maternal exposure to brief periods of strobe light at regular intervals during gestation (4 occasions in late gestation, every 5 days from GA50; term GA71) [49, 50]). Strobe light exposure consistently leads to activation of the maternal HPA axis and increased cortisol concentrations in maternal plasma and saliva [50, 51] and fetal plasma [52] (Fig. 7). Salivary cortisol is representative of circulating cortisol concentrations relieving the potentially confounding effect of blood collection and guinea pigs readily produce copious amounts of saliva enabling easy collection that does not result in elevated cortisol levels (unpublished data). We have shown that prenatal light stress in pregnant guinea pigs results in reduced myelin basic protein (MBP), glial fibrillary acidic protein, and microtubule-associated protein-2 (MAP-2) expression in late gestation male fetal hippocampi, suggesting reduced myelination, changes in astrocyte reactivity and fewer mature neurons at term in pregnancies exposed to the following prenatal stress procedure [50]. These sexually dimorphic changes were found to remain at 21 days of age and were associated with increased anxiety as assessed by open field analysis (unpublished observations). Matthews and colleagues extensively studied the effects of prenatal stress on offspring and found disruption of HPA function,

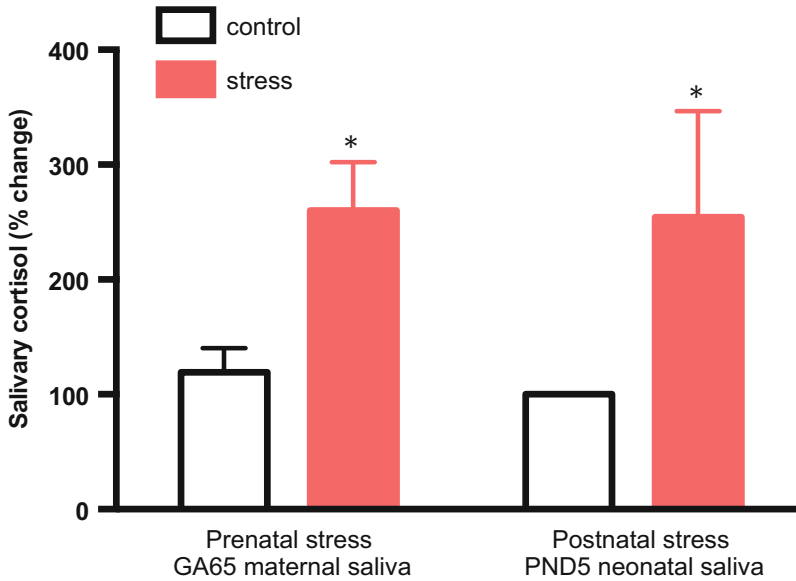


Fig. 7 Maternal salivary cortisol before (*open*) and after (*filled*) prenatal strobe light stress at 65 days of gestational age (Prenatal stress GA65 maternal saliva, $n = 11$) and neonatal salivary cortisol before (*open*) and after (*filled*) maternal separation at 5 days of postnatal age (Postnatal stress PND5 neonatal saliva, $n = 10$). Bars represent mean \pm SEM. Asterisks indicate significant differences between before and after groups ($*p < 0.05$)

endocrine and behavioral changes which exist into adulthood [40, 53]. The consequences of prenatal stress depend not only on the frequency, type/severity, and timing of the stress episodes but also on the sex of offspring and time at which they are assessed. For example, chronic maternal stress in guinea pigs was found to decrease ambulatory activity in PND25 male offspring, increased activity in PND80 male offspring, and had no effect on the ambulatory activity of female offspring at either age [40, 53, 54]. Acute periods of stress at 50–52 or 60–62 days of gestation did not alter locomotor activity in young adult male offspring. Whereas, acute periods of stress at either 50 or 60 days of gestation were found to have sexually dimorphic effects on post weaning body weight, basal cortisol and testosterone levels, and anxiety in guinea pig offspring [48, 49]. These studies in guinea pigs have shown that critical aspects of brain development occur in utero, as in the human, and are sensitive to maternal endocrine perturbations caused by an anxiety-like stress [51]. Moreover, these effects show sex differences with the most marked effects observed in male guinea pig offspring [50, 55]. Consistent with these findings we observed marked sex differences in behavior patterns following prenatal stress in our guinea pig studies [56] and similar differences have been reported in children; i.e., more marked hyperactivity problems in boys compared to girls [35].

We, and others, have proposed that suppression of neurosteroid synthesis and disruptions of neurosteroid action represents a key mechanistic link by which maternal stress leads to neurodevelopmental and behavioral abnormalities in offspring [23, 57]. As indicated above our findings show that increased exposure to elevated glucocorticoids caused suppression of neurosteroid synthesis. Importantly, we found that repeated maternal synthetic glucocorticoid treatment suppressed expression of key enzymes in allopregnanolone pathway suggesting high glucocorticoids have a disrupting effect on gestational neurosteroid production processes [32].

These studies examining the effect of exogenous and endogenous elevations in cortisol support the contention that the stress-induced disruption of neurosteroid production adversely affects key neurodevelopmental processes. Clinical studies show that allopregnanolone concentrations in plasma increase transiently in response to acute stress, but may be reduced with chronic anxiety [58]. This is consistent with studies showing that repeated glucocorticoid exposure suppresses allopregnanolone levels [32, 59]. Reduced allopregnanolone synthesis would in turn rob the fetus of a key endogenous neuroprotective mechanism and disrupt normal apoptotic processes in the brain, in a similar manner to that seen when 5α -reductase-2 activity is inhibited [5]. Pharmacologically reduced neurosteroid levels in pregnancy have been shown to impair cognitive ability in juvenile rats [60]. We contend that stress-induced suppression of neurosteroids and disruption of their receptor actions continue in the neonatal brain and contribute further to the hyperactivity and related adverse behaviors [58]. Ongoing studies by ourselves and others are now focusing on the benefit of allopregnanolone replacement therapy, both pre- and postnatally, in pregnancies affected by prenatal stress. In recent studies [56], we administered allopregnanolone to maternal guinea pigs after prenatal stress exposure in order to replace potentially depressed levels. Interestingly, this treatment did not affect postnatal behavior, however, the findings showed that while maternal allopregnanolone levels were increased by allopregnanolone treatment, there was an increase in fetal levels in control fetuses (non-stressed dams), and there was no rise in levels in the stress-exposed fetuses (Fig. 8, [50]). These results suggest placental metabolism of exogenously administered allopregnanolone may be increased in pregnancies exposed to prenatal stress. Furthermore, the findings suggest that there may be marked changes in neurosteroid metabolic pathways in the placenta following exposure to stress-induced elevation in cortisol concentrations. Our ongoing studies are assessing the timing of stress during pregnancy and how this affects neurosteroid levels in the fetus and potential neurodevelopmental consequences.

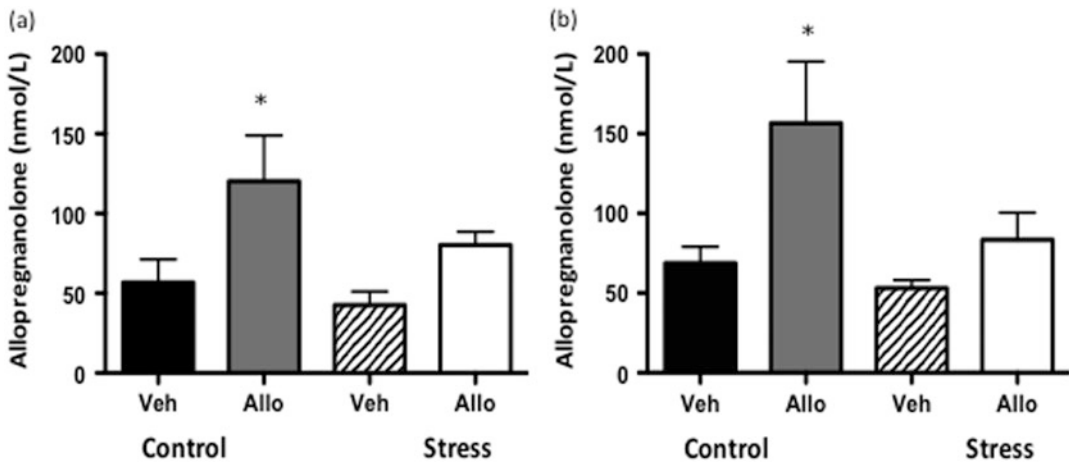


Fig. 8 Fetal plasma allopregnanolone concentrations at the time of post mortem shown in males (a) and females (b). Values are for non-stressed (Control) and prenatally stressed animals (Stress) that were treated with vehicle (Veh) or allopregnanolone (Allo). *Black bars* indicated Control + Veh (males $n = 5$; females $n = 5$), *grey bars* indicate Control + Allo (males $n = 6$; females $n = 5$), *hatched bars* indicate Stress + Veh as *hatched bars* (males $n = 5$; females $n = 5$) and *open bars* indicate Stress + Allo (males $n = 6$; females $n = 6$). Bars represent mean \pm SEM. *Asterisks* indicate significance difference in fetal plasma allopregnanolone levels in the Control + Allo treated group compared to all other groups [50]

7 Potentiating Effects of Postnatal Stress

Many pregnant women suffer stress during pregnancy due to natural or manmade disasters, chronic interpersonal tensions, adverse conditions in the home or work place or other factors frequently associated with low socioeconomic status. Unfortunately, the causes of the stressors often continue after birth so that the infant also faces similar early life stress. Recent studies suggest effects of such stressors continue into adolescence and may have additive effects on stress experiences before birth [61] and make a major contribution to the incidence of behavioral disorders such as hyperactivity, anxiety, and depression in childhood and adolescence.

Identification of the mechanisms by which early life stress (caused by maternal separation) leads to these behavioral disorders and how this may be potentiated by maternal psychosocial stress in pregnancy is important as the resulting behavioral disorders are a major health problem [62]. There is now extensive evidence that these stresses cause increased responsiveness of the HPA axis in the newborn that persists into adult life [47]. The comprehensive studies of Meaney and co-workers [63, 64] have demonstrated that the amount and quality of the mother–neonate interaction has a major influence over the long-term activity of the HPA axis; there is marked up-regulation of postnatal HPA axis activity where mothers display a low level of maternal care and nursing. Lower

maternal care also has a major influence on glutamatergic pathways with increased glutamate-NMDA receptor signaling [65]. Postnatal experience was further found to result in marked changes in plasticity of the hippocampus, leading to effects on adult behaviors such as learning, memory, and attention [64]. However, using rats to study the mother–neonate interaction has some disadvantages, because, unlike humans, GABA_A receptors undergo transition from excitatory to inhibitory status only after birth [66, 67], and therefore the effects of prenatal and/or postnatal stress on neurosteroid-GABAergic inhibitory activity is unclear.

The guinea pig neonate is most appropriate for studies on the effects of stress-induced disruption of neurosteroid pathways in the perinatal period due to the maturity of GABAergic signaling which exerts inhibitory actions from the second half of gestation [68] similar to humans [69]. In addition, while these neonates are more independent in terms of the absolute necessity for maternal care compared to nest-bound rat pups, newborn guinea pigs do demonstrate primate-like attachment [3] with maternal–neonatal separation leading to a pronounced stress response. Indeed we have seen a marked increased plasma cortisol concentration in neonates following separation from their mothers, work that is supported by previous studies showing strong attachment (Fig. 7). Matthews and colleagues [70] have demonstrated that maternal stress in late pregnant guinea pigs had the effect of increasing the hypothalamo-pituitary-adrenal (HPA) axis activity, and this persisted after birth so that these offspring showed higher cortisol responses to stress as adults. Furthermore, they showed that this was due to reduced negative feedback by glucocorticoids on the HPA, implicating a long-lasting change in hippocampus–hypothalamus signaling in these offspring. We have previously shown that acute stress induced by episodes hypoxic stress raises allopregnanolone synthesis in the newborn fetal sheep brain [18]. In contrast we have found that chronic exposure to stress during pregnancy has a suppressive action of synthetic capacity, but it is currently unclear if chronic stress after birth also disrupts neurosteroid pathways [50]. The sensitivity of GABA_A receptors to modulation by allopregnanolone is governed by the subunit composition (including: $\alpha 4$, $\alpha 5$, $\alpha 6$, and δ ; [11]) of the receptor. GABA_A receptors present in the fetal brain are highly sensitive to modulation by allopregnanolone with sensitivity decreasing in adulthood [71], however, little is known regarding the early neonate–childhood period. We have recently found that prenatal stress resulted in marked changes in GABA_A receptor subunit expression, with offspring that were exposed to stress showing markedly lower GABA_A receptor δ -subunit and $\alpha 6$ -subunit mRNA expression after birth with the changes in the $\alpha 6$ -subunit still present at 21 days of age in the guinea pig [72]. These findings suggest that steroid sensitivity is also influenced by stress and these changes can continue a considerable time after

birth. Whether these changes can be further influenced by postnatal stress is currently under investigation.

8 Conclusions and Directions

We contend that the pregnant guinea pig with its long gestation and with the fetus undergoing major brain development in utero is an appropriate model for examining the effects of compromised pregnancy and preterm birth on neurosteroid pathways. We used a model of intrauterine growth restriction to show this chronic stress that raised cortisol levels tended to lower neurosteroid synthetic capacity. This was in contrast to the marked increase in neurosteroid synthesis which we have reported to occur with acute stress. We have also delivered guinea pig pups prematurely and shown we can maintain these preterm pups until 24 h of age and are now extending this out to term equivalent age. These studies showed that the preterm pups undergo brain development in a neurosteroid deficient environment between preterm delivery and term equivalence. Previous evidence suggests that this deficiency will contribute to suboptimal neurodevelopment during this time. We further showed that progesterone replacement can restore allopregnanolone levels in the brain and has potential as a future neuroprotective therapy following preterm birth. Prenatal maternal stress during pregnancy can be readily modeled in the guinea pig by stress treatments that raise salivary cortisol levels. We showed that repeated prenatal stress exposure disrupted the transfer of allopregnanolone to the fetus and this may involve changes to neurosteroid metabolism in the placenta. The role of these neurosteroid changes in the ongoing behavior problems seen in the offspring following prenatal stress requires further investigation. Postnatal stress may potentiate the effects of prenatal stress on neurosteroid pathways and the effects of elevated cortisol levels in the neonatal period on these pathways warrant further study. Overall, these findings suggest that many perinatal compromises lead to disrupted neurosteroid signaling. In addition, prenatal and postnatal stress events may also potentiate suppression of neurosteroid pathways. These findings suggest that neurosteroid supplementation or replacement therapy may be a new therapeutic direction that should be explored as a way to improve neurodevelopmental outcomes following these adverse events.

Acknowledgements

This work was funded by the NHMRC (grant numbers 1003517 and 1044846).

References

- Mitchell BF, Taggart MJ (2009) Are animal models relevant to key aspects of human parturition? *Am J Physiol Regul Integr Comp Physiol* 297(3):R525–R545
- Hirst JJ, Walker DW, Yawno T, Palliser HK (2009) Stress in pregnancy: a role for neuroactive steroids in protecting the fetal and neonatal brain. *Dev Neurosci* 31(5):363–377
- Hennessy MB, O’Leary SK, Hawke JL, Wilson SE (2002) Social influences on cortisol and behavioral responses of preweaning, periadolescent, and adult guinea pigs. *Physiol Behav* 76(2):305–314
- Dobbing J, Sands J (1970) Growth and development of the brain and spinal cord of the guinea pig. *Brain Res* 17(1):115–123
- Kelleher MA, Palliser HK, Walker DW, Hirst JJ (2011) Sex-dependent effect of a low neurosteroid environment and intrauterine growth restriction on foetal guinea pig brain development. *J Endocrinol* 208(3):301–309
- Motzel SL, Wagner JE (1989) Diagnostic exercise: fetal death in guinea pigs. *Lab Anim Sci* 39(4):342–344
- Peaker M, Taylor E (1996) Sex ratio and litter size in the guinea-pig. *J Reprod Fertil* 108(1):63–67
- Palliser HK, Kelleher MA, Welsh TN, Zakar T, Hirst JJ (2014) Mechanisms leading to increased risk of preterm birth in growth-restricted guinea pig pregnancies. *Reprod Sci* 21(2):269–276
- Mesiano S, Wang Y, Norwitz ER (2011) Progesterone receptors in the human pregnancy uterus: do they hold the key to birth timing? *Reprod Sci* 18(1):6–19
- Palliser HK, Zakar T, Symonds IM, Hirst JJ (2010) Progesterone receptor isoform expression in the guinea pig myometrium from normal and growth restricted pregnancies. *Reprod Sci* 17(8):776–782
- Herd MB, Belelli D, Lambert JJ (2007) Neurosteroid modulation of synaptic and extrasynaptic GABA(A) receptors. *Pharmacol Ther* 116(1):20–34
- Schumacher M, Baulieu EE (1995) Neurosteroids: synthesis and functions in the central and peripheral nervous systems. *Ciba Found Symp* 191:90–106, discussion 106–112
- Hirst JJ, Palliser HK, Yates DM, Yawno T, Walker DW (2008) Neurosteroids in the fetus and neonate: potential protective role in compromised pregnancies. *Neurochem Int* 52(4–5):602–610
- Mellon SH, Griffin LD, Compagnone NA (2001) Biosynthesis and action of neurosteroids. *Brain Res Brain Res Rev* 37(1–3):3–12
- Zwain IH, Yen SS (1999) Neurosteroidogenesis in astrocytes, oligodendrocytes, and neurons of cerebral cortex of rat brain. *Endocrinology* 140(8):3843–3852
- Kelleher MA, Hirst JJ, Palliser HK (2013) Changes in neuroactive steroid concentrations after preterm delivery in the Guinea pig. *Reprod Sci* 20(11):1365–1375
- Nguyen PN, Billiards SS, Walker DW, Hirst JJ (2003) Changes in 5alpha-pregnane steroids and neurosteroidogenic enzyme expression in the perinatal sheep. *Pediatr Res* 53(6):956–964
- Nguyen PN, Yan EB, Castillo-Melendez M, Walker DW, Hirst JJ (2004) Increased allopregnanolone levels in the fetal sheep brain following umbilical cord occlusion. *J Physiol* 560(Pt 2):593–602
- Yawno T, Yan EB, Hirst JJ, Walker DW (2011) Neuroactive steroids induce changes in fetal sheep behavior during normoxic and asphyxic states. *Stress* 14(1):13–22
- Wang JM, Liu L, Irwin RW, Chen S, Brinton RD (2008) Regenerative potential of allopregnanolone. *Brain Res Rev* 57(2):398–409
- Ghoumari AM, Ibanez C, El-Etr M, Leclerc P, Eychenne B, O’Malley BW, Baulieu EE, Schumacher M (2003) Progesterone and its metabolites increase myelin basic protein expression in organotypic slice cultures of rat cerebellum. *J Neurochem* 86(4):848–859
- Schule C, Nothdurfter C, Rupprecht R (2014) The role of allopregnanolone in depression and anxiety. *Prog Neurobiol* 113:79–87
- Darbra S, Modol L, Llido A, Casas C, Vallee M, Pallares M (2014) Neonatal allopregnanolone levels alteration: effects on behavior and role of the hippocampus. *Prog Neurobiol* 113:95–105
- Yawno T, Yan EB, Walker DW, Hirst JJ (2007) Inhibition of neurosteroid synthesis increases asphyxia-induced brain injury in the late gestation fetal sheep. *Neuroscience* 146(4):1726–1733
- Kaufmann P, Davidoff M (1977) The guinea-pig placenta. *Adv Anat Embryol Cell Biol* 53(2):5–91
- Tolcos M, Rees S (1997) Chronic placental insufficiency in the fetal guinea pig affects neurochemical and neuroglial development but not neuronal numbers in the brainstem: a new method for combined stereology and

- immunohistochemistry. *J Comp Neurol* 379 (1):99–112
27. Tolcos M, Bateman E, O'Dowd R, Markwick R, Vrijksen K, Rehn A, Rees S (2011) Intrauterine growth restriction affects the maturation of myelin. *Exp Neurol* 232(1):53–65
 28. Turner AJ, Trudinger BJ (2009) A modification of the uterine artery restriction technique in the guinea pig fetus produces asymmetrical ultrasound growth. *Placenta* 30(3):236–240
 29. Heap RB, Deanesly R (1966) Progesterone in systemic blood and placentae of intact and ovariectomized pregnant guinea-pigs. *J Endocrinol* 34(4):417–423
 30. Mackenzie R, Walker M, Armson A, Hannah ME (2006) Progesterone for the prevention of preterm birth among women at increased risk: a systematic review and meta-analysis of randomized controlled trials. *Am J Obstet Gynecol* 194(5):1234–1242
 31. Ruiz RJ, Fullerton JT (1999) The measurement of stress in pregnancy. *Nurs Health Sci* 1 (1):19–25
 32. McKendry AA, Palliser HK, Yates DM, Walker DW, Hirst JJ (2010) The effect of betamethasone treatment on neuroactive steroid synthesis in a foetal Guinea pig model of growth restriction. *J Neuroendocrinol* 22(3):166–174
 33. Van den Bergh BR, Mulder EJ, Mennes M, Glover V (2005) Antenatal maternal anxiety and stress and the neurobehavioural development of the fetus and child: links and possible mechanisms. A review. *Neurosci Biobehav Rev* 29(2):237–258
 34. Van den Bergh BR, Marcoen A (2004) High antenatal maternal anxiety is related to ADHD symptoms, externalizing problems, and anxiety in 8- and 9-year-olds. *Child Dev* 75 (4):1085–1097
 35. Loomans EM, van der Stelt O, van Eijsden M, Gemke RJ, Vrijkotte T, den Bergh BR (2011) Antenatal maternal anxiety is associated with problem behaviour at age five. *Early Hum Dev* 87(8):565–570
 36. O'Connor TG, Heron J, Golding J, Beveridge M, Glover V (2002) Maternal antenatal anxiety and children's behavioural/emotional problems at 4 years. Report from the Avon Longitudinal Study of Parents and Children. *Br J Psychiatry* 180:502–508
 37. Buss C, Davis EP, Muftuler LT, Head K, Sandman CA (2010) High pregnancy anxiety during mid-gestation is associated with decreased gray matter density in 6-9-year-old children. *Psychoneuroendocrinology* 35(1):141–153
 38. Laplante DP, Brunet A, Schmitz N, Ciampi A, King S (2008) Project Ice Storm: prenatal maternal stress affects cognitive and linguistic functioning in 5 1/2-year-old children. *J Am Acad Child Adolesc Psychiatry* 47 (9):1063–1072
 39. King S, Mancini-Marie A, Brunet A, Walker E, Meaney MJ, Laplante DP (2009) Prenatal maternal stress from a natural disaster predicts dermatoglyphic asymmetry in humans. *Dev Psychopathol* 21(2):343–353
 40. Emack J, Kostaki A, Walker C-D, Matthews SG (2008) Chronic maternal stress affects growth, behaviour and hypothalamo-pituitary-adrenal function in juvenile offspring. *Horm Behav* 54(4):514–520
 41. Newnham JP, Jobe AH (2009) Should we be prescribing repeated courses of antenatal corticosteroids? *Semin Fetal Neonatal Med* 14 (3):157–163
 42. Quinlivan JA, Dunlop SA, Newnham JP, Evans SF, Beazley LD (1999) Repeated, but not single, maternal administration of corticosteroids delays myelination in the brain of fetal sheep. *Prenat Neonatal Med* 4:47–55
 43. Dunlop SA, Archer MA, Quinlivan JA, Beazley LD, Newnham JP (1997) Repeated prenatal corticosteroids delay myelination in the ovine central nervous system. *J Matern Fetal Med* 6 (6):309–313
 44. Huang WL, Harper CG, Evans SF, Newnham JP, Dunlop SA (2001) Repeated prenatal corticosteroid administration delays myelination of the corpus callosum in fetal sheep. *Int J Dev Neurosci* 19(4):415–425
 45. Seckl JR, Holmes MC (2007) Mechanisms of disease: glucocorticoids, their placental metabolism and fetal “programming” of adult pathophysiology. *Nat Clin Pract Endocrinol Metab* 3(6):479–488
 46. McTernan CL, Draper N, Nicholson H, Chalder SM, Driver P, Hewison M, Kilby MD, Stewart PM (2001) Reduced placental 11beta-hydroxysteroid dehydrogenase type 2 mRNA levels in human pregnancies complicated by intrauterine growth restriction: an analysis of possible mechanisms. *J Clin Endocrinol Metab* 86(10):4979–4983
 47. Matthews SG, Phillips DIW (2010) Minireview: transgenerational inheritance of the stress response: a new frontier in stress research. *Endocrinology* 151(1):7–13
 48. Kapoor A, Petropoulos S, Matthews SG (2008) Fetal programming of hypothalamic-pituitary-adrenal (HPA) axis function and behavior by

- synthetic glucocorticoids. *Brain Res Rev* 57 (2):586–595
49. Kapoor A, Matthews SG (2005) Short periods of prenatal stress affect growth, behaviour and hypothalamo-pituitary-adrenal axis activity in male guinea pig offspring. *J Physiol* 566 (Pt 3):967–977
 50. Bennett GA, Palliser HK, Saxby B, Walker DW, Hirst JJ (2013) Effects of prenatal stress on fetal neurodevelopment and responses to maternal neurosteroid treatment in Guinea pigs. *Dev Neurosci* 35(5):416–426
 51. Kapoor A, Dunn E, Kostaki A, Andrews MH, Matthews SG (2006) Fetal programming of hypothalamo-pituitary-adrenal function: prenatal stress and glucocorticoids. *J Physiol* 572 (Pt 1):31–44
 52. Dauprat P, Monin G, Dalle M, Delost P (1984) The effects of psychosomatic stress at the end of pregnancy on maternal and fetal plasma cortisol levels and liver glycogen in guinea-pigs. *Reprod Nutr Dev* 24(1):45–51
 53. Kapoor A, Matthews SG (2008) Prenatal stress modifies behavior and hypothalamic-pituitary-adrenal function in female guinea pig offspring: effects of timing of prenatal stress and stage of reproductive cycle. *Endocrinology* 149 (12):6406–6415
 54. Emack J, Matthews SG (2011) Effects of chronic maternal stress on hypothalamo-pituitary-adrenal (HPA) function and behavior: no reversal by environmental enrichment. *Horm Behav* 60(5):589–598
 55. Kapoor A, Leen J, Matthews SG (2008) Molecular regulation of the hypothalamic-pituitary-adrenal axis in adult male guinea pigs after prenatal stress at different stages of gestation. *J Physiol* 586(Pt 17):4317–4326
 56. Palliser HK, Bennett GA, Walker DW, Hirst JJ (2014) Prenatal stress causes sex specific persistent reductions in myelination and reactive astrocytes in adolescent guinea pig offspring, International Congress on Neuroendocrinology, Sydnese, p A371
 57. Paris JJ, Frye CA (2011) Juvenile offspring of rats exposed to restraint stress in late gestation have impaired cognitive performance and dysregulated progesterone formation. *Stress* 14 (1):23–32
 58. Wirth MM (2011) Beyond the HPA axis: progesterone-derived neuroactive steroids in human stress and emotion. *Front Endocrinol* 2:1–14
 59. Yawno T, Mortale M, Sutherland AE, Jenkin G, Wallace EM, Walker DW, Miller SL (2014) The effects of betamethasone on allopregnanolone concentrations and brain development in preterm fetal sheep. *Neuropharmacology* 85:342–348
 60. Berry NM, Robinson MJ, Bryan J, Buckley JD, Murphy KJ, Howe PR (2011) Acute effects of an *Avena sativa* herb extract on responses to the Stroop Color-Word test. *J Altern Complement Med* 17(7):635–637
 61. Robinson M, Mattes E, Oddy WH, Pennell CE, van Eekelen A, McLean NJ, Jacoby P, Li J, de Klerk NH, Zubrick SR, Stanley FJ, Newnham JP (2011) Prenatal stress and risk of behavioral morbidity from age 2 to 14 years: The influence of the number, type, and timing of stressful life events-. *Dev Psychopathol* 23:507–520
 62. Gibb BE, Chelminski I, Zimmerman M (2007) Childhood emotional, physical, and sexual abuse, and diagnoses of depressive and anxiety disorders in adult psychiatric outpatients. *Depress Anxiety* 24(4):256–263
 63. Meaney MJ, Szyf M, Seckl JR (2007) Epigenetic mechanisms of perinatal programming of hypothalamic-pituitary-adrenal function and health. *Trends Mol Med* 13(7):269–277
 64. Champagne DL, Bagot RC, van Hasselt F, Ramakers G, Meaney MJ, de Kloet ER, Joels M, Krugers H (2008) Maternal care and hippocampal plasticity: evidence for experience-dependent structural plasticity, altered synaptic functioning, and differential responsiveness to glucocorticoids and stress. *J Neurosci* 28 (23):6037–6045
 65. Bagot RC, Zhang TY, Wen X, Nguyen TT, Nguyen HB, Diorio J, Wong TP, Meaney MJ (2012) Variations in postnatal maternal care and the epigenetic regulation of metabotropic glutamate receptor 1 expression and hippocampal function in the rat. *Proc Natl Acad Sci U S A* 109(Suppl 2):17200–17207
 66. Tyzio R, Holmes GL, Ben-Ari Y, Khazipov R (2007) Timing of the developmental switch in GABA(A) mediated signaling from excitation to inhibition in CA3 rat hippocampus using gramicidin perforated patch and extracellular recordings. [Erratum appears in *Epilepsia*. 2007;48 (12):2380], *Epilepsia* 48(Suppl 5):96–105
 67. Ben-Ari Y (2002) Excitatory actions of gaba during development: the nature of the nurture. *Nat Rev Neurosci* 3(9):728–739
 68. Coleman HJ, Parkington HC (2013) The GABAA excitation-to-inhibition switch in the hippocampus of the perinatal guinea pig. *Fetal Neonatal Pysiol Soc Proc Abstract* 40
 69. Ben-Ari Y, Khalilov I, Kahle KT, Cherubini E (2012) The GABA excitatory/inhibitory shift

- in brain maturation and neurological disorders. *Neuroscientist* 18(5):467–486
70. Matthews SG (2007) Foetal experience: life-long consequences. *J Neuroendocrinol* 19(1):73–74
71. Crossley KJ, Nitsos I, Walker DW, Lawrence AJ, Beart PM, Hirst JJ (2003) Steroid-sensitive GABAA receptors in the fetal sheep brain. *Neuropharmacology* 45(4):461–472
72. Walker DW, Hirst JJ, Bennett GA, Cumberland AL, Shaw JC, Palliser HK (2015) Loss of steroid-mediated neuroprotection following stress in fetal life. 7th International Meeting on Steroids and the Nervous System, Proceedings pA6

Chapter 12

Placental Transport and Metabolism: Implications for the Developmental Effects of Selective Serotonin Reuptake Inhibitors (SSRI) Antidepressants

Juan C. Velasquez and Alexandre Bonnin

Abstract

A host of neurodevelopmental processes are modulated by serotonin (5-HT), a molecule also implicated in the etiology of diverse psychiatric disorders. Prenatal exposures that affect serotonergic signaling and the developing 5-HT system are increasingly associated with multiple long-term repercussions for the offspring. Both maternal depression and antidepressant treatments have been shown to affect fetal neurodevelopment during pregnancy, possibly through alterations of 5-HT levels that are otherwise precisely set by placental and endogenous sources. The result of such dysregulation impacts a variety of critical signaling pathways, and eventually leads to long-term effects on postnatal brain function. This chapter provides investigators with details of recently developed methods that can be applied to the study of how maternal–fetal transfer of therapeutic drugs, such as selective serotonin reuptake inhibitors (SSRIs), cross the placenta and impact fetal brain circuit development.

Key words Placenta, Serotonin, Tryptophan, SSRI, Depression, Fetal programming, Placental transfer

1 Background and Overview

Serotonergic signal transduction throughout the nervous system involves 17 different serotonin (5-hydroxytryptamine; 5-HT) receptors subtypes, each unique in cellular and molecular aspects, tissue distribution, and gene expression [1, 2]. Despite innate differences within the serotonergic receptor family, they all have 5-HT as their ligand in common. The structural and functional features of the serotonergic system, namely its abundant and widespread anatomical projections, along with diverse receptor subtypes, provide great insight into how 5-HT is involved in almost every imaginable developmental, physiological, and behavioral process throughout life. It follows that altered 5-HT tissue concentration may potentially lead to generalized aberrant signaling through

more than one receptor subtype simultaneously, having widespread effects across several domains.

Many drugs indicated for the treatment of symptoms observed in neuropsychiatric conditions such as major depression, anxiety, schizophrenia and obsessive-compulsive disorder target serotonergic mechanisms [3–6]. This befits the notion that 5-HT is implicated in the regulation of multiple processes orchestrating cognitive, behavioral, and physiological functions. Most interestingly, before its role in adult neurotransmission, 5-HT signaling plays critical functions during brain development—an idea that stems from the early appearance of serotonergic neurons, axons, and receptors in the brain [7–12]. Consistent with a potential role in the fetal programming of adult mental disorders, basic and epidemiological findings have linked developmental disruption of 5-HT signaling to diverse functional disorders in adulthood [13–19]. In particular, animal studies have shown that prenatal and early postnatal exposure to selective serotonin reuptake inhibitors (SSRIs), which inhibit the 5-HT transporter (SERT; *Slc6a4*) activity and reuptake of 5-HT in neurons and other cell types, induces anxious behaviors much later in the adult offspring [8, 20–24]. As discussed in the next sections, the molecular mechanisms by which this early developmental exposure has long-term consequences on adult brain function remain largely unknown. As more mechanistic influences of 5-HT signaling on various aspects of fetal brain development and their long-term consequences are being uncovered, this signaling pathway will undoubtedly become a central tenet of the developmental programming of adult mental disorders [25–27].

This chapter also provides brief discussions on the development of the serotonergic system and its relevance to the fetal programming of adult mental disorders. Of particular interest is prenatal exposure to maternal depression and antidepressants, both suggested to alter fetal brain development. Additionally, it outlines innovative techniques that can be applied to study the effects of gestational exposure to therapeutic drugs such as SSRIs on placental physiology and fetal brain development.

1.1 Serotonin and Fetal Brain Development

Serotonergic development is a complex, multi-organ process with specific spatial and temporal patterns of receptors expression, which has emerged as a powerful influence on the causality of several neuropsychiatric disorders [16, 17, 28]. This focus has increased further in light of the early presence of 5-HT and the recent discovery of the placental origin of 5-HT in the fetal brain [16, 29]. Serotonergic neurons generate one of the most ubiquitous circuits in the mammalian brain. 5-HT cell bodies emerge early in fetal development (~embryonic day (E)10 in mice) and cluster in the raphe nuclei; over the following days of murine fetal development, 5-HT neurons rapidly form vast axonal projections that

essentially innervate all regions of the neural axis in a caudal-to-rostral gradient [30, 31]. Intriguingly, 5-HT itself and several of its receptors are already present in the rostral part of the fetal forebrain before a single 5-HT axon has reached the area (prior to E14.5) [28, 32, 33]. This led to the discovery that the fetal forebrain accumulates placentally synthesized 5-HT during early pregnancy [16, 29]. Thus, the placenta acts as an exogenous source of 5-HT for the forebrain at a time when the endogenous 5-HT system has yet to fully mature.

1.2 Prenatal Exposures and Effects on Fetal Brain Development

5-HT is a key trophic factor during fetal and early postnatal development, modulating critical histogenic processes such as neuronal cell proliferation, migration, and brain circuit wiring [14, 32, 34–38]. Transient genetic (e.g., 5-HT_{1A} receptor knockout) and pharmacological (e.g., exposure to SSRIs) disruption of 5-HT signaling during critical periods of fetal and early postnatal brain development lead to long-term behavioral abnormalities, such as increased anxiety in adulthood [39–41]. These far-reaching functional consequences may arise due to abnormal serotonergic system development leading to, or originating from, altered 5-HT concentration and aberrant ligand/receptor interactions in fetal brain tissue. Thus, genetic and environmental factors that alter tissue levels of 5-HT during pregnancy may lead to abnormal signaling in the developing fetal brain, a potential mechanism for the developmental origins of adult mental disorders. Such is a possibility for about 15 % of pregnant women that are diagnosed with Major Depression Disorder (MDD) during gestation, a leading cause of disability worldwide [42–44]. Despite an unclear safety profile, a lack of well-controlled safety studies, and assignments to Pregnancy Categories C and D by the US Food and Drug Administration, about 9 % of pregnant women diagnosed with MDD in the USA are prescribed a SSRI antidepressant during all or part of their pregnancy, a figure that has been steadily on the rise [45, 46].

In the adult brain, SSRIs inhibit SERT-mediated 5-HT reuptake activity, resulting in increased 5-HT concentration at the synapse, which contributes to relieving symptoms of maternal depression [47]. For the fetus however, since SERT is expressed early in the brain (e.g., E12 in raphe serotonergic neurons and E14 in thalamic neurons) [10, 48], early exposure to SSRIs is likely to alter overall fetal tissue concentrations of 5-HT, resulting in broad effects on 5-HT signaling [9, 11, 12]. Developmental alterations of 5-HT signaling *in vivo* have been shown to affect the formation of major axonal circuits in the fetal brain. For instance, the genetic manipulation of two G_i-protein coupled 5-HT receptors (*htr1b* and *htr1d*) expression by *in utero* electroporation at E12.5, specifically in developing thalamic neurons, led to abnormal thalamocortical axon (TCA) pathway formation 4–6 days later [32]. This was shown to arise from 5-HT receptor-mediated changes in

intracellular cAMP in thalamic neurons, which modulates the response of growing TCAs to guidance cues during initial pathway formation. Together with the finding that the commonly prescribed SSRI Citalopram directly affects the response of TCAs to guidance cues in vitro independently of 5-HT signaling [49], these results suggest that fetal brain exposure to SSRIs may directly or indirectly alter the formation of TCA pathways. Thus, fetal brain exposure to maternally ingested SSRIs may potentially lead to functional alterations of the circuits that underlie social, emotional, and cognitive higher functions in the offspring [49].

For the fetus, the maternal depressive state is one of the earliest adverse experiences resulting in poor pregnancy outcomes and an induction of long-term adverse effects [40, 42, 45, 50–53] (Fig. 1a). The dilemma arises when both the pharmacological intervention to alleviate the maternal condition and the illness itself pose serious risks to fetal health, an unfavorable scenario in which a

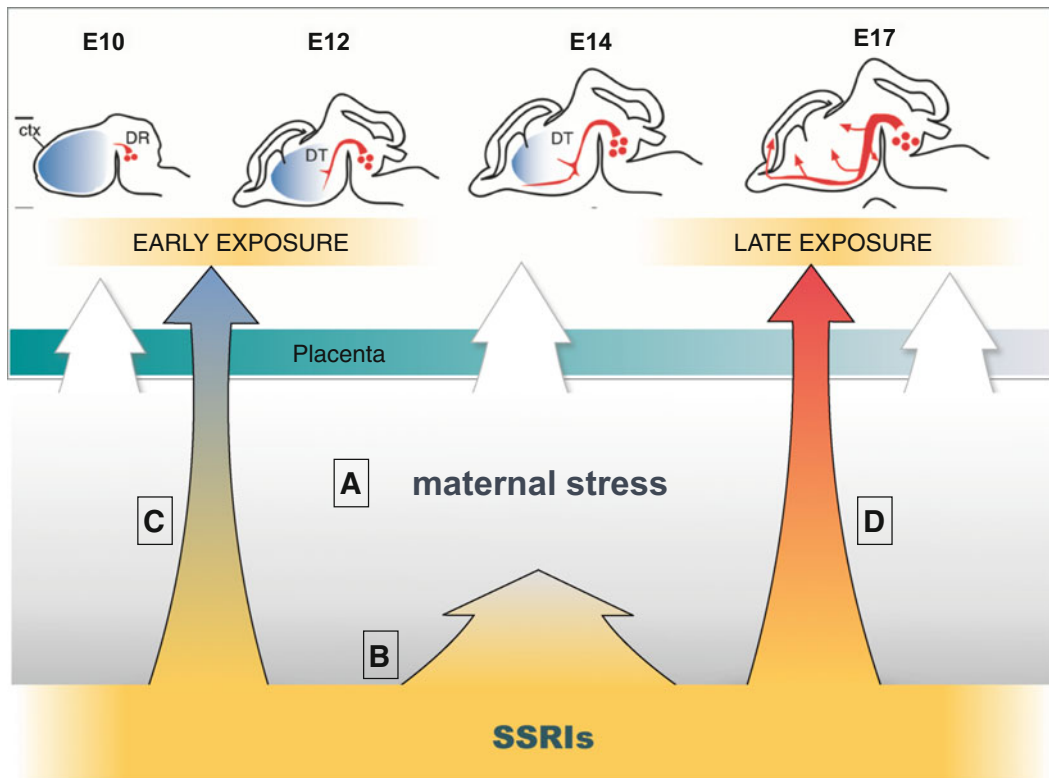


Fig. 1 Effects of prenatal exposures to stress and SSRIs on the fetal brain. Effects of SSRIs on fetal brain development may be through direct or indirect pathways. (A) In untreated maternal depression, the fetal brain may be continuously exposed to maternal stress effects. (B) SSRIs may relieve maternal stress and indirectly prevent its effects on fetal brain development. At the same time, SSRIs may transfer through the placenta, reach the fetal brain, and alter (C) early (e.g., neuronal differentiation; or (D) late (e.g., axon growth and guidance) phases of fetal brain development. SSRIs selective serotonin reuptake inhibitors, ctx cortex, DR dorsal raphe, DT dorsal thalamus

risk-benefit decision must be made. Accumulating epidemiological studies show increased risks for a variety of physiological, cognitive, and developmental disorders (extensively reviewed here [17, 43]), including the recent increased associated risk for Autism Spectrum Disorders [19, 54]. Although important, these studies cannot delineate between the risks brought about by SSRIs from those attributed to the underlying maternal depressive disorder (Fig. 1a, b).

As with maternal depression, SSRI use during pregnancy has often been associated with poor pregnancy outcomes [55–59]. To explain how maternal SSRI therapy may affect brain development in the offspring of mothers coping with depression, some studies suggest that they cross the placenta into the fetal circulation, although this evidence is based on drug measures taken from umbilical cord blood at birth and transfer studies at term in the human perfused placental cotyledon model [58, 60–62]. Like the fetus, the placenta is in a state of developmental flux in both structure and function, and its progressive remodeling has yet to be considered in the context of transplacental transport earlier in gestation when highly sensitive developmental milestones are taking place [63–65]. In any event, once in the fetal compartment, SSRIs may directly target brain SERT and affect baseline 5-HT levels and signaling, thereby impacting early (neuronal differentiation) or late (axon growth and guidance) phases of brain development (Fig. 1c, d).

Alternatively, SSRIs may impact placental physiology in such a way that the effects indirectly impact the fetus. Since the fetal brain acquires placenta-derived 5-HT during a critical period of widespread axonal outgrowth, the effects of SSRIs on fetal brain development may be through an indirect pathway that affects placental tryptophan metabolism to 5-HT, resulting in downstream effects on the fetus. Although it is not clear whether SSRI exposure induces physiological changes in the placenta, its high expression of SERT support the notion that SSRIs would have high binding affinity in this organ [66–69]. If blocking SERT function alters placental 5-HT synthesis and/or transport to the fetus, the placenta's key function of maintaining fetal homeostasis may be compromised by SSRIs.

In summary, the impact of SSRIs on fetal brain development may result from direct actions on the fetal brain, indirect actions on placental or maternal physiology or, more likely, a combination of all these routes. Exposure to SSRIs at a time surrounding critical developmental milestones may very well have profound, long-lasting implications on offspring brain function; most importantly, these effects have yet to be considered in the context of the underlying maternal depression, which may significantly impact brain development and function if left untreated. Thus, the question arises as to whether SSRIs cross the placenta, and if so, to what

extent do they access the fetal blood compartment and reach the fetal brain at different stages of pregnancy? The next sections describe innovative *ex vivo* and *in vivo* methods to explore these questions and to begin to assess the mechanisms by which *in utero* exposure to antidepressants may alter neurodevelopmental processes.

2 Materials, Equipment, and Setup

One of the major challenges of studying how extrinsic factors impact development during pregnancy is its physiologically dynamic state. Developmental programs are precisely modulated both in time and space; a particular developmental process may thus be affected at certain time points and locations but not others. A rigorous, multifaceted set of techniques, all done at various developmental time-points of interest, are necessary to gain meaningful insight into gestational conditions. The *ex vivo* perfusion of the mouse placenta procedure provides the framework for studying placental drug transport, independently of maternal and fetal metabolism. In contrast, *in vivo* studies of SSRI exposures are designed to quantify the pharmacokinetics of drug transfer to the fetal compartment, and the influences of maternal and fetal metabolism on these parameters. These observations can be correlated with immunohistochemical analyses of fetal brain architecture. The sections that follow detail experimental protocols for performing perfusion of the mouse placenta, *in vivo* exposures of SSRIs, and immunohistochemical analysis. Any animal tissue should be collected in compliance with legislative and institutional requirements.

2.1 Ex Vivo Perfusion of the Mouse Placenta for Bidirectional Drug Transport Studies

This procedure provides the framework for directly studying transplacental passive/active molecular transport and the downstream consequences this might have for the developing fetus. *Ex vivo* perfusion systems offer a reliable, reproducible method for studying acute physiological responses of an organ to various environmental manipulations while maintaining the cellular organization, compartmentalization and three-dimensional structure intact. The perfusion procedure, which can be completed in 4–5 h, allows for integrated, physiological studies of *de novo* synthesis and metabolism and transport of materials across the live mouse placenta.

The system can be used to measure the short-term maternal–fetal transfer pharmacokinetics of individual SSRIs at different stages of gestation, independent of maternal and fetal metabolism. Following microcannulations of placental vasculature, perfusion solutions of known composition are infused into the maternal and fetal sides of an isolated mouse placenta that is maintained in a thermostated, oxygenated chamber (Fig. 2). Peristaltic pumps keep perfusion media flowing at steady, physiological rates uniquely

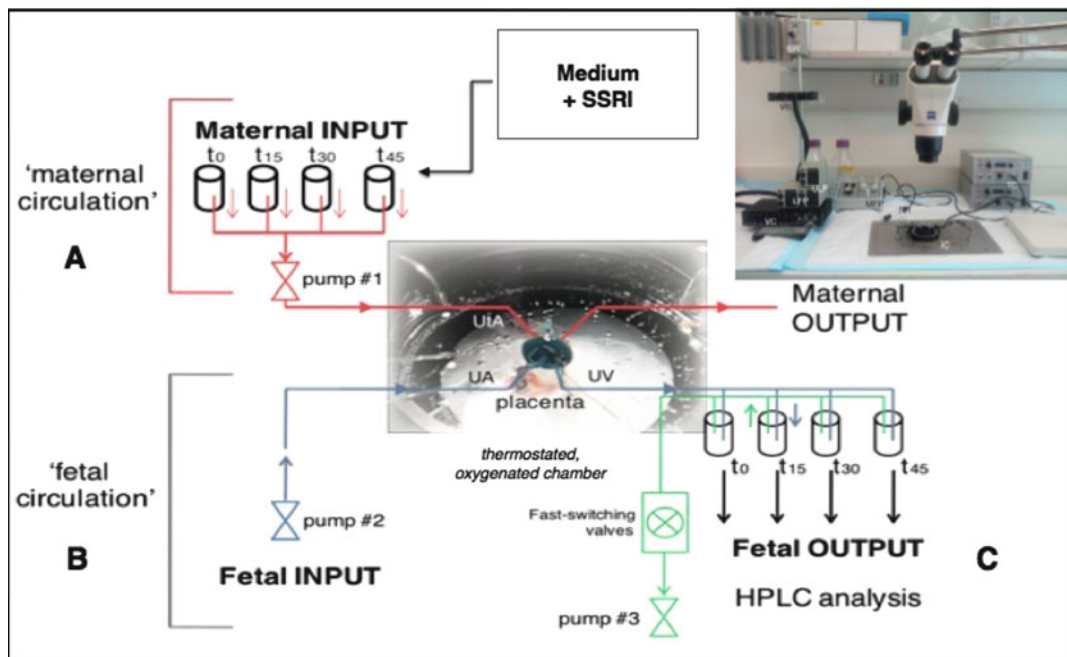


Fig. 2 Schematics of the ex vivo dual perfusion system. The artificial maternal circulation consists of a multichannel, fast-switching peristaltic perfusion system (pump #1) (a) connected to the uterine artery on the maternal side of the placenta. The artificial fetal circulation consists of a single-channel peristaltic perfusion system (pump #2) connected to the umbilical artery (b) and a multichannel negative-pressure peristaltic collection system (pump #3) connected to the umbilical vein (c) on the fetal side of the placenta. *SSRI*, selective serotonin reuptake inhibitor, *HPLC-FLD* high pressure liquid chromatography coupled with fluorescence detection

adapted to the maternal and fetal circulations. For maternal–fetal transfer, the fetal perfusion output can be collected through the umbilical vein for analysis (Fig. 2c).

The perfusion system theory and setup, along with a list of equipment, materials, procedural notes, and troubleshooting guidelines, have been extensively detailed in both a protocols publication [70] and a textbook chapter [71]. This chapter thus focuses on customizing this technique for the pharmacokinetic study of transplacental transfer of SSRIs.

2.1.1 Reagents

1. M199 medium without phenol red (Corning Cellgro, Cat. No. 90-050-PB).
2. Bovine Serum Albumin (AMRESCO, Cat. No. 0332).
3. Heparin (Sigma-Aldrich, Cat. No. H3149).
4. Glucose (BDH, Cat. No. BDH8005).
5. Dextran40 (TCI, Cat. No. D1448).
6. Sodium bicarbonate (BDH, Cat. No. BDH0280).

7. L-glutamine (Alfa Aesar, Cat. No. A14201).
8. Fast green dye (Haleco, Cat. No. 19143).
9. Phosphoric acid (EMD Millipore, Cat. No. 4809391000).
10. Citalopram hydrobromide (Tocris, Cat. No. 1427).
11. Desmethylcitalopram hydrobromide (Sigma-Aldrich, Cat. No. D-047).
12. Fluoxetine hydrochloride (Sigma-Aldrich, Cat. No. F132).
13. Norfluoxetine hydrochloride (Sigma-Aldrich, Cat. No. F133).
14. Paroxetine hydrochloride (Sigma-Aldrich, Cat. No. 1500218).
15. Antipyrine (Sigma-Aldrich, Cat. No. 10790).
16. Potassium phosphate monobasic (Sigma-Aldrich, Cat. No. P0662).
17. Acetonitrile, HPLC Grade (EMD Millipore, Cat. No. AX0145).
18. Perchloric acid (EMD Millipore, Cat. No. 1005171000).

2.1.2 Equipment

1. SpeedVac Concentrator (Thermo-Savant SPD1010, Thermo Fisher Scientific, Massachusetts, USA).
2. High Pressure Liquid Chromatography System (Eicom 700, Eicom Corporation, Kyoto, Japan).
3. Fluorescence Detector (Shimadzu RF-20A-XS, Shimadzu, Kyoto, Japan).

2.2 *In Vivo Studies of SSRI Transfer to the Fetal Compartment*

SSRIs given during pregnancy may reach the fetal brain and alter various critical phases of fetal brain development. Direct drug action on the fetal brain requires that SSRIs cross the maternal–fetal placental barrier. In this context, the effect of SSRIs on brain development largely depends on the transfer of SSRIs to the fetal compartment. In vivo maternal–fetal transfer measures following timed drug exposures are useful to measure detailed profiles of maternal metabolism and the disposition of the drug of interest and its metabolites to the fetus.

2.2.1 Reagents

1. Physiological saline (BD, Cat. No. 221819).
2. Citalopram hydrobromide (Tocris, Cat. No. 1427).
3. Desmethylcitalopram hydrobromide (Sigma-Aldrich, Cat. No. D-047).
4. Fluoxetine hydrochloride (Sigma-Aldrich, Cat. No. F132).
5. Norfluoxetine hydrochloride (Sigma-Aldrich, Cat. No. F133).
6. Paroxetine hydrochloride (Sigma-Aldrich, Cat. No. 1500218).
7. Antipyrine (Sigma-Aldrich, Cat. No. 10790).
8. Perchloric acid (EMD Millipore, Cat. No. 1005171000).

9. Potassium phosphate monobasic (Sigma-Aldrich, Cat. No. P0662).
10. Acetonitrile, HPLC Grade (EMD Millipore, Cat. No. AX0145).

2.2.2 Equipment

1. High Pressure Liquid Chromatography System (Eicom 700, Eicom Corporation, Kyoto, Japan).
2. Fluorescence Detector (Shimadzu RF-20A-XS, Shimadzu, Kyoto, Japan).

3 Methods

3.1 *Ex Vivo Perfusion of the Mouse Placenta for Bidirectional Drug Transport Studies*

The placenta perfusion setup, method, and procedure should be followed according to previous publications [70, 71]. This section focuses on the media preparation customized for the simulated maternal and fetal blood supplies for transfer studies, in addition to instructions for perfusion sample preparation and analysis using High Pressure Liquid Chromatography coupled with Fluorescence Detection (HPLC-FLD).

3.1.1 *Perfusion Solutions*

Maternal Solution

1. M199 Medium without phenol red.
2. Bovine serum albumin (2.9 g/dL).
3. Heparin (20 IU USP/mL).
4. Dextran40 (7.5 g/L).
5. Glucose (1 g/L).
6. Sodium bicarbonate (2.2 g/L).
7. L-glutamine (100 mg/L).
8. Fast-green dye (0.001 %).
9. pH 7.3 with 1 M phosphoric acid.

Fetal Solution

1. M199 Medium without phenol red.
2. Bovine serum albumin (2.9 g/dL).
3. Heparin (20 IU USP/mL).
4. Dextran40 (30 g/L).
5. Glucose (0.5 g/L).
6. Sodium bicarbonate (2.2 g/L).
7. L-glutamine (100 mg/L).
8. Fast-green dye (0.001 %).
9. pH 7.3 with 1 M phosphoric acid.

Pharmacological substances of interest may be added to either maternal or fetal solutions above according to the directional

transfer study of interest. Unlike *in vivo* studies which would have to rely on the use of radioactively labeled molecules, this technique and detection method allow the versatility for maternal–fetal or fetal–maternal transplacental transfer of native (unlabeled) compounds. Antipyrine (1 µg/mL), a freely diffusible substance across the placental barrier, should also be included as a measure of perfusion efficiency and as an internal positive control [72, 73].

3.1.2 Perfusion Sample Preparation and Analysis

Once perfusion samples have been collected at the desired intervals, these can be stored at -80°C until time of analysis. Investigators should be aware of drug degradation resulting from freeze–thaw cycles and length of storage (which should be measured independently). This section outlines sample preparation procedure and HPLC–FLD chromatographic conditions.

Sample Preparation

1. Thaw perfusion sample on ice.
2. Measure sample volume and add acetonitrile (1:1 v/v) to deproteinate the sample.
3. Vortex sample and incubate at room temperature for 10-min.
4. Separate the precipitated proteins by centrifugation at 5000-rpm for 10-min.
5. Collect and measure the supernatant volume.
6. Evaporate sample in SpeedVac concentrator at room-temperature. Evaporation time will vary depending on sample starting volume.
7. Using a 0.2 M perchloric acid with 100 µM EDTA-2Na solution, resuspend evaporated sample in half of the supernatant volume (**Step 5**) following acetonitrile extraction (this corresponds to the original sample volume).
8. Analyze sample by HPLC–FLD.
9. Standard calibration curves can be made using stock compounds appropriately diluted in a solution composed of 0.2 M perchloric acid with 100 µM EDTA-2Na.

HPLC–FLD Chromatographic Conditions

HPLC–FLD analysis can be performed using an Eicom 700 system coupled to a Shimadzu RF-20AX fluorescence detector. An Eicom-pak SC-30DS C₁₈ reversed-phase column packed with 3-µm silica particles (3.0 × 100 mm I.D.) is used as the analytical column. A 10 µL aliquot of extracted sample is injected onto the column and eluted with a mobile phase of 10 mM KH₂PO₄–acetonitrile (3:1 v/v) (pH = 4.0 with 1 M phosphoric acid), at a flow rate of 500 µL/min. Using the same system, other analytic conditions can be customized for each SSRI, each molecule having a specific chromatographic profile (Fig. 3).

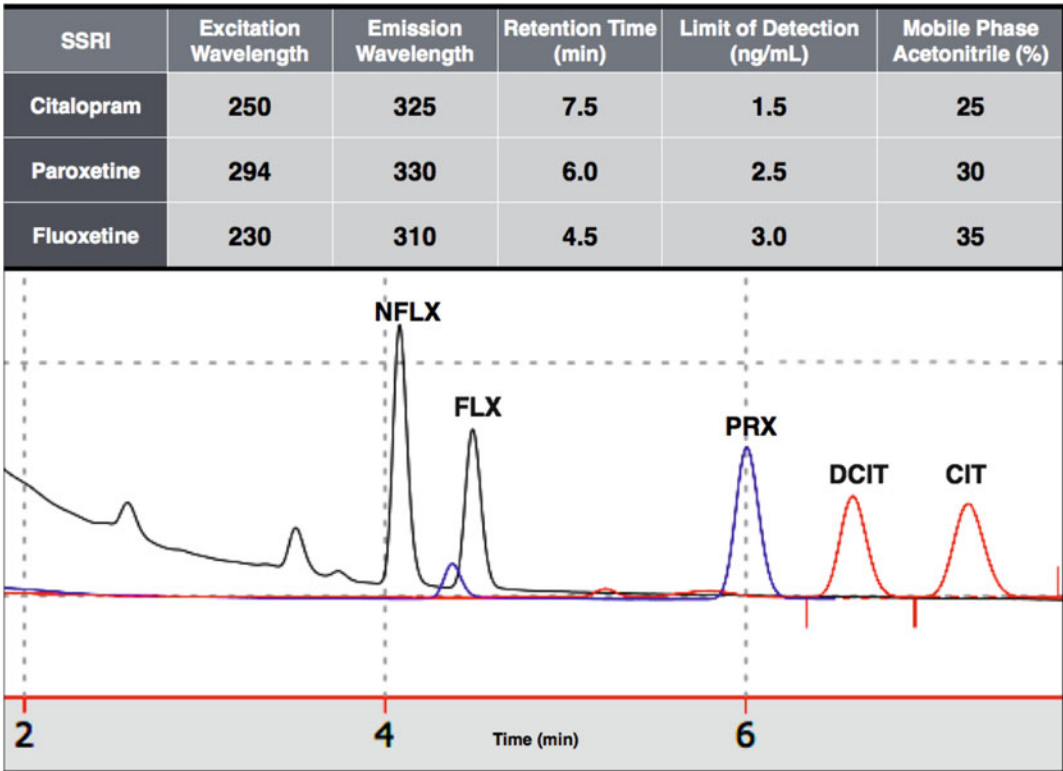


Fig. 3 Chromatographic conditions for the detection of SSRIs. Different drugs in the SSRI class can be detected by making minor modifications to the detection wavelengths of the HPLC-FLD system and the acetonitrile composition of the mobile phase. Each compound will have a specific chromatographic signature varying in retention time and sensitivity. The technique allows for highly sensitive assays that grant investigators great versatility for quantifying different species of interest. *SSRI* selective serotonin reuptake inhibitor, *NFLX* norfluoxetine, *FLX* fluoxetine, *PRX* paroxetine, *CIT* citalopram, *DCIT* desmethylcitalopram

Determination of Antipyrine

The perfusion samples can be assessed for antipyrine concentration with the use of a spectrophotometer. Since the perfusion samples consist of a modified cell culture medium, several endogenous molecular species may generate interfering, background measures. Therefore, to quantify maternal–fetal transfer of antipyrine, fetal solution without antipyrine must be extracted and prepared as above in the “[Sample Preparation](#)” section. This solution should be used as a blank and to prepare the calibration standard dilutions from stock antipyrine. The spectrophotometer detection wavelength should be set at 240 nm. This method provides a quick, reliable assay of antipyrine quantification with a limit of detection of ~10 ng/mL. If needed, higher sensitivity can be achieved with an HPLC system coupled to ultraviolet (UV) detection [74].

3.2 In Vivo Studies of SSRI Transfer to the Fetal Compartment

3.2.1 Treatment

Working with a timed-pregnant dam at a developmental time of interest, administer drug of interest at a dosage shown to provide efficacious therapeutic effects in mice. For the SSRI Citalopram, our lab performs intraperitoneal (i.p.) injections with 20 mg/kg of body weight resuspended and filter-sterilized in a physiological saline volume of 0.01 mL/g of drug [75, 76]

3.2.2 Dissection

Following a timed exposure to the drug, pregnant dams are anesthetized with a lethal dose of isofluorane. Before performing a cervical dislocation and caesarean section, the dam is assessed for loss of corneal reflex and lack of responsiveness to toe pinch. A midline incision is then made through the skin over the abdomen using sterile scissors. Using a second pair of sterile scissors and forceps, the underlying muscle layer is cut, exposing the uterine horns, which are then carefully removed and placed in a sterile petri dish with cold Phosphate Buffer Saline (PBS). As a secondary measure to ensure euthanasia, the diaphragm of the dam is severed following removal of the uterus. A cardiac puncture is performed with a 25 G syringe needle to collect a maternal blood sample for drug metabolism analysis (usually ~1 mL per dam). Using new sterile instruments and under a dissection microscope, the fetuses are removed from the uterine horns, placentas isolated and flash frozen in liquid nitrogen prior to storage at -80°C . The embryos are then decapitated and the fetal blood collected through the exposed carotid and jugular vasculature using a pipette; the blood from at least ten embryos per dam is collected and pooled into a tube on ice. The brains can then be dissected and flash-frozen before storing at -80°C . Both the maternal and the fetal blood should be left on ice for 30-min prior to centrifuging at $2000 \times g$ for 10-min at 4°C . The sera (supernatant) is then collected and stored at -80°C .

3.2.3 Sample Preparation

1. Prepare extraction buffer, composed of 0.2 M perchloric acid, 100 μM EDTA-2Na and 100 ng/mL isoproterenol, to use as an internal standard.
2. Add 0.5 mL of ice-cold extraction buffer per 100 mg of tissue. For fetal blood serum, add equal amounts of sample and extraction buffer (1:1 v/v). Maternal blood serum requires a higher dilution with extraction buffer (1:3 v/v).
3. Tissue should be homogenized or sonicated until it is fully suspended in a homogeneous solution. Time and sonication power will vary depending on the age and tissue type, but consistency across similar samples must be maintained.
4. Denature the protein by keeping the homogenate in an ice bath for 30 min
5. Spin at $20,000 \times g$ for 15-min at 4°C .
6. Remove and measure the supernatant volume, analyze by HPLC-FLD using the chromatographic conditions outlined in Sect. 3.1.2 above.

7. Standard curves can be made using stock compounds appropriately diluted in the extraction buffer solution (**Step 1**).
8. Quantify drug measures, adjust for sample dilutions and internal standard.
9. Measure protein concentration in each sample using a bovine serum albumin (BSA) assay to normalize drug measures to protein content.

4 Notes and Expected Results

4.1 *Ex Vivo* Perfusion of the Mouse Placenta for Bidirectional Drug Transport Studies

Analysis of perfusion samples can be used to study the pharmacokinetic profile of bidirectional transfer of drugs across the placenta. Following HPLC-FLD analysis, the transplacental transfer percentage (TPT) of each drug and associated metabolite is calculated using the following equation: $TPT = (C_f \times S_f \times 100) / (C_m \times S_m)$; where C_f is the concentration in fetal venous outflow, S_f is the fetal flow rate (3–5 $\mu\text{L}/\text{min}$ —depending on age [70]), C_m is the SSRI concentration in maternal arterial inflow, and S_m is the maternal flow rate (16–20 $\mu\text{L}/\text{min}$). The transplacental transfer index (TI) (i.e., the ratio of transfer between SSRI and antipyrine—used as internal standard) is calculated by dividing the $TPT_{(\text{SSRI})}$ by the $TPT_{(\text{antipyrine})}$. Based on preliminary data obtained with the SSRI CIT *ex vivo* (Fig. 4), we observe differential transfer between the parent drug and its metabolite throughout the perfusion at E18. *Ex vivo* maternal–fetal TPT measures can then be correlated to short-term *in vivo* measures of fetal blood and brain tissue drug concentrations (see below) for the estimation of drug metabolism and disposition to the fetal compartment.

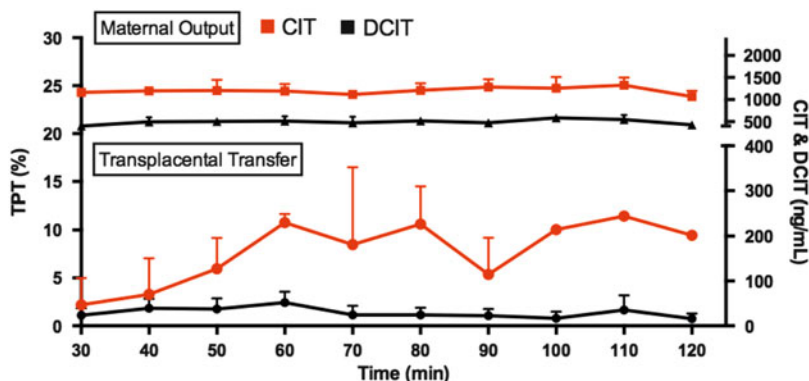


Fig. 4 Transplacental transfer of CIT and DCIT. An E18 CD-1 mouse placenta was perfused with 1500 ng/mL of CIT and 500 ng/mL of DCIT through the maternal input side (uterine artery) for 120 min. The fetal perfusion outputs were collected through the umbilical vein and analyzed for quantification of CIT and DCIT. Transplacental transfer (TPT) ratios were measured every 10 min for 120 min after a 30 min stabilization period (*lower traces*). *Upper traces*: steady input of CIT and DCIT measured simultaneously through the output side of the uterine artery; $n = 2$ independent perfusions. *CIT* citalopram, *DCIT* desmethylcitalopram

4.2 In Vivo Studies of SSRI Transfer to the Fetal Compartment

Measures of in vivo maternal–fetal transfer from our lab show that maternal CIT and its metabolite DCIT reach the fetal blood stream and fetal brain within 15-min following i.p. injection of 20 mg/kg CIT at E18 (Fig. 5). This technique can be applied to obtain a comprehensive pharmacokinetic profile of maternal metabolism and transfer to the fetus across several time points. Furthermore, it can be used to assess gestational differences in terms of drug disposition to the fetal compartment.

While the determination of SSRI concentrations in the fetal blood and brain is an indication of in vivo exposures, the question of the biological impact that different exposure paradigms and maternal treatment regimens have on fetal development still remains. Examination of the fetal brain architecture is one way to determine how SSRIs and maternal stress affect the development of the serotonergic system and TCA formation. Immunohistochemical (IHC) imaging studies (Fig. 6) and quantification of immunofluorescence distribution allow high-resolution visualization and accurate identification of 5-HT neurons (5-HT+) and axons and TCAs (netrin-G1a+) throughout the rostro-caudal extent of the fetal brain [32]. These measures can be done in 20 μ m-thick

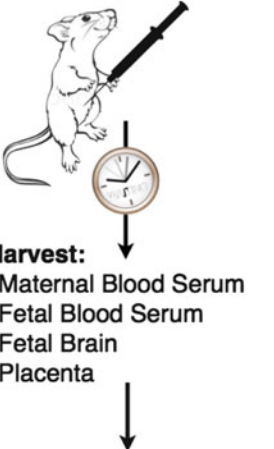
i.p injection of timed-pregnant E18 mouse with 20mg/kg CIT	Sample	CIT (ng/mg of protein)	DCIT (ng/mg of protein)
 <p>Harvest:</p> <ul style="list-style-type: none"> • Maternal Blood Serum • Fetal Blood Serum • Fetal Brain • Placenta <p>HPLC-FLD Analysis</p>	Maternal Blood Serum	1078	94.1
	Placenta	139.4	7.89
	Fetal Blood Serum	753.4	39.2
	Fetal Brain	131.1	3.67

Fig. 5 In vivo maternal–fetal transfer of CIT and DCIT. A CD-1 timed-pregnant mouse was injected i.p. with 20 mg/kg of Citalopram (CIT). After 15-min, maternal and fetal blood serum along with placental and fetal brain tissue was harvested. These samples were prepared for HPLC-FLD analysis for quantification of CIT and its metabolite desmethylcitalopram (DCIT). *i.p.* intraperitoneal, *HPLC-FLD* high pressure liquid chromatography coupled with fluorescence detection

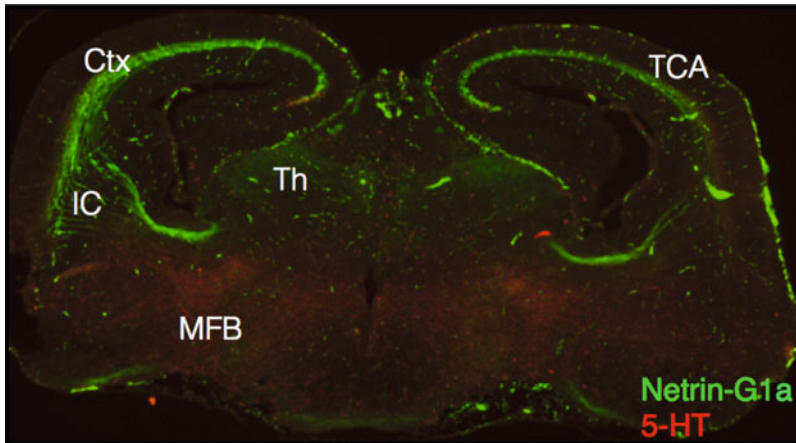


Fig. 6 Immunohistochemistry of the fetal brain. Antibody staining for 5-HT (red) and Netrin-G1a expressing thalamocortical axons (TCA; green) of CD-1 fetal mouse brain at E18. After dissection, brains were fixed overnight and dehydrated through sucrose gradients prior to embedding. The fetal brain was then sliced in 20- μ m sections and stained. Netrin-G1a signal has been amplified with a Tyramide Signal Amplification (TSA) kit. In the rostral forebrain, 5-HT-positive axons can be visualized in the medial forebrain bundle (MFB). The path of thalamocortical axons from the thalamus (Th), through the internal capsule (IC) to the cortex (Ctx) is clearly visible. Relative immunofluorescence distribution analysis can be used to quantify the effects of drug treatment on 5-HT and TCA axonal pathway formation

coronal and sagittal sections encompassing the whole fetal brain, as previously described [29, 32, 77]. Specific regions of interest can be delimited for quantification: relevant structures include (1) from the medial cortex to the claustrum (for netrin-G1a+ TCAs), and (2) from the hypothalamus midline to the internal capsule, including the medial forebrain bundle (for 5-HT+ axons) (Fig. 6).

5 A Concluding Perspective on the Effects of Prenatal Exposures on Fetal Brain Development

Transient disruptions of essential signaling events during critical developmental periods may have lasting effects that are expressed throughout life. The ubiquitous role of 5-HT signaling in brain development and adult brain function befits that early perturbations of the serotonergic system are increasingly implicated in the etiology of several neuropsychiatric conditions. In particular, developmental perturbations of serotonergic signaling by in utero exposure to maternal depression and SSRIs may affect the formation of functional somatosensory circuits such as thalamocortical axon pathways. The techniques described in this chapter were designed to provide direct functional correlation between in utero exposure to therapeutic drugs such as SSRIs and developmental perturbations resulting in abnormal formation of serotonergic/thalamocortical axon pathways that may ultimately have far-reaching functional consequences throughout life.

References

1. Hoyer D, Hannon JP, Martin GR (2002) Molecular, pharmacological and functional diversity of 5-HT receptors. *Pharmacol Biochem Behav* 71:533–554
2. American College of Neuropsychopharmacology (2002) *Neuropsychopharmacology: the fifth generation of progress: an official publication of the American College of Neuropsychopharmacology*. Lippincott Williams & Wilkins, Philadelphia, PA
3. Blasi G, De Virgilio C, Papazacharias A et al (2013) Converging evidence for the association of functional genetic variation in the serotonin receptor 2a gene with prefrontal function and olanzapine treatment. *JAMA Psychiatry* 70:921–930
4. Stein MB, Seedat S, Gelernter J (2006) Serotonin transporter gene promoter polymorphism predicts SSRI response in generalized social anxiety disorder. *Psychopharmacology (Berl)* 187:68–72
5. Hu X-Z, Lipsky RH, Zhu G et al (2006) Serotonin transporter promoter gain-of-function genotypes are linked to obsessive-compulsive disorder. *Am J Hum Genet* 78:815–826
6. Gorman JM, Kent JM (1999) SSRIs and SNRIs: broad spectrum of efficacy beyond major depression. *J Clin Psychiatry* 60(Suppl 4):33–38, discussion 39
7. Lidov HG, Molliver ME (1982) An immunohistochemical study of serotonin neuron development in the rat: ascending pathways and terminal fields. *Brain Res Bull* 8:389–430
8. Gaspar P, Cases O, Maroteaux L (2003) The developmental role of serotonin: news from mouse molecular genetics. *Nat Rev Neurosci* 4:1002–1012
9. Lebrand C, Cases O, Wehrlé R et al (1998) Transient developmental expression of monoamine transporters in the rodent forebrain. *J Comp Neurol* 401:506–524
10. Lebrand C, Cases O, Adelbrecht C et al (1996) Transient uptake and storage of serotonin in developing thalamic neurons. *Neuron* 17:823–835
11. Brüning G, Liangos O (1997) Transient expression of the serotonin transporter in the developing mouse thalamocortical system. *Acta Histochem* 99:117–121
12. Brüning G, Liangos O, Baumgarten HG (1997) Prenatal development of the serotonin transporter in mouse brain. *Cell Tissue Res* 289:211–221
13. Chugani DC, Muzik O, Behen M et al (1999) Developmental changes in brain serotonin synthesis capacity in autistic and nonautistic children. *Ann Neurol* 45:287–295
14. Whitaker-Azmitia PM (2001) Serotonin and brain development: role in human developmental diseases. *Brain Res Bull* 56:479–485
15. Sodhi MSK, Sanders-Bush E (2004) Serotonin and brain development. *Int Rev Neurobiol* 59:111–174
16. Bonnin A, Levitt P (2012) Placental source for 5-HT that tunes fetal brain development. *Neuropsychopharmacology* 37:299–300
17. Velasquez JC, Goeden N, Bonnin A (2013) Placental serotonin: implications for the developmental effects of SSRIs and maternal depression. *Front Cell Neurosci* 7:47
18. Harrington RA, Lee L-C, Crum RM et al (2013) Serotonin hypothesis of autism: implications for selective serotonin reuptake inhibitor use during pregnancy. *Autism Res* 3:149–168
19. Harrington RA, Lee L-C, Crum RM et al (2014) Prenatal SSRI use and offspring with autism spectrum disorder or developmental delay. *Pediatrics*. doi:10.1542/peds.2013–3406
20. Holmes A, Li Q, Murphy DL et al (2003) Abnormal anxiety-related behavior in serotonin transporter null mutant mice: the influence of genetic background. *Genes Brain Behav* 2(6):365–380
21. Holmes A, Yang RJ, Lesch K-P et al (2003) Mice lacking the serotonin transporter exhibit 5-HT(1A) receptor-mediated abnormalities in tests for anxiety-like behavior. *Neuropsychopharmacology* 28:2077–2088
22. Ansorge MS, Zhou M, Lira A et al (2004) Early-life blockade of the 5-HT transporter alters emotional behavior in adult mice. *Science* 306:879–881
23. Nordquist N, Orelund L (2010) Serotonin, genetic variability, behaviour, and psychiatric disorders – a review. *Ups J Med Sci* 115:2–10
24. Malkova NV, Yu CZ, Hsiao EY et al (2012) Maternal immune activation yields offspring displaying mouse versions of the three core symptoms of autism. *Brain Behav Immun* 26:607–616
25. Oberlander TF (2012) Fetal serotonin signaling: setting pathways for early childhood development and behavior. *J Adolesc Health* 51: S9–S16
26. Bonnin A, Levitt P (2011) Fetal, maternal, and placental sources of serotonin and new implications for developmental programming of the brain. *Neuroscience* 197:1–7

27. Ganu RS, Harris RA, Collins K et al (2012) Early origins of adult disease: approaches for investigating the programmable epigenome in humans, nonhuman primates, and rodents. *ILAR J* 53:306–321
28. Bonnin A, Peng W, Hewlett W et al (2006) Expression mapping of 5-HT₁ serotonin receptor subtypes during fetal and early postnatal mouse forebrain development. *Neuroscience* 141:781–794
29. Bonnin A, Goeden N, Chen K et al (2011) A transient placental source of serotonin for the fetal forebrain. *Nature* 472:347–350
30. Pattyn A, Simplicio N, van Doorninck JH et al (2004) *Ascl1/Mash1* is required for the development of central serotonergic neurons. *Nat Neurosci* 7:589–595
31. Hawthorne AL, Wylie CJ, Landmesser LT et al (2010) Serotonergic neurons migrate radially through the neuroepithelium by dynamin-mediated somal translocation. *J Neurosci* 30:420–430
32. Bonnin A, Torii M, Wang L et al (2007) Serotonin modulates the response of embryonic thalamocortical axons to netrin-1. *Nat Neurosci* 10:588–597
33. van Kleef ESB, Gaspar P, Bonnin A (2012) Insights into the complex influence of 5-HT signaling on thalamocortical axonal system development. *Eur J Neurosci* 35:1563–1572
34. Brezun J, Daszuta A (1999) Depletion in serotonin decreases neurogenesis in the dentate gyrus and the subventricular zone of adult rats. *Neuroscience* 89:999–1002
35. Brezun JM, Daszuta A (2000) Serotonergic reinnervation reverses lesion-induced decreases in PSA-NCAM labeling and proliferation of hippocampal cells in adult rats. *Hippocampus* 10:37–46
36. Brezun J, Daszuta A (2008) Serotonin may stimulate granule cell proliferation in the adult hippocampus, as observed in rats grafted with foetal raphe neurons. *Eur J Neurosci* 12:391–396
37. Kindt KS, Tam T, Whiteman S et al (2002) Serotonin promotes G(o)-dependent neuronal migration in *Caenorhabditis elegans*. *Curr Biol* 12:1738–1747
38. Banasr M, Hery M, Printemps R et al (2004) Serotonin-induced increases in adult cell proliferation and neurogenesis are mediated through different and common 5-HT receptor subtypes in the dentate gyrus and the subventricular zone. *Neuropsychopharmacology* 29:450–460
39. Ansoorge MS, Morelli E, Gingrich JA (2008) Inhibition of serotonin but not norepinephrine transport during development produces delayed, persistent perturbations of emotional behaviors in mice. *J Neurosci* 28:199–207
40. Oberlander TF, Gingrich JA, Ansoorge MS (2009) Sustained neurobehavioral effects of exposure to SSRI antidepressants during development: molecular to clinical evidence. *Clin Pharmacol Ther* 86:672–677
41. Gross C, Zhuang X, Stark K et al (2002) Serotonin_{1A} receptor acts during development to establish normal anxiety-like behaviour in the adult. *Nature* 416:396–400
42. Oberlander TF, Warburton W, Misri S et al (2006) Neonatal outcomes after prenatal exposure to selective serotonin reuptake inhibitor antidepressants and maternal depression using population-based linked health data. *Arch Gen Psychiatry* 63:898–906
43. Olivier JDA, Akerud H, Kaihola H et al (2013) The effects of maternal depression and maternal selective serotonin reuptake inhibitor exposure on offspring. *Front Cell Neurosci* 7:73
44. Suri R, Altshuler L, Helleman G et al (2007) Effects of antenatal depression and antidepressant treatment on gestational age at birth and risk of preterm birth. *Am J Psychiatry* 164:1206–1213
45. Cooper WO, Willy ME, Pont SJ et al (2007) Increasing use of antidepressants in pregnancy. *Am J Obstet Gynecol* 196:544.e1–5
46. Bourke CH, Stowe ZN, Owens MJ (2014) Prenatal antidepressant exposure: clinical and preclinical findings. *Pharmacol Rev* 66:435–465
47. Hiemke C, Härtter S (2000) Pharmacokinetics of selective serotonin reuptake inhibitors. *Pharmacol Ther* 85:11–28
48. Narboux-Nême N, Pavone LM, Avallone L et al (2008) Serotonin transporter transgenic (SERT^{cre}) mouse line reveals developmental targets of serotonin specific reuptake inhibitors (SSRIs). *Neuropharmacology* 55:994–1005
49. Bonnin A, Zhang L, Blakely RD et al (2012) The SSRI citalopram affects fetal thalamic axon responsiveness to netrin-1 in vitro independently of SERT antagonism. *Neuropsychopharmacology* 37:1879–1884
50. Moses-Kolko EL, Bogen D, Perel J et al (2005) Neonatal signs after late in utero exposure to serotonin reuptake inhibitors: literature review and implications for clinical applications. *JAMA* 293:2372–2383
51. Bonari L, Pinto N, Ahn E et al (2004) Perinatal risks of untreated depression during pregnancy. *Can J Psychiatry* 49:726–735

52. Davis EP, Sandman CA (2012) Prenatal psychological predictors of anxiety risk in preadolescent children. *Psychoneuroendocrinology* 37: 1224–1233
53. Deave T, Heron J, Evans J et al (2008) The impact of maternal depression in pregnancy on early child development. *BJOG* 115: 1043–1051
54. Croen LA, Grether JK, Yoshida CK et al (2011) Antidepressant use during pregnancy and childhood autism spectrum disorders. *Arch Gen Psychiatry* 68:1104–1112
55. Simon GE (2002) Outcomes of prenatal antidepressant exposure. *Am J Psychiatry* 159:2055–2061
56. Källén B (2004) Neonate characteristics after maternal use of antidepressants in late pregnancy. *Arch Pediatr Adolesc Med* 158: 312–316
57. Lund N, Pedersen LH, Henriksen TB (2009) Selective serotonin reuptake inhibitor exposure in utero and pregnancy outcomes. *Arch Pediatr Adolesc Med* 163:949–954
58. Sit D, Perel JM, Wisniewski SR et al (2011) Mother-infant antidepressant concentrations, maternal depression, and perinatal events. *J Clin Psychiatry* 72:994–1001
59. Yonkers KA, Norwitz ER, Smith MV et al (2012) Depression and serotonin reuptake inhibitor treatment as risk factors for preterm birth. *Epidemiology* 23:9
60. Hostetter A, Ritchie JC, Stowe ZN (2000) Amniotic fluid and umbilical cord blood concentrations of antidepressants in three women. *Biol Psychiatry* 48:1032–1034
61. Hendrick V (2003) Placental passage of antidepressant medications. *Am J Psychiatry* 160:993–996
62. Heikkine T, Ekblad U, Laine K (2002) Transplacental transfer of citalopram, fluoxetine and their primary demethylated metabolites in isolated perfused human placenta. *BJOG* 109:1003–1008
63. Uusküla L, Männik J, Rull K et al (2012) Mid-gestational gene expression profile in placenta and link to pregnancy complications. *PLoS One* 7:e49248
64. Sitras V, Fenton C, Paulssen R et al (2012) Differences in gene expression between first and third trimester human placenta: a microarray study. *PLoS One* 7:e33294
65. Mikheev AM, Nabekura T, Kaddoumi A et al (2008) Profiling gene expression in human placentae of different gestational ages: an OPRU Network and UW SCOR Study. *Reprod Sci* 15:866–877
66. Ganapathy V, Ramamoorthy S, Leibach F (1993) Transport and metabolism of monoamines in the human placenta – a review. *Placenta* 35–51
67. Yavarone MS, Shuey DL, Sadler TW et al (1993) Serotonin uptake in the ectoplacental cone and placenta of the mouse. *Placenta* 14:149–161
68. Shearman LP et al (1998) Relationship between [¹²⁵I]RTI-55-labeled cocaine binding sites and the serotonin transporter in rat placenta. *Am J Physiol* 275:1621–1629
69. Verhaagh S, Barlow DP, Zwart R (2001) The extraneuronal monoamine transporter Slc22a3/Orc13 co-localizes with the Maa0 metabolizing enzyme in mouse placenta. *Mech Dev* 100:127–130
70. Goeden N, Bonnin A (2013) Ex vivo perfusion of mid-to-late-gestation mouse placenta for maternal-fetal interaction studies during pregnancy. *Nat Protoc* 8:66–74
71. Goeden N, Bonnin A (2014) Ex vivo perfusion of the mouse placenta for maternal-fetal interaction studies. In: Anecorry B et al (eds) *The guide to investigation of mouse pregnancy*, 1st edn. Elsevier, Amsterdam
72. Heikkinen T, Ekblad U, Palo P et al (2003) Pharmacokinetics of fluoxetine and norfluoxetine in pregnancy and lactation. *Clin Pharmacol Ther* 73:330–337
73. Mathiesen L, Mose T, Mørck TJ et al (2010) Quality assessment of a placental perfusion protocol. *Reprod Toxicol* 30:138–146
74. Menjoge AR, Rinderknecht AL, Navath RS et al (2011) Transfer of PAMAM dendrimers across human placenta: prospects of its use as drug carrier during pregnancy. *J Control Release* 150:326–338
75. Crowley JJ, Brodtkin ES, Blendy JA et al (2006) Pharmacogenomic evaluation of the antidepressant citalopram in the mouse tail suspension test. *Neuropsychopharmacology* 31:2433–2442
76. Cryan JF, O’Leary OF, Jin S-H et al (2004) Norepinephrine-deficient mice lack responses to antidepressant drugs, including selective serotonin reuptake inhibitors. *Proc Natl Acad Sci U S A* 101:8186–8191
77. Eagleson KL, Bonnin A, Levitt PAT (2005) Region- and age-specific deficits in γ -aminobutyric acidergic neuron development in the telencephalon of the uPAR $-/-$ mouse. *J Comp Neurol* 466:449–466

Studies on the Effects Prenatal Immune Activation on Postnatal Behavior: Models of Developmental Origins of Schizophrenia

Udani Ratnayake and Rachel Anne Hill

Abstract

Human epidemiological studies have indicated an association between infection during pregnancy and an increased risk of neurodevelopmental disorders such as schizophrenia in offspring. As infections arising from various causes have a similar debilitating effect in later life, it is thought that the maternal response, common to most infections, may be the critical factor altering fetal brain development. In this chapter, we discuss various animal models of prenatal exposure to an infection, that have aimed to cause neurobiological, pharmacological and behavioral abnormalities in offspring comparable to those seen in schizophrenic patients. We propose that one such model, the prenatal treatment with the viral mimetic, polyriboinosinic-polyribocytidylic acid (Poly I:C) successfully demonstrates critical features of the human disorder. Therefore, this model is ideal to further investigate the neurodevelopmental basis of schizophrenia and, importantly, may provide a useful tool for testing treatment strategies.

Key words Prenatal immune activation, Poly I:C, Behavior, Schizophrenia, Symptoms, Animal model

1 Background

Schizophrenia is a debilitating disease that affects 1 % of the population worldwide [1]. Although it is known that genetic and environmental factors can predispose an individual to this disease, the exact etiology of schizophrenia remains unknown, as these factors alone cannot account for its prevalence [1, 2]. It has been suggested that schizophrenia is a neurodevelopmental disorder, with aberrations in fetal life thought to increase the susceptibility of individuals to the disorder [3, 4]. Considerable epidemiological evidence supports this hypothesis. For example, researchers investigating the long term impact of exposure to the 1964 rubella epidemic, using serological testing and clinical examination, have shown an association between prenatal infectious exposure and the development of mental retardation in postnatal life [5, 6]. Also, a significant number of epidemiological studies that focused on the '1968 Hong

Kong' influenza epidemic, showed an association between exposure during fetal development and an increased risk of developing mental illness in later life, specifically schizophrenia [7–12], with second trimester exposure being of particular significance [7, 10, 13]. Prenatal exposure to other infections, such as herpes simplex virus type 2 [14], toxoplasmosis [15, 16], poliovirus [17, 18], measles [18], varicella-zoster [18] and maternal genital and reproductive infections [19], have also been linked with the development of neuropsychiatric disorders in postnatal life. As varying infections during pregnancy can lead to similar outcomes, it has been suggested that factors common to the immune system, and induced by any pathogen, viral or bacterial, may be affecting fetal brain development. Specifically, research has suggested maternal induction or a change in the balance of pro- and anti-inflammatory cytokines may be a key mechanism involved in altering the normal course of fetal brain development [20].

2 Animal Models of the Prenatal Immune Activation Hypothesis of Schizophrenia

Due to the debilitating nature of schizophrenia, the relatively high incidence worldwide, and public health burden on society, it is important to understand the mechanisms and factors involved in the etiology of this disease in order to develop interventions or treatments. Schizophrenia is characterized by a spectrum of symptoms including positive symptoms such as hallucinations and delusions and negative symptoms such as social withdrawal. Schizophrenia is also associated with severe cognitive deficits, specifically working memory, executive function, and verbal memory. Although no animal model of a complex human disorder is ever likely to replicate the deficits in all aspects of structure and function observed in patients with a neuropsychiatric illness, animal models that demonstrate individual mental illness-like behavioral symptoms and neuropathology can be nonetheless useful for understanding the etiology of the disease and testing treatments. As such, studies have attempted to demonstrate the association between exposure to a prenatal infection and the development of schizophrenia in later life by investigating long-term behavioral outcomes, and neuro-molecular and morphological changes in rodents infected either with live viruses, or a viral-mimetic agent.

2.1 *Human Influenza Virus*

As exposure to influenza epidemics during prenatal life have been identified as a risk factor for the development of schizophrenia in later life [7–11], animal studies have attempted to demonstrate this association. It is possible to argue this model is epidemiologically relevant; however, the use of a live human virus requires stringent biosafety practices, and therefore makes the establishment and study of this model difficult. Studies that administered influenza

to pregnant rodents predominantly focused on the impact of maternal human influenza virus on the brain of offspring, finding morphological alterations in neuronal and glial cell types [21–23], similar to changes found in the brains of schizophrenic patients [24]. However, a study found that offspring prenatally exposed to human influenza virus present with behavioral abnormalities that are similar to those that characterize schizophrenia in human patients, including hyper-anxiety in novel or stressful situations, deficiencies in social interaction, and deficits in sensorimotor gating, which could be attenuated with the treatment of antipsychotics [25]. It is important to note that the response by the maternal immune system to influenza-specific pathogens may be critical in determining the outcomes mentioned above. Studies have shown that viral RNAs for influenza do not pass the placenta and are not found in the brain of offspring where the mother had been exposed to influenza [26, 27]. In a nonhuman primate study, which used magnetic resonance imaging to show a reduction in cortical grey matter, authors concluded that direct exposure of the fetus to influenza virus does not occur as immunoglobulin M, an antibody associated with an initial exposure to a pathogen, were not present in these brains. These studies support the idea that it is not the virus that directly infects the fetal brain, but a substance released in either the maternal or placental compartments that enters the fetal compartment and alters fetal brain development.

2.2 Bacterial Endotoxin, LPS

To evoke a bacteria-induced immune response without having to use live bacteria, administration of lipopolysaccharide (LPS) has been commonly used in pregnant rodents. Recognition of LPS by the innate immune receptors toll-like receptor (TLR)-2 and TLR-4 elicits a strong inflammatory response including the production of cytokines in maternal serum, amniotic fluid and the fetal brain [28–31]. As previously mentioned, TLRs are a family of innate pathogen recognition receptors, recognizing the structures present on microbial pathogens and inducing antimicrobial immune responses [32]. The activation of these receptors by LPS in a pregnant rodent has been shown to alter the production of cytokines, including IL-1 β , IL-6, and TNF- α in maternal serum, amniotic fluid and the fetal brain [28–31]. Similar to influenza, LPS was only detected in maternal tissue and the placenta, but not the fetus, and therefore, authors concluded that the actions of LPS on the developing fetal brain were not the direct actions of LPS, but indirect actions that were initiated at the level of maternal circulation or mediated by the placenta [31].

Studies that investigated the behavioral outcome of offspring prenatally exposed to LPS identified deficits in auditory and visual prepulse inhibition (PPI) [33, 34], and learning and memory deficits [28, 35, 36], which are abnormalities also seen in schizophrenic patients. PPI deficits in offspring prenatally exposed

to LPS were found to be less when the offspring were treated with antipsychotics, thus providing predictive validity for this model [33, 34]. Neurological abnormalities associated with schizophrenia have been identified in the brains of adult offspring prenatally exposed to LPS, including glial activation [34, 35], and alterations in dopaminergic function [33, 34, 37, 38]. It is important to note that many of these studies involved chronic administration of LPS during gestation [33–37], with up to 20 daily injections [33]. In addition, there is a high rate of preterm delivery with the use of LPS during pregnancy [30], and therefore, this model may not appropriately replicate outcomes that follow a clinically manageable infection in pregnant women.

2.3 Exogenous Cytokines

As cytokines are thought to play a critical role in the development of schizophrenia, studies have determined postnatal behavioral and neurological dysfunctions in offspring following the administration of the cytokine interleukin(IL)-6 to pregnant rodents. Offspring prenatally exposed to exogenous IL-6 demonstrate deficits in learning and memory, PPI and latent inhibition (LI), and altered exploratory behavior in an open field [39–41]. Although these studies are worthwhile in identifying key mediators, they do not model the full spectrum of the human paradigm, such as activating receptors of the innate immune system, and therefore may not be the ideal models to investigate the developmental origins of human disorders.

2.4 Viral Mimetic, Poly I:C

Perhaps the most commonly used and well established model of prenatal immune activation involves the administration of **Polyinosinic:polycytidylic acid** (Poly I:C) to pregnant rodents.

Poly I:C, a synthetic analogue of double stranded RNA, is referred to as a viral-mimetic as most viruses produce double stranded RNA during their replication phase [42]. Poly I:C is recognized by the mammalian innate immune receptor TLR-3 [43]. The activation of the TLR-3 induces an acute, time-limited cytokine response in the maternal host a critical link between maternal infection and the disruption of fetal brain development. Furthermore, studies have shown clear dose-dependent alterations in cytokine levels due to Poly I:C administration [44, 45], indicating that it is possible to control the level of activation of the maternal immune system. In adult animals, Poly I:C has been shown to cause an increase in inflammatory cytokines and plasma corticosterone, induce sickness behaviors including a febrile response, decrease in body weight, and reduced appetite [42, 45, 46].

Poly I:C administration during pregnancy is a highly appropriate model to investigate the impact of immunological mediators, specifically inflammatory cytokines, as the critical mediator altering fetal brain development and leading to neuropsychiatric disorders

in later life. Numerous studies have shown increases in maternal serum cytokines, including IL-1 β , IL-6, IL-10 and TNF- α , by 6 h after Poly I:C administration in pregnant animals [44, 47–50]. Studies have also shown alterations in protein levels of the same inflammatory cytokines and others in the fetal brain within 12 h after Poly I:C administration of the pregnant rodent [44, 47–49, 51]. In a study which found increased protein levels of cytokines in the fetal brain, gene expression of some cytokines (IL-1 β , IL-6, IL-10 and TNF- α) were increased at 6 h after Poly I:C exposure [49], showing that these cytokines are transcribed rapidly after Poly I:C exposure. In pregnant animals, a single dose of Poly I:C (5 mg/kg) is able to produce a greater severity of sickness behaviors compared to 3 days of LPS administration [52]. Cytokine levels in maternal serum and the fetal brain were generally increased in the studies mentioned, even though the dose of Poly I:C, time of administration in pregnancy and species used were different between the separate studies. These differences may account for the different times and duration of cytokine increase between studies, and suggests that small changes in experimental design will have significant effects on cytokine expression in the fetus compared to the mother, and possibly, explain the resulting phenotype of the offspring due to these factors.

The use of Poly I:C has the advantage that it is able to elicit a nonspecific immune response, without the production of specific antibodies that arise with the use of alternative virulent pathogens such as the influenza virus, and it leads to more consistent responses and outcomes compared to the volatile actions of infectious agents and the unpredictable response to pathogens by different species [51]. Although this can also be considered to be a disadvantage as prenatal Poly I:C administration does not mimic the full spectrum of a viral infection. However, as the effects of Poly I:C are time-limited, lasting approximately 48 h [53], it allows the effects of prenatal immune activation to be studied at specific stages of fetal development, and therefore, it is a valuable tool for investigating neurodevelopmental disorders.

Neuroanatomical, neurochemical, and morphological disruptions that have been previously implicated in the neuropathology of schizophrenia have also been found to be altered in various brain regions of offspring prenatally exposed to Poly I:C. Briefly, changes in neuronal cells, including cell death, cell loss, and altered neurogenesis, and glial cells, such as abnormalities in microglial and astrocyte activation, have been found in the hippocampus, cortex, and cerebellum of offspring prenatally exposed to Poly I:C [23, 35, 49, 54–59]. Altered development of neurotransmitter systems, including dopamine (DA) levels [60–63], glutamate and gamma-aminobutyric acid (GABA) [64, 65], have been found in offspring prenatally exposed to Poly I:C. Finally, MRI studies have also shown ventricular enlargement relevant to schizophrenia in adult

mice and rats born to mothers treated with Poly I:C [66, 67]. In addition to similarities in neuropathology to schizophrenia, prenatal Poly I:C studies have also found schizophrenia-like behavioral and cognitive abnormalities in the offspring including changes of sensorimotor gating, latent inhibition, anxiety, memory, and learning, as detailed in the following section.

3 Modeling Symptoms of Schizophrenia in Offspring Prenatally Exposed to Poly I:C

Compared to other infectious agents, prenatal Poly I:C administration is able to produce a greater spectrum of schizophrenia-like behaviors in offspring, as shown in Table 1. Similar to other animal models of schizophrenia, studies characterizing the behavioral outcome of offspring prenatally exposed to Poly I:C have attempted to identify cognitive and behavioral endophenotypes of relevance to schizophrenia, in the hope to investigate the underlying mechanisms involved. The aim of this chapter is to evaluate behavioral tests of psychosis and cognition that can be used to assess specific symptoms of the human condition, with a focus on paradigms previously used in prenatal immune activation models of schizophrenia.

3.1 Social Behaviors

Abnormal social interaction and social withdrawal is one of the most important negative symptoms of schizophrenia, but also involves cognitive domains [68]. Offspring born to mothers treated with Poly I:C display abnormal levels of interaction with a stranger mouse, suggesting a dysfunction in social behaviors, regardless of species or dose [40, 57, 69]. These studies have utilized the three chamber social interaction paradigm, where the amount of time a subject mouse interacts with an enclosed age and sex matched stranger mouse is compared to an empty enclosure, as shown in Fig. 1. Although an important feature of the disease, surprisingly few studies have fully examined this symptom in rodent, prenatal immune activation models of schizophrenia. Unlike rodents, a longer term study in rhesus monkeys found juvenile offspring born to mothers administered with a modified form of Poly I:C show an increase in their interactions with unfamiliar peers [70]. The authors of this study emphasize that excessive social approach is in fact a non-stereotypical behavior of nonhuman primates and a deviation from normal social protocol, which is to approach after considerable evaluation at distance and with caution. Therefore, the authors conclude that the nonhuman primate prenatal Poly I:C model is comparable to rodent models, as offspring display a deviation from normal social behavior. Although a recent study showed that differences in social behavior in the three chamber interaction test can be found between strains of mice that were prenatally exposed to Poly I:C [71], other social behaviors that could also be investigated in rodents, including

Table 1
The behavioral outcome of rodent offspring exposed to varying prenatal infections and infection-like agent

Infectious agent	Species	Route of maternal administration (dose)	Timing of insult	Memory and reversal learning	Exploratory activity	Sensitivity to AMPH/ NMDA ligands	Latent inhibition	Prepulse inhibition	Social interaction	Reference
Poly I:C	Mice	IV (2.5–20 mg/kg)	GD 9, 12 or 17	✘	✘	✘	✘	✘	✘	[44, 49, 65, 66, 73]
Poly I:C	Spiny Mice	SC (0.5–5 mg/kg)	GD 20	✘	✘			✘	✘	[58, 69]
Poly I:C	Rats	IV (4 mg/kg)	GD15 or GD 17	✘		✘	✘	✘		[53, 78, 87]
Influenza virus (H)	Mice	IN (6×10^3 pfu)	GD 9.5					✘	✘	[25]
LPS	Rats	SC (0.5–2 mg/kg)	GD 8–20 ^a	✘				✘		[33–36, 90]
LPS	Mice	IP (0.12 µg/g mouse/100 µl)	GD 17	✘						[28]
Human IL-6	Rats	IP (9 µg/kg)	GD 16, 18 and 20	✘						[39]

IN, intranasal; IP, Intraperitoneal; IV, intravenous; SC, subcutaneous; ✘ Indicates offspring showed a deficit or abnormality in this behavior ^a3–4 times alternate days

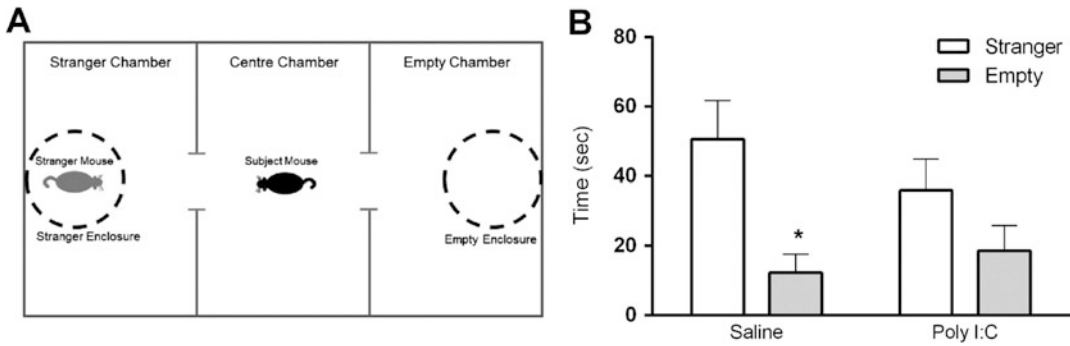


Fig. 1 Social behaviors assessed in the three chamber social interaction test. The three chamber social interaction test assesses the subject mouse's interaction with an enclosed, age and sex matched stranger mouse (a). Control (saline) spiny mice spend significantly greater time exploring the social enclosure containing the stranger mouse compared to the empty enclosure; however, this is not found in male offspring prenatally exposed to Poly I:C (b), suggesting an abnormality in social behavior. * $p < 0.05$ compared to stranger chamber (Adapted from [69])

home cage social interaction, nesting, and aggressive behaviors, may provide a more consistent behavioral endophenotype in prenatal Poly I:C exposed offspring.

3.2 Memory and Learning

Seven cognitive domains have been identified to be impaired in schizophrenia including: verbal learning and memory, visual learning and memory, working memory, attention and vigilance, processing speed, reasoning and problem solving, and social cognition [72]. Although offspring of Poly I:C treated dams show a normal ability to learn a spatial context [53, 73], they have been consistently found to have deficits in reversal learning as assessed in the Morris water maze [44, 49, 65, 73, 74], suggesting difficulties in adapting to a change in a previously learned context and thus executive dysfunction. A recent study found reversal learning is altered in male but not female rats prenatally exposed to Poly I:C [75], which supports consistent findings of sex differences in human studies with men showing a more severe course of illness, particularly with respect to cognitive impairments [76]. Abnormalities in non-spatial memory, assessed in the novel object recognition test or alternatives of this test, have been found in offspring prenatally exposed to Poly I:C [58, 69, 73, 77, 78]. Also a far greater number of studies showed this memory deficit, than studies which found no differences between groups [79].

3.3 Latent Inhibition

Attentional deficits commonly found in schizophrenic patients can be measured with the latent inhibition test (LI) in both humans and animals. The LI test is an assessment of an organism's ability to ignore irrelevant stimulation, and is commonly used in animal and human studies of mental illness. LI refers to a poorer performance on a stimulus associated task, when that stimulus has been

previously conditioned [80]. A disruption in LI is generally considered as a positive symptom of schizophrenia; however, abnormally persistent LI is thought to model a negative symptom of the disease [81]. LI was abnormal in adult mouse and rat offspring following Poly I:C treatment at early-mid and late gestation respectively [44, 53]. Zuckerman and Weiner [82] showed that a delay occurs in the development of LI, with deficits not appearing until adulthood, an important feature of schizophrenia. In addition, these abnormalities were lessened when adult offspring were treated with antipsychotic drugs. However, Meyer, Feldon [48] found that LI deficits were only present in adult offspring that were prenatally exposed to a single infection of Poly I:C between 6 and 13 days of gestation, but not day 17, suggesting that the stage of brain development is critical in determining the vulnerability of the fetus to injury caused by maternal immune activation.

3.4 Enhanced Locomotor Hyperlocomotor Activity

Drug-induced hyperlocomotion via administration of psychomimetics such as amphetamine and dizocilpine are commonly viewed as animal models of psychosis and have been previously investigated to determine if the dopaminergic and *N*-methyl-D-aspartate (NMDA) systems have been altered by the Poly I:C treatments. It is known that an abnormal modulation of dopamine and glutamate neurotransmitter systems has a role in the psychotic symptoms of schizophrenia. For example, increased dopaminergic release has been found to correlate with the severity of psychosis in schizophrenic patients. In addition, the administration of amphetamine, a dopamine agonist, is able to induce psychotic episodes in healthy subjects, similar to those seen in schizophrenic patients [83, 84]. Therefore, an enhancement in amphetamine induced hyperlocomotor activity can be used as a measure of psychosis [85], as shown by a prototypical example in Fig. 2a. Offspring from Poly I:C treated dams have an enhanced sensitivity to dopamine releasing drugs, displayed by their increased locomotor activity following amphetamine treatment to control treated littermates. These studies suggest that the development of the dopaminergic system is altered by this viral-mimetic treatment during pregnancy [44, 65]. This enhanced sensitivity to amphetamine treatment was found in juvenile and adult offspring prenatally exposed to Poly I:C. Rat and mice offspring prenatally exposed to Poly I:C also display increased sensitivity to the effects of the NMDA-receptor antagonist, dizocilpine, as these offspring show enhanced locomotor response to the drug [53, 62, 65].

3.5 Prepulse Inhibition

Another test commonly used in animal and human studies of mental illness is the prepulse inhibition (PPI) test, an assessment of sensorimotor gating, which is commonly impaired in schizophrenic patients. Prenatal Poly I:C rodent studies have consistently found deficits in PPI, despite the usual differences in dose, timing and

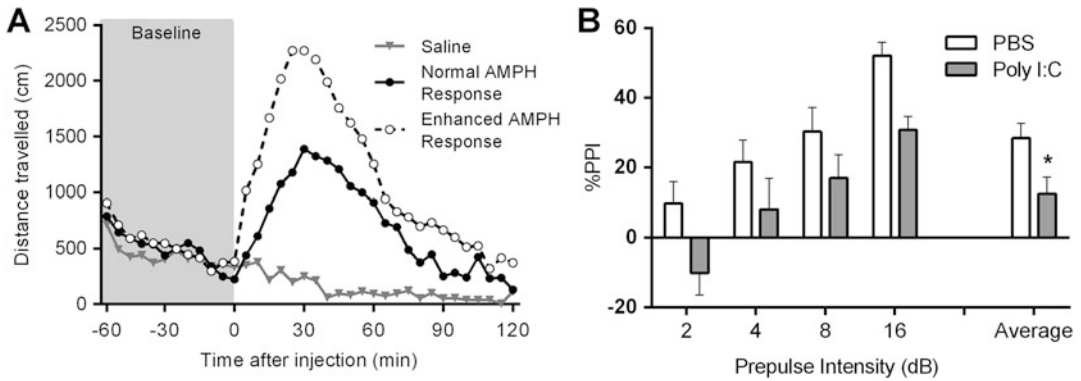


Fig. 2 Locomotor hyperactivity and prepulse inhibition (PPI) as paradigms of psychosis. A prototypical example of hyperactivity induced by amphetamine (AMPH) treatment, that is greater than the normal drug induced response (control), is suggested to model the positive symptoms of schizophrenia (A). A reduction in normal PPI, an endophenotype of schizophrenia, has been found in juvenile spiny mice offspring (male and female combined) prenatally exposed to Poly I:C. **p* < 0.05 compared to Saline (B) (Adapted from [69])

species. Many studies which administered Poly I:C at early-mid gestation, in varying doses, found PPI impairments in adult offspring [44, 86]. In addition, similar studies found that the timing of Poly I:C administration is essential, as adult offspring exposed to an early-mid gestation but not a mid-late gestation insult presented with PPI deficits [65, 66]. However, in other studies where Poly I:C was administered in late gestation in conventional rodents, not only were PPI deficits present in adulthood, but in juvenile offspring as well [78, 87]. Unfortunately, the former studies, which showed an early-mid gestation infection resulted in more severe outcomes in terms of PPI, did not assess the behavior of the offspring at an early postnatal age, and therefore, it is difficult to make comparisons between these studies. PPI deficits have also been found in juvenile spiny mice, that are born at a more advanced stage of brain development compared to conventional rodents, and that have been prenatally exposed to Poly I:C at mid gestation, shown in Fig. 2b. Although full expression of schizophrenia symptoms generally appears clinically in early adulthood, the emergence of these deficits in adolescence may present as the prodromal signs of the disease. It is of interest that treatment with a dopamine receptor antagonist such as SCH23390 and raclopride [61], or with the NF-κB inhibitor pyrrolidine dithiocarbamate [50], are able to normalize PPI deficits in adult offspring after the prenatal Poly I:C treatment, suggesting possible pathways of injury.

3.6 Two-Hit Hypothesis

It is thought that the full development of schizophrenia disease is caused by the combination of a subsequent life event following an early genetic or environmental event, i.e., the ‘two hit’ hypothesis. After the “first hit” susceptible individuals may present with prodromal signs and symptoms of schizophrenia, but will only develop

full expression of schizophrenia symptoms with a “second hit” in later life, such as a social stressor, inflammatory insult or drug abuse. As prodromal-like behavioral deficits have been identified in juvenile offspring prenatally exposed to Poly I:C, this lead researchers to believe that these offspring will present with exacerbated expression of schizophrenia symptoms in adulthood if exposed to a subsequent insult.

A spectrum of schizophrenia-like behavioral abnormalities, including deficits in prepulse inhibition and drug induced hyperlocomotor activity, as well as alterations in neurotransmitter levels and glial cell expression in the hippocampus, were found in adult offspring only if animals were exposed to both prenatal Poly I:C and to repeated and unpredictable adolescent stressors [59]. A study which administered restraint stress for 3 consecutive days, found prepulse inhibition deficits and neurotransmitter alterations in the prefrontal cortex and striatum, only in prenatal Poly I:C exposed offspring that also received the adolescent stress [88]. Prenatal Poly I:C exposure also increased the vulnerability of the neonatal brain to an early hypoxic-ischemic insult, as shown by more severe white matter injury [89].

4 Methodological Considerations for Establishing the Prenatal Poly I:C Model of Schizophrenia

This section provides methodological details for establishing the prenatal Poly I:C model of schizophrenia in a rodent model. We suggest maternal treatment with a final dose of 5 mg/kg for mice and 4 mg/kg for rats of Poly I:C as these doses have been previously shown to be effective in producing schizophrenia-like behaviors in offspring (Table 1). To prevent batch to batch differences in potency, an amount of Poly I:C (Sigma-Aldrich) should be ordered so that a singular batch should be enough to treat all animals for a single study (at least an extra 10 % is required for unforeseeable errors or factors). A stock solution should be made at a concentration of at least ten times higher than the working concentration. Working solutions should be made for at least 10 % above the predicted number of animals to be treated. In addition, the working solution should be made to a final volume (working volume) that takes into account the maximum weight of a pregnant mouse or rat at the chosen gestation age of injection plus 10 %. Working sterile saline solutions should also be made to take into account the number of animals treated and volume required to inject. All Poly I:C working solutions and stock solution, as well as the working saline solutions should be frozen at -20°C until just prior to use.

An immunological challenge at different times during prenatal development may have important, varying neurodevelopmental

consequences. Epidemiological studies investigating various prenatal infections found that the risk of developing mental illness disorders can be dependent on the timing of exposure to an infection [9, 12]. Studies investigating the administration of the viral mimetic, Poly I:C during gestation have also provided further evidence that the time of prenatal exposure critically determines the patterns of behavioral and neurological abnormalities displayed in the offspring [48, 49, 65]. These studies found alterations in latent inhibition [48], exploratory activity [49], and sensorimotor gating [65] in offspring exposed to Poly I:C in early to mid-gestation. Whereas reversal learning deficits [49] and impairments in spatial working memory [65] were only demonstrated in mid-late prenatally exposed offspring. As human epidemiological and animal studies have highlighted that activation of the maternal immune system in the second trimester is a critical risk factor for the emergence of abnormal behaviors in later life, we suggest mid-gestation as the timing for maternal treatment.

Pregnant animals should be handled and weighed prior to the treatment day and an inclusion criterion for gestational weight should be set, to reduce confounding factors. The route of administration varies between previous studies, with intraperitoneal injection being the most common. The route of administration selected should be the least stressful; therefore, this may vary between species and strains. Maternal treatment should always be conducted at the same time of the day. After treatment with Poly I:C or saline, pregnant animals should be returned to their home cage and allowed to give birth naturally. During this time ensure to monitor the pregnant animals for sickness behaviors.

Offspring can be left in their home cage until the time of weaning or cross-fostered to other mothers to reduce the effect of maternal sickness behaviors. Most studies behaviorally assess offspring at adulthood, as schizophrenia symptoms clinically appear in late adolescence or early adulthood. Moreover behaviors such as prepulse inhibition are still being established in juvenile animals and are therefore difficult to accurately measure. However, the assessment of other behaviors in juvenile animals can be useful to assess the postpubertal emergence or exacerbation of schizophrenia-like behaviors. Behavioral tests should be ordered from least to most stressful, and an adequate break should be allowed between behavioral testing days. It is recommended that all animals are habituated in their home cage in the testing room at least 30 min prior to the start of each test.

5 Conclusion

Modeling a human condition in an animal undoubtedly has limitations. This is particularly challenging in the case of schizophrenia, which is characterized by a wide spectrum of symptoms. Models of

prenatal immune activation have identified behavioral endophenotypes and molecular anomalies that strongly correlate to symptoms and pathophysiology of schizophrenia. We propose that Poly IC treatment during pregnancy is a robust and clinically relevant model in which to study the basis of symptomology of schizophrenia. Furthermore, this model may be ideal for testing therapeutic treatments and interventions, although for these studies, accurate and appropriate behavioral characterization of Poly I:C offspring will be essential.

References

1. Tandon R et al (2008) Schizophrenia, "Just the Facts": what we know in 2008 part 1: overview. *Schizophr Res* 100(1-3):4–19
2. Williams JG et al (2006) The epidemiology of autistic spectrum disorders: is the prevalence rising. *Arch Dis Child* 91:8–15
3. Cannon TD (1998) Neurodevelopmental influences in the genesis and epigenesis of schizophrenia: an overview. *Appl Prev Psychol* 7:47–62
4. Cannon M, Murray RM (1998) Neonatal origins of schizophrenia. *Arch Dis Child* 78(1):1–3
5. Brown AS et al (2001) Prenatal rubella, premorbid abnormalities, and adult schizophrenia. *Biol Psychiatry* 49(6):473–486
6. Brown AS et al (2000) Nonaffective psychosis after prenatal exposure to rubella. *Am J Psychiatry* 157(3):438–443
7. Mednick SA et al (1988) Adult schizophrenia following prenatal exposure to an influenza epidemic. *Arch Gen Psychiatry* 45(2):189–192
8. O'Callaghan E et al (1991) Schizophrenia after prenatal exposure to 1957 A2 influenza epidemic. *Lancet* 337(8752):1248–1250
9. Brown AS et al (2000) Maternal exposure to respiratory infections and adult schizophrenia spectrum disorders: a prospective birth cohort study. *Schizophr Bull* 26(2):287–295
10. Machon RA et al (2002) Adult schizotypal personality characteristics and prenatal influenza in a Finnish birth cohort. *Schizophr Res* 54(1-2):7–16
11. Limosin F et al (2003) Prenatal exposure to influenza as a risk factor for adult schizophrenia. *Acta Psychiatr Scand* 107(5):331–335
12. Brown AS et al (2004) Serologic evidence of prenatal influenza in the etiology of schizophrenia. *Arch Gen Psychiatry* 61(8):774–780
13. Kendell RE, Kemp IW (1989) Maternal influenza in the etiology of schizophrenia. *Arch Gen Psychiatry* 46(10):878–882
14. Buka SLS et al (2001) Maternal infections and subsequent psychosis among offspring. *Arch Gen Psychiatry* 58(11):1032–1037
15. Brown AS et al (2005) Maternal exposure to toxoplasmosis and risk of schizophrenia in adult offspring. *Am J Psychiatry* 162(4):767–773
16. Mortensen PB et al (2007) *Toxoplasma gondii* as a risk factor for early-onset schizophrenia: analysis of filter paper blood samples obtained at birth. *Biol Psychiatry* 61(5):688–693
17. Suvisaari J et al (1999) Association between prenatal exposure to poliovirus infection and adult schizophrenia. *Am J Psychiatry* 156(7):1100–1102
18. Fuller Torrey E et al (1988) Schizophrenic births and viral diseases in two states. *Schizophr Res* 1(1):73–77
19. Babulas V et al (2006) Prenatal exposure to maternal genital and reproductive infections and adult schizophrenia. *Am J Psychiatry* 163(5):927–929
20. Watanabe Y et al (2010) Cytokine hypothesis of schizophrenia pathogenesis: evidence from human studies and animal models. *Psychiatry Clin Neurosci* 64(3):217–230
21. Fatemi SH et al (1999) Defective corticogenesis and reduction in Reelin immunoreactivity in cortex and hippocampus of prenatally infected neonatal mice. *Mol Psychiatry* 4(2):145–154
22. Fatemi SH et al (2002) Prenatal viral infection leads to pyramidal cell atrophy and macrocephaly in adulthood: implications for genesis of autism and schizophrenia. *Cell Mol Neurobiol* 22(1):25–33

23. Fatemi SH et al (2002) Human influenza viral infection in utero alters glial fibrillary acidic protein immunoreactivity in the developing brains of neonatal mice. *Mol Psychiatry* 7 (6):633–640
24. Bayer TA et al (1999) Evidence for activation of microglia in patients with psychiatric illnesses. *Neurosci Lett* 271(2):126–128
25. Shi L et al (2003) Maternal influenza infection causes marked behavioral and pharmacological changes in the offspring. *J Neurosci* 23 (1):297–302
26. Shi L et al (2005) Maternal influenza infection is likely to alter fetal brain development indirectly: the virus is not detected in the fetus. *Int J Dev Neurosci* 23(2-3):299–305
27. Fatemi SH et al (2012) The viral theory of schizophrenia revisited: abnormal placental gene expression and structural changes with lack of evidence for H1N1 viral presence in placentae of infected mice or brains of exposed offspring. *Neuropharmacology* 62 (3):1290–1298
28. Golan HM et al (2005) Specific neurodevelopmental damage in mice offspring following maternal inflammation during pregnancy. *Neuropharmacology* 48(6):903–917
29. Urakubo A et al (2001) Prenatal exposure to maternal infection alters cytokine expression in the placenta, amniotic fluid, and fetal brain. *Schizophr Res* 47(1):27–36
30. Fidel PL Jr et al (1994) Systemic and local cytokine profiles in endotoxin-induced preterm parturition in mice. *Am J Obstet Gynecol* 170 (5):1467–1475
31. Ashdown H et al (2006) The role of cytokines in mediating effects of prenatal infection on the fetus: implications for schizophrenia. *Mol Psychiatry* 11(1):47–55
32. Takeda K, Akira S (2005) Toll-like receptors in innate immunity. *Int Immunol* 17(1):1–14
33. Romero E et al (2007) Neurobehavioral and immunological consequences of prenatal immune activation in rats. Influence of antipsychotics. *Neuropsychopharmacology* 32 (8):1791–1804
34. Borrell J et al (2002) Prenatal immune challenge disrupts sensorimotor gating in adult rats: implications for the etiopathogenesis of schizophrenia. *Neuropsychopharmacology* 26 (2):204
35. Hao LY et al (2010) Prenatal exposure to lipopolysaccharide results in cognitive deficits in age-increasing offspring rats. *Neuroscience* 166(31):763–770
36. Graciarena M et al (2010) Prenatal inflammation impairs adult neurogenesis and memory related behavior through persistent hippocampal TGFbeta1 downregulation. *Brain Behav Immun* 24(8):1301–1309
37. Bakos J et al (2004) Prenatal immune challenge affects growth, behavior, and brain dopamine in offspring. *Ann N Y Acad Sci* 1018:281–287 (Stress: Current Neuroendocrine and Genetic Approaches)
38. Quinn TA et al (2014) Adrenal steroidogenesis following prenatal dexamethasone exposure in the spiny mouse. *J Endocrinol* 221:347
39. Samuelsson A-M et al (2006) Prenatal exposure to interleukin-6 results in inflammatory neurodegeneration in hippocampus with NMDA/GABAA dysregulation and impaired spatial learning. *Am J Physiol Regul Integr Comp Physiol* 290(5):R1345–R1356
40. Smith SEP et al (2007) Maternal immune activation alters fetal brain development through interleukin-6. *J Neurosci* 27(40):10695–10702
41. Hsiao EY, Patterson PH (2011) Activation of the maternal immune system induces endocrine changes in the placenta via IL-6. *Brain Behav Immun* 25(4):604–615
42. Fortier ME et al (2004) The viral mimic, polyinosinic:polycytidylic acid, induces fever in rats via an interleukin-1-dependent mechanism. *Am J Physiol Regul Integr Comp Physiol* 287 (4):R759–R766
43. Alexopoulou L et al (2001) Recognition of double-stranded RNA and activation of NF- κ B by Toll-like receptor 3. *Nature* 413 (6857):732(7)
44. Meyer U et al (2005) Towards an immunoprecipitated neurodevelopmental animal model of schizophrenia. *Neurosci Biobehav Rev* 29(6):913–947
45. Cunningham C et al (2007) The sickness behaviour and CNS inflammatory mediator profile induced by systemic challenge of mice with synthetic double-stranded RNA (poly I:C). *Brain Behav Immun* 21(4):490–502
46. Gandhi R et al (2007) Influence of poly I:C on sickness behaviors, plasma cytokines, corticosterone and central monoamine activity: moderation by social stressors. *Brain Behav Immun* 21(4):477–489
47. Gilmore JH et al (2005) Maternal poly I:C exposure during pregnancy regulates TNF [alpha], BDNF, and NGF expression in neonatal brain and the maternal-fetal unit of the rat. *J Neuroimmunol* 159(1-2):106–112
48. Meyer U et al (2006) Immunological stress at the maternal-foetal interface: a link between neurodevelopment and adult psychopathology. *Brain Behav Immun* 20(4):378–388

49. Meyer U et al (2006) The time of prenatal immune challenge determines the specificity of inflammation-mediated brain and behavioral pathology. *J Neurosci* 26(18):4752–4762
50. Song X et al (2011) The nuclear factor-kappaB inhibitor pyrrolidine dithiocarbamate reduces polyinosinic-polycytidilic acid-induced immune response in pregnant rats and the behavioral defects of their adult offspring. *Behav Brain Funct* 7(1):50
51. Arrode-Bruses G, Bruses JL (2012) Maternal immune activation by poly(I:C) induces expression of cytokines IL-1beta and IL-13, chemokine MCP-1 and colony stimulating factor VEGF in fetal mouse brain. *J Neuroinflammation* 9:83
52. Arsenaault D et al (2014) The different effects of LPS and poly I:C prenatal immune challenges on the behavior, development and inflammatory responses in pregnant mice and their offspring. *Brain Behav Immun* 38:77–90
53. Zuckerman L, Weiner I (2005) Maternal immune activation leads to behavioral and pharmacological changes in the adult offspring. *J Psychiatr Res* 39:311–323
54. Zuckerman L et al (2003) Immune activation during pregnancy in rats leads to a postpubertal emergence of disrupted latent inhibition, dopaminergic hyperfunction, and altered limbic morphology in the offspring: a novel neurodevelopmental model of schizophrenia. *Neuropsychopharmacology* 28(10):1778–1789
55. De Miranda J et al (2010) Induction of Toll-like receptor 3-mediated immunity during gestation inhibits cortical neurogenesis and causes behavioral disturbances. *MBio* 1(4):e00176410
56. Meyer U et al (2010) Chronic clozapine treatment improves prenatal infection-induced working memory deficits without influencing adult hippocampal neurogenesis. *Psychopharmacology (Berl)* 208(4):531–543
57. Shi L et al (2009) Activation of the maternal immune system alters cerebellar development in the offspring. *Brain Behav Immun* 23(1):116–123
58. Ratnayake U et al (2012) Behaviour and hippocampus-specific changes in spiny mouse neonates after treatment of the mother with the viral-mimetic Poly I:C at mid-pregnancy. *Brain Behav Immun* 26(8):1288–1299
59. Giovanoli S et al (2013) Stress in puberty unmasks latent neuropathological consequences of prenatal immune activation in mice. *Science* 339(6123):1095–1099
60. Winter C et al (2009) Prenatal immune activation leads to multiple changes in basal neurotransmitter levels in the adult brain: implications for brain disorders of neurodevelopmental origin such as schizophrenia. *Int J Neuropsychopharmacol* 12(04):513–524
61. Vuillermot S et al (2010) A longitudinal examination of the neurodevelopmental impact of prenatal immune activation in mice reveals primary defects in dopaminergic development relevant to schizophrenia. *J Neurosci* 30(4):1270–1287
62. Meyer U et al (2008) Relative prenatal and postnatal maternal contributions to schizophrenia-related neurochemical dysfunction after in utero immune challenge. *Neuropsychopharmacology* 33(2):441–456
63. Ozawa KK et al (2006) Immune activation during pregnancy in mice leads to dopaminergic hyperfunction and cognitive impairment in the offspring: a neurodevelopmental animal model of schizophrenia. *Biol Psychiatry* 59(6):546–554
64. Nyffeler M et al (2006) Maternal immune activation during pregnancy increases limbic GABAA receptor immunoreactivity in the adult offspring: implications for schizophrenia. *Neuroscience* 143(1):51–62
65. Meyer U et al (2008) Adult brain and behavioral pathological markers of prenatal immune challenge during early/middle and late fetal development in mice. *Brain Behav Immun* 22(4):469–486
66. Li Q et al (2009) Prenatal immune challenge is an environmental risk factor for brain and behavior change relevant to schizophrenia: evidence from MRI in a mouse model. *PLoS One* 4(7):e6354
67. Piontkewitz Y et al (2011) Abnormal trajectories of neurodevelopment and behavior following in utero insult in the rat. *Biol Psychiatry* 70(9):842–851
68. Wilson CA, Koenig JI (2014) Social interaction and social withdrawal in rodents as readouts for investigating the negative symptoms of schizophrenia. *Eur Neuropsychopharmacol* 24(5):759–773
69. Ratnayake U et al (2014) Prenatal exposure to the viral mimetic Poly I:C alters fetal brain cytokine expression, and postnatal behaviour. *Dev Neurosci* 36:83
70. Bauman MD et al (2014) Activation of the maternal immune system during pregnancy alters behavioral development of rhesus monkey offspring. *Biol Psychiatry* 75(4):332–341
71. Schwartzer JJ et al (2013) Maternal immune activation and strain specific interactions in the

- development of autism-like behaviors in mice. *Transl Psychiatr* 3:e240
72. Nuechterlein KH et al (2004) Identification of separable cognitive factors in schizophrenia. *Schizophr Res* 72(1):29–39
 73. Ito HT et al (2010) Maternal immune activation alters nonspatial information processing in the hippocampus of the adult offspring. *Brain Behav Immun* 24(6):930–941
 74. Savanthrapadian S et al (2013) Enhanced hippocampal neuronal excitability and LTP persistence associated with reduced behavioral flexibility in the maternal immune activation model of schizophrenia. *Hippocampus* 23(12):1395–1409
 75. Zhang Y et al (2012) Prenatal exposure to a viral mimetic alters behavioural flexibility in male, but not female, rats. *Neuropharmacology* 62(3):1299–1307
 76. Han M et al (2012) Gender differences in cognitive function of patients with chronic schizophrenia. *Prog Neuropsychopharmacol Biol Psychiatry* 39(2):358–363
 77. Wolff AR et al (2011) Behavioural deficits associated with maternal immune activation in the rat model of schizophrenia. *Behav Brain Res* 225(1):382–387
 78. Howland JG et al (2012) Altered object-in-place recognition memory, prepulse inhibition, and locomotor activity in the offspring of rats exposed to a viral mimetic during pregnancy. *Neuroscience* 201:184–198
 79. Abazyan B et al (2010) Prenatal interaction of mutant DISC1 and immune activation produces adult psychopathology. *Biol Psychiatry* 68(12):1172–1181
 80. Feldon J, Weiner I (1992) From an animal model of an attentional deficit towards new insights into the pathophysiology of schizophrenia. *J Psychiatr Res* 26(4):345–366
 81. Weiner I (2003) The “two-headed” latent inhibition model of schizophrenia: modeling positive and negative symptoms and their treatment. *Psychopharmacology (Berl)* 169(3–4):257–297
 82. Zuckerman L, Weiner I (2003) Post-pubertal emergence of disrupted latent inhibition following prenatal immune activation. *Psychopharmacology (Berl)* 169(3/4):308
 83. Ellinwood EH Jr et al (1973) Evolving behavior in the clinical and experimental amphetamine (model) psychosis. *Am J Psychiatry* 130(10):1088–1093
 84. Snyder SH (1973) Amphetamine psychosis: a “model” schizophrenia mediated by catecholamines. *Am J Psychiatry* 130(1):61–67
 85. van den Buuse M et al (2005) Importance of animal models in schizophrenia research. *Aust N Z J Psychiatry* 39(7):550–557
 86. Makinodan M et al (2008) Maternal immune activation in mice delays myelination and axonal development in the hippocampus of the offspring. *J Neurosci Res* 86(10):2190–2200
 87. Wolff AR, Bilkey DK (2008) Immune activation during mid-gestation disrupts sensorimotor gating in rat offspring. *Behav Brain Res* 190(1):156–159
 88. Deslauriers J et al (2014) Preventive effect of alpha-lipoic acid on prepulse inhibition deficits in a juvenile two-hit model of schizophrenia. *Neuroscience* 272:261
 89. Stridh L et al (2013) Toll-like receptor-3 activation increases the vulnerability of the neonatal brain to hypoxia-ischemia. *J Neurosci* 33(29):12041–12051
 90. Romero E et al (2010) Ontogeny of sensorimotor gating and immune impairment induced by prenatal immune challenge in rats: implications for the etiopathology of schizophrenia. *Mol Psychiatry* 15(4):372–383

Part III

Brain Damage—Causes and Consequences

Oligodendrocytes: Cells of Origin for White Matter Injury in the Developing Brain

Mary Tolcos, David H. Rowitch, and Justin Dean

Abstract

A prominent pattern of brain injury in preterm born infants involves damage to white matter with impaired oligodendrocyte maturation. This results in diffuse deficits in myelination that are associated with later development of cerebral palsy. While numerous experimental animal models of perinatal white matter injury have been developed, they show a spectrum of effects. This review proposes that adopting a more standard approach to defining white matter injury is important for validating experimental findings against the *bona fide* human condition. This chapter will describe the pathology of perinatal white matter injury and a general methodological approach for assessing white matter injury experimentally.

Key words Oligodendrocyte, Perinatal white matter injury, Myelination, Neuropathology, Astrogliosis, Microgliosis, Preterm, Immunohistochemistry, Histopathology, Methodology

1 Background

The white matter tracts of the brain comprise bundles of axons that establish connections between different regions. The wrapping of axons with a myelin sheath (myelination) is a cornerstone of human neurodevelopment. Myelin acts as an insulator for axons, and enables the rapid transfer of electrical information required for normal brain activity including coordinated sensory, cognitive, and motor functions. In humans, myelination begins in the second half of gestation, and progresses from deep to superficial regions of the brain in a caudal-to-rostral gradient [1]. After birth, the process of myelination progresses rapidly and peaks during the first postnatal year, but continues into adolescence and adulthood [2].

In the central nervous system (CNS), myelin is produced by oligodendrocytes. At least four stages of oligodendrocyte maturation have been described in the human brain: oligodendrocyte progenitor cells (OPCs), pre-oligodendrocytes (preOLs), immature oligodendrocytes and mature oligodendrocytes (Fig. 1) [3–5]. OPCs are highly proliferative, and develop from multipotent

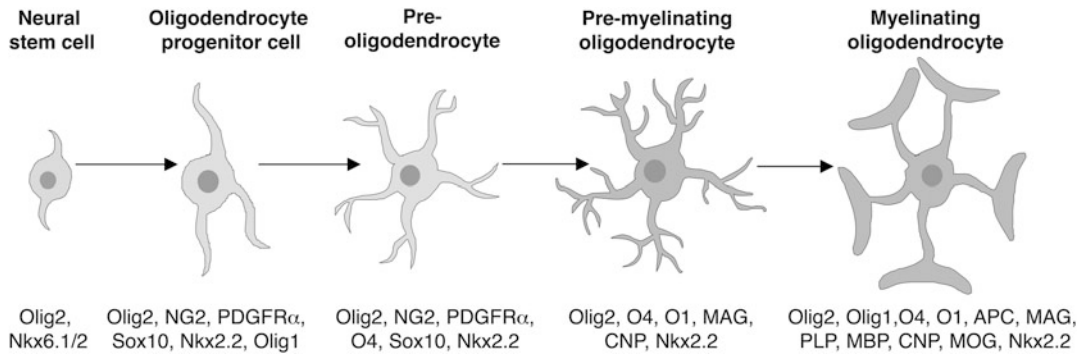


Fig. 1 Lineage and stage-specific antigens of oligodendrocytes. During development, oligodendrocytes are generated by multipotent stem cells in the proliferative zones of the brain and spinal cord. These give rise to oligodendrocyte progenitor cells that divide and migrate through the parenchyma to reach their final destination. These progenitor cells terminally differentiate into pre-oligodendrocytes, pre-myelinating oligodendrocytes and then mature myelinating oligodendrocytes that form the myelin sheath of axons (Figure provided by Dr Anzari Atik). *APC*, adenomatous polyposis coli; *CNP*, 2',3'-cyclic-nucleotide 3'-phosphodiesterase; *MAG*, myelin-associated glycoprotein; *MBP*, myelin basic protein; *MOG*, myelin oligodendrocyte glycoprotein; *NG2*, NG2 chondroitin sulfate proteoglycan; *Nkx2.2*, NK2 homeobox 2; *Nkx6.1/2*, NK6 homeobox 1 and 2; *O1*, O1 antigen; *O4*, O4 antigen; *Olig1*, oligodendrocyte transcription factor 1; *Olig2*, oligodendrocyte transcription factor 2; *PDGFR α* , platelet-derived growth factor receptor- α ; *PLP*, proteolipid protein; *Sox10*, sex-determining region Y-box 10

stem cells in sequential waves during fetal and early postnatal life from restricted periventricular zones. OPCs first appear in the ganglionic eminence around 9 weeks of gestation in humans, and continue to be produced throughout intrauterine life, after birth and into adulthood [6–10]. Thus, even where oligodendrocyte development has been disturbed, an endogenous pool of OPCs may remain available for therapeutic targeting of repair and remyelination. Once OPCs migrate to reach their final destination, they can terminally differentiate into post-mitotic pre-myelinating oligodendrocytes, before finally forming mature oligodendrocytes capable of producing myelin and initiating axonal myelination.

2 Pathology of Perinatal White Matter Injury

Injury to the cerebral white matter resulting in deficits in myelination is the major pattern of brain injury observed in survivors of preterm birth, although white matter injury can also occur in term born infants, typically in combination with overt grey matter damage [11–14]. The classical pattern of perinatal white matter injury involves focal regions of macroscopic and microscopic cystic necrosis, associated with reactive gliosis [15–20]. The myelination deficits observed in these cystic lesions are related to degeneration of all cellular elements, including oligodendrocytes and axons [5, 15, 21–24]. However, in more modern cohorts of preterm infants,

imaging studies suggest that the incidence and overall burden of cystic white matter lesions is very low [25, 26], while a pattern of less severe but widespread diffuse white matter injury is now prevalent [17, 27–29].

Pathologically, diffuse white matter injury is characterized by a pattern of diffuse myelination failure associated with reactive astrogliosis and microgliosis, without major primary axonal injury [17, 22, 30, 31]. While selective death of preOLs was previously considered the predominant mechanism leading to these diffuse deficits in white matter myelination [32–34], the major consensus finding in humans is that oligodendrocytes can become arrested in their maturation, likely at the O4/O1 transition stage, and thus fail to differentiate into myelin producing cells [16, 17, 35]. Maturation arrest of oligodendrocytes has also been reported in several perinatal animal models of hypoxia-ischemia [30, 36, 37], chronic hyperoxia [38] or hypoxia [39–41], intrauterine growth restriction [42, 43], and infection/inflammation [44–46]. Thus, a role of loss of oligodendrocytes in this chronic stage of injury is unlikely [17]. Indeed, experimentally, the acute loss of oligodendrocytes in response to hypoxia-ischemia in neonatal rats [37] and preterm fetal sheep [30] is recovered by a rapid proliferative response of the OPC population. Further, the human neonatal brain exhibits vast numbers of migratory OPCs that can easily repopulate the area of injury to replace dying oligodendrocytes [47, 48]. Experimental models of neonatal white matter injury have also shown OPC proliferation and impaired maturation in the absence of acute oligodendrocyte cell death [40, 41, 45, 46]. Overall, these findings suggest that understanding the mechanisms of arrested oligodendrocyte development should be a particular focus for studies examining the pathogenic basis of neonatal white matter injury and therapeutic strategies.

3 Assessment of Experimental Perinatal White Matter Injury

As described, perinatal white matter injury is comprised of a spectrum of disorders that includes focal cystic micro/macrosopic necrotic lesions, diffuse non-cystic lesions, axonal injury, astrogliosis, microgliosis, oligodendrocyte cell death, oligodendrocyte maturation arrest, and deficits in myelination. Such injury can be assessed using a variety of techniques including magnetic resonance imaging (MRI), in particular diffusion tensor imaging (DTI), neuropathological assessment using histochemistry and immunohistochemistry, and electron microscopy, as well as molecular techniques (qPCR and *in situ* hybridization) to examine mechanistic injury pathways. The advantages and disadvantages of these common techniques are listed in Table 1. Below we provide an outline of neuropathological procedures that should be considered for

Table 1
Techniques used to assess experimental perinatal white matter injury: advantages and disadvantages

Technique	Application	Advantages	Disadvantages
Magnetic Resonance Imaging	Used to assess white matter volumes and macrostructure.	Noninvasive; provides details of injury (extent and localization) without having to terminate the experiment; can investigate time-course or progression of injury.	Does not provide details of cellular changes associated with the injury; animal requires sedation.
Diffusion Tensor Imaging	Used to assess white matter microstructure. e.g., integrity of axonal fibers, coherence of axon bundles, trajectory of fiber tracts.	Noninvasive	Does not provide details of cellular changes associated with the injury; animal requires sedation. Does not definitively identify myelin.
Magnetic Resonance Spectroscopy	Used to study metabolic changes in the brain.	Noninvasive	Does not provide details of cellular changes associated with the injury; animal requires sedation.
Neuropathology: Histology	Identification of gross morphological changes and injury within the brain at the microscopic level.	Provides information on degree, severity, and location of injury; quantifiable; quick.	Information on injury at one point in time. i.e., unable to assess progression of injury in the same animal; provides no information on alterations at the protein level; unable to distinguish between different specific cell types (e.g., microglia and astrocytes).
Neuropathology: Immunohistochemistry	Microscopic identification of alterations to specific cell types or protein levels.	Able to assess various neural populations (neuron, microglia, astrocyte, oligodendrocyte), subpopulations (e.g., preOL, mature oligodendrocyte), or activation states (e.g., reactive microglia: M1 or M2 phenotype).	Only provides information on changes at one point in time; densitometry assessment of immunoreactivity may not completely reflect actual protein content in tissue.

<p>Electron microscopy</p>	<p>Ultrastructural assessment of myelin sheath thickness, axon diameter, axon number, ratio of myelinated to unmyelinated axons.</p> <p>“Gold standard” quantitative assessment of myelination; high power visualization of the myelin sheath and axons; requires very small tissue pieces.</p> <p>Large areas of the white matter cannot be assessed, and therefore, nonuniform changes may be missed.</p>
<p>Molecular techniques: qPCR</p>	<p>Analysis of regulators of oligodendrocyte maturation at the mRNA level.</p> <p>Provides information on the putative molecular mechanisms underlying impaired oligodendrocyte development.</p> <p>mRNA changes do not always translate to changes in protein; does not provide details on cellular localization.</p>
<p>In situ hybridization</p>	<p>Analysis of regulators of oligodendrocyte maturation at the mRNA level in tissue sections.</p> <p>Provides information on the putative molecular mechanisms underlying impaired oligodendrocyte development; allows for phenotype analysis due to cellular localization of mRNA; works well in PFA fixed tissue.</p> <p>mRNA changes do not always translate to changes in protein.</p>

complete assessment of experimental white matter injury, focusing specifically on the use of histology, immunohistochemistry and electron microscopy.

3.1 General Considerations

3.1.1 Tissue Preparation

The most common brain fixation methods involve perfusion or immersion fixation with 10 % formalin or 4 % paraformaldehyde (PFA), followed by either (1) tissue processing (dehydration) and paraffin embedding, (2) equilibration in sucrose solution (cryoprotectant) and sectioning using the cryostat or freezing microtome, or (3) sectioning of fixed brains using a vibratome. The majority of antibodies used to assess white matter injury (*see* Table 2) will work successfully in tissues processed with any of these methods (e.g., *see* [16, 30, 37, 42, 49]). However, staining for the stage-specific cell surface antigens O4 and O1 can be markedly reduced by use of formalin solutions (likely due to methanol impurities), alcohols, solvents including xylenes, and antigen retrieval techniques, making assessment of oligodendrocyte morphology and cell counts difficult or impossible. Increasing time intervals in post-mortem fixation can also markedly reduce immunostaining for oligodendrocyte O4 and NG2 markers due to postmortem autolysis [50, 51]. Immersion fixation of blocks of brain tissues or whole rodent brains with fresh ice-cold 4 % PFA, followed by sucrose equilibration/cryostat cutting or direct vibratome cutting, then free floating immunofluorescence provides excellent staining using O4/O1 antibodies, as well as the majority of other markers required to assess white matter injury (*see* Table 1 and Sect. 3.5 for more details) [30, 37–41, 49, 52–55].

3.1.2 White Matter Assessment

White matter injury in the developing brain primarily occurs in the deep dorsal and lateral aspects to the lateral ventricles at the frontal, parietal and occipital levels, and may extend into adjacent external capsule, corona radiata, corpus callosum, and centrum ovale [5]. In rodents, the white matter constitutes only a small proportion of total brain volume, and the connecting white matter tracts encompassing the corpus callosum, overlying supracallosal radiation, and the external capsule at the level of the midseptal nuclei (frontal white matter) and the anterior hippocampal formation/anterior nuclei of the thalamus (parietal white matter) are typically used for assessment of white matter injury [37, 42, 52, 56–58]. In larger species such as sheep, white matter injury can be regionally divided into deep periventricular and more superficial regions (e.g., corona radiata, centrum ovale) at the frontal (e.g., mid-striatum) and parietal (e.g., mid-thalamic) levels [36, 59–62], while a medial versus lateral approach has also been reported [63]. Critically, irrespective of species, given that oligodendrocytes develop in a caudal to rostral direction, and can exhibit marked regional and level differences in density, maturation, and myelination, it is key

Table 2
Antibodies used for assessing perinatal white matter injury using immunohistochemistry

Antigen/marker	Labels
<i>Oligodendrocytes</i>	
Olig1	OPCs (nuclear) and mature oligodendrocytes (cytoplasmic)
Olig2	Nuclear pan-oligodendrocyte marker of OPCs, preOLs, pre-myelinating and myelinating oligodendrocytes. Also expressed in multipotent neural stem cells and some transit amplifying astrocyte progenitors.
O4	preOLs, pre-myelinating oligodendrocytes
O1	Pre-myelinating and myelinating oligodendrocytes
PDGFR α	OPCs and preOLs
Nkx2.2	OPCs, preOLs, pre-myelinating and myelinating oligodendrocytes
Sox10	Nuclear marker for OPCs, preOLs
NG2	OPCs and preOLs
CC1/APC	Myelinating oligodendrocyte marker; but can show overlap in cycling and NG2-positive cells.
CNP	Pre-myelinating and myelinating oligodendrocytes
NogoA	Myelinating oligodendrocytes
<i>Myelin proteins</i>	
MBP	Mature myelin, myelinating oligodendrocytes
MAG	Mature myelin, Pre-myelinating and myelinating oligodendrocytes
PLP	Mature myelin, myelinating oligodendrocytes
<i>Astrocytes</i>	
GFAP	Astrocytes (cell body and processes), radial glia, Bergman glia
S100 β	Astrocytes
Glutamine synthetase	Astrocyte cell body
GLT-1	Astrocytes (and neurons)
GLAST (aka ACSA-1)	Astrocyte specific glutamate transporter; astrocytes, radial glia, Bergmann glia
AldoC	Astrocytes (and Purkinje cells)
CD44	High levels in astrocyte precursors, astrocytes; expression in other cell types including oligodendrocytes
<i>Microglia</i>	
Lectin	Microglia/macrophages (and blood vessels)
Iba1	Microglia/macrophages
ED1/CD68	Resting (low expression) and reactive (high expression) microglia/macrophages

(continued)

Table 2
(continued)

Antigen/marker	Labels
F4/80	Mature microglia/macrophages
CD40	Microglia/macrophages
CD45	Microglia/macrophages
CX3CR1	High levels in microglia/macrophages; lower expression in other cells types including neurons
<i>Axons</i>	
NF200	Phosphorylated and/or dephosphorylated 200 kDa neurofilament (high molecular weight)
SMI 312	Phosphorylated neurofilament (medium and high molecular weight)
SMI 31	Phosphorylated neurofilament (high molecular weight)
SMI 32	Non-phosphorylated neurofilament (high molecular weight)
β -APP	Damaged neurons/axons
Fractin	Apoptotic neurons/axons
Tubulin Δ Csp6	Damaged neurites/axons

that white matter injury be assessed at equivalent levels and region matched areas between groups.

3.2 Basic Histopathology

If the experimental insult is severe, white matter injury may be detected macroscopically at the time of tissue processing. However, it is more routine and informative to assess the tissue sections microscopically using a range of histochemical or immunohistochemical methods. Tissue sections can be stained histochemically using a neural specific stain such as thionine or cresyl violet (in acetate buffer, pH 4); these stains will detect Nissl substance, or RNA within the neurons and dendrites, but not in axons. However, conventional hematoxylin and eosin (H&E) can be used and is often beneficial for detecting the presence of other cell types within the parenchyma or meninges such as blood and inflammatory cells. Nissl stains and H&E also allow for the assessment of global injury in the brain, rather than that specific to the white matter. Alternatively, histochemical stains such as luxol fast blue (LFB) [64], eriochrome cyanine R (also called chromoxane cyanine R, solochrome cyanine R, or Mordant blue 3) [65], or Gallyas silver stain [66] can be used to specifically stain myelin. However, caution must be taken when interpreting a reduction in staining intensity as a reduction in myelin content. Silver-staining methods such as Bielschowsky or Bodian [67] identify axons within the white

matter, and provide a useful technique for the identification of axonal pathologies (*see* Sect. 3.4 for more detail).

Tissue sections stained histochemically are used to assess overt white matter injury in the form of necrotic lesions, focal or diffuse non-destructive lesions, acute axonal injury and/or areas of pallor, or for the determination of white matter volume. White matter lesions can be scored based on severity (e.g., necrotic vs. non-destructive), incidence (e.g., the proportion of experimental animals with lesions) and distribution (e.g., periventricular white matter, subcortical white matter, corpus callosum, external capsule, cingulum). The neuropathological assessment of white matter injury in human neonates is considerably more detailed [17], and often requires review by a pathologist.

The volume of the white matter also provides a surrogate measure of white matter injury and can be assessed quantitatively using imaging processing software packages such as ImageJ or Fiji (www.fiji.sc/Fiji). It must be acknowledged, however, that a reduction in the volume of the white matter (or regional volume reductions) can indicate a reduction in myelination or myelin thickness, and/or a reduction in the number of myelinated/unmyelinated axons. Therefore, to distinguish between these phenomena, further assessment using electron microscopy (*see* Sect. 3.6.3 below) is required.

3.3 Assessment of Astrogliosis and Microgliosis

Reactive astrocytosis and microglial activation are common features observed in human and experimental postmortem studies of perinatal white matter injury. Identification of areas of white matter gliosis also provides a basis for regional analysis of oligodendrocyte survival, maturation, and myelination in the lesion environment (*see* Sect. 3.5) [17, 30]. The classical antibodies used to assess astrocyte morphology include glial fibrillary acid protein (GFAP; stains major processes) and S100 β (cytosolic protein), as well as glutamine synthetase and the glutamate transporters GLT-1 (aka EAAT2) and GLAST (aka EAAT1). Note that these markers do not all selectively label astrocytes. For example, GFAP is also expressed by radial glia within the cerebral cortex and Bergmann glial within the cerebellum. Further, these markers are not selective for reactive astrocytes, and thus morphological assessment is required to assess reactivity. Nevertheless, a wide range of alternative markers of normal and reactive astrocytes, including aldolase C (AldoC) and CD44 [17, 68] have been reported [69–72].

The most common markers or antibodies used to assess macrophages/microglia include lectins (e.g., biotinylated tomato lectin; lectins also stain blood vessels), ionized calcium-binding adapter molecule 1 (Iba1), ED1/CD68, as well as F4/80, CD40, CD45, and CX3CR1. It is important to note that these markers do not differentiate between macrophages (such as those entering from the periphery) versus resident CNS microglia, although new panels of

unique microglia markers are being developed [73]. Further, only ED1/CD68 is considered a marker of reactive microglia/macrophages, and morphological assessment is generally required to assess reactivity. Interestingly, there is increasing evidence that microglia can acquire multiple activation phenotypes that may have differing functions in perinatal brain injury [74, 75], as observed in adults [76–81]. The key phenotypes include the M1 classic phenotype (cytotoxic), M2a alternate phenotype (repair and regeneration), and M2b Type II-deactivating phenotype (immunomodulatory) [82, 83]. Using panels of markers for these phenotypes validated *in vitro* [84–86], it is possible to examine the temporal patterns and roles of activated microglia phenotypes with respect to evolution and mechanisms of perinatal white matter injury [87].

By single or double staining markers of astrocytes or microglia (e.g., GFAP/Iba1), necrotic foci can be observed microscopically as focal areas of dense astrocyte or microglial staining, with cells typically exhibiting a reactive morphology [17, 30]. Similarly, diffuse white matter injury can be characterized neuropathologically by areas of diffuse accumulation of reactive microglia and astrocytes. In the early developing white matter, the expression of GFAP-positive astrocytes is very low. For example, in our experience, widespread staining of GFAP-positive astrocytes is not present in the normal brain until around postnatal day 7 in neonatal rodents. Thus, brain lesions containing reactive astrocytes can easily be identified at these younger ages. With increasing expression of GFAP-positive astrocytes in the white matter with development, it can become difficult to assess areas of reactive astrogliosis over the normal dense astrocytic background. In such cases, low-power image montages or digital scanning (e.g., Leica Aperio ePathology) of entire brain sections can be useful in determining areas of gliosis. Counting numbers of astrocytes in brain lesions is also difficult, as astrocytes are intrinsically connected with other cell types, making accurate selection of the astrocyte cell body problematic. Further, astrocytes do not typically proliferate in response to injury, but rather exhibit thickening of their main processes with elevated GFAP expression [88]. Unbiased quantification of astrogliosis in neonatal white matter lesions has been recently reported using point-counting methods such as the Cavalieri approach [17]. In this technique, the area fraction of GFAP-positive cell soma and/or processes can be determined by overlay of a grid of known size onto a microscope image, and then counting of the grid points that fall on the item to be quantified [89].

In contrast to astrocytes, microglia can be easily visualized in the white matter during early brain development, where they exhibit an amoeboid morphology, before developing into a ramified state. Microglia typically accumulate in areas of white matter injury by migration and proliferation, and demonstrate a reactive morphology. For quantification of reactive microgliosis, counts of

numbers of microglia in white matter lesions can be determined, although with excessive microgliosis this can be challenging. An alternative approach is to use the Cavalieri approach described above for astrocytes. More detailed assessment of the temporal changes in reactive microglial phenotypes may also provide important details on potential roles of microglia in the injury process. Importantly, small clusters of amoeboid microglia can be found in the white matter during normal development in patterns that may resemble areas of injury. Thus, care needs to be taken to have appropriate matched level controls sections for assessment of injury.

3.4 Assessment of Axonal Injury

During human cortical development, growing axons (growth-associated protein 43-positive) are detected as early as 20 weeks of gestation, with extensive expression by 37 weeks [90]; thus, axons are highly vulnerable to developmental injury in preterm infants. Axonal injury is present within the focal cystic necrotic lesions in human periventricular leukomalacia (PVL) and has been established as a feature in experimental models of perinatal hypoxic-ischemic brain injury. Using fractin as a marker of apoptotic axons, degenerating axons have also been detected in diffuse non-cystic lesions within human PVL [22]; however, this finding was not replicated in a preterm fetal sheep model of global ischemia [30]. It is still unclear whether the axonal injury associated with diffuse non-cystic lesions occurs as a consequence of the underlying injury (e.g., neuronal injury) or is the primary source of the injury. Nonetheless, if axons degenerate it is reasonable to assume that myelination would also be affected leading to cerebral hypomyelination and regional volume reductions.

3.4.1 Staining Methods

One of the most well-known and utilized techniques for the pathological assessment of axonal injury is Bielschowsky's silver stain, which identifies argyrophilic axons, and is thought to stain all neurofilaments regardless of their molecular weight. This method, applied to paraffin-embedded tissue, has undergone numerous modifications, but one of the most recognizable protocols is that of Yamamoto and Hirano [91]. In models of perinatal brain injury, Bielschowsky's silver stain is used to identify regions of axonal degeneration and the presence of axonal spheroids [92]. Antibodies directed against the neurofilament proteins are also used to examine axonal pathology in human preterm brains [90] and models of perinatal white matter injury [31, 59, 93]. Neurofilaments are components of the axonal cytoskeleton and consist of a family of three polypeptide subunits: NFL (low molecular weight neurofilament; ~ 68 kDa), NFM (medium molecular weight neurofilament; 90–168 kDa), and NFH (high molecular weight neurofilament; 100–200 kDa). During axonal development, neurofilament subunits, in particular NFM and NFH, are phosphorylated at the same time that neurofilament is transported down the axon. Thus,

phosphorylated NFH in particular, is a marker for axonal maturity [94]. Listed in Table 2 are four antibodies used to label neurofilaments: SMI 31 recognizes phosphorylated NFH; SMI 32 recognizes non-phosphorylated NFH; SMI 312 recognizes phosphorylated NFM and NFH and NF200, a pan-axonal marker that labels all 200 kDa neurofilaments (phosphorylated and dephosphorylated). Other antibodies for axonal injury/degeneration include β -amyloid precursor protein (β -APP), caspase-cleaved forms of the cytoskeletal elements actin (fractin; N-terminal fragment of actin) and tubulin (Tubulin Δ Csp6) (Table 2), or β -APP in combination with Caspase 6 [95, 96]. β -APP is a membrane glycoprotein present in low levels in normal neurons, but is rapidly upregulated within axons following neuronal damage [97, 98]. The fractin antibody recognizes caspase-cleaved but not intact actin, and labels apoptotic but not necrotic neurons/axons [99], and Tubulin Δ Csp6 labels degenerating neurites in human hypoxic-ischemic injury [100]. In human diffuse non-necrotic lesions, fractin-immunoreactivity is present, while β -APP immunostaining is rarely seen [31, 90], highlighting the need to use more than one marker of axonal injury.

3.4.2 Neuropathological Analysis

Neuropathological assessment of axonal injury in perinatal white matter injury involves analysis for the presence of reduced staining/immunoreactivity, axonal swellings and axonal spheroids. Such analysis is semi-quantitative and can involve the use of a grading system to score the amount immunoreactivity, or the proportion of cases/animals with axonal injury [22, 31, 90]. However, neither method is quantitative and thus suitable for statistical analysis. Densitometry of neurofilament immunoreactivity may be used but must be interpreted with caution for reasons outlined in Sect. 3.6.2 below.

3.4.3 Electron Microscopy

The ultrastructural assessment of axonal structure and injury is more informative and quantifiable using electron microscopy. The processing of tissue for electron microscopy is different to that for histochemistry or immunohistochemistry. Ideally, the brain is first transcardially perfused with 2.5 % glutaraldehyde in 0.1 M cacodylate buffer (pH 7.4). Alternatively, blocks (approximately 1 mm³) can be dissected from tissue perfused with 4 % paraformaldehyde for histology, and quickly immersed in 2.5 % glutaraldehyde in 0.1 M cacodylate buffer (pH 7.4), reducing the need for additional animals. Briefly, tissue blocks are then post-fixed in 1 % osmium tetroxide in 0.2 M cacodylate buffer (pH 7.4) and stained with uranyl acetate in maleate buffer (pH 6), before being embedded in epon-araldite. Semi- and/or ultrathin sections are then cut using an ultramicrotome. These sections can be used to assess the areal density of myelinated and unmyelinated axons in non-overlapping fields from a number of sections using ImageJ software. Of note,

osmium tetroxide treatment makes many epitopes unstable, and reduces the efficacy of superimposed immunogold labeling of electron microscopy samples. New and more stable epitope tags, resistant to effects of osmium tetroxide fixation, are therefore needed to overcome this problem.

3.5 Assessment of Oligodendrocyte Stages, Death, and Maturation

3.5.1 Stage Specific Oligodendrocyte Markers

Oligodendrocytes express a range of cell surface and myelin-specific antigens that can be used to precisely identify the various stages of oligodendrocyte maturation (Fig. 1; Table 2) [4]. The pan-lineage marker *Olig2* is widely used for identification of oligodendrocytes at all maturational stages. As a nuclear marker, it is particularly useful for assessing changes in total numbers of oligodendrocytes in the white matter in injury models. The OPC is the earliest stage of the committed oligodendrocyte lineage, and exhibits a simple bipolar morphology. For identification of OPCs, antibodies against platelet-derived growth factor receptor- α (PDGFR α), nuclear *Olig1*, *Sox10*, or *NG2* chondroitin sulfate proteoglycan are commonly used, although some of these markers can also label a population of preOLs. As described, OPCs often exhibit marked proliferative responses in many models of white matter injury, which can be assessed by combination with cell cycle markers such as *Ki67* or proliferating cell nuclear antigen (PCNA).

The next stage of oligodendrocyte maturation, the preOL, is also mitotically active, and exhibits a simple multipolar morphology. preOLs are most commonly identified by expression of the O4, but not O1, antibodies, although they may also express a range of markers similar to OPCs. Double staining using the mouse-monoclonal O4 and O1 IgM antibodies has been achieved by sequential primary/secondary antibody staining with a fixation step between primaries, or utilizing a biotinylated O4 antibody [3, 37, 52]. The immature oligodendrocyte is postmitotic and exhibits a complex multipolar morphology. Immature oligodendrocytes express both O4 and O1 antigens, but lack the complex myelinating morphology of mature oligodendrocytes, and do not express myelin proteins such as myelin basic protein (MBP). The progression to immature oligodendrocyte is also characterized by expression of myelin-associated glycoprotein (MAG) and 2', 3'-cyclic-nucleotide 3'-phosphodiesterase (CNP). Mature oligodendrocytes can be identified by expression of cytoplasmic *Olig1* [101], adenomatous polyposis coli (APC, aka CC-1), and myelin-associated markers, including MBP and proteolipid protein (PLP). In human tissue, *NogoA* is also a useful mature oligodendrocyte marker [49].

An important consideration when examining the oligodendrocyte lineage is that with advancing white matter myelination, it becomes progressively difficult to identify oligodendrocyte cell bodies using markers such as O4 and O1, due to the expression

of these antigens in oligodendrocyte processes. In such cases, double labeling using the mature oligodendrocyte marker APC with Olig2 can provide an estimate of the number of mature cells [41].

3.5.2 Oligodendrocyte Cell Death

Degenerating oligodendrocytes can be identified by cellular pyknosis (nuclear chromatin condensation) and karyorrhexis (nuclear fragmentation). When stained with the nuclear marker Hoechst 33342 or 4',6-diamidino-2-phenylindole (DAPI), pyknotic cells in the white matter are easily identified by intensely stained, condensed nuclei. Cellular degeneration and DNA fragmentation can also be assessed with the Terminal deoxynucleotidyl transferase dUTP nick end labeling (TUNEL) assay. Confirmation of oligodendrocyte lineage or specific developmental stage can be achieved by double labeling with Olig2 or O4/O1 for example [17, 30, 32, 37]. In addition, markers of dying oligodendrocytes labeled with O4 for example, will show morphological condensation of the cell body, fragmentation of the processes, and O4-labeling of cell membrane and cytoplasm due to loss of plasma membrane integrity [57]. Note that these methods do not distinguish between apoptotic or non-apoptotic modes of cell death. Co-localization of oligodendrocyte antibodies with apoptotic cascade markers such as activated-caspase-3, along with assessment of cellular pyknosis or TUNEL, can also be used to give a broad indication of the relative contributions of different cell death pathways.

3.6 Assessment of Myelination

The white matter within the CNS is composed of ~40–50 % myelin (dry weight) [4]. Of this myelin dry weight, 70 % is composed of glycolipids and the remaining 30 % is proteins; these myelin constituents are formed within the oligodendrocyte. Oligodendrocytes and myelin are rich in glycosphingolipids, in particular galactosylceramides (GalC/O1) and their sulfate derivatives (sulfatides/O4). Each of these lipids can be localized immunohistochemically and are used to identify stages of maturation of the oligodendrocyte lineage (*see* Sect. 3.5.1).

3.6.1 Myelin Proteins

There are numerous myelin proteins, which are located at different positions within the lipid bilayer and play different roles in myelination. Thus, the choice of myelin marker is an important consideration when assessing changes in myelination. MBP and PLP are the two major CNS myelin proteins, and constitute 30 % and 50 % of the total myelin proteins, respectively [4]. MBP plays a role in myelin compaction and is localized to the major dense line, while PLP spans the entire thickness of the lipid bilayer and is localized to both the intraperiodic line and major dense line. Minor myelin constituents include: 2',3'-cyclic-nucleotide 3'-phosphodiesterase (CNP, 4 %) localized to oligodendrocyte membranes during early stages of axonal ensheathment and not to compact myelin [102]; MAG (1 %) localized to periaxonal membranes of the myelin

internodes, and is thus in direct contact with the axon; myelin/oligodendrocyte glycoprotein (MOG), located on the oligodendrocyte membrane, in particular the oligodendrocyte cell processes and on outer most lamellae of the myelin sheath; and myelin associated oligodendrocyte basic protein (MOBP), located in major dense lines and involved in myelin compaction. Interestingly, MBP and MOBP mRNA are initially found within the soma of the oligodendrocyte, but once myelination proceeds they move distally into the oligodendrocyte cell processes [103, 104]. In human PVL cases [16] and in an experimental model of intrauterine growth restriction [42], MBP expression is retained with the oligodendrocyte cell soma, reflecting a deficit in the trafficking of MBP to the processes for myelin sheath wrapping. Thus, aberrant cellular localization of these two proteins should also be a consideration when assessing perinatal white matter injury in experimental models.

The large majority of experimental studies investigating the impact of perinatal insults on white matter development use MBP as a marker of myelin, and thus, any reduction in expression or aberrant cellular localization is interpreted as hypomyelination. However, MBP is only one of many myelin proteins, and myelination should be investigated in combination with other markers such as PLP or MAG. Indeed, in a model of intrauterine growth restriction in the guinea pig, we have noted a striking lack of MBP expression (i.e., trapping of MBP within the cell soma), which could be interpreted as a lack in myelination, but the presence of both PLP and MAG immunoreactivity, albeit at reduced levels [42]. Thus, conclusions on the state of myelination should not be drawn based on MBP staining alone.

3.6.2 *Immunohistochemical Analysis of Myelination*

Immunocytochemistry is commonly used to detect changes in the expression of myelin proteins. This can be performed using tissue sections to assess for deficits in spatial distribution and localization, as well as potentially for changes in the intensity of myelin proteins. Semi-quantification of myelin proteins localized to tissue sections may be performed using densitometry, although the sensitivity and reproducibility of this technique remain controversial. The reaction between an antibody and its antigen is not stoichiometric; therefore, the intensity of the staining product does not directly translate to the amount of that product (i.e., protein) within the tissue. This phenomenon is particularly applicable when assessing immunoreactivity using 3',3'-diaminobenzidine (DAB) as the chromogen, because DAB does not follow the Beer-Lambert law; the brown reaction product does not absorb light but rather scatters it. Despite this, studies have shown a positive linear relationship between the intensity of immunoreactivity and the antigen concentration [105], although this may not apply to all antibodies [106]. Other chromogens such as Liquid

Permanent Red show very similar spectral profiles at both high and low levels of expression, and are considered more suitable for densitometry [107]. It should be noted that densitometry is typically used to assess relative differences in immunoreactivity between control and experimental cohorts rather than quantification of absolute protein levels.

If densitometry is the chosen form of analysis, certain technical steps need to be considered. First, it is imperative that all tissue is fixed and processed in the same way, including fixative used, duration of fixation, and section thickness. Secondly, immunohistochemistry should be performed on all tissue sections to be compared at the same time and using the same protocol. This often results in a large number of slides undergoing simultaneous immunostaining, and it is thus important that incubation times (particular of the chromogen) are consistent. Thirdly, if possible a counterstain should not be used to prevent the need for spectral unmixing [107]. Lastly, imaging should ideally be performed in a single day to maintain identical microscope parameters (e.g., intensity of light source, condenser position).

Densitometry is then performed on captured images using software packages such as Image-Pro Plus (Media Cybernetics). In preparation for densitometry measurements, the image analysis system is first calibrated using an image of a blank section of the glass slide (incident light) and an obscured section of the slide (infinite optical density). Images are then taken from matched regions of interest from immunostained tissue sections at comparable levels of the brain, converted to greyscale and the optical density (absorbance) determined. A correction is then applied to each of these images by subtracting the optical density measurement of the immunostaining from the optical density measurement from a region of background staining. Optical density units have no dimension and are logarithmic, and the value reflects the amount of photons absorbed or transmitted; an optical density of zero indicates all photons are transmitted, and an optical density of 1.0 indicates that 90 % of all photons are absorbed, while an optical density of 2.0 indicates that 99 % of all photons are absorbed.

3.6.3 *Electron Microscopy*

While immunohistochemical localization of myelin proteins (and oligodendrocytes) provides essential microscopic data when assessing white matter injury, electron microscopy is considered the “gold standard” technique for assessing myelination as it detects changes at the ultrastructural level. The methodology for preparing tissue for electron microscopy is presented in Sect. 3.4.3. Semi-thin and/or ultrathin sections can be used to assess the areal density of myelinated and unmyelinated axons, as well as inner axon diameter and outer axon diameter (axon + myelin sheath) in nonoverlapping fields from a number of sections using ImageJ software. The

conduction velocity of an axon is closely related to the axon diameter and myelin sheath thickness [108], thus dividing the inner axon diameter by the outer axon diameter (known as the g-ratio) provides a measure of conduction velocity. It is thought that the g-ratio of a myelinated axon is optimized to reach maximal efficiency and physiological function. A theoretical g-ratio value of 0.6 was first described by Rushton [109]; however, it is now acknowledged that different central white matter tracts have different optimal g-ratios [110].

While there is much focus on the myelinated axon, the assessment of unmyelinated tracts should not be overlooked. In a recent study in the rabbit model of cerebral palsy induced by antenatal hypoxia-ischemia, a decrease in the number and function of unmyelinated fibers was associated with hypertonia, with the loss of myelinated fibers occurring secondary to the motor deficits [111].

4 Conclusion

Here we have described a variety of methodological approaches that should be considered for the detection and assessment of perinatal white matter injury. Although not described in this chapter, a wide range of molecular techniques (e.g., qPCR and in situ hybridization) and transgenic animal models are available to complement these methods, as well as provide detailed mechanistic data of the pathogenesis of perinatal white matter injury, including regulators of oligodendrocyte proliferation and maturation [49, 54]. Behavioral assessment should also be considered in order to provide functional outcomes associated with experimental white matter injury and treatment strategies. A battery of behavioral tests, including motor, cognitive, and somatosensory paradigms, that can be used in rodents to investigate long-term outcomes are detailed in Chapter 11. Use of such combination approaches will further our understanding of the cellular and molecular mechanisms of perinatal white matter injury, with the aim to develop regenerative strategies to promote normal brain development and function in this group of infants.

Acknowledgments

MT is supported by the National Health and Medical Research Council of Australia and a Career Development Grant awarded by the Research Foundation, Cerebral Palsy Alliance. DHR is a HHMI investigator. JD is supported by grants from the Health Research Council of New Zealand, the Marsden Fund, and the Auckland Medical Research Foundation.

References

1. Jakovcevski I, Zecevic N (2005) Sequence of oligodendrocyte development in the human fetal telencephalon. *Glia* 49(4):480–491
2. Volpe J (2008) *Neurology of the newborn*, 5th edn. Saunders Elsevier, Philadelphia, PA
3. Back SA et al (2001) Late oligodendrocyte progenitors coincide with the developmental window of vulnerability for human perinatal white matter injury. *J Neurosci* 21(4):1302–1312
4. Baumann N, Pham-Dinh D (2001) Biology of oligodendrocyte and myelin in the mammalian central nervous system. *Physiol Rev* 81(2):871–927
5. Kinney HC, Back SA (1998) Human oligodendroglial development: relationship to periventricular leukomalacia. *Semin Pediatr Neurol* 5(3):180–189
6. El Waly B et al (2014) Oligodendrogenesis in the normal and pathological central nervous system. *Front Neurosci* 8:145
7. Jakovcevski I et al (2009) Oligodendrocyte development and the onset of myelination in the human fetal brain. *Front Neuroanat* 3:5
8. Rakic S, Zecevic N (2003) Early oligodendrocyte progenitor cells in the human fetal telencephalon. *Glia* 41(2):117–127
9. Richardson WD, Kessaris N, Pringle N (2006) Oligodendrocyte wars. *Nat Rev Neurosci* 7(1):11–18
10. Young KM et al (2013) Oligodendrocyte dynamics in the healthy adult CNS: evidence for myelin remodeling. *Neuron* 77(5):873–885
11. Lasry O, Shevell MI, Dagenais L (2010) Cross-sectional comparison of periventricular leukomalacia in preterm and term children. *Neurology* 74(17):1386–1391
12. Li AM et al (2009) White matter injury in term newborns with neonatal encephalopathy. *Pediatr Res* 65(1):85–89
13. Martinez-Biarge M et al (2012) White matter and cortical injury in hypoxic-ischemic encephalopathy: antecedent factors and 2-year outcome. *J Pediatr* 161(5):799–807
14. Pagliano E et al (2007) Cognitive profiles and visuo-perceptual abilities in preterm and term spastic diplegic children with periventricular leukomalacia. *J Child Neurol* 22(3):282–288
15. Banker BQ, Larroche JC (1962) Periventricular leukomalacia of infancy. A form of neonatal anoxic encephalopathy. *Arch Neurol* 7:386–410
16. Billiards SS et al (2008) Myelin abnormalities without oligodendrocyte loss in periventricular leukomalacia. *Brain Pathol* 18(2):153–163
17. Buser JR et al (2012) Arrested preoligodendrocyte maturation contributes to myelination failure in premature infants. *Ann Neurol* 71(1):93–109
18. Dubowitz LM, Bydder GM, Mushin J (1985) Developmental sequence of periventricular leukomalacia. Correlation of ultrasound, clinical, and nuclear magnetic resonance functions. *Arch Dis Child* 60(4):349–355
19. Iida K, Takashima S, Ueda K (1995) Immunohistochemical study of myelination and oligodendrocyte in infants with periventricular leukomalacia. *Pediatr Neurol* 13(4):296–304
20. Pierson CR et al (2007) Gray matter injury associated with periventricular leukomalacia in the premature infant. *Acta Neuropathol* 114(6):619–631
21. Deguchi K, Oguchi K, Takashima S (1997) Characteristic neuropathology of leukomalacia in extremely low birth weight infants. *Pediatr Neurol* 16(4):296–300
22. Haynes RL et al (2008) Diffuse axonal injury in periventricular leukomalacia as determined by apoptotic marker fractin. *Pediatr Res* 63(6):656–661
23. Hirayama A et al (2001) Early immunohistochemical detection of axonal damage and glial activation in extremely immature brains with periventricular leukomalacia. *Clin Neuropathol* 20(2):87–91
24. Marin-Padilla M (1997) Developmental neuropathology and impact of perinatal brain damage. II: white matter lesions of the neocortex. *J Neuropathol Exp Neurol* 56(3):219–235
25. Counsell SJ et al (2003) Diffusion-weighted imaging of the brain in preterm infants with focal and diffuse white matter abnormality. *Pediatrics* 112(1 Pt 1):1–7
26. Hamrick SE et al (2004) Trends in severe brain injury and neurodevelopmental outcome in premature newborn infants: the role of cystic periventricular leukomalacia. *J Pediatr* 145(5):593–599
27. Inder TE et al (2003) Defining the nature of the cerebral abnormalities in the premature infant: a qualitative magnetic resonance imaging study. *J Pediatr* 143(2):171–179
28. Miller SP et al (2005) Early brain injury in premature newborns detected with magnetic resonance imaging is associated with adverse

- early neurodevelopmental outcome. *J Pediatr* 147(5):609–616
29. Woodward LJ et al (2006) Neonatal MRI to predict neurodevelopmental outcomes in preterm infants. *N Engl J Med* 355(7):685–694
 30. Riddle A et al (2011) Histopathological correlates of magnetic resonance imaging-defined chronic perinatal white matter injury. *Ann Neurol* 70(3):493–507
 31. Riddle A et al (2012) Differential susceptibility to axonopathy in necrotic and non-necrotic perinatal white matter injury. *Stroke* 43(1):178–184
 32. Back SA et al (2005) Selective vulnerability of preterm white matter to oxidative damage defined by F2-isoprostanes. *Ann Neurol* 58(1):108–120
 33. Gerstner B et al (2008) Hyperoxia causes maturation-dependent cell death in the developing white matter. *J Neurosci* 28(5):1236–1245
 34. Schmitz T et al (2011) Cellular changes underlying hyperoxia-induced delay of white matter development. *J Neurosci* 31(11):4327–4344
 35. Verney C et al (2012) Microglial reaction in axonal crossroads is a hallmark of noncystic periventricular white matter injury in very preterm infants. *J Neuropathol Exp Neurol* 71(3):251–264
 36. Davidson JO et al (2014) Connexin hemichannel blockade is neuroprotective after asphyxia in preterm fetal sheep. *PLoS One* 9(5):e96558
 37. Segovia KN et al (2008) Arrested oligodendrocyte lineage maturation in chronic perinatal white matter injury. *Ann Neurol* 63(4):520–530
 38. Ritter J et al (2013) Neonatal hyperoxia exposure disrupts axon-oligodendrocyte integrity in the subcortical white matter. *J Neurosci* 33(21):8990–9002
 39. Jablonska B et al (2012) Oligodendrocyte regeneration after neonatal hypoxia requires FoxO1-mediated p27Kip1 expression. *J Neurosci* 32(42):14775–14793
 40. Scafidi J et al (2014) Intranasal epidermal growth factor treatment rescues neonatal brain injury. *Nature* 506(7487):230–234
 41. Yuen TJ et al (2014) Oligodendrocyte-encoded HIF function couples postnatal myelination and white matter angiogenesis. *Cell* 158(2):383–396
 42. Tolcos M et al (2011) Intrauterine growth restriction affects the maturation of myelin. *Exp Neurol* 232(1):53–65
 43. Reid MV et al (2012) Delayed myelination in an intrauterine growth retardation model is mediated by oxidative stress upregulating bone morphogenetic protein 4. *J Neuropathol Exp Neurol* 71(7):640–653
 44. Brehmer F et al (2012) Interaction of inflammation and hyperoxia in a rat model of neonatal white matter damage. *PLoS One* 7(11):e49023
 45. Favrais G et al (2011) Systemic inflammation disrupts the developmental program of white matter. *Ann Neurol* 70(4):550–565
 46. Nobuta H et al (2012) STAT3-mediated astrogliosis protects myelin development in neonatal brain injury. *Ann Neurol* 72(5):750–765
 47. Franklin RJ, Ffrench-Constant C (2008) Remyelination in the CNS: from biology to therapy. *Nat Rev Neurosci* 9(11):839–855
 48. Franklin RJ, Gallo V (2014) The translational biology of remyelination: past, present, and future. *Glia* 62(11):1905–1915
 49. Fancy SP et al (2011) Axin2 as regulatory and therapeutic target in newborn brain injury and remyelination. *Nat Neurosci* 14(8):1009–1016
 50. Lyck L et al (2008) Immunohistochemical markers for quantitative studies of neurons and glia in human neocortex. *J Histochem Cytochem* 56(3):201–221
 51. Sommer I, Schachner M (1981) Monoclonal antibodies (O1 to O4) to oligodendrocyte cell surfaces: an immunocytological study in the central nervous system. *Dev Biol* 83(2):311–327
 52. Dean JM et al (2011) Strain-specific differences in perinatal rodent oligodendrocyte lineage progression and its correlation with human. *Dev Neurosci* 33(3-4):251–260
 53. Dean JM et al (2011) An organotypic slice culture model of chronic white matter injury with maturation arrest of oligodendrocyte progenitors. *Mol Neurodegener* 6:46
 54. Fancy SP et al (2009) Dysregulation of the Wnt pathway inhibits timely myelination and remyelination in the mammalian CNS. *Genes Dev* 23(13):1571–1585
 55. Ruckh JM et al (2012) Rejuvenation of regeneration in the aging central nervous system. *Cell Stem Cell* 10(1):96–103
 56. Back SA et al (2007) Hypoxia-ischemia preferentially triggers glutamate depletion from oligodendroglia and axons in perinatal cerebral white matter. *J Cereb Blood Flow Metab* 27(2):334–347

57. Back SA et al (2002) Selective vulnerability of late oligodendrocyte progenitors to hypoxia-ischemia. *J Neurosci* 22(2):455–463
58. Craig A et al (2003) Quantitative analysis of perinatal rodent oligodendrocyte lineage progression and its correlation with human. *Exp Neurol* 181(2):231–240
59. Atik A et al (2014) Impact of daily high-dose caffeine exposure on developing white matter of the immature ovine brain. *Pediatr Res* 76(1):54–63
60. Dean JM et al (2011) Delayed cortical impairment following lipopolysaccharide exposure in preterm fetal sheep. *Ann Neurol* 70(5):846–856
61. Drury PP et al (2014) nNOS inhibition during profound asphyxia reduces seizure burden and improves survival of striatal phenotypic neurons in preterm fetal sheep. *Neuropharmacology* 83:62–70
62. Rees S et al (2010) Erythropoietin is neuroprotective in a preterm ovine model of endotoxin-induced brain injury. *J Neuropathol Exp Neurol* 69(3):306–319
63. Riddle A et al (2006) Spatial heterogeneity in oligodendrocyte lineage maturation and not cerebral blood flow predicts fetal ovine periventricular white matter injury. *J Neurosci* 26(11):3045–3055
64. Kluver H, Barrera E (1953) A method for the combined staining of cells and fibers in the nervous system. *J Neuropathol Exp Neurol* 12(4):400–403
65. Page KM (1965) A stain for myelin using solochrome cyanin. *J Med Lab Technol* 22(4):224–225
66. Gallyas F (1979) Silver staining of myelin by means of physical development. *Neurol Res* 1(2):203–209
67. Uchihara T (2007) Silver diagnosis in neuropathology: principles, practice and revised interpretation. *Acta Neuropathol* 113(5):483–499
68. Sosunov AA et al (2014) Phenotypic heterogeneity and plasticity of isocortical and hippocampal astrocytes in the human brain. *J Neurosci* 34(6):2285–2298
69. Bachoo RM et al (2004) Molecular diversity of astrocytes with implications for neurological disorders. *Proc Natl Acad Sci U S A* 101(22):8384–8389
70. Cahoy JD et al (2008) A transcriptome database for astrocytes, neurons, and oligodendrocytes: a new resource for understanding brain development and function. *J Neurosci* 28(1):264–278
71. Tsai HH et al (2012) Regional astrocyte allocation regulates CNS synaptogenesis and repair. *Science* 337(6092):358–362
72. Zamanian JL et al (2012) Genomic analysis of reactive astrogliosis. *J Neurosci* 32(18):6391–6410
73. Butovsky O et al (2014) Identification of a unique TGF-beta-dependent molecular and functional signature in microglia. *Nat Neurosci* 17(1):131–143
74. Perry VH, Nicoll JA, Holmes C (2010) Microglia in neurodegenerative disease. *Nat Rev Neurol* 6(4):193–201
75. Ransohoff RM, Perry VH (2009) Microglial physiology: unique stimuli, specialized responses. *Annu Rev Immunol* 27:119–145
76. David S, Kroner A (2011) Repertoire of microglial and macrophage responses after spinal cord injury. *Nat Rev Neurosci* 12(7):388–399
77. Hu X et al (2012) Microglia/macrophage polarization dynamics reveal novel mechanism of injury expansion after focal cerebral ischemia. *Stroke* 43(11):3063–3070
78. Kigerl KA et al (2009) Identification of two distinct macrophage subsets with divergent effects causing either neurotoxicity or regeneration in the injured mouse spinal cord. *J Neurosci* 29(43):13435–13444
79. Miron VE et al (2013) M2 microglia and macrophages drive oligodendrocyte differentiation during CNS remyelination. *Nat Neurosci* 16(9):1211–1218
80. Olah M et al (2012) Identification of a microglia phenotype supportive of remyelination. *Glia* 60(2):306–321
81. Wang G et al (2013) Microglia/macrophage polarization dynamics in white matter after traumatic brain injury. *J Cereb Blood Flow Metab* 33(12):1864–1874
82. Colton C, Wilcock DM (2010) Assessing activation states in microglia. *CNS Neurol Disord Drug Targets* 9(2):174–191
83. Mantovani A, Sica A, Locati M (2007) New vistas on macrophage differentiation and activation. *Eur J Immunol* 37(1):14–16
84. Chhor V et al (2013) Characterization of phenotype markers and neuronotoxic potential of polarised primary microglia in vitro. *Brain Behav Immun* 32:70–85
85. Lund S et al (2006) The dynamics of the LPS triggered inflammatory response of murine microglia under different culture and in vivo conditions. *J Neuroimmunol* 180(1-2):71–87
86. Michelucci A et al (2009) Characterization of the microglial phenotype under specific

- pro-inflammatory and anti-inflammatory conditions: effects of oligomeric and fibrillar amyloid-beta. *J Neuroimmunol* 210(1-2): 3-12
87. Faustino JV et al (2011) Microglial cells contribute to endogenous brain defenses after acute neonatal focal stroke. *J Neurosci* 31 (36):12992-13001
 88. Wilhelmsson U et al (2006) Redefining the concept of reactive astrocytes as cells that remain within their unique domains upon reaction to injury. *Proc Natl Acad Sci U S A* 103(46):17513-17518
 89. Mouton P (2002) Principles and practices of unbiased stereology: an introduction for bioscientists. Johns Hopkins University Press, Baltimore, MD
 90. Haynes RL et al (2005) Axonal development in the cerebral white matter of the human fetus and infant. *J Comp Neurol* 484(2): 156-167
 91. Yamamoto T, Hirano A (1986) A comparative study of modified Bielschowsky, Bodian and thioflavin S stains on Alzheimer's neurofibrillary tangles. *Neuropathol Appl Neurobiol* 12 (1):3-9
 92. Duncan JR et al (2002) White matter injury after repeated endotoxin exposure in the pre-term ovine fetus. *Pediatr Res* 52(6):941-949
 93. Duncan JR et al (2006) Chronic endotoxin exposure causes brain injury in the ovine fetus in the absence of hypoxemia. *J Soc Gynecol Investig* 13(2):87-96
 94. Martin R et al (1999) Neurofilament phosphorylation and axon diameter in the squid giant fibre system. *Neuroscience* 88(1): 327-336
 95. Harrington EP et al (2010) Oligodendrocyte PTEN is required for myelin and axonal integrity, not remyelination. *Ann Neurol* 68(5): 703-716
 96. Nikolaev A et al (2009) APP binds DR6 to trigger axon pruning and neuron death via distinct caspases. *Nature* 457(7232):981-989
 97. Bendotti C et al (1988) Neuroanatomical localization and quantification of amyloid precursor protein mRNA by in situ hybridization in the brains of normal, aneuploid, and lesioned mice. *Proc Natl Acad Sci U S A* 85 (10):3628-3632
 98. Otsuka N, Tomonaga M, Ikeda K (1991) Rapid appearance of beta-amyloid precursor protein immunoreactivity in damaged axons and reactive glial cells in rat brain following needle stab injury. *Brain Res* 568(1-2): 335-338
 99. Rossiter JP et al (2000) Caspase-cleaved actin (fractin) immunolabelling of Hirano bodies. *Neuropathol Appl Neurobiol* 26(4):342-346
 100. Sokolowski JD et al (2014) Caspase-mediated cleavage of actin and tubulin is a common feature and sensitive marker of axonal degeneration in neural development and injury. *Acta Neuropathologica Commun* 2:16
 101. Kitada M, Rowitch DH (2006) Transcription factor co-expression patterns indicate heterogeneity of oligodendroglial subpopulations in adult spinal cord. *Glia* 54(1):35-46
 102. Trapp BD et al (1988) Cellular and subcellular distribution of 2',3'-cyclic nucleotide 3'-phosphodiesterase and its mRNA in the rat central nervous system. *J Neurochem* 51 (3):859-868
 103. Montague P et al (1997) Developmental expression of the murine Mobp gene. *J Neurosci Res* 49(2):133-143
 104. Pedraza L et al (1997) The active transport of myelin basic protein into the nucleus suggests a regulatory role in myelination. *Neuron* 18 (4):579-589
 105. Huang X, Chen S, Tietz EI (1996) Immunocytochemical detection of regional protein changes in rat brain sections using computer-assisted image analysis. *J Histochem Cytochem* 44(9):981-987
 106. Watanabe J, Asaka Y, Kanamura S (1996) Relationship between immunostaining intensity and antigen content in sections. *J Histochem Cytochem* 44(12):1451-1458
 107. van der Loos CM (2008) Multiple immunoenzyme staining: methods and visualizations for the observation with spectral imaging. *J Histochem Cytochem* 56(4): 313-328
 108. Waxman SG (1980) Determinants of conduction velocity in myelinated nerve fibers. *Muscle Nerve* 3(2):141-150
 109. Rushton WA (1951) A theory of the effects of fibre size in medullated nerve. *J Physiol* 115 (1):101-122
 110. Chomiak T, Hu B (2009) What is the optimal value of the g-ratio for myelinated fibers in the rat CNS? A theoretical approach. *PLoS One* 4 (11):e7754
 111. Drobyshevsky A et al (2014) Unmyelinated axon loss with postnatal hypertonia after fetal hypoxia. *Ann Neurol* 75(4):533-541

Prenatal Determinants of Brain Development: Recent Studies and Methodological Advances

Stephen A. Back and A. Roger Hohimer

Abstract

Despite advances in neonatal intensive care, survivors of premature birth remain highly susceptible to unique patterns of developmental brain injury that manifest as cerebral palsy and cognitive-learning disabilities. Whereas preterm infants were previously at high risk for destructive brain lesions that resulted in cystic white matter injury and secondary cortical and subcortical gray matter degeneration, contemporary cohorts of preterm survivors commonly display less severe injury that does not appear to involve pronounced glial or neuronal loss. Cerebral development in fetal sheep shares many anatomical and physiological similarities with human. Thus, the fetal sheep has provided unique experimental access to the complex pathophysiological processes that contribute to injury to the human brain during successive periods in development. Recent refinements have resulted in models that replicate major features of acute and chronic human cerebral injury and which have provided access to complex clinically relevant studies of cerebral blood flow and neuro-imaging that are not feasible in smaller laboratory animals. We focus here on emerging insights and methodologies from studies in fetal sheep that have begun to define cellular and vascular factors that contribute to preterm white and gray matter injury. Despite the higher costs and technical challenges of instrumented preterm fetal sheep models, they provide powerful access to clinically relevant studies that provide a more integrated analysis of the spectrum of insults that appear to contribute to cerebral injury in human preterm infants.

Key words Hypoxia-ischemia, White matter injury, Oligodendrocyte, Neuron, Dendrite, Cerebral blood flow, MRI, Necrosis, Apoptosis

1 Introduction

1.1 Overview of the Clinical Problems to be Addressed in Preterm Fetal Sheep

The last decade has seen a resurgence of interest in instrumented preterm fetal sheep preparations to study the complex pathophysiological processes that contribute to preterm brain injury and mechanisms of regeneration and repair. The considerable merits of a large preclinical animal model have become increasingly recognized as it has become apparent that rodent models have significant limitations to study injury to the developing human brain [1]. Not only do preterm fetal sheep preparations closely replicate major

features of acute and chronic human preterm brain injury, but they also provide access to complex clinically relevant studies of cerebral blood flow and neuro-imaging that are not feasible in smaller laboratory animals.

Until recently, the extensive brain abnormalities in preterm neonates appeared to be related mostly to destructive processes that lead to substantial deletion of neurons, axons and glia from insults that often resulted in cystic necrotic lesions. However, advances in neonatal care have yielded a growing body of evidence that preterm cerebral gray and white matter frequently sustain less severe insults where tissue destruction is the minor component. During the last decade, there has been increasing recognition that cerebral injury in human preterm survivors has shifted from more severe patterns of injury dominated by necrosis to milder forms of injury that nevertheless affect motor control, cognition, language, behavior, vision, and hearing [2].

Although now much less common, severe white matter injury results in cystic periventricular leukomalacia (PVL), which manifests as spastic diplegic cerebral palsy and visual dysfunction, as well as deficits in cognition and learning. Necrotic injury to axons and myelin is accompanied by secondary cortical and subcortical gray matter degeneration [3], which provides an explanation for the broad spectrum of neurobehavioral disabilities that accompany PVL.

There is increasing recognition that following milder forms of cerebral injury, cognitive deficits can occur in the absence of significant motor impairments and cerebral palsy [4]. This diverse spectrum of neurocognitive and motor outcomes following preterm birth, has supported the notion that more widespread cellular maturational disturbances occur that target both cerebral gray and white matter. These milder insults primarily result in cerebral injury that involves aberrant cellular responses that disrupt the maturation of certain populations of glial progenitors and neurons. Late oligodendrocyte progenitors (preOLs) are highly susceptible to early ischemic cell death that triggers a maladaptive regeneration and repair response where the surviving progenitor pool expands but fails to differentiate and myelinate [5]. By contrast, cortical and subcortical immature projection neurons are much more resistant to cell death [6, 7], but nevertheless fail to generate a normal arbor of dendritic processes and spines [8, 9]. These emerging findings suggest that a major component of brain injury in many contemporary preterm survivors involves a primary cerebral dysmaturation disorder that may ultimately be amenable to strategies directed at promoting brain maturation and improved neurological outcome [10].

1.2 Hypoxia-Ischemia (H-I) in Fetal Sheep Generates Pathological Features of Human White Matter Injury (WMI)

The ovine fetus offers significant advantages to analyze systemic hemodynamic disturbances that regulate cerebral blood flow and metabolism in preterm cerebral white matter. The sheep fetus displays cerebral hemodynamics similar to human and permits repeated physiological measurements in utero in the unanesthetized state. Measurements of blood pressure, electroencephalography, blood oxygenation and other vital variables can be correlated with acute changes in cerebral blood flow and metabolism. Importantly, like the human fetus [11–14], the fetal sheep displays a very limited range of cerebral autoregulation under normal conditions and a pressure-passive cerebral circulation when subjected to systemic hypoxia and associated hypotension [15–19].

Multiple lines of evidence support a role for cerebral ischemia in the pathogenesis of WMI in very low birth weight human infants [20–22]. Given the limitations of human studies to directly link blood flow disturbances with WMI, studies in fetal sheep have greatly strengthened our understanding of the contribution of cerebral H-I to WMI. These experimental studies support that a complex interplay of factors related to cerebrovascular immaturity predispose preterm cerebral white matter to injury from H-I. A model of global cerebral hypoperfusion found that the mid-gestation animal displayed a predilection to subcortical WMI, whereas the near term animal displayed predominantly parasagittal cortical neuronal injury [23, 24]. A variable degree of WMI was also detected after systemic hypotension arising from intermittent or partial umbilical cord occlusion [25, 26]. By contrast, in the near term animal, repeated umbilical cord occlusion produced injury to both the periventricular white matter and the cerebral cortex [27]. Systemic hemorrhagic hypotension in the 0.75 gestation fetus resulted in mostly necrotic WMI with focal necrotic lesions or axonal swellings in the periventricular white matter [28]. Preterm ovine white matter lesions were detected after repeated systemic fetal endotoxin exposure that triggered both transient hypoxemia and hypotension [29, 30]. The importance of cerebral ischemia is supported by studies where WMI was detected only infrequently in models of hypoxemia in which a restriction in uteroplacental blood flow resulted in decreased oxygen delivery and mild acidemia to the fetus without systemic hypotension or cerebral hypoperfusion [31–33]. A model of fetal metabolic acidemia induced by maternal hypoxemia similarly produced mild-to-moderate injury in mid-gestation and near-term sheep [34]. Hence, since cerebral hypoperfusion in conjunction with hypoxia appears to be a critical factor to generate significant WMI in the preterm fetal sheep, we will describe below several global cerebral hypoxia-ischemia protocols that model human WMI [35–37].

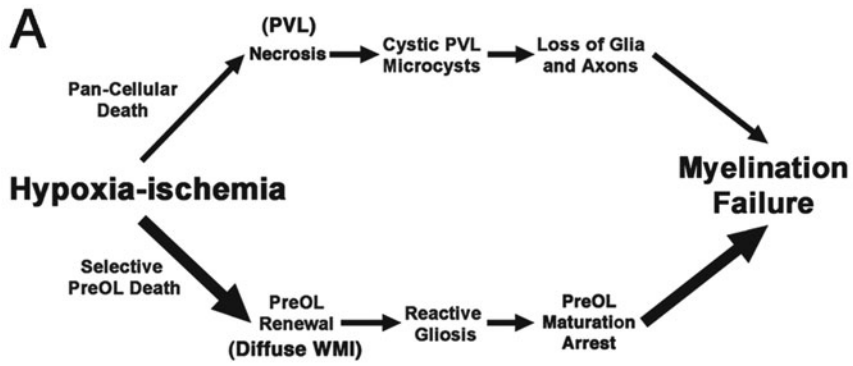
Fetal sheep have also provided an important model to define mechanisms of oxidative injury from cerebral H-I. This is in part

due to the large fetal cerebral hemispheres, which permit blood sampling from the venous sagittal sinus and placement of intracerebral probes for dialysis studies. Initial studies found that reperfusion after cerebral ischemia was an important source of free radical formation in the near term fetal sheep brain [38]. Partial umbilical cord occlusion resulted in a delayed increase in lipid peroxidation in frontal and parietal white matter in near term fetal sheep [39]. Dialysis studies in near term [40] and preterm [41] sheep have both demonstrated the enhanced generation of stable adducts of reactive oxygen species.

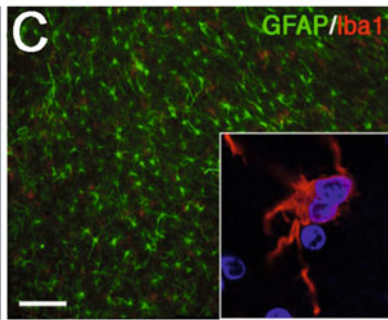
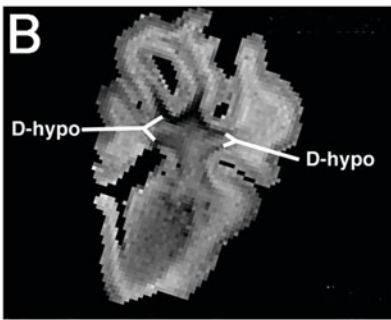
1.3 Spectrum of Injury and Dysmaturation in Preterm WMI

Using the protocol described below, the WMI generated by global cerebral ischemia in our preterm fetal sheep model reproduces the spectrum of WMI (Fig. 1a) that we have observed in a series of human preterm autopsy brains [42]. We have employed ex vivo ultrahigh field (12 Tesla; T) MRI to align images of white matter lesions at high resolution with white matter lesions defined by histopathological data [35]. At this ultrahigh field strength, three types of white matter lesions were observed during the subacute phase of injury, at 1 and 2 weeks after hypoxia-ischemia. Each lesion type displays distinct astroglial and microglial responses that correspond to forms of necrotic or diffuse WMI that also occur in human preterm neonates:

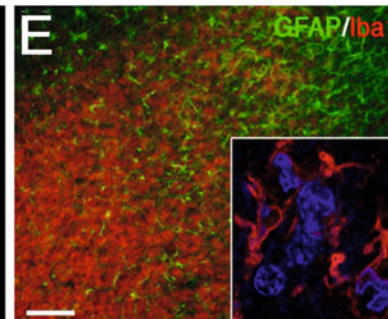
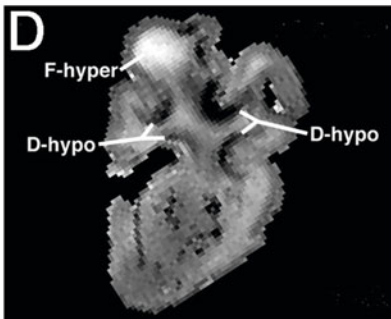
1. *Diffuse WMI*: In preterm fetal sheep, diffuse WMI is visualized on ultrahigh field MRI as diffuse hypo-intense signal abnormalities on T₂W images (Fig. 1b). These diffuse hypointense signal changes are observed in the early chronic phase of WMI at 1–2 weeks after H-I and correspond to reactive astrogliosis and myelination disturbances related to maturation arrest of preOLs on histopathology (Fig. 1c). In early diffuse WMI, there is selective degeneration of late OL progenitors (preOLs), while axonal degeneration is restricted to foci of microscopic necrosis [37, 43]. Importantly, the imaging characteristics of diffuse WMI differ substantially at clinical field strengths compared to at high field. Unlike at ultrahigh field strength where diffuse WMI lesions are large (>2.5 mm³) and detected with high sensitivity and specificity, this spectrum of WMI is not as directly evident on diagnostic MRI. At clinical MRI field strengths, WMI is indicated by discrete focal or multifocal areas of MR signal abnormalities. The importance of diffuse WMI must be emphasized, as this is the major form of WMI in autopsy studies of contemporary human cohorts and in fetal ovine WMI. In chronic lesions in fetal sheep, diffuse WMI comprised nearly 90 % of the total volume of WMI. While the extent of diffuse WMI is difficult to define by conventional neuropathology, recent studies have quantified the extent of reactive astrocytes and microglia in chronic human WMI and



Diffuse WMI



Focal Necrotic WMI



Microscopic Necrotic WMI

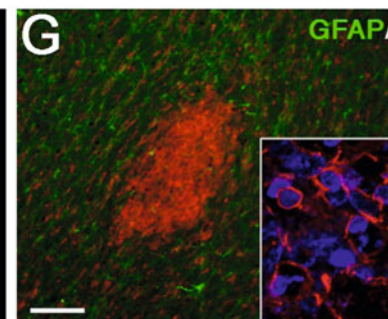
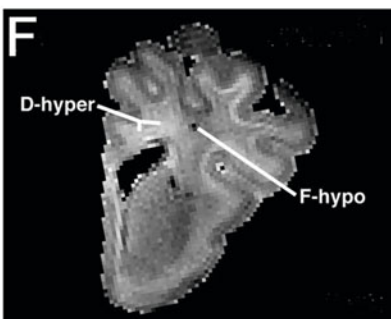


Fig. 1 (a) Distinctly different pathogenetic mechanisms mediate abnormal myelination in necrotic lesions (PVL; *upper pathway*) vs. lesions with diffuse WMI (*lower pathway*). Hypoxia-ischemia(H-I) is illustrated as one

determined that these lesions displayed a robust inflammatory reaction that extended considerably beyond the apparent lesion boundaries defined by non-quantitative approaches [42]. These chronic lesions evolve from early WMI where the human oligodendrocyte (OL) lineage is particularly susceptible to oxidative damage [6] of a severity consistent with hypoxia-ischemia [7, 44].

2. *Cystic necrotic WMI*: Banker and Larroche described cystic necrotic WMI in the preterm neonate over 50 years ago and defined the pathological features of periventricular leukomalacia (PVL) [45–51]. Cystic PVL describes foci of necrosis that are typically larger than one millimeter in diameter with degeneration of all cell types including glia and axons on pathological examination [37, 43]. In fetal sheep, pronounced necrotic WMI is visualized on MRI (Fig. 1d) as hyperintense signal abnormalities on T2-weighted images (T₂W) or as volume loss of major white matter tracts such as the corpus callosum or optic radiations. These large necrotic lesions on MRI

Fig. 1 (Continued) potential trigger for WMI. More severe H-I triggers white matter necrosis (*upper pathway*) with pan-cellular degeneration that depletes the white matter of glia and axons. Severe necrosis results in cystic PVL, whereas milder necrosis results in microcysts. Milder H-I (*lower pathway*) selectively triggers early preOL death. PreOLs are rapidly regenerated from a pool of early OL progenitors that are resistant to H-I. Chronic lesions are enriched in reactive glia (astrocytes and microglia/macrophages) that generate inhibitory signals that block preOL differentiation to mature myelinating OLs. Myelination failure in diffuse WMI thus results from preOL arrest rather than axonal degeneration. Note that the *lower pathway* is the dominant one in most contemporary preterm survivors, whereas the minor upper pathway reflects the declining burden of white matter necrosis that has accompanied advances in neonatal intensive care. **(b, c)** Diffuse WMI in chronic lesions. **(b)** Representative appearance and distribution of diffuse hypointense (D-hypo) lesions seen on a T₂w image at 1 week after injury. **(c)** Diffuse WMI had pronounced astrogliosis defined by immunohistochemical staining of reactive astrocytes with glial fibrillary acidic protein (GFAP; *green*) and a lesser population of Iba1-labeled microglia/macrophages (*red*) with a reactive morphology (*inset*). Nuclei in the *inset* are visualized with Hoechst 33342 (*blue*). **(d, e)** Focal Necrotic WMI. **(d)** Representative appearance from the largest focal hyperintense (F-hyper) lesion seen on a T₂w image at 1 week after injury. These lesions typically localized to subcortical white matter. Note the substantial difference in the F-hyper lesion relative to the diffuse gliotic lesions, which appears much more hypointense (D-hypo). **(e)** A typical focal macroscopic necrotic lesion defined by diffuse dense staining for reactive microglia and macrophages with Iba1 (*red* and *inset*) and a paucity of GFAP-labeled astrocytes. Nuclei in the *inset* are visualized with Hoechst 33342 (*blue*). **(f, g)** Microscopic necrotic WMI. **(f)** Representative appearance of a focal hypointense (F-hypo) lesion seen on a T₂w image at 2 weeks after injury. Note the substantial difference in the F-hypo lesion relative to a diffuse gliotic lesion at 2 weeks, which appears more hyperintense (D-hyper). **(g)** A typical microscopic necrotic lesion (microcyst) defined by a discrete focus of immunohistochemical staining for reactive microglia and macrophages with Iba1 (*red* and *inset*) and a paucity of staining for astrocytes with glial fibrillary acidic protein (GFAP; *green*). Nuclei in the *inset* are visualized with Hoechst 33342 (*blue*). Bars in **(c)**, **(e)**, **(g)**, 100 μm

correspond to lesions highly enriched in macrophages and activated microglia on histopathology (Fig. 1e).

3. *Microscopic necrotic WMI*: Whereas cystic PVL was previously the major form of WMI in preterm survivors, the occurrence of these large cystic lesions has markedly declined in preterm survivors such that they are detected by MRI in less than 5 % of preterm neonates at 24–32 weeks gestation—an almost tenfold decline in some cohorts [52–55]. Despite this pronounced reduction in cystic PVL, small foci of necrosis that measure less than a millimeter continue to be evident on human neuropathological examination (i.e., microcysts) [56]. As in the larger cystic lesions of PVL, in their mature stages, human microcysts are enriched in cellular debris, degenerating axons, and phagocytic macrophages [42]. The extent to which microcysts contribute to disability or are clinically silent is unclear, because they are poorly visualized by MRI at clinical field strengths. However, in preterm fetal sheep, high field MRI (Fig. 1f) identified microcysts in at least one third of brains analyzed [35], which is similar to the incidence observed in recent human autopsy cases [42]. Yet, because of their size and extent, microcysts comprised only a small proportion, <5 %, of lesion burden in sheep and human. These microcysts on MRI correspond to lesions highly enriched in macrophages and activated microglia on histopathology (Fig. 1g).

1.4 Mechanisms of Degeneration and Dysmaturation of Oligodendrocyte Progenitors

In early diffuse WMI, abnormal myelination is initiated by selective degeneration of late oligodendrocyte (OL) progenitors (preOLs) that are normally present in the white matter during the early third trimester of gestation, which coincides with the high-risk period for WMI [57]. The magnitude and distribution of acute WMI in several experimental models corresponds to the spatial distribution of these susceptible OL lineage cells. Unlike other stages of OL lineage cells, preOLs are highly vulnerable to hypoxia-ischemia and inflammation [5, 58].

Despite the pronounced selective degeneration of preOLs in acute WMI, abnormal myelination in chronic WMI is defined by a more complex process of cellular dysmaturation. Recent findings suggest that myelination disturbances involve a potentially reversible process linked to arrested pre-OL maturation rather than an irreversible loss of pre-OLs. Despite substantial preOL degeneration after hypoxia-ischemia, surviving preOLs in preterm-equivalent rats [59] and fetal sheep [35] rapidly increased in number to compensate for depleted preOLs. This response was driven primarily by OL progenitors that proliferate locally at the sites of WMI [59] or cortical injury [60] rather than from the subventricular zone [59, 61–65]. A robust expansion of human preOLs is also observed in chronic lesions [42] despite the significant loss of these

cells during the acute phase of WMI [6]. However, these newly generated preOLs fail to myelinate intact axons and display persistent arrested differentiation, whether in human studies or experimental models. Arrested maturation of preOLs is the main contributor to myelination failure in diffuse WMI [35, 42]. Thus, diffuse WMI is characterized by an aberrant response to acute injury, whereby preOLs are regenerated but fail to mature.

1.5 Mechanisms of Gray Matter Volume Loss in Association with Preterm White Matter Injury

1.5.1 Gray Matter Dysmaturation in Preterm WMI

Brain injury in the preterm neonate involves both destructive and developmental disturbances of the cerebral gray matter and white matter [10, 66]. It is now apparent that gray matter abnormalities are prevalent among preterm neonates and must be considered as an important component of diffuse brain injury in this population. Reduced volumes of cortical and subcortical gray matter structures that include the basal ganglia, thalamus, hippocampus and cerebellum are now recognized in preterm survivors, even in the absence of significant overt focal WMI [67–71]. As discussed below, necrotic WMI may be accompanied by impaired growth of cortical or subcortical gray matter that results from primary neuronal degeneration or secondary neuronal degeneration related to axonal injury in foci of white matter necrosis. In more common diffuse WMI, we have recently proposed that impaired cerebral growth involves disrupted neuronal maturation of large distinct populations of neurons in multiple cortical and subcortical structures.

1.5.2 Neuronal Degeneration in Preterm WMI

Neurons in the neonatal brain at term are highly vulnerable to hypoxic-ischemic death that is mediated by excitotoxic neuronal necrosis and apoptosis [72–77]. In contrast, preterm neurons have a more variable susceptibility to hypoxia-ischemia that is related to the severity of the insult, as well as the severity of concurrent WMI. White matter necrosis is accompanied by degeneration of neurons in cerebral gray and white matter. In preterm fetal sheep, the severity and extent of neuronal degeneration increases with the duration of hypoxia-ischemia; prolonged hypoxia-ischemia triggers widespread neuronal death related to cystic necrotic WMI [7]. In the human preterm brain with necrotic WMI, significant neuronal loss is recognized in the cortex, basal ganglia, thalamus and cerebellum [56, 78–80]. In addition to this primary neuronal death, necrotic WMI may also be accompanied by secondary neuronal loss from retrograde axonal degeneration [37, 43].

In contrast to necrotic WMI, diffuse WMI spares axons. Despite similar degrees of ischemia in the superficial cortex and periventricular white matter, diffuse WMI in preterm fetal sheep is characterized by acute preOL degeneration but preserved neurons in gray and white matter [7, 8]. In human preterm autopsy cases with early diffuse WMI, neither the gray matter nor white matter displayed significant degeneration of neurons or axons, despite a significant magnitude of oxidative stress, comparable to that observed in the term neonate with severe hypoxic-ischemic

encephalopathy [6]. Thus, in the preterm neonate, neuronal loss is primarily associated with destructive WMI, whereas neuronal loss does not appear to be a prominent feature of diffuse WMI.

*1.5.3 Neuronal
Dysmaturation in Preterm
WMI*

Our preterm fetal sheep model of diffuse WMI has provided unique access to the mechanisms of cortical and subcortical gray matter volume loss that have been described in human preterm survivors. Unbiased quantitative studies using stereology, found that volume loss can occur in the absence of significant neuronal loss, but involves an increased packing density of neurons [9]. This unexpected finding is explained by a significant reduction in the complexity of the dendritic arbor of pyramidal neurons, the major population of cortical projection neurons. In the cerebral cortex of preterm sheep, pyramidal neurons are normally immature with a simplified arbor. During normal cortical development in near term animals, the dendritic arbor becomes highly arborized, which accompanies a marked increase in cortical volume. The disruption in the normal development of the dendritic arbor following cerebral hypoxia-ischemia was most pronounced closer to the cell body where synaptic integration occurs.

Neuronal dysmaturation has also been observed in preterm sheep in the caudate nucleus, which also displays reduced growth without any apparent loss of GABAergic medium spiny projection neurons or interneurons [8]. As with the cerebral cortex, reduced growth of the caudate was not explained by loss of GABAergic neurons, but rather by a reduced dendritic arbor of caudate projection neurons. Hence, widespread disturbances in maturation of cortical and caudate projection neurons occur with diffuse WMI even in the absence of significant neuronal loss.

*1.5.4 Synaptic Activity
with Neuronal
Dysmaturation in Preterm
Neonates*

Disturbances in maturation of dendrites are accompanied by reduced numbers of spines on both projection neurons in the caudate [8] and the cortex [9]. Neuronal dysmaturation in the preterm cerebrum occurs during a sensitive window in the establishment of neuronal connections and may thus have long-lasting consequences. In the fetal sheep model of diffuse WMI following cerebral ischemia, significant abnormalities in excitatory synaptic activity mediated by NMDA and AMPA receptors were observed in electrophysiological studies of medium spiny neurons (MSNs) in the caudate, consistent with reduced spine density on MSNs [8]. These disturbances in spine density and excitatory synaptic activity of MSNs may impact the long-term maturation of the caudate's neuronal circuitry. Reduced afferent excitation of MSNs occurs with a shorter time window for integration of multiple synaptic inputs onto these projection neurons. Furthermore, disturbed NMDA receptor mediated synaptic activity alters neuronal migration, synapse formation, and dendritic pruning [81–84]. Thus,

neuronal dysmaturation may precipitate a vicious cycle with further alteration of neuronal circuitry maturation. The resultant widespread disturbances in neuronal maturation may contribute to the global disturbances in cerebral connectivity and the diverse spectrum of neurodevelopmental impairment seen in preterm-born children.

1.6 Advantages and Disadvantages of the Fetal Sheep to Model Preterm Cerebral Injury

Fetal sheep preparations require considerable cost and infrastructure to support the surgical instrumentation and post-operative care of large laboratory animals. Fetal sheep studies require a highly skilled surgical team, a large animal operating facility suitable for sterile operations, specialized veterinary care, and access to reliable breeders. Despite these challenges, many preparations have yielded very reproducible results with low morbidity and mortality, thereby limiting the number of animals required. Presently, the ovine genome has not been fully sequenced and the molecular tools available to study ovine brain injury are more limited than in rodents. Rodent models, including transgenic rodents, are ideal to provide more rapid, cost-effective access to cellular and molecular mechanisms that subsequently can be validated in a large pre-clinical animal model, such as the instrumented fetal sheep.

Preterm (0.65 gestation or 95 days) fetal sheep models have multiple distinct advantages relative to small fetal and neonatal animals, which are limited by a lissencephalic brain that does not resemble the gyrencephalic human cerebrum. In terms of its neurodevelopment, the immature ovine brain is similar to preterm human between approximately 24–28 weeks in terms of the completion of neurogenesis, the onset of cerebral sulcation, and the detection of the cortical component of the auditory and somatosensory evoked potentials [85–88]. The long gestation of fetal sheep (145 days) allows selection of an appropriate developmental stage over which brain insults can be induced and evaluated.

The abundance of cerebral white matter and its anatomic similarities to that of the preterm infant make the fetal sheep ideal for neuropathological correlation with human [89, 90]. Rodents, have a paucity of cerebral white matter that differs markedly from human, whereas the fetal sheep generates acute [7] and chronic [35] WMI that is very similar to human in histopathological features. White matter maturation in fetal sheep can be defined relative to human through assessment of oligodendrocyte lineage progression and myelination. Oligodendrocyte development in the 0.65 gestation sheep fetus is similar to that of 24–28 week human [7]. The late gestation ovine fetus (0.9 gestation; 135 days) displays oligodendrocyte development similar to term human [91]. Thus, the investigator can choose the appropriate developmental timing for the insult to be given and evaluated.

In contrast to the fetal sheep, the cerebrovascular supply of the rodent white matter is also structurally and physiologically very

dissimilar to human, which is an additional factor that is likely to contribute to the markedly different patterns of cerebral injury in rodents and fetal sheep. Whereas the fetal sheep cerebrum has a predilection for relatively selective WMI under conditions of moderate cerebral ischemia [7], rodents have a propensity for mixed cerebral injury such that substantial gray matter injury accompanies WMI [44, 59, 92–95]. This shortcoming, for example, limits the relevance of rodent hypoxia-ischemia models for the study of myelination disturbances associated with chronic human WMI. Necrotic injury to cerebral gray matter contributes substantially to neuro-axonal degeneration as a cause of dysmyelination, which is not a prominent feature of WMI in either fetal sheep [35] or contemporary human cases of WMI [35]. In contrast to fetal sheep preparations, the small size of rodents is also a major technical limitation for a wide range of invasive physiological measurements as well as for studies that seek to achieve high resolution neuroimaging by MRI [35, 96].

The size of the preterm sheep fetus allows for chronic instrumentation to enable hemodynamic measurements, repeated access to blood and CSF and chronic electrophysiological recording of the fetal electroencephalogram [97]. Thus, it is feasible to study well-defined brain insults with reliable measurements of blood pressure, oxygenation, and cerebral blood flow. Chronic instrumentation also allows a wide range of practical and clinically pertinent cerebral insults to be administered. These include global cephalic ischemia [23], systemic hypotension or hypoxemia [17, 32, 98], single or repeated cord occlusion [99–101], increased intracranial pressure [102], and administration of infectious agents or exogenous inflammatory mediators [29, 103, 104]. These insults can be graded in intensity and duration to mimic the human situation. In each case, the stressor can be well described if not regulated by conventional monitoring measurements. Thus, a wide range of pathogenetic events can be evaluated physiologically and correlated neuropathologically with the distribution and extent of white matter damage. Moreover, the natural progression of various types of WMI can be evaluated in a time frame ranging from days-to-weeks-to-months after the insult.

From a practical standpoint, the availability, cost and ease of breeding of the sheep makes it a more practical large animal model than the nonhuman primate. In addition, the size and docile nature of the sheep supports the feasibility of both in utero and ex vivo neuro-imaging studies [35, 105]. Finally, fetal sheep preparations provide powerful access to large animal preclinical testing as exemplified by preclinical studies in near term fetal sheep that lead to the head cooling trials for neonatal encephalopathy [106].

2 Materials and Setup

2.1 Catheters and Other Materials

Each fetus has a non-occlusive polyvinyl carotid artery catheter (0.023" ID × 0.039" OD), which is inserted at the inguinal branch and advanced about 4 cm centrally; and an amniotic catheter (0.030" ID × 0.048" OD) tied to the fetal skin. A 4 mm hydraulic occluder is placed around the brachiocephalic artery or a 2 mm occluder is placed around each carotid artery. V3 and V4 catheters are 7' in length and are made from medical grade micro vinyl manufactured by Scientific Commodities, Lake Havasu City, Arizona. The occluders are silastic and manufactured by In Vivo Metric, Healdsburg, California.

2.2 Animals

Time-bred sheep of mixed western breed (88–91 days gestation; term, 145 days) are raised on a farm from a reliable breeder before being transported and housed in the animal care facility for 3–7 days to acclimate the animals prior to surgery. The large animal facility is climate-controlled (ambient temperature $20 \pm 1^\circ\text{C}$) with a 12 h light/dark cycle (light hours 06:00–18:00). Twin pregnancies are studied so that each experimental fetus has a twin control. Digital X-rays are performed at 87 days of gestation to confirm the ewe's pregnancy. Loose-fitting collars are routinely used as part of the preoperative procedure (to aid shearing surgical sites) and the ewes take no special notice of the collars.

2.3 Biohazard Precautions When Handling Sheep

Pregnant sheep may be infected with the human pathogen, *Coxiella burnetii* (Q-Fever), the organisms of which can be found in urine, feces, amniotic fluid and placental tissue. Given that pregnant sheep cannot be reliably tested for these organisms, we assume that all pregnant sheep may be infected. A vaccine for Q fever has been developed and used successfully in humans overseas, but the vaccine is not currently available for commercial use in the USA. Several procedures should be implemented to minimize infection with Q-Fever while working with pregnant sheep:

1. Animals are restricted to designated areas with Biosafety Level 2 practices for the containment of pregnant sheep. Specialized carts ("Q carts") are used for transport of animals outside the designated containment area. "Q-carts" are used for the safe transport of sheep between buildings, for example, between the loading docks at the time of delivery from the farm to their housing runs. The carts are fitted with air filters and are large enough for the sheep to stand or lie down. These carts are used for transport only and sheep are in the carts for the minimum amount of time possible.
2. All personnel are required to wear protective clothing when handling animals or their waste products. These include a disposable gown and shoe covers, surgical mask, and exam gloves.

3. Procedure rooms and other items in contact with the animals are routinely cleaned with a bleach solution (1 part 5 % hypochlorite to 30 parts water, changed daily). These include all equipment, carts, cages, and other items that need to be moved outside of the designated Q-fever containment area. Animal carcasses are “double bagged” before cremation.

2.4 Preoperative Care and Anesthesia

At 90 days of their 145 day gestation time-dated pregnant sheep with twin fetuses are prepared for sterile surgery. At ~15–18 h prior to surgery, food is withheld but the pregnant ewe has free access to water. The ewe’s jugular vein is cannulated with a 20 G intravenous (i.v.) cannula and injected with atropine (7.5 mg i.m.), ketamine (400 mg, i.v.), and diazepam (10 mg, i.v.) to allow tracheal intubation. If necessary, an additional half dose of each agent is given prior to anesthesia. The ewe is placed in a U-shaped trough on the surgery table in a supine position with its legs restrained caudally and cranially to prevent rotation during surgery. Intubation is performed with a 8.5 mm Mallinckrodt inflatable endotracheal tube (Covidien-Nellcor, Boulder, Colorado) that is connected to the anesthesia mixer and ventilator. Under positive pressure ventilation (Norkovet II Anesthesia machine with a Hallowell Veterinary Ventilator, Hallowell EMC, Pittsfield, MA), isoflurane (1–2 % in a 70:30 mixture of oxygen and nitrous oxide) is initiated to maintain anesthesia during surgery with the isoflurane concentration adjusted to ensure a surgical level of anesthesia for the ewe and fetus. A continuous isotonic saline drip (500 ml/h) is administered to maintain maternal fluid balance.

3 Methods

3.1 Surgical Procedures

3.1.1 Maternal and Fetal Surgery for Fetal Global Cerebra Ischemia Protocols

Provided here are details pertinent to the generation of preterm fetal global cerebral ischemia. The maternal abdomen is shaved, disinfected with betadine and the operative site covered with sterile drapes. The abdomen is opened through a midline incision. A purse-string suture is placed around the uterine incision and is tightened to reduce amniotic fluid loss after the head and neck of the fetus are exposed.

We have employed two different approaches to achieve global cerebral ischemia. The first is to place an occluder on each of the carotid arteries in the neck. The second is to place a single occluder around the brachiocephalic artery in the chest. The relative advantages and disadvantages of each approach are discussed below. For placement of the carotid occluders, a small (less than 3 cm) midline incision is made in the fetal neck to expose the carotid arteries. To confine the cerebral blood supply to the carotid arteries, the

vertebro-occipital arteries are ligated bilaterally. These anastomoses connect the vertebral arteries, supplied by the thoracic aorta, with the external carotid arteries that are fed by the brachiocephalic [107]. Silastic hydraulic occluders (2 mm diameter) are placed around each carotid artery. A non-occlusive indwelling polyvinyl catheter is placed in one carotid artery. A catheter is also attached to the fetal skin to allow subsequent measurement of amniotic fluid pressure. The fetal neck incision is closed with suture.

For placement of the brachiocephalic occluder (4 mm diameter), an incision is made at the second intercostal space on the left side. The brachiocephalic artery is isolated and an occluder placed to allow subsequent controlled reduction of fetal cephalic blood pressure distal to the occluder in order to cause global brain ischemia. The chest incision is closed in two layers.

After placement of either set of occluders, all catheters are anchored to the fetal skin on the neck and head or back to prevent them from pulling out or kinking off. The fetus is then gently returned to the uterus with special care taken to preserve and reseal the membranes. The uterine incision is closed and then oversewn to prevent leakage. The twin fetus is either left as an un-instrumented control or can be similarly instrumented. The maternal abdominal incision is closed in anatomical layers, and all catheters are tunneled subcutaneously to emerge on the flank of the ewe. Catheters are bundled and stored in a pouch stitched to the flank of the ewe, to prevent them from pulling out. One million units of penicillin-G are administered to the amniotic fluid (through a catheter) for the specific prevention of clostridia; no other antibiotics are routinely necessary (post-operative cultures have amply demonstrated the adequacy of this regime).

3.1.2 Placement of EEG Electrodes and EEG Recording Studies

EEG electrodes are placed via 2 cm scalp incisions on the fetal dura by making small holes in the fetal skull. One or two pairs of EEG electrodes (AS633-5SSF, Cooner Wire, Chatsworth, CA) are secured on the dura over the parasagittal parietal cortex (5 mm and 10 mm anterior to bregma and 5 mm lateral) with a reference electrode attached over the occiput. The electrodes are connected to high impedance amplifiers to provide a filtered input to a Stellate Systems (Montreal, Quebec) digital EEG recording and analysis system. We have recorded 2–5 channels of continuous EEG from ten animals for up to 16 h before and after global ischemia [108]. Seizure detection was done both by visual analysis and confirmed with a newborn seizure detection algorithm from Stellate Systems.

3.2 Postoperative Care

After surgery, the ewe is returned to a recovery pen for at least 24 h. The pen is covered with clear bedding material. The ewe is checked at least every half-hour until the animal is standing and feeding, usually within 0.5–1 h after surgery. Buprenex (buprenorphine,

0.3–0.6 mg, s.c.) is routinely administered after surgery and for the next 1.5 days, twice daily. The surgical incision site is assessed at least once daily and post-surgical infections are treated, as required in consultation with the veterinary staff. Fetal catheters are maintained patent by a daily infusion of 300 U/cc of heparinized saline. Ewes are monitored daily for normal ruminal function and for signs of pain and distress including a hunched posture, reluctance to move around, unwillingness to lie down or decreased appetite. Animals are assessed regularly for these signs after surgical procedures and at least once daily thereafter. A requirement for parenteral fluids or electrolytes is unusual in our experience, but their administration is at the discretion of veterinary staff, in consultation with investigators. In the rare situation that pain cannot be adequately managed, and treatments are proving to be ineffective, the animal is removed from the study and euthanized.

3.3 Specific Study Protocols

Restraint of the animals. After a minimum of 72 h of recovery, the ewe is placed in a mobile self-contained rolling cart and taken to the study room. In the cart, the ewe is loosely tethered to the cart via a collar and chain and has access to food and water. Typically, the maximum amount of time that the ewe is loosely restrained in the cart is 3 h. If the ewe is uneasy in the cart, a second sheep is put in a cart and brought into the study room for company. Alternatively, a mirror is placed in front of the study cart so that the ewe sees another apparent companion.

Cerebral hypoperfusion studies: bilateral carotid occlusion. Animals are typically studied no earlier than the third post-operative day to allow fetal recovery from surgery. Pressure transducers are connected to appropriate amplifiers (TA 6000; Gould Instruments, Valley View, OH) to record mean arterial blood pressure (MABP) in the fetal artery relative to amniotic fluid pressure using ADI Powerlab software (Dagan Corp., Minneapolis, MN). Fetal heart rate (HR) is calculated from triplicate measurements of the arterial pressure pulse intervals over a continuous recording of >20 s. Fetuses are studied only if they demonstrated normal oxygenation (>6 ml O₂/100 ml blood) and blood indices [109]. Sustained cerebral hypoperfusion is initiated by bilateral carotid artery occlusion after inflation of the carotid occluders. Cerebral reperfusion is established by deflation of the occluders and was studied at either 15 or 60 min of restored flow. Verification of successful inflation of the occluders is verified by measurement of an increase in pressure proximal to the occluders with an indwelling carotid or axillary artery catheter. Fetal heart rate and MAP traces are monitored continuously throughout the occlusion and arterial blood gas analysis is done at standard time points prior to, during and after the occlusion to assess the fetal response.

Cerebral hypoperfusion and hypoxia studies: brachiocephalic artery occlusion coupled with reduced inspired oxygen. To reduce fetal oxygen delivery, the ewe inspires a reduced content oxygen mixture. After a basal period where room air is inspired, a clear plastic bag is placed over the ewes head and the ewe inspires a 10–12 % oxygen mixture that flushes the bag at 20 l/min. Ewes respond by increasing their ventilation and generally tolerate the procedure well. After 4 min of lowered inspired oxygen, the fetus also becomes moderately hypoxic. At this time the occluder, which has been placed around the brachiocephalic artery, is inflated to reduce the perfusion pressure to the fetal head and arms for 25 min. Thereafter, the occluder is released to restore normal fetal cephalic blood pressure. The bag is removed and the ewe returns to breathing room air so that oxygenation of the ewe and fetuses oxygenation returns to normal.

Blood analysis. One milliliter blood samples are taken anaerobically from the fetal carotid artery and analyzed for arterial p_{aH} , P_{aO_2} , P_{aCO_2} (corrected to 39 °C), hemoglobin content, arterial oxygen content (CaO_2), arterial oxygen saturation, glucose and lactate (ABL 700 pH/Blood Gas Analyzer; Radiometer, Westlake, OH), and hematocrit (capillary microfuge). Fetuses are only studied if they demonstrate normal fetal oxygenation, defined as >6 ml $O_2/100$ ml blood, at a 24 h recovery from the operation.

Microsphere injection protocol. Fetal brain blood flow is measured spatially by the fluorescent microsphere distribution and reference sample method [110]. Fluorescent microspheres with four different colors (15 μ m diameter; F-17047, F-17048, F-17048, F-17050; Molecular Probes, Eugene, OR) have the following peak excitation and emission: green (450/480) yellow (515/534), red (580/605) and scarlet (650/685). Approximately 3×10^6 microspheres suspended in 1 ml of saline with 0.05 % Tween are sonicated and then injected over 30 s into the fetal hindlimb vein followed by a 2 ml flush with saline. Starting just before and continuing 2 min after each injection, a reference blood sample is drawn at 0.75 ml/min into a syringe mounted in a syringe pump (Harvard Apparatus Co., Dover, MA).

Tissue handling. The ewe and fetuses are killed by intravenous injection of the ewe with Euthasol (~10 ml/50 kg body weight.; Virbac Inc., Ft. Worth, TX). After fetal brains are removed, we employ a variety of protocols for tissue preservation depending on the study criteria. These include immersion fixation at 4 °C in 4 % paraformaldehyde in 0.1 M phosphate buffer, pH 7.4 for 2 days followed by storage in PBS. Brains to be analyzed for microspheres or for MRI-histopathological correlation are subsequently immersed in 20 % sucrose until they sink and then rapidly frozen in OCT for acquisition of frozen sections with a cryostat.

4 Discussion

4.1

Pathophysiological Mechanisms of Preterm Cerebral Injury Related to the Brachiocephalic Vs. Carotid Occlusion Models of Global Cerebral Ischemia

The dominant factors related to the generation of WMI in most if not all models are: (1) the content of oxygen and glucose in the blood; (2) the driving or perfusion pressure and hence cerebral blood flow (CBF); and (3) the duration of the insult. In preterm fetal sheep, it is often feasible for these important variables to be manipulated and measured either in groups of animals or in single individuals. The pathophysiological disturbances associated with these factors are variously weighted depending upon the model employed.

With models of maternal hypoxemia (e.g., high altitude or a low inspired oxygen fraction) fetal oxygenation falls while blood pressure (BP) rises transiently but then returns to normal and then falls below normal [32, 34, 98, 111–114]. Likewise systemic asphyxia models that utilize umbilical cord occlusion cause a reduced fetal arterial oxygen tension and content [100, 115, 116]. In cord occlusion models, BP initially increases to compensate for diminished oxygenation, but as systemic and cardiac hypoxia progressively intensify, hemodynamic and cardiac decompensation occurs with a resultant fall in BP. It appears that significant brain damage occurs only when the hypoxia and hypotension are allowed to progress until near death conditions occur. However, as cardiovascular compensations fail with time, substantial albeit variable reductions in BP occur. The residual brain blood flow has seldom been measured, but for brain injury to occur, pressures must fall below 1/3 normal for 10–15 min depending on the animal's age. The importance of the central autonomic system as well as adrenal stress hormones remains unclear as do systemic blood concentrations of metabolic substrates like glucose and products like lactate. The fetal sheep brain, in particular when immature and hypoxemic, has essentially no ability to autoregulate [15, 16, 18]. Hence, in asphyxia models, the fall in BP exacerbates the fetal brain hypoxia with a consequent reduction in CBF that leads to partial ischemia.

Occlusive cerebral ischemia models differ from asphyxia models in several significant ways. A major practical advantage of the occlusive models is that the heart is largely unaffected. Essentially, cerebral damage can be reliably generated without the significant fetal deaths and morbidity that are inherently associated with other models that require near death conditions to ensure brain damage. Injury in the umbilical cord occlusion models can be modulated by adjusting the duration of occlusion relative to the onset of systemic hypotension.

Unlike in utero systemic hypoxemia or asphyxia models, models that utilize carotid or brachiocephalic artery occlusions cause an immediate fall in perfusion pressure and CBF, and thus have a

well-defined onset of the insult [7, 23, 109]. Cerebral ischemia in these models is generally global and severe but not complete, especially when collateral circulation is left intact (discussed further below). Importantly, some CBF persists and the oxygenation and glucose levels of this residual flow have important influence on the extent of damage. The residual blood flow is the most difficult parameter to quantify. Even in fetal sheep models, CBF is only infrequently measured and BP is often used as a surrogate marker of CBF.

There are a number of considerations that guide the selection of a model that utilizes carotid versus common brachiocephalic artery occlusion. However, the differences between bi-carotid and brachiocephalic artery occlusion are not as great as the difference between either of those models and cord occlusion models. The carotid arteries in the 0.65 sheep fetus are small and there is a relatively greater risk that commercially available occluders can inadvertently obstruct flow chronically if placement and routing techniques are not optimal. By contrast, the brachiocephalic artery is a larger and much more stable vessel for the placement of a single occluder [19, 111]. In sheep, the brachiocephalic artery supplies the entire head including the carotids as well as both axillary arteries, which supply the forelegs. The brachiocephalic artery is the only major artery that supplies the upper body. Occlusion of the brachiocephalic artery is similar to bilateral carotid occlusion in terms of perfusion to the head and brain, but different in that forelimb perfusion is also reduced, which does not occur if flow to both carotids is completely restricted.

One important consequence of the brachiocephalic artery occlusion model is that proximal BP to the rest of the fetal body and the placental circulation is subject to an elevated pressure. This probably results in an increase in flow that causes a moderate but significant rise in arterial oxygenation. The same effect probably occurs with bi-carotid occlusion, but would be expected to be smaller. Either preparation can be coupled with a lowered maternal inspired oxygen fraction to counteract elevations in arterial oxygenation or even generate a fetal hypoxemia in addition to cerebral ischemia.

The occipital-vertebral arteries are small but potentially important in models where cephalic occlusions are studied [23, 107]. They provide an important anastomosis between the anterior circulation provided by the carotid arteries and the posterior circulation derived from the vertebral arteries. Occipital-vertebral arteries are likely to be variable in size from animal to animal, perhaps linked to variations in anatomy related to their supply at or near the Circle of Willis. They connect to the carotids near the lingual branch and are, thus, distal to the brachiocephalic artery occluder as well as to all but the most rostral placements of carotid occluders. Hence, they act to support brain blood flow when systemic pressure is normal but BCA or carotid occlusions are used.

Hence, in both the bi-carotid and BCA occlusion models, it is important to ligate these vessels to achieve near complete global cerebral ischemia. The exact amount of flow they provide, especially to the preterm fetus, has not been carefully determined. In normal sheep, it is not even clear whether there is a net flow and, if so, in what direction. During either carotid or BCA occlusions, flow is certainly from the vertebrals to the carotids distal to the site of placement of occluders. The amount of flow in the occipital-vertebral arteries, while likely to be variable from animal to animal, is clearly sufficient to cause variability in brain damage in the cephalic ischemia models unless they are ligated.

4.2 Final Conclusions

The preterm human infant displays unique patterns of cerebral injury that now can be closely replicated in the preterm fetal sheep. Despite the higher costs and technical challenges of preterm fetal sheep models, they provide powerful access to preclinical questions related to the pathophysiology of WMI. Recent advances include spatially defined measurements of cerebral blood flow in utero, the definition of cellular-maturational factors that define the topography of WMI and the application of high field neuro-imaging to define MRI signatures for specific types of chronic WMI. There is a critical need to further define the cellular and molecular mechanisms that mediate the progression of cerebral white and gray matter injury. Such information is critical for the rationale design of therapies targeted to block the initial phase of injury or to promote regeneration and repair during the chronic phase. With few exceptions, most studies have focused on models of cerebral hypoxia-ischemia or maternal fetal infection. Future improved fetal sheep models are needed that more closely reproduce the spectrum of insults that are likely to converge to generate cerebral injury in human preterm infants.

Acknowledgments

Supported by the National Institutes of Neurological Diseases and Stroke: 1RO1NS054044, R37NS045737-06S1/06S2 to SAB, the American Heart Association (SAB) and the March of Dimes Birth Defects Foundation (SAB).

References

1. Back S, Riddle A, Hohimer A (2012) The instrumented fetal sheep as a model of cerebral white matter injury in the preterm infant. *Neurotherapeutics* 9:359–370
2. Marlow N, Wolke D, Bracewell MA, Samara M (2005) Neurologic and developmental disability at six years of age after extremely preterm birth. *N Engl J Med* 352:9–19
3. Kinney H, Back S (1998) Human oligodendroglial development: relationship to periventricular leukomalacia. *Semin Pediatr Neurol* 5:180–189
4. Gonzalez FF, Miller SP (2006) Does perinatal asphyxia impair cognitive function without cerebral palsy? *Arch Dis Child Fetal Neonatal Ed* 91:F454–F459

5. Back SA, Rosenberg PA (2014) Pathophysiology of glia in perinatal white matter injury. *Glia* 62:1790–1815
6. Back SA, Luo NL, Mallinson RA, O'Malley JP, Wallen LD et al (2005) Selective vulnerability of preterm white matter to oxidative damage defined by F₂-isoprostanes. *Ann Neurol* 58:108–120
7. Riddle A, Luo N, Manese M, Beardsley D, Green L et al (2006) Spatial heterogeneity in oligodendrocyte lineage maturation and not cerebral blood flow predicts fetal ovine periventricular white matter injury. *J Neurosci* 26:3045–3055
8. McClendon E, Chen K, Gong X, Sharifnia E, Hagen M et al (2014) Prenatal cerebral ischemia triggers dysmaturation of caudate projection neurons. *Ann Neurol* 75:508–524
9. Dean J, McClendon E, Hansen K, Azimi-Zonooz A, Chen K et al (2013) Prenatal cerebral ischemia disrupts MRI-defined cortical microstructure through disturbances in neuronal arborization. *Sci Transl Med* 5:101–111
10. Back S, Miller S (2014) Brain injury in premature neonates: a primary cerebral dysmaturation disorder? *Ann Neurol* 75:469–486
11. Pyrdy O (1991) Control of cerebral circulation in the high-risk neonate. *Ann Neurol* 30:321–329
12. Menke J, Michel E, Hildebrand S (1997) Cross-spectral analysis of cerebral autoregulation dynamics in high risk preterm infants during the perinatal period. *Pediatr Res* 42:690–699
13. du Plessis A (2008) Cerebrovascular injury in premature infants: current understanding and challenges for future prevention. *Clin Perinatol* 35:609–641
14. Soul J, Hammer P, Tsuji M, Saul J, Bassan H et al (2007) Fluctuating pressure-passivity is common in the cerebral circulation of sick premature infants. *Pediatr Res* 61:467–473
15. Papile L, Rudolph AM, Heymann M (1985) Autoregulation of cerebral blood flow in the preterm fetal lamb. *Pediatr Res* 19:159–161
16. Tweed W, Cote J, Pash M, Lou H (1985) Arterial oxygenation determines autoregulation of cerebral blood flow in fetal lamb. *Pediatr Res* 17:246–249
17. Szymonowicz W, Walker A, Yu V, Stewart M, Cannata J et al (1990) Regional cerebral blood flow after hemorrhagic hypotension in the preterm, near-term, and newborn lamb. *Pediatr Res* 28:361–366
18. Helou S, Koehler RC, Gleason CA, Jones MD, Traystman RJ (1994) Cerebrovascular autoregulation during fetal development in sheep. *Am J Physiol* 266:H1069–H1074
19. Hohimer AR, Bissonnette JM (1989) Effects of cephalic hypotension, hypertension, and barbiturates on fetal cerebral blood flow and metabolism. *Am J Obstet Gynecol* 161:1344–1351
20. Greisen G (2009) To autoregulate or not to autoregulate—that is no longer the question. *Semin Pediatr Neurol* 16:207–215
21. Tsuji M, Saul J, du Plessis A, Eichenwald E, Sobh J et al (2000) Cerebral intravascular oxygenation correlates with mean arterial pressure in critically ill premature infants. *Pediatrics* 106:625–632
22. Volpe JJ (2008) *Neurology of the newborn*. W.B. Saunders, Philadelphia, pp 399–407
23. Reddy K, Mallard C, Guan J, Marks K, Bennet L et al (1998) Maturation change in the cortical response to hypoperfusion injury in the fetal sheep. *Pediatr Res* 43:674–682
24. Raad RA, Tan WK, Bennet L, Gunn AJ, Davis SL et al (1999) Role of the cerebrovascular and metabolic responses in the delayed phases of injury after transient cerebral ischemia in fetal sheep. *Stroke* 30:2735–2741
25. Clapp J III, Peress N, Wesley M, Mann L (1988) Brain damage after intermittent partial cord occlusion in the chronically instrumented fetal lamb. *Am J Obstet Gynecol* 159:504–509
26. Ikeda T, Murata Y, Quilligan E, Choi B, Parer J et al (1998) Physiologic and histologic changes in near-term fetal lambs exposed to asphyxia by partial umbilical cord occlusion. *Am J Obstet Gynecol* 178:24–32
27. Ohyu J, Marumo G, Ozawa H, Takashima S, Nakajima K et al (1999) Early axonal and glial pathology in fetal sheep brains with leukomalacia induced by repeated umbilical cord occlusion. *Brain Dev* 21:248–252
28. Matsuda T, Okuyama K, Cho K, Hoshi N, Matsumoto Y et al (1999) Induction of antenatal periventricular leukomalacia by hemorrhagic hypotension in the chronically instrumented fetal sheep. *Am J Obstet Gynecol* 181:725–730
29. Duncan J, Cock M, Scheerlinck J, Westcott K, McLean C et al (2002) White matter injury after repeated endotoxin exposure in the preterm ovine fetus. *Pediatr Res* 52:941–949
30. Dalitz P, Harding R, Rees S, Cock M (2003) Prolonged reductions in placental blood flow and cerebral oxygen delivery in preterm fetal sheep exposed to endotoxin: possible factors in white matter injury after acute infection. *J Soc Gynecol Investig* 10:283–290

31. Rees S, Stringer M, Just Y, Hooper S, Harding R (1997) The vulnerability of the fetal sheep brain to hypoxemia at mid-gestation. *Dev Brain Res* 103:103–118
32. Rees S, Breen S, Loeliger M, McCrabb G, Harding R (1999) Hypoxemia near mid-gestation has long-term effects on fetal brain development. *J Neuropathol Exp Neurol* 58:932–945
33. Mallard E, Rees S, Stringer M, Cock M, Harding R (1998) Effects of chronic placental insufficiency on brain development in fetal sheep. *Pediatr Res* 43:262–270
34. Penning D, Grafe J, Hammond R, Matsuda Y, Patrick J et al (1994) Neuropathology of the near-term and midgestation ovine fetal brain after sustained in utero hypoxemia. *Am J Obstet Gynecol* 170:1425–1432
35. Riddle A, Dean J, Buser JR, Gong X, Maire J et al (2011) Histopathological correlates of magnetic resonance imaging-defined chronic perinatal white matter injury. *Ann Neurol* 70:493–507
36. Riddle A, Maire J, Cai V, Nguyen T, Gong X et al (2013) Hemodynamic and metabolic correlates of perinatal white matter injury severity. *PLoS One* 8:e82940
37. Riddle A, Maire J, Gong X, Chen K, Kroenke C et al (2012) Differential susceptibility to axonopathy in necrotic and non-necrotic perinatal white matter injury. *Stroke* 43:178–184
38. Bagenholm R, Nilsson U, Gotborg C, Kjellmer I (1998) Free radicals are formed in the brain of the fetal sheep during reperfusion after cerebral ischemia. *Pediatr Res* 43:271–275
39. Ikeda K, Murata Y, Quilligan EJ, Parer J, Doi S et al (1998) Brain lipid peroxidation and antioxidant levels in fetal lambs 72 hours after asphyxia from partial umbilical cord occlusion. *Am J Obstet Gynecol* 178:474–478
40. Castillo-Melendez M, Chow J, Walker D (2004) Lipid peroxidation, caspase-3 immunoreactivity, and pyknosis in late-gestation fetal sheep brain after umbilical cord occlusion. *Pediatr Res* 55:864–871
41. Welin A-K, Sandberg M, Lindblom A, Arvidsson P, Nilsson U et al (2005) White matter injury following prolonged free radical formation in the 0.65 gestation fetal sheep brain. *Pediatr Res* 58:100–105
42. Buser J, Maire J, Riddle A, Gong X, Nguyen T et al (2012) Arrested pre-oligodendrocyte maturation contributes to myelination failure in premature infants. *Ann Neurol* 71:93–109
43. Haynes RL, Billiards SS, Borenstein NS, Volpe JJ, Kinney HC (2008) Diffuse axonal injury in periventricular leukomalacia as determined by apoptotic marker fractin. *Pediatr Res* 63:656–661
44. Back SA, Han BH, Luo NL, Chrichton CA, Tam J et al (2002) Selective vulnerability of late oligodendrocyte progenitors to hypoxia-ischemia. *J Neurosci* 22:455–463
45. Banker B, Larroche J (1962) Periventricular leukomalacia of infancy. A form of neonatal anoxic encephalopathy. *Arch Neurol* 7:386–410
46. DeReuck J, Chattha A, Richardson E (1972) Pathogenesis and evolution of periventricular leukomalacia in infancy. *Arch Neurol* 27:229–236
47. Rorke LB (1982) Pathology of perinatal brain injury. Raven, New York, pp 45–63
48. Leviton A, Gilles F (1984) Acquired perinatal leukoencephalopathy. *Ann Neurol* 16:1–10
49. Haynes RL, Folkert RD, Keefe RJ, Sung I, Swzeda LI et al (2003) Nitrosative and oxidative injury to premyelinating oligodendrocytes in periventricular leukomalacia. *J Neuropathol Exp Neurol* 62:441–450
50. Iida K, Takashima S, Ueda K (1995) Immunohistochemical study of myelination and oligodendrocyte in infants with periventricular leukomalacia. *Pediatr Neurol* 13:296–304
51. Robinson S, Li Q, Dechant A, Cohen M (2006) Neonatal loss of gamma-aminobutyric acid pathway expression after human perinatal brain injury. *J Neurosurg* 104:396–408
52. Hamrick S, Miller SP, Leonard C, Glidden D, Goldstein R et al (2004) Trends in severe brain injury and neurodevelopmental outcome in premature newborn infants: the role of cystic periventricular leukomalacia. *J Pediatr* 145:593–599
53. Counsell S, Allsop J, Harrison M, Larkman D, Kennea N et al (2003) Diffusion-weighted imaging of the brain in preterm infants with focal and diffuse white matter abnormality. *Pediatrics* 112:176–180
54. Miller SP, Cozzio CC, Goldstein RB, Ferriero DM, Partridge JC et al (2003) Comparing the diagnosis of white matter injury in premature newborns with serial MR imaging and transfontanel ultrasonography findings. *AJNR Am J Neuroradiol* 24:1661–1669
55. Inder TE, Anderson NJ, Spencer C, Wells S, Volpe JJ (2003) White matter injury in the premature infant: a comparison between serial cranial sonographic and MR findings at term. *AJNR Am J Neuroradiol* 24:805–809

56. Pierson CR, Folkerth RD, Billiards SS, Trachtenberg FL, Drinkwater ME et al (2007) Gray matter injury associated with periventricular leukomalacia in the premature infant. *Acta Neuropathol* 114:619–631
57. Back SA, Luo NL, Borenstein NS, Levine JM, Volpe JJ et al (2001) Late oligodendrocyte progenitors coincide with the developmental window of vulnerability for human perinatal white matter injury. *J Neurosci* 21:1302–1312
58. Favrais G, van de Looij Y, Fleiss B, Ramanantsoa N, Bonnin P et al (2011) Systemic inflammation disrupts the developmental program of white matter. *Ann Neurol* 70:550–565
59. Segovia K, McClure M, Moravec M, Luo N, Wang Y et al (2008) Arrested oligodendrocyte lineage maturation in chronic perinatal white matter injury. *Ann Neurol* 63:517–526
60. Sizonenko SV, Camm EJ, Dayer A, Kiss JZ (2008) Glial responses to neonatal hypoxic-ischemic injury in the rat cerebral cortex. *Int J Dev Neurosci* 26:37–45
61. Zaidi A, Bessert D, Ong J, Xu H, Barks J et al (2004) New oligodendrocytes are generated after neonatal hypoxic-ischemic brain injury in rodents. *Glia* 46:380–390
62. Felling RJ, Snyder MJ, Romanko MJ, Rothstein RP, Ziegler AN et al (2006) Neural stem/progenitor cells participate in the regenerative response to perinatal hypoxia/ischemia. *J Neurosci* 26:4359–4369
63. Yang Z, Levison SW (2006) Hypoxia/ischemia expands the regenerative capacity of progenitors in the perinatal subventricular zone. *Neuroscience* 139:555–564
64. Zhiheng H, Liu J, Cheung P-Y, Chen C (2009) Long-term cognitive impairment and myelination deficiency in a rat model of perinatal hypoxic-ischemia brain injury. *Brain Res* 1301:100–109
65. Wright J, Zhang G, Yu T-S, Kernie S (2010) Age-related changes in the oligodendrocyte progenitor pool influence brain remodeling after injury. *Dev Neurosci* 32:499–509
66. Volpe JJ (2009) Brain injury in premature infants: a complex amalgam of destructive and developmental disturbances. *Lancet Neurol* 8:110–124
67. Srinivasan L, Dutta R, Counsell SJ, Allsop JM, Boardman JP et al (2007) Quantification of deep gray matter in preterm infants at term-equivalent age using manual volumetry of 3-tesla magnetic resonance images. *Pediatrics* 119:759–765
68. Keunen K, Kersbergen KJ, Groenendaal F, Isgum I, de Vries LS et al (2012) Brain tissue volumes in preterm infants: prematurity, perinatal risk factors and neurodevelopmental outcome: a systematic review. *J Matern Fetal Neonatal Med* 25(Suppl 1):89–100
69. Tam EW, Ferriero DM, Xu D, Berman JI, Vigneron DB et al (2009) Cerebellar development in the preterm neonate: effect of supratentorial brain injury. *Pediatr Res* 66:102–106
70. Nossin-Manor R, Chung AD, Whyte HE, Shroff MM, Taylor MJ et al (2012) Deep gray matter maturation in very preterm neonates: regional variations and pathology-related age-dependent changes in magnetization transfer ratio. *Radiology* 263:510–517
71. Vinall J, Grunau RE, Brant R, Chau V, Poskitt KJ et al (2013) Slower postnatal growth is associated with delayed cerebral cortical maturation in preterm newborns. *Sci Transl Med* 5:168ra168
72. Johnston MV (2001) Excitotoxicity in neonatal hypoxia. *MRDD Res Rev* 7:229–234
73. Cheng Y, Deshmukh M, D'Costa A, Demaro J, Gidday J et al (1998) Caspase inhibitor affords neuroprotection with delayed administration in a rat model of neonatal hypoxic-ischemic brain injury. *J Clin Invest* 101:1992–1999
74. Han BH, DeMattos RB, Dugan LL, Kim-Han JS, Brendza RP et al (2001) Clusterin contributes to caspase-3-independent brain injury following neonatal hypoxia-ischemia. *Nat Med* 7:338–343
75. Holtzman D, Sheldon R, Jaffè W, Cheng Y, Ferriero D (1996) NGF protects the neonatal brain against hypoxic-ischemic brain injury. *Ann Neurol* 39:114–122
76. Stone BS, Zhang J, Mack DW, Mori S, Martin LJ et al (2008) Delayed neural network degeneration after neonatal hypoxia-ischemia. *Ann Neurol* 64:535–546
77. Northington FJ, Ferriero DM, Flock DL, Martin LJ (2001) Delayed neurodegeneration in neonatal rat thalamus after hypoxia-ischemia is apoptosis. *J Neurosci* 21:1931–1938
78. Andiman SE, Haynes RL, Trachtenberg FL, Billiards SS, Folkerth RD et al (2010) The cerebral cortex overlying periventricular leukomalacia: analysis of pyramidal neurons. *Brain Pathol* 20:803–814
79. Nagasunder AC, Kinney HC, Bluml S, Tavare CJ, Rosser T et al (2011) Abnormal microstructure of the atrophic thalamus in preterm survivors with periventricular leukomalacia. *AJNR Am J Neuroradiol* 32:185–191
80. Kinney H, Haynes R, Xu G, Andiman S, Folkerth R et al (2012) Neuron deficit in the white

- matter and subplate in periventricular leukomalacia. *Ann Neurol* 71:397–406
81. Komuro H, Rakic P (1993) Modulation of neuronal migration by NMDA receptors. *Science* 260:95–97
 82. Zhang ZW, Peterson M, Liu H (2013) Essential role of postsynaptic NMDA receptors in developmental refinement of excitatory synapses. *Proc Natl Acad Sci U S A* 110:1095–1100
 83. Luthi A, Schwyzler L, Mateos JM, Gahwiler BH, McKinney RA (2001) NMDA receptor activation limits the number of synaptic connections during hippocampal development. *Nat Neurosci* 4:1102–1107
 84. Gambrill AC, Barria A (2011) NMDA receptor subunit composition controls synaptogenesis and synapse stabilization. *Proc Natl Acad Sci U S A* 108:5855–5860
 85. Barlow R (1969) The foetal sheep: morphogenesis of the nervous system and histochemical aspects of myelination. *J Comp Neurol* 135:249–262
 86. Bernhared C, Kolmodin G, Meyerson B (1967) On the prenatal development of function and structure in the somesthetic cortex of the sheep. *Prog Brain Res* 2:60–77
 87. Cook C, Gluckman P, Johnston B, Williams C (1987) The development of the somatosensory evoked potential in the unanaesthetized fetal lamb. *J Dev Physiol* 9:441–456
 88. Cook C, Williams C, Gluckman P (1987) Brainstem auditory evoked potential in the fetal lamb, in utero. *J Dev Physiol* 9:429–440
 89. Gluckman P, Parsons Y (1983) Stereotaxic method and atlas for the ovine fetal forebrain. *J Dev Physiol* 5:101–128
 90. Vanderwolf C, Cooley R (1990) The sheep brain: a photographic series. A.J. Kirby Co., London, Ontario, Canada
 91. Back SA, Riddle A, Hohimer AR (2006) Role of instrumented fetal sheep preparations in defining the pathogenesis of human periventricular white matter injury. *J Child Neurol* 21:582–589
 92. Follet PL, Rosenberg PA, Volpe JJ, Jensen FE (2000) NBQX attenuates excitotoxic injury to the developing white matter. *J Neurosci* 20:9235–9241
 93. Uehara H, Yoshioka H, Kawase S, Nagai H, Ohmae T et al (1999) A new model of white matter injury in neonatal rats with bilateral carotid artery occlusion. *Brain Res* 837:213–220
 94. Olivier P, Baud O, Evrard P, Gressens P, Verney C (2005) Prenatal ischemia and white matter damage in rats. *J Neuropathol Exp Neurol* 64:998–1006
 95. Marret S, Mukendi R, Gadsisieux J-F, Gressens P, Evrard P (1995) Effect of ibotenate on brain development: an excitotoxic mouse model of microgyria and posthypoxic-like lesions. *J Neuropathol Exp Neurol* 54:358–370
 96. Lodygensky G, West T, Moravec M, Back S, Dikranian K et al (2011) Diffusion characteristics associated with neuronal injury and glial activation following hypoxia-ischemia in the immature brain. *Magn Reson Med* 66:839–835
 97. Gunn AJ, Bennet L (2009) Fetal hypoxia insults and patterns of brain injury: insights from animal models. *Clin Perinatol* 36:579–593
 98. Gleason CA, Hamm C, Jones MD Jr (1990) Effect of acute hypoxemia on brain blood flow and oxygen metabolism in immature fetal sheep. *Am J Physiol* 258:H1064–1069
 99. Falkowski A, Hammond R, Han V, Richardson B (2002) Apoptosis in the preterm and near term ovine fetal brain and the effect of intermittent umbilical cord occlusion. *Dev Brain Res* 136:165–173
 100. Bennet L, Rossenrode S, Gunning MI, Gluckman PD, Gunn AJ (1999) The cardiovascular and cerebrovascular responses of the immature fetal sheep to acute umbilical cord occlusion. *J Physiol* 517(Pt 1):247–257
 101. Welin AK, Svedin P, Lapatto R, Sultan B, Hagberg H et al (2007) Melatonin reduces inflammation and cell death in white matter in the mid-gestation fetal sheep following umbilical cord occlusion. *Pediatr Res* 61:153–158
 102. Harris AP, Koehler RC, Gleason CA, Jones MD Jr, Traystman RJ (1989) Cerebral and peripheral circulatory responses to intracranial hypertension in fetal sheep. *Circ Res* 64:991–1000
 103. Rees S, Hale N, De Matteo R, Cardamone L, Tolcos M et al (2010) Erythropoietin is neuroprotective in a preterm ovine model of endotoxin-induced brain injury. *J Neuropathol Exp Neurol* 69:306–319
 104. Dean J, van de Looij Y, Sizonenko S, Lodygensky G, Lazeyras F et al (2011) Delayed cortical impairment following lipopolysaccharide exposure in preterm fetal sheep. *Ann Neurol* 70:846–856
 105. Sorensen A, Pedersen M, Tietze A, Ottosen L, Duus L et al (2009) BOLD MRI in sheep fetuses: a non-invasive method for measuring changes in tissue oxygenation. *Ultrasound Obstet Gynecol* 34:687–692

106. Gunn A, Bennet L (2008) Brain cooling for preterm infants. *Clin Perinatal* 35:735–748
107. Baldwin B, Bell F (1963) The anatomy of the cerebral circulation of the sheep and ox. The dynamic distribution of the blood supplied by the carotid and vertebral arteries to cranial regions. *J Anat* 97:203–215
108. McClure M, Riddle A, Manese M, Luo N, Rorvik D et al (2008) Cerebral blood flow heterogeneity in preterm sheep: lack of physiological support for vascular boundary zones in fetal cerebral white matter. *J Cereb Blood Flow Metab* 28:995–1008
109. Chao CR, Hohimer AR, Bissonnette JM (1991) Fetal cerebral blood flow and metabolism during oligemia and early postoligemic reperfusion. *J Cereb Blood Flow Metab* 11:416–423
110. Bernard SL, Ewen JR, Barlow CH, Kelly JJ, McKinney S, Frazer DA, Glenn RW (2000) High spatial resolution measurements of organ blood flow in small laboratory animals. *Am J Physiol Heart Circ Physiol* 279:H2043–H2052
111. Hohimer AR, Chao CR, Bissonnette JM (1991) The effect of combined hypoxemia and cephalic hypotension on fetal cerebral blood flow and metabolism. *J Cereb Blood Flow Metab* 11:99–105
112. Iwamoto HS, Kaufman T, Keil LC, Rudolph AM (1989) Responses to acute hypoxemia in fetal sheep at 0.6–0.7 gestation. *Am J Physiol* 256:H613–H620
113. Rurak DW, Richardson BS, Patrick JE, Carmichael L, Homan J (1990) Oxygen consumption in the fetal lamb during sustained hypoxemia with progressive acidemia. *Am J Physiol* 258:R1108–R1115
114. Richardson BS, Rurak D, Patrick JE, Homan J, Carmichael L (1989) Cerebral oxidative metabolism during sustained hypoxaemia in fetal sheep. *J Dev Physiol* 11:37–43
115. Yan EB, Baburamani AA, Walker AM, Walker DW (2009) Changes in cerebral blood flow, cerebral metabolites, and breathing movements in the sheep fetus following asphyxia produced by occlusion of the umbilical cord. *Am J Physiol Regul Integr Comp Physiol* 297:R60–R69
116. Richardson BS (1993) The fetal brain: metabolic and circulatory responses to asphyxia. *Clin Invest Med* 16:103–114

Using Pregnant Sheep to Model Developmental Brain Damage

Lotte G. van den Heuij, Guido Wassink, Alistair J. Gunn,
and Laura Bennet

Abstract

In order to develop more effective ways of identifying, managing, and treating preterm asphyxial brain injury, stable experimental models are essential. The present review describes the key experimental factors that determine the pattern and severity of brain injury in chronically instrumented fetal sheep, including the depth (“severity”) and duration of asphyxia, and the maturity, and condition of the fetus. These models are valuable to dissect the pathogenesis of key clinical patterns of brain injury in a stable thermal and biochemical environment, and to test therapeutic interventions.

Key words Fetal sheep, Perinatal asphyxia, Hypoxic-ischemic encephalopathy, Hypotension, Cerebral blood flow

1 Introduction

Premature birth is one of the leading causes of morbidity and mortality. Around 6–13 % of all births are preterm [1]. Preterm survivors have a high risk of neurobehavioral disturbances and intellectual disabilities related to learning, cognition, visuospatial integration, attention deficit, and socialization [2–4]. Early imaging and postmortem data suggest that cerebral injury in preterm infants occurs in the immediate perinatal period in approximately two thirds of cases, while an appreciable number of cases occur before the onset of labor; in contrast, injury after the early neonatal period represents only approximately 10 % of cases [5, 6]. Consistent with this, acute EEG abnormalities are reported in the early perinatal period in the majority of infants and are highly predictive of long-term outcome [7]. The precise etiology of injury remains surprisingly unclear; however, it is highly likely to involve both hypoxia-ischemia and infection/inflammation [8].

Acute neonatal encephalopathy associated with asphyxia remains a significant cause of death and long-term disability at all ages [9]. Early onset neonatal encephalopathy is highly associated with evidence of asphyxia as shown by non-reassuring fetal heart rate tracings and severe metabolic acidosis on umbilical cord blood [10, 11], with acute brain lesions on magnetic resonance imaging, and ultimately with subsequent neurodevelopmental impairment [12]. In term infants, large clinical trials have established that mild brain cooling significantly reduces cerebral palsy and improves survival without disability at 18 months of age after acute hypoxic-ischemic encephalopathy [13]. However, therapeutic hypothermia is only partially protective, such that nearly half of affected babies still die or survive with disability despite treatment. Moreover, it is effective only within a relatively limited window of time, and current protocols may not be appropriate for preterm infants. There is a strong historical link between mild hypothermia and increased mortality in preterm newborns [14], and recently a phase I trial of cooling for preterm infants was stopped by the US Food and Drug Administration because of potential concerns about intracerebral hemorrhage. Thus, it is vital to find specific treatments for brain injury in the preterm brain.

Many drugs have been shown to be neuroprotective in neonatal rodent models; however, none have yet shown clinical improvement [15]. In order to translate promising treatments, it is essential to validate them in large animal translational models before considering clinical trials. Such models are also useful to help understand the many factors that affect outcome from an event, including the fetal sex, weight, and degree of hypotension.

1.1 What Initiates Neuronal Injury?

Before discussing the experimental approach, it is helpful to reflect on the triggers of asphyxial injury to the brain and other organs. Fundamentally, injury requires a period of insufficient oxygen and substrate delivery (glucose and other substances such as lactate) such that neurons (and glia) cannot maintain internal homeostasis and become depolarized [16]. At least broadly, the extent of injury is related to the duration of tissue depolarization [17]. Since organ perfusion is essential for maintaining oxygen and substrate delivery to tissues, not surprisingly, there is now considerable evidence to suggest that brain perfusion is the key factor that determines whether or not neural injury occurs after severe hypoxia/asphyxia [18–20]. Conversely, it is critical to appreciate that the fetus can fully adapt to mild to moderate reductions in oxygen tension without injury, from normal values of greater than 20 mmHg down to 10–12 mmHg [21]. Thus, in general, hypotension during a severe hypoxic challenge is a central requirement to reliably induce asphyxial neural injury.

Compression of the umbilical cord due to knots or entanglements of the cord or prolapse after rupture of the amniotic

membranes in labor are known potential causes of fetal asphyxia. Further, if amniotic fluid is reduced, e.g., in the growth retarded fetus, or lost after rupture of the amniotic membranes in an early stage of labor, or even worse, if the cord becomes trapped in the birth canal, physiologic uterine contractions can compress the umbilical cord between the fetus and uterine wall, giving rise to fetal hypoxemia, anaerobic glycolysis, and acidemia, with repeated or fixed deceleration of the fetal heart rate [22]. In view of these considerations, the present review focuses on induction of severe asphyxia using umbilical cord occlusion in preterm fetal sheep.

1.2 Choice of Experimental Species: Why Use the Sheep?

The species that is chosen for experimental studies must be appropriate to the scientific question. Rodent models are relatively cheap, and have an extensive repertoire of behavioral tests and molecular probes. However, such lissencephalic small animal species, with relatively small white matter tracts, are very unsatisfactory for studies of white matter injury and subsequent impaired cortical development. The absence of a gyral structure distorts the distribution of injury and makes it impossible to assess effects on cortical complexity. In contrast, the gyrencephalic structure of the fetal sheep brain, with large white matter volumes, is highly advantageous for studies of intracerebral white matter injury. No other experimental paradigms have so clearly mimicked the common pathological finding of diffuse white matter injury, with subcortical neural damage, as well as the model of asphyxia in the preterm fetal sheep [23, 24]. Equally important, the larger size of the fetal sheep enables intensive physiological, cerebrovascular and electrophysiological monitoring, which are not possible in newborn rodents. The relatively large size of the sheep fetus enables extensive implantation of instrumentation to allow continuous measurement of fetal heart rate, blood pressure (arterial and venous) [25], behavior (body movements) [26], blood flow to the brain and periphery and brain metabolism [27], intracerebral oxygenation as measured by near infrared spectroscopy [24], sympathetic activity, temperature [23, 28], and more. Catheters in the ewe and fetus also allow access for blood sampling, treatments and euthanasia. This comprehensive approach permits a significant physiological assessment of multiple organ systems in utero in a stable environment, without the confounding effects of anesthesia, ventilation, and changes in temperature.

2 Materials

2.1 Experimental Population and Procedures

Many potentially suitable breeds of sheep are available, although there is little information on whether this affects responses to asphyxia. For reference, our studies are currently conducted using pregnant Romney ewes, time-mated with Suffolk rams at

approximately 3–4 years of age. This breed has a typical gestational period of 145–147 days.

Sheep are highly precocial. Neural development of the fetal sheep at 0.8–0.85 of gestation is broadly similar to the full-term human infant [29, 30], while the 0.7 gestation fetus is broadly equivalent to the late preterm infant at 30–34 weeks, before the onset of cortical myelination, and at 0.6 gestation the sheep fetus is similar to the 26–28 week gestation human infant.

Experimentation should be begun 3–5 days after surgical instrumentation to allow fetal stress responses to resolve and for normal behavior to return. Ideally, all physiological data should be recorded continuously from 24 h or more before study and continued until the end of the study. Even if this is not possible, it is absolutely essential to display continuous ECG and blood pressure measurements during and immediately after umbilical cord occlusion to assess the onset and rate of fall of fetal blood pressure and to detect cardiac arrhythmias.

2.2 Experimental Procedures

2.2.1 Complete Occlusion of the Umbilical Cord

Complete compression of the umbilical cord is performed by inflating the occluder with a volume known to completely occlude the umbilical cord. This may be verified in pilot experiments with a Transonic flow probe placed around an umbilical vein [31]. Pragmatically, successful complete occlusion can be routinely confirmed by rapid onset of fetal bradycardia and arterial hypertension, within the first minute. Blood composition measurements are taken at standard time points to assess fetal condition. Upon completion of the occlusion protocol the occluder is deflated. It is unknown whether rapid deflation of the occluder has any material effect on fetal recovery compared for example with controlled deflation over 10 s.

The total duration of occlusion required to induce hypotension and neural injury is a function of maturity, and may need to be fine-tuned in different settings or with different breeds of sheep. For reference, in our studies we found that the optimal durations of near-terminal single periods of complete occlusion were as follows: 30 min at 0.6 gestation [26, 31], 25 min at 0.7 gestation [27, 32, 33], and 15 min at 0.85 gestation [34–36].

2.2.2 Phases of Fetal Adaptation to Umbilical Cord Occlusion

As shown in Fig. 1, distinct phases of fetal adaptation may be clearly distinguished. There is an initial vagally mediated bradycardia, and an increase in mean arterial blood pressure, associated with intense peripheral vasoconstriction (the “compensation” phase). At this time carotid blood flow is maintained at around baseline values by vasoconstriction (Fig. 2), in contrast with an increase cerebral blood flow during moderate hypoxia [21]. During this phase EEG activity is profoundly suppressed [25, 31, 37], reducing metabolic demand. Microsphere studies in term fetal sheep have shown that although total brain flow does not change in this initial phase,

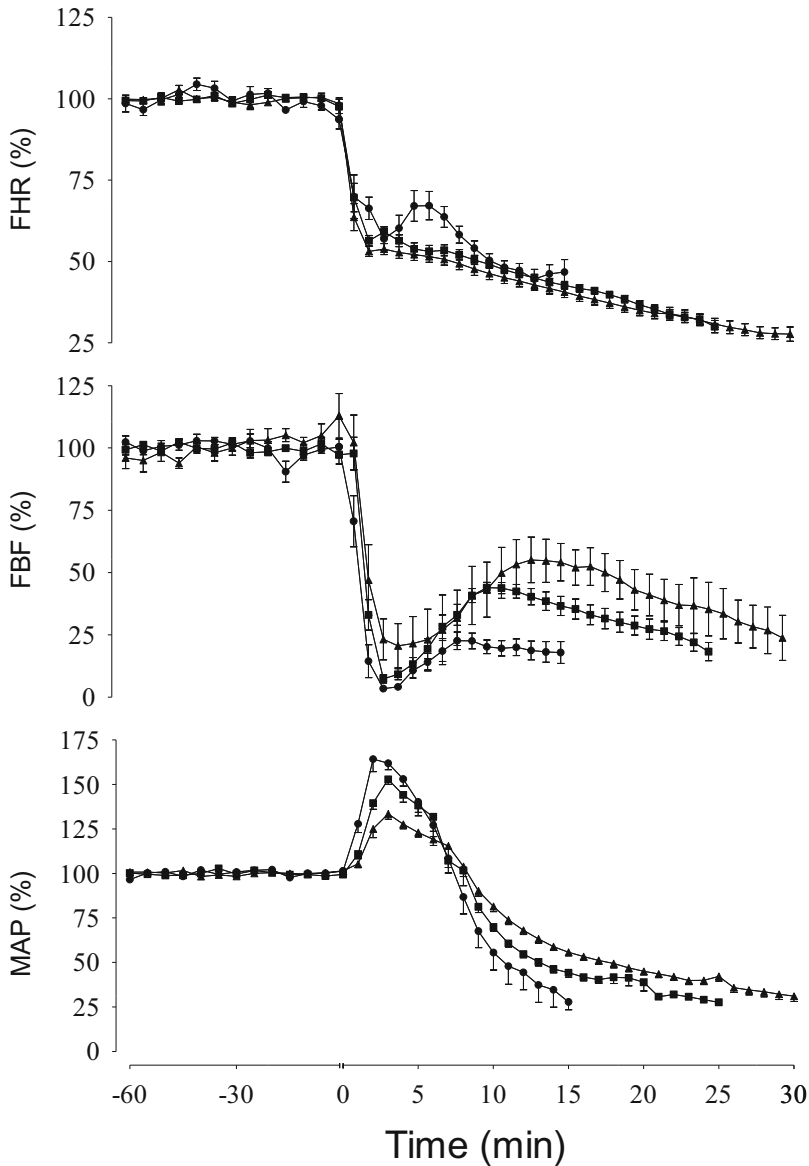


Fig. 1 Cardiovascular responses to prolonged umbilical cord occlusion in fetal sheep at 0.6, 0.7, or 0.85 gestation. Fetal heart rate (FHR, bpm, *top panel*), femoral blood flow (FBF, ml/min, *second panel*) and mean arterial pressure (MAP, mmHg, *bottom panel*) data represent 5 min averages before asphyxia, and 1 min averages during asphyxia and are expressed as percentages of baseline. The period of umbilical cord occlusion for each group starts at time zero; recovery data are not shown. Data are mean \pm SE. Data modified from Wassink et al. [25]

fetal blood flow is redistributed within the brain, away from the cerebrum and choroid plexus, towards the brain stem [38].

As asphyxia continues these compensatory responses are attenuated (Figs. 1 and 2). There is a progressive fall in heart rate as

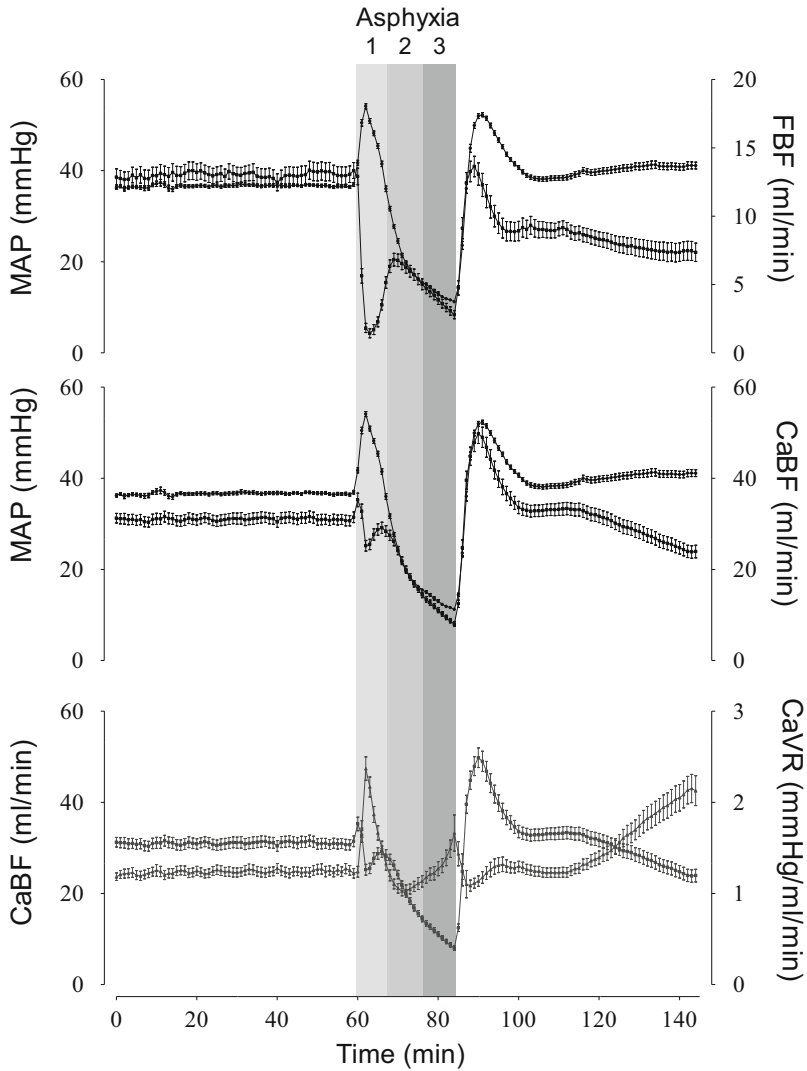


Fig. 2 Data before, during and after 15 min of complete umbilical cord occlusion in 0.7 gestation fetal sheep. 1 min averages \pm SEM. The *top panel* shows time sequence changes in mean arterial blood pressure (MAP (filled circle, left axis)) and femoral blood flow (FBF (filled square, right axis)), the *middle panel* shows MAP (filled circle, left axis) and carotid blood flow (CaBF (filled square, right axis)) and the *bottom panel* shows carotid blood flow (filled square, left axis) and carotid vascular resistance (CaVR (filled triangle, right axis)). The asphyxial period is broken into three phases: compensation (1), the start of decompensation (2), with pressure passive blood flow, and the final stages of decompensation (3), where the fall in blood pressure is slowed by increased central and peripheral vascular resistance, which in turn leads to further compromised brain and peripheral organ perfusion

cardiac function becomes impaired secondary to hypoxia, acidosis, depletion of myocardial glycogen, and cardiomyocyte injury (Fig. 1) [39]. Peripheral vasoconstriction, which had functioned to maintain blood pressure in the face of the profound

bradycardia, is lost with partial or near complete vasodilatation occurring depending on the vascular bed in question (Figs. 1 and 2) [25, 40]. Recent telemetry studies of renal sympathetic nerve activity show that failure to maintain vascular resistance is at least in part related to a failure to maintain neural control of peripheral vascular tone [41].

Once MAP falls below baseline in a so-called “decompensation” phase [22, 25, 40], cerebral perfusion falls in parallel, consistent with the known relatively narrow low range of autoregulation of cerebral blood flow in the fetus (Fig. 2) [42]. This loss of autoregulation has been proposed to be a key factor mediating injury, particularly in preterm infants [40]. However, experimental data show that loss of peripheral vascular resistance is not complete. As Fig. 2 shows, in preterm fetal sheep, peripheral vasoconstriction begins to be attenuated around 4–5 min of asphyxia, in association with a progressive fall in arterial blood pressure. Cerebral perfusion falls below baseline values from around 7–8 min, and there is partial restoration of peripheral perfusion that is greatest at 12 min (Fig. 2). However, the precipitous fall in blood pressure is attenuated through by stabilisation of the cerebral and peripheral vascular resistance at baseline values from around 12 min. The effect of this shown by slowing of the fall in blood pressure after about 15 min, such that perfusion no longer mirrors the fall in pressure.

The observation that the preterm fetus is able to partially maintain vascular resistance throughout prolonged complete umbilical cord occlusion [25], argues that total loss of autoregulation control is not required for injury. Further research is required to define the role of autoregulation in the processes mediating injury. The redistribution of blood flow to the brainstem is likely progressively lost, although this has not been extensively quantified for the term or preterm fetus. Given that the preterm fetus can survive asphyxia for longer and is thus exposed to a greater period of hypoperfusion, this likely underpins injury to brainstem regions [26, 43].

2.2.3 Prolonged Partial Umbilical Cord Occlusion

Prolonged periods of partial asphyxia in utero can be produced by partial compression of the umbilical cord. Partial cord compression for 90 min induced severe asphyxial insults in near-term fetal sheep [44], similar in nature to those following uterine hypoperfusion [45] except for some relatively minor haemodynamic differences, followed by delayed development of seizures. Although this approach might seem to be less controllable than occlusion of the uterine blood supply, in practice it is easy to vary the degree of occlusion, and umbilical venous flow can be measured directly with an ultrasonic flow probe. Both methods produce similar levels of asphyxia and evidence of encephalopathy with typically relatively variable neural injury [44, 46].

3 Technical Notes

Umbilical cord occlusion is a very simple experimental technique. The most common experimental problem is failure to recovery after release of occlusion. In term fetuses, moderate insults, such as 10 min of complete umbilical cord occlusion in the near-term fetal sheep, are associated with little risk of mortality in healthy fetuses, who then go on to develop selective neuronal loss [37, 47]. In contrast, more prolonged, complete occlusion is intrinsically associated with the development of severe hypotension [25, 35, 36, 48].

Successful recovery from complete occlusion is confirmed by a rapid, overshoot increase of FHR and MAP. If bradycardia persists for more than 30 s or blood pressure does not increase to over 50 % of baseline in the first 60 s after release of occlusion then a dose of epinephrine (0.1 ml/kg estimated weight, 1:10,000 epinephrine) should be given to the fetus via the brachial vein by slow i.v. push. Even before this stage, fetal cardiovascular status can sometimes be stimulated using a non-pharmaceutical method of making the ewe move abruptly, by nudging or generally touching her flank or back for example. This can have the effect of promoting a changing fetal position and rapidly improving fetal perfusion. More often than not, this facilitates resuscitation such that epinephrine may not be required.

Fetal death may be associated either with asystole or with more rapid onset of hypotension as previously described [26, 49]. Fortunately, because hypotension develops progressively, it is possible to identify warning signs such as more rapid fall in blood pressure, or marked blood pressure or heart rate instability before it becomes terminal by continuously monitoring fetal arterial blood pressure. If the goal of the study is to test post-insult treatment it may be reasonable to stop occlusion a little earlier (1–2 min) in such cases to avoid cardiac death, provided that the experimenters use consistent criteria and robustly randomize all fetuses between groups before occlusion.

Examples of such criteria are the level to which blood pressure falls beyond which the fetus is seldom able to reestablish perfusion. In the preterm, 0.7 gestation fetus, for example, our experience suggests it is appropriate to stop occlusion when mean arterial blood pressure falls from baseline values of 35–40 mmHg down to a cut-off level of 8 mmHg or below. Equally, occlusion should stop if there is fetal asystole or arrhythmia. Even before this point, we observed that fetuses that reached mean arterial blood pressure below 15 mmHg by 15 min of occlusion reached the terminal cut-off blood pressure before 25 min, thus giving the experimenter early warning of impending problems [49].

4 Determinants of Outcome

4.1 Sensitisation and Tolerance to Injury

It is widely speculated that adverse conditions such as preexisting hypoxia and infection may impair the ability of the fetus to mount an effective defense response to hypoxia and render neurons and glia more sensitive to hypoxia [50]. The most common metabolic disturbance to the fetus is intrauterine growth retardation (IUGR) associated with placental dysfunction. Indeed, mild maternal undernutrition that does not alter fetal growth may still affect development of the fetal hypothalamic–pituitary–adrenal function, with reduced pituitary and adrenal responsiveness to moderate hypoxia [51]. Clinically, overt IUGR is usually associated with a greater risk of brain injury, albeit the risks have fallen over time [10]. Consistent with this observation, chronically hypoxic fetuses from multiple pregnancies developed much more severe, progressive metabolic acidosis than previously normoxic fetuses during brief (1 min) umbilical cord occlusions repeated every 5 min (pH 7.07 ± 0.14 vs. 7.34 ± 0.07) and hypotension (a nadir of 24 ± 2 mmHg vs. 45.5 ± 3 mmHg after 4 h of repeated occlusion) [52]. Fetuses with preexisting hypoxia were smaller on average, and had lower blood glucose values and higher PaCO₂ values. Similarly, in normally grown fetuses, 5 days of induced chronic hypoxemia was associated with increased striatal damage after acute exposure to repeated umbilical cord occlusion for 5 min every 30 min for a total of four occlusions [53]. Together, these data support the clinical concept that fetuses with chronic placental insufficiency are vulnerable even to relatively infrequent periods of brief asphyxia in early labor. However, under some circumstances at least, this appears not to be the case. In spontaneously hypoxic fetuses, we have observed, for example, that the initial chemoreflex response to asphyxia induced by umbilical cord occlusion is enhanced [48].

Exposure to the endotoxin lipopolysaccharide (LPS) can cause neural injury [54–56]. We have recently shown, rather intriguingly, that exposure to asphyxia after 4 days of chronic LPS exposure actually reduced white matter injury in the preterm fetal sheep [56]. However, timing between insults is important. Studies in newborn rats have shown a single injection of LPS (which does not normally cause injury) given within 6 h or more than 72 h before an hypoxic-ischemic insult (carotid artery ligation plus hypoxia) increases neural injury [57, 58]. In contrast, injection of LPS at intermediate times such as 24 h before hypoxia-ischemia reduced subsequent neural injury, i.e., preconditioned the brain [58]. The critical effect of timing suggests that LPS exposure protection requires transcriptional changes. For example, a recent study suggests that the transcription factor nuclear factor E2-related factor 2, and the transcription cofactor, peroxisome proliferator-activated

receptor- γ coactivator 1 α play a key role in mediating LPS induced neuroprotection in the neonatal rat [59].

4.2 Brain Maturity

Maturation of the brain and body have dramatic and underappreciated effects on cardiac and neural sensitivity to asphyxia [25, 26, 60]. Boyle's experiments with Hooke and others in the seventeenth century, elegantly demonstrated that younger animals have much greater tolerance to hypoxia [61]. Extensive work by perinatal scientists such as Dawes, Mott, and Heather in the 1950s and 1960s demonstrated that anaerobic capacity during fetal life underpinned greater fetal tolerance to hypoxia. We and others have shown that the younger the fetus, the greater the tolerance to hypoxia [62]. For example, the premature sheep fetus at 90 days gestation (term is 147 days), prior to the onset of cortical myelination, can tolerate extended periods of up to 20 min of umbilical cord occlusion without neuronal loss [26, 31, 60]. As Fig. 1 demonstrates, the initial adaptation to severe hypoxia, is consistent at all ages, but the critical difference is that the preterm fetus can keep its heart going for longer and thus, the younger the fetus, the longer the survival time.

This is consistent with the observation by Shelley that cardiac glycogen peaks during preterm-equivalent life in a wide variety of mammalian species [63]. In the fetal sheep for example, at 0.6 gestation the majority of fetuses survived up to 30 min of complete umbilical cord occlusion and did not require resuscitation with epinephrine and did not develop cardiac injury at 3 days post-insult [31]. In contrast, near-term fetuses can tolerate 10–12 min, typically without requiring resuscitation [64]. A near-terminal insult is around 15–18 min, with most fetuses requiring resuscitation, and showing subsequent severe cardiac dysfunction [25, 35, 39, 65, 66].

Critically, as a consequence of this extended survival during severe asphyxia, the premature fetus is exposed to extremely prolonged and profound hypotension and hypoperfusion. At 0.6 gestation, for example, no injury occurs after 20 min of complete umbilical cord occlusion even though hypotension is already present (Fig. 1) [26, 60], but severe subcortical injury occurs if the occlusion is continued for 30 min [26]. Speculatively, there may be failure of redistribution of blood flow within the fetal brain during the phase of severe hypotension, which places previously protected areas of the brain such as the brainstem at risk of injury [67].

4.2.1 The Effect of Fetal sex

Numerous studies have confirmed that there is an increased risk of perinatal mortality and morbidity in boys compared to girls at all stages of gestation [68]. The mechanisms mediating the influence of gender on perinatal death and disability are poorly understood and likely to be multifactorial. There is increasing evidence in the developing brain that estradiol may play a neuroprotective role [69]. There is evidence of sex-related differences in the pathways

leading to apoptosis [70], and in cell sensitivity to excitotoxins [70, 71]. Recent data in human infants shows sex-related differences in the CSF levels of IL-8 and antioxidants after asphyxia, with higher levels in newborn females that may contribute to the greater vulnerability to brain injury in males than females [72].

There are also data that male fetuses may be less able to adapt to hypoxic stress. Male fetuses have higher rates of abnormal fetal heart rate recordings, metabolic acidosis, and need for operative intervention or resuscitation in labor [73–77]. Male fetuses are on average bigger, grow faster, and have a higher metabolic rate than females [78, 79], suggesting that when oxygen is limited they might deplete available resources more rapidly. Further, there is evidence that males have relatively delayed maturation of some aspects of autonomic nervous system function, such as for example, adrenal medullary and lung beta-receptor maturation in fetal rabbits [80]. Clinically, after exposure to asphyxia at birth preterm boys are reported to have lower plasma catecholamine levels than girls [81]. Moreover, data from pregnancies complicated by placental insufficiency before 34 weeks, showed that cardiac troponin levels are significantly greater in male than female fetuses [82].

The sex of the fetus per se did not significantly alter the cardiovascular responses of healthy singleton preterm (0.7 gestation) fetal sheep to an acute, profound asphyxial insult [49]. Neither the average responses, nor the incidence or timing of failure to complete the full period of umbilical cord occlusion were significantly different between the sexes. However, overall, significantly more male fetuses developed profound hypotension (<8 mmHg) before the end of the occlusion period. Further, blood pressure at 15 min correlated with fetal weight for male fetuses, but not female fetuses suggesting a role for metabolic reserve in facilitating this capacity [49]. These data further support the idea that metabolic substrate availability has a greater impact on male fetuses.

The causes of failure to complete the full target duration of occlusions differed markedly between male and female sheep fetuses. These differences were associated in turn with changes that suggest altered chemoreflex and cardiac responses between the genders. The short-occlusion-males demonstrated slower and reduced initial peripheral vasoconstriction compared with the full-occlusion fetuses. This was followed by earlier and significantly greater hypotension, associated with greater falls in heart rate and carotid and femoral blood flow. In contrast, short-occlusion-females showed a markedly more rapid onset of initial vasoconstriction of the femoral bed, and subsequent falls in blood pressure and heart rate that were intermediate between the full-occlusion fetuses and short-occlusion-males. It is improbable that these differences relate to placental function, since fetal body weight (measured 3 days after occlusion) and pH, blood gas, glucose and lactate values before occlusion were not different between the groups.

5 Final Conclusions

The experimental models outlined in this chapter will continue to be developed and refined, aiming to mimic human pathophysiology as closely as possible at the whole body level, while allowing the factors contributing to the wide variability in outcomes observed after perinatal asphyxia to be dissected. Both systemic and cerebral factors are important in real life, and include respectively the determinants of cardiovascular decompensation and factors that modulate the intrinsic vulnerability of the brain, such as environmental temperature, metabolic status and expression of neurotrophic factors. In turn, these factors are highly likely to affect responses to treatment. As the critical events which precipitate significant perinatal hypoxic-ischaemic encephalopathy are better understood, our ability to identify and intervene in clinical asphyxia will also improve.

Acknowledgments

The authors' work reported in this review has been supported by the Health Research Council of New Zealand, Lottery Health Board of New Zealand, the Auckland Medical Research Foundation, the National Institutes of Health, and the March of Dimes Birth Defects Trust.

References

1. Committee on Understanding Premature Birth and Assuring Healthy Outcomes. Preterm birth: causes, consequences, and prevention. In: Behrman RE, Butler AS (eds). Washington DC: Institute of Medicine of the National Academies, 2007. http://books.nap.edu/openbook.php?record_id=11622&page=1. Accessed on 1 March 2013
2. Mullen KM, Vohr BR, Katz KH et al (2011) Preterm birth results in alterations in neural connectivity at age 16 years. *Neuroimage* 54:2563–2570
3. Marlow N, Hennessy EM, Bracewell MA et al (2007) Motor and executive function at 6 years of age after extremely preterm birth. *Pediatrics* 120:793–804
4. Rogers CE, Anderson PJ, Thompson DK et al (2012) Regional cerebral development at term relates to school-age social-emotional development in very preterm children. *J Am Acad Child Adolesc Psychiatry* 51:181–191
5. de Vries LS, Eken P, Groenendaal F et al (1998) Antenatal onset of haemorrhagic and/or ischaemic lesions in preterm infants: prevalence and associated obstetric variables. *Arch Dis Child Fetal Neonatal* Ed 78: F51–F56
6. Bell JE, Becher JC, Wyatt B et al (2005) Brain damage and axonal injury in a Scottish cohort of neonatal deaths. *Brain* 128:1070–1081
7. Kubota T, Okumura A, Hayakawa F et al (2002) Combination of neonatal electroencephalography and ultrasonography: sensitive means of early diagnosis of periventricular leukomalacia. *Brain Dev* 24:698–702
8. Perlman JM (1998) White matter injury in the preterm infant: an important determination of abnormal neurodevelopment outcome. *Early Hum Dev* 53:99–120
9. Gunn AJ, Gunn TR (1997) Changes in risk factors for hypoxic-ischaemic seizures in term infants. *Aust N Z J Obstet Gynaecol* 37:36–39
10. Westgate JA, Gunn AJ, Gunn TR (1999) Antecedents of neonatal encephalopathy with fetal acidemia at term. *Br J Obstet Gynaecol* 106:774–782

11. Wyatt JS, Gluckman PD, Liu PY et al (2007) Determinants of outcomes after head cooling for neonatal encephalopathy. *Pediatrics* 119: 912–921
12. MacLennan A, The International Cerebral Palsy Task Force, Gunn AJ et al (1999) A template for defining a causal relation between acute intrapartum events and cerebral palsy: international consensus statement. *BMJ* 319:1054–1059
13. Edwards AD, Brocklehurst P, Gunn AJ et al (2010) Neurological outcomes at 18 months of age after moderate hypothermia for perinatal hypoxic ischaemic encephalopathy: synthesis and meta-analysis of trial data. *BMJ* 340: c363
14. Gunn AJ, Bennet L (2008) Brain cooling for preterm infants. *Clin Perinatol* 35:735–748
15. Robertson NJ, Tan S, Groenendaal F et al (2012) Which neuroprotective agents are ready for bench to bedside translation in the newborn infant? *J Pediatr* 160:544–552.e544
16. Wassink G, Gunn ER, Drury PP et al (2014) The mechanisms and treatment of asphyxial encephalopathy. *Front Neurosci* 8:40
17. Dijkhuizen RM, Beekwilder JP, van der Worp HB et al (1999) Correlation between tissue depolarizations and damage in focal ischemic rat brain. *Brain Res* 840:194–205
18. Gunn AJ, Parer JT, Mallard EC et al (1992) Cerebral histologic and electrocorticographic changes after asphyxia in fetal sheep. *Pediatr Res* 31:486–491
19. Mallard EC, Williams CE, Johnston BM et al (1994) Increased vulnerability to neuronal damage after umbilical cord occlusion in fetal sheep with advancing gestation. *Am J Obstet Gynecol* 170:206–214
20. Fujii EY, Takahashi N, Kodama Y et al (2003) Hemodynamic changes during complete umbilical cord occlusion in fetal sheep related to hippocampal neuronal damage. *Am J Obstet Gynecol* 188:413–418
21. Giussani DA, Spencer JAD, Hanson MA (1994) Fetal and cardiovascular reflex responses to hypoxaemia. *Fetal Matern Med Rev* 6:17–37
22. Westgate JA, Wibbens B, Bennet L et al (2007) The intrapartum deceleration in center stage: a physiological approach to interpretation of fetal heart rate changes in labor. *Am J Obstet Gynecol* 197:e1–e11.236
23. Bennet L, Roelfsema V, George S et al (2007) The effect of cerebral hypothermia on white and grey matter injury induced by severe hypoxia in preterm fetal sheep. *J Physiol* 578:491–506
24. Bennet L, Roelfsema V, Pathipati P et al (2006) Relationship between evolving epileptiform activity and delayed loss of mitochondrial activity after asphyxia measured by near-infrared spectroscopy in preterm fetal sheep. *J Physiol* 572:141–154
25. Wassink G, Bennet L, Booth LC et al (2007) The ontogeny of hemodynamic responses to prolonged umbilical cord occlusion in fetal sheep. *J Appl Physiol* 103:1311–1317
26. George S, Gunn AJ, Westgate JA et al (2004) Fetal heart rate variability and brainstem injury after asphyxia in preterm fetal sheep. *Am J Physiol Regul Integr Comp Physiol* 287: R925–R933
27. Bennet L, Roelfsema V, Dean J et al (2007) Regulation of cytochrome oxidase redox state during umbilical cord occlusion in preterm fetal sheep. *Am J Physiol Regul Integr Comp Physiol* 292:R1569–R1576
28. Gunn AJ, Gunn TR, de Haan HH et al (1997) Dramatic neuronal rescue with prolonged selective head cooling after ischemia in fetal lambs. *J Clin Invest* 99:248–256
29. Barlow RM (1969) The foetal sheep: morphogenesis of the nervous system and histochemical aspects of myelination. *J Comp Neurol* 135:249–262
30. McIntosh GH, Baghurst KI, Potter BJ et al (1979) Foetal brain development in the sheep. *Neuropathol Appl Neurobiol* 5: 103–114
31. Bennet L, Rossenrode S, Gunning MI et al (1999) The cardiovascular and cerebrovascular responses of the immature fetal sheep to acute umbilical cord occlusion. *J Physiol* 517: 247–257
32. Quaedackers JS, Roelfsema V, Heineman E et al (2004) The role of the sympathetic nervous system in post-asphyxial intestinal hypoperfusion in the preterm sheep fetus. *J Physiol* 557:1033–1044
33. Quaedackers JS, Roelfsema V, Hunter CJ et al (2004) Polyuria and impaired renal blood flow after asphyxia in preterm fetal sheep. *Am J Physiol Regul Integr Comp Physiol* 286: R576–R583
34. Wibbens B, Westgate J, Bennet L, et al. The relationship between changes in the ST complex and the development of hypotension during prolonged asphyxia in the near term fetal sheep. Paper presented at Proceedings, IUPS Fetal Physiology Satellite Meeting, 2001, Auckland, New Zealand
35. Wibbens B, Westgate JA, Bennet L et al (2005) Profound hypotension and associated ECG changes during prolonged cord occlusion in

- the near term fetal sheep. *Am J Obstet Gynecol* 193:803–810
36. Drury PP, Davidson JO, van den Heuij LG et al (2014) Status epilepticus after prolonged umbilical cord occlusion is associated with greater neural injury fetal sheep at term-equivalent. *PLoS One* 9:e96530
 37. Hunter CJ, Bennet L, Power GG et al (2003) Key neuroprotective role for endogenous adenosine A1 receptor activation during asphyxia in the fetal sheep. *Stroke* 34:2240–2245
 38. Jensen A, Hohmann M, Kunzel W (1987) Dynamic changes in organ blood flow and oxygen consumption during acute asphyxia in fetal sheep. *J Dev Physiol* 9:543–559
 39. Gunn AJ, Maxwell L, de Haan HH et al (2000) Delayed hypotension and subendocardial injury after repeated umbilical cord occlusion in near-term fetal lambs. *Am J Obstet Gynecol* 183:1564–1572
 40. Bennet L, Booth LC, Drury PP et al (2012) Preterm neonatal cardiovascular instability: does understanding the fetus help evaluate the newborn? *Clin Exp Pharmacol Physiol* 39:965–972
 41. Booth LC, Malpas SC, Barrett CJ et al (2012) Renal sympathetic nerve activity during asphyxia in fetal sheep. *Am J Physiol Regul Integr Comp Physiol* 303:R30–R38
 42. Parer JT (1998) Effects of fetal asphyxia on brain cell structure and function: limits of tolerance. *Comp Biochem Physiol A Mol Integr Physiol* 119:711–716
 43. Logitharajah P, Rutherford MA, Cowan FM (2009) Hypoxic-ischemic encephalopathy in preterm infants: antecedent factors, brain imaging, and outcome. *Pediatr Res* 66:222–229
 44. Ball RH, Espinoza MI, Parer JT et al (1994) Regional blood flow in asphyxiated fetuses with seizures. *Am J Obstet Gynecol* 170:156–161
 45. Ikeda T, Murata Y, Quilligan EJ et al (1998) Fetal heart rate patterns in postasphyxiated fetal lambs with brain damage. *Am J Obstet Gynecol* 179:1329–1337
 46. Ikeda T, Murata Y, Quilligan EJ et al (1998) Physiologic and histologic changes in near-term fetal lambs exposed to asphyxia by partial umbilical cord occlusion. *Am J Obstet Gynecol* 178:24–32
 47. Mallard EC, Williams CE, Johnston BM et al (1995) Neuronal damage in the developing brain following intrauterine asphyxia. *Reprod Fertil Dev* 7:647–653
 48. Wibbens B, Bennet L, Westgate JA et al (2007) Pre-existing hypoxia is associated with a delayed but more sustained rise in T/QRS ratio during prolonged umbilical cord occlusion in near-term fetal sheep. *Am J Physiol Regul Integr Comp Physiol* 293:R1287–R1293
 49. Bennet L, Booth LC, Ahmed-Nasef N et al (2007) Male disadvantage? Fetal sex and cardiovascular responses to asphyxia in preterm fetal sheep. *Am J Physiol Regul Integr Comp Physiol* 293:R1280–R1286
 50. Gunn AJ, Bennet L (2009) Fetal hypoxia insults and patterns of brain injury: insights from animal models. *Clin Perinatol* 36:579–593
 51. Hawkins P, Steyn C, McGarrigle HH et al (2000) Effect of maternal nutrient restriction in early gestation on responses of the hypothalamic-pituitary-adrenal axis to acute isocapnic hypoxaemia in late gestation fetal sheep. *Exp Physiol* 85:85–96
 52. Westgate J, Wassink G, Bennet L et al (2005) Spontaneous hypoxia in multiple pregnancy is associated with early fetal decompensation and greater T wave elevation during brief repeated cord occlusion in near-term fetal sheep. *Am J Obstet Gynecol* 193:1526–1533
 53. Pulgar VM, Zhang J, Massmann GA et al (2007) Mild chronic hypoxia modifies the fetal sheep neural and cardiovascular responses to repeated umbilical cord occlusion. *Brain Res* 1176:18–26
 54. Dean JM, van de Looij Y, Sizonenko SV et al (2011) Delayed cortical impairment following lipopolysaccharide exposure in preterm fetal sheep. *Ann Neurol* 70:846–856
 55. Mathai S, Booth LC, Davidson JO et al (2013) Acute on chronic exposure to endotoxin in preterm fetal sheep. *Am J Physiol Regul Integr Comp Physiol* 304:R189–R197
 56. van den Heuij LG, Mathai S, Davidson JO et al (2014) Synergistic white matter protection with acute-on-chronic endotoxin and subsequent asphyxia in preterm fetal sheep. *J Neuroinflammation* 11:89
 57. Yang L, Sameshima H, Ikeda T et al (2004) Lipopolysaccharide administration enhances hypoxic-ischemic brain damage in newborn rats. *J Obstet Gynaecol Res* 30:142–147
 58. Eklind S, Mallard C, Arvidsson P et al (2005) Lipopolysaccharide induces both a primary and a secondary phase of sensitization in the developing rat brain. *Pediatr Res* 58:112–116
 59. Correa F, Ljunggren E, Patil J et al (2013) Time-dependent effects of systemic lipopolysaccharide injection on regulators of antioxidant defence Nrf2 and PGC-1alpha in the neonatal rat brain. *Neuroimmunomodulation* 20:185–193

60. Keunen H, Blanco CE, van Reempts JL et al (1997) Absence of neuronal damage after umbilical cord occlusion of 10, 15, and 20 minutes in midgestation fetal sheep. *Am J Obstet Gynecol* 176:515–520
61. Boyle R (1670) New pneumatical experiments about respiration. *Phil Trans Roy Soc Lond* 62:2011–2031
62. Gunn AJ, Quaedackers JS, Guan J et al (2001) The premature fetus: not as defenseless as we thought, but still paradoxically vulnerable? *Dev Neurosci* 23:175–179
63. Shelley HJ (1961) Glycogen reserves and their changes at birth and in anoxia. *Br Med Bull* 17:137–143
64. Mallard EC, Gunn AJ, Williams CE et al (1992) Transient umbilical cord occlusion causes hippocampal damage in the fetal sheep. *Am J Obstet Gynecol* 167:1423–1430
65. Ley D, Oskarsson G, Bellander M et al (2004) Different responses of myocardial and cerebral blood flow to cord occlusion in exteriorized fetal sheep. *Pediatr Res* 55:568–575
66. Drury PP, Booth LC, Bennet L et al (2013) Dopamine infusion for post-resuscitation blood pressure support after profound asphyxia in near-term fetal sheep. *Exp Physiol* 98:699–709
67. Barkovich AJ, Sargent SK (1995) Profound asphyxia in the premature infant: imaging findings. *AJNR Am J Neuroradiol* 16:1837–1846
68. Joseph KS, Wilkins R, Dodds L et al (2005) Customized birth weight for gestational age standards: perinatal mortality patterns are consistent with separate standards for males and females but not for blacks and whites. *BMC Pregnancy Childbirth* 5:3
69. McCarthy MM (2008) Estradiol and the developing brain. *Physiol Rev* 88:91–134
70. Renolleau S, Fau S, Charriaut-Marlangue C (2008) Gender-related differences in apoptotic pathways after neonatal cerebral ischemia. *Neuroscientist* 14:46–52
71. Johnston MV, Hagberg H (2007) Sex and the pathogenesis of cerebral palsy. *Dev Med Child Neurol* 49:74–78
72. Hussein MH, Daoud GA, Kakita H et al (2007) The sex differences of cerebrospinal fluid levels of interleukin 8 and antioxidants in asphyxiated newborns. *Shock* 28:154–159
73. Dawes NW, Dawes GS, Moulden M et al (1999) Fetal heart rate patterns in term labor vary with sex, gestational age, epidural analgesia, and fetal weight. *Am J Obstet Gynecol* 180:181–187
74. Ingemarsson I, Herbst A, Thorngren-Jerneck K (1997) Long term outcome after umbilical artery acidemia at term birth: influence of gender and duration of fetal heart rate abnormalities. *Br J Obstet Gynaecol* 104:1123–1127
75. Bekedam DJ, Engelsbel S, Mol BW et al (2002) Male predominance in fetal distress during labor. *Am J Obstet Gynecol* 187:1605–1607
76. Sheiner E, Levy A, Katz M et al (2004) Gender does matter in perinatal medicine. *Fetal Diagn Ther* 19:366–369
77. Thorngren-Jerneck K, Herbst A (2001) Low 5-minute Apgar score: a population-based register study of 1 million term births. *Obstet Gynecol* 98:65–70
78. Clarke CA, Mittwoch U (1995) Changes in the male to female ratio at different stages of life. *Br J Obstet Gynaecol* 102:677–679
79. Mittwoch U (2004) The elusive action of sex-determining genes: mitochondria to the rescue? *J Theor Biol* 228:359–365
80. Padbury JF, Hobel CJ, Lam RW et al (1981) Sex differences in lung and adrenal neurosympathetic development in rabbits. *Am J Obstet Gynecol* 141:199–204
81. Greenough A, Lagercrantz H, Pool J et al (1987) Plasma catecholamine levels in preterm infants. Effect of birth asphyxia and Apgar score. *Acta Paediatr Scand* 76:54–59
82. Nomura RM, Ortigosa C, Fiorelli LR et al (2011) Gender-specific differences in fetal cardiac troponin T in pregnancies complicated by placental insufficiency. *Gend Med* 8:202–208

Origin and Detection of Neonatal Seizures: Animal and Clinical Studies

S. Tracey Bjorkman

Abstract

Neonatal seizures remain a major clinical problem worldwide and are harmful to the developing brain. Seizures are associated with poor neurodevelopmental outcomes and significant risk of death requiring urgent diagnosis and intervention. Current antiepileptic drugs however have limited efficacy and are potentially harmful to the developing newborn brain. Despite this, standard clinical practice for the treatment of neonatal seizures remains unchanged. This chapter describes a clinically relevant neonatal animal model of HI-induced seizures.

Key words Neonatal seizures, aEEG, Hypoxia–ischemia, Brain injury, Pig

1 Background

Seizures are more common in the newborn period than at any other time in life [1]. They are among the most prominent and distinctive signs of neurological dysfunction in the human newborn and are associated with significant risk of morbidity and mortality [2]. As many as 5 per 1000 term newborns are at risk of seizures, however the true incidence is likely to be higher with preterm infants at an even greater risk [3]. Hypoxic–ischemic encephalopathy (HIE) is the most frequent underlying reason for seizures during the neonatal period (>50 %); however, seizures may result from a number of other causes including stroke, intracranial hemorrhage, congenital malformations, infection, metabolic disturbances, and genetic disorders [2, 4–6]. Neonatal seizures are strong predictors of long-term cognitive and neurodevelopmental impairment. Outcomes following neonatal seizures are often poor, resulting in permanent impairments to learning, memory, and cognition in up to 47 % of survivors, and an increased risk of post-neonatal epilepsy, cerebral palsy, and death [7].

In animal models, there is growing evidence that recurrent seizures are harmful to the developing brain [8]. In neonatal rats,

kainic acid-induced seizures following hypoxia–ischemia (HI) injury result in significantly greater brain injury than in rat pups with HI injury alone [9]. In our piglet model of HI described in this chapter, we have shown that the presence of seizures following HI is associated with increased brain injury as detected *in vivo* by magnetic resonance imaging (MRI) and magnetic resonance spectroscopy (MRS) and, at post-mortem by a greater degree of neuropathological injury [10]. In human newborns, several studies have reported a significant and independent association of seizures with brain injury and adverse neurodevelopmental outcomes [11, 12]. Even in the absence of underlying brain injury, seizures have been shown to perturb brain architecture and function [13].

Detection of neonatal seizures has traditionally relied on clinical signs although more than 80 % of neonatal seizures are sub-clinical (no clinical manifestations) and cannot be detected without the aid of electroencephalographic (EEG) monitoring [14, 15]. Conventional full-channel EEG with video is the gold standard for detecting and diagnosing seizures although this is not always routinely available. The advent of amplitude-integrated EEG (aEEG), while using fewer channels and time-compression of the EEG signal, has made continuous bedside EEG monitoring more accessible and aided in detection and diagnosis of neonatal seizures [16]. An example of the types of background aEEG patterns and seizures observed in the term newborn pig is illustrated in Figs. 1 and 2, respectively.

Elucidating the mechanisms of seizure susceptibility and investigating novel therapeutic strategies in the developing brain however remains a challenge. Although a number of neonatal seizure models exist mainly in rodents, many of these genetically, chemically, or electrically induce seizures [8, 9, 17, 18]. The advantages of such models are numerous and while some of them do result in spontaneous seizures a major disadvantage of these models is the lack of clinical relevance especially to the neonate. In most of these models seizures are induced in an otherwise normal healthy brain with little evidence of neuronal cell loss, in the human neonate seizures are usually associated with significant underlying brain pathology [19]. As well as considering underlying brain injury, normal age-specific developmental brain changes will impact seizure generation and evolution [1]. Seizures may also alter the way in which antiepileptic drugs work in the brain. It has been suggested that the lack of efficacy of current antiepileptic drug treatments for neonatal seizures may be the result of seizure-induced alterations of brain receptors; there is also evidence that AEDs harm the developing brain [2, 20].

While there are several models of HI-induced neonatal seizures in rodents that utilize both hypoxia alone and hypoxia with carotid ligation, there are some distinct advantages of using a larger pre-clinical animal model such as the pig [21–23]. Firstly, the pig is

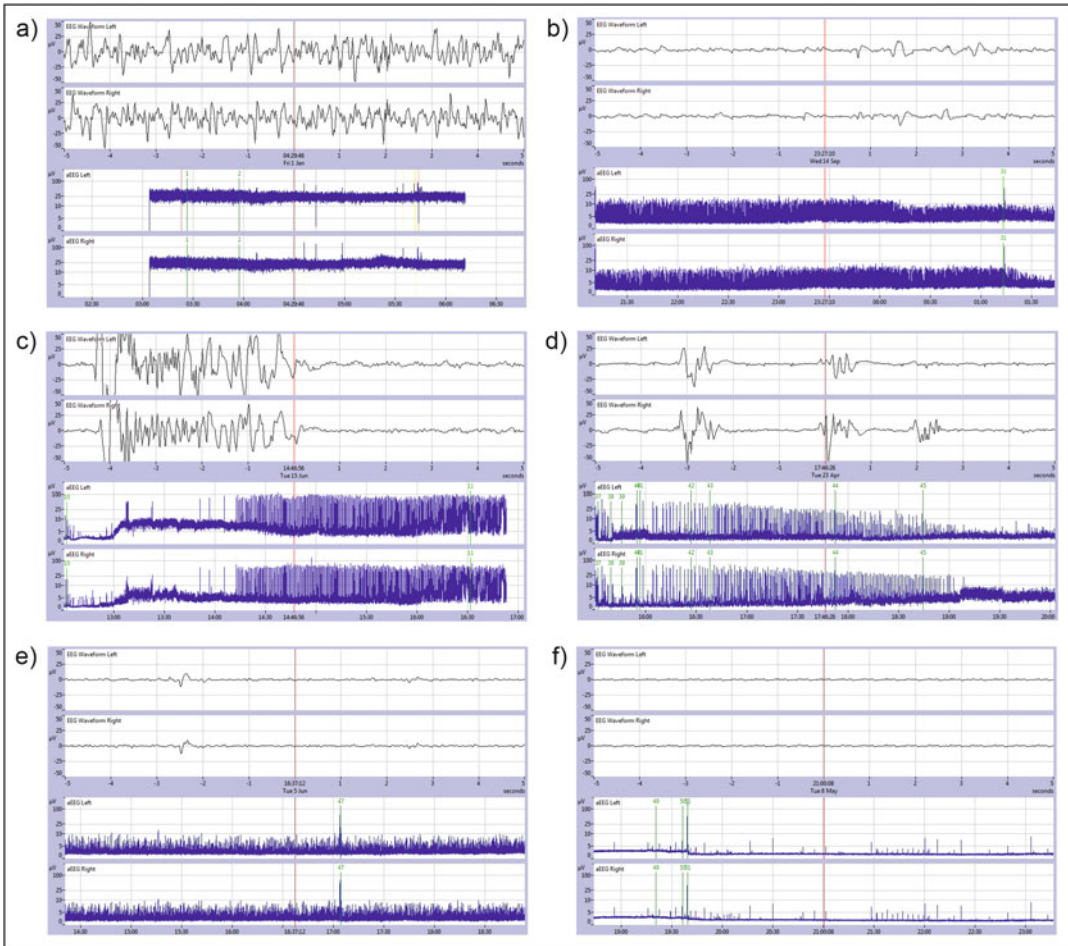


Fig. 1 Classification of background aEEG patterns, example traces from newborn pigs. **(a)** Continuous normal voltage (CNV); minimum amplitude (*lower margin*) of 7–10 μV and maximum amplitude (*upper margin*) of 10–25 μV . **(b)** Discontinuous normal voltage (DNV) has a variable minimum amplitude but $<5 \mu\text{V}$ and maximum amplitude $>10 \mu\text{V}$; minimum amplitude $<5 \mu\text{V}$ and maximum amplitude $>10 \mu\text{V}$. Burst suppression (BS) is characterized by a discontinuous background with minimum amplitude of 0–1 μV and bursts with amplitudes $>25 \mu\text{V}$. **(c)** BS with ≥ 100 bursts per hour. **(d)** BS ≤ 100 bursts per hour. **(e)** Continuous low voltage (CLV)—continuous background pattern but with very low voltage $\leq 5 \mu\text{V}$. **(f)** Flat trace (FT); a predominantly inactive (isoelectric) trace $<5 \mu\text{V}$

comparable to the human neonate in size, brain development, and maturation allowing for easy and continuous measurement of numerous physiological parameters including EEG; obtaining continuous measurements from immature rodents such as arterial blood gases (ABGs) to monitor pH, pO_2 , and pCO_2 for example is impossible and can only be achieved by terminal collections at specific time-points thus requiring large groups of animals [24]. Where required, the ability to continuously monitor our animals enables us to titrate the HI insult according to the animal's response to hypoxia, ensuring that we achieve a moderate to severe

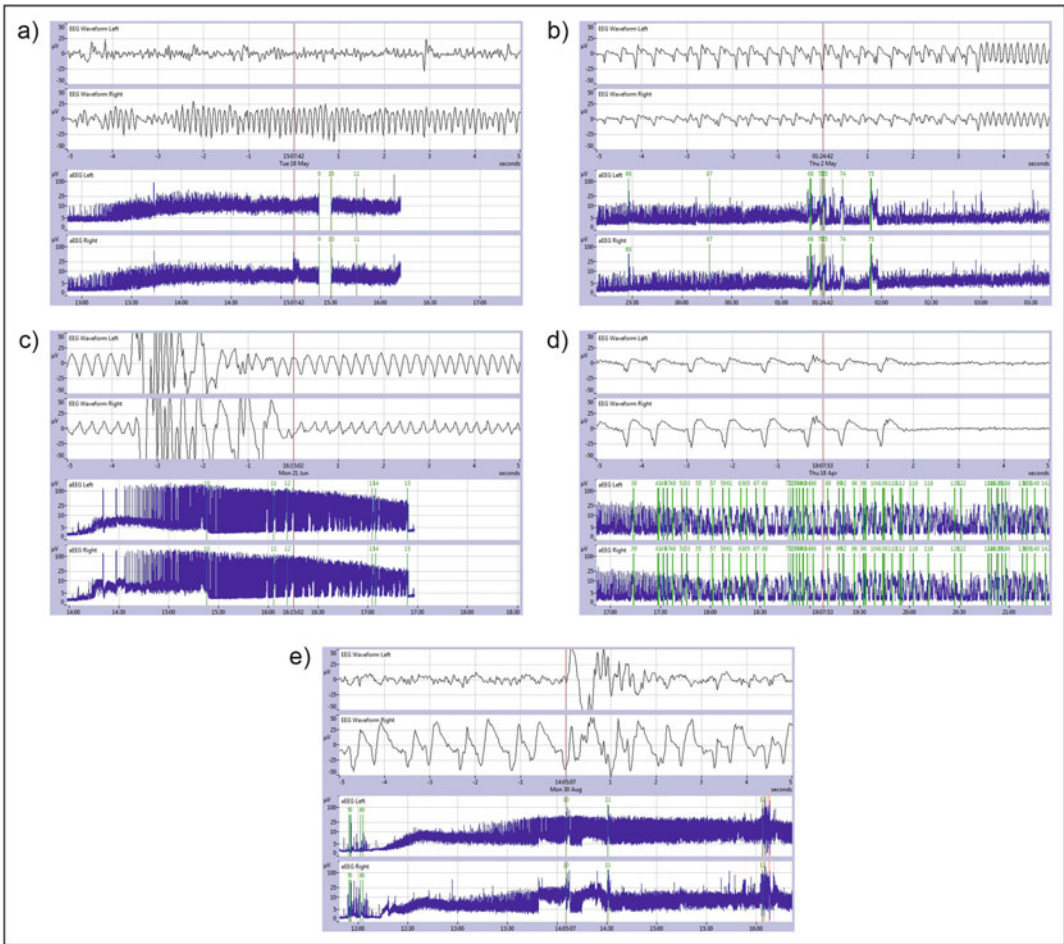


Fig. 2 Classification of seizure activity, example traces from newborn pigs. On the aEEG, seizures present as a significant rise from baseline of both the minimum and maximum amplitude. The raw trace should show simultaneous seizure activity identified as repetitive, rhythmic waveforms with a distinct beginning and end >10 s duration and with a gradual build-up in both amplitude and frequency of spike-wave discharges. **(a)** Single seizure (SS); one seizure within a 30 min period. Repetitive seizures (RS) are defined as more than one seizure within a 30 min period. **(b)** Repetitive seizures on continuous low voltage background. **(c)** Repetitive seizures on a burst suppression background. **(d)** Status epilepticus (SE) ongoing seizure activity of >30 min. **(e)** Piglet movement—not seizure. The aEEG pattern resembles seizure activity with the rise in minimum and maximum amplitude; however, inspection of the raw trace does not reveal the tell-tale repetitive rhythmic waveform pattern. This animal started to shake due to recovery from anesthesia

survivable brain injury. Secondly, our model is a global hypoxic–ischemic insult and does not require invasive interventions such as ligation of carotid vessels. A key aspect of our model is the loss of blood pressure (hypotension) which more likely resembles the ischemia that occurs in the human neonate; carotid ligation results in a total loss of blood flow. In the hypoxia alone model while these animals do develop seizures, end insult physiological parameters do

not mimic those of the human HIE neonates [22]. Although very low % concentrations of O₂ were used, pH, pO₂, and pCO₂ values do not reflect those observed in the human HIE neonate, where acidosis is a significant criteria for determining a HI event. Furthermore, this rodent model does not result in any abnormal brain pathology. Thirdly, seizures arise spontaneously following neonatal HI and do not require chemical or electrical induction. Although latency to seizure onset (typically around 12 h after the insult) can make for arduous experiments, this most closely mimics the human clinical situation; in the human HIE newborn seizures typically arise around 12–24 h after birth [25]. Fourth, the neurological deficits and neuropathology are similar to those that occur in the human HIE neonate [10].

2 Equipment, Materials, and Setup

The experiments detailed here ideally require a dedicated, and if possible permanent, theatre space and recovery area as animals are undergoing intensive care procedures and continuous monitoring.

2.1 Equipment

- Open cot or table with mattress.
- Servo-controlled heater (overhead or blanket).
- Neonatal ventilator—humidifier and ventilation circuits.
- Patient monitoring system (Marquette, GE Healthcare).
- Cerebral function monitor (CFM) with synchronized video.
- Arterial blood gas analyzer (Radiometer).
- Syringe pumps.
- Laptop for data collection.
- Quiet recovery room.

2.2 Drugs and Fluids

- Propofol.
- Alfentanil.
- Dopamine.
- Adrenaline.
- Antibiotics (Gentamicin, Cephalothin).
- Isotonic saline (0.9 % NaCl).
- 10 % Glucose.
- Phenobarbital.
- Midazolam.
- Heparin ampoules (1000 IU/ml).
- Heparin saline ampoules (50 IU/5 ml).

- Sterile water for injection (10 ml amps).
- 1–2% Isoflurane.
- Zoletil.
- Xylocaine Gel.

2.3 Consumables and Other Equipment

- Syringes (1–50 ml).
- Arterial blood gas (ABG) syringes.
- 24G cannulas.
- Short and long extension lines.
- Three way taps.
- Scalpels (#11 and #22).
- Chromic gut sutures (3.0).
- Rectal probes.
- Swabs.
- Umbilical artery catheters (UAC—single lumen 3.5FG).
- Sterile surgical kit (scalpel handle, 2× fine forceps, 2× curved clamps, scissors, small sterile dish, drape).
- EEG electrodes (needle).
- Micropore tape (thick and thin).
- Brown tape (thick and thin).
- Disposable waterproof mattress cover (Blueys).
- Nasogastric feed tubes (8FG).
- Nitrogen cylinder (100 % D size).
- Endotracheal (ET) tube (3.5).
- Laryngoscope and introducer.
- Facemask and Goldman vaporizer.
- Suction tubing.
- Needles.
- BP transducer.
- ECG leads.
- Permanent marker.

3 Procedures

On the day of the experiment and prior to initiating anesthesia, ensure that all equipment is assembled and turned on (i.e., ventilator/humidifier, radiant heater, CFM). Prepare all i.v. fluids, prime lines, and setup in syringe pumps.

3.1 Animals

Newborn piglets <24 h of age (large white) are obtained from the University of Queensland Gatton Piggery. Average piglet weight should be 1.5 ± 0.3 kg and the umbilical cord should still be present. Approvals for all studies are obtained from the University of Queensland Animal Experimentation Ethics Committee and are carried out in accordance with National Health and Medical Research Council guidelines (Australia).

3.2 Anesthesia and Ventilation

1. Induce initial anesthesia by isoflurane inhalation via a facemask.
2. Cannulate an ear vein (24G cannula), tape in place and administer a 5 mg/kg propofol induction dose.
3. Attach the propofol (9 mg/ml)/alfentinal (50 µg/ml) mixture and deliver at a rate of 10 mg/kg/h propofol until intubation. Once the animal is intubated increase the rate to 20 mg/kg/h propofol for 15 min, then reduce to 15 mg/kg/h propofol for 15 min followed by reduction and maintenance at 10 mg/kg/h.
4. Intubate piglets using a 3.0 cuffed ET tube and attach to a neonatal ventilator with settings as follows: 21 % fraction of inspired O₂ (FiO₂), 30 breaths per minute (bpm), peak inspiratory pressure (PIP) 12 cm, positive end expiratory pressure (PEEP) 5 cm, and inspiratory time 0.75 s. Inflate the cuff on the ET tube.

3.3 Surgical Preparation and Physiological Monitoring of Animals

1. Place the animal in supine position (sandbags can be placed at either side to prevent rolling). Attach electrocardiograph (ECG) leads to record and monitor heart rate (HR) and an oximeter to the hind trotter to record oxygen saturation (SaO₂). Position a rectal temperature probe (~3 cm) and tape to the tail to monitor and maintain core body temperature (CBT) at 38.5 °C. Monitor and record HR, SaO₂, and CBT using the Marquette data acquisition system (*see* Table 1 for normal values).
2. Cannulate a mammary vein (24G cannula) and tape in place with the thin micropore tape (Fig. 1). Attach a long extension with a three-way tap and short extension to the cannula, tape securely with thick micropore tape and infuse 10 % glucose at a rate of 3 ml/kg/h.
3. Umbilical artery catheterization should be performed under sterile surgical conditions. Prior to the surgery prepare a sterile surgery tray with the following: unwrapped sterile surgical pack—fill small dish with 2 % chlorhexidine, 5 ml syringe, three-way tap, UAC, swabs, #22 scalpel blade, sutures. Draw up 5 ml of heparinized saline, attach the three-way tap to the syringe and then to UAC and prime the catheter. Remove the

Table 1
Normal physiological status

Physiological variables	Normal value/range
MABP	>30 mmHg
HR	>130 bpm
SaO ₂	>95–100 %
Temperature	38.5 ± 0.2 °C
<i>Arterial blood gas variables</i>	
pH	7.35–7.45
pO ₂	80–100 mmHg
pCO ₂	35–45 mmHg
HCO ₃ ⁻	22–26 mEq/L
Base excess	-2 to +2 mmol/L
Glucose	1.5–6 mmol/L
Lactate	1.0–3.0 mmol/L

excess umbilical cord to reveal the umbilical vessels and aseptically catheterize an umbilical artery advancing the UAC approximately 11 cm. Suture UAC in place and fasten securely with brown tape. Attach the UAC to the blood pressure transducer, zero the waveform, and start recording the blood pressure (Marquette). Assess ABG regularly to monitor pO₂, pCO₂ and pH and adjust the ventilation settings as necessary to maintain normal values (Table 1).

- Administer 0.2 mg/kg cephalothin and 0.25 mg/kg gentamicin (via glucose line) following umbilical catheterization.

3.4 Amplitude-Integrated Electroencephalography (aEEG)

- Place the head and front limbs of the piglet in the prone position.
- For 2-channel aEEG insert five needle electrodes sub-dermally at C3-P3, C4-P4 (plus ground electrode) as defined by the neonatal modification of the International 10–20 system [26]. Electrodes can be taped in place (thin brown tape) to minimize movement. Position video to capture piglet movement.
- Initiate monitoring, check electrode impedance is minimal and start the video-aEEG recording using a cerebral function monitor (CFM).
- Normal aEEG voltage (continuous normal voltage—CNV) prior to the hypoxic–ischemic insult should be in the range of 10–25 µV depending on degree of anesthesia (see notes).

3.5 Hypoxic–Ischemic Protocol

1. Allow 90 min following initial anesthetic induction for the animal to stabilize, check blood gases to ensure that animal is stable and within normal ranges (Table 1) prior to inducing hypoxia.
2. Set timer for 30 min, detach oxygen line and attach to the nitrogen cylinder.
3. Turn on nitrogen and induce hypoxia by decreasing fraction of inspired O₂ (FiO₂) to 4 % (~85 % O₂ on ventilator = 4 % O₂ when blended with nitrogen).
4. If low amplitude EEG (laEEG; <5 μV) is not reached within the first 4 min, decrease FiO₂ to 2 %. Return FiO₂ to 4 % once laEEG is achieved.
5. Modify FiO₂ (range 2–10 %) as necessary to maintain laEEG for the duration of the HI insult and to maintain HR > 130 bpm and MABP >70 % baseline (i.e., above ~30 mmHg) for the first 20 min.
6. For the final 10 min of the insult, decrease FiO₂ until MABP is <70 % of baseline (<30 mmHg).
7. Terminate the insult and resuscitate the animal by returning to 21 % FiO₂ (air), detach the hose from the nitrogen cylinder and re-attach to the oxygen gas outlet.
8. Decrease the anesthetic infusion to 6 mg/kg/h. Adjust as necessary (4–10 mg/kg/h) to keep the piglet sedated and to minimize movement. Continue to monitor physiological variables (HR, MABP, etc.) and routinely check ABG.
9. Administer inotropic support as necessary, e.g., dopamine.
10. When required, cease the anesthesia infusion and slowly wean the piglet from ventilatory support. Once spontaneous breathing is established, the piglet can be moved to a quiet recovery area. Maintain CBT and feed 40–50 ml of artificial pig milk every 3–4 h.

3.6 Post-Insult aEEG and Seizure Analysis

When evaluating EEG activity (either in real time or offline), both the aEEG and raw EEG traces should be reviewed. The aEEG can be classified and described by determining background pattern of the aEEG and the presence or absence of seizures. Background aEEG pattern is defined as the dominant aEEG pattern in the trace at a given epoch and is classified in the following five categories:

- Continuous normal voltage (CNV) with minimum amplitude >5 μV and maximum amplitude >10 μV.
- Discontinuous normal voltage (DNV) with a variable minimum amplitude although <5 μV and a maximum amplitude >10 μV.

- Burst suppression (BS) is a discontinuous background with minimum amplitude of 0–1 μV and bursts with amplitudes $>25 \mu\text{V}$.
- Continuous low voltage (CLV) is characterized by a continuous background pattern but with very low voltage $\leq 5 \mu\text{V}$.
- Flat trace (FT) which is a predominantly inactive (isoelectric) trace $<5 \mu\text{V}$ [27].

Figure 1 illustrates background aEEG patterns in our pigs, these patterns are very similar to those observed in the term human newborn.

On the aEEG seizures are identified as a rise in the minimum and maximum amplitude (*see* Fig. 2), however actual electrographic seizure activity should be confirmed by analyzing the raw EEG trace. Electrographic seizures are defined as repetitive, rhythmic waveforms with a distinct beginning and end with a duration $>10 \text{ s}$ [14, 28]. They can be identified as a gradual build-up in both amplitude and frequency of spike-wave discharges with an abrupt cessation or may begin abruptly and decline gradually [27]. Electrographic seizure activity can present as:

- Epileptiform activity (Epi) which is seizure-like activity $<10 \text{ s}$ duration.
- Single seizure (SS) which is one seizure within a 30 min period.
- Repetitive seizures (RS) which consist of multiple seizures (more than one) within a 30 min period.
- Status epilepticus (SE) which is continuous seizure activity where return to baseline between seizures rarely occurs [27].

Figure 2 illustrates the types of seizures we observe in our pigs which are very similar to those observed in term human newborns [27]. We have devised a seizure scoring system taking into account both background aEEG pattern and type of seizure (Table 2) to enable us to analyze severity of EEG changes with brain injury measures (MRI and neuropathology).

The piglet should also be visually observed in real time for clinical seizure activity and evidence documented for the purposes of seizure classification, i.e., clinical or sub-clinical (electrographic only—no clinical signs). The synchronized video-EEG should be utilized to assess clinical seizures offline. While there is documented evidence of clinical only seizure activity (no electrographic correlate), clinical seizure activity should be accompanied by an electrographic seizure activity to confirm clinical seizures. Clinical seizures are identified by motor manifestations that can be subtle; eyes opening and closing, lip-smacking/tongue poking or by more overt signs such as myoclonic jerks, rhythmic pathologic movements (cycling), or tonic postures including hyperextension of the neck and of the front and hind limbs; in some instances there may

Table 2
aEEG classification score

Background pattern	Seizure activity			
	No Sz	Epi/SS	RS	SE
CNV	4	4	3	2
DNV	4	3	3	2
BS	3	3	2	1
CLV	2	2	1	1
FT	0	0	0	0

CNV continuous normal voltage, DNV discontinuous normal voltage, BS burst suppression, CLV continuous low voltage, FT flat trace

NoSz no electrographic seizure and/or clinical correlate, Epi/SS epileptiform activity or single seizure, RS repetitive seizures, SE status epilepticus

also be vocalization. In the conscious animal clinical seizures can manifest as the overt signs described above. However in the anesthetized animal, if clinical seizure signs are evident, they are often much more subtle.

Animals are constantly monitored for clinical seizures and if persistent clinical seizures develop, the animal is treated with phenobarbital (20 mg/kg). Animals are administered an initial dose and observed for termination of clinical seizure activity, if after 20 min clinical seizure activity has not resolved a second dose is given. If clinical seizures persist the animals are treated with a third dose of antiepileptic drug, in our case midazolam (0.2 mg/kg). If clinical seizures did not resolve following the third dose, the animal is euthanized as required by The University of Queensland Animal Experimentation Ethics Committee. As for human infants, administration of antiepileptic drugs can result in termination of clinical seizure activity but electrographic activity may persist—a phenomenon referred to as electro-clinical dissociation [15]. Depending on the experimental question however, treatment of clinical and/or electrographic seizures should be considered. For experiments addressing mechanisms of neonatal seizures it would be preferable that animals are not treated with antiepileptic drugs, however the welfare of the animal must be duly considered and suitable animal ethics sought.

3.7 Neurobehavioral Scoring

Animals can be assessed for neurobehavior once anesthesia has been ceased. Animals should be assessed from 8 h post-anesthesia to determine degree of neurobehavioral impairment. Animals should be assessed at 4 h intervals until 24 h post-anesthesia and then at 24 h intervals thereafter. Animals are assessed on nine neurologic measures such as the level of consciousness, respiration, ability to

stand and walk (both front and hind limbs should be assessed), the righting reflex, and the presence of clinical seizures. Each neurologic measure is assigned a score of 2 (normal), 1 (moderately abnormal), or 0 (pathologic). The nine neurologic measures are totaled to achieve a maximal score of 18 = normal.

3.8 Magnetic Resonance (MR) Studies

The gold standard for assessing HI brain injury in the human newborn is with MR imaging and MR spectroscopy. While MR was performed in our animals at a slightly earlier time-point (72 h post-HI) than that used in the H/I human infant (5–7 days post-birth), MR imaging and MR spectroscopy findings from our animal studies reveal changes similar to those observed in the human HI neonate [10, 29].

1. Piglets are sedated with an intramuscular injection of Zoletil (Tiletamine/Zolazepam 10 mg/kg).
2. The animal is placed in an evacuated beanbag and positioned supine in a new coil within the magnet.
3. Heart rate and oxygen saturation are continuously monitored using MR compatible equipment.
4. Images are obtained using the same methods used for human neonates; see our previous work for detailed methods [10]. Sagittal and coronal high-resolution T₂-weighted images are acquired using a multi-echo, fast spin-echo sequence and a series of multi-slice coronal diffusion-weighted images (DWI) acquired at the same slice position. Apparent Diffusion Coefficient (ADC) and T₂-weighted maps are generated and average ADC values for cortical and sub-cortical regions are calculated for comparison across animals.
5. ¹H-MR spectra is acquired in the fronto-parietal region from a 15-mm³ voxel. Lactate (Lac) is represented as an inverted broad peak (no doublet character) and is thus quantified 180° out of phase with the other metabolite peaks using a Gaussian peak. Peak area ratios are calculated for NAA/Lac, NAA/Cho, NAA/Cr, Lac/Cr, Lac/Cho, Lac/NAA, and Cho/Cr.

3.9 Tissue Collection/Brain Investigations

At 72 post-insult, animals are euthanized with a peritoneal injection of Lethobarb (650 mg/kg) until respiration ceases. The brain is transcardially perfused with 0.9 % sterile saline and then removed and coronally sectioned (3–4 mm). Brain regions of interest (frontal, temporal, parietal and occipital cortex, basal ganglia, hippocampus, thalamus, cerebellum, and brainstem) are dissected from the left hemisphere, snap frozen and stored at –80 °C. The right hemisphere is fixed for 24 h with agitation in 4 % paraformaldehyde/0.1 M phosphate buffered saline pH 7.2 (PBS) and the sections then stored in PBS/sodium azide (0.05 %).

3.10 Basic Neuropathology

Paraffin-embedded tissue sections (4 μm) are stained with hematoxylin and eosin to assess neuronal injury. Blinded examination of brain regions of interest is undertaken and injury graded from 0 to 9 with 0 representing no injury and 9 representing severe damage [30]. Total histological injury score is the sum of all brain region scores (maximum possible score = 81).

4 Troubleshooting and Notes

- Developmental stage is an important consideration when investigating seizures in neonatal models as the EEG changes dramatically between the preterm and term brain; pigs should be <24 h age which is equivalent to the term human brain [24].
- Pigs do produce spontaneously growth restricted piglets. As a guide weight should be >1.2 kg and <2.0 kg however this is dependent on litter size. In our experience, piglets <1.2 kg born at term are considered growth restricted (chronic hypoxia) and therefore should be excluded from acute hypoxia studies.
- The umbilical cord should still be present and attached and relatively fresh. A very dry or absent cord can (1) indicate that animals are most likely older than 24 h and therefore not considered “newborn” and (2) make finding and catheterizing the umbilical artery difficult. The umbilical stump can be cut down to access the umbilical vessels, however caution should be exercised so as not to perforate the abdominal wall. Extra care should also be taken with male piglets in such cases.
- Use of a timer is advised to ensure correct amount of anesthetic is administered.
- An easily visible anesthetic and drug chart (dopamine, adrenaline, etc.) with animal weights and doses is useful for quick reference.
- If possible, arterial blood gas analyzer with additional metabolites is useful to monitor glucose and lactate levels. Glucose levels can be monitored with a portable glucometer.
- If aEEG is below 10 μV prior to insult check the level of anesthesia administration is correct. If required anesthesia rate can be reduced for a short period.
- During the insult it is important to ensure an adequate period of hypotension (MABP < 70 % baseline; ~30 mmHg) is achieved for animals to develop moderate to severe brain injury and to increase the likelihood of developing seizures.
- It is preferable to have continuous aEEG with video for offline analysis of seizures. Most CFM systems will have event marker capability to allow a written comment in the file in real time. This

should be used in addition to the video, however it is vital if there is no access to video so that all movements and activity are recorded to clearly differentiate between seizure and non-seizure activity.

- Administration of drugs may differentially influence outcomes of seizures and changes in receptor populations, especially in the developing brain where AEDs have been shown to cause apoptosis and is an important consideration.
- In human neonates, normal jittery movements can be misdiagnosed as clinical seizures. If repositioning of the baby stops the seizure activity then it is unlikely to be a seizure; this also holds true in our seizure model.
- Electrographic seizures can also be misinterpreted. Identification of seizures must involve inspecting both the aEEG and raw trace. Rises in the minimum and maximum amplitude of the aEEG as well as patterns resembling repetitive waveforms on the raw trace may result from causes other than seizures. If the suspected artifact can be adjusted and the seizure activity ceases then it is not seizure. Other causes that resemble electrographic seizure activity can include:

- Movement artifact.

Recovery or inadequate level of anesthesia. The piglet can start to move or shake resulting in a raised aEEG margin.

Cycling of front and/or hind limbs may become apparent during recovery and is due to the innate righting reflex in animals. If you can place the pig in an upright position and cycling ceases then it is not seizure activity (see point above). The rhythmic waveform on the raw trace that accompanies this will also cease.

Human intervention, i.e., administering procedures (raised aEEG margin).

- Ventilation artifact (can be either or both aEEG and raw trace alterations).
- ECG artifact (can be either or both aEEG and raw trace alterations).

5 Conclusion

Significant progress in recent years had led to a much better understanding of the mechanisms that underlie seizures. The ultimate goal however is that animal models of human disease more closely mimic the human condition. This is critical to ensure both appropriate development of new therapies, especially in the developing brain, and to enable efficient translation to clinical care of the

human newborn. Management of seizures in the newborn is a significant clinical challenge. The harmful effects of seizures as well as the relative ineffectiveness and potentially adverse consequences of current AEDs provides a compelling need for relevant animal models to develop safe and effective seizure therapies for the developing newborn brain.

Acknowledgments

This work was supported by the National Health and Medical Research Council and The Lions Medical Research Foundation.

References

1. Silverstein FS, Jensen FE (2007) Neonatal seizures. *Ann Neurol* 62(2):112–120
2. Glass HC (2014) Neonatal seizures: advances in mechanisms and management. *Clin Perinatol* 41(1):177–190
3. Bassan H, Bental Y, Shany E, Berger I, Fromm P, Levi L et al (2008) Neonatal seizures: dilemmas in workup and management. *Pediatr Neurol* 38(6):415–421
4. Ramantani G (2013) Neonatal epilepsy and underlying aetiology: to what extent do seizures and EEG abnormalities influence outcome? *Epileptic Disord* 15(4):365–375
5. Badawi N, Kurinczuk JJ, Keogh JM, Alessandri LM, O'Sullivan F, Burton PR et al (1998) Intrapartum risk factors for newborn encephalopathy: the Western Australian case-control study. *BMJ* 317(7172):1554–1558
6. Prasad M, Chow G (2012) Neonatal seizure: what is the cause? *BMJ* 345, e6003
7. Tekgul H, Gauvreau K, Soul J, Murphy L, Robertson R, Stewart J et al (2006) The current etiologic profile and neurodevelopmental outcome of seizures in term newborn infants. *Pediatrics* 117(4):1270–1280
8. Wasterlain CG (1997) Recurrent seizures in the developing brain are harmful. *Epilepsia* 38(6):728–734
9. Wirrell EC, Armstrong EA, Osman LD, Yager JY (2001) Prolonged seizures exacerbate perinatal hypoxic-ischemic brain damage. *Pediatr Res* 50(4):445–454
10. Bjorkman ST, Miller SM, Rose SE, Burke C, Colditz PB (2010) Seizures are associated with brain injury severity in a neonatal model of hypoxia-ischemia. *Neuroscience* 166(1):157–167
11. McBride MC, Laroia N, Guillet R (2000) Electrographic seizures in neonates correlate with poor neurodevelopmental outcome. *Neurology* 55(4):506–513
12. Miller SP, Weiss J, Barnwell A, Ferriero DM, Latal-Hajnal B, Ferrer-Rogers A et al (2002) Seizure-associated brain injury in term newborns with perinatal asphyxia. *Neurology* 58(4):542–548
13. Schmid R, Tandon P, Stafstrom CE, Holmes GL (1999) Effects of neonatal seizures on subsequent seizure-induced brain injury. *Neurology* 53(8):1754–1761
14. Clancy RR, Legido A, Lewis D (1988) Occult neonatal seizures. *Epilepsia* 29(3):256–261
15. Murray DM, Boylan GB, Ali I, Ryan CA, Murphy BP, Connolly S (2008) Defining the gap between electrographic seizure burden, clinical expression and staff recognition of neonatal seizures. *Arch Dis Child Fetal Neonatal Ed* 93(3):F187–F191
16. Thoresen M, Hellstrom-Westas L, Liu X, de Vries LS (2010) Effect of hypothermia on amplitude-integrated electroencephalogram in infants with asphyxia. *Pediatrics* 126(1):e131–e139
17. Loscher W (2011) Critical review of current animal models of seizures and epilepsy used in the discovery and development of new antiepileptic drugs. *Seizure* 20(5):359–368
18. White HS, Loscher W (2014) Searching for the ideal antiepileptogenic agent in experimental models: single treatment versus combinatorial treatment strategies. *Neurotherapeutics* 11(2):373–384
19. Glass HC, Wirrell E (2009) Controversies in neonatal seizure management. *J Child Neurol* 24(5):591–599
20. Bittigau P, Siffringer M, Genz K, Reith E, Pospischil D, Govindarajulu S et al (2002) Antiepileptic drugs and apoptotic neurodegeneration

- in the developing brain. *Proc Natl Acad Sci U S A* 99(23):15089–15094
21. Helmy MM, Tolner EA, Vanhatalo S, Voipio J, Kaila K (2011) Brain alkalosis causes birth asphyxia seizures, suggesting therapeutic strategy. *Ann Neurol* 69(3):493–500
 22. Jensen FE, Applegate CD, Holtzman D, Belin TR, Burchfiel JL (1991) Epileptogenic effect of hypoxia in the immature rodent brain. *Ann Neurol* 29(6):629–637
 23. Rice JE 3rd, Vannucci RC, Brierley JB (1981) The influence of immaturity on hypoxic-ischemic brain damage in the rat. *Ann Neurol* 9(2):131–141
 24. Dobbing J, Sands J (1979) Comparative aspects of the brain growth spurt. *Early Hum Dev* 3(1):79–83
 25. Lynch NE, Stevenson NJ, Livingstone V, Murphy BP, Rennie JM, Boylan GB (2012) The temporal evolution of electrographic seizure burden in neonatal hypoxic ischemic encephalopathy. *Epilepsia* 53(3):549–557
 26. Fisch BJ (1999) *Fisch and Schlmann's EEG primer, basic principles digital and analog EEG*, 3rd edn. Elsevier, New York
 27. Hellstrom-Westas L, Rosen I (2006) Continuous brain-function monitoring: state of the art in clinical practice. *Semin Fetal Neonatal Med* 11(6):503–511
 28. Clancy RR, Legido A (1987) The exact ictal and interictal duration of electroencephalographic neonatal seizures. *Epilepsia* 28(5):537–541
 29. Munkeby BH, De Lange C, Emblem KE, Bjornerud A, Kro GA, Andresen J et al (2008) A piglet model for detection of hypoxic-ischemic brain injury with magnetic resonance imaging. *Acta Radiol* 49(9):1049–1057
 30. Bjorkman ST, Foster KA, O'Driscoll SM, Healy GN, Lingwood BE, Burke C et al (2006) Hypoxic/ischemic models in newborn piglet: comparison of constant FiO₂ versus variable FiO₂ delivery. *Brain Res* 1100(1):110–117

INDEX

A

- Actocardiograph 104, 106
 AD. *See* Alzheimer's disease (AD)
 Adenomatous polyposis coli (APC) ...282, 287, 293, 294
 Adenosine 95, 112
 ADHD. *See* Attention deficit hyperactivity disorder (ADHD)
 Adjacency matrix62, 63
 aEEG. *See* Amplitude-integrated electroencephalography (aEEG)
 Allopregnanolone...95, 127, 224–226, 228–233, 236–239
 Alzheimer's disease (AD).....42, 206–209, 211
 Amphetamine 271, 272
 Amplifiers.....54, 55, 91, 121, 316, 317
 Amplitude-integrated electroencephalography (aEEG)..... 344–346, 350–353, 355, 356
 Amygdala 4, 205–207, 209, 211
 Anaerobic glycolysis 329
 Antidepressants 245–259
 Antipyrine252, 254, 255, 257
 Anxiety207, 212, 213, 225, 233–237, 246, 247, 268
 APC. *See* Adenomatous polyposis coli (APC)
 apoD 204
 Apoptosis204, 205, 310, 337
 Apparent diffusion coefficient (ADC) 354
 Arcuate nucleus 191, 205
 Arousal ...92, 94–96, 102, 103, 112, 122, 123, 127, 225
 Artefact sensitivity 55
 Arterial spin labeled perfusion-magnetic resonance imaging (ASL-pMRI)..... 71–72, 81
 ASD. *See* Autism spectrum disorders (ASD)
 ASL-pMRI. *See* Arterial spin labeled perfusion-magnetic resonance imaging (ASL-pMRI)
 Astrocytes ...205, 209–214, 226–228, 234, 267, 284, 287, 289–291, 306, 308
 Astrocytosis..... 211, 289
 Attention deficit hyperactivity disorder (ADHD)...204, 214
 Autism spectrum disorders (ASD)41, 204, 213, 249
 Autoregulation 73, 77, 305, 333
 Axonal injury283, 289, 291–293, 310

B

- Basal ganglia21, 206, 310, 354
 BDNF. *See* Brain-derived neurotrophic factor (BDNF)
 BFI. *See* Blood flow index (BFI)

- Bielschowsky's silver stain.....291
 Blood flow index (BFI).....80–82
 Blood oxygenation level-dependent (BOLD)....54, 57–60, 72, 78
 Bmal1 148–152
 BMI.....169, 204, 206, 207, 213
 BOLD. *See* Blood oxygenation level-dependent (BOLD)
 Brain-derived neurotrophic factor (BDNF) 210, 213
 Brain injury... 70, 77, 82, 226, 282, 290, 291, 303, 304, 310, 312, 319, 328, 335, 337, 344, 346, 352, 354, 355

C

- Cafeteria-style diet 192
 Cajal-Retzius cells 4, 5, 16, 17, 33
 Carbamazepine211
 Carbocyanine dyes 22
 CBF. *See* Cerebral blood flow (CBF)
 CBF autoregulation73, 77, 333
 Centrum ovale.....286
 Cephalic ischemia 313, 321
 Cerebellum 113, 205, 215, 267, 289, 354
 Cerebral blood flow (CBF) ... vii, viii, ix, 69–83, 305, 313, 319–321, 333
 Cerebral injury282, 304, 312–313, 319–321, 327
 Cerebral metabolic rate.....72, 77
 Cerebral metabolic rate of oxygen (CMRO₂).....72, 81
 Cerebral oxygenation 70, 72, 74, 77–83
 Cerebral palsy vii, 304, 328, 343
 Cerebral perfusion.....70, 72, 77, 83, 333
cFos..... 156
 CFP 42
 Channelrhodopsin.....31–34
 Chick..... vii, 35
 Chronodisruption viii, 147, 148, 156–158, 161, 162
 Circadian..... viii, 90, 118, 128–129, 137, 147–162
 Circadian clock148–150, 155, 157
 Circadian rhythms 118, 128–129, 137, 147–162
 Citalopram.....248, 252, 255–258
 Clock..... 148–151, 153, 155, 159–161
 Clock genes 148–151, 153, 156, 157, 160
 CLoNe29–30
 CMRO₂. *See* Cerebral metabolic rate of oxygen (CMRO₂)
 CNP. *See* 2',3'-Cyclic-nucleotide 3'-phosphodiesterase (CNP)

Conjugated linoleic acid 190
 Connectivityvii, 53–63, 65, 197, 312
 Continuous wave (CW) spectroscopy.....74, 75
 Cord occlusion... 124, 305, 306, 313, 319, 320, 329–337
 Corpus callosum..... 15, 182, 286, 289, 308
 Cortical development 4, 19, 21–36, 291, 311
 Cortical plate5, 15, 16, 18, 19, 27, 29, 30, 48
 Corticogenesis..... vii, 27, 36
 Corticotrophin-releasing hormone (CRH)..... 212
 Cortisol.... 128, 131, 157, 160, 212, 233–236, 238, 239
 Cosinor analysis..... 161
 CRH. *See* Corticotrophin-releasing hormone (CRH)
 Cryptochrome1-2 148
 2',3'-Cyclic-nucleotide 3'-phosphodiesterase
 (CNP)282, 287, 293, 294
 Cystic necrosis 282
 Cystic necrotic lesions..... 291, 304

D

DCS. *See* Diffuse optical correlation spectroscopy (DCS)
 Dementia206–208, 215
 Deoxycorticosterone (DOC) 224
 Deoxyhaemoglobin..... 214
 Depression 207, 210, 212, 225, 233, 237,
 246–249, 259
 Diaphragmatic EMG 108, 111, 114–116
 Diet170–175, 177, 182–187, 189–193, 196–198,
 205–207, 210
 Diffuse optical correlation spectroscopy (DCS).....80–82
 Diffusion correlation spectroscopy 80–82
 3 α -Dihydroprogesterone 224
 Dizocilpine 271
 DOC. *See* Deoxycorticosterone (DOC)
 Docosahexaenoic acid..... 212
 Dopamine 170, 180, 267, 271, 272, 347, 351, 355
 D2 receptor 170, 180

E

Echo-planar imaging (EPI) 57, 58, 60, 63
 ECoG.....91–93, 95, 99–101, 105–107, 109–114, 121,
 122, 128, 132
 EEG. *See* Electroencephalography (EEG)
 Electroocortical91, 93, 94, 96–101
 Electroencephalography (EEG)... vii, 53–65, 81, 99–103,
 106, 107, 119, 316, 327, 330, 344, 345, 348, 351,
 352, 355
 Electron microscopy 283, 285, 286, 289, 292–293,
 296–297
 Electroporation ... vii, 4–6, 10–13, 15–18, 22–32, 34–36
 EMG activity 91, 92, 95, 108, 111, 114–116, 122,
 126, 129
 EPI. *See* Echo-planar imaging (EPI)
 Epilepsy.....41, 42, 204, 207, 208, 211, 212, 343
 Epileptic seizures 206

Epileptiform activity..... 207, 352, 353
 Eriochrome cyanine R 288
 Estradiol..... 157, 212, 336
 External capsule..... 286, 289
 Ex vivo perfusion 250–255
 Eye movements91, 92, 94–96, 101–104, 111, 112,
 117, 121–123

F

FACS. *See* Fluorescence-activated cell sorting (FACS)
 False detection rate (FDR) 61
 Fast Fourier analysis98, 99
 Fast Green8, 9, 11, 13, 24, 252, 253
 FDR. *See* False detection rate (FDR)
 Ferret 35, 107
 Fetal baboons95, 100, 101, 128
 Fetal breathing movements 107–114, 117–119, 130,
 134, 137
 Fetal electroencephalogram 313
 Fetal lambs ...91–103, 106–113, 115–119, 121, 124–128,
 130–136
 Fetal programming 246
 Fetal SCN149, 150, 153, 154
 Fetal sheep... 90, 93, 126, 231, 238, 283, 291, 303–306,
 308–313, 319–321, 329–336
 Fetal sleep statesviii, 90, 91, 96, 101, 109, 122
 Fick principle70, 76
 Finasteride 225, 226, 229
 Fluorescence-activated cell sorting (FACS)..... 42–47, 49,
 50
 fMRI. *See* Functional magnetic resonance imaging (fMRI)
 FOS 156
 Fractin 288, 291, 292
 Frequency resolved spectroscopy 74
 Functional brain connectome..... 62
 Functional magnetic resonance imaging (fMRI) ...vii, 53,
 54, 57–60, 62–65, 72, 77–78

G

GABA_A receptor.....208, 209, 224, 238
 GABAergic neurons41–50, 170, 208, 209, 311
 GAD65 42
 GAD6742–44, 46, 49, 208
 Gallyas silver stain 288
 Gamma-amino butyric acid 224
 Germinal matrix haemorrhage70, 77
 GFAP. *See* Glial fibrillary acidic protein (GFAP)
 GFP. *See* Green fluorescent protein (GFP)
 GFP+42–50
 Ghrelin..... 205, 209
 GLAST..... 287, 289
 Glial fibrillary acidic protein (GFAP)..... 226, 228, 229,
 234, 287, 289, 290, 308
 GLT-1 287, 289

Glucocorticoid receptors (GR) 150, 196, 212, 224
 Glucocorticoids 148, 150, 156, 157, 196, 234, 236, 238
 GR. *See* Glucocorticoid receptors (GR)
 Green fluorescent protein (GFP) 5, 42–50
 Growth restriction 137, 191, 225–228, 239, 283
 Gyrencephalic vii, 312, 329

H

Head cooling 313
 HIE. *See* Hypoxic–ischemic encephalopathy (HIE)
 High fat diet 170, 191, 192, 205, 210
 HPA axis. *See* Hypothalamic–pituitary–adrenal (HPA) axis
 5-HT. *See* 5-Hydroxytryptamine (5-HT)
 Human fetus 101–107, 118, 119, 128, 132, 213, 305
 Human influenza virus 264–265
 5-Hydroxytryptamine (5-HT) viii, 245–249, 258, 259
 Hyperphagia 197
 Hypotensio 79, 131, 132, 305, 313, 319, 328, 330, 334–337, 346, 355
 Hypothalamic–pituitary–adrenal (HPA) axis 196, 197, 233, 234, 237, 238, 335
 Hypothalamus 109, 148, 191, 197, 204–206, 215, 259
 Hypoxia 70, 77, 110, 111, 225, 283, 305, 318, 319, 328, 330, 332, 335, 336, 344–346, 351, 355
 Hypoxia-ischemia 70, 283, 297, 305–311, 313, 321, 327, 335, 344
 Hypoxic–ischemic encephalopathy (HIE) 328, 343, 347

I

Iba1 287, 289, 290, 308
 Ibotenic acid 111
 ICA. *See* Independent component analysis (ICA)
 Immunohistochemistry 48–50, 174, 178, 180, 182, 259, 284, 286, 287, 292
 Independent component analysis (ICA) 57, 60, 61, 63
 Infection viii, 264–267, 269, 271, 272, 274, 283, 314, 317, 321, 327, 335, 343
 Inflammation 204, 205, 210–213, 283, 309, 327
 In situ hybridization 113, 159, 174, 180–182, 186, 283, 285
 Insulin 157, 158, 190, 205, 209
 Interhemispheric synchrony 55, 56
 Interneurons vii, 4, 21, 22, 41, 42, 44, 48, 49, 208, 211, 311
 Intrauterine growth restriction/retardation (IUGR) 137, 226, 229, 239, 283, 295, 335
 Intraventricular haemorrhage 70, 77, 82
 In utero electroporation (IUE) vii, 3–19, 21–36, 247
 In utero growth restriction 191
 In utero labeling 22
 In utero transplantation 44
 IUE. *See* In utero electroporation (IUE)
 IUGR. *See* Intrauterine growth restriction/retardation (IUGR)

J

Junk food 169–172, 174, 175, 177, 182–185, 187

K

Kainic acid 207, 344
 Ketogenic diet 206
 Kv4.2 channel 208

L

Lectins 287, 289
 Leptin 156, 157, 196, 197, 205, 209
 LFB. *See* Luxol fast blue (LFB)
 Lipopolysaccharide (LPS) 197, 265–267, 269, 335, 336
 Litter 27, 50, 184, 185, 193–197, 222
 Litter size 4, 50, 171, 175, 193–198, 225, 355
 LPS. *See* Lipopolysaccharide (LPS)
 Luxol fast blue (LFB) 288

M

Macronutrient 172, 173, 176, 177, 183
 MAG. *See* Myelin-associated glycoprotein (MAG)
 Magnetic resonance imaging (MRI) 53–65, 72, 78, 81, 214, 265, 267, 283, 284, 306, 308, 309, 313, 318, 321, 328, 344, 352, 354
 Magnetic resonance spectroscopy (MRS) 284, 344, 354
 Magnetoencephalography (MEG) 56, 105, 106
 MAP-2 234
 Maternal diet 170, 185, 190, 192
 Maternal-fetal transfer viii, 252, 255, 258
 Maternal obesity 192, 203–215
 Maternal stress viii, 175, 185, 186, 233, 235, 236, 238, 239, 248, 258
 MBP. *See* Myelin basic protein (MBP)
 Medial ganglionic eminence (MGE) 21, 42–50
 MEG. *See* Magnetoencephalography (MEG)
 Melatonin 128, 129, 149, 150, 153–158, 160
 Mesolimbic viii, 169–187
 Metabolic syndrome 157, 158, 204
 MGE. *See* Medial ganglionic eminence (MGE)
 Microcapillary 6, 8, 9, 13, 17, 18
 Microglia 209–210, 213, 284, 287–291, 306, 308, 309
 Microgliosis 283, 289–291
 microRNA regulome viii, 148, 162
 Midazolam 347, 353
 Mineralocorticoid receptors (MR) 212
 miRNAs 155
 MOG. *See* Myelin oligodendrocyte glycoprotein (MOG)
 Morphogen 4
 MR. *See* Mineralocorticoid receptors (MR)
 MRI. *See* Magnetic resonance imaging (MRI)
 MRS. *See* Magnetic resonance spectroscopy (MRS)

mu-opioid receptor 170, 180, 182
Muscimol 33
Myelin-associated glycoprotein (MAG)..... 282, 287,
293–295
Myelination 120, 211, 215, 222, 225, 226,
228, 230, 232, 234, 281–283, 285, 286, 289, 291,
293–297, 306–310, 312, 313, 330
Myelin basic protein (MBP)..... 226, 229, 230, 234,
282, 287, 293–295
Myelin oligodendrocyte glycoprotein (MOG)... 282, 295
Myelin sheath 281, 282, 285, 295–297
Myosin heavy chain isoforms..... 115, 116

N

NA. *See* Noradrenaline (NA)
NAc. *See* Nucleus accumbens (NAc)
NADPH oxidase 210, 211
Naloxone 182, 183, 185, 186
Near infrared spectroscopy (NIRS) 70, 73–82, 329
Necrosis 155, 304, 306, 308–310
Neocortex..... vii, 3, 4, 16, 21, 35, 41, 42,
44, 206
Neonatal ix, 53–57, 59, 62, 64–65, 69–83, 95, 103,
106, 115, 116, 120, 128, 173, 180–182, 192,
193, 195–197, 204, 229–233, 235, 236, 239,
273, 283, 290, 304, 308, 310, 312, 313, 327,
328, 336, 343–357
EEG 54–57
rats..... 120, 173, 180–182, 283, 336, 343
seizures..... ix, 343–357
Nerve growth factor (NGF)..... 196, 213
Netrin-G1a 258, 259
Neuro-imaging 304, 313
Neurosteroid(s)..... viii, 127, 221–239
Neurovascular coupling vii, 53, 64, 65
NG2 282, 286, 287, 293
NGF. *See* Nerve growth factor (NGF)
NIRS. *See* Near infrared spectroscopy (NIRS)
Nitric oxide synthase (NOS) 210
Nitrous oxide..... 70, 315
Non REM sleep..... 91, 225
Noradrenaline (NA)..... 212
NOS. *See* Nitric oxide synthase (NOS)
NPY..... 208, 209
Nucleus accumbens (NAc) 170, 173, 174, 178–182,
184, 186

O

O1 282, 283, 286, 287, 293, 294
O4 282, 283, 286, 287, 293, 294
Obesity..... 157, 169, 187, 189–192, 198, 203–215
Olig1 282, 287, 293
Olig2 282, 287, 293, 294

Oligodendrocyte progenitor 282, 309–310
Oligodendrocyte progenitor cells
(OPCs)..... 281–283, 287, 293
Oligodendrocytes ix, 281–297, 304, 308–310, 312
Omega-3..... 190
OPCs. *See* Oligodendrocyte progenitor cells (OPCs)
Opioids 170, 180–183
Opsins 31
Optogenetics 22, 31–34, 214

P

Paraventricular nucleus of the hypothalamus (PVN)... 191,
196, 197
Per2..... 149–152, 156
Perinatal asphyxia 169–338
Perinatal programming 189–191
Perinatal white matter injury ix, 282–291, 295, 297
Period1-3 148
Periventricular leukomalacia (PVL) 70, 291, 295, 304,
307–309
Peroxisome proliferator-activated receptor- γ coactivator
1 α 335–336
PET. *See* Positron emission tomography (PET)
Phenobarbital 211, 347
Phenytoin 211
Photoperiod viii, 147, 149
Pig...ix, 96, 106, 107, 116, 117, 121, 123, 124, 129, 132,
221–239, 344–346, 351, 352, 355, 356
Piglet 344, 346, 349–352, 354–356
Pinelectomy 128, 153
Pineal gland 153
Placenta... viii, 17, 24, 47, 95, 112, 128, 129, 133, 134,
150, 153, 222–224, 226–228, 234, 236, 239,
247–255, 257, 265
Placental insufficiency 223, 227, 335, 337
Placental transfer 254, 257
Plasmids 4, 6, 8, 9, 11–15, 17–19, 22–24, 27–30,
33, 34
PLP. *See* Proteolipid protein (PLP)
Polygraph..... 91, 93, 94, 96, 100, 108, 134
Polyribonucleosinic-polyribocytidilic acid (Poly I:C).....ix,
266–275
Positron emission tomography (PET)..... 70, 71
Post traumatic stress disorder (PTSD) 212
PPI. *See* Prepulse inhibition (PPI)
PR. *See* Progesterone receptor (PR)
PRA..... 223
PRB 223
Prefrontal cortex 206, 212, 273
Prenatal immune activation 263–275
Pre-oligodendrocytes (preOLs) 281, 283, 284, 287,
293, 304, 306, 308–310
Preplate layer 15
Prepulse inhibition (PPI)..... 265, 266, 269, 271–274

Preterm birth 69, 121, 225, 228–232, 239, 282
 Proenkephalin 180
 Progesterone 127, 156, 157, 222–224, 228–232, 239
 Progesterone receptor (PR) 223
 Prostaglandin E₂ 112
 Prostaglandin H-synthase-1 113
 Proteolipid protein (PLP) 282, 287, 293–295
 PTSD. *See* Post traumatic stress disorder (PTSD)
 PVL. *See* Periventricular leukomalacia (PVL)
 PVN. *See* Paraventricular nucleus of the hypothalamus (PVN)
 Pyknosis 294
 Pyramidal neurons vii, 21, 23, 41, 42, 204, 311

R

Radial glia 22, 30, 287, 289
 Raphe nuclei 246
 Reactive gliosis 282
 Reactive oxygen species (ROS) 211, 306
 Real-time ultrasound 102, 104, 115, 118, 122, 124–126, 130
 Regional cerebral oxygen saturation (rScO₂) 76, 81
 Region of interest 23, 25, 59
 REM sleep 91–93, 96–98, 102–104, 107, 111, 115, 117, 121–123, 130, 132
 Remyelination 282
 Reptile 35
 ROS. *See* Reactive oxygen species (ROS)
 rScO₂. *See* Regional cerebral oxygen saturation (rScO₂)

S

Satiety 189, 191, 197, 205
 Schizophrenia viii, 41, 210, 246, 263–275
 SCN. *See* Suprachiasmatic nucleus (SCN)
 Seizures ix, 42, 206–207, 211, 316, 333, 343–357
 Selective serotonin reuptake inhibitors (SSRIs) 245–259
 Sensorimotor gating 268, 271
 Serotonin viii, 196, 245–247
 SERT 246, 247, 249
 Sex vii, 174, 184, 185, 212, 235, 268, 270, 328, 336–337
 Sickness behaviours 266, 267, 274
 Single photon emission computed tomography (SPECT) 71
Slc6a4 246
 Sleep epochs 56
 SOM. *See* Somatostatin-positive (SOM)
 Somatostatin 42
 Somatostatin-positive (SOM) 208
 Spastic diplegic 304
 SPECT. *See* Single photon emission computed tomography (SPECT)
 Spectral edge frequency analysis 97–101, 132

SSRIs. *See* Selective serotonin reuptake inhibitors (SSRIs)
 STK24 204, 210, 212
 Stress ... vii, viii, 155, 156, 161, 175, 185, 186, 193–197, 204, 210–214, 222, 223, 232–239, 248, 258, 273, 310, 319, 330, 337
 Subcortical injury 336
 Subplate 5, 15, 16, 19, 30, 33
 Suprachiasmatic nucleus (SCN) 148–150, 152–156, 158
 Surrogate signals 61
 Synaptotagmin 204

T

TCD. *See* Transcranial Doppler (TCD)
 tdTomato 42
 Temporal lobe epilepsy (TLE) 207, 211
 5 α -Tetrahydrocorti-costerone (THDOC) 224
 Tetrodotoxin 33
 THDOC. *See* 5 α -Tetrahydrocorti-costerone (THDOC)
 Therapeutic hypothermia 82, 328
 Time resolved spectroscopy 74, 75
 Tissue oxygenation index (TOI) 76–78
 TLE. *See* Temporal lobe epilepsy (TLE)
 TLR. *See* Toll-like receptor (TLR)
 TLR-3 266
 TLR-4 265
 TOI. *See* Tissue oxygenation index (TOI)
 Toll-like receptor (TLR) 210, 265
 Transcranial Doppler (TCD) 70, 73
 Transfection vii, 4, 15, 18, 19, 23, 28, 34, 214
 TrkB 210
 Tryptophan 249
 TUNEL 294
 Tyrosine hydroxylase 180

U

Ultrasound 73, 81, 102–105, 115–128, 130
 Umbilical cord occlusion 124, 305, 319, 329–337

V

Valproic acid 211
 Ventral tegmental area (VTA) 170, 173, 174, 178–182, 184
 Ventricular zone (VZ) 5, 15, 16, 21, 27, 29, 30, 42, 156
 Vibroacoustic stimulation 104
 VTA. *See* Ventral tegmental area (VTA)
 VZ. *See* Ventricular zone (VZ)

W

Wakefulness 58, 92–95, 103, 107

White matter injury (WMI)..... ix, 273, 281–297, 304–313, 319, 321, 329, 335	Y YFP 42
X	Z
Xenon-133 70–71	Zeitgeber 152–154, 161